University of Oxford

The role of aquatic systems and the re-occupation and settlement of the North European Plain during the Lateglacial

Cassian Bramham Law

Thesis submitted for degree of D.Phil

Research Laboratory for Archaeology and the History of Art

August 2013

Declaration

I declare that the work in this thesis is my own

Cassian Bramham Law

University of Oxford

Hertford College

Archaeological Science

The role of aquatic systems and the re-occupation and settlement of the North European Plain during the Lateglacial

Cassian Bramham Law

The Lateglacial between ~14,600 - 11,500 cal yr BP is characterised by the rapid fluctuation of climatic conditions following the termination of the Last Glacial Maximum. During this period, the North European Plain (NEP) was re-occupied and settled by hunter-gather groups utilising a succession of lithic technocomplexes. Contrasting models of population expansion exist to explain the re-occupation of the NEP by ~14,600 cal yr BP. Both rapid climatic amelioration and increased food resource availability on the NEP are suggested as possible stimuli. Studies of food resource availability as a stimulus for re-occupation and settlement of the NEP have long been dominated by the prevailing view that large mammal hunting was the dominant subsistence strategy. A number of archaeological finds across the NEP however, suggest that the exploitation of aquatic resources such as fish may have played a role in a more varied subsistence strategy during the period ~14,600 - 11,500 cal yr BP.

This thesis sets out to examine the development of palaeolake systems and examine their potential as a resource base for Lateglacial hunter-gatherers. This is achieved through the analysis of sedimentary organic matter and cladoceran records from five Lateglacial sites in northern Germany and southern Denmark, providing important information on basin development and the presence or absence of fish. The results suggest that significant variability existed in the development and resource availability of the basins over a local scale. Observed variability in the organic matter and cladoceran records within chronozone boundaries suggests that the Lateglacial – Holocene development of aquatic systems across the NEP cannot be solely explained by external climate

change, and that local environmental and ecological factors are likely to have played a major part in their development.

This thesis demonstrates that the local variance in aquatic conditions and fish populations would have offered, at best, limited and ephemeral resource availability and were therefore unlikely to have formed a major resource base for hunter-gatherer groups across the NEP. It is more likely that lakes were exploited opportunistically and as such formed only a minor component of a subsistence strategy more focussed on large mammal hunting.

Table of Contents

		Page
List of figures		**xii - xvi**
List of tables		**xvii - xviii**
Acknowledgements		**xix**
	Chapter 1: The Lateglacial of the North European Plain	**1**
1.1	The Lateglacial	2
1.1.1	*Lateglacial chronostratigraphic classification*	2 - 5
1.1.2	*Chronostratigraphic synchronicity*	5 - 6
1.2	Conventions adopted	6 - 7
1.3	The North European Plain – floral record	8 - 12
1.4	The North European Plain – faunal record	12 - 16
1.5	The North European Plain – aquatic record	16 - 18
1.5.1	*Aquatic fauna*	18 - 19
1.6	Thesis structure	19 - 21
1.7	Aims and objectives	21
1.8	Chapter summary	21 - 22
	Chapter 2: Human dispersal and archaeology during the Lateglacial	**23**
2.1	Structure of Lateglacial expansion	23 - 24
2.1.1	*Population event 1 - refugium*	24 - 26
2.1.2	*Population event – initial expansion*	26 - 27
2.1.3	*Population event 3 – expansion II*	27 - 30
2.1.4	*Population event 4 – expansion III*	30 - 31
2.1.4.1	*The significance of dating population event 4*	31 - 33
2.1.5	*Population event 5 – consolidation*	33- 36
2.1.6	*Population event 6 – hiatus*	36 - 37
2.2	Models of population expansion	37 - 38

2.2.1	*Population 'pull' model*	38
2.2.2	*Population 'push' model*	39
2.3	The technocomplexes and subsistence strategies of population events 4-6	40 - 41
2.3.1	*Conventions adopted*	41 - 42
2.3.2	*The Hamburgian – Population event 4*	42 - 46
2.3.2.1	*The cause of variation between the classic Hamburgian and Havelte Group*	46 - 47
2.3.2.2	*Hamburgian subsistence strategies*	47 - 50
2.3.3	*The Federmesser – Population event 5*	50 - 55
2.3.3.1	*Federmesser subsistence strategies*	55- 57
2.3.4	*The Brømme – Population event 5*	57 - 59
2.3.4.1	*Bromme subsistence strategies*	59 - 60
2.3.5	*The Ahrensburgian – Population event 6*	60 - 63
2.3.5.1	*Ahrensburgian subsistence strategies*	63 - 64
2.4	Chapter summary	64
	Chapter 3: Understanding aquatic exploitation during the Lateglacial	**65**
3.1	Understanding the basis of aquatic exploitation	65 - 67
3.1.1	*Evidence from modern hunter-gatherers*	68 - 70
3.1.2	*A model of aquatic exploitation for the NEP*	70 - 71
3.2	Microtephra analysis	71 - 75
3.3	Stable isotope analysis	75 - 76
3.4	Cladoceran sub-fossil analysis	76 - 78
3.5	Study sites	78
3.5.1	*Slotseng*	78 - 80
3.5.1.1	*Site stratigraphy*	81 - 82
3.5.1.2	*Tephrochronology and tephrostratigraphy of the Slotseng kettle hole*	83
3.5.1.3	*Radiocarbon dates for Slotseng*	83 - 85
3.5.2	*Endinger Bruch*	85 - 88
3.5.2.1	*Site stratigraphy*	89
3.5.2.2	*Tephrochronology and tephrostratigraphy of the Endinger Bruch kettle hole*	89 - 90
3.5.2.3	*Radiocarbon dates and age models for Endinger Bruch*	90 - 92

3.5.3	*Potremser Moor*	92 - 94
3.5.3.1	*Site stratigraphy*	95
3.5.4	*Kieshofer Moor*	95 - 96
3.5.4.1	*Site Stratigraphy*	96 - 98
3.5.5	*Daschower Moor*	99 - 100
3.5.5.1	*Site stratigraphy*	101
3.6	Chapter Summery	101
	Chapter 4: Field and laboratory Methodology	102
4.4	Field sampling	102
4.4.1	*Slotseng, Denmark*	102
4.4.2	*Endinger Bruch, Germany*	102
4.4.3	*Potremser Moor, Kieshofer Moor and Daschower Moor*	103
4.4.4	*Lundby Mose, Denmark*	103
4.4.5	*Gedser, Denmark*	103
4.4.6	*Tolk, Germany*	103
4.4.7	*Gorinsee, Germany*	103
4.4.8	*Weitsche, Germany*	104
4.5	Laboratory methods: Cryptotephra	104 - 105
4.5.1	*Sediment sampling*	105 - 106
4.5.2	*Sieving*	106
4.5.3	*Density separation of samples*	106
4.5.4	*Alterations to density separation method (4.5.3)*	106
4.5.5	*Scanning*	106 - 107
4.5.6	*EPMA*	107
4.5.7	*LA-ICP-MS*	107 - 108
4.5.8	*Alterations to LA-ICP-MS (4.5.7)*	108
4.6	Laboratory methods: sedimentary stable isotope analysis	108 - 109
4.6.1	*Sediment sampling*	109
4.6.2	*Mass spectrometry*	110
4.6.3	*Total organic carbon*	110 - 111

4.6.4	*Total nitrogen*	111 - 112
4.6.5	*C:N ratios*	112 - 113
4.7	Laboratory methods: cladoceran analysis	113 - 114
4.7.1	*Sediment sampling*	114
4.7.2	*Identification*	114 - 115
4.8	Laboratory methods: radiocarbon dating	115
4.9	Laboratory methods: additional sedimentary analysis	115
4.9.1	*Loss on ignition*	115
4.9.2	*$CaCO_3$ content*	116
4.9.3	*Dry bulk density*	116
4.10	Chapter summary	117
	Chapter 5: Results I Chronology	118
5.1	Potremser Moor tephrochronology	118
5.1.1	*POT-455*	119 - 121
5.1.2	*POT-446*	121
5.1.3	*Geochemical comparison of POT-455*	121 - 124
5.1.4	*Potremser Moor radiocarbon dates*	125
5.1.5	*An age model for Potremser Moor*	125 - 126
5.2	Kieshofer Moor tephrochronology	127
5.2.1	*KHM-796*	128 - 129
5.2.2	*KHM-749*	130
5.2.3	*KHM-622*	130
5.2.4	*Geochemical comparison of KHM-796*	130 - 131
5.2.5	*Kieshofer Moor radiocarbon dates*	131 - 132
5.2.6	*An age model for Kieshofer Moor*	132 - 134
5.3	Daschower Moor tephrochronology	135
5.3.1	*DAM-263*	136
5.3.2	*Geochemical comparison of DAM-263*	136 - 138
5.3.3	*Daschower Moor radiocarbon dates*	138 - 139
5.3.4	*An age model for Daschower Moor*	139 - 140

5.4	Chapter summary	140 - 141
	Chapter 6: Results II	**142**
6.1	Slotseng, Denmark	142
6.1.1	*Isotope and organic content record*	142 - 147
6.1.2	*Deviation of TN record*	147 - 148
6.1.3	*Distinction of OM zones*	148 - 149
6.1.4	*Chronozone distinction*	149 - 150
6.1.5	*Cladoceran record*	150 - 156
6.1.6	*Palaeoevolution of Slotseng*	156 - 160
6.2	Endinger Bruch, Germany	160
6.2.1	*Isotope and organic content record*	160 - 166
6.2.2	*Distinction of OM zones*	166 - 167
6.2.3	*Chronozone distinction*	168 - 169
6.2.4	*Cladoceran record*	169 - 176
6.2.5	*Palaeoevolution of Endinger Bruch*	176 - 180
6.3	Potremser Moor, Germany	180
6.3.1	*Isotope and organic content record*	180 - 185
6.3.2	*Deviation of TN record*	185 - 186
6.3.3	*Distinction of OM zones*	186 - 187
6.3.4	*Chronozone distinction*	187 - 189
6.3.5	*Cladoceran record*	189 - 194
6.3.6	*Palaeoevolution of Potremser Moor*	194 - 196
6.4	Kieshofer Moor	196
6.4.1	*Isotope and organic content record*	196 - 200
6.4.2	*Deviation of TN record*	299 - 201
6.4.3	*Distinction of OM zones*	201 - 202
6.4.4	*Chronozone distinction*	202 - 203
6.4.5	*Cladoceran record*	204 - 209
6.4.6	*Palaeoevolution of Kieshofer Moor*	209 - 211
6.5	Daschower Moor, Germany	211

6.5.1	*Isotope and organic content record*	211 - 216
6.5.2	*Distinction of OM record*	216 - 217
6.5.3	*Distinction of chronozones*	217 - 218
6.5.4	*Cladoceran record*	218 - 224
6.5.5	*Palaeoevolution of Daschower Moor*	224 - 226
6.6	Chapter summary	226
	Chapter 7: Discussion	**227**
7.1	Site chronologies	227 - 233
7.2	Comparison of OM and cladoceran response to climatic boundaries across study sites	233 - 234
7.2.1	*Variability between study sites*	234 - 249
7.2.2	*The impact of the Laacher See eruption on Lateglacial aquatic systems*	249 - 260
7.2.3	*Inter-site correlation and wider implications*	260 - 263
7.2.3.1	*Lake productivity at 12,880 ± 40 cal yr BP: The LST*	263 - 269
7.2.3.2	*Lake productivity at 12,121 ± 114 GICCO5 yr BP: The Vedde Ash*	270 - 273
7.3	What potential did the Lateglacial lakes of the NEP have of supporting hunter gatherer groups?	274 - 275
7.3.1	*Hypothesis 1: aquatic systems within the NEP during the Lateglacial responded synchronously to AETs making them a predictable resource base*	275 - 276
7.3.2	*Hypothesis 2: levels of productivity within aquatic systems are consistent across all systems regardless of the surrounding terrestrial environment*	276 - 277
7.3.3	*Hypothesis 3: aquatic systems were sufficiently productive to support hunter-gatherer groups during the Lateglacial of the NEP*	277 - 279
7.8	Chapter summary	279 - 280
	Chapter 8: Conclusions	**281 - 283**
	Bibliography	**284 - 347**
	Appendix I: Additional study sites	**348 - 356**
	Appendix II: Stable isotope and selected organic matter data	**357 - 361**
	Appendix III: Cladoceran counts	**362 - 381**

Appendix IV: Additional sedimentary data **382**

Appendix V: Selected cladoceran images **283 - 384**

Appendix VI: Bramham Law *et al*., 2013; New findings regarding the Saksunarvatn Ash in Germany **385 - 395**

List of Figures

		Page
1.1	The area of the NEP during the Lateglacial	9
1.2	Limit of the Fennoscandinavian Ice Sheet during the LGM ~22,000 cal yr BP	17
2.1	The main area of Franco-Cantabrian refugium	26
2.2	Population event 2	27
2.3	Population event 3	29
2.4	Population event 4	33
2.5	Population event 5	35
2.6	Population event 6	37
2.7	Distribution of the Classic and Havelte Hamburgian technocomplexes	43
2.8	Tools from the classical phase of the Hamburgian technocomplex	44
2.9	Typical tanged points of the Havelte technocomplex	45
2.10	Distribution of the Federmesser technocomplex	53
2.11	Tools and artefacts from the Federmesser technocomplex	54
2.12	Points from the site of Bützee	55
2.13	Distribution of the Bromme technocomplex	58
2.14	Tools from the Bromme technocomplex	59
2.15	Tools from the Ahrensburgian technocomplex	61
2.16	Distribution of the Ahrensburgian technocomplex	62
3.1	Location of Slotseng	79
3.2	Orthogonal photograph of the transect through the Slotseng kettle hole	80
3.3	Lithological diagram of Slotseng	82
3.4	Comparison of Bayesian P_Sequence depositional models for Slotseng	85
3.5	Location of Endinger Bruch	86
3.6	Lithological diagram of Endinger Bruch	88
3.7	Comparison of Bayesian P_Sequence depositional models for Endinger Bruch	92
3.8	Location of Potremser Moor	93

3.9	Lithological diagram of Potremser Moor	94
3.10	Location of Kieshofer Moor	96
3.11	Lithological diagram of Kieshofer Moor	98
3.12	Location of Daschower Moor	99
3.13	Lithological diagram of Daschower Moor	100
4.1	Density separation procedure for the extraction of tephra shards from sediments	105
4.2	Schematic representation of methodological approaches employed within the isotopic investigation of this thesis	109
4.3	Bi-plots of the realtionship between TOC (%) and TN (%)	112
4.4	Schematic representation of methodological approaches employed within the cladoceran investigation of this thesis	114
5.1	Tephra shard counts for Potremser Moor	118
5.2	Major and minor element plots of POT-455 with selected major northern European Lateglacial tephras	122
5.3	POT-455, Saksunarvatn Ash, GRIP 1528.61 m and LINK 14:185 trace element plots	123
5.4	Distribution envelope of the Saksunarvatn Ash	124
5.5	Bayesian P_Sequence depositional model for Potremser Moor	126
5.6	Tephra shard counts for Kieshofer Moor	127
5.7	Major and minor element plots of KHM-796 with selected major northern European Lateglacial tephras	131
5.8	Comparison of Bayesian P_Sequence depositional models for Kieshofer Moor and the neighbouring core from the site	134
5.9	Tephra shard counts for Daschower Moor	135
5.10	Major and minor element plots of DAM-263 with selected major northern European Lateglacial tephras	138
5.11	Bayesian P_Sequence depositional model for Daschower Moor	140
6.1	Stable isotope profiles and selected organic properties for Slotseng	144

6.2	Bi-plots of stable isotope values and selected organic properties for Slotseng	145 - 146
6.3	Bi-plot of TN – TOC for SOZ I – SOZ V	147
6.4	PCA bi-plots of selected isotopic and organic properties for Slotseng	149
6.5	PCA bi-plots of selected isotopic and organic properties for Slotseng	149
6.6	Cladoceran profile for Slotseng	153
6.7	Box plots of *B. longirostris* mucro length and *D. pulex* ephippia length for Slotseng	154 - 155
6.8	Stable isotope profiles and selected organic properties for Endinger Bruch	162
6.9	Bi-plots of stable isotope values and selected organic properties for Endinger Bruch	163 - 164
6.10	PCA bi-plots of selected isotopic and organic properties for Endinger Bruch	167
6.11	PCA bi-plots of selected isotopic and organic properties for Endinger Bruch	168
6.12	Cladoceran profile for Endinger Bruch	171
6.13	Box plots of *B. longirostris* mucro length for Endinger Bruch	173
6.14	Stable isotope profiles and selected organic properties for Potremser Moor	182
6.15	Bi-plots of stable isotope values and selected organic properties for Potremser Moor	183 - 184
6.16	Bi-plots of TN – TOC for POZ I – POZ III and TN – $\delta^{15}N_{org}$ for all OM zones in Potremser Moor	185
6.17	PCA bi-plots of selected isotopic and organic properties for Potremser Moor	186 - 187
6.18	PCA bi-plots of selected isotopic and organic properties for Potremser Moor	188
6.19	Cladoceran profile for Potremser Moor	191
6.20	Box plots of *B. longirostris* mucro length for Potremser Moor	192
6.21	Stable isotope profiles and selected organic properties for Kieshofer Moor	198
6.22	Bi-plots of stable isotope values and selected organic properties for Kieshofer Moor	199 - 200
6.23	Bi-plots of TN – TOC for KOZ I – KOZ II and TN – $\delta^{15}N_{org}$ for all OM zones in Kieshofer Moor	201
6.24	PCA bi-plots of selected isotopic and organic properties for Kieshofer Moor	202
6.25	PCA bi-plots of selected isotopic and organic properties for Kieshofer Moor	203
6.26	Cladoceran profile for Kieshofer Moor	206
6.27	Box plots of *B. longirostris* mucro length for Kieshofer Moor	207
6.28	Stable isotope profiles and selected organic properties for Daschower Moor	213
6.29	Bi-plots of stable isotope values and selected organic properties for Daschower Moor	214 - 215

6.30	PCA bi-plots of selected isotopic and organic properties for Daschower Moor	217
6.31	PCA bi-plots of selected isotopic and organic properties for Daschower Moor	218
6.32	Cladoceran profile for Daschower Moor	221
6.33	Box plots of *B. longirostris* mucro length for Daschower Moor	222
7.1	Onset of lacustrine sedimentation and peat formation in lake basins of northeast Germany	229
7.2	PCA bi-plots of $\delta^{13}C_{org}$, $\delta^{15}N_{org}$, TOC, TN and C:N plotted by chronozones for the five sites presented in this thesis	235
7.3	Composite diagram showing the five sites presented in this thesis plotted with OM derived productivity levels and cladoceran inferred fish populations	237
7.4	Distribution of the LST following the eruption of the Laacher See volcano	250
7.5	The visible LST layer recorded in Daschower Moor	253
7.6	$CaCO_3$ response to the deposition of the LST from Endinger Bruch, Kieshofer Moor and Daschower Moor	254
7.7	Single grain glass shards from the LST recorded in Kieshofer Moor	258
7.8	Distribution envelopes of the Vedde Ash and LST	261
7.9	$\delta^{13}C$ and $\delta^{15}N$ records from Endinger Bruch, Kieshofer Moor, Daschower Moor and Meerfelder Maar linked through the LST	265
7.10	Cladoceran records from Soppensee, Endinger Bruch, Kieshofer Moor and Daschower Moor linked through the LST	268
7.11	Cladoceran records from Kieshofer Moor, Daschower Moor, Endinger Bruch and Hämelsee linked through the LST	269
7.12	Younger Dryas in Kråkenes compared with the $\delta^{13}C_{org}$, $\delta^{15}N_{org}$, C:N and total cladoceran records from Endinger Bruch. The sites are linked through the Vedde Ash	271
7.13	Cladoceran records from Kråkenes, Endinger Bruch and Slotseng linked through the Vedde Ash	273
I.1	Additional study sites not used in this thesis	348
I.2	Tephra shard counts for Lundby Mose	350
I.3	Tephra shard counts for Tolk	353
I.4	Tephra shard counts for Gorinsee	354
I.5	Tephra shard counts for Weitsche	356

IV.1 Additional sedimentary data for Slotseng, Endinger Bruch, Potremser Moor, Kieshofer Moor and Daschower Moor 382

V Selected cladoceran sub-fossil images 383 - 384

List of Tables

		Page
1.1	Commonly cited terminologies for the various chronozones of the Lateglacial period of northern Europe	3
1.2	Chronozones of the Lateglacial with the NGRIP equivalents for the Lateglacial period of northern Europe	7
1.3	Fauna of the NEP during the Lateglacial – Holocene period	13 - 14
2.1	Lateglacial population history of western Europe with associated technocomplexes	24
2.2	The four technocomplexes of the NEP during the Lateglacial period with associated vegetation and climatic variables	42
3.1	Relationship between increasing mean annual temperature and fishing as shown by ethnographic hunter-gatherer groups	69
3.2	Key tephra horizons associated with northern Europe during the Lateglacial – Holocene transition	73
3.3	Tephras discovered within the Slotseng kettle hole as part of the tephrochronological study of the basin by Dr Alison MacLeod	83
3.4	^{14}C dates and modelled ages for samples from Slotseng	84
3.5	Tephras discovered within the Endinger Bruch kettle hole as part of the tephrochronological study of the basin by Lane *et al*., (2011b).	90
3.6	^{14}C date and modelled age for the sample from core KZA	91
4.1	Error ranges for in-house alanine standards	110
5.1	Non-normalised major and minor elemental oxide compositions for POT-455	120
5.2	LA-ICP-MS results for POT-455 from Potremser Moor	121
5.3	^{14}C dates and modelled ages for samples from Potremser Moor	125
5.4	Non-normalised major and minor elemental oxide compositions for KHM-796	129
5.5	^{14}C dates and modelled ages for samples from Kieshofer Moor and the neighbouring core	132
5.6	Modelled age comparisons for the Kieshofer Moor and neighbouring core	133
5.7	Non-normalised major and minor elemental oxide compositions for DAM-263	136
5.8	^{14}C dates and modelled ages for samples from Daschower Moor	139

6.1	List of cladoceran species recorded for Slotseng	151
6.2	List of cladoceran species recorded from Endinger Bruch	170
6.3	List of cladoceran species recorded for Potremser Moor	189
6.4	List of cladoceran species recorded for Kieshofer Moor	204
6.5	List of cladoceran species recorded for Daschower Moor	219
7.1	Summary of the age ranges for the basins presented in this thesis	228
7.2	Modelled ^{14}C ages for the Lateglacial chronozones represented in this thesis	231
7.3	Summary table showing the tephra layers found at the five sites studied in this thesis	260
II.1	Stable isotope and selected organic properties for Slotseng	357
II.2	Stable isotope and selected organic properties for Endinger Bruch	358
II.3	Stable isotope and selected organic properties for Potremser Moor	259
II.4	Stable isotope and selected organic properties for Kieshofer Moor	360
II.5	Stable isotope and selected organic properties for Daschower Moor	361
III.1	Cladoceran counts for Slotseng	362 - 363
III.2	Cladoceran counts for Endinger Bruch	364 - 369
III.3	Cladoceran counts for Potremser Moor	370 - 373
III.4	Cladoceran counts for Kieshofer Moor	374 - 377
III.5	Cladoceran counts for Daschower Moor	378 - 381

Acknowledgements

This research would not have been possible without the help and support from a number of people, who have guided and supported me during the past four years. To my supervisors, Dr Christine Lane, Professor Clive Gamble and Professor Nick Barton I am indebted for all the advice, guidance, inspiration and support that has enabled me to fully explore this project and bring it to fruition. This research project has been a fantastic journey and I cannot express my gratitude enough for academic and personal support my supervisors have provided. I would also like to extend my thanks to a number of academic colleagues who have helped shape this research project; Dr Rupert Housley, Victoria Cullen, Dr Victoria Smith, Dr Peter Ditchfield, Dr Allison MacLeod, Dr Ruth Rawcliffe, Dr Mara Weber, Dr Martin Theuerkauf, Professor Felix Riede, Dr Morten Mortensen and Dr Falko Turner.

I would also like to take this opportunity to express my gratitude to my family and friends. To my parents Judith and Jeremy who first kindled my interest in the natural world and provided me with the all the support possible to complete this research, I could not wish for better parents and role models, thank you. To my girlfriend Alicia who has been on this journey with me every step of the way, I cannot thank you enough. Without your support I would not have completed this project, and I owe you more than it is possible to say, I look forward to the next adventure. To my Grandparents Pamela Sykes and Frieda Law who have supported and encouraged me throughout the last four years. To the rest of my family and friends, thank you. You have all provided love, support and welcome distraction. I would also like to thank Oxford University Rugby Football Club, who helped make my time at Oxford that bit more special.

I would lastly like to thank NERC for providing the funding that allowed this project to take shape and all members of the RESET team.

Chapter 1: The Lateglacial of the North European Plain

Following the termination of the Last Glacial Maximum (~ 16,000 cal yr BP) large areas of the North European Plain (NEP, Figure 1) became accessible for re-occupation by hunter-gatherer populations moving out of pockets of Iberian refugia. Chronological and archaeological investigations indicate that hunter-gatherer populations were present within southern and central Germany by the later stages of Oldest Dryas (Street *et al*., 1994). New ^{14}C evidence appears to confirm that expansion onto the NEP occurred prior to the prominent temperature rise of the Bølling (see Grimm and Weber, 2008). Vegetation reconstructions, based on pollen and plant macro fossils, give a detailed picture of how the terrestrial environment developed following the termination of the Last Glacial Maximum (See Erikesen, 2002). There is in contrast comparatively little understanding of how the aquatic systems of the NEP responded to this period of climate change. Following deglaciation the NEP would have been very much influenced by aquatic systems. The retreating Fennoscandinavian ice sheet would have left thousands of pro-glacial lakes and kettle holes ranging in size from less than 1 hectare to over 100 hectares in size across much of the Schleswig-Holstein and Mecklenburg-Vorpommern regions of northern Germany as well as large areas of Denmark, in what was during the Lateglacial, the northern boundaries of the NEP (Kaiser *et al*., 2012). Archaeological evidence suggests that within some areas of the NEP, aquatic systems were regularly exploited as sources of food. For example, recent excavations at sites such as Mirkowice, Poland (Kabaciński *et al*., 1999), Slotseng, Denmark (Holm 2003) and Poggenwisch, Germany (Bratlund 1996); show hunter-gatherer settlement sites associated with the large scale exploitation of freshwater fish and other aquatic resources, whilst bone and ivory fish hooks, prongs, harpoons and points have also been found in association with Lateglacial sediments throughout the NEP (see Cziesla, 2004); Chapter 3). These finds challenge the established view that large mammal hunting formed the sole subsistence strategy used by people on the NEP during the Lateglacial. This thesis specifically aims to address key questions how these lakes developed during a period of abrupt climatic change, thus contributing to our understanding of how aquatic environments may have influenced human reoccupation events across the NEP.

The expansion and colonisation period of the NEP coincides with a series of Abrupt Environmental Transitions (AETs), characterising Lateglacial (~14,600 – 11,500 cal yr BP) ecological, cultural, social

and technological regimes within Europe. In Chapter 1 I will begin by outlining the Lateglacial framework of this thesis. I will also briefly address its chronostratigraphic position and associated issues of chronostratigraphic synchronicity. The Chapter will follow with further commentary on the floral, faunal and aquatic response within the area of research to AETs during the Lateglacial. Chapter 1 will conclude with the structure of thesis contained herein as well as this project's aims and objectives.

1.1 The Lateglacial

The Lateglacial *sensu stricto* refers to the 'Weichselian' (mainland Europe), 'Devensian' (Britain) and 'Midlandian' (Ireland) periods between ~14,600 – 11,500 cal yr BP. The period of rapidly fluctuating climatic conditions is defined by two geological-climatic units: the 'Lateglacial Interstadial' a period of climatic amelioration between ~14,600 – 12,900 cal yr BP; and the 'Younger Dryas Stadial' a sharp climatic downturn between ~12,900 – 11,500 cal yr BP (Walker *et al*., 1994). The Lateglacial is dated by various different techniques, including ^{14}C dating (Kitagawa and van der Plicht, 1998; Turney *et al*., 2000), varve chronology (Merkt and Müller, 1999; Brauer *et al*., 1999) and tephrochronology (Turney *et al,* 2006; Mortensen *et al*., 2005; Lowe *et al*., 2008). Among these, ^{14}C dating has proved to be the most widely used in Quaternary science for developing Lateglacial chronologies. Early understanding of the timing and order of Lateglacial climate events was based largely upon conventional ^{14}C dating, usually from bulk organic samples (Walker *et al*., 1994). Recently however the augmentation of AMS ^{14}C dating on individual plant macrofossils has greatly improved the application of this approach, particularly when combined with high resolution varve counting (Nakagawa *et al*., 2012). Despite these advances it has proved challenging in making temporal correlations between Lateglacial sequences due to the variability in the precision and accuracy of many ^{14}C age determinations and age models (Blockley *et al*., 2004).

A major challenge for chronological studies of the Lateglacial is the unification of chronostratigraphic classification. This has implications not only for North Atlantic and northern European terminology, but also for the synchronisation of terrestrial, marine and ice-core records. These issues will be discussed within section 1.1.1 and 1.1.2.

1.1.1 Lateglacial chronostratigraphic classification

The principles underlying the classification of the Lateglacial stratigraphic record of northern Europe were introduced by Mangerud *et al*., (1974). Since his early lead, a number of terrestrial classification systems have been postulated for northern Europe (e.g. Van der Hammen, 1957; Mangerud *et al*., 1974; Lowe and Gray, 1980; Van Geel *et al*., 1989; Hoek 1997; Usinger, 1998) Table 1.1).

<table>
<tr><th colspan="2">Van der Hammen (1957</th><th colspan="2">Mangerud et al., (1974)</th><th>Hoek (1997); cf, Van Geel et al., (1989)</th><th>Usinger (1998)</th><th>Lowe and Gray (1980)</th></tr>
<tr><td rowspan="2">Holocene</td><td rowspan="2"></td><td rowspan="2">Early Flandrian</td><td rowspan="2">Preboreal</td><td>Late Preboreal</td><td rowspan="2"></td><td rowspan="2"></td></tr>
<tr><td>Early Preboreal</td></tr>
<tr><td rowspan="4">Lateglacial</td><td>Younger Dryas</td><td rowspan="4">Late Weichselian</td><td>Younger Dryas</td><td>Late Dryas</td><td></td><td>Younger Dryas Stadial</td></tr>
<tr><td>Allerød - Interstadial</td><td>Allerød</td><td>Allerød</td><td>Allerød - Interstadial</td><td rowspan="3">Lateglacial Interstadial</td></tr>
<tr><td>Older Dryas</td><td>Older Dryas</td><td>Earlier Dryas</td><td></td></tr>
<tr><td>Bølling - Interstadial</td><td rowspan="2">Bølling</td><td>Bølling</td><td rowspan="2">Meiendorf - Interstadial</td></tr>
<tr><td>Pleniglacial</td><td></td><td>Middle Weichselian</td><td></td><td>Late Pleniglacial</td><td></td><td></td></tr>
</table>

Table 1.1 – Commonly cited terminologies for the various chronozones of the Lateglacial period of northern Europe. Van der Hammen (1957); Mangerud *et al*., (1974); Lowe and Gray (1980); Van Geel *et al*., (1989); Hoek (1997); Usinger (1998).

The original 1974 classification was based largely upon conventional stratigraphic techniques whereby units of stage or rank and the boundaries of chronostratigraphic units, were defined by reference to stratotypes (Björck *et al*., 1998). A major problem with this early approach was the definition of chronozone boundaries in radiocarbon years that lacked proper reference to type-sequences or sections (Björck *et al*., 1998). According to this scheme the Lateglacial – Holocene period was sub-divided into the following chronozones : Bølling (including Oldest Dryas) 14,670-14,

100 cal yr BP, Older Dryas 14,100 – 13,900 cal yr BP, Allerød 13,900 – 12,900 cal yr BP and Younger Dryas 12,900 – 11,500 cal yr BP. This approach was developed to reflect key changes in pollen or plant macrofossil records in a number of early studies (Hartz and Milthers 1901; Jessen, 1935; Iversen, 1942; Iversen, 1954; Nilsson, 1961). However the adoption and utilisation of early botanical studies has sometimes led to confusion and ambiguity, for example in comparing environmental records as defined in the original 1974 classification with those far outside those areas where it was initially conceived (Straus, 1996). There is also ambiguity in the strict definitions of chronostratigraphic terms. For instance, continuing debate exists over the use of the term 'Bølling'. The definition of the 'Bølling' given by Mangerud *et al*., (1974) states:

"*The Bølling chronozone thus comprises the Oldest Dryas and Bølling periods or pollen zones Ia and Ib of Iversen (1954)*"

In southern Scandinavia however, the Bølling may be used to designate a specific pollen zone (Eriksen, 2002). Therefore, the Bølling may be separated from the Allerød by the Older Dryas, or in areas where the Older Dryas is not present in the palynological record, the Bølling forms part of the early Allerød (Berglund, 1979; Lowe and Gray, 1980; Menke, 1983; Kolstrup, 1991; de Klerk, 2008). Due to the ambiguity surrounding the definition of the Bølling, some researchers have suggested dropping the term altogether (Usinger, 1997). Other scholars in contrast, have suggested incorporating the Bølling within the Allerød; the Bølling thus forming the earliest part of the Allerød, with the Meiendorf representing the initial warming associated with GI-1e (Terberger *et al*., 2009). While this new sub-division may help resolve some of these chronostratigraphical issues, there is still no general consensus (Baales, 2002). For instance in northeastern Germany, researchers regularly apply the term "*Hippophaë-Phase*" to describe the latter Bølling/Meiendorf (Kaiser *et al*., 1999; de Klerk, 2002; Terberger *et al*., 2004a).

A potential solution to these issues has been through the proposed utilisation of a single high resolution record as the regional stratotype for northern Europe. Early advances using this notion employed the GRIP SS08C isotopic record, which at the time was considered to provide the best resolved and most complete template for climatic events during the Lateglacial – Holocene in the North Atlantic region (Lowe *et al*., 2008). A revision of this approach employs a new Greenland ice-

core record from North GRIP (GICC05; Table 1). The record, based upon layer counting with robust quantification of counting errors, offers a chronology of significantly improved temporal resolution and precision (Rasmussen *et al*., 2006). As a means of ensuring consistency between environmental and archaeological sites within northern Europe, the INTIMATE group recommended that all site records should initially be designated using appropriate local or regional terminologies (e.g. Bølling or Allerød) and that palaeoenvironmental, climatic or archaeological events be established independently of the GICC05 record (Lowe *et al*., 2008).

1.1.2 Chronostratigraphic synchronicity

High resolution palaeoclimate archives, such as the Greenland ice core records have demonstrated that climatic oscillations during the Lateglacial – Holocene transition were both complex *and* abrupt, occurring over centennial and even decadal intervals (Alley *et al*., 1993; Dansgaard *et al*., 1993; Kapsner *et al*., 1995; Rasmussen *et al*., 2006; Steffensen *et al*., 2008). This poses a significant challenge for scientists of how to determine the phasing of the palaeoenvironmental responses recognised across ice core, terrestrial and marine archives. As discussed in section 1.1.1, ambiguity still exists within regional and local chronostratigraphic terminologies. Thus, while various chronozone boundaries in northern Europe are believed to have been synchronous, there is an increasing body of evidence to show that they were in fact diachronous during the Lateglacial (e.g. Coope *et al*., 1998; Blockley *et al*., 2004). Two major implications arise from this: first, a palaeoenvironmental, climatic or archaeological site or unit assigned for instance to the Bølling, will not necessarily be contemporary with other Bølling age sites. Second, the boundaries between chronozones will not be synchronous throughout the whole of northern Europe, with onset and terminations varying temporally and spatially (Erikesen, 2002).

The problem of synchronisation between local records and the GICC05 stratotype is compounded by dating/modelling errors within specific archives and also whether the climatic events in GICC05 were regionally significant or whether significant ‘leads’ and ‘lags’ existed between Greenland and the records of northern Europe. As a counter to this problem it has been proposed that inter-site chronologies should firstly be established independently at a local level and along a common timescale with age-model uncertainties smaller than the durations of the studied transitions (Lane *et*

al., 2011a). Such an approach requires rigorous independent dating of archives with high levels of precision and accuracy, to ensure the accurate alignment of such archives. Such high levels of precision and accuracy for aligning records at decadal timescales is however often difficult to achieve due to the variability of dating techniques used and inherent uncertainties associated with the calibration of radiocarbon ages (Blockley *et al*., 2004). The use of fixed isochronous marker horizons of known age is one method that can be employed in order to reduce errors associated with age models. One of the most widely employed methods is to construct chronological tie-points within sites using non-visible layers of volcanic ash (microtephra). Such tephra can be deposited thousands of kilometres from the volcanic source forming widespread isochronous layers over wide areas. Recent research has extended the application of microtephra within the Greenland ice-core records (e.g. Abbot *et al*., 2012; Davies *et al*., 2012) allowing climatic teleconections between terrestrial, marine and ice-core records to be assessed and further allowing the elucidation of 'lead/lag' effects within the northern European environmental record. The further use of microtephra, and its application to sites in this thesis, will be discussed in detail in Chapter 3.

1.2 Conventions adopted

The climatic and environmental complexity of the Lateglacial has led to the proliferation of numerous classification systems (see section 1.1.1 and 1.1.2). To avoid confusion throughout this thesis only the most cited and readily used classification systems have been employed for greater clarity (Table. 1.1). As a result, and following INTIMATE protocol this thesis utilises local chronozones in order to describe site chronology. The exception to this will be when discussing tephra layers when in association with the Greenland ice-core record. The Bølling – Allerød *sensu stricto* is punctuated by at least two minor periods of colder conditions in northern Europe (Blockley *et al*., 2006). Their presence is however is not always visible within the sedimentary and palynostratigraphic record and as such will only be discussed if of relevance at a site specific level. These two cooler events will be referred to as the 'Older Dryas' and GI-1b (Walker *et al*., 1999).

Chronozone	cal yr BP	NGRIP event stratigraphy equivalent	Onset GICC05 age b2k
Holocene	11,500 –		11,703
Younger Dryas	12,900 – 11,500	GS-1	12,896
Allerød	13,900 – 12,900	GI-1c – GI-1a	13,954
Pre-Bølling – Bølling	14,670 – 14,100	GS-2a - GI-1e	14,692
Oldest Dryas	19,000 – 14,670	GS-2a	Not clear in NGRIP
		GS-2b	20,900
Last Glacial Maximum		GS-2c	22,900[a]

Table 1.2 – Chronozones of the Lateglacial with the NGRIP equivalents for the Lateglacial period of northern Europe. Dates taken from Rasmussen *et al*., (2006). [a] defined from midpoint of $\delta 18^{O}$ transition in combined NGRIP, GRIP, and GISP2 records following the approach of Andersen *et al*., (2006).

To ensure consistency between age estimates the following dating conventions will be applied: (1) ^{14}C ages will be referred to as '^{14}C yr BP' (radiocarbon years before present). (2) calibrated ^{14}C ages will be referred to as 'cal yr BP' (calibrated years before present). (3) Greenland ice core years will be referred to as 'GICC05 yr b2k' (GICC05 years before 2000) (Rasmussen *et al*., 2006). Published uncalibrated ^{14}C dates will be (re)calibrated with OxCal 4.2 (Bronk Ramsey, 2009a) using IntCal09 (Reimer *et al*., 2009) with 2σ age ranges quoted within the text.

The term '*Aquatic System'* used throughout this thesis will refer specifically to lake environments. During the Lateglacial – Holocene other aquatic systems would have been present across the NEP, such as river, stream and marine environments. However the scope of this thesis is concerned with addressing only lake environments across the NEP.

1.3 The North European Plain – floral record

The region known as the NEP formed a large part of northern Europe during the Lateglacial (Figure 1.1). The area was extensively shaped by Quaternary glaciations, with the ice terminal zones of the Saalian and Weichselian (Last glacial period) advances traversing the region (Kaiser *et al*., 2012). The complex glacial and interglacial processes that shaped the landscape of this area have led to a mosaic type sedimentary record that comprises glacial, fluvial, lacustrine, colluvial, marine and aeolian sediments (Kaiser *et al*., 2012). Following the termination of the Last Glacial Maximum (LGM) and the retreat of the Fennoscandinavian ice sheet, the area again became accessible for occupation by hunter-gatherer groups. The oldest date for a human presence on the NEP currently stands at 16,194 – 14,057 cal yr BP (12,680 ± 230 ^{14}C yr BP; Olbrachcice 8, Poland) suggesting much of the area was habitable by at least 14,057 cal yr BP (Kanwiszer and Trzeciak, 1984).

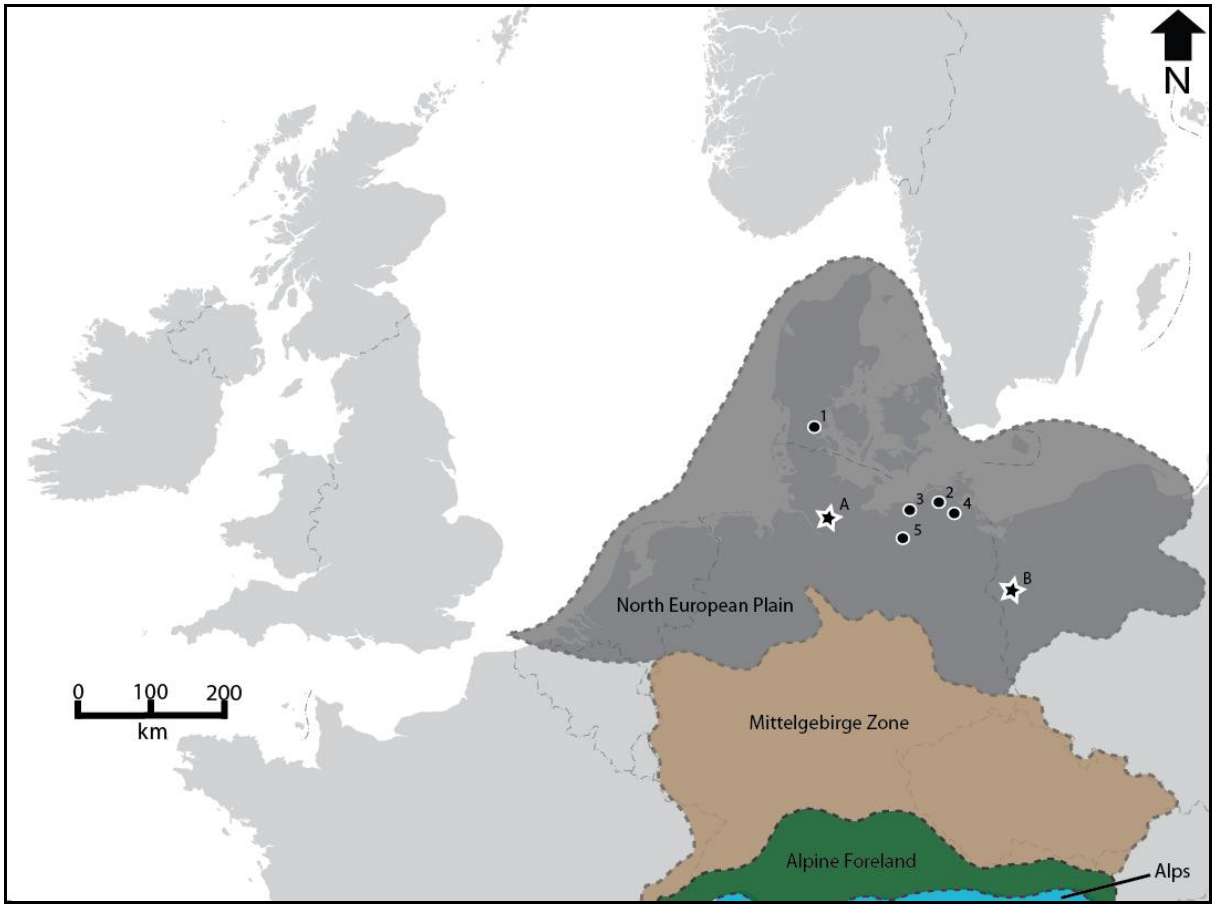


Figure 1.1 – The area of the NEP during the Lateglacial. Areas of the North and Baltic Seas that formed substantial parts of the landmass during this time are also shown. Sites presented within this thesis are as follows: 1 – Slotseng, 2 – Endinger Bruch, 3 – Potremser Moor, 4 – Kieshoffer Moor, 5 – Daschower Moor. Star "A" represents the sites of Stellmoor, Meiendorf and Poggenwisch within the Ahrensburgian Tunnel Valley. Star "B" represents the site of Mirkowice.

The floral history of the NEP has been intensively studied for over 100 years (Bratlund, 1996) and although there is a general consensus as to the main vegetational phases, more recent studies (e.g. de Klerk, 2002; Veski *et al*., 2012) have demonstrated that subtle, regional differences exist in the terrestrial responses to climatic amelioration following de-glaciation. The Oldest Dryas (Table 1.1) is characterised in particular by traces of early pioneer vegetation consisting of heliophilous herbs and dwarf-shrubs, notably *Juniperus*, *Betula nana*, *Salix* and *Dryas* (de Klerk, 2002). However, the early Lateglacial landscape was prone to disruption caused by aeolian and peri-glacial processes, and remained unstable until the transition to Bølling (Bratlund, 1996). With further climatic amelioration

during the Bølling, this period is classically characterised by *Hippophaë* expansion. With limited competitive taxa to check its expansion *Hippophaë* likely would have formed high, dense stands across large areas of the NEP (Skogen, 1972). *Hippophaë* seeds are highly tolerant to wind and cold temperatures (Pearson and Rodgers, 1962; Bat *et al*., 1988) therefore it is possible that stands of *Hippophaë* existed prior to the Bølling, however likely only vegetatively, as it needs relatively high summer temperatures to flower (Iversen, 1954). Evidence from the eastern (e.g. Veski *et al*., 2012) northern, (e.g. de Klerk, 2002; Mortensen *et al*., 2011) and western (e.g. Hoek, 2001; Bos *et al*., 2006) margins of the NEP all indicate that the Bølling was relatively homogenous and open, dominated by *Hippophaë* and heliophilous herbs and dwarf-shrubs. This period of gradual climatic improvement was interrupted by, the Older Dryas. The Older Dryas, correlated commonly to GI-1d, was a short cooling episode covering 125 years within NGRIP ice core record (Lowe *et al*., 2008). Landscape response to the Older Dryas within the NEP is often difficult to gauge, with apparent disparities between areas. Vegetation records however generally indicate that the landscape during the Older Dryas became progressively more open, with a reduction in *Hippophaë* and an increase in open taxa species such as *Poaceae* and Birch *nana* (Mortensen, 2007). It has been suggested that the shift to more open conditions during the Bølling was the result of dryer conditions across the NEP (e.g. Van Greel and Kolstrup 1978; Kolstrup, 1982). A number of records appear to support this hypothesis, with increases in drought tolerant species such as *Lychnis alpine* and *Saxifraga aizoides* as well as reduction in lake levels (Mortensen *et al*., 2011; Veski, 2012). An alternate argument is however presented by de Klerk *et al*., (2001) who suggests that the disappearance of *Hippophaë* is more likely to be the result of cooler conditions as *Hippophaë* are drought tolerant. This is supported by data from the Reinberg Basin in Vorpommern, Germany, that indicates that the climate during the Bølling was in fact relatively moist (de Klerk, 2002).

The transition to the Allerød was marked by the closure of Birch and Pine forests. The classical interpretation of the period Allerød is that of dense forest coverage brought about by the stabilisation of soils and the introduction of warmer climatic conditions (Iversen, 1954, 1973; Noe-Nygaard *et al*., 2006). It is possible however, that the NEP was never fully 'closed' (see Kolstrup, 1999; Bennike *et al*., 2004) and that the Allerød was characterised by more heterogeneous vegetation cover, varying

between Birch and Pine forest, interspersed by open herb and dwarf-shrub type communities (Mortensen *et al*., 2011).

The final stage in the Lateglacial development of the NEP before the major climatic transition to the Preboreal was that of the Younger Dryas. The Younger Dryas was the longest of the stadial events following the LGM, lasting ~1100-1250 years (Goslar *et al*., 1998; Rasmussen *et al*., 2006; Schaub *et al*., 2008). The Younger Dryas can be seen as a tripartite event in the NEP (Weber *et al*., 2011). An initial cold phase of the Younger Dryas, with minimal temperatures, was followed by a period of warmer temperatures which were generally stable and similar to those of the Allerød (von Grafenstein *et al*., 1999; Schwark *et al*., 2002). The terminal portion of the Younger Dryas is characterised by a rise in temperature, culminating in the onset of Holocene (Rasmussen *et al*., 2006). The vegetation response to The Younger Dryas appears to be consistent throughout the NEP, with a loss of Birch and Pine forest and a return to open conditions. There is evidence to suggest that Birch and Pine did not completely disappear from the landscape, and may have existed as isolated tress rather than forming dense stands (de Klerk, 2002). A prominent feature of The Younger Dryas is that of increased aeolian activity (Isarin, 1997; Isarin and Bohncke 1999; Brauer *et al*., 2008) with dry windy conditions prevailing throughout the NEP, this seems to have been associated with an increase in *Empetrum* which is recognised as a widespread phenomenon of the Younger Dryas (Hoek, 1997). An additional impact of The Younger Dryas would have been the formation of separate soil zones. Northern boundaries of the NEP would have sat inside a zone of continuous permafrost, which, with progression into southerly areas of the NEP would have developed into a zone of discontinuous permafrost with deep seasonal frosts (Weber *et al*., 2011).

The transition from the Lateglacial to the Holocene was characterised by the replacement of the open shrub type conditions and the rapid expansion of Birch and Pine forest throughout the NEP as a result of warming at the Younger Dryas – Preboreal boundary. Low non-arboreal pollen (NAP) values within early Preboreal sediments likely indicate the rapid expansion of Birch and Pine, probably from remnant stands that survived throughout the Younger Dryas (de Klerk *et al*., 2008). The increase in temperatures is also indicated by the appearance of thermophilous plants such as *Filipendula* (Iversen, 1954). The early Preboreal was however also characterised by a period of climatic

deterioration, with an decrease in Birch and subsequent rise in *Poaceae*, thus possibly indicating a return to open conditions like those experienced during the Younger Dryas (Jahns, 2000). Other authors have suggested a second period of climatic deterioration across the NEP. Usinger (2004) working at the site of Kubitzbergmoor in the Schleswig-Holstein region of Germany, documented a second period of Birch decline which, unlike the first, he attributed to drier conditions, but this pattern however has yet to be observed elsewhere. It has proved difficult to accurately quantify the Preboreal oscillations and their effect on vegetation development within the northern margins of the NEP. For example, reconstructions from the southern Mecklenburg and Berlin-Brandenburg regions of Germany however, the Preboreal *sensu stricto* is characterised by two distinct peaks in Birch, separated by a period of climatic deterioration (Brande, 1980; Wolters, 2002; Brande, 2003).

1.4 The North European Plain – faunal record

As discussed in section 1.3, the floral record indicates that during GS-2a the NEP became ice-free and a pioneer landscape began to develop. Prior to deglaciation, reindeer (*Rangifer tarandus*), saiga (*Saiga tatarica*) and mammoth (*Mammuthus primigenius*) are likely to have followed the retreating ice sheet and were possibly present in northerly reaches of the NEP before the OD (Degerbøl and Krog, 1959; Lagerlund and Houmark-Nielsen, 1993; Berglund *et al*., 1976; Aaris-Sørensen, 1992).

	Region	Bølling	Allerød	Late Allerød	Younger Dryas (early)	Younger Dryas (late)	Preboreal
Rangifer tarandus - (Linnaeus) Reindeer	1 2 3	+ + +	 + +	 + 	+ + +	+ + +	+ +
Equus caballus ferus – (Linnaeus) Horse	1 2 3	+ 	 + 	 +	 +	+ 	 + +
Bison bonasus arbusto-tundrarum - (Dgrbl) Bison	1 2 3	 	 	 	+ 	 	
Desmana moschata hungarica - (Kormos) Desman	1 2 3	+ 	 	 	+ 	 	
Citellus major – (Pallas) Ground Squirrel	1 2 3	+ 	 	 	 +	 	
Lepus timidus – (Linnaeus) Arctic Hare	1 2 3	+ 	 	 	+ +	+ +	
Lemmus – (Link) Lemming	1 2 3	+ 	 	 	+ 	+ 	
Vulpes - Fox sp.	1 2 3	+ 	 	 	 	 	
Canis lupus – (Linnaeus) Wolf	1 2 3	 +	 	 	 	+ 	
Gulo gulo spelaeus - (Rosenmüller) Wolverine	1 2 3	+ 	 +	 	 	 	
Lynx lynx - (Linnaeus) Lynx	1 2 3	 	 	 	+ 	+ 	
Castor fiber - (Linnaeus) Beaver	1 2 3	 	 +	 	 	 	
Sus scrofa ferus – (Linnaeus) Wild Boar	1 2 3	 	 	 	 	 	 +
Alces alces - (Linnaeus) Elk	1 2 3	 +	+ + +	 +	 	+? +	+ + +
Megaloceros giganteus - (Blumenbach) Giant Elk	1 2 3	 	 + +	 +	 +?	+? 	
Ochotona pusilla – (*Pall*as) Steppe Pika	1 2 3	 	 	 	 +	 +	

Bos primigenius - (Bojanus) Aurochs	1 2 3						+ +
Ursus arctos – (Linnaeus) Brown Bear	1 2 3			+			+ +
Cervus elaphus – (Linnaeus) Red Deer	1 2 3						+ +
Capreolus capreolus – (Linnaeus) Roe Deer	1 2 3						+ +

Table 1.3 – Fauna of the NEP during the Lateglacial – Holocene period. + refers to presence of listed species. 1 – Schleswig-Holstein 2- Mecklenburg-Vorpommern 3-Denmark. Regional data is taken from original sources (Degerbøl, (1964); Bratlund, (1996); Terberger, (2006) and is not used to define areas within this thesis.

Climatic amelioration associated with the Bølling (section 1.3) coincided with an increase in the abundance and variance of fauna on the NEP. Reindeer (*Rangifer tarandus*), horse (*Equus caballus ferus)*, desman (*Desmana moschata hungarica*), ground squirrel (*Citellus major*), hare (*Lepus timidus*), lemming (*Lemmus*), fox (*Vulpes*), wolf (*Canis lupis*), wolverine (*Gulo gulo spelaeus*) and elk (*Alces alces)* all are present within the Bølling (Table 1.3). Of this new influx, reindeer were by far the most ubiquitous in the archaeozoological record. According to Degerbøl and Krog, (1959) the morphology of the Danish reindeer indicates affinity with the Eurasian tundra reindeer (*Rangifer tarandus taranadus*) as does those from the Schleswig-Holstein region (Gripp, 1937; 1943; Kollau, 1943; Krause, 1937). Recent radiocarbon dating of reindeer remains from Danish sites indicate a prolonged presence of reindeer from the Bølling into the early Preboreal (Liljegren and Ekström 1996; Sorensen *et al*., 2007). The best evidence of this early faunal advance comes from the north German sites of Meiendorf and Stellmoor hunting camps, excavated in 1932-1936 by Alfred Rust. The sites, located in the Ahrensburgian tunnel valley, north of Hamburg, give a detailed insight into not only the prevailing fauna of the period but also the hunting strategies of early hunter-gatherers on the NEP. A commentary on the hunting strategies will be discussed in Chapter 3, so the following paragraphs deal exclusively with describing the faunal component present. Excavations in the Ahrensburgian

tunnel valley record faunal assemblages that strongly support the floral record of an open shrub-tundra type environment. Reindeer dominate Bølling age faunal assemblages with 1931 bone and 320 antler fragments at Meiendorf and 1904 bone and 80 antler fragments at Stellmoor (Bratlund, 1996). Coupled with this are finds of horse, hare, fox, wolverine and other small mammals such as the desman as well relatively large numbers of migratory birds such as the whooper swan (*Cygnus Cygnus*) and the greylag goose (*Anser anser)*. The presence of such birds suggests possible summer migrations into the NEP as well as large areas of wetlands necessary to support such populations. Whilst it must be noted that the faunal assemblages at Meiendorf and Stellmoor are heavily influenced by human selection, they do give an intriguing view of the landscape of the Bølling.

The development of Birch and Pine forests throughout the NEP during the Allerød gave rise to a homogenous environment, composed of forest interspersed by more open shrub type conditions. The appearance of forests within the NEP caused the re-ordering in the dominance of species within faunal assemblages. The Allerød was characterised by a dominance of elk (*Alces alces*) in the faunal record, whereas reindeer are found only in the regions of Mecklenburg-Vorpommern and Denmark. Giant deer (*Megaloceros giganteus*) are also found with Mecklenburg-Vorpommern as well as Denmark, while horse (*Equus caballus ferus*) is confined to the former (Table 1.3). The transition into the Late Allerød coincides with a reduction in the number of species present across the NEP. Reindeer appear only in the Mecklenburg-Vorpommern region, while elk, giant deer and horse are all confined to Denmark (Table 1.3). Unfortunately the faunal record of the Allerød is relatively limited, with only a few sites yielding information on species composition. One such site is Kleinnordende in Schleswig-Holstein, where 88 bones from a minimum of two elk were recovered from Allerød age sediments (Bokelmann *et al.,* 1983). Perhaps the most diverse and characteristic fauna of this period comes from the eponymous site of Bromme in Denmark. The site which lends its name to the subsequent Bromme technocomplex was excavated in the 1940s and palynologically dated to the Allerød (Mathiassen, 1946; Fischer and Sonne Nielsen, 1986). As with many Lateglacial archaeozoological sites the faunal remains are sparse and not particularly well preserved, nevertheless the following species can be attributed to the site: reindeer, elk, wolverine (*Gulo gulo spelaeus*), beaver (*Castor fiber*), Swan (unspecified) and Pike (*Esox lucius*) (Bratlund, 1996).

The opening of the landscape and subsequent climatic deterioration associated with the Younger Dryas again reshuffled the faunal assemblage of the NEP. Reindeer returned as the dominant ungulate on the NEP, whilst the geographical range of horse shifted southward into the Schleswig-Holstein region (Table 1.3). The survival of elk and giant deer on the NEP during the Younger Dryas is still debated; however there seems to be good evidence for the survival of elk at least in southern Scandinavia (Degerbøl and Krog, 1959; Aaris-Sørensen, 1988; Liljegren, 1994). The fauna of the Younger Dryas largely resembles that of the Bølling, aside from the return of the ubiquitous reindeer and other species indicative of open tundra such as arctic hare (*Lepus timidus*) and lemming (*Lemmus*) that reappeared in parts of northern Germany and Denmark.

The termination of the Younger Dryas and onset of the Preboreal is marked by a dramatic change in the fauna of the NEP. Reindeer, which had been prominent throughout the Lateglacial, began to retreat to higher latitudes, before finally becoming locallyextinct. Dates from southwestern Germany (10,500-10,270 cal yr BP; Drucker *et al*., 2011) and Denmark (10,559-10,222 cal yr BP; Sorensen *et al*., 2007) indicate the almost contemporaneous local of extinction of reindeer during the Preboreal. The onset of the Preboreal coincided with the appearance of classical Holocene fauna, including aurochs (*Bos primigenius*) as well as red and roe deer (*Cervus elaphus* and *Capreolus capreolus*) horse, wild boar (*Sus scrofa ferus*) and bear (*Ursus arctos)* in the Mecklenburg-Vorpommern region and Denmark (Table 1.3).

1.5 The North European Plain – aquatic record

The northern and eastern margins of the NEP that had been subjected to the LGM advance of the Fennoscandinavian Ice Sheet (Figure 1.2) are characterised by numerous lakes of varying sizes and of different genetic, hydrological and ecological type (Kaiser *et al*., 2012). Based on estimates from the adjacent Polish young morainic zone, only one-third to half of all Lateglacial lakes remain today due to aggradation or anthropogenic processes (Starkel, 2003). Coupled with this, a large portion of the northeastern NEP is covered by peatland, with ~5800 km^2 located in Germany alone (Joosten, 2008). These two factors indicate that northeastern areas of the NEP were heavily characterised by aquatic environments such as lakes, kettle-holes or wetlands during the Lateglacial.

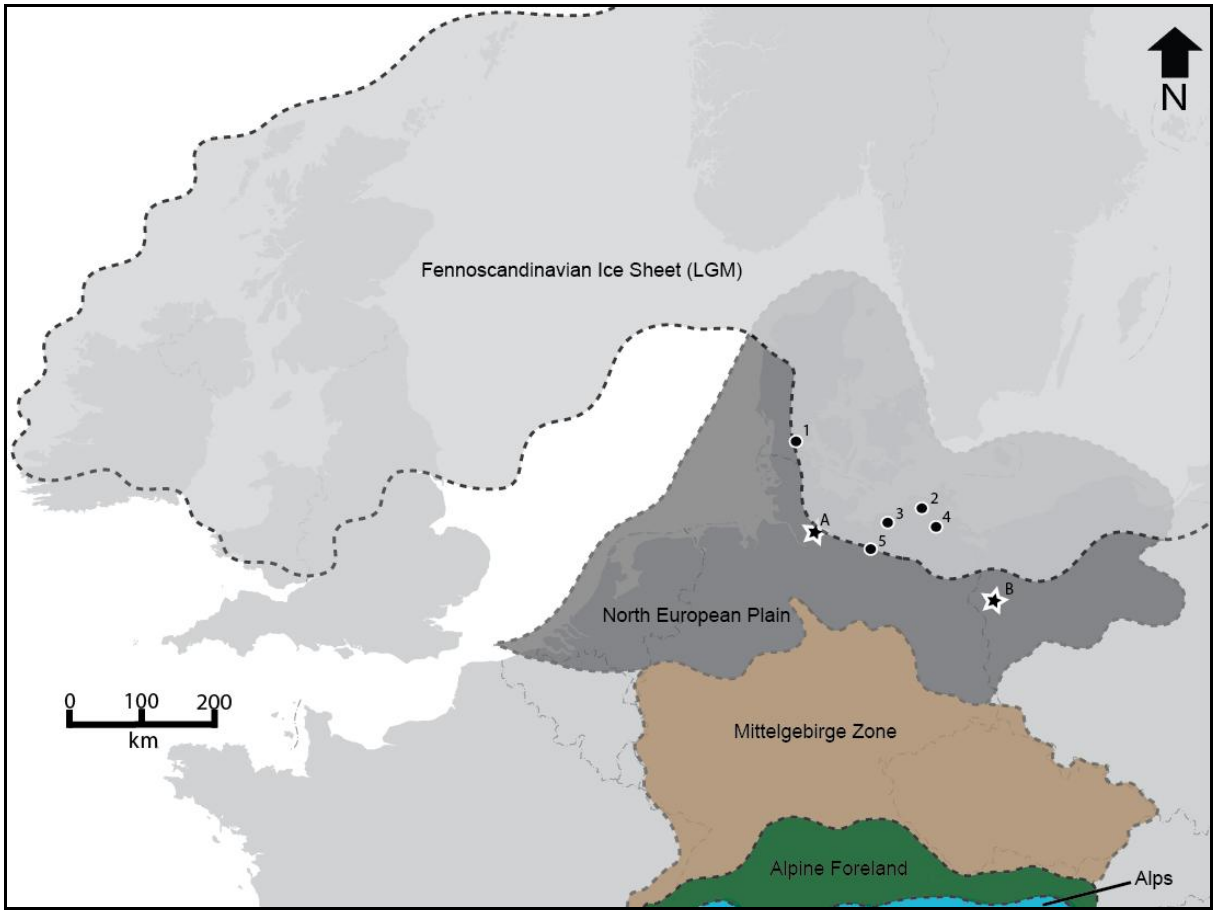


Figure 1.2 – Limit of the Fennoscandinavian Ice Sheet during the LGM ~22,000 cal yr BP (adapted from Terberger *et al*., 2004).

The lake systems of the NEP can be subdivided into large glaciolacustrine basins (>10,000 hectare), medium sized lakes (3-10,000 hectare) and kettle holes (<3 hectare) (Terberger *et al*., 2004). The relative abundance of each lake system type is not well know, however it is likely that lake abundance was inversely related to size. With the onset of deglaciation across northern Europe ~14,600 cal yr BP large proglacial lakes were formed in the coastal region of the northeast margins of the NEP. Sedimentary records show that the early phases of large lake development were characterised by clay and silt sedimentation with thick layers (~15m) of fine and medium grained sand deposited on top (Terberger *et al*., 2004b). During the Allerød soil and peat formation within these large lake basins indicate fragmented conditions with smaller lakes forming in the deeper parts of the basin and telemetric or fully terrestrial conditions occurring in shallower areas (Kaiser, 2001). With progress into

the later stage of the Younger Dryas, increased aeolian activity redeposited basin sands leading to complete terrestrialisation of these large lakes by the Early Holocene.

The development of medium sized lakes can be demonstrated by the sites of Endinger Bruch (section 3.5.2, Chapter 3) and the Biesenthal basin, Germany. The Endinger Bruch basin (~12km^2) is one of the most extensively studied Lateglacial basins and is composed of at least five separate lacustrine systems (see Terberger, 1998; de Klerk, 2002, Kaiser *et al*., 2004 and Lane *et al*., 2011b) and shows similarities with the Biesenthal basin. Both Endinger Bruch and the Biesenthal basin and the majority of medium size lake basins at northeast margins of the NEP show the beginning of sedimentation, composed of clastic gyttja overlying fine sand (section 3.5.2, Chapter 3), and dated to the early part of the Bølling. The Allerød is characterised by organic and calcareous gyttjas, thus suggesting, at least within the Endinger Bruch profile, that by this time it was a 'closed' system with no fluvial input.

The large majority of these aquatic systems originated from the melting of buried stagnant ice or 'dead ice' (Nitz *et al*., 1995; Juschus, 2003; Kaiser, 2004; Błaszkiewicz, 2010, 2011). The term 'dead ice' refers to the local conservation or incorporation of ice within topographic depressions; either derived from the freezing of pre-existing water bodies or the burial of glacial ice (Kaiser *et al*., 2012). The variety in topographic depressions within northeastern areas of the NEP therefore allowed the development of a wide range of aquatic systems. Prior to melting of dead ice within the depressions of the NEP, swamps and shallow lakes had already begun to form within these basins. A comprehensive study of the excising lakes of Mecklenburg-Vorpommern and northern Brandenburg by Kaiser, (2001) concluded that in ~90% of the studied lakes, sedimentation began within the Lateglacial, with 38% during the Allerød.

1.5.1 Aquatic fauna

The evolution of the aquatic fauna of the NEP is somewhat harder to unravel than that of its terrestrial counterpart. Many of the key archaeozoological sites within the study area such as Meiendorf and Stellmoor were excavated during the 1930's and 1940's when excavation techniques were far less rigorous by contemporary standards. A consequence of this is the likely loss of the bones of fish and other small aquatic vertebrates that do not readily preserve as frequently as other, larger terrestrial

animal remains and are also far harder to spot. Despite this under representation a number of recently excavated sites show the existence of well established aquatic assemblages. Firstly, recent excavations at the Polish site of Mirkowice have uncovered a hunter-gatherer hearth, dated to the Bølling, in association with fish bones belonging to pike and members of the cyprinidae family (Kabaciński *et al*., 1999). Coupled with the evidence from the hearth, a detritus layer, also assigned to the Bølling, contained ~3000 thousand bones of pike, perch (*Perca fluviatillis*), cyprinid fish and salmonid fish, possibly brown trout (*Salmo trutta*) (Kabaciński *et al*., 1999; Kabaciński and Sobkowiak-Tabaka, 2009). Secondly, at the site of Poggenwisch, Germany, aside from the remains of reindeer, polecat (*Mustela putorius*), ground squirrel (*Citellus rufescens*), swan (*Cygnus olor*) and grouse, numerous fish bones belonging to pike (*Esox lucius*) have also been uncovered (Herre and Requate, 1958; Bratlund, 1996). Finally, the site of Slotseng, Denmark, again shows the presence of cyprinid fish and birds coupled with reindeer during the Bølling (Holm, 2003).

1.6 Thesis structure

This thesis will explore the evolution of aquatic systems during the Lateglacial, within 7 Chapters as follows:

Chapter 2: Human dispersal and archaeology during the Lateglacial – will address the major population dispersal events that occurred within northern Europe during the Lateglacial. The Chapter will explore the timing and pattern of dispersal of these events that ultimately led to the resettlement of the NEP. Population expansion onto the NEP is subject to contrasting hypotheses as to the stimulus for northern expansion. The two leading arguments will be discussed as well as the implications of each within the remit of this thesis. Chapter 2 will also introduce the four cultural groups that span the Lateglacial of the NEP as well as discussing their associated hunting and subsistence strategies. The period of occupation on the NEP during the Lateglacial was relatively short; however there was considerable cultural and technological evolution during this period. These changes will be discussed for each cultural group, and possible reasons for cultural transitions explored. The Chapter will also explore the variations in hunting and subsistence strategies present within the NEP.

Chapter 3: Understanding aquatic exploitation during the Lateglacial – will address the potential of aquatic exploitation with Lateglacial hunter-gatherers from an archaeological, palaeoenvironmental and ethnographic standpoint. The Chapter will continue with the development of a model of aquatic exploitation for the NEP during the Lateglacial, and how this can be tested using the proxies used by this thesis. The Chapter will conclude by introducing the sites studied within this thesis. Five final sites have been used to evaluate the evolution of aquatic systems within the NEP. These sites will be discussed in full and published site information presented.

Chapter 4: Field and laboratory methodology – will outline the field and laboratory methods included within this thesis. The two laboratory methods used in the reconstruction of aquatic systems; stable isotopes and cladocera sub-fossils, will be introduced as will chronological methods, including microtephra analysis and ^{14}C dating,

Chapter 5: Results I chronology – will present the chronological results of this project. The tephrochronological record for each site will be discussed in turn. This will involve the presentation of geochemical data and subsequent interpretations based upon said data. To accompany the independent age estimates provided by microtephra, the results of the ^{14}C dating will also be presented for those sites with a ^{14}C chronology produced by this thesis. Age models for the studied sites will also be presented within Chapter 5.

Chapter 6: Results II stable isotopes and palaeoecology – will present the isotopic and palaeoecological results of this project. The isotopic record for each site will be discussed in turn. Variations in isotopic values will be highlighted and the importance of such variations analysed through numerical analysis. In addition, the cladoceran record for each studied site will be presented. This will involve the presentation of cladoceran sub-fossil records as interpreted through changes in cladoceran abundance and species composition throughout the studied sites evolution. Morphological changes in certain species of cladoceran will also be presented. Finally, each site will be summarised in a chronological discussion of the palaeoevolution of the lake system present during the Lateglacial – Holocene.

Chapter 7: Discussion and interpretation – will present an interpretation of Chapter 6 I and II, and will discuss the outcomes of the data and its implication for the development of aquatic systems and the relationship with Lateglacial hunter-gatherer groups. Specifically Chapter 7 assesses two main issues. Firstly, the potential of aquatic systems in supporting hunter-gatherer groups, and comparison of the exploitation of aquatic systems with terrestrial based subsistence strategies. Secondly, the impact of AETs on aquatic system development and its relation to the patterns of change witnessed in the isotopic and cladoceran record. Both lines of discussion will be assessed over temporal and spatial scales, therefore providing information on whether aquatic system development was contemporaneous or whether it differed over local scales.

Chapter 8: Conclusion – draws together the main conclusions from this thesis and will present them in a context of Lateglacial social and environmental change.

1.7 Aims and objectives

Through the use of isotopic and palaeoecological proxies, investigate the development of aquatic systems within the North European Plain during the Lateglacial.

This primary aim can be sub-dived into four additional objectives

1. To assess the impact of abrupt environmental transitions on the development of aquatic systems in the NEP.
2. To evaluate whether aquatic system development was contemporaneous or whether it differed over local scales.
3. To evaluate the impact environmental events such as the Laacher See eruption had on the aquatic record.
4. To evaluate the potential aquatic systems had in supporting hunter-gatherer groups, and to what degree they might have played in Lateglacial subsistence strategies.
5. To establish a detailed tephrochronological and tephrostratigraphic record for the studied sites.

1.8 Chapter summary

The Lateglacial period between ~14, 600 - 11, 500 cal yr BP is characterised by the rapid fluctuation of climatic conditions within the Northern Hemisphere following the termination of the LGM. The floral and faunal response of the NEP follows that of the climate with open type vegetation and animals consistent with colder conditions and closed type vegetation and animals consistent with warmer conditions. There is also evidence to suggest that a well established aquatic faunal record was developing within the NEP during this time, with a few well excavated sites showing the presence of fish and aquatic birds. The rapid climatic fluctuations during this period poses a direct challenge to Quaternary scientists to investigate the phasing of the palaeoenvironmental responses recognised across ice core, terrestrial and marine archives. Determining phasing and synchronisation of events within local, regional and continental records is compounded by dating and modelling errors within specific archives or whether significant 'leads' and 'lags' existed between records. Elucidating whether such 'leads' and 'lags' existed requires high levels of precision and accuracy to align records along often decadal timescales, which is often unattainable due to the variability of dating techniques used and associated inherent uncertainties.

This thesis is therefore an attempt to integrate different lines of evidence, each with varying degrees of importance and influence, in order to develop better understanding of Lateglacial aquatic systems and their associated role in supporting hunter-gatherer occupation of the NEP. The strength of this project is that it provides the first multiple site analysis of aquatic systems, and through tephrostratigraphy, has the ability to compare variations between sites at fixed isochronous points. This approach will allow greater understanding of how aquatic systems developed, and subsequently will further our knowledge of a resource base, that through archaeological evidence, we know was utilised by hunter-gatherer groups within the NEP during the Lateglacial.

Chapter 2: Human dispersal and archaeology during the Lateglacial

The following chapter will discuss patterns of human dispersal, technology and subsistence during the Lateglacial of northern Europe. Chapter 2 will begin by discussing human dispersal patterns during the Lateglacial of northern Europe, before introducing the competing models of human dispersal (characterised as population events 2 - 4). Chapter 2 will conclude with a review of the technocomplexes and subsistence strategies of population events 4 -6. The Lateglacial is composed of a series of population dispersals into increasingly more northern areas of Europe. It is necessary to discuss these as they not only provide the background to the eventual resettlement of the NEP, but also enable a period characterised by complex archaeological transitions to be viewed as a series of population events. Furthermore the population events present within sections 2.1.1 - 2.1.6 may also serve to help us better understand the models of population expansion presented in section 2.2.

2.1 Structure of Lateglacial expansion

Following Gamble *et al*., (2005) six main population events (1 - 6) can be suggested for the Lateglacial of western Europe (Table 2.1). In this chapter I will continue with a brief comment on each of the six proposed population events; in turn focussing principally on the timing and general dispersal patterns of the events.

Population event	Chronozone	GRIP event stratigraphy	Onset cal yr BP	End cal yr BP	Technocomplex
1. Refugium	Last Glacial Maximum	GS-2c		20,000	Solutrean
2. Initial expansion			20,000	19,000	Protomagdalenian – Badegoulian
3. Expansion II	Oldest Dryas	GS-2	19,000	14,670	Magdalenian
4. Expansion III	Pre-Bølling – Bølling	GS-2a - GI-1e	14,670	14,100	Hamburgian
	Older Dryas	GI-1d	14,100	13,900	
5. Consolidation	Allerød	GI-1c – GI-1a	13,900	12,900	Federmesser – Brømme
6 Hiatus	Younger Dryas	GS-1	12,900	11,500	Ahrensburgian – Brømme

Table 2.1 – Lateglacial population history of western Europe with associated technocomplexes (after Gamble *et al*., 2005). Population events and technocomplexes highlighted in grey are discussed in reference to the NEP only. Dating is presented as cal yr BP to allow comparison with ^{14}C age determinations discussed within the text (Miller, 2012).

2.1.1 Population event 1 - refugium

The term refugium *senso stricto* incorporates two potential concepts (Gamble *et al*., 2005, 2006) both of which may ultimately influence our understanding of population event 1.

Refugium^{1} – This concept refers to the minimum geographic distribution of a population, irrespective of population size

Refugium^{2} – This concept refers to the minimum population size, irrespective of geographic distribution

Through careful application of these definitions it is possible to view Lateglacial refugia, not as an geographically isolated pocket with a reduced population size, but rather one in which smaller 'satellite' populations exist on the periphery of the larger population groups as suggested by *Refugium*^{1}. The utility of distinguishing two refugia can be illustrated by the human expansion of population event 2 (section 2.1.2). While such sites are still relatively isolated and the majority of contemporary occupation is still found in the Franco-Cantabrian region, the observed spread of humans beyond the main area of refugia points to the problems in accurately specifying the geographical limits of a refuge (Gamble *et al*., 2005).

While it is highly likely that human populations were not contracted into an isolated pocket, but rather remained within small satellite' populations on the periphery of larger groups; the locations of these 'satellite' centres is still a source of debate. Phylogeographic analysis based on molecular-genetic evidence suggests that a population expansion occurred from southwest to northern Europe (Gamble, 1986; 2005; Achilli *et al*., 2004; Soares *et al*., 2010; Schwendler, 2012). It has been suggested that the decline of hunter-gatherer populations, between the Upper Palaeolithic and the Bølling Interstadial was caused by dietary breadth contraction leading to population stress and recurring population

bottlenecks within Franco-Cantabria (Cavalli-Sforza *et al*., 1994; (Morin, 2008). Recent research by Pardinas *et al*., (2012) correlates well with this view, and suggests that population expansion originated from the Franco-Cantabria region (Figure 2.1) with smaller dispersed populations not significantly contributing to the genetic pool. Spatial restrictions and small carrying capacities of the Franco-Cantabrian refuge would have given rise to low genetic diversity; however with rapid expansion within population events 3 and 4 would give rise to a positive association of genetic diversity and distance to the refuge, as seen in the European Postglacial haplogroup record (Pardinas *et al*., 2012).

The notion of a southwestern refugium has however been challenged and it is has been argued that whilst the frequencies of European Postglacial haplogroups are highest within Franco-Cantabrian populations, they also exhibit the lowest molecular diversities (Garcia *et al*., 2011). This suggests that the Franco-Cantabrian genetic pool may have evolved discreetly and differently from the rest of Europe, and therefore may not be sufficient for inferring continental dispersal patterns (Pardinas *et al*., 2012). It is therefore suggested by some authors that the singular area of refugia was in fact more fragmented and that re-population was aligned along a number of different axes such as those in southern France, Italy and the Balkan Peninsula (Richard *et al*., 2007; Pala *et al*., 2009; Malyarchuk *et al*., 2010).

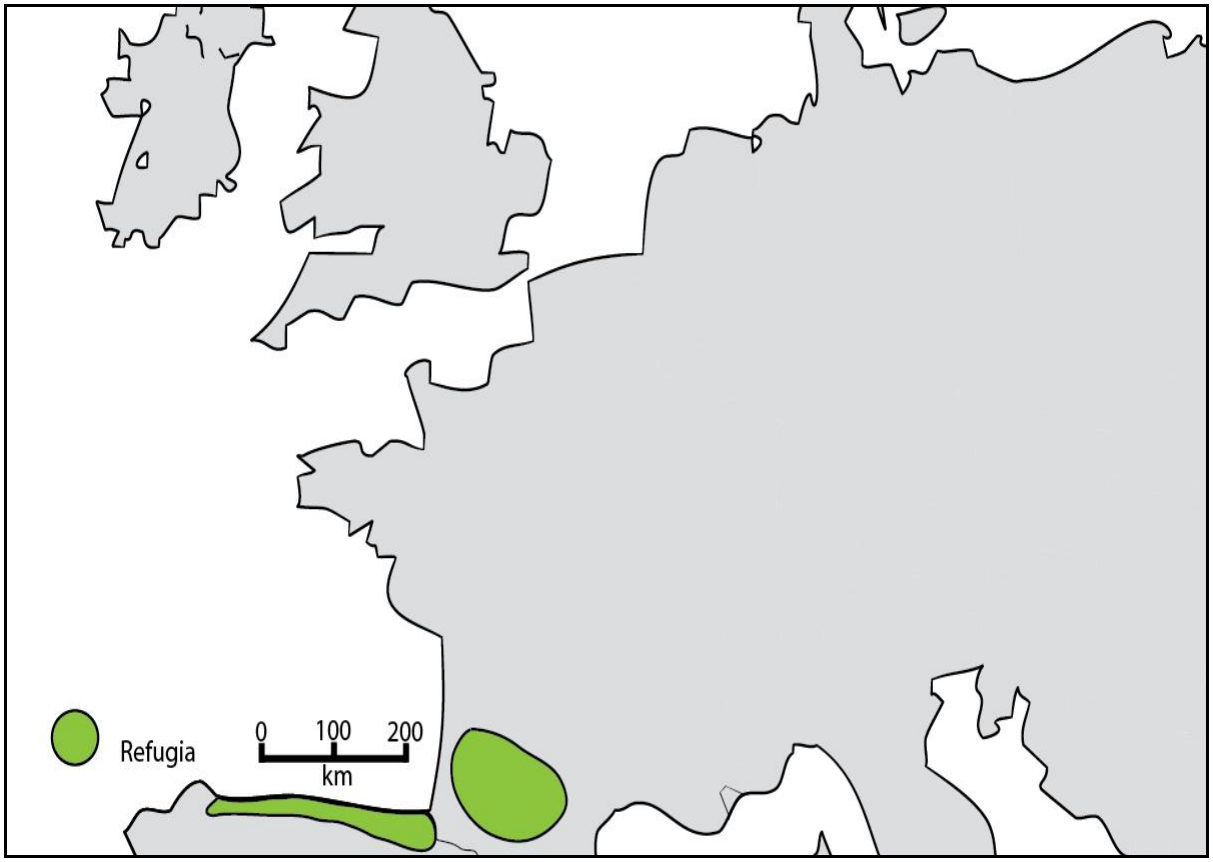


Figure 2.1 – The main area of Franco-Cantabrian refugium inhabited by Solutrean populations during the LGM forming population event 1 (Gamble *et al*., 2005). This follows the notion of a singular region of refugium as predicted by genetic evidence (Pardinas *et al*., 2012).

2.1.2 Population event 2 – initial expansion

Between 20 – 19 ka cal BP there was a small initial expansion of Protomagdalenian and Badegoulian populations beyond the area of Franco-Cantabria into southwest and central France as well as southern Germany (Figure 2.2; Miller, 2012). Evidence of occupation at sites such as Abri Fritsch, 22,020 – 19,385 cal yr BP (17,130 ± 550 ^{14}C yr BP); Abri Pataud, 22,170 – 20,012 cal yr BP (17,605 ± 420 ^{14}C yr BP); Solutré I-11, 21,805 – 19,474 cal yr BP (17,310 ± 470 ^{14}C yr BP); Monthaud, 21,082 – 19,470 cal yr BP (16,970 ± 300 ^{14}C yr BP) and Wiesbaden-Igstadt 19,000 – 17,000 cal yr BP, all indicate an initial movement away from the area of Franco-Cantabrian refugium (Miller, 2012).

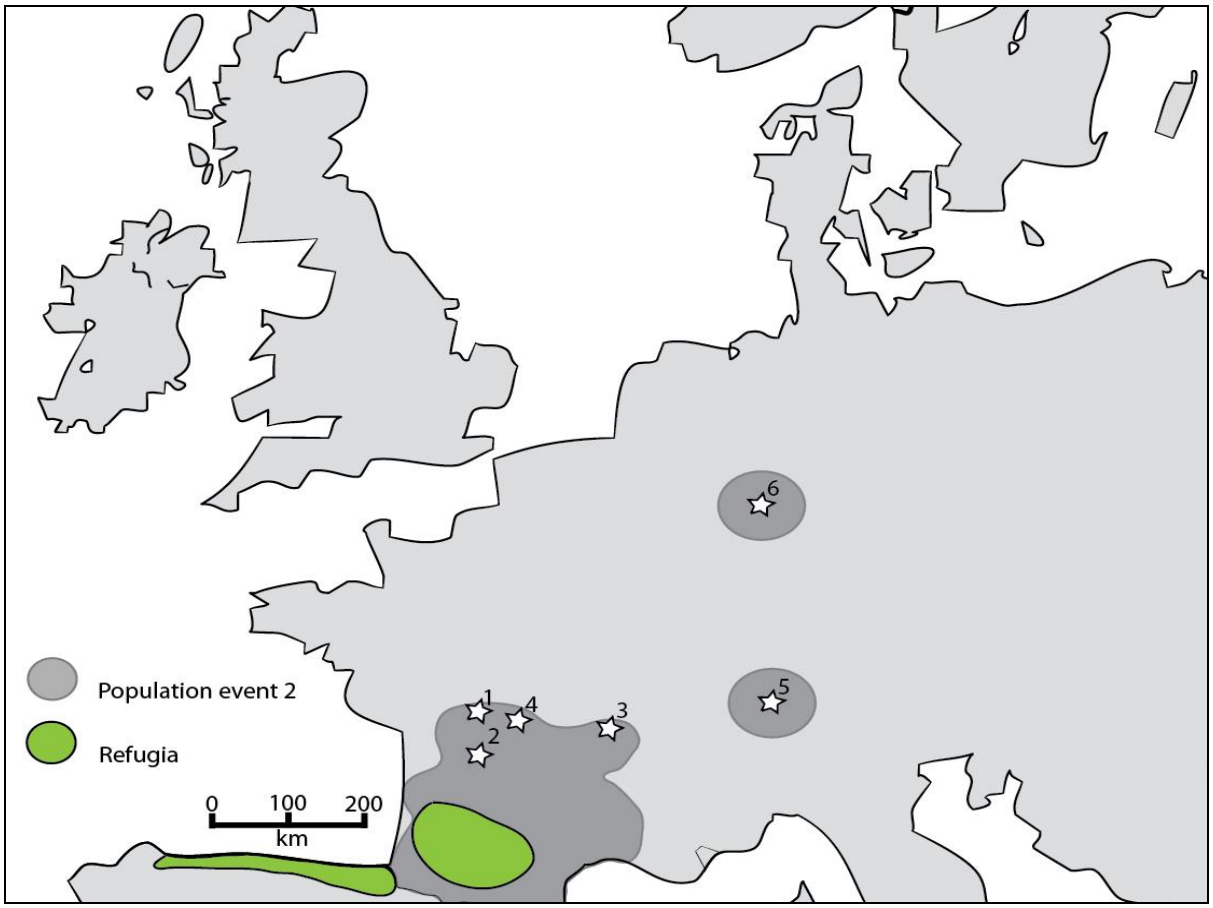


Figure 2.2 – Population event 2 forms the first initial expansion outside the main zone of Franco-Cantabrian refugium. Populations are still small during this period, but the geographic range of expansion has been furthered. Key sites referred to in the text; 1 – Abri Fritsch; 2 – Abri Pataud; 3 – Solutré; 4 – Monthaud; 5 – Kastelhöhle; 6 – Wiesbaden-Igstadt

2.1.3 Population event 3 – expansion II

Population event 3 may be seen as a prolonged period of northward expansion punctuated by a short (~1 ka) period of stasis associated with the Oldest Dryas (Figure 2.3). A slight warming phase between 19 – 17.5 ka cal BP initiates increased dispersal along a southwest – northeast axis, with occupation sites from Munzingen, Hohle Fels Schelkilngen, Spitzbubenhöhle and Regensburg in southern Germany (Terberger *et al*., 2009; Street *et al*., 2012) and also into southern Poland at

Maszycka Cave (Kozłowski *et al*., 2012). There is an increase in population density within the Franco-Cantabrian region coupled with expansion into more northern areas of France such as Oisy and Arcy-sur-Cure (Miller, 2012). The sharp climatic downturn associated with the Oldest Dryas (~17 ka cal BP) appears to stall northeast dispersal with only Munzingen dated to 17,780 – 16,975 cal yr BP (14,270 ± 120 ^{14}C yr BP) and Spitzbubenhöhle dated to 17,974 – 17,210 cal yr BP (14,510 ± 110 ^{14}C yr BP) in Germany and Kesslerloch dated to 17,585 – 16,900 cal yr BP (14,150 ± 100 ^{14}C yr BP) and Kastelhöhle dated to 16,878 – 16,216 cal yr BP (13,435 ± 50 ^{14}C yr BP) in Switzerland remaining occupied during this stage (Leesch *et al*., 2012; Miller, 2012). The termination of the Oldest Dryas coincides with a rapid rise in temperatures as well as occupation sites throughout Europe. The density of population in southern Germany is argued to have increased, with new occupations at sites such as Petersfels, Hohle Fels, Bockstein-Törle, Hohlenstein-Kleine Scheuer and Ofnet, as well as continuing occupation at Munzingen and Spitzbubenhöhle (Miller, 2012). Within this population event there was also the first occupation of sites within the Paris Basin such as Etiolles 17,010 – 16,456 cal yr BP (13,625 ± 105 ^{14}C yr BP) and Grand Canton 16,289 – 14,942 cal yr BP (12,880 ± 115 ^{14}C yr BP) as well as occupation further north into Belgium and the Upper Meuse basin (Street 2000; Valentin and Pigeot 2000; Miller, 2012; Schwendler, 2012).

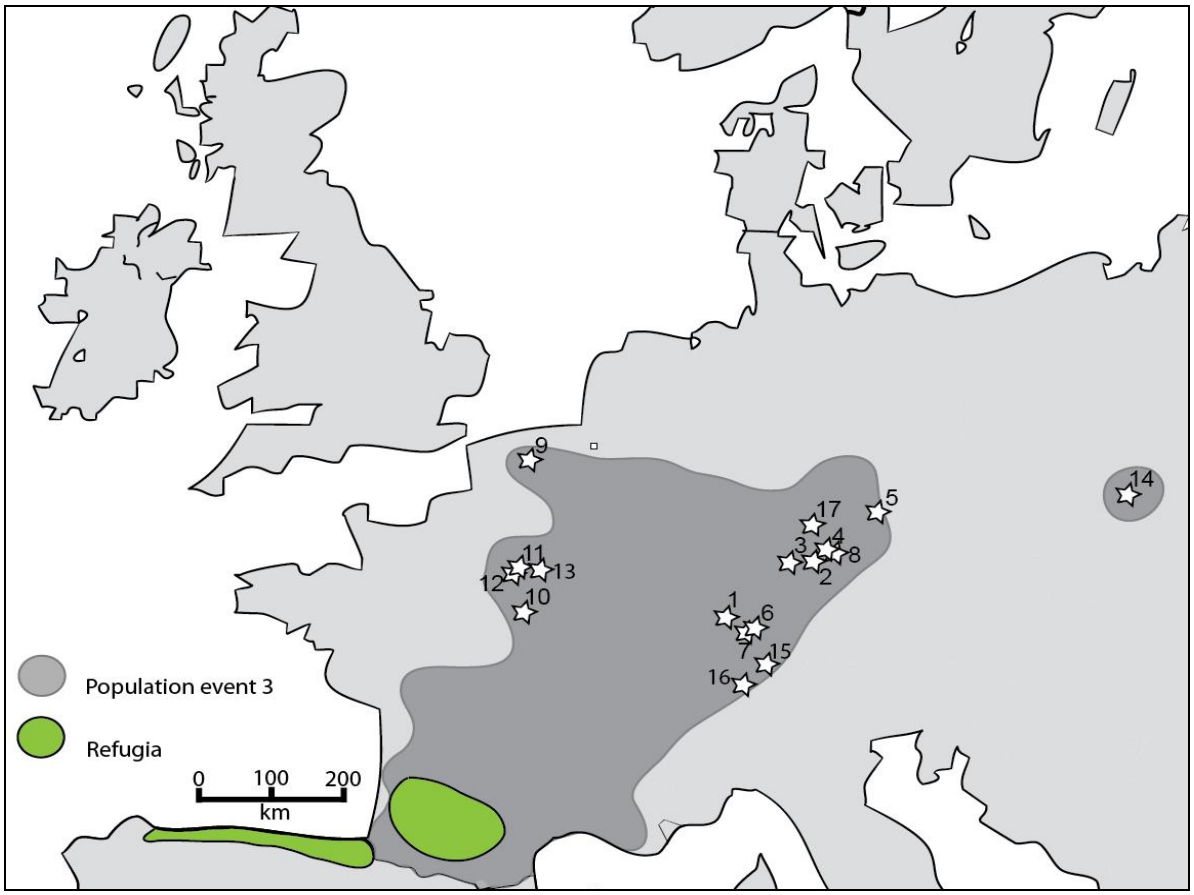


Figure 2.3 – Population event 3 forms the main demic expansion into southern and central areas of Europe. There is increasing population density within southern German uplands throughout this phase, but no expansion onto the NEP. Key sites referred to in the text; 1 – Munzingen; 2 – Hohle Fels; 3 – Schelkilngen; 4 – Spitzbubenhöhle; 5 – Regensburg; 6 – Petersfels; 7 – Bockstein-Törle; 8 – Hohlenstein-Kleine Scheuer; 9 –Pas-de-Calais; 10 – Oisy; 11 – Arcy-sur-Cure; 12 – Etiolles; 13 – Grand Canton; 14 – Maszycka Cave; 15 – Kesslerloch; 16 – Kastelhöhle; 17 – Ofnet

The dispersal associated with population event 3 led to an increasing presence of Magdalenian populations within the Rhineland, Thuringia, southern Poland and the southern upland region of Germany; the so called "*Mittelgebirge*" zone. This however marked the limit of northern Magdalenian expansion onto the NEP. The southern German uplands mark the edge of a cultural divide between the Magdalenian to the south and the Hamburgian on the NEP. Excavations of rock shelters in the mountains north of Göttingen yielded several sites of Magdalenian occupation (Grote, 1993) while in Gadenstedt, Landkreis Peine, a Magdalenian site was located at the transition to the northern

German lowlands (Simoneit and Veil, 1999), there is however at present no evidence for the Magdalenian on the NEP.

The history of the re-occupation of the NEP can be seen as commencing with population event 4, and involved the rapid propagation of archaeological sites within this region that are culturally separate from the Magdalenian to the south. The following three population events deal directly with cultural groups entering onto the NEP.

2.1.4 Population event 4 – expansion III

Whilst it is now accepted that Magdalenian populations had moved into the southern German uplands by the later phases of the Older Dryas, early models of expansion onto the NEP suggested that further settlement was restricted until the climatic amelioration of the Bølling chronozone (e.g. Housley *et al*., 1997; Figure 2.4). However, there is now new evidence to challenge this view. The oldest date for the Hamburgian, and therefore human presence on the NEP, comes from Olbrachcice 8, Poland (Kanwiszer and Trzeciak, 1984) with an age of 16,194 – 14,057 cal yr BP (12,680 ± 230 ^{14}C yr BP) and Querenstede, Netherlands (Lanting and Plicht 1996) with an age of 16,421 – 13,943 cal yr BP (12,650 ± 320 ^{14}C yr BP). Although represented only by single charcoal dates from two separate sites, thus making any discussion on their validity problematic, they do suggest the possibility that expansion onto the NEP occurred prior to the Bølling. Coupled with this is a date on an anthropogenically modified reindeer antler from Slotseng, Denmark (Aaris-Sørensen *et* al., 2007) with a weighted mean age of 14,994 – 14,120 cal yr BP (12,423 ± 66^{14}C yr BP). Such early dates from the northern edge of the NEP may suggest an expansion prior to the climatic amelioration of the Bølling. Without further dating, this theory is un-supportable, however if proved to be correct with additional dating, then the earliest settlement within the NEP was contemporaneous with the Late Magdalenian of the Paris Basin (Street, 2000; Valentin and Pigeot, 2000) and the Creswellian of the British Isles (Barton *et al*., 2003; Jacobi and Higham, 2009).

The general increase in archaeological sites associated with population event 4 (and also population event 5) must however be treated with caution. The settlement of the NEP coincides with a dramatic increase in ^{14}C dates, which have been utilised in the past as proxies for archaeological events (see

Housley *et al*., 1997). An apparent increase in ^{14}C dates does not however necessarily mean an increase in people/population. First is the issue of contemporaneity. Whilst preceding population event 4, an example from the Gravettian of southwestern Germany shows how separate occupation sites, can in fact be archaeologically contemporaneous and as such do not indicate an increase in population but merely reflect the multiple use of different sites by the same band of people. Out of a total of five Gravettian sites from the Swabian Alb, three were directly connected through refitting of lithic artifacts (Scheer, 1993). The close clustering of dates within the NEP (section 2.1.4.1) may therefore represent a small number of groups utilising multiple sites, therefore increasing the number of ^{14}C dates but without an associated rise in population (Eriksen, 2002). Secondly, ethnographic studies of hunter-gatherer groups within inland areas of varying environmental conditions, all have population densities between 0.1 – 0.01 individuals per km^2 (Krzywicki, 1934; Kroeber, 1939). This would indicate that the expansion of population event 3 into central Europe with an area of ~900,000 km^2, would have had a population density of 9000 – 90,000 individuals. In contrast the later expansion of population event 4 and 5 onto the NEP, which has an area of ~150,000 km^2, implies a population density of 1500 – 15,000 individuals. These figures require that every km^2 is occupied within the two areas, which of course will not have been the case; however it does serve to illustrate that the NEP had a far lower capacity for supporting larger populations than central Europe. With improving climatic conditions and new resource availability on the NEP, a population increase is most probably a logical outcome between 14,670 – 13,900 cal yr BP. What these studies show however is that the NEP may not have been as rapidly and intensively occupied as previously believed.

2.1.4.1 The significance of dating population event 4

Based upon current research there are approximately 100 ^{14}C dates for the Hamburgian (population event 4). Unfortunately, critical evaluation of these dates (see Pettitt *et al*., 2003) shows there are problems. Whilst many dates obtained by conventional (β-) methods are generally acceptable, assuming no significant contamination issues or bulked samples, they often carry large standard deviations (Grimm and Weber, 2008). Conversely, many recent AMS dates on small amounts of material may have failed to fulfil the minimum carbon yield (>1.4 mg C, Wohlfahrt *et al*., 1998; > 1-

wt% collagen/ 10 mg pre-treatment yield, Higham *et al*., 2006). Unfortunately such information is rarely given in publications making it difficult to evaluate the reliability of published dates.

As discussed in section 2.1.4 the earliest dates for population event 4 are represented by single charcoal dates with no close association with lithic material. The earliest unequivocally human dates can be found at sites in Denmark and northern Germany. The site of Slotseng has a date taken from humanly modified antler. A single date from an antler in association with tools and cut marked bones, from Meiendorf, is dated at 15,001 – 13,999 cal yr BP (12,360 ± 110^{14}C yr BP; Fischer and Tauber, 1986). Lastly, a cluster of eight dates on humanly modified bone from Poggenwisch give a mean age of 14, 894 – 14, 093 cal yr BP (12, 375 ± 25^{14}C yr BP; Fischer and Tauber, 1986). The close grouping of dates for this period can however be divided according to geographic position. Sites that yield older ages for population event 4 are typically found to the east, while younger dates lie further to the west (Grimm and Weber, 2008). This pattern may have implications for the direction of expansion. As highlighted in section 2.1.4, the earliest settlement of the NEP is believed to be contemporaneous with the Late Magdalenian of the Paris Basin and the Creswellian of the Britain. The Creswellian may be seen as the easterly extent of the population event 4, as the NEP would have extended across the dry North Sea region during this time. A grouping of older dates within the eastern region of the NEP would suggest a pattern of re-settlement from a southeasterly direction, possibly following the Oder Valley. This dating evidence would therefore call into question a western origin for population event 4 (see Burdukiewicz, 1989) and chronologically speaking, an easterly direction would seem to be most

plausible.

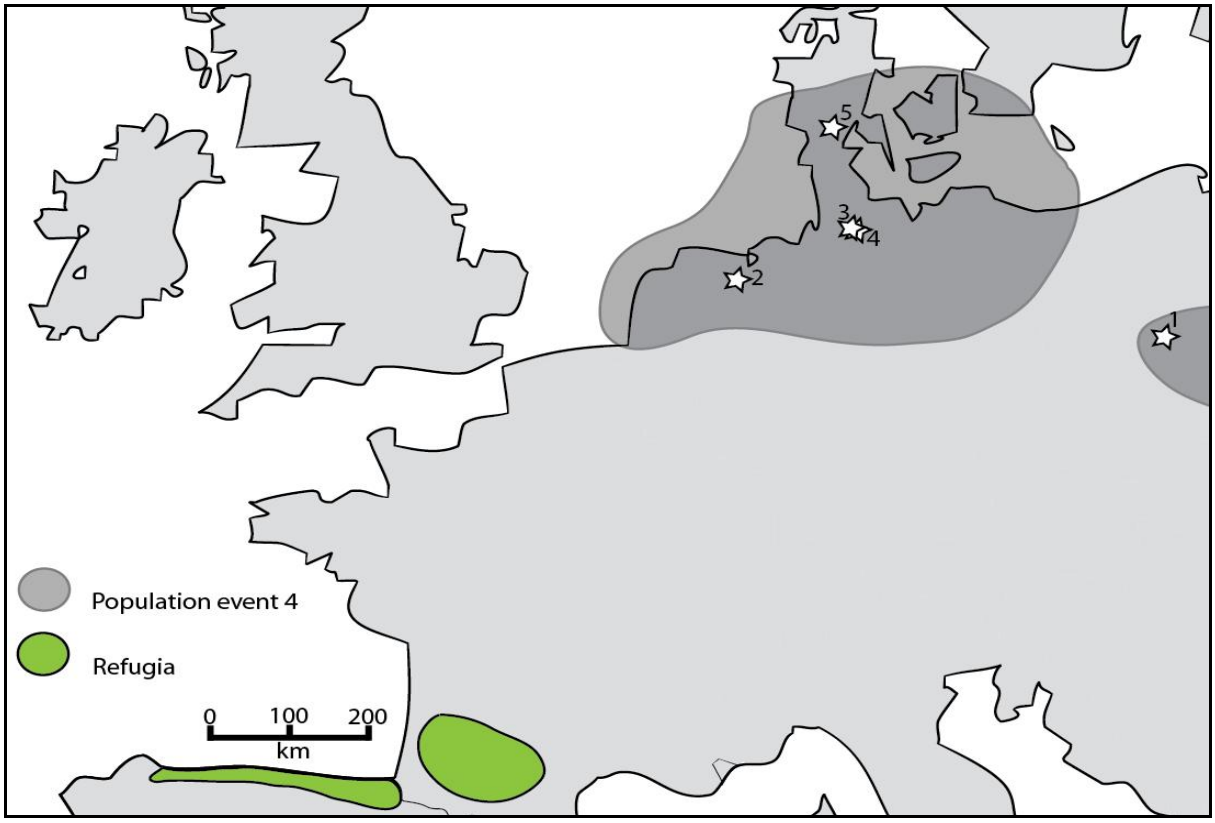


Figure 2.4 – Population event 4 indicates the first expansion of hunter-gatherer populations onto the NEP. Expansion during this phase is rapid with confirmed expansion in all areas of the NEP within ~ 1.6 ka of the first arrival of populations. Population event 4 is characterised by an increase in ^{14}C dates throughout the NEP. This however may be more of a result of a bias in the number of ^{14}C dates undertaken rather than a large in increase in population (see section 2.1.4). Key sites referred to in the text; 1 – Olbrachcice; 2 – Querenstede; 3 – Meiendorf; 4 – Poggenwisch; 5 – Slotseng.

2.1.5 Population event 5 – consolidation

Population event 5 can effectively be divided into two dispersal events; the first from the southwest and the second from the east, west or an entirely separate local origin. The first phase of population event 5 (emergence of the Federmesser) appears to have entered the NEP as part of a population dispersal from the southwest by 14,138 ± 287 cal yr. BP, based on evidence from the site of Reichwalde, Germany (Friedrich *et al*., 2001; Brinch Petersen, 2009; Riede *et al*., 2010), Further dates from Klein Nordende, 13,096 – 12,720 cal yr BP (11,035 ± 50 ^{14}C yr BP) and Querenstede,

13,701 – 12,222 cal yr BP (11,070 ± 320 ^{14}C yr BP) indicate a rapid spread of populations during this time (Riede and Edinborough, 2012). The second phase of population event 5 coincides with the emergence of the tanged point group (TPG) of the Bromme. The origin of the TPG on the NEP is still uncertain and open to debate and interpretation, currently three main concepts have been proposed. 1) a local origin 2) an eastern origin 3) a western origin. The local origin hypothesis was first proposed by Schwabedissen (1937) and argued for the evolution of the Ahrensburgian (and earlier Bromme) to be founded in the Havelte Hamburgian due to the similarity of Havelte points with Bromme and Ahrensburgian points (Šatavičius, 2004). This version of the local origin has been questioned by some (see Fischer, 1991) who claims that the chronological gap between the Havelte Hamburgian and the Bromme and Ahrensburgian is too great to allow technological continuity without any intermediary technological stage. As a counter to this argument it has been suggested that the technological and chronological overlap between the Havelte Hamburgian and the TPG Bromme stage was filled by the Arch Backed Points (ABP) of the Federmesser (Eriksen, 1999). A second possible option for the local origin hypothesis was recently proposed by Riede (2008), suggesting that the eruption of the Laacher See volcano 12880 ± 40 varve year BP (Brauer *et al*., 1999). The eruption, approximately 200 years before the onset of the Younger Dryas, is argued to have caused the loss of ABP and the subsequent emergence of TPG through significant population reorganisation (Riede, 2008). This author also suggests that the simplification within the TPG, and in particular Bromme technologies, including the loss of bow and arrow technology, was the direct result of geographic and social isolation, caused by divisions within the landscape as a result of volcanic ash fall out.

An eastern origin for the appearance of the TPG can be seen as a plausible alternative given the continuous occupation of southeastern Europe during the LGM and Lateglacial. Several sites in Belarus, northern Ukraine and western Russia have yielded tanged points that are either morphologically similar to Bromme and Ahrensburgian ones or have actually been classified as such (Burdukiewicz, 2011). The eastern origin of the TPG on the NEP implies that TPG groups had their basis in the Eastern Epigravettian of western Ukraine and Russia, and that local mammoth hunting was eventually superseded by reindeer exploitation during the Lateglacial. Establishing a chronology for this eastern European area is difficult, as at present there are no secure chronologies for the sites

with tanged points (Burdukiewicz, 2011). Pollen data suggest a possible Allerød age for sites such as Podol 1 and 2 and Ust-Tudovka in western Russsia (Sinitsyna, 2002), but without further chronological data from other sites, any link between the east and the NEP is difficult to ascertain. Recent genetic studies open the door for the third possible hypothesis: the western origin. Work by Passarino *et al*., (2002) suggests that the first settlers of the NEP had their origins in the southeastern European Gravettian; whilst Torroni *et al*., (1998) and Dupuy *et al*., (2006) suggest a southwestern origin associated with Magdalenian expansion from southwestern France and northern Spain. Both areas conceivably could have contributed to the appearance of ABP and TPG; with ABP closely aligned with the Azilian (see section 2.3.3) and TPG with the southwestern Magdalenian.

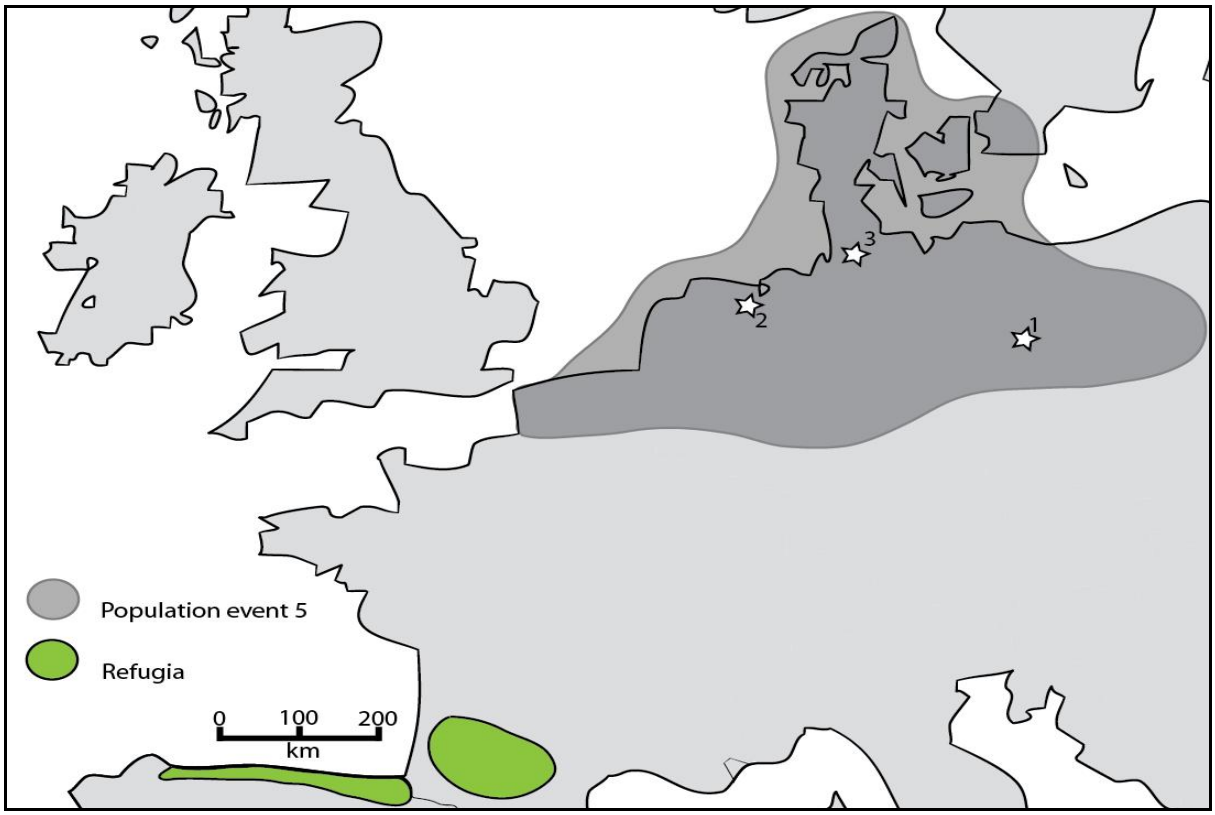


Figure 2.5 – Population event 5 is characterised by a rapid spread of populations within central, western and northern areas of the NEP. Population event 5 can be further divided into two separate, further expansions of hunter-gatherers onto the NEP (see section 2.1.5). Key sites referred to in the text; 1 – Reichwalde; 2 – Querenstede; 3 – Klein Nordene.

2.1.6 Population event 6 – hiatus

Early studies into population event 6, suggest that during the Younger Dryas there was a considerable contraction in hunter-gatherer populations on the NEP (see Housley *et al*., 1997; Gamble *et al*., 2005; Figure 2.6). Subsequent archaeological surveys (see Straus *et al*., 1996) and radiocarbon determinations, suggested that the NEP was neither fully abandoned nor used any less than in previous population events. Attempts to elucidate the population history of the NEP during the Younger Dryas is hampered by poor preservation, such as that at the site of Nahe, northern Germany (Weber *et al*., 2011). With optimum temperatures for the Younger Dryas recorded during the middle of the stadial (Rasmussen *et al*., 2006) it is plausible that the warmer conditions led to the melting and destabilisation of frozen soils (von Grafenstein *et al*., 1999). Coupled with Holocene induced melting, it is possible that mid – terminal archaeological deposits were either destroyed or re-worked, particularly in southern portions of the NEP with discontinuous permafrost (e.g. Kaiser *et al*., 1999; Bos, 2001; Dewez *et al*., 2008). When considered in a climatic and environmental context, the presence of a true hiatus for the mid – terminal Younger Dryas seems unlikely (Weber *et al*., 2011). It is therefore likely that there is no true hiatus in NEP settlement during the Younger Dryas, however further work is needed in refining this chronologically complex population event.

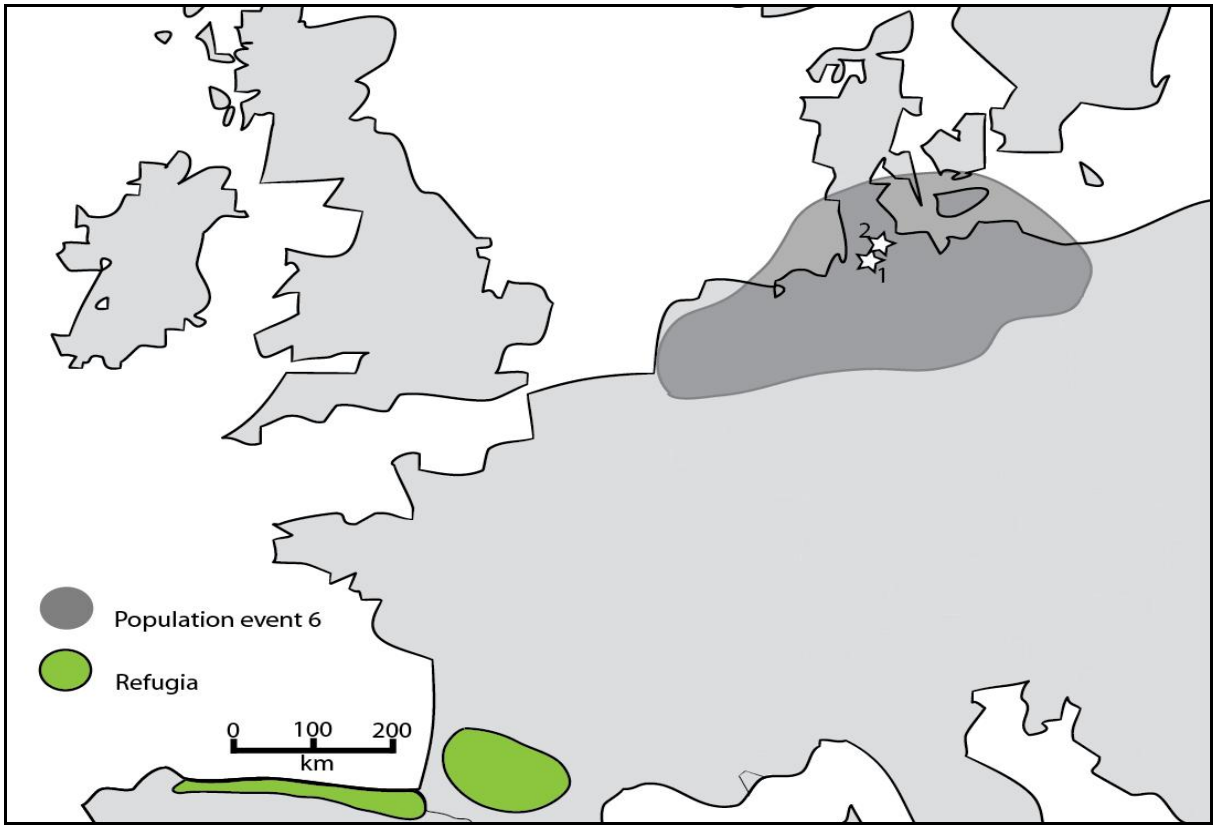


Figure 2.6 – Population event 6 coincides with the Younger Dryas. Archaeological and chronological data suggests that there was a shift away from more northerly margins of the NEP, with parts of Denmark abandoned. The hypothesis that the NEP was largely abandoned during the Younger Dryas is not supported, with the majority of anthropogenic ^{14}C dates attributed to the earliest part of the Younger Dryas when the climate was at its harshest. Key sites referred to in the text; 1 – Stellmoor; 2 – Nahe.

2.2 Models of population expansion

The models of population expansion discussed in section 2.2.1 and 2.2.2 are directly tied to our perception of a refugium (see section 2.1.1). If the model *Refugium*[1] is considered, our understanding in determining whether resource richness or consistency formed its principle biotic feature, is key in elucidating this mode of refugium (Gamble *et al*., 2005). With this in mind two models of population

expansion exist, i) a population 'pull' model where resource richness provided the necessary stimulus for expansion into central and northern areas of Europe; ii) a population 'push' model where changes in resource richness and/or consistency within *Refugium*[1] led to a net population expansion, radiating from pockets of refugia.

2.2.1 Population 'pull' model

The population 'pull' model (following Gamble *et al*., 2005) hypothesises that resources such as game and fish attracted and expedited the re-occupation of the NEP following the LGM.. The population 'pull' model is tied to the ability of hunter-gatherer groups to adapt to, and exploit any given area. It can be argued that;

"*a society with a subsistence strategy based solely upon hunting and gathering, will only exploit a region to the degree made possible by the natural preconditions reflected in the biostratigraphical record of climate, flora and fauna*" (Eriksen, 2002).

In the context of the population 'pull' model, this statement implies that, floral and faunal developments on the NEP influenced the northward movement of hunter-gatherer groups during population event 2 and 3. However, as discussed in section 2.1.3, the movement of hunter-gatherer populations effectively stalled in the southern German uplands and only moved onto the NEP during the later stages of the Oldest Dryas and early Bølling. Comparison of temperature reconstructions for the Bølling indicates that changes in temperature alone cannot explain population event 4. Increased northward expansion onto the NEP during the Bølling coincides with mean January temperatures of -5 °C in northern Europe, while Iberian temperatures remained close to 5 °C, based on multi-proxy climate reconstructions (see Björk *et* al., 1998; Renssen and Isarin, 2001; Walker *et al*., 2003 and Gamble *et al*., 2004). If population event 4 is considered outside of a temperature context, then the 'local opportunities' introduced by the model need to be fully determined. It is on this point that present research is deeply divided, it is nevertheless becoming clear that the 'local resources' of the NEP and subsistence strategies used to exploit them, are more complex than previously thought.**2.2.2 Population 'push' model**

With the associated climate amelioration following the termination of the LGM, the population 'push' model (following Gamble *et al*., 2005) argues for floral and faunal changes within the zones of south-western refugium forcing northward expansion towards the NEP.. This differs crucially from the pull model as changes occur within the pockets of refugia as opposed to on the NEP. As discussed in section 2.1.3 there is a significant increase in the number of Late Magdalenian ascribed calibrated radiocarbon ages observed in western and central Europe between ~18 – 15 ka cal BP (Gamble *et al*., 2005; Alonso, 2007; Miller, 2012). It is likely that the floral and faunal responses to AETs during this period largely contributed to the control of hunter-gatherer dispersal during population events 2 and 3. Terrestrial records from western Europe show a distinct palynological response to the termination of the LGM (Pons and Reille, 1986; Turner and Hannon, 1988; Lowe *et al*., 1994; Allen *et al*., 1996). Prior to the Pre-Bølling the vegetation cover over much of Iberia consisted of open, shrub like conditions with *Juniperus* and *Artemisia* dominant (Roucoux *et al*., 2005; Garzón *et al*., 2007). With a rise in mid-latitude temperatures by the onset of the Pre-Bølling, the vegetation of Iberia underwent large scale changes. *Quercus*, *Betula*, *Corylus* and *Alnus* concentrations all rose dramatically at the expense of the shrub like plants (Boessenkool 2002; Roucoux *et al*., 2005; Naughton *et al*., 2007). The relative climate amelioration of the Pre-Bølling coincides with a major switch in the cultural and social aspects of Late Magdalenian life. There is an increased shift away from a heavy dependence on red deer and ibex towards the exploitation of a broader diversity of foods including birds and marine shell fish (Davidson, 1989; Aura and Pérez, 1992; Villaverde and Martinez, 1992). Secondly, in this phase there is a reduction in the distance travelled to collect raw materials for lithic production, while widespread figurative art also disappears (Aura *et al.*, 1998). It is argued that this dramatic shift in behaviour is related to increased restrictions in the ranges of population events 2 and 3 due to rapid reforestation and sea level rise (Straus, 1991; 1992).

The 'push' model therefore hypothesises that climate-induced responses in the flora and fauna of Iberia forced hunter-gatherer populations northward out of pockets of refugia during population events 2 and 3.

2.3 The technocomplexes and subsistence strategies of population events 4-6

The following section will discuss the archaeological technocomplexes and associated subsistence strategies of population events 4 - 6 (Table 2.1). The Lateglacial of the NEP is characterised by different technocomplexes often overlapping both temporally and spatially. This is particularly evident with the classic Hamburgian and Havelte Hamburgian as well as the emergence of the Federmesser and Bromme technocomplexes (section 2.3.2.1 and 2.3.3). This section will therefore discuss each technocomplex sequentially, and where necessary explore the possible reasons behind the variations or overlaps in technocomplexes. This section will also discuss the variations in subsistence strategies associated with each of the technocomplexes of population events 4 - 6. When considered at a regional scale, the archaeological groups discussed in sections 2.3.2 – 2.3.5 must have inhabited a great variety of local environments, each with its own varying resource potential (Bratlund, 1996). As introduced in section 2.2.1 hunter-gatherer societies, whose subsistence strategy is based solely on local resource availability, i.e. resources that can be obtained within a day's hunting (Kelly, 1995) can only exploit a region to the degree made possible by the local flora and fauna (see Eriksen, 2002). With this in mind, and the close association and alignment of archaeological groups with the major ecozones of the NEP, it is pertinent to ask: what were these local floral and faunal resources and how were they exploited? A simplistic view of the floral and faunal record presented in sections 1.3 – 1.4 (Chapter 1) would suggest the predominance of more or less open conditions of the Bølling and Younger Dryas chronozones, and thus the Hamburgian *sensu stricto* and Ahrensburgian, were associated with reindeer hunting, whereas forested conditions of the Allerød characterised the Federmesser and Bromme and these were predominantly associated with elk exploitation. This over-simplification however has several problems. Firstly, it assumes that there was social continuity in the ways in which hunting methods were practiced. Thus for instance, the hunting tradition of the Ahrensburgian is assumed to replicate that of the Hamburgian which preceded it by ~ 2500 cal yr BP. Secondly, little emphasis is placed on a diversity of subsistence strategies. As discussed in section 1.4 (Chapter 1), the faunal record of the NEP is largely biased towards large mammals which more readily preserve, whilst small mammal and fish bones do not. Unfortunately, the large majority of archaeological excavations in the NEP have not been excavated to modern standards (only 15% of Hamburgian sites have been excavated to modern standards; Grimm and Weber, 2008) whilst many others are found with limited or no faunal representation. Therefore it is highly likely that the

contribution of fishing and small mammal exploitation are largely understated in the hunting economies of the NEP.

2.3.1 Conventions adopted

In order to ensure consistency in this thesis, the archaeological groups discussed within sections 2.3.2 – 2.3.5 will be referred to as technocomplexes. The term 'cultural' will only be used when in reference to a particular behavioural trait, such as the transmission of knowledge from successive generations, for instance:

"*The consistency in bone and ivory fishing equipment from the Magdalenian through to the Mesolithic may therefore be suggestive of a consistent* ***cultural*** *thread spanning Lateglacial hunter-gatherer groups*" – section 3.1, Chapter 3

When discussing the development and nature of Lateglacial subsistence strategies it is necessary to deviate from the term 'technocomplex' when addressing hunter-gatherer behaviour. Hunting and gathering is by definition dynamic and driven by social, economic and cultural needs. It is required therefore to refer to these people as 'groups', for instance:

"*The little we know of the seasonal exploitation of game during the Lateglacial comes from the Hamburgian and Ahrensburgian (sections 2.3.2 and 2.3.5) while Federmesser and Bromme* ***groups*** *are argued to have less pronounced seasonality in their hunting practices caused by a shift away from reindeer based subsistence strategies*" – section 3.1, Chapter 3

Therefore this thesis will utilise the term 'group' e.g. Federmesser group, when referring to active nature of hunting and gathering or when discussing subsistence strategies in general.

As discussed within section 1.2 (Chapter 1) this thesis utilises local chronozones (Table 2.2). The overall appearance of the four main technocomplexes of the NEP Lateglacial will be discussed in reference to this chronological record. The only exception to this will be the discussion of ^{14}C dates which date occurrences of specific technocomplexes at site level.

Technocomplex	Chronozone	Climate	Vegetation
Hamburgian	Bølling	Cool temperate	Park tundra with dwarf birch, rowan, willow, wormwood, grasses and herbs
Federmesser	Allerød	Cool temperate	Park tundra with birch and pine forest
Bromme	Late Allerød	Cool temperate	Park tundra with birch and pine forest
Ahrensburgian	Younger Dryas	Subarctic	Park tundra with willow, dwarf birch, juniper, wormwood, crowberry, grasses and sedges

Table 2.2 – The four technocomplexes of the NEP during the Lateglacial period with associated vegetation and climatic variables. Table adapted from Eriksen, (2002). For approximate ^{14}C cal yr BP ages refer to Table 2.1.

2.3.2 The Hamburgian – Population event 4

The oldest firm evidence for prolonged human presence on the NEP comes from sites of the classic Hamburgian. Research suggests this early technocomplex was broadly contemporary with and possibly derived from the latest Magdalenian to the south (Schwantes, 1932; Rust, 1937; Street *et al*., 2001). Various sources suggest that the *Mittelgebirge* zone in southern Germany marks the divide between the Magdalenian to the south and the Hamburgian to the north. Excavations of rock shelters in the mountains north of Göttingen yielded several sites of Magdalenian occupation (Grote, 1993) while in Gadenstedt, Landkreis Peine, a Magdalenian site was located in the transitional zone with the northern German lowlands (Simoneit and Veil, 1999), there is as yet, no evidence for the Hamburgian within the *Mittelgebirge* zone (Figure 2.7).

The Hamburgian technocomplex was defined in 1932 based on a number of surface scatters in the Hamburg area; the appearance and form of which was different to previously recognised lithic industries, but with a distinctly Upper Palaeolithic appearance (Clark, 1938). This new lithic industry was termed the '*Wellingsbütteler Stufe'* (Welling Bütteler stage) by Schwantes, (1932) who regarded it as a preceding stage of the Ahrensburgian, that he himself had just defined (Burdukiewicz, 1986). A year later the term '*Hamburger Stufe*' was proposed by Schwantes, (1933) after which the name

became gradually more accepted. A defining form of the newly discovered Hamburgian was the excellence in blade production (Clark, 1938) with tool forms including: 'atypical' shouldered points, burins, end scrapers and perforators with a curved prong termed '*Zinken*' (Rust, 1937; Clark, 1938; Burdukiewicz, 1986) (Figure 2.8).

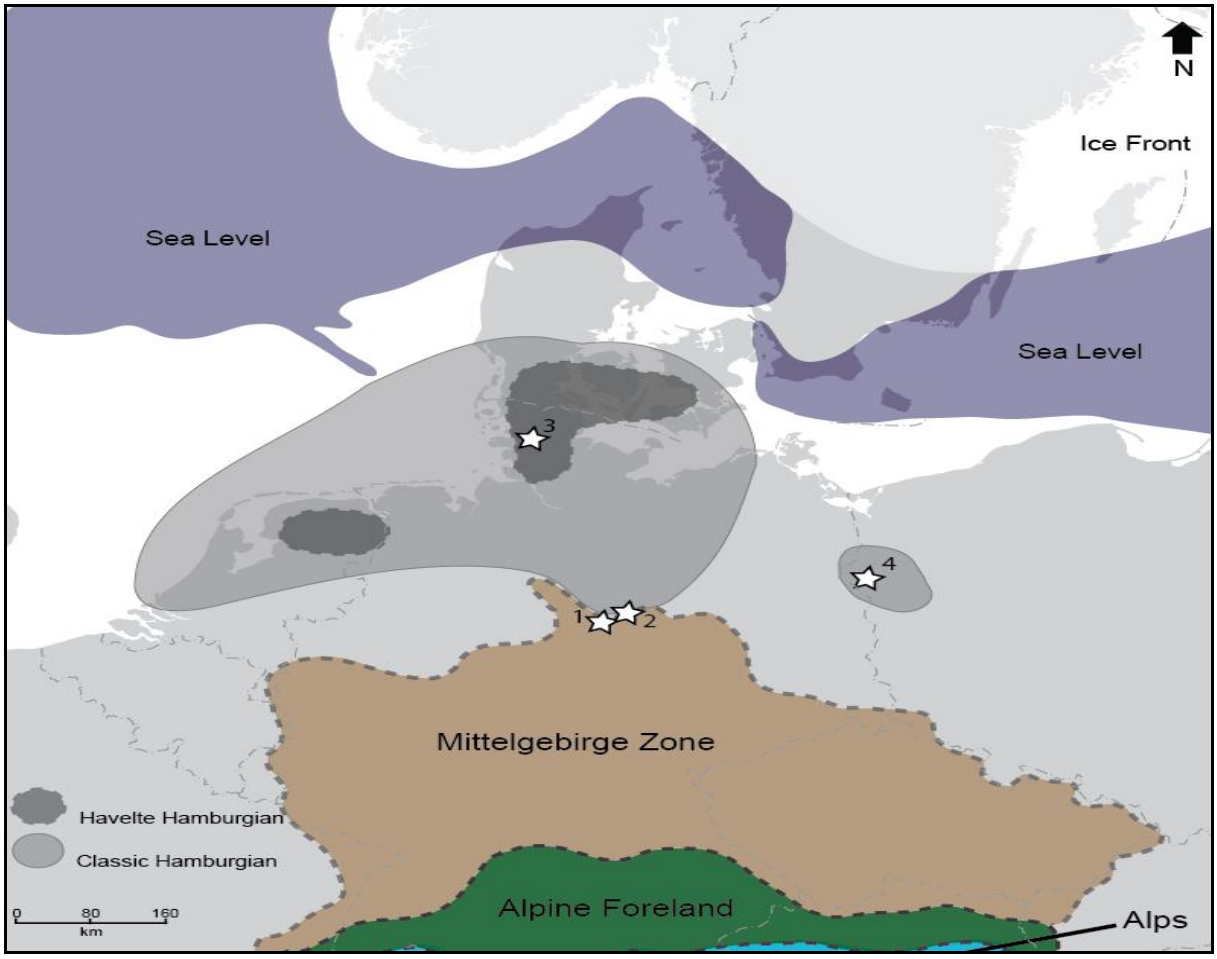


Figure 2.7 – Distribution of the Classic and Havelte Hamburgian technocomplexes during the Bølling and postulated areas of occupation within North and Baltic Sea zones. The relative position of the Fennoscandinavian ice-sheet as well as the palaeocoastline are also shown. Figure adapted from Terbeger, (2006); Grimm and Weber, (2008). Key sites referred to in the text; 1 – Göttingen; 2 – Gadenstedt; 3 – Ahrenshöft; 4 – Mirkowice.

Following numerous attempts to define the Hamburgian into typologically distinct groups (Schwabedissen, 1937; Rust, 1941-42; 1943) Bohmers (1947) sub-divided the Hamburgian into 'Hamburg I' and 'Hamburg II' groups. Today this division is known as the classical Hamburgian group (Hamburg I) and the Havelte group (Hamburg II). Sites associated with the classical Hamburgian are characterised by the presence of shouldered points and by a predominance of *Zinken* over end scrapers and burins (Burdukiewicz, 1986). Havelte Group lithics are also associated with shouldered points but the most distinguishing artefacts are elongate tanged points of the Havelte type (Figure 2.9) and end scrapers predominate over burins and *Zinken* (Burdukiewicz, 1986).

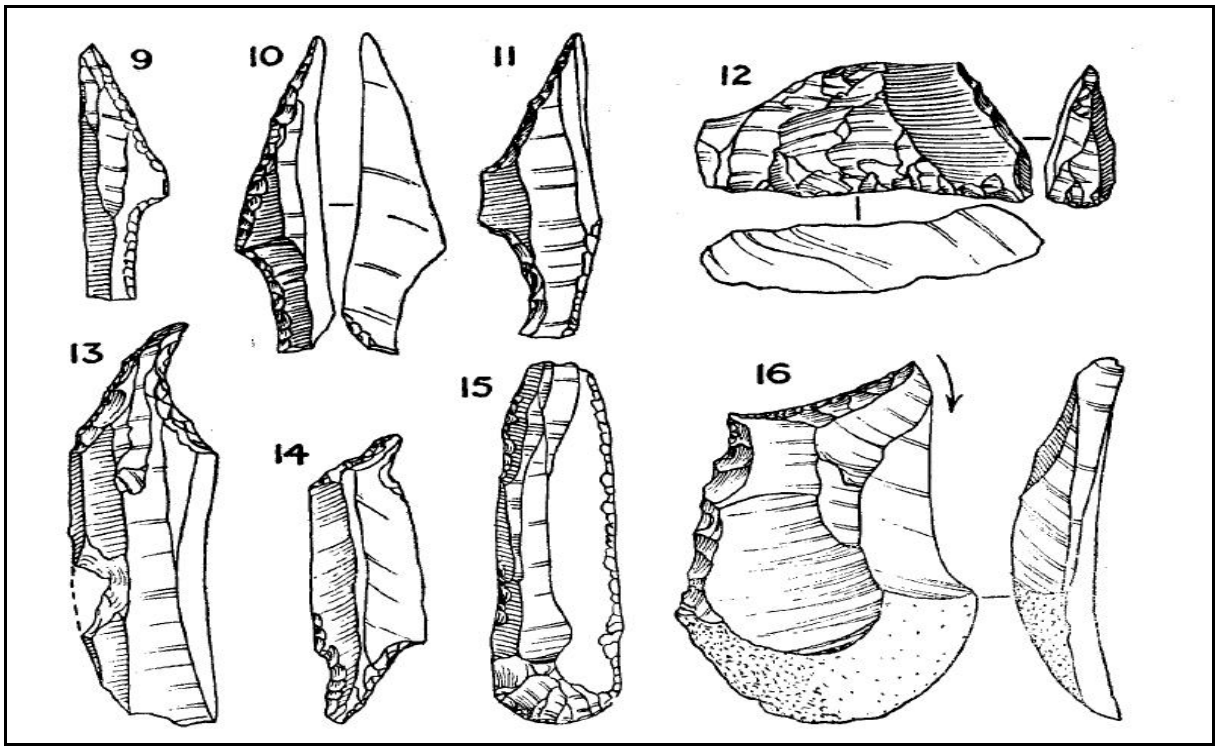


Figure 2.8 – Tools from the classical phase of the Hamburgian technocomplex. 9-11 - shouldered points; 12 and 16 - development of blanks; 13 and 14 - *Zinken*; 15 - backed piece. Items drawn to scale 1:1. (Clark, 1938).

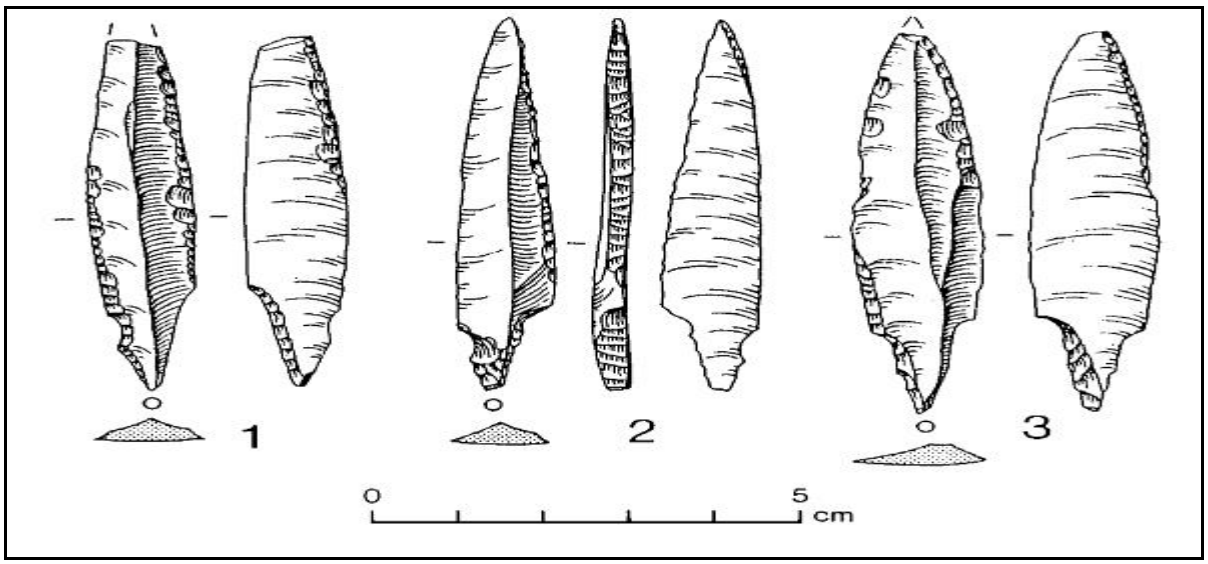


Figure 2.9 – 1-3 - Typical tanged points of the Havelte technocomplex. (Clausen, 1997).

Within the Hamburgian, the relationship between the classic phase and the Havelte Group has been a source of debate for a number of decades (Schwabedissen, 1937; Rust, 1941-42; 1943; Bohmers, 1947; Tromnau, 1975).Typologically the main difference between the classic Hamburgian and the Havelte group lies in the different form of their lithic points; while shouldered points are characteristic of the classic Hamburgian, tanged points dominate the Havelte group (Grimm and Weber, 2008). There are also some subtle differences in blade manufacture (e.g. Hartz, 1987) but a major distinction is in differential distribution of these groups across the NEP. A total of 150 Hamburgian sites (including surface finds and scatters) are so far recognised in the archaeological record (Burdukiewicz, 1986; Eriksen, 1999; Terberger and Lübke, 2004; Bobrowski and Sobkowiak-Tabaka, 2006). The classic Hamburgian is found over most of the NEP from the Netherlands to western Poland, while Havelte Group sites are predominantly distributed along the western margins of the NEP (Grimm and Weber, 2008).To date therefore, the only geographic areas of overlap between the classic Hamburgian and the Havelte Group are located in the Netherlands, southern Denmark and northern Germany (Figure 2.7).

Dating the earliest evidence of the Hamburgian in northern Germany and southern Scandinavia is still a matter of controversy (Terberger *et al*., 2009). Housley *et al* (1997) and later Grimm and Weber (2008) using calibrated radiocarbon dates, argued that humans re-occupied the NEP prior to the onset of the warming associated with the Bølling chronozone. Grimm and Weber (2008) suggest a

weighted mean age of 14,602 ± 326 cal. yr BP (12,390 ± 25 ^{14}C yr BP) for the classic Hamburgian; and 14,232 ± 218 cal yr. BP for the Havelte. Evidence from the site of Ahrenshöft does appear to support a chronological division between the classic Hamburgian and the Havelte. Palynological analysis from Ahrenshöft Site LA73 shows stratigraphic succession from the classic Hamburgian to the Havelte Group (Clausen, 1997). Excavations have shown the association of the classic Hamburgian within the early Meiendorf, prior to the increased temperature rise of the Bølling. The Havelte Group is stratigraphically above *Meiendorf* age sediments, located within Bølling age sediments and firmly associated with a rise in *Hippophaë* (Clausen, 1997; Usinger, 1997).

2.3.2.1 The cause of variation between the classic Hamburgian and Havelte Group

The reasons behind the typological variation of the classic Hamburgian and the Havelte Group are still unclear. Functional, chronological and regional differences have all been postulated (Burdukiewicz, 1987; Bratlund, 1996; Grimm and Weber, 2008). The lack of archaeozoological data associated with the Hamburgian as a whole frustrates any attempt to link tool production with intended function. At present much of our knowledge of the classic Hamburgian comes from sites within the Ahrensburg tunnel valley (Bratlund, 1996). Evidence shows a heavy bias towards reindeer (*Rangifer tarandus*) exploitation (Bratlund, 1996; Street *et al*., 2001) and follows a pattern of classic Hamburgian association with autumn reindeer kills. Conversely, the only known Havelte site with preserved faunal material comes from Slotseng (Kabaciński and Sobkowiak-Tabaka, 2009). Evidence from Slotseng again shows a faunal record dominated by reindeer, with seasonal indicators varying from spring to early winter, broadly comparable with that of classic Hamburgian (Grimm and Weber, 2008; Kabaciński and Sobkowiak-Tabaka, 2009). Conversely, the Hamburgian site of Mirkowice, Poland, has a faunal record dominated by pike (*Esox lucius*) and various cyprinid fish (Kabaciński *et al*., 1999). Arguments as to whether this represents a different local economy, seasonal variation or the result of preservation or sampling techniques are thus far unresolved (Grimm and Weber, 2008). What is clear however is that at least within the German and Danish Hamburgian record, different

prey species or hunting seasons do not appear to be linked to typological variation between the classic Hamburgian and Havelte groups.

There has been some suggestion that the Havelte Group marks a transition to bow and arrow technology within the Hamburgian (Burdukiewicz, 1987; Grimm and Weber, 2008; Kabaciński and Sobkowiak-Tabaka, 2009). Bratlund (1990) analysed faunal remains with projectile lesions from the sites of Meiendorf and Stellmoor, and observed that the injuries were inflicted from a lateral shooting position. However, the projectile delivery system could not be defined. A conservative approach would be to suggest that the Hamburgian as a whole primarily utilised the spear thrower (Bokelmann, 1991) with bow and arrow technology becoming more prevalent with the development of the Federmesser and Ahrensburgian technocomplexes.

2.3.2.2 Hamburgian subsistence strategies

Current research into Hamburgian subsistence strategies on the NEP is dominated by the prevailing view of large mammal exploitation, most notably that of reindeer. Early work by Clark (1938) referred to the Upper Magdalenian and Hamburgian hunter-gatherers as "*the reindeer hunting tribes of northern Europe*" and for many, early hunter-gatherer populations were previously seen as comparable to present day arctic and subarctic reindeer/caribou hunters (Gordon, 1988; Schuler, 1994; Sturdy, 1975; White, 1985). It is well known from the faunal record that reindeer dominated the open scrub environments of the Bølling, best demonstrated at the sites of Meiendorf and Stellmoor, Germany (Krause, 1937; Kabaciński and Sobkowiak-Tabaka, 2009). Such is the dominance of reindeer in the faunal record that the Lateglacial - Holocene transition has, in the past, been referred to as the "age of reindeer" (Weinstock, 2000) and has sparked numerous papers about reindeer exploitation (Bouchud, 1966; Weniger, 1982; Bratlund, 1991; Enloe, 1991; Baales, 1992; Mellars, 1996).

It is presently hypothesised that Hamburgian subsistence strategies were based on seasonal population migrations in response to migrating reindeer herds (Gordon, 1998; Sorensen *et al.,* 2007; Kabaciński and Sobkowiak-Tabaka, 2009). Current research however does not seem to agree on the

preferred season of reindeer exploitation. Research by Sturdy (1975) and Bokelmann (1979) interpret sites within northern Germany as winter camps following reindeer hunts in the autumn. According to this model, reindeer were hunted in autumn as they crossed the river Elbe to the north; surplus or cached meat was utilised during the winter, followed by summer movement into the Netherlands and the now submerged area of the North Sea (Sturdy, 1975; Bokelmann, 1979; 1991; Bratlund, 1990; Bratlund, 1996; Street, 1998). Conversely, Rust (1943) and Tromnau (1976) interpreted these Hamburgian sites as summer camps therefore, implying that northern Germany was the summer destination for migrating reindeer herds before wintering in the south and southwest of Germany. Direction and seasonality of reindeer migration, inferred from shed antlers should, however, not be accepted uncritically. Firstly, the faunal record is too fragmentary to fully support such dynamic reconstructions (Bratlund, 1996). Secondly, archaeological context and interpretation must be considered when developing seasonal migration routes. Shed antlers, used to infer seasonality, are fairly ubiquitous in the archaeological record, making any inference about migration direction hypothetical (Johansen, 2000; Petersen and Johansen, 1993; Petersen, 2006).

The reconstruction of hunting practices for Hamburgian groups is difficult for archaeologists as there is no record of wooden artefacts until the Ahrensburgian (Bratlund, 1996). Undoubtedly Hamburgian and later groups would have utilised wood within hunting practices, however to what degree remains uncertain. The similarity of Hamburgian lithics with central European Magdalenian tools however, may suggest that the same spearthrower technology was used for large mammal hunting (Schwantes, 1932; Street *et al*., 2001), whilst others have suggested the use of the bow and arrow (Bosinski, 1984).

Comparison of archaeozoological data from Meiendorf and Stellmoor allows an examination of the level of social continuity in reindeer hunting practices between Hamburgian and later Ahrensburgian groups (see Rust, 1937; 1943; Möller, 1975; Bratlund, 1990; 1991). Both Hamburgian and Ahrensburgian layers at Meiendorf and Stellmoor indicate that four basic principles were practiced by both sets of hunter-gatherers: reindeer kill, carcass butchery, body part selection and antler storage or disposal. Within these categories however subtle differences exist. Analysis of skeletal remains from both Meiendorf and Stellmoor show differences in the position of wounds inflicted on reindeer by

Hamburgian and Ahrensburgian hunters. Wounds attributed to Hamburgian hunters were all found to be made from the same level as the reindeer from a position to the side or slightly behind the animals. In contrast, wounds attributed to the Ahrensburgian were spread all over the reindeer, from the front, side and behind the animals (Bratlund, 1996). The random pattern of the Ahrensburgian wounds may suggest indiscriminate hunting or 'shooting' of large groups of reindeer as they passed through the site, whereas the Hamburgian hunting pattern may represent a more controlled pattern of stalking smaller groups or single individuals (Bratlund, 1996). The level of intensity in carcass butchery differs widely between Hamburgian and Ahrensburgian groups, as indicated by the frequency of cut-marked bone, with Hamburgian butchery showing a very high percentage of cut-marked bone for all skeletal parts, whereas Ahrensburgian butchery shows low percentages on fewer skeletal parts (Bratlund, 1996). Following work by Grønnow, (1985) it is possible to delineate the differences between Hamburgian and Ahrensburgian butchery. Of the ~130 reindeer carcasses from Meiendorf and Stellmoor attributed to Hamburgian hunter-gatherers, only about 50 individuals were consumed locally, with the remaining individuals butchered and removed to another location. In both cases there is a large emphasis on the meaty parts such as the hind legs and back. In contrast, Ahrensburgian butchery remains show far less emphasis on work-intensive parts of the carcass such as the neck and sacrum, and instead there appears to be a more methodological approach to butchery with fewer cut-marks. Hamburgian reindeer hunts appear to be confined to the Ahrensburgian Tunnel Valley during a brief period in the autumn, with birds and possibly horse exploited during the late summer (Bokelmann, 1991).

As demonstrated by the sites of Meiendorf and Stellmoor, reindeer and large mammal exploitation was undoubtedly an important part of Hamburgian subsistence strategies, not only for food, but in terms of raw material for tool production and shelter construction e.g. hides (Gramsch, 2004). A number of sites throughout the NEP are however shedding light on a more varied foraging strategy. As discussed in sections 1.4 and 1.5.1 (Chapter 1) various sites are associated with small mammals, birds and fish. The sites of Meiendorf and Stellmoor well known for their reindeer assemblages, also contain the remains of hare, fox, wolverine, whooper swan and greylag goose, whilst at Stellmoor, fish may also have been present (Bratlund, 1996). The site of Mirkowice, Poland offers a complete contrast to reindeer dominated sites of the Ahrensburg tunnel valley. The Hamburgian hearth site

located 80 km inside the young moranic zone is completely dominated by fish remains, specifically those of the cyprinid family, pike and perch (Kabaciński *et al*., 1999; Kabaciński and Sobkowiak-Tabaka, 2009). Poggenwisch, northern Germany shows a similar pattern to Mirkowice, with a greater bias towards fish and small mammals as opposed to reindeer (Herre and Requate, 1958; Bratlund, 1996).

Fish remains, unlike reindeer remains, do not preserve any record of how they were caught. We are therefore reliant on a fragmentary archaeological record to determine how Hamburgian hunter-gatherers exploited them. Fish hooks and harpoons are well-known from the Federmesser period as well as the Solutrean and Magdalenian of southwestern Europe (Manne *et al*., 2012). It is reasonable to assume transfer of knowledge within Hamburgian populations of the NEP.

2.3.3 The Federmesser – Population event 5

The transition from the Hamburgian to Federmesser on the NEP is believed to have occurred by 14,016 ± 210 cal yr. BP as indicated by the occurrence of a *Zinken* and a backed point obtained from the Ahrenshöft inventory LA 58 (12,030 ± 60 ^{14}C yr BP; Clausen, 1997). It has been suggested by Terberger (2006) that prior to the appearance of the Federmesser in the northern margins of the NEP a contemporary pan-regional change in technocomplex was already underway. Evidence from Reichwalde, Saxony, shows the emergence of an early Federmesser inventory dated to 14,138 ± 287 cal yr BP (Friedrich *et al*., 2001). The northward spread of the Federmesser can be dated within the region of Dithmarschen, north Germany to 13,697 ± 174 cal yr BP (Terberger, 2006) and to Mecklenburg-Vorpommern, northeast Germany within the same period (Street, 1996; Terberger, 1996; Kaiser *et al*., 1999). The cultural development of the Federmesser within central Europe from the Magdalenian into the Early Mesolithic can be followed with some certainty (Bodu, 1998). At many Federmesser sites, the diagnostic arch-backed point is found in association with very small scrapers, tanged scrapers and different burin forms, thus placing the origins of the Federmesser within a wider central European Late Magdalenian or Early Azilian context (De Bie and Caspar, 2000; Riede and Edinborough, 2012). On a regional scale, the existence of a well attested Federmesser occupation in

southern Scandinavia is limited (Eriksen, 2002; Terberger *et al*., 2009) with the few potential sites still giving unclear ages. This however may be attributed to misidentification and confusion with the Bromme culture of southern Scandinavia. Particularly good evidence of the Federmesser is known from the Netherlands, with clusters of Federmesser sites often located on moranic ridges in close association with kettle holes, for example Een-Schipsloot (Houtsma *et al*., 1981). The spread of the Federmesser is thought to represent the first significant adaption to forested environments (Bratlund, 1996) with the NEP settled up to the Baltic and the southern fringes of southern Scandinavia (Figure 2.11) (Schwabedissen, 1954; Schild, 1984; Fischer, 1988).

The Federmesser technocomplex saw a shift to a simpler blade technology with shorter and irregular blades (Terberger *et al*., 2004) and is believed to show similarities with the more southerly Azilian technocomplex (Stapert and Street, 1997). Steeply backed points and bladelets are a common feature as is the reduction in the quality of raw material (Schwabedissen, 1954; Taute, 1968) (Figure 2.11). It has been suggested that Federmesser backed points were probably used as arrow tips (Bosinski, 1984; Baales, 2002) and that roe deer antler was preferentially used as a raw organic material (Pelegrin, 2000; Fagnart and Coudret, 2000). Bone and antler appears to be widely used in the production of barbed points, harpoons and fish hooks. A previously held interpretation of fishhook and harpoon finds on the NEP was that they were typically Mesolithic (Gramsch, 1973) with no evidence of production in the Late Palaeolithic. More recent research, however, has uncovered these tools in stratigraphic association with Federmesser finds, as for example at Klein Lieskow, northeast Germany, where a fragment of bone fishhook was recovered (Pasda, 2001). Another example is at the site of Wustermark near Berlin, where six bone fish hooks are pre-Mesolithic and can be correlated, based upon pollen assemblages, to before the onset of the Younger Dryas (Beran, 2001; Gramsch *et al*., 2013). There is even greater evidence of fish hook production within other areas of Europe; the sites of Pont d'Ambon and Bois-Ragot in southwesten France attributed to the Azilian, have produced a total of four fishhooks (Chollet *et al*., 1980), while the site of Zigeunerhöhle in Austria, has produced one fish hook in association with a backed point/Federmesser complex (Pittioni, 1955). Aside from fish hooks, 'leister prongs' are perhaps the most ubiquitous of the Late Palaeolithic finds attributed to fishing practices. "Type-2-Duvensee" prongs appear during the Federmesser period, and although closer to the harpoon/point tradition, may represent a unique

development with no precedent in the Magdalenian (Cziesla, 2004). However, a clear evolution can be seen in other tool forms from the Late Magdalenian and Federmesser forms. Clark (1936) recognised that harpoons ("Havelte-type 12a and 12b) became larger and more gracile with the transition from the Magdalenian to the Federmesser, and biserial barbed harpoons become very rare in Federmesser assemblages (Cziesla, 2004). Firstly, double pointed gorges of the Magdalenian seem to have been replaced by more finely produced fish hooks during the Federmesser. There is also evidence from bone and antler harpoons from the North Sea and areas of East Anglia dating to the Allerød chronozone The famous point from the "Leman and Ower Bank" in the North Sea was trawled up in 1932 off the Norfolk coast (Evans, 1932; Godwin and Godwin, 1933) was later AMS dated to give an age range of 13,890 – 13,295 cal yr BP (Smith, 1992). Secondly, finds from "Devils Wood Pit" in Ipswich yielded two notched points dated to 13,472 – 13,200 cal yr BP (11,485 ± 60 ^{14}C yr BP) and 13,063 – 12,654 cal yr BP (10,960 ± 50 ^{14}C yr BP) (Jacobi *et al*., 2009). While lastly, a point recovered from Dümmer See near Osnabrück, Germany gives an age of 13,480 – 12,065 cal yr BP (Veil *et al*., 1991). The greatest concentration of Type-2-Duvensee prongs are found in the area known as Havelland, northwest of Berlin, Germany and on the northwestern margins of the NEP in the Mecklenburg-Vorpommern region (see Cziesla, 2000; 2001; 2004). Type-2-Duvensee prongs have also often been found in stratigraphical association with some of the larger, gracile biserially barbed harpoon forms (Figure 2.12).

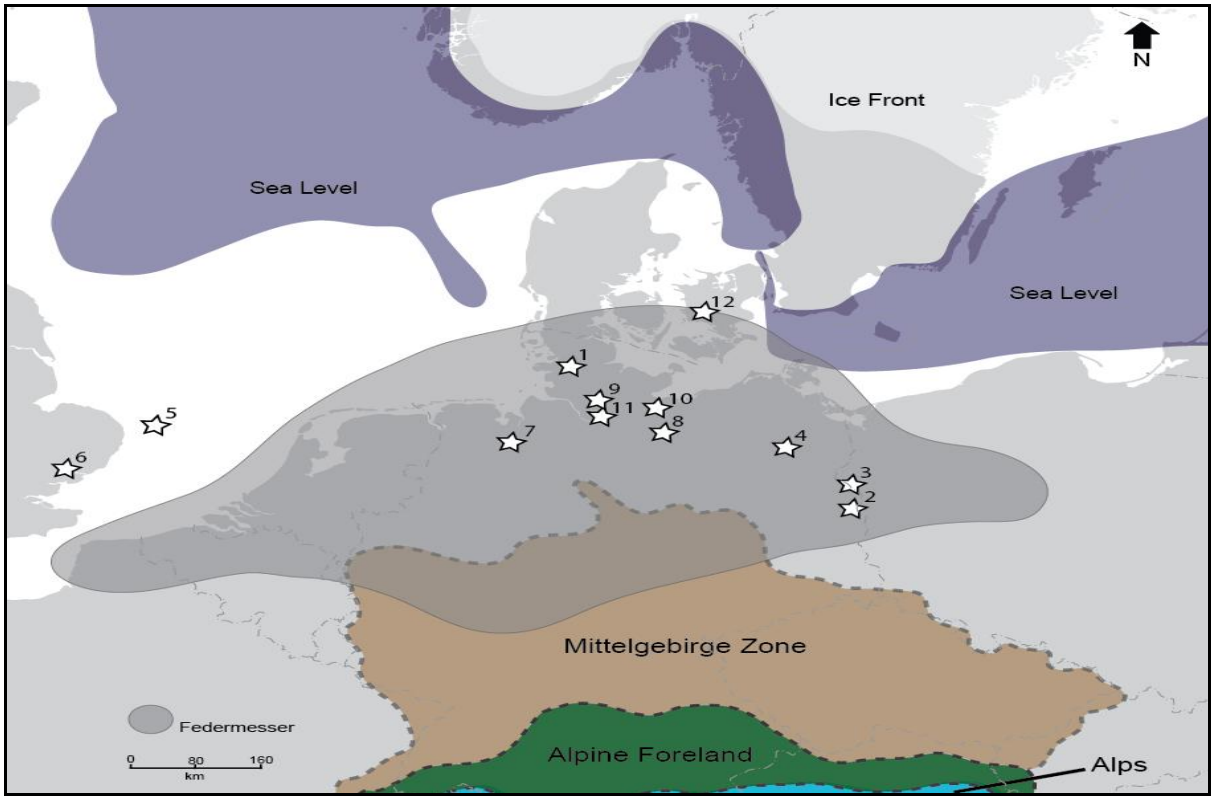


Figure 2.10 – Distribution of the Federmesser technocomplex during the Allerød within the NEP and postulated areas of occupation within North and Baltic Sea zones. The relative positions of the Fennoscandinavian ice-sheet and palaeocoastlines are also shown. Figure adapted from Terberger, (2006); Grimm and Weber, (2008). Key sites referred to in the text; 1 – Ahrenshöft; 2 – Reichwalde; 3 – Klein Lieskow; 4 – Wustermark; 5 – Leman and Ower Bank; 6 – Devils Wood Pit; 7 – Osnabrück; 8 – Weitsche; 9 – Klein Nordende; 10 – Lüdersdorf; 11 – Stellmoor; 12 – Bromme.

An important aspect of Federmesser groups on the NEP concerns the exploitation of amber, best demonstrated at the site of Weitsche, Germany (Veil and Breest, 2000). The site, located on a sandy ridge next to several palaeochannels (Veil and Breest, 2000) has produced numerous worked pieces of amber, including beads and an 8.2 cm elk (*Alces alces*) sculpture (Veil and Breest, 1995; Terberger, 2006).

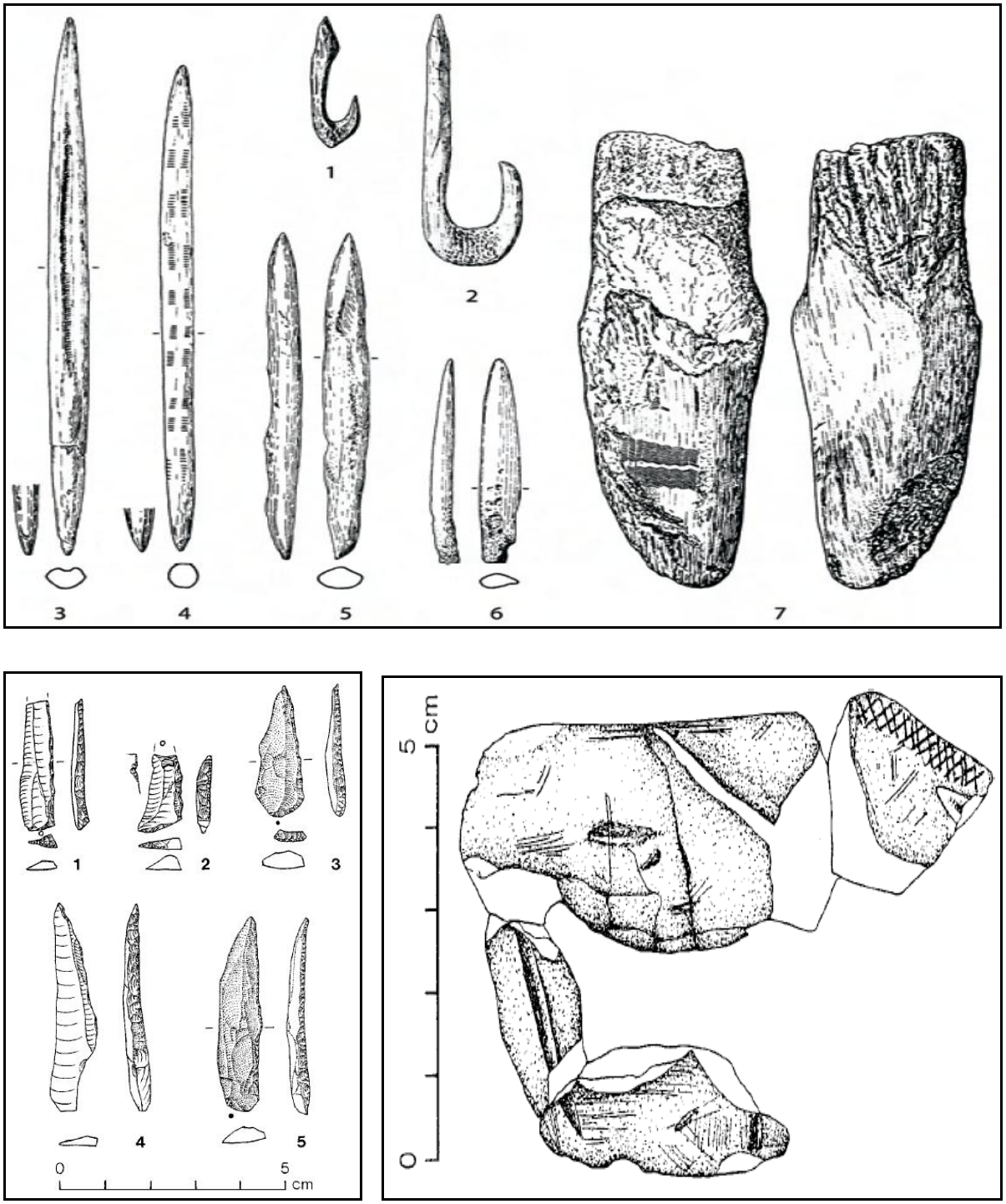


Figure 2.11 – Tools and artefacts from the Federmesser technocomplex. Top: 1-2 - fishooks from Wustermark (Beran, 2001); 3-6 - bone points; 7 - elk antler axe (Terberger, 2006). Bottom left: 1-3 - backed points of Federmesser tradition; 1, 4 and 5 - backed points with basal retouch (Waldmann *et al*., 2001). Bottom right: refitted amber figurine from Weitsche (Veil and Breest, 1995; Terberger and Ansorge, 2000).

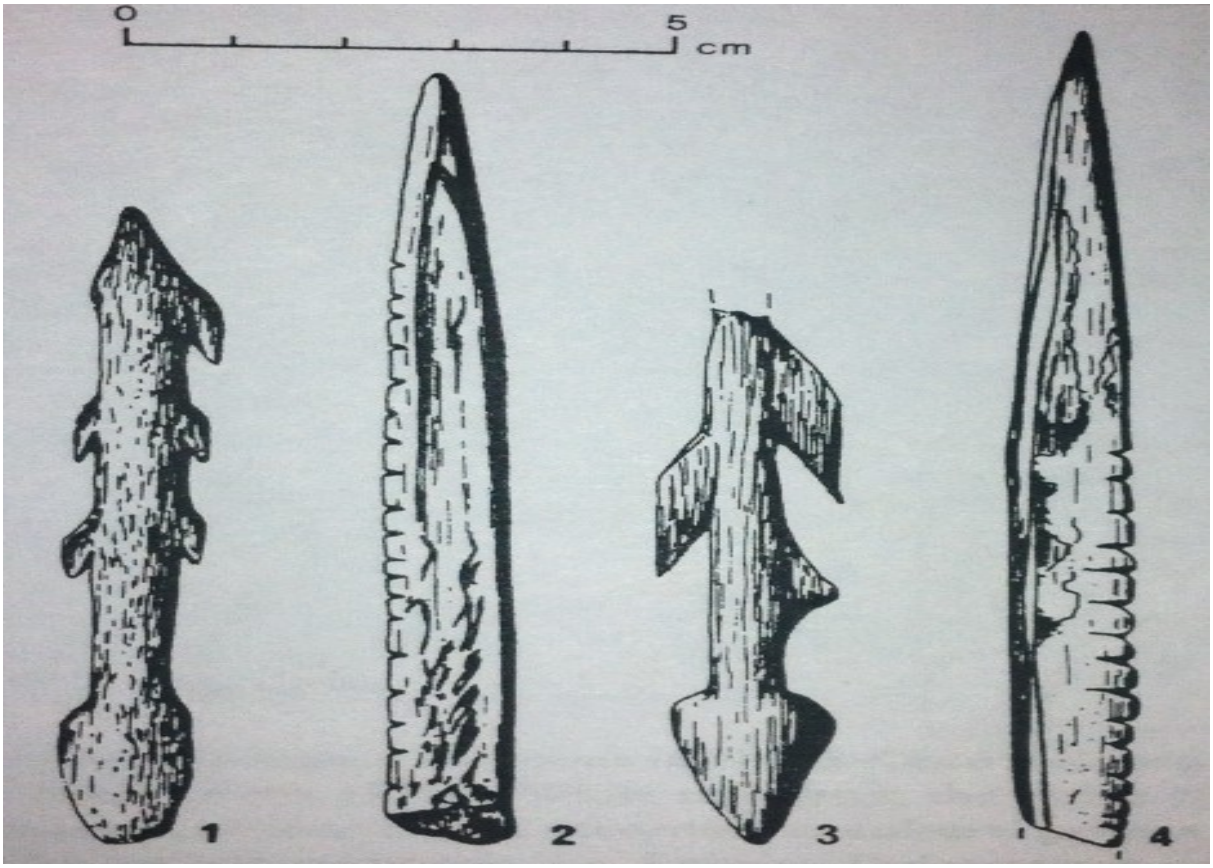


Figure 2.12 – Points from the site of Bützee. 1 – Biserially barbed harpoon; 2 – Leiester of "Type-2-Duvensee" form; 3 – Biserially barbed harpoon; 4 – Leiester of "Type-2-Duvensee" form. Adapted from Cziesla (2004).

2.3.3.1 Federmesser subsistence strategies

The transition to the Federmesser witnessed a shift away from the reindeer dominated economies of the Hamburgian towards one more dependent on forest adapted species such as elk. Unfortunately the faunal evidence for the Allerød is rather sparse making inferences about actual hunting practices difficult, with direct evidence of hunting practices revealed by skeletal remains not available during the Federmesser. On the other hand, evidence of bone blanks produced from an elk metapodials from the site of Klein Nordende, Germany and worked antler from the site of Lüdersdorf also in Germany, both indicate the use of organic raw materials (Bokelmann *et al.,* 1983; Bratlund *et al*., 1993; Hedges *et al*., 1993) but give very little evidence of hunting strategy. Analysis of Federmesser lithics can however give some indication as to the method of the weapon delivery system. The ABP of the

Federmesser has long been seen as an industry adapted for the use in bow and arrow, and spear thrower technology (Mace, 1959; Barton, 1992; Breest, 1999; Bagniewski, 1999; Gerken, 2001). The Federmesser shows a bi-modal distribution in its lithic modes, with the subsidiary mode composed of large tanged points which have been identified as dart points through discriminant analysis (see Riede, 2008). The parallel use of hunting systems is evident within modern ethnographical studies (see Churchill, 1993) and may suggest local adaption to varying resources. Spearthrower technology offers a far higher impact potential than the bow and arrow and as such may have been more suited for hunting larger cervids in open conditions at the borders of the emerging forests on the NEP (Bokelmann, 1978; Churchill, 1993; Baugh, 1998). Bow and arrow technology would have been more useful in the confines of forested areas (with the reduced impact potential of bow and arrow technology mitigated by greater cover afforded by the forests) allowing hunters to get closer to their prey.

A number of recent excavations of Federmesser sites throughout northern Europe have been conducted at a suitable level to allow the recovery of fish remains. Based upon the ichthyofaunal remains from 50 sites, it has been possible to track the development of fish species composition. What this record shows is a dramatic difference in species from the Late Magdalenian to the Federmesser. Late Magdalenian sites (none present on the NEP, see section 2.1.3) show that fish populations were dominated by grayling (*Thymallus thymallus*), burbot (*Lota lota*), trout (*Salmo trutta*) and huchen (*Hucho hucho*). Analysis of habitat tolerance of these species suggests that they come from cold and clear water bodies with high oxygen levels (Böhme, 1997), consistent with river and lake conditions in northern Europe during the early Interstadial (see Torke, 1998). The transition to the Allerød marks a dramatic shift in fish composition. Evidence from southern fringes and also from three sites (Klein-Nordende, Germany; Stellmoor, Germany; Bromme, Denmark) in the northern margins of the NEP show that pike made up 75 % of the fish remains, followed by chub (*Leuciscus cephalus*), perch and grayling (Cziesla, 2004). The presence of pike, chub and perch indicate still or slow moving water, with high nutrient levels (Böhme, 1997).

The large scale modification in fishing equipment between Magdalenian and Federmesser technocomplexes may therefore have been prompted by the dramatic shift in fish species present

throughout northern Europe and the NEP. Interestingly the stability of fish species composition between the Allerød and Pre-Boreal (particularly amongst pike) is matched by an almost unbroken tradition of fish hooks and leister points from the Federmesser to the Mesolithic (Cziesla, 2004). It can be postulated therefore, that during the Federmesser, line fishing with hooks and stick fishing with harpoons and prongs, became more prevalent, with a shift towards the exploitation of freshwater (and marine) resources.

2.3.4 The Bromme – Population event 5

The Bromme technocomplex is the oldest variant of the tanged point group (TPG) and is recognised from a relatively restricted area in northerly reaches of the NEP within the young morainic zone (Clausen, 2004; Figure 2.13). The Bromme technocomplex was first recognised in Scandinavia, when in 1912 a large tanged point was discovered at the site of Nørre Lyngby, Denmark (Jessen and Nordmann, 1915). Further finds became known throughout northern Germany and Denmark (e.g. Rust, 1938) collectively becoming known as the 'Lyngby culture'. Subsequent excavation at the site of Bromme, Denmark (Figure 2.13) uncovered the first settlement site attributed to the Lyngby culture (Mathiassen, 1946). Recent AMS dating of an elk vertebrae from the site of Bromme gives an age of 12,861 – 12,431 cal yr BP (10,720 ± 90 ^{14}C yr BP; Riede and Edinborough, 2012). These finds were initially interpreted as an earlier stage of the Lyngby culture, however today no such division is upheld, with the term 'Bromme' the favoured cultural classification (Riede and Edinborough, 2012) The Bromme is defined by comparatively simply technology when compared with the Federmesser (Barton, 1992). Tool preparation is characterised by the preparation of cores with either big with broad, conical or sub-cylindrical shapes, usually with only a single striking platform (Madsen, 1996). Distinctive bulbs on the flint debitage indicate that blades and flakes were produced by direct hard hammer percussion (Burdukiewicz, 2011). Typically, Bromme assemblages are composed of large (up to 12 cm long) tanged points, end scrapers and burins with rarer examples of retouched pieces and perforators (Madsen, 1996; Burdukiewicz, 2011). In contrast Bromme assemblages in southerly parts of its distribution are often associated with curved back points and scrapers with lateral retouch more characteristic of the Federmesser (Taute, 1968; Burdukiewicz, 2011).

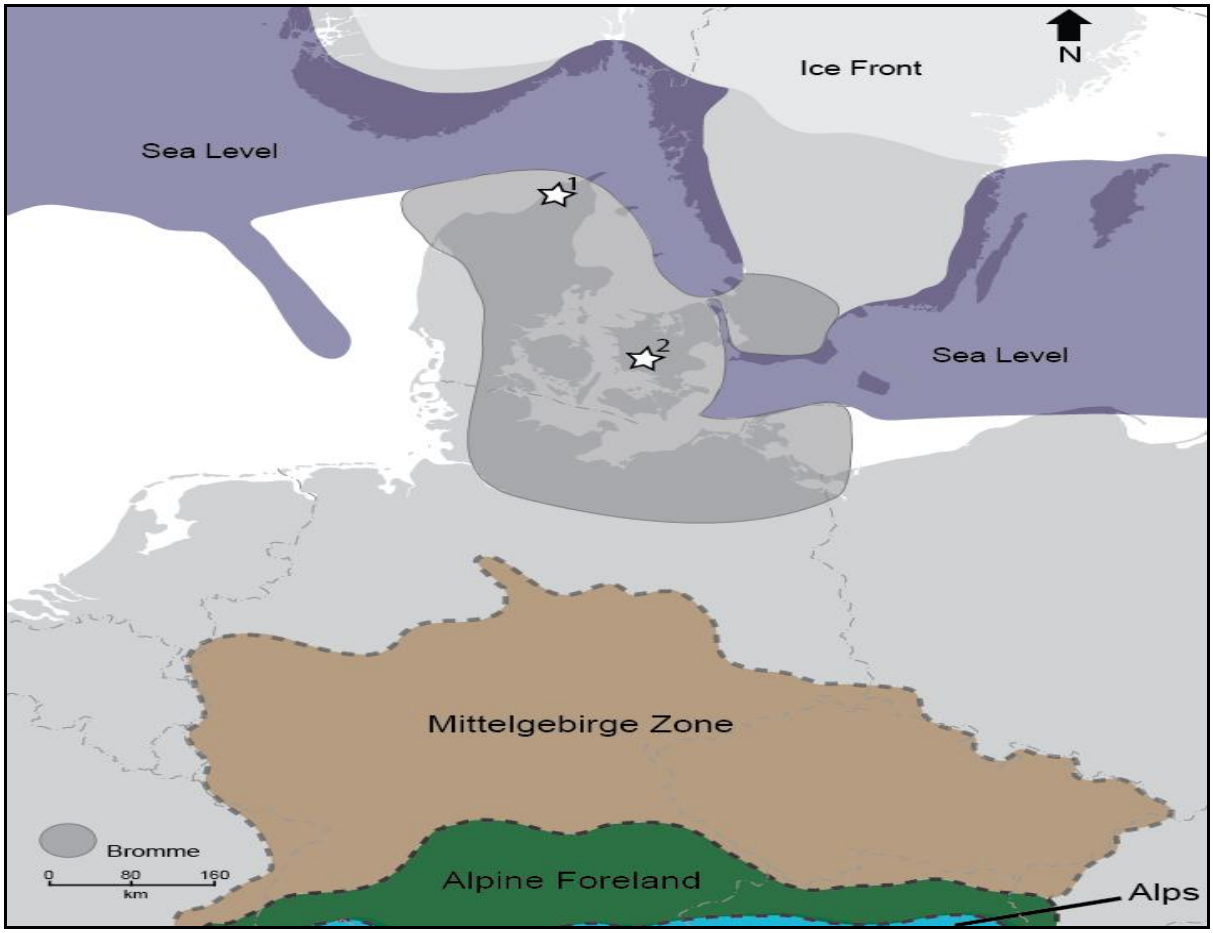


Figure 2.13 – Distribution of the Bromme technocomplex during the Allerød within the NEP and postulated areas of occupation within North and Baltic Sea zones. The relative position of the Fennoscandinavian ice-sheet as well as the palaeocoastline are also shown. Figure adapted from Terberger, (2006); Grimm and Weber, (2008). Key sites referred to in the text; 1 – Nørre Lyngby; 2 – Bromme.

The distribution of Bromme sites within the NEP is patchy, with the majority of finds coming from northern Germany and Denmark; 75 settlement sites alone are known from Denmark (Eriksen, 1999). It has been suggested (see Schild, 1984; Bratlund, 1996) that Bromme hunter-gatherers preferred open areas or those of light woodland associated with the young morainic zone and that this zone acted as a causeway between Bromme populations in the east and west. Reliable dating of the Bromme has proved difficult due to the relative paucity of sites with organic material. As discussed in section 2.1.5; it has been postulated that the Bromme emerged within the northern reaches of the NEP during the Allerød before disappearing by the early Younger Dryas (Fischer, 1991; Ikinger, 1998;

Eriksen, 2002). More recent research suggests however that the Bromme may in fact have only emerged during the terminal phases of the Allerød and that it was short-lived archaeological phenomenon on the NEP (Riede, 2008).

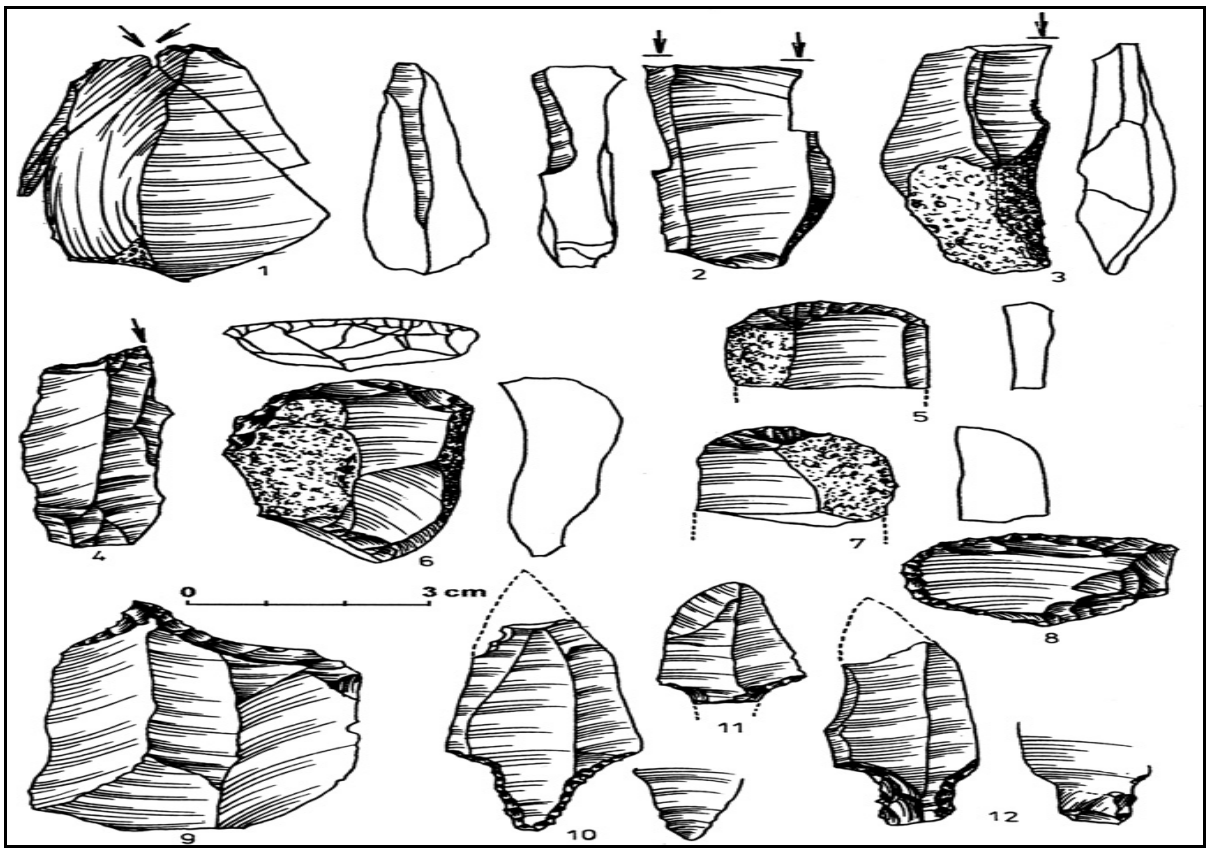


Figure 2.14 – Tools from the Bromme technocomplex. 1-4 - burins; 5-8 - end scrapers; 9 - perforator; 10-12 – Bromme tanged points (Schild, 1975).

2.3.4.1 Bromme subsistence strategies

As with the Federmesser, the lack of Bromme lithic assemblages with associated faunal remains makes it difficult to elucidate hunting practices. It has been suggested that the Bromme represents the loss of bow and arrow technology and a return to simpler spearthrower technology (Riede, 2008) with the large tanged points of the Bromme certainly more suited for delivery by spearthrower. As we have seen, Bromme sites are often associated with open areas or those composed of light woodland, and within Denmark especially, lakes (Eriksen, 2002). The restriction of the Bromme to open areas and the use of large tanged points seems to suggest that larger cervids, e.g. elk, were hunted using

spearthrowing technology. However, the relationship of the Bromme with lakes in the northern margins of the NEP may suggest fishing as another subsistence strategy. A number of uniserialy and biserially barbed harpoons are known from Denmark, with association to Federmesser technologies (Cziesla, 2004). These finds may however relate to Bromme artefacts, due to close technological similarity, and thus may be wrongly represented as a northern variant of Federmesser technologies. Unfortunately it is impossible to robustly reconstruct hunting strategies of the Bromme based on the available evidence, what is apparent however, is the close overlap of Bromme sites with ecozone boundaries suggesting a culture dependent on open habitats or available lake systems (Bokelmann, 1978).

2.3.5 The Ahrensburgian – Population event 6

The Ahrensburgian was first distinguished by Schwantes (1932) in the Ahrensburg Tunnel valley and represents the western variant of the Tanged Point Group TPG (*Stielspitzen-Gruppen*) as defined by Taute (1968). The technocomplex follows on from the Bromme in the continuation of the TPG tradition, and is characterised by a well-made laminar technology produced from single or opposed platform cores (Figure 2.15). End scrapers form the most numerous tool group in the Ahrensburgian, and are either found as long or short scrapers with transverse, rounded retouched ends (Burdukiewicz, 2011). Burins are also found within the Ahrensburgian, as are small truncations called ‘Zonhoven’ points which are found within younger Ahrensburgian assemblages (Taute, 1968). The most diagnostic tools within the Ahrensburgian are however tanged points (7 - 9; Figure 2.15). Smaller than Bromme points, they have a distinctive tang on either the distal or proximal end and are retouched on the dorsal face of the blade (Burdukiewicz, 2011).

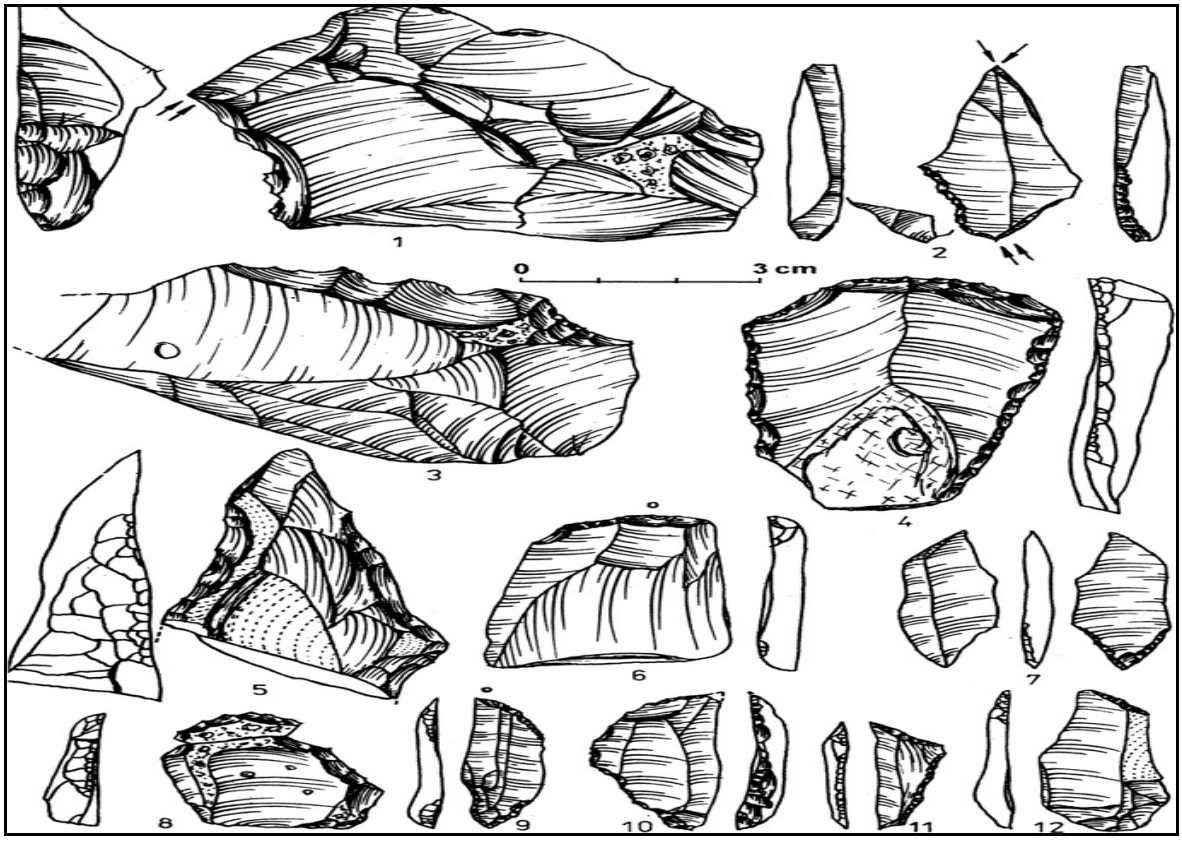


Figure 2.15 – Tools from the Ahrensburgian technocomplex. 1-3 - burins; 4, 6 and 8 - end scrapers; 5 and 10 - side scraper; 7 and 9 - tanged points; 11 - geometric microlith; 12 - truncation (Burdukiewicz, 1989)

The small tanged points have been interpreted as arrowheads, exemplified by wooden arrow shafts (unfortunately now destroyed) from the Ahrensburgian horizon at Stellmoor (Rust, 1943; Bokelmann, 1991). Supporting evidence for this bow and arrow technology during the Younger Dryas comes from channelled shaft smoothers, impact scars on tanged points and possible adhesive residues found on a single Ahrensburgian point from Stellmoor (Bokelmann, 1999). Otherwise organic finds are rare within the Ahrensburgian group. Bone and ivory fishhooks and harpoons are occasionally found in such assemblages (Hanik and Jahns, 2010), as are Lyngby (antler) axes (Clausen, 2004). The Ahrensburgian shows some continuity with the Federmesser, with Type-2-Duvensee prongs found in association with Ahrensburgian or late Allerød assemblages (Cziesla, 2004). Ahrensburgian harpoons record the dramatic evolution in size from their Magdalenian predecessors. The longest complete Magdalenian harpoon comes from Kesserloch Cave, Switzerland and has a total length of 15.6 cm

(Julien, 1982) whilst the younger Ahrensburgian equivalents have been known to exceed 25 cm in length (Cziesla, 2004).

The geographic distribution of the Ahrensburgian across the NEP is confined to Belgium and the Netherlands in the west, the river Oder in the east, and as far north as Zealand in Denmark (Petersen and Johansen, 1993; Pedersen, 2009; Figure 2.16). Small tanged points from Avington VI, Berkshire, confirm a presence of the Ahrensburgian type industries to the west of the NEP and well into Britain (Barton and Froom, 1986; Froom, 2005). Currently there are approximately 300 sites attributed to the Ahrensburgian across the NEP, with the earliest appearance occurring just prior to the onset of the Younger Dryas (Burdukiewicz, 2011).

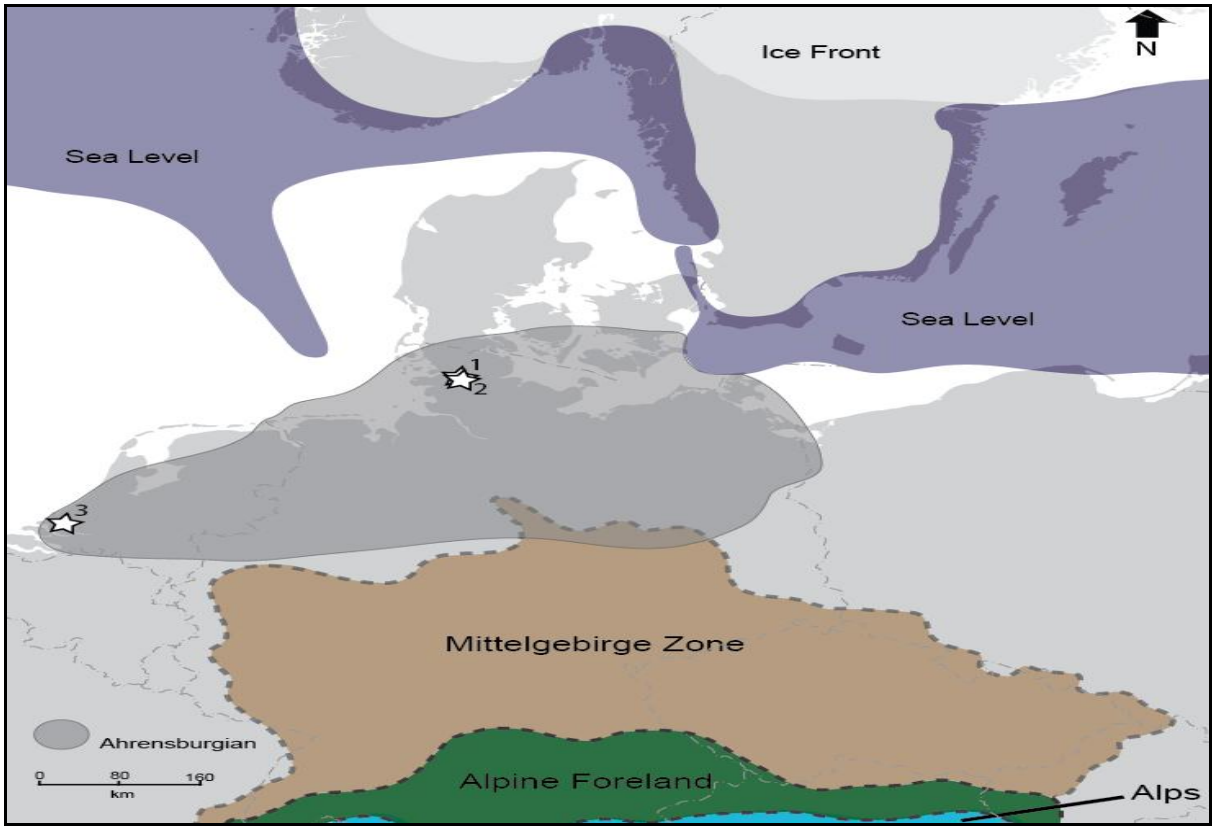


Figure 2.16 – Distribution of the Ahrensburgian technocomplex during the Younger Dryas within the NEP and postulated areas of occupation within North and Baltic Sea zones. The relative position of the Fennoscandinavian ice-sheet as well as the palaeocoastline are also shown. Figure adapted from Terbeger, (2006); Grimm and Weber, (2008). Key sites referred to in the text; 1 – Stellmoor; 2 – Meiendorf; 3 – Europoort.

2.3.5.1 Ahrensburgian subsistence strategies

Like the Hamburgian of the Bølling, the Ahrensburgian of the Younger Dryas has previously been regarded as synonymous with reindeer hunting in an open landscape. The Ahrensburgian however clearly shows a different rationale to large mammal exploitation, primarily utilising bow and arrow technology. Excavations of Ahrensburgian layers at Stellmoor uncovered arrows made of pine wood with flint tips. The arrows, with a foreshaft 20 cm long, can be considered specialized, highly developed and adaptive weapons (Bratlund, 1996). Due to the time and skill needed to craft such implements, they are likely to have been a major part of the Ahrensburgian hunting kit. To date no indisputable bow fragments have been found within the NEP, however the wounds on reindeer remains from Stellmoor indicate bows with sufficient power to bring down or disable reindeer (Bratlund, 1990; 1991). The excavations at Stellmoor and Meiendorf indicate that with the opening of the landscape, the Ahrensburgian Tunnel Valley again became an important strategic area for reindeer hunting. The reconstruction of butchery practices from the reindeer remains indicates massive, indiscriminate hunting drives, with only selective parts of the reindeer removed as opposed to the more whole-sale butchery experienced in the Hamburgian. Unlike the Hamburgian, Ahrensburgian groups appear to have spent more of the year hunting reindeer, largely made possible by the colder conditions of the Younger Dryas. Faunal analysis from the Ahrensburgian Tunnel Valley indicates that reindeer were taken possibly in the spring, late summer and autumn (Bratlund, 1996). What is also apparent is a heavy bias towards raw material procurement, with the incomplete butchery of carcasses based around the removal of skins, antlers and back sinew (Bratlund, 1996) with work by Grønnow (1985) further suggesting that Ahrensburgian hunters discarded lean animals during autumn hunts after the removal of raw materials.

As with the preceding Federmesser and Bromme technocomplexes, the Ahrensburgian shows evidence that fishing was practiced during the Younger Dryas. A notched point with a date of 11,957 – 11,187 cal yr BP from the Europoort, Netherlands (Verhart, 1988) indicates the survival of bone and antler harpoons, prongs and points well into the late Younger Dryas. The ichthyofaunal record suggests that the Ahrensburgian period is associated with pike, perch and grayling (Cziesla, 2004). This continuity within the ichthyofaunal record is matched by very little modification of fishing tools,

with the form of Type-2-Duvensee prongs as well as biserial harpoon points remaining relatively constant.

2.4 Chapter summary

The onset of warming associated with the termination of the LGM served to expedite the re-occupation of central Europe. By the later stages of the Oldest Dryas, Magdalenian populations had expanded out of southwesterly pockets of refugia into southern and central areas of Europe. ^{14}C dates from northern areas of the NEP appear to confirm that hunter-gatherers associated with population event 4 had moved back onto the NEP prior to the prominent temperature rise associated with the Bølling. The population history of the NEP is characterised by the ebb and flow of technocomplexes, with the population event 5 associated with either a second population dispersal from the southwest or independent autochthonous development amongst resident groups. The role of rapid climatic amelioration cannot be discounted in aiding the movement of hunter-gatherer groups into more northerly latitudes, however as highlighted within section 2.2.1 other 'local' factors may have played a part in the final settlement of the NEP.

The archaeological history of the NEP during the Lateglacial is characterised by a rapid changes in tool form either becoming more complex and advanced or in the case of the Bromme, regressing into more basic tool forms. Faunal remains from the Ahrensburgian Tunnel Valley appear to indicate a close correlation between prevailing environmental conditions and prey selection. As indicated within Chapter 1, reindeer dominate the open environments of the Bølling and Younger Dryas, and as such they appear to have been the dominant prey item for Hamburgian and Ahrensburgian hunters. Our knowledge of the subsistence strategies of the Allerød is hampered by the lack of reliably dated faunal and archaeological sites from this period; the few sites from this period however suggest elk were exploited by Federmesser and Bromme groups. While there is an undoubted heavy exploitation of large mammals during the Lateglacial period, the presence of bone and ivory (see Gramsch *et al*., 2013) fishing equipment dated to at least the Federmesser, and fish remains associated with a Hamburgian settlement site, indicates that aquatic exploitation was practiced during this time. The uniformity in fishing equipment production and form within the NEP suggests that aquatic exploitation was a consistent feature of Lateglacial subsistence strategies.

Chapter 3: Understanding aquatic exploitation during the Lateglacial

The following chapter will address the potential contribution of aquatic exploitation in Lateglacial hunter-gatherering societies from archaeological, palaeoenvironmental and ethnographic standpoints. The archaeological record indicates that aquatic exploitation and fishing regularly occurred from as early as the Middle-Upper Palaeolithic in Europe. However, due the paucity of archaeozoological remains relating to this aspect of hunter-gatherer subsistence, it is difficult to gauge the extent to which this may have contributed to overall subsistence strategies during the Lateglacial. Thus, it is therefore first necessary to understand the basis of aquatic exploitation in the context of the NEP. The ethnographic study of modern hunter-gatherer groups allows a better understanding of the situations in which aquatic exploitation would have been more advantageous than solely hunting large mammals. Secondly, it is necessary to reconstruct the aquatic environments in palaeoenvironmental terms. By studying how these systems evolved during the Lateglacial we are better able to develop our understanding about the level to which these systems could have contributed to hunter-gatherer subsistence patterns. Chapter 3 will continue with the development of a model of aquatic exploitation for the NEP during the Lateglacial, and how this can be tested using the proxies used by this thesis. The chapter will conclude by introducing the sites studied within this thesis.

3.1 Understanding the basis of aquatic exploitation

The aim of this thesis is to better understand the aquatic environment of the NEP during the Lateglacial period. The archaeological record indicates that fishing and other methods of aquatic exploitation formed part of hunter-gatherer subsistence strategies during the Lateglacial. The importance of fishing to Lateglacial hunter-gatherers is evident from the time invested in the production of fish hooks, prongs, harpoons and points. It is also interesting to note, that while stone tool forms changed and evolved during the Lateglacial, fishing equipment appears to have stayed the same and was largely unaffected by the various climatic and environment transitions that characterise this period. This level of continuity requires the temporal and spatial transfer of knowledge through successive generations, which is suggestive of a highly valued social and economic trait.

If we are to understand the role aquatic exploitation played in hunter-gatherer existence on the NEP, we must firstly understand the basis on which aquatic systems developed. This thesis aims to characterise the development of aquatic systems within the northern-most reaches of NEP, an area where numerous fishing implements have been recovered. It is well known that Middle-Upper Palaeolithic groups regularly exploited aquatic resources within southwestern areas of Europe (see Pokines and Krupa, 1997; Richards and Trinkaus, 2009). The tradition of aquatic exploitation appears consistently within European hunter-gather groups from this period until the emergence of farming (see Zvelebil and Rowley-Conwy, 1984; Bogucki, 1996). The sheer wealth of fishing implements found in the NEP Lateglacial, has led some to refer to these people as "hunters, gatherers and fishers" (Cziesla, 2004). The addition of 'fisher' to 'hunter-gatherer' in a number of permutations e.g. fisher, gatherer and hunter or hunter, fisher and gatherer; underlies however some of the uncertainty over the importance of the role of aquatic systems or the variability in their use (Bailey and Milner, 2003). Unfortunately the contribution of aquatic exploitation in European hunter-gatherer societies was for a long time influenced by Charles Darwin's disparaging descriptions of the Indian tribes of Tierra del Fuego and their primitive use of marine resources (Darwin, 1839). By the mid 20th century, and with the wealth of Upper Palaeolithic and Mesolithic finds coming out of northern Europe including the NEP, many authors suggested the association of hunter-gatherer groups with aquatic resources was evidence of a transition into an inferior stage of development and was indicative of a "low level of culture" (Clark, 1952; Wheeler, 1954; Evans, 1969). New excavations and archaeological research in the NEP at sites such as Mirkowice, Poland (section 2.3.2.1) focuses our attention on a developed method of subsistence in area that at the time would have presented challenges to hunter-gatherer groups. This contrasts markedly with previous interpretations of aquatic exploitation during the last stages of the Upper Palaeolithic as interpreted by mid 20th century authors. If we refer back to a quote from Chapter 2:

"*a society with a subsistence strategy based solely upon hunting and gathering, will only exploit a region to the degree made possible by the natural preconditions reflected in the biostratigraphical record of climate, flora and fauna*" (Eriksen, 2002).

It is possible to view aquatic exploitation therefore as an adaptive response to the environmental and ecological stresses placed upon Lateglacial hunter-gatherers. Diachronic variations in tool form and production, subsistence patterns and other adaptive traits are most commonly explained as cultural developments (Gamble, 1982). The consistency in bone and ivory fishing equipment from the Magdalenian through to the Mesolithic may therefore be suggestive of a consistent cultural thread spanning Lateglacial hunter-gatherer groups.

If we accept the archaeological evidence of a fishing culture in the Lateglacial of the NEP, then we must also look at the economic benefit it would have provided. The little we know of the seasonal exploitation of game during the Lateglacial comes from the Hamburgian and Ahrensburgian, while Federmesser and Bromme groups are argued to have less pronounced seasonality in their hunting practices caused by a shift away from reindeer based subsistence strategies. By focussing on Hamburgian and Ahrensburgian groups it is however possible to infer possible situations, that are applicable also to Federmesser and Bromme groups, when fishing would be highly beneficial. While seasonality patterns in the Hamburgian and Ahrensburgian differed, what is clear is that reindeer hunting would not have been a prime activity all year round. This raises a key point. At present there is no conclusive evidence of the use of storage pits on the NEP. It has been suggested that some of the Stellmoor and Meiendorf assemblages represent cached meat (Bratlund, 1996) while the drying of meat has also been proposed (Grønnow, 1985), however in both cases there is no definitive evidence of such practices. If reindeer hunting was seasonally limited, could aquatic exploitation and fishing have been utilised in the months reindeer was not hunted? Consequently, aquatic exploitation may have been used as a supplementary food base during periods of food stress (Straus, 1991). With the more mosaic type environment of the Allerød and subsequent local variability in food resources, this adaption is equally applicable to Federmesser and Bromme groups.

The complexity in subsistence strategies and in particular aquatic exploitation, present within the NEP Lateglacial requires a ‘bottom-up’ approach to their interpretation. The basis for aquatic exploitation must focus on the aquatic environments themselves as separate entities from archaeological and cultural interpretations. This thesis will aim to provide information on these systems and their availability to potential fishers within the NEP.

3.1.1 Evidence from modern hunter-gatherers

Subsistence studies have long been a part of hunter-gatherer anthropology, whereby the study of the present (or documented historical past) may serve to further our knowledge of past prehistoric groups. Prior to the “Man the Hunter” symposium held in 1966, it was generally considered that meat (given in this context as that from terrestrial animals) was the primary constituent of the hunter-gatherer diet (Kelly, 1995). Following this symposium, Lee (1968) proposed that while meat forms part of hunter-gatherer diets, it can however be only a minor part. In his study Lee concluded that the mean contribution of meat to hunter-gatherer subsistence, across all latitudes, is only 35%. This important observation overturned the long-held belief that meat was dominant, and opened up alternative dietary contributions, such as fish, to hunter-gatherer subsistence strategies. Though there is great diversity within the hunter-gatherer foraging spectrum and over generalisation must be avoided, a key aspect of ethnographic subsistence strategy is the influence of environment. The role of environment and temperature was first developed by Bailey (1960) before being furthered by Binford (1980) in a series of studies. The concept of this approach is that the annual mean temperature will ultimately influence the pattern of subsistence strategies (Table 3.1). Lee (1968) noted that the use of aquatic resources tended to be greater in colder environments, because aquatic environments are typically more productive than the adjacent terrestrial environment. Modern ethnographic studies (see Kelly 1995) show that the dependence on aquatic resources only accounts for a small difference between the expected and actual dependence on other gathered foods.

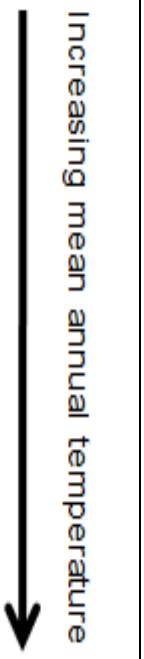
Group	Region	Hunting (%)	Gathering (%)	Fishing (%)	
Tareumiut	Alaska - 70° 34′ 17″ N, 153° 30′ 51″ W	30	0	**70**	
Copper Inuit	Canada (Northwest Territory) - 68° 31′ 0″ N, 110° 51′ 0″ W	40	0	**60**	
Slavey	Canada (Northwest Territory) - 61° 35′ 49.63″ N, 125° 51′ 7.92″ W	**50**	10	40	
Cree	Canada - 57° 46′ 26″ N, 93° 22′ 17″ W	**60**	20	20	
Crow	North America - 47° 30′ 13″ N, 111° 17′ 11″ W	**80**	20	0	

Table 3.1 – Relationship between increasing mean annual temperature and fishing as shown by ethnographic hunter-gatherer groups. Fishing is shown to dominate subsistence strategies when groups are subject to lower mean annual temperatures. Adapted from Kelly (1995).

Interestingly however, dependence on aquatic resources accounts for more variability in the expected hunted food, as opposed to gathered food (Kelly, 1995). Therefore, groups that have a higher dependence on fishing are actually hunting terrestrial animals less than predicted for that group. This has two implications, firstly, it has been suggested that fishing and the utilisation of aquatic resources may be a function of a group's inability to hunt as much as necessary (Yesner, 1980; Keeley, 1988; Binford, 1990). Hamburgian and Ahrensburgian groups appear to have operated within the Ahrensburgian Tunnel Valley ambushing reindeer groups in open conditions, most probably during migration events (Grønnow, 1985; Bratlund, 1996); whilst Federmesser and Bromme groups, from the limited faunal evidence, appear to have hunted under forested conditions. Hamburgian and Ahrensburgian groups only appear to have exploited reindeer at certain times of the year, therefore leaving the question of what resources or methods of storage could have been employed to supplement access to fresh meat. Likewise within Federmesser and Ahrensburgian groups, the newly

expanding forests of the NEP as well as large scale events such as the eruption of the Laacher See Volcano would have led to local variability in food resources. In both cases, the inability to hunt, either at certain times of the year or for environmental reasons, may have led to the utilisation of aquatic resources. Secondly, is the issue of food sharing and predictability: there, ethnographic studies (e.g. Hawkes *et al*., 1989) have demonstrated that meat from large animals is widely shared, not only within the hunters own camp, but with other associated camps, based on the conservative assumption that a camp defines the sharing limits and that each hunter represents a family. In their study of the Hadza, Hawkes *et al*., (1989) discovered that out of a typical kill of a medium sized animal; each hunter within a group of eight is left with approximately 900 cal/day. When compared to smaller resources that can be gathered, in this case tubers, but in other studies fish and shellfish (e.g. Kelly, 1995), it was found that the calorific content increases to between 3,900-10,000 cal/day. Therefore, within sharing groups, gathering of smaller resources such as fish can offer a far higher calorific return than hunting. A second point is that of resource predictability and success rate. Further studies of Hadza groups indicate that the probability of killing or scavenging a large animal on any given day is only 0.03, therefore Hadza hunters have a 0.97 risk of failure each day (Hawkes *et al*., 1991). This raises an interesting point, the Hadza of eastern Africa, inhabit a region where numerous large prey items are available e.g. antelope and gazelle, yet their diet is biased towards gathering (65%). The Hadza therefore negate the risk of hunting failure by diversifying their subsistence strategies where the gathering of smaller resources fails far less often. It has also been noted that ethnographic groups who have been observed to hunt more than expected all inhabit areas where there is limited or no access to aquatic resources e.g. inland areas such as the Great Plains in North America (Kelly, 1995).

3.1.2 A model of aquatic exploitation for the NEP

If we consider the faunal evidence from the NEP together with ethnographic evidence presented in section 3.1.1, it is possible to make several statements about the role of aquatic exploitation in both modern and ancient hunter-gatherer groups. This can be surmised as follows:

- Hunter-gatherer groups in cold climates tend to rely more heavily on aquatic resources than they do on large animal hunting.

- Evidence from the Ahrensburgian Tunnel Valley indicates that reindeer hunting was not a year round practice in the Bølling and Younger Dryas, while during the Allerød resources were locally variable. Coupled with this is the suggestion that large animal hunting would have entailed high risk as indicated by modern ethnographic studies, implying that other, lower risk, resources would have been utilised for at least part of the year.

- Gathering of lesser resources and fishing can offer a far higher calorific return per day then large animal hunting alone.

In order to validate these statements, the model of aquatic exploitation therefore proposes the following hypotheses:

1. That aquatic systems within the NEP during the Lateglacial responded synchronously to AETs making them a predictable resource base.

2. Aquatic systems offered greater resources during environmental events such as the Laacher See eruption.

3. Levels of productivity within aquatic systems are consistent across all systems regardless of the surrounding terrestrial environment.

4. Aquatic systems contained fish populations necessary to support hunter-gatherers during the Lateglacial of the NEP.

The proxies employed in this thesis will allow the hypotheses above to be addressed. The following sections will therefore discuss these proxies and how they can be utilised to develop our knowledge of aquatic system evolution and therefore further our knowledge of aquatic exploitation.

3.2 Microtephra analysis

High resolution palaeoclimate archives, such as the Greenland ice core records have demonstrated that climatic oscillations during the Lateglacial were both complex and abrupt, occurring over centennial and even decadal timeframes (Alley *et al*., 1993; Dansgaard *et al*., 1993; Kapsner *et al*., 1995; Rasmussen *et al*., 2006; Steffensen *et al*., 2008). In order to fully understand the impact these

climatic shifts had on the environment and the development of aquatic systems within the NEP, a precise correlation between geographically widespread environmental archives is needed (Blockley *et al*., 2005; 2006). The abrupt nature of these AETs poses a challenge to scientists; the most frequent age models for this period are generated through ^{14}C dating in the terrestrial and marine realm. These models typically have centennial age uncertainties, at best, and are therefore unable to accurately define the phasing of the palaeoenvironmental responses to AETs (Bramham Law *et al*., 2013). One of the approaches recommended by the INTIMATE group in resolving this geochronological uncertainty is through the use of, often invisible, volcanic ash layers (tephra, or microtephra) (Davies *et al*., 2002; Turney *et al*., 2004). Explosive volcanic eruptions produce large volumes of volcanic ash which can be dispersed over many thousands of kilometres as visible or invisible ash layers (Lane *et al*., 2011a). Crucially this ash is deposited as a geologically instantaneous isochrone, which allows the alignment of records at discrete, fixed points in time, thus reducing the uncertainties associated with record alignment (Mangerud *et* al., 1984; Turney *et* al., 2006; Lane *et al*., 2011b; Brooks *et al*., 2012).

The use of tephra within Quaternary research can be divided into two approaches; tephrochronology and tephrostratigraphy. Tephrochronology uses the import of externally dated eruptions into a site chronology (see Lowe *et* al., 2007; Blockley *et* al., 2008; Lane *et al*., 2011b). The accuracy of externally dated eruptions is dependent on the method of dating, with ^{14}C (see Mangerud *et al.,* 1984), varve counting (see Brauer *et al*., 1999), Ar/Ar (Mark *et al*., 2013) and ice core stratigraphy (Rasmussen *et al*., 2006) all utilised. Tephrostratigraphy relies on the presence of isochronous tephra layers to align records at fixed points in time (see Wastegård *et al*., 2000; Bogaard and Schminke, 2002). Initially, stratigraphic records of northern European tephra layers were limited to observations of visible tephra horizons; with the subsequent development of microtephra analysis the range and applicability of tephrochronology and tephrostratigraphy has been dramatically extended. Distal deposits, invisible to the naked eye, have now been used to link terrestrial, marine and ice core records of the palaeoenvironment across Europe (Lowe and Turney, 1997; Turney *et al*., 1997; Turney, 1998; Wastegård *et al*., 1998, 2000; Lowe *et al*., 2001).

Tephra	Source	Date	Reference for age estimate
Saksunarvatn Ash	Iceland	10,297 ± 45 GICC05 yrs b2k' [1] 10,210 ± 35 cal yr BP[2]	Rasmussen *et al*., 2006 Lohne *et al*., 2013
Askja	Iceland	10,570 – 11,050 cal. yr BP	Wohlfahrt *et al*., 2006
Hasseldalen	Iceland	11,543 – 11,232 cal. yr BP[3] 11,596 – 11,164 cal. yr BP[4]	Wohlfahrt *et al*., 2006
Vedde Ash	Iceland	12,121 ± 114 GICCO5 yr BP	Rasmussen *et al* 2006
Laacher See Tephra (LST)	Eifel Region, Germany	12,880 varve years. BP	Brauer *et al*., 1999
Borrobol	Iceland	13,667 – 14,331 cal. yr BP	Davies *et al*., 2004

Table 3.2 – Key tephra horizons associated with northern Europe during the Lateglacial – Holocene transition. The LST has the only local source from within Germany; the other three tephra horizons are from Icelandic sources.[1] and [2] the two ages given for the Saksunarvatn Ash. Based on trace element analysis the Saksunarvatn Ash is argued to be represented by two separate eruptions dispersing tephra to the NW and SE (see Bramham Law *et al*., 2013). [3] and [4] the two age models constructed for the Hasseldalen tephra (Wohlfarth *et al*., 2006).

As indicated by Table 3.2, the most important volcanic centres for northern European, Lateglacial records are located in Iceland and the Eifel Volcanic Field. An important issue to resolve is the extent to which the various magmas and ashes generated by these volcanic centres can be geochemically identified. This has far reaching importance in distinguishing eruptions originating from the same volcanic centre, in which there may have been limited geochemical evolution of magmas over time (Davies *et al*., 2002). Geochemical identification of tephra deposits is based on the premise that glass shards formed by rapidly cooling magma have a composition that is comparable to the bulk

geochemistry of the parent magma immediately before the eruption event (Barker, 1983). If a tephra deposit can be shown to have a distinct and identifiable geochemical signature, it can be used to correlate the stratigraphic unit/s in which it is found (tephrostratigraphy) and also to date those unit/s if the age of the tephra is known (tephrochronology) (Westgate and Gorton, 1981; Blockley *et al*., 2005; 2006). In order to establish a detailed tephrostratigraphic and tephrochronological record for the NEP, the geochemical properties of individual tephra layers found in the region must be assessed. The most commonly employed techniques for determining glass chemical composition is electron probe micro-analysis (EPMA) and laser ablation inductively coupled plasma mass spectrometry (LA-ICP-MS). EPMA enables single grain determinations of major elements within glass shards (Davies *et al.*, 2002), a process which is of particular use to microtephra layers with low shard concentrations (shards per gram dry weight of sediment) which only preserve glass shards as minerals fall out closer to the eruptive centre (Hunt and Hill, 1993). One of the main issues with the European Lateglacial tephra record is the lack of proximal outcrops for distally described tephra layers. The identification of distal tephras, particularly those from Iceland, relies on the compositional and stratigraphic correlation to other distal deposits. It is possible to identify tephra deposits based solely on major element data when there is secure stratigraphy and additional chronological information, however many of the Icelandic volcanoes that erupted frequently during the Lateglacial and Holocene are known to have produced tephra with almost identical major elemental profiles from multiple eruptive events (Larsen *et al*., 2001; Lowe *et al*., 2008; Housley *et al*., 2012; Lane et al., 2012c). Due to this it is necessary to firmly establish correlations using LA-ICP-MS. The utilisation of trace element analysis can also be used to delineate individual eruptions. For instance the Saksunarvatn Ash is found within both the NGRIP ice core record as well as within European environmental records. Since its discovery on the Faroe Islands (Waagstein and Jóhansen, 1968; Jóhansen, 1975) occurrences of the Saksunarvatn Ash within Greenland and Europe has been considered representative of a single eruption. However recent LA-ICP-MS analysis of the Saksunarvatn Ash by Davies *et al*., (2012) and Bramham Law *et al*., (2013) has now confirmed that the Saksunarvatn Ash is actually representative of two separate eruptions with dispersal axis to the NW and SE.

Tephrostratigraphy and tephrochronology have both been used extensively within Lateglacial palaeoenvironmental research. The use of tephra to synchronise isotopic records within northern

Europe however, has been relatively under used, with the few studies utilising tephra only as a chronological tool (see Mayer and Schwark, 1999; Lücke *et al*., 2003; Lücke and Brauer, 2004). Work by Lücke *et al.,* (2007) raised the potential of synchronising isotopic records in his study of two Lateglacial varved lakes, demonstrating the potential of tephra in evaluating aquatic responses to AETs at sub-centennial scales. The tephrostratigraphic and tephrochronological framework provided by this thesis allows the direct synchronisation of isotopic and palaeoecologcial records. Additionally, the presence of well dated tephra layers within each of this thesis studied sites, allows increased precision within the age models produced.

3.3 Stable isotope analysis

Variations in aquatic primary productivity provide a good, first order measurement of a lacustrine system's health during periods of significant environmental change (Hyodo and Longstaffe, 2011). Geochemical element contents such as total organic carbon and total nitrogen as well as the stable isotope compositions of carbon and nitrogen derived from organic matter can be used to reconstruct past changes in lake productivity and nutrient cycling in relation to climatic and environmental change (Parplies *et al*., 2008). Stable isotopes have been utilised in my thesis based on the premise that terrestrial or aquatic plants and algae show differences in their $\delta^{13}C$ and $\delta^{15}N$ compositional ranges due to the differences in photosynthetic mechanism or sources of carbon and nitrogen used. The $\delta^{13}C$ values of freshwater algae are typically controlled by the composition of dissolved CO_2 and the level of photosynthetic activity. When lacustrine organic matter is comprised of algal matter its isotopic composition can used to describe the cycling of dissolved CO_2 as well as the primary aquatic productivity (Hyodo and Longstaffe, 2011). Higher, vascular plants contain large amounts of cellulose and waxy hydrocarbons, both of which are rich in carbon. Non-vascular plants e.g. phytoplankton, have low cellulose and lignin contents and are high in N-rich proteins (Hyodo and Longstaffe, 2011). The result of this is that it is possible to differentiate between these sources of organic carbon based on the combination of $\delta^{13}C$ range and C/N ratio (algal C/N <10; terrestrial C/N >20; Lücke et al., 2003). The nitrogen source for lacustrine, non-nitrogen fixing algae is dissolved inorganic nitrogen (DIN, NO_3^-, NO_2^-, NH_4^+) derived from soil and /or nitrogen fixed microbially in lake water (Goericke et al., 1994; Hyodo and Longstaffe, 2011). The $\delta^{15}N$ values of algae typically range from +2 to +13 ‰

(Nichols and Garling, 2000, Johannsson et al, 2001, Vuorio et al., 2006) depending on the nitrogen isotopic composition of the DIN source and algal productivity (Meyers, 2003). In contrast terrestrial higher plants utilize inorganic nitrogen (NO_3, NO_2, NH_4) available in soil, mainly derived through the nitrification of microbially fixed atmospheric N_2 (Fogel and Cifuentes, 1993). The $\delta^{15}N$ values of land plants therefore are typically much lower than those derived from an algal source in the range of-5 to +3 ‰.

The use of geochemical element contents and stable isotope compositions is well established within Lateglacial research both as a standalone technique (e.g. Parplies *et al*., 2008; Cook *et al*., 2012; Street *et al*., 2012) or as part of a multi-proxy approach (e.g. Shen *et al*., 2005; Wennrich *et al*., 2005; Veski *et al*., 2012). The key strength of stable isotopes for this research is their speed of response to changes in environmental conditions. Lacustrine organic matter reacts rapidly to changes in aquatic and terrestrial conditions, providing information on vegetation shifts and the level of productivity within an aquatic system (Hyodo and Longstaffe, 2011). Stable carbon and nitrogen isotopes in lacustrine organic matter record variations in aquatic primary productivity with almost no lag phase to environmental change (Lücke *et al.,* 2007). It is well known that terrestrial vegetation response to AETs lags behind the climatic record (e.g. Pennington, 1986; Williams *et al*., 2002; Müller *et al*., 2003). Isotopic changes within aquatic systems therefore offer the chance to assess whether these changes are consistent between each studied site or whether changes in aquatic productivity were more locally variable. The level of consistency in the evolution of an aquatic system would have had far reaching consequences for hunter gatherer groups during the Lateglacial of the NEP (see section 3.1.1). Resources that have a unified response to environmental changes are predictable, therefore allowing hunter-gatherer groups to plan subsistence strategies accordingly. Conversely, inconsistency amongst resource basis makes them unpredictable and therefore less likely to form a core part of any subsistence strategy (e.g. Bousman, 1993).

3.4 Cladoceran sub-fossil analysis

Cladocera, commonly referred to as water fleas, are a major component of the micro-crustacean fauna in freshwater lakes. Cladocera are found within both offshore (pelagic) regions, where the families *Bosminidae* and *Daphniidae* predominate, as well as shallow water (benthic) regions where

members of the Chydoridae family preferentially inhabit different substrates such as mud, sand, gravel or shallow water aquatic macrophytes (Hann, 1988). These shallow water cladocerans may also be referred to as “littoral”; however in the context of this thesis these species will be referred to as benthic to highlight the importance of substrate to cladoceran abundance. Cladoceran remains are composed of chitin, and as such readily preserve within lake sediments (Frey, 1962; 1986; 1988). Cladocera, throughout their life cycle, shed their exoskeletons a number of times, this therefore produces abundant chitinous remains within the sediment in direct proportion to the species community in the water column, Cladocera are a key proxy of ecological and environmental change within an aquatic system (e.g. Korhola, 1999; Hofman, 1987; Duigan and Birks, 2000; Korhola and Rautio, 2001; Hofmann, 2003; Korponai *et al*., 2011; Kattel and Sirocko, 2011) as well as indicators of predation pressure and food web dynamics (e.g. Amsinck *et al*., 2003; Sweetman and Finney, 2003; Amundsen *et al*., 2009; Alexander and Hotchkiss, 2010).

Cladocera have been utilised within this thesis for two key reasons. Firstly, Individual cladoceran species have different habitat tolerances, and as such can be used to infer existing conditions within an aquatic system. Therefore, by assessing species composition it is possible to assess basin conditions such as water level, dominant substrate, pH and vegetation levels. The ratio between planktonic and littoral species is a widely used proxy in the reconstruction of water depth (e.g. Sarmaja-Korjonen and Alhonen, 1999; Korhola *et al*., 2005). A decrease in water depth causes an increase in the remains of littoral species relative to planktonic species; an increase in water depth therefore causes a reverse in this pattern (Sarmaja-Korjonen, 2001). This process is due to the compositional and area changes of the littoral zone, therefore allowing shallow water species to predominate at lower water levels with an increased littoral zone and planktonic open water species to dominate during periods of deeper, more open water (Whiteside *et al*., 1978). Secondly, cladocera have been shown to be excellent indicators of predation pressure and changes in food web dynamics, particularly fish predation (e.g. Jeppesen *et al*., 2002). Numerous studies (Frey, 1986; Jeppesen et al., 1996; Alexander and Hotchiss, 2010) has shown that predation by planktivorous fish significantly influences the community structure and morphology of cladocerans through size selective predation. With high predation pressure from planktivorous fish, larger bodied cladocerans such as *D. pulex* will be preferentially preyed upon, causing a reduction in numbers. Conversely smaller cladoceran

species such as *B. longirostris* will increase due to reduced grazing competition with *D. pulex*. Additionally, changes in *Bosmina* morphology can be used to infer past changes in predation pressure both from fish and aquatic invertebrates. Longer morphological features such as mucrone (tail spine) length reduce predation pressure from invertebrate predators (Kerfoot, 1974; 1977; 1981). Conversely predation from fish has been shown to reduce *Bosmina* mucrone length (Salo *et al*., 1989; Kerfoot, 1981; Alexander and Hotchiss, 2010). As discussed within section 1.5.1 (Chapter 1) fish remains do not readily preserve or are missed within Lateglacial environmental investigations. As such cladocerans provide an important tool for determining food webs and as such whether fish were present within Lateglacial lakes of the NEP.

3.5 Study sites

The following section will present site and stratigraphic information for each of the sites studied within this thesis. As discussed within Chapter 1, a total of five final sites have been used to evaluate the evolution of aquatic systems within the NEP. A further five sites have also been analysed within this thesis; however these proved to be problematic due to chronological issues and do not form a major part of this thesis. Additional information can be found on these sites in Appendix I.

3.5.1 Slotseng

The site of Slotseng lies to the east of the former stationary line of the Fennoscandinavian Ice Sheet (55°19´43"N - 9°16´8.24"E; Figure 1.2, Chapter 1). During the LGM the Fennoscandinavian Ice Sheet reached its maximum extent in Denmark by ~22,000 cal yr BP covering all areas apart from western Jutland (Houmark-Nielsen and Kjaer, 2003. The main stationary line of the Fennoscandinavian Ice Sheet within Denmark formed the Jutland Ridge, which after deglaciation ~19,000 cal yr BP, acted as a major watershed divide within the Jutland Peninsula (Mortensen *et al*., 2011). The retreat of the Fennoscandinavian Ice Sheet by ~19,000 cal yr BP left a landscape characterised by undulating dead ice features such as kettle holes to the east of the stationary line and extended outwash plains to the west (Houmark-Nielsen and Kjaer, 2003).The site of Slotseng is composed of a palaeolake (~4 hectares), a small kettle hole (~0.5 hectares) and an area of former Hamburgian and Federmesser occupation. The kettle hole (this study was only granted access to the small kettle hole) is located ~30

meters south of the former lake and ~50 meters north of the area of Hamburgian and Federmesser occupation (Figure 3.1). Today the area is part of extensive farmland, with the former basin deposits covered by colluvial soil (Mortensen *et al*., 2011).

The Slotseng kettle hole, studied as part of this thesis, was first excavated in 1991 after fragments of a reindeer antler were found within cored sediments 450 cm below the surface. A trench covering ~2 m^2 was excavated at the site leading to the additional finding of reindeer antler and bone fragments with associated cut marks as well as a *Zinken*-like implement of the Hamburgian technocomplex (Mortensen, 2007).

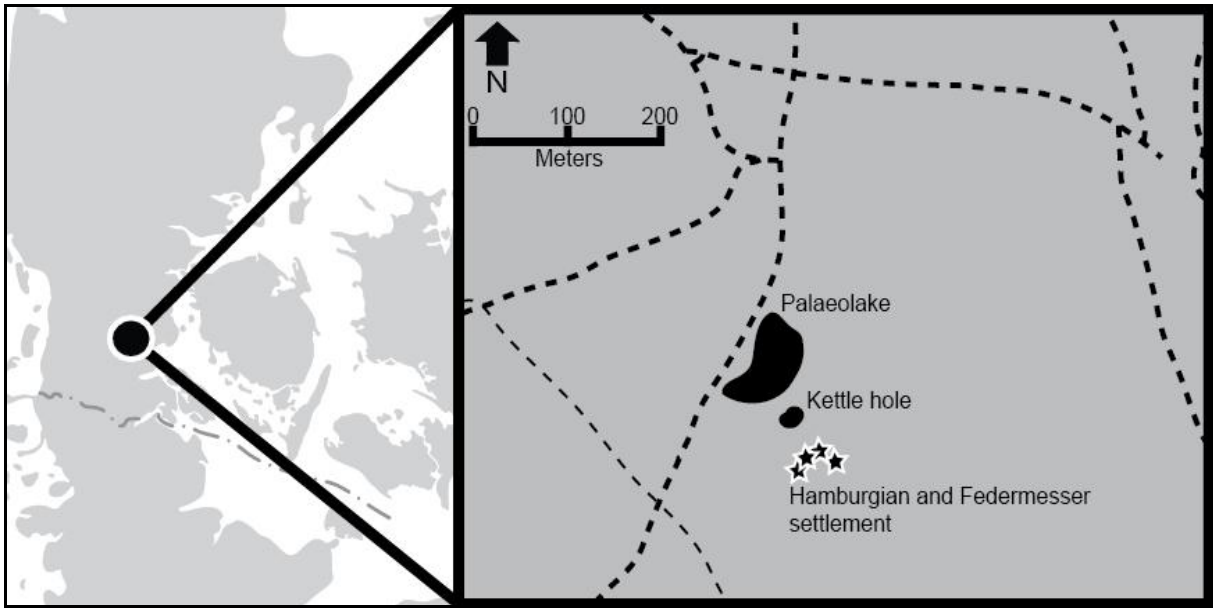


Figure 3.1 – Location of Slotseng within southeast Jutland. Insert: the position of the Slotseng kettle hole in relation to the larger palaeolake to the north and the area of Hamburgian and Federmesser occupation to the south. The larger dotted lines indicate main 'A' roads, while the smaller dotted lines indicate minor 'B' roads. Adapted from Mortensen *et al*., (2011).

Following these early finds, a complete excavation of the kettle hole was conducted in 2000 and 2001 by the Danish National Museum, when two thirds of the former basin was excavated. During this phase of the Slotseng excavations, at least 12 reindeer were uncovered as well as flint implements (Holm *et al*., 2002; Aaris-Sørensen *et al*., 2007) dated to 14,190 – 13, 980 cal yr BP (12, 222 ± 29 ^{14}C yr BP; Mortensen, 2007). The Slotseng kettle hole was formed by dead ice melt within a topographic

depression during the early Bølling period. During the later Bølling – Older Dryas period, ice that was trapped beneath the kettle hole floor further melted leading to a collapse of the basin's floor causing slumping within the kettle hole (Mortensen, 2007). Today the lacustrine sediments of the Slotseng kettle hole are capped by almost 200 cm of peat and a further 200 - 300 cm of colluvial soil which has washed down into the depression from the surrounding landscape (Mortensen, 2007). These accumulations have protected the Lateglacial lacustrine sediments from modern ploughing.

A comprehensive study of the Slotseng vegetation record was conducted by Mortensen (2007) and Mortensen *et al*., (2011). The record for Slotseng presented here was conducted on the same core material as that from the previous two studies by Mortensen. A tephrochronological study of the Slotseng material was also undertaken by Dr Alison MacLeod and will be presented in section 3.5.1.2. Two monoliths covering a total of 218 cm were taken from the former kettle hole. Due to disturbances in the sediment, the lower monolith was sampled ~300 cm to the east of the central basin therefore avoiding the disturbed sediments (Mortensen, 2007; Figure 3.2). The monoliths were correlated using dry density measurements and a distinctive sedimentary boundary within both sequences (Mortensen *et al*., 2011).

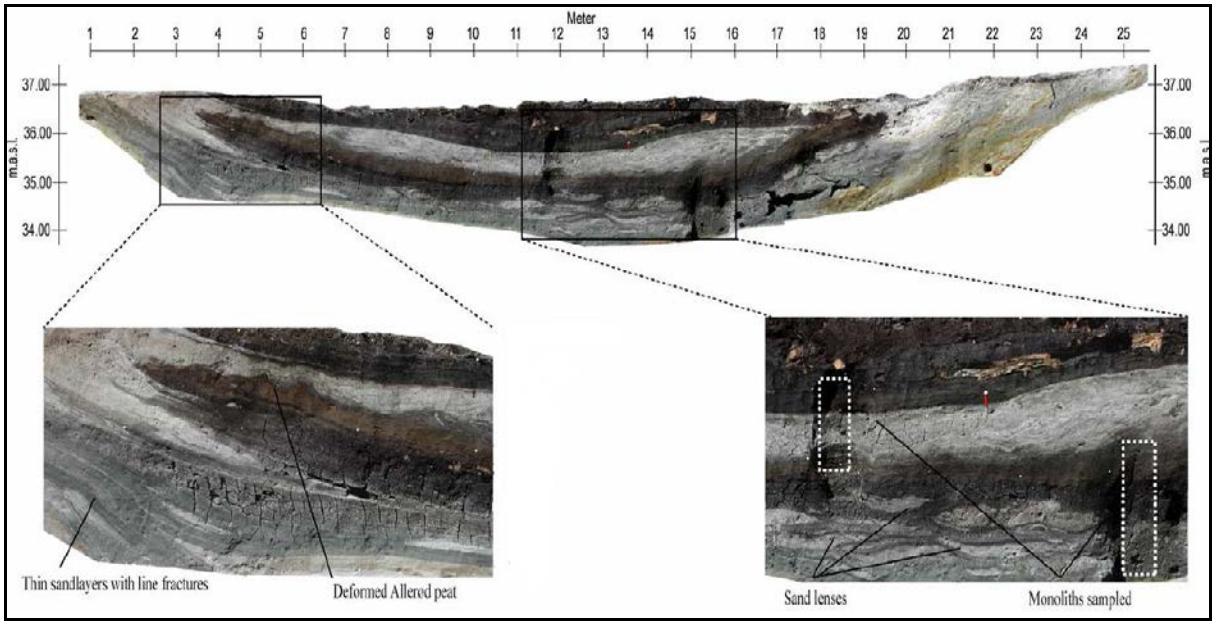


Figure 3.2 – Orthogonal photograph of the transect through the Slotseng kettle hole showing the basins stratigraphy. The position of the two monoliths used within this study are shown as white dotted boxes on the lower right hand image. Adapted from Mortensen *et al*., (2011).

3.5.1.1 Site stratigraphy

The complex depositional history of the Slotseng kettle hole has produced a sedimentary sequence with a number of highly variable units (Figure 3.3). The Bølling – Older Dryas period (0 - 47 cm) is characterised by limnic clayey silty gyttjas that were deposited during the early phases of the basin's formation. The formation of *Sphagnum* peat during the Allerød period (97 - 120 cm) indicates that the basin is now within a partial telmatic phase with semi terrestrial sedimentation occurring. The transition into the Younger Dryas (120 - 162 cm) coincides with renewed deposition of limnic silts and clayey gyttjas; sand layers within this zone may indicate some inwash events or heightened aeolian activity around the basin. The last main sedimentary stage coincides with a final telmatic phase, as indicated by the deposition of peat and the formation of birch/pine woodland over the basin during the Holocene (182 - 218 cm). The unique preservation of Bølling – Holocene age sediments within Slotseng allow not only the palaeoecological record to be reconstructed (see section 6.1, Chapter 6) but also the effect dead ice melt within Slotseng had on the basin evolution.

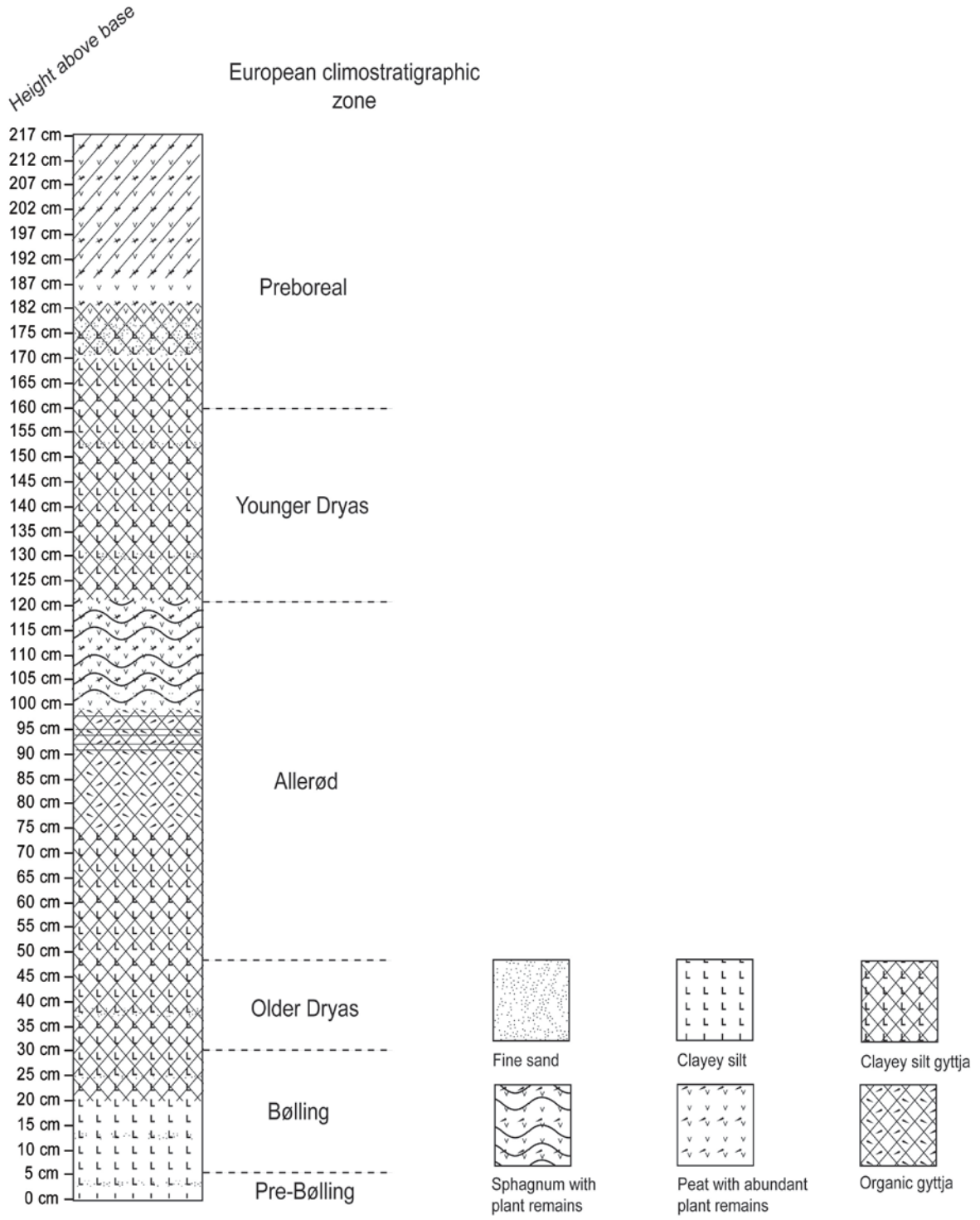


Figure 3.3 – Lithological diagram of the sedimentary units that form the Lateglacial sequence within the Slotseng kettle hole.

3.5.1.2 Tephrochronology and tephrostratigraphy of the Slotseng kettle hole

The analysis of the Slotseng tephra record was previously conducted by Dr Alison MacLeod at Royal Holloway, University of London. The Vedde Ash was located between 153 - 158 cm allowing comparison with Endinger Bruch and other sites across Europe which will be discussed further in Chapter 7.

Tephra	Depth	Chronozone	Reference for age estimate
Vedde Ash	153 - 158 cm	Younger Dryas	12, 121 ± 114 GICC05 yr b2k[1]

Table 3.3 - Tephras discovered within the Slotseng kettle hole as part of the tephrochronological study of the basin by Dr Alison MacLeod. Dates for the discovered tephras are given as thus: [1] – Rasmussen *et al*., (2006).

3.5.1.3 Radiocarbon dates for Slotseng

A radiocarbon chronology was previously developed for Slotseng by Mortensen *et al*. (2011), with the resulting model constructed using OxCal 4.1 with a model parameter *k* = 100 (Bronk Ramsey, 2008). The ^{14}C dates reported by Mortensen *et al*. (2011) have been used to re-run the original model using 4.2.2 (Bronk Ramsey, 2009a) and IntCal09 (Reimer *et al*., 2009) and are presented in Table 3.4. The original boundaries have been utilised to ensure consistency however with a *k* = 1, in order to reflect variable depositional rates associated with Slotseng's development (Figure 3.4). The model produced as part of this thesis provides age estimates that agree with the previously published ages of major chronozone boundaries as reported by Mortensen *et al*. (2011). The lower *k* value used in the model produced by this thesis allows for more variable sedimentation rates and thus likely provides more accurate age ranges. The agreement of the dates from Slotseng will be further discussed in section 7.1 (Chapter 7).

Height above base (cm)	Lab Code	Material	δC (‰ VPDB)	^{14}C age (yr BP)	Model age (cal yr BP)	A
196	AAR-9834	4 twigs probably *B. pubescens*	-29.15	9650 ± 60	11,139 - 10,019	98%
185	AAR-9833	3 twigs probably *B. pubescens*	-27.71	9600 ± 70	11,237 - 10,774	78%
179	AAR-9849	2 twigs probably *B. pubescens*	-27.41	9935 ± 60	11,397 - 11,186	111%
173	AAR-9832	1 *betula* fruit and 1 *betula* bud scale	-28	9960 ± 90	11,540 - 11,226	125%
159	AAR-9831	3 *B. nana* fruit and 1 b*etula* bud scale	-26.94	10635 ± 70	12,113 - 11,424	2%
128	AAR-9830	*B. nana* fruit and *B. nana* leaf fragment. 4 twigs	-28.18	10390 ± 65	12,897 - 12,253	51%
114	AAR-9882	*B. pubescens* twig	-27.57	11120 ± 60	13,166 - 12,807	110%
106	AAR-9827	*B. pubescens leaf fragment*	-26.76	11400 ± 75	13,360 - 13,115	103%
102	AAR-9826	*Betula pubescens / nana* leaf fragment	-29.44	11305 ± 75	13,512 - 13,151	Outlier
89	AAR-9825	7 twigs - terrestrial. 2 *B. nana* fruit	-26.72	11680 ± 80	13,747 - 13,428	99%
74	AAR-9824	Twigs	-27.21	11890 ± 70	13,827 - 13,604	119%
55	Ua-19898	Twigs	-27.4	12115 ± 120	13,956 - 13,783	118%
54	Ua-19897	Twigs	-27	12125 ± 135	13,970 - 13,798	132%
53	Ua-19896	Twigs	-27.8	12145 ± 120	13,980 - 13,805	121%
46	AAR-9850	8 fruit and 12 catkin scales of B. *nana* , 6 twigs possibly of *B. nana* and leaf fragment of *D. octopetala*	-27.62	11830 ± 70	14,025 - 13,855	3%
40	Ua-19895	Twigs	-28.2	12280 ± 125	14,104 - 13,908	108%
39	Ua-19894	Twigs	-28.4	12390 ± 160	14,116 - 13,917	55%
38	Ua-19893	Twigs	-27.6	12185 ± 130	14,120 - 13,921	157%
32	Ua-19892	Twigs	-27.7	12035 ± 130	14,205 - 13,962	63%
31	Ua-19891	Twigs	-26.8	12200 ± 135	14,222 - 13,966	Outlier
30	Ua-19222	Twigs	-28	12425 ± 115	14,253 - 13,978	50%
27	Ua-19809	Twigs	-28.9	12175 ± 120	14,328 - 13,993	122%
23	Ua-19889	Twigs	-29	11965 ± 120	14,452 - 14,019	11%
21	Ua-19220	Twigs	-27.8	12365 ± 110	14,485 - 14,034	115%
14	Ua-19888	Twigs	-25.6	12265 ± 120	14,682 - 14,054	95%
13	Ua-19219	Twigs	-28.6	12640 ± 190	14,683 - 14,056	77%
10	Ua-19887	Twigs	-22.5	12620 ± 200	15,573 - 14,194	107%
9	Ua-19886	Twigs	-28	13270 ± 125	16,100 - 15,117	48%
3	Ua-19218	Twigs	-28.8	12730 ± 265	16,829 - 15,773	40%
1	Ua-19217	Twigs	-17.7	14180 ± 165	17,584 - 16,809	98%

Table 3.4 – ^{14}C dates and modelled ages for samples from Slotseng re-calibrated using OxCal 4.2.2 (Bronk Ramsey, 2009a) and IntCal 09 (Reimer *et al*., 2009). Original un-calibrated dates from Mortensen *et al*. (2011).

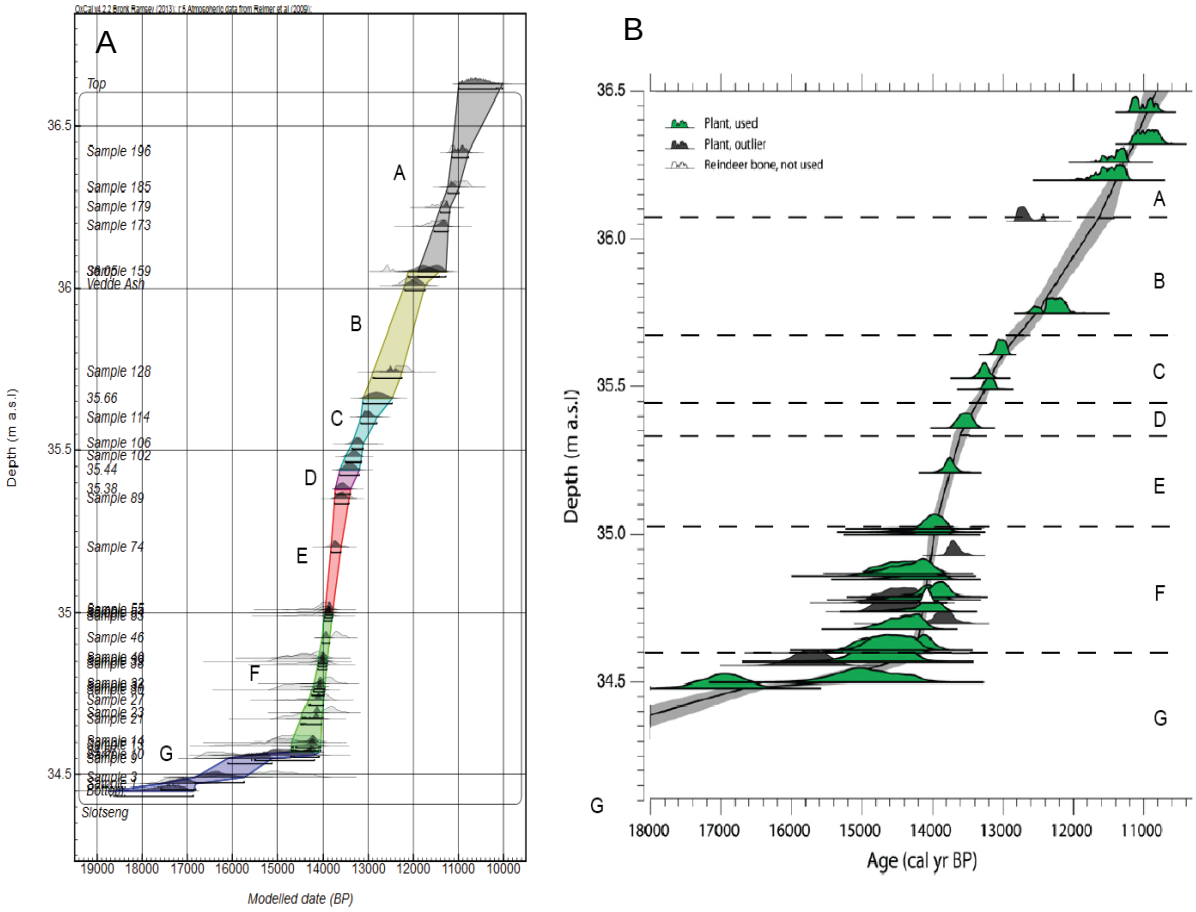


Figure 3.4 – (A) Bayesian P_Sequence depositional model for Slotseng, based upon ^{14}C dates published in Mortensen *et al*., (2011) and the Vedde Ash. Model was constructed following Bronk Ramsey, (2008) using OxCal 4.2.2 and IntCal 09 (Reimer *et al*., 2009). An outlier probability of 0.05 was used within a *General* outlier model coupled with a *k* value = 1 to allow for variations in sedimentation rates. (B) Previous age model for Slotseng produced by Mortensen *et al*. (2011). Model was constructed using OxCal 4.1 following Bronk Ramsey, (2008) using OxCal 4.1 and a *k* value = 100 (Bronk Ramsey, 2001). A – G define age model boundaries used within the original model produced by Mortensen *et al*., (2011), these are reproduced on the age model produced by this thesis to ensure consistency between both models.

3.5.2 Endinger Bruch

The site of Endinger Bruch lies north of the former stationary line of the Fennoscandinavian Ice Sheet (Figure 1.2, Chapter 1) in the Mecklenburg-Vorpommern region of NE Germany (54°14'53"N, 12°53'15"E). The landscape surrounding the Endinger Bruch basin was heavily influenced by glacial and periglacial processes during the LGM and also during deglaciation ~19,000 cal yr. BP, and as such there are numerous lacustrine basins within the region (Terberger *et al*., 2004b). The Endinger Bruch site is composed of at least five separate lacustrine basins (Figure 3.5). The discovery of the remains of a giant deer antler with human modifications first brought this site scientific attention in 1900 (Deecke, 1900). Recent AMS dating of the giant deer remains to 13,675 – 13,215 cal yr BP (11,555 ± 100 ^{14}C yr BP; Terberger, 1996) provides evidence for a human presence within the region during the early Allerød period. The Endinger Bruch basin has been extensively studied since the early archaeological finds in 1900 (e.g. Junke, 1996; Kaiser and Terberger, 1996; Kaiser, 2001). A recent palynological study of the site by de Klerk (2002) provided important, high resolution information about the vegetation response within the Endinger Bruch region to AETs during the Lateglacial and as such became an important palynological reference site for vegetation changes in the Mecklenburg-Vorpommern region (de Klerk, 2002).

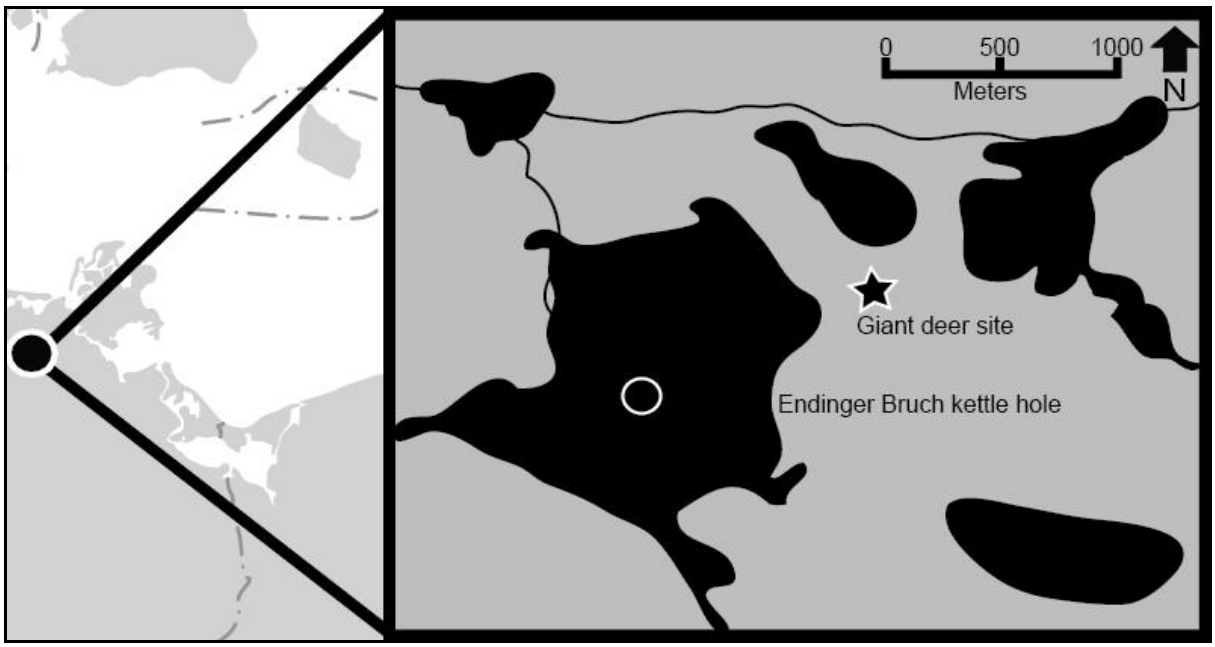


Figure 3.5 – Location of Endinger Bruch with northeast Germany. Insert: the position of the larger Endinger Bruch basin in relation to the other smaller basins which collectively make up the Endinger Bruch site. The location of the coring site is marked with a white circle which is located in a small basin forming one of many topographic hollows within the larger basin as shown by the figure. Adapted from de Klerk (2002).

The record for Endinger Bruch presented in my research was conducted on the same core material as de Klerk (2002) and the tephrochronological study of Lane *et al*. (2011b). The tephrochronological record will be further discussed in section 3.5.2.2. The Endinger Bruch site is a large alder carr located within the till plains of the Mecklenburg-Vorpommern region (de Klerk, 2002). The kettle hole (this study) is ~ 500 meters in diameter is located within a larger basin ~ 1 kilometre in diameter that is composed of the kettle hole itself and several smaller basins (de Klerk, 2002). The area immediately surrounding the kettle hole is composed of several mineral ridges, possibly eskers deposited by meltwater streams within the original dead ice body (Schulz, 1998). The kettle hole which forms the central part of the basin is ~15 meters deep and is now filled with alternating layers of silty sandy gyttja and detritus gyttja (Figure 3.6). From this kettle hole a 660 cm core was removed from the central part of the basin (Figure 3.5) as part of de Klerks (2002) study spanning 1511 – 851 cm. The core, like that from Slotseng, is rare in that it records undisturbed sediments from the Bølling through to the Holocene. Unlike Slotseng however the stratigraphy of the core is relatively simple

being composed of two alternating sedimentological units (Figure 3.6). The relatively large size of the Endinger Bruch kettle hole appears to have insulated it from dead ice melt deformation events such as slumping, which are prevalent within Slotseng.

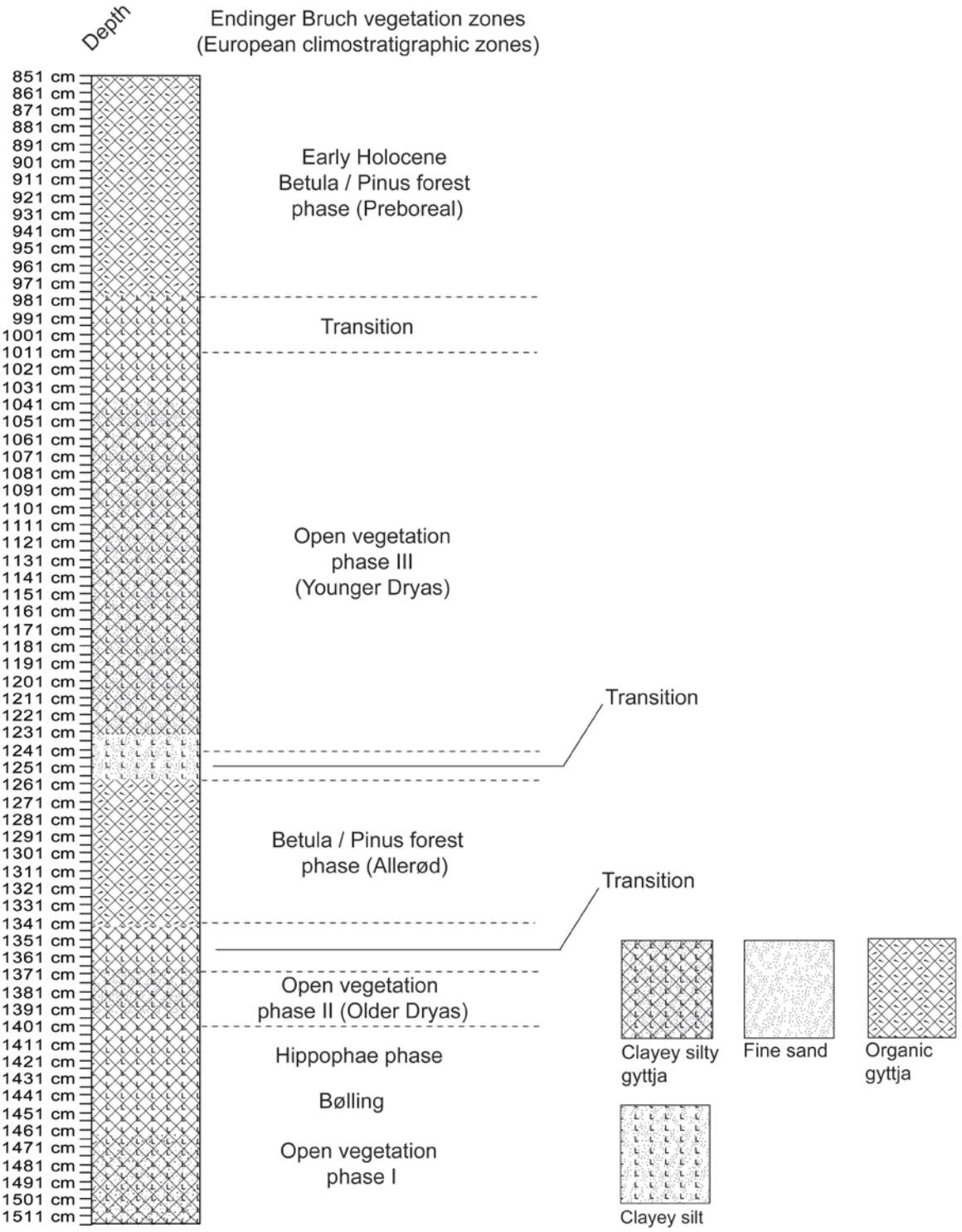


Figure 3.6 – Lithological diagram of the sedimentary units that form the Lateglacial sequence within the Endinger Bruch kettle hole.

3.5.2.1 Site stratigraphy

The Endinger Bruch kettle hole has a relatively simple stratigraphy being composed of five major units interspersed by three sedimentary transition zones (Figure 3.6). The first main sedimentary unit is attributed to the Bølling chronozone within the kettle hole (1511 - 1371 cm) and is represented by clastic sediments, primarily composed of silty sandy gyttja. A transitional zone (1371 - 1342 cm) separates the first main sedimentary unit from the second, where clastic sediments give way to detrital gyttjas. The second major sedimentary unit is that of the deposition of organic gyttjas between 1342 - 1257 cm coinciding with the Allerød chronozone. A second transitional zone (1257 - 1242 cm) separates the detrital gyttjas of the Allerød from the more clastic sediments of the Younger Dryas. The Younger Dryas within the kettle hole is represented by clastic sediments again comprising silty sandy gyttjas similar to those recorded within the Bølling chronozone. A third transitional zone (1011 - 981 cm) marks the boundary between the Younger Dryas and the Holocene. Following this the last sedimentary unit (981 - 851 cm) within the Endinger Bruch core is that of organic gyttjas representative of the early Holocene.

3.5.2.2 Tephrochronology and tephrostratigraphy of the Endinger Bruch kettle hole

The tephrochronological record of the Endinger Bruch kettle hole is well documented; Table 3.5 lists the known tephras reported by Lane *et al*. (2011b). As with Slotseng, this previous tephrochronological study within the Endinger Basin allows direct comparison with other sites in my thesis. This therefore augments the microtephra analysis conducted as part of my thesis for the sites of Kieshoffer Moor, Daschower Moor and Potremser Moor. Crucially the Endinger Bruch record has the Laacher See and Vedde Ash tephras. Firstly, as discussed with section 3.5.1.2 Slotseng also has the Vedde Ash present; thus allowing direct comparison of these two, spatially disparate, basins during the Younger Dryas. Secondly, the presence of the Laacher See tephra allows Endinger Bruch to be linked with the sites of Kieshoffer Moor and Daschower Moor, again allowing spatial synthesis of records.

Tephra	Depth	Endinger Bruch vegetation phase	Chronozone	Reference for age estimate
Askja Tephra	886 cm	Early Holocene *Betula*/ *Pinus* forest phase	Holocene	10, 846 ± 145 cal yrBP[1]
Hässeldalen Tephra	937 cm	Early Holocene *Betula*/ *Pinus* forest phase	Holocene	11, 380 ± 216 cal yr BP[2]
Vedde Ash	1118 cm	Open vegetation phase III	Younger Dryas	12, 121 ± 114 GICC05 yr b2k[3]
Laacher See Tephra	1300 cm	*Betula*(/*Pinus*) phase	Allerød	12, 880 ± 40 varve yr BP[4]

Table 3.5 – Tephras discovered within the Endinger Bruch kettle hole as part of the tephrochronological study of the basin by Lane *et al*. (2011b). Dates for the discovered tephras are given as thus: [1] – Wohlfarth *et al*. (2006), [2]- Wohlfarth *et al*. (2006), [3] – Rasmussen *et al*., (2006), [4] – Brauer *et al*. (1999).

3.5.2.3 Radiocarbon dates and age models for Endinger Bruch

Two ^{14}C dates are available for the Endinger Bruch core, these however are taken from two sister cores (DTV and KZA; see de Klerk, 2002). The dates (DTV - 11,930 ± 70 ^{14}C yr BP and KZA - 11950 ± 70 ^{14}C yr BP) located at the end of the *Hippophaë* phase were transported across into the Endinger Bruch core using exciting pollen stratigraphies (see Lane *et al*., 2011b). The KZA date has been re-calibrated with OxCal 4.2.2 (Bronk Ramsey, 2009a) using IntCal09 (Reimer *et al*., 2009) and is presented in Table 3.6.

Depth (cm)	Lab Code	Material	Core	^{14}C age (yr BP)	Model age
151.5-152.5	UtC 6939	*Carex* seeds	KZA	11950 ± 70	14001-13500

Table 3.6 – ^{14}C date and modelled age for the sample from core KZA. Date calibrated using OxCal 4.2.2 (Bronk Ramsey, 2009a) and IntCal 09 (Reimer *et al*., 2009).

An age model for Endinger Bruch was previously constructed by Lane *et al*., (2011b) this has been re-run using OxCal 4.2.2 to ensure consistency with other sites in this thesis (Figure 3.7). New modelled ages for the onset and termination of the Younger Dryas (Open vegetation phase III) agree (within errors) with the model produced previously produced. The new model gives the onset of the Younger Dryas a modelled age of 12,886 – 12,416 cal yr BP and the termination an age of 12,174 – 11307 cal yr BP.

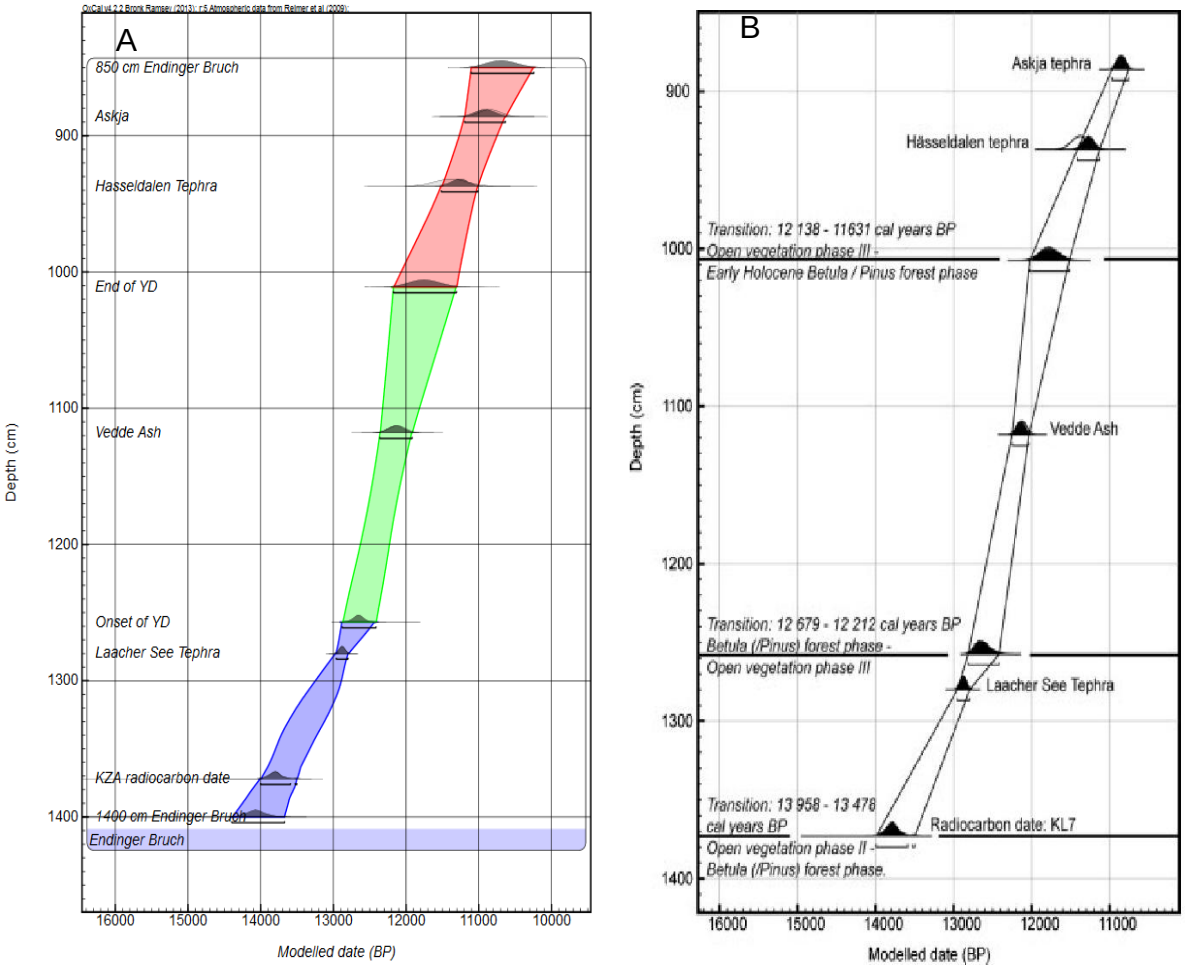


Figure 3.7 – (A) Bayesian P_Sequence depositional model for Endinger Bruch, based upon the single ^{14}C date from core KZA and the known ages of the LST, Vedde Ash, Hässeldalen tephra and Askja tephra. Model was constructed following Bronk Ramsey, (2008) using OxCal 4.2.2 and IntCal 09 (Reimer *et al*., 2009). An outlier probability of 0.05 was used within a *General* outlier model coupled with a *k* value = 1 to allow for variations in sedimentation rates. (B) Previous age model produced by Lane *et al*., (2011b). Model is a Bayesian P_Sequence depositional model constructed using single ^{14}C date from core KZA and the known ages of the LST, Vedde Ash, Hässeldalen tephra and Askja tephra. Model was constructed following Bronk Ramsey, (2008) using OxCal 4.1 (Bronk Ramsey, 2001) and IntCal 09 (Reimer *et al*., 2009).

3.5.3 Potremser Moor

The site of Potremser Moor lies north of the former stationary line of the Fennoscandinavian Ice Sheet (Figure 1.2, Chapter 1) in the Mecklenburg-Vorpommern region of NE Germany (53°59'40"

12°16'57"). As with the site of Endinger Bruch, Potremser Moor is located within the till plains of the Mecklenburg-Vorpommern region, a region heavily characterised by lacustrine systems (see Terberger *et al*., 2004). The Potremser Moor basin is a medium sized palaeolake of ~15 hectares in size (Figure 3.8). The basin was formed by dead ice melt during the Lateglacial, with the onset of sedimentation occurring within the Allerød chronozone. Today the site is mostly forested, covered by a mesotrophic open birch forest with *Sphagnum* peat covering the ground (Theuerkauf, *pers comm*.). The former basin is surrounded by arable farmland and fallow grassland, with the extent of the basin a protected nature reserve. To the east of Potremser Moor is the larger basin of Göldenitzer Moor. Like Potremser Moor it was formed by dead ice melt during the Lateglacial and is capped by several meters of Holocene peats.

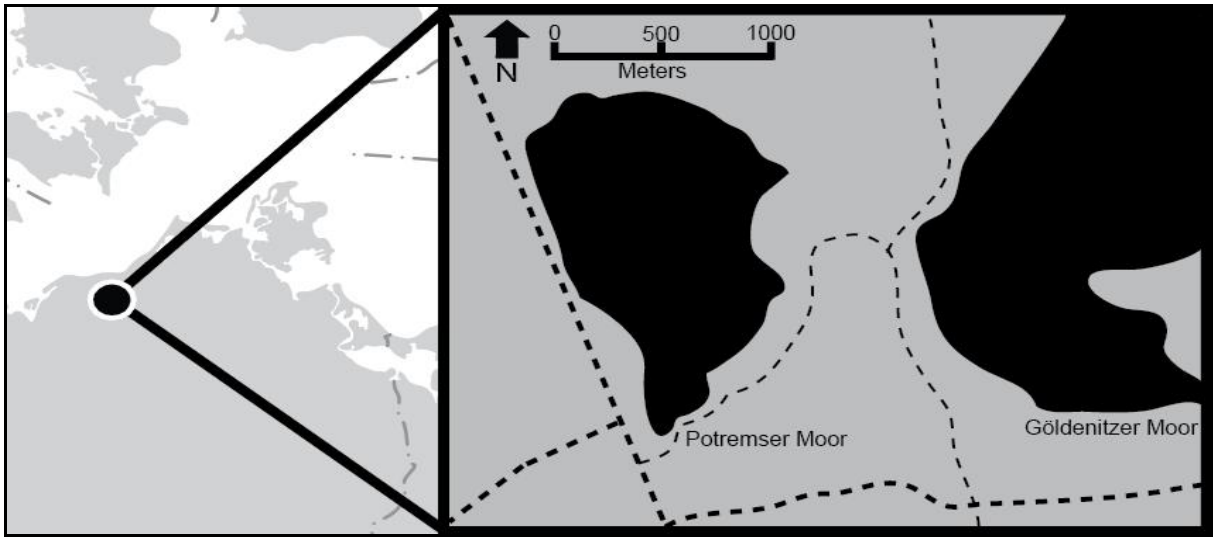


Figure 3.8 – Location of Potremser Moor within northeast Germany. Insert: the position of the Potremser Moor basin. To the east lies the large former palaeolake of Göldenitzer. The larger dotted lines indicate main 'A' roads, while the smaller dotted lines indicate minor 'B' roads.

Potremser Moor was cored in 2007 by Martin Theuerkauf, University of Greifswald. Several coring attempts were made, with the longest at 570 cm being used by this thesis. The upper 400 cm of the core are composed of Late Holocene peats interspersed by layer of organic gyttja between 120 - 280 cm. Due to their recent age; the upper 400 cm of the Potremser Moor core were not sampled by the collectors. The remaining 170 cm of Lateglacial sediment are composed of detrital and clastic sediments, primarily made up of organic, silicious and clayey gyttjas (Figure 3.9).

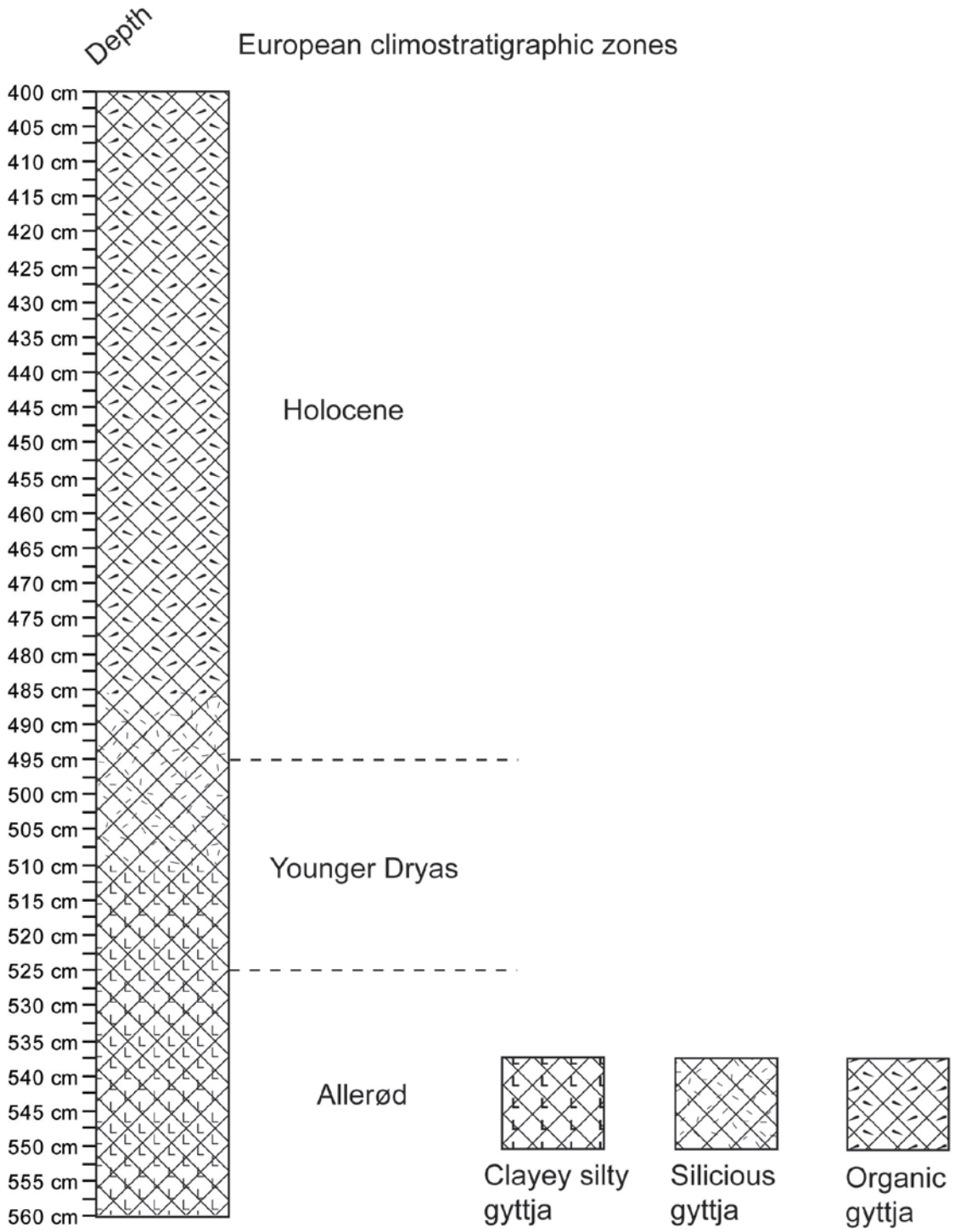


Figure 3.9 – Lithological diagram of the sedimentary units that form the Lateglacial sequence within the Potremser Moor basin.

3.5.3.1 Site stratigraphy

Potremser Moor is characterised by a simple sedimentary stratigraphy of three, primarily gyttja, units. The lower most unit is composed of clayey gyttjas and represents the Allerød chronozone within Potremser Moor (560 - 525 cm). The deposition of clayey gyttjas continues into the Younger Dryas chronozone (525 - 495 cm), however at 510 cm, there is a change in sedimentation with silicious gyttja deposited. The deposition of silicious gyttja continues into the early Holocene (495 cm) where at 485 cm there is a sharp transition to organic gyttjas that predominate until the formation of later Holocene peats.

3.5.4 Kieshofer Moor

The site of Kieshofer Moor lies on the till plains north of the former stationary line of the Fennoscandinavian Ice Sheet (Figure 1.2) in the Mecklenburg-Vorpommern region of NE Germany (54°07'53" 13°20'31"). As with the previous sites of Endinger Bruch and Potremser Moor, Kieshofer Moor is located in region that is heavily characterised by Lateglacial lacustrine systems. Kieshofer Moor was formed by dead ice melting during the Lateglacial, with the onset of sedimentation occurring during the Allerød chronozone.

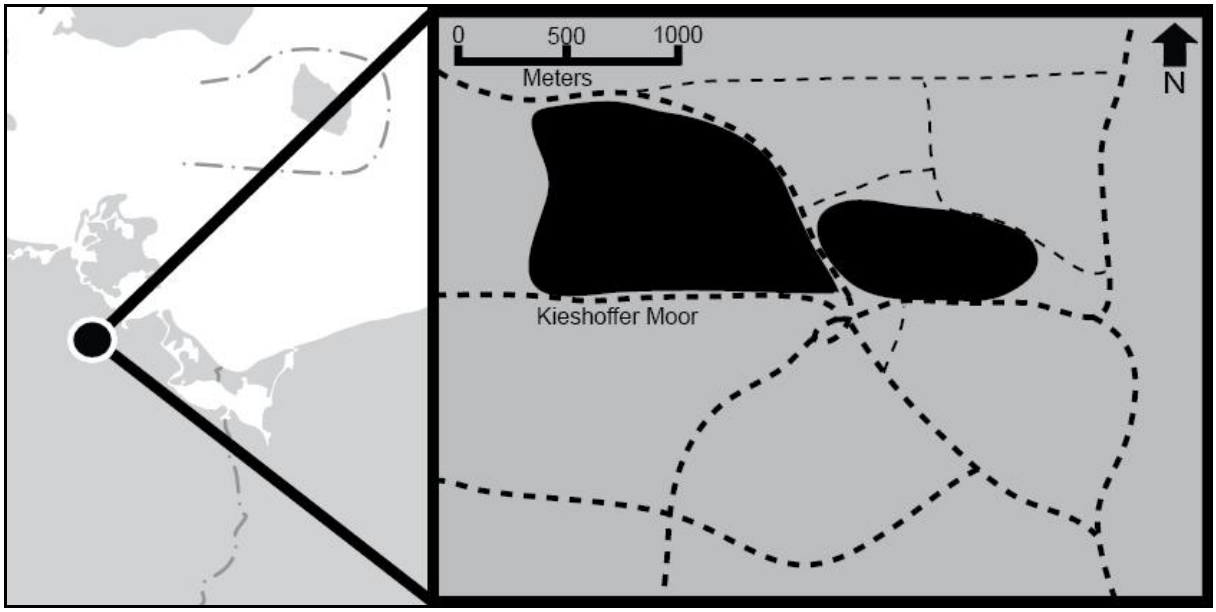


Figure 3.10 – Location of Kieshofer Moor with northeast Germany. Insert: the position of the Kieshofer Moor basin. Extensive farming and road building have reduced the visible size of the site, with only the area shown now protected as nature reserve. The larger dotted lines indicate main 'A' roads, while the smaller dotted lines indicate minor 'B' roads

Kieshofer Moor is a medium sized palaeolake of ~ 40 hectares. The extent of the former lake may have been much larger, however due to extensive farming and road building within its catchment, much of the basin has been lost (Figure 3.10). The former lake became fully terrestrial within medieval times, and like many of the lakes in this region, former lacustrine sediments are capped by peat deposits. The basin today is covered by a mesotrophic, acidic peatland with open vegetation dominated by peat mosses such as *Sphagnum* and cotton grass (*Eriophorum*).

Kieshofer Moor was cored in 2011 by Martin Theuerkauf, University of Greifswald. A core totalling 830 cm was recovered from the site. The upper two meters of the core were composed of *Sphagnum* peat with gyttjas comprising the remaining 630 cm. This thesis was granted access to a section of core spanning 600 – 800 cm, which included organic and clastic sediments of the Lateglacial (Figure 3.11).

3.5.4.1 Site Stratigraphy

Kieshofer Moor is characterised by a simple sedimentary stratigraphy of three, primarily gyttja, units. The lower most unit comprising of organic gyttja with some clayey silt represents the onset of

sedimentation within the Kieshofer Moor basin during the Allerød chronozone (800-790 cm). The Younger Dryas located at 790 - 755 cm, is represented initially by organic gyttja, this however gives way to clayey gyttja at 780 cm forming the second sedimentary unit. The final sedimentary unit coincides with the onset of the Holocene at 755 cm, whereby highly organic gyttjas are deposited.

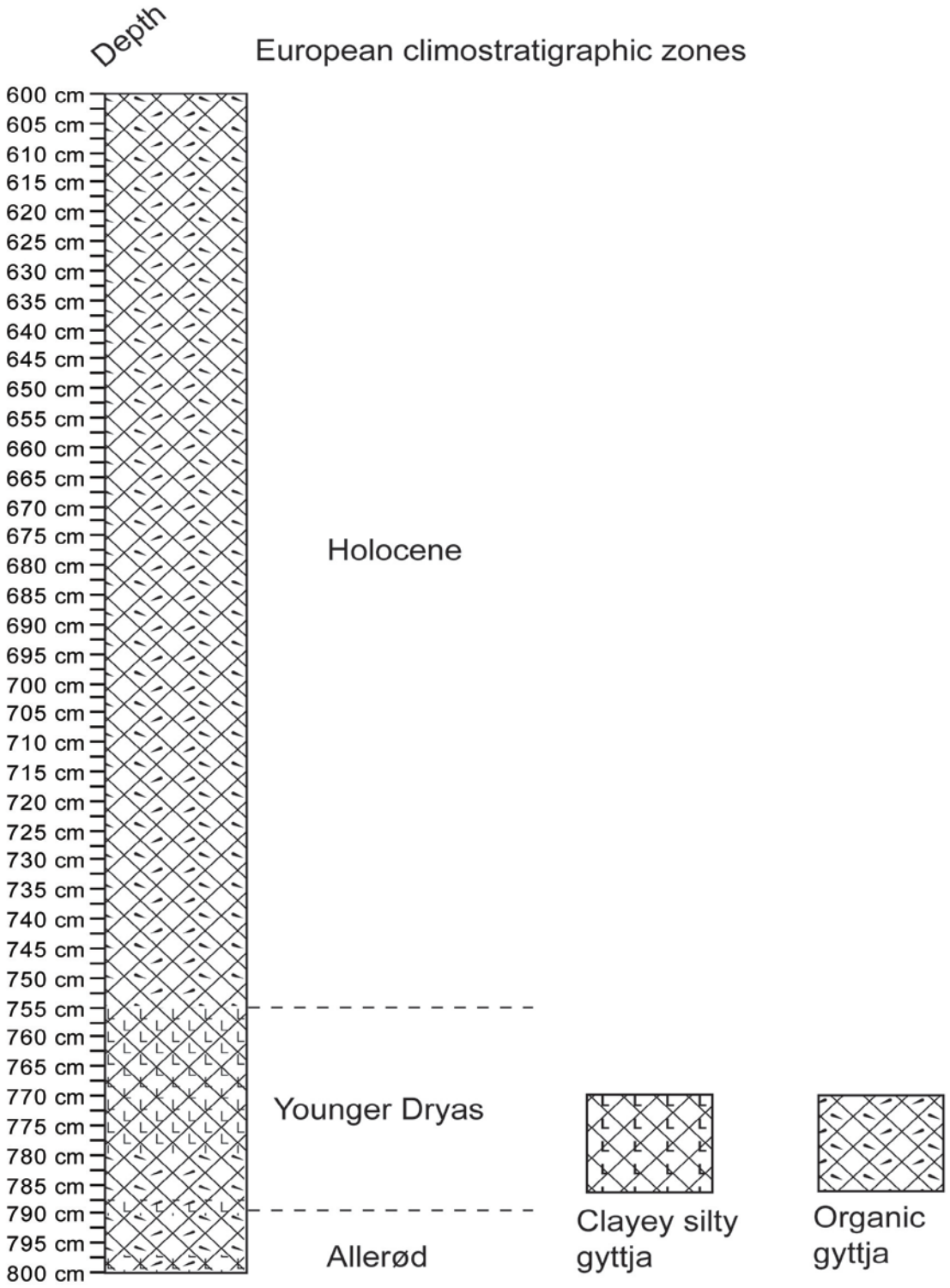


Figure 3.11 – Lithological diagram of the sedimentary units that form the Lateglacial sequence within the Kieshofer Moor basin.

3.5.5 Daschower Moor

The site of Daschower Moor lies within the till plains north of the former stationary line of the Fennoscandinavian Ice Sheet (Figure 1.2, Chapter 1) in the Mecklenburg-Vorpommern region of NE Germany (53° 30′ 28″, 12° 9′ 23″). As with the other sites within this thesis, Daschower Moor is located in an area heavily characterised by Lateglacial lacustrine systems, with the onset of sedimentation occurring during the Allerød. Daschower Moor is a kettle hole of approximately 2 hectares in size (Figure 3.12), with the former lacustrine sediments capped by peat. The present day vegetation is open fenn vegetation (sedge fenn) with some birch trees, surrounded by Salix shrubs.

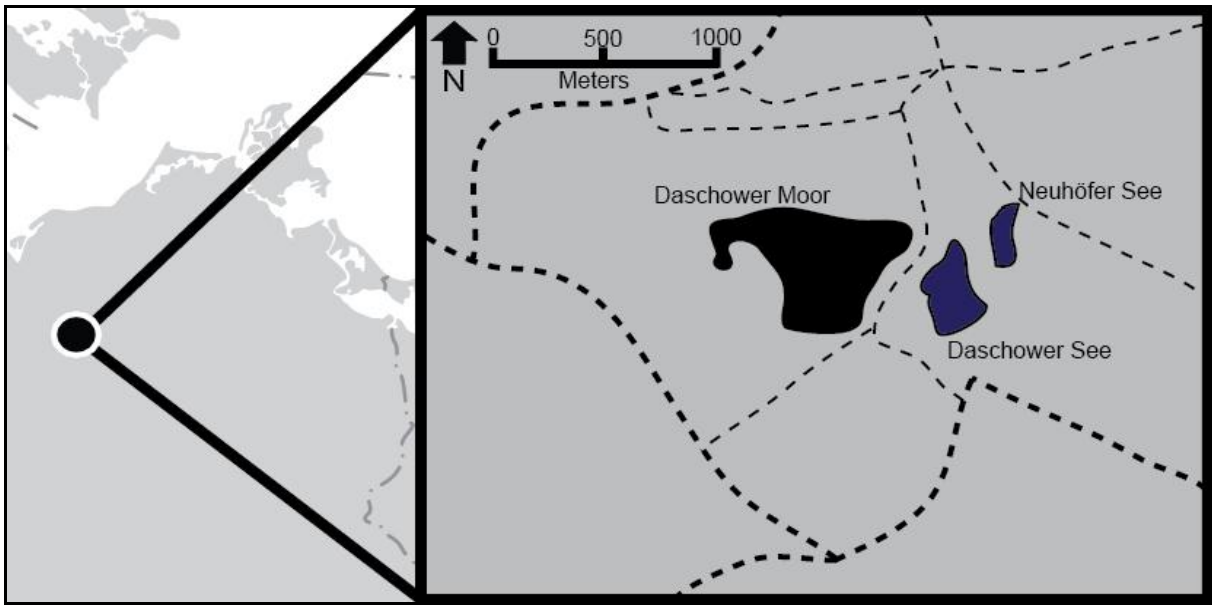


Figure 3.12 – Location of Daschower Moor with northeast Germany. Insert: the position of the Daschower Moor basin. To the east of the former basin lie the extant lakes of Daschower See and Neuhöfer See. The larger dotted lines indicate main 'A' roads, while the smaller dotted lines indicate minor 'B' roads.

Daschower Moor was cored in 2007 by Martin Theuerkauf, University of Greifswald. A core totalling 300 cm was recovered from the site. The upper 100 cm of the Daschower Moor core is composed of Late Holocene peat and therefore was not included within sampling. The lower 20 cm composing of clayey gyttja was also not included due to disturbances within the sediment. This thesis therefore sampled material between 100 – 280 cm, allowing analysis of Lateglacial lacustrine sediments (Figure 3.11).

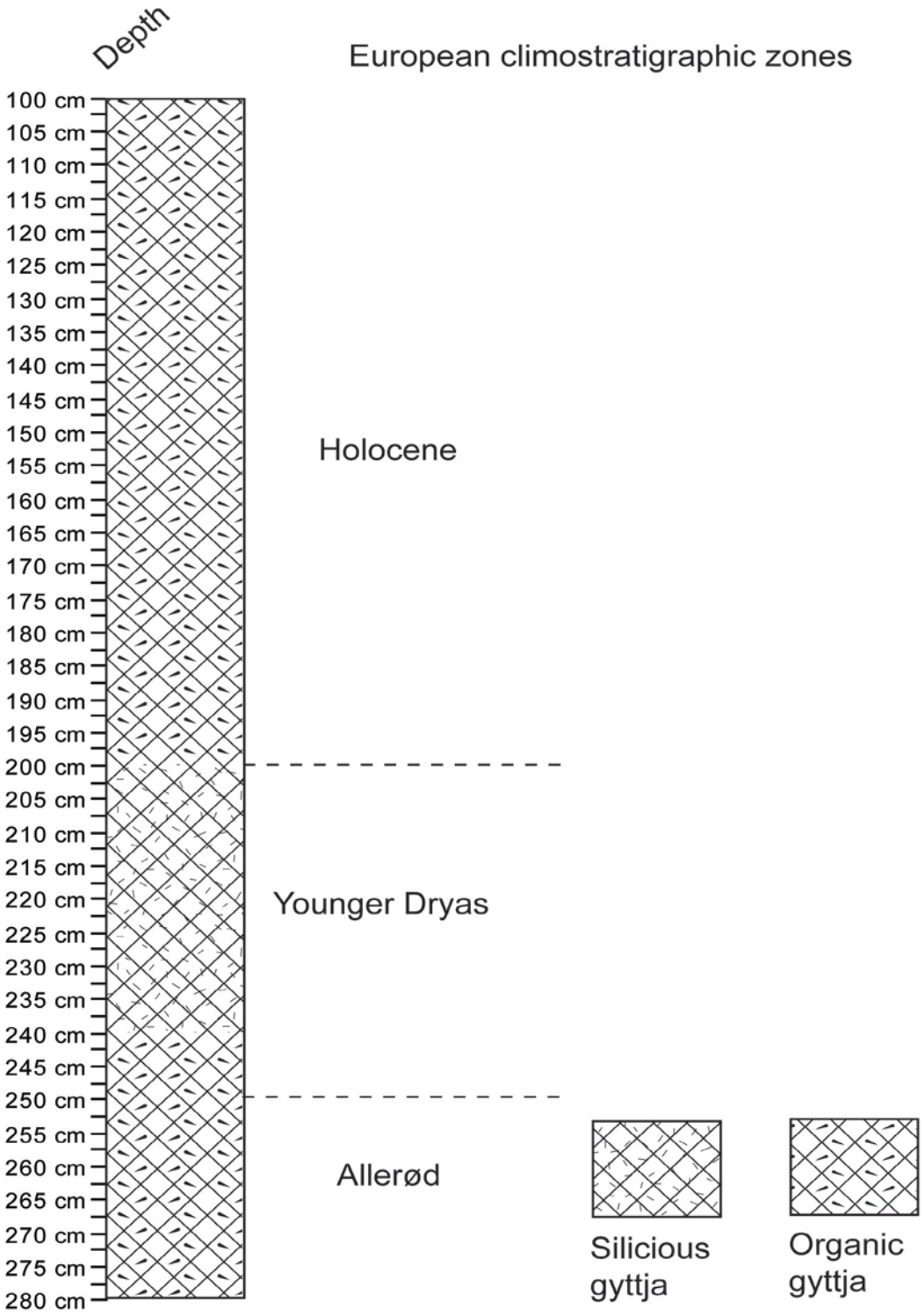


Figure 3.13 – Lithological diagram of the sedimentary units that form the Lateglacial sequence within the Daschower Moor basin

3.5.5.1 Site stratigraphy

Daschower Moor is characterised by a simple sedimentary stratigraphy of three, primarily gyttja, units. The lower most unit comprising of organic gyttja represents the onset of sedimentation within Daschower Moor during the Allerød chronozone (280 - 250 cm). The Younger Dryas located at 250 - 200 cm, is represented initially by organic gyttja, this however gives way to silicious gyttja at 240 cm forming the second sedimentary unit. The final sedimentary unit coincides with the onset of the Holocene at 200 cm, whereby highly organic gyttjas are deposited within the basin.

3.6 Chapter Summary

Modern ethnographic studies highlight the fact that hunter-gatherer groups within colder environments rely more heavily on the exploitation of aquatic resources as a mode of subsistence than hunting alone. Coupled with this is the high risk of hunting, with the 0.97 chance in failure of any given trip and the lower potential calorific reward of hunting compared to gathering and fishing. The aquatic model of exploitation proposes therefore that fishing and the utilisation of aquatic resources could have served as an alternative or additional subsistent strategy to hunter-gatherers on the NEP.

The utilisation of stable isotopes and cladoceran sub-fossils allows the evolution of the five studied sites to be reconstructed. This bottom up method gives crucial information about the relative health of the aquatic systems presented within this thesis during the Lateglacial. Coupled with the addition of tephrochronology and tephrostratigraphy it is possible to compare the responses of these systems to AETs. This level of information provides the first step in understanding how these systems could have contributed to hunter-gatherer subsistence strategies during the Lateglacial.

Chapter 4: Field and laboratory Methodology

The following chapter discusses the field and laboratory methods employed within this thesis. Due to the variation in protocols across all methods, Chapter 4 will discuss each method separately and discuss each stage sequentially.

4.4 Field sampling

The sites presented in this thesis are the result of collection by the author or through collaboration with European co-workers. The following section will briefly address the field methods used in the collection of material.

4.4.1 Slotseng, Denmark

During the archaeological investigation of Slotseng, an east-west transect of the basin was uncovered, showing a complex pattern of sedimentation affected by dead ice melt, water-level changes, erosion, slumping and ice rafted debris (Mortensen *et al*., 2011). The central portion of the basin however was observed to contain undisturbed sediments. From this central section two monoliths were removed by Dr Morten Mortensen, National Museum of Denmark, covering a total of 218 cm of Lateglacial and early Holocene deposits. The monoliths used by this thesis are the same as those used for the pollen and plant macro fossil reconstruction of the site as presented by Mortensen *et al*. (2011).

4.4.2 Endinger Bruch, Germany

The Endinger Bruch core was recovered from the central portion of the former basin using a Usinger Corer (modified Livingstone corer) by Dr Pim de Klerk, University of Greifswald. The core was then sub-sampled and stored in 1 cm contiguous sections. The samples used by thesis are taken from the same core as used in the sites pollen reconstruction (de Klerk 2002) and microtephra investigation (Lane *et al*., 2011b).

4.4.3 Potremser Moor, Kieshofer Moor and Daschower Moor

Cores from all three sites were recovered by Dr Martin Theuerkauf, University of Greifswald, from the central portion of the former basins using a chamber corer of 1 meter in length and 8 cm in diameter. The samples used by the thesis are taken from the same core as the pollen reconstructions by Theuerkauf (unpublished data).

Unused sites

These sites were sampled as part of this thesis for the presence of microtephra. No tephra was identified therefore precluding these sites from further study. Additional site information can be found in Appendix I.

4.4.4 Lundby Mose, Denmark

A 377 cm core was recovered from the western edge of the former basin using a chamber corer by the author and Dr Rupert Housley. The core was taken from two core holes to ensure complete sediment recovery. The sediment was then transferred to 1 meter sections of plastic drainpipe before being wrapped in clingfilm and labelled for transportation.

4.4.5 Gedser, Denmark

A large trench was mechanically dug by the author and Dr Rupert Housley forming a transect across the former basin, exposing the Lateglacial sequence. From this a series of five 50 cm tins were for microtephra and palaeoproductivity analysis.

4.4.6 Tolk, Germany

A 496 cm core was recovered by Mara Weber, Schleswig-Holstein Museum, from the former lake shore using a Usinger corer in 2010. The sediment was transferred to 1 meter plastic drainpipe sections and wrapped in clingfilm for storage. The author sub-sampled these sections in August 2010, taking 20 cm ‘L’ channel sections for cryptotephra investigation.

4.4.7 Gorinsee, Germany

The Gorinsee profile was recovered by Dr Martin Theuerkauf, University of Greifswald, from the central portion of the former basin using a chamber corer of 1 meter in length and 8 cm in diameter. The samples used by the thesis are taken from the same core as the pollen reconstructions by Theuerkauf (unpublished data).

4.4.8 Weitsche, Germany

A series of two cores were recovered by Falko Turner, University of Hannover, from the former river channels at Weitsche using a chamber corer. The first (WVI) had a total length of 268 cm, whilst the second (WVIII) had a length of 98 cm. Both sets of cores were stored in plastic drainpipe sections and wrapped in clingfilm. The samples used by this thesis are taken from the same cores as the sites pollen reconstruction by Turner (unpublished PhD thesis).

4.5 Laboratory methods: Cryptotephra

All sites presented within this thesis were sampled by the author for cryptotephra, following the non-destructive density separation technique of Blockley *et al*., (2005). The only two exceptions to this are the site of Endinger Bruch which was sampled by Dr Christine Lane, University of Oxford (Lane *et al*., 2011b) and Slotseng which was sampled by Dr Alison Macleod, Royal Holloway, University of London. The methodologies employed within the cryptotephra investigation of this thesis are summarised within Figure 4.1 and will be discussed sequentially through 4.5.1 – 4.5.7.

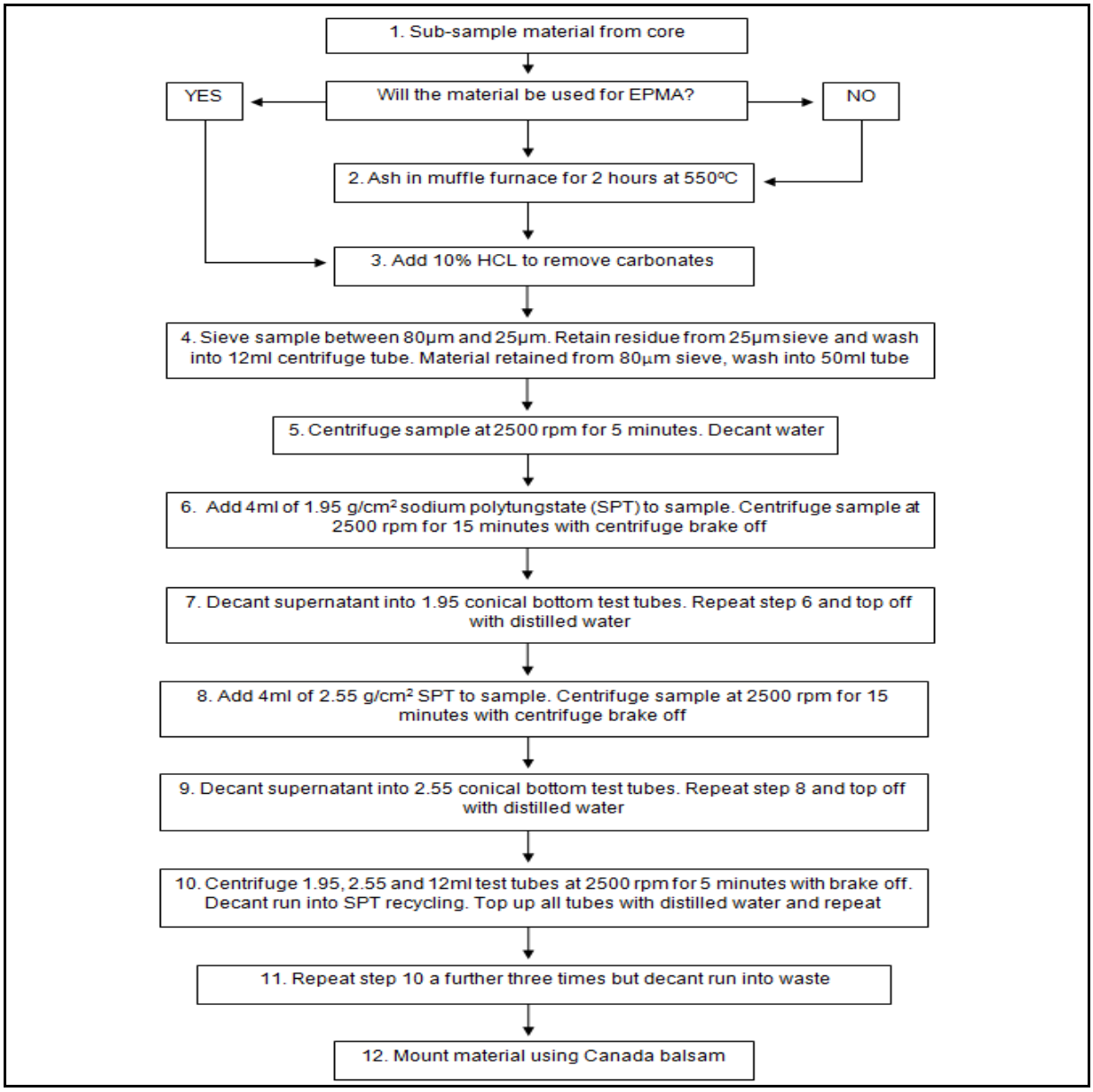


Figure 4.1 – Density separation procedure for the extraction of tephra shards from sediments within this thesis (after Blockley *et al*., 2005).

4.5.1 Sediment sampling

Sediment cores and monoliths were initially sampled at 10 cm contiguous and continuous intervals. 10 cm sections of sediment were bulked to form a single sample, for initial analysis at low depth resolution. Samples were then air dried at 60°C in a drying cabinet before being weighed, to allow eventual estimation of the total number of glass shards per gram of dry sediment (sg^{-1}).

Where glass shards were detected within the 10 cm scan samples, further contiguous 1 cm samples were taken at the corresponding depths of the greatest glass shard concentration in order to further refine the stratigraphic position of the cryptotephra.

4.5.2 Sieving

Prior to sieving, organic samples were ashed at 550°C for two hours to remove organics, carbonates were removed from the samples using 1 M HCl and left to react in a fume cupboard. De-calcified samples were then passed through 80 and 25 µm nylon mesh sieves using a plastic spatula to agitate samples where necessary. The residue from the 80 µm sieve, representing the course fraction of the sample, is then returned to the 50 ml test tubes and checked if tephra is found. The remaining 25 µm residue is washed into 12 ml round bottom test tubes and retained for extraction.

4.5.3 Density separation of samples

The method of extraction follows that of the non-destructive, heavy liquid flotation method outlined in Blockley *et* al., (2005) and is presented in Figure 4.1.

4.5.4 Alterations to density separation method (4.5.3)

An addition to the method outlined in Blockley *et al*., (2005) was made at the sites of Potremser Moor and Gorinsee. 10 cm scan samples showed a small presence of basaltic looking shards within the 1.95 – 2.55 g cm^{-3} fraction. Due to the presence of dense basaltic glass shards within both sites only a cleaning float of 1.95 g cm^{-3} was implemented before the remaining sediment was mounted for scanning.

4.5.5 Scanning

The 1.95 – 2.55 g cm^{-3} fraction is transferred onto glass slides using disposable plastic pipettes and allowed to dry over a hot plate. Once all water has evaporated from the glass slide, glass cover slips are placed on the slides using Canada balsam as a mounting medium. Glass slides are then examined using high powered (100 – 200X) optical microscopy under plane and crossed polarised light. Identified cryptotephra shards were counted and any morphological features noted. Shard

counts reported within chapter 6 are expressed as sg^{-1}, an exception to this is if absolute counts are < 5 and thus will be expressed in absolute numbers.

4.5.6 EPMA

Further 1cm depth samples were taken from where peaks in cryptotephra concentration were observed, and these prepared for geochemical analysis following the extraction methods described as above, with omission of ashing as this is known to alter glass chemistry (Blockley *et al*., 2005). In order to concentrate glass shards for analysis, shards were picked manually using a gas chromatography syringe with a transparent silica glass needle under high powered microscopy and mounted on epoxy resin stubs. Stubs were ground and polished to expose flat internal glass shard sections. Major element analysis was carried out using the JEOL JXA8600 electron microprobe, in wavelength dispersive mode (WD-EMPA) at the Research Laboratory for Archaeology and the History of Art (RLAHA), University of Oxford. EPMA is carried out in line with the recommended protocols set out in Kuehn *et al*., (2011). Nine major elements were analysed with varying analysis times (count times: Na, 10s; Mg, Al, Si, K, Ca and Fe, 30s; Ti and Mn, 40s) using an accelerating voltage of 15kV, a beam current of 6nA and a beam diameter of 10μm. The MPI-DING secondary standards of fused volcanic glass: KL2-Basalt (basaltic), ATHO-G (rhyolite) and STHS6/80-G (andesite), (Jochum *et al*., 2005; 2006) were used to monitor the precision of the data output and to ensure analytical accuracy. Single grain glass totals <95% were discarded, with all accepted data normalised to 100% for comparative purposes.

4.5.7 LA-ICP-MS

Trace element analysis was performed by laser ablation inductively coupled plasma mass spectrometry (LA-ICP-MS), using an Agilent 7500 ICP-MS coupled to a Resonetics 193 nm ArF eximer laser ablation system, with a two volume ablation chamber, at the Department of Earth Sciences, Royal Holloway University of London (Müller *et al*., 2009). LA-ICP-MS operating protocols and data quantification followed Tomlinson et al (2010). A 5 Hz repetition rate was used with a 40s count time on the sample and the gas blank. NIST 612 was used as the standard for calibration and ^{29}Si as the internal standard element, having previously been measured by single grain WD-EMPA. A

laser spot size of 25 µm was used due to the relatively small size of glass shards. As with WD-EMPA, ATHO-G and STHS6/80-G MPI-DING secondary standards were also analysed to monitor instrumental accuracy and precision.

4.5.8 Alterations to LA-ICP-MS (4.5.7)

In order to validate the correlation of POT-455 to the Saksunarvatn Ash (see section 5.1.3, Chapter 5) a sample from the type site at Saksunarvatn, as described by Mangerud *et al*., (1986) was also analysed by WD-EMPA, and for the first time, by LA-ICP-MS to determine the trace element composition of the volcanic glass. The Saksunarvatn Ash, located at 29.85 – 30.30 m within Lake Saksunarvatn, was sieved to > 63 µm then prepared and analysed following the same methods outlined above excepting a larger LA-ICP-MS spot size of 34 µm.

4.6 Laboratory methods: sedimentary stable isotope analysis

Sedimentary stable isotope analysis was performed at 5 cm intervals within the sites of Slotseng and Endinger Bruch and at 2 cm intervals within the sites of Potremser Moor, Kieshoffer Moor and Daschower Moor due to varying core lengths. All bulk sedimentary stable isotope analysis was conducted by the author with the assistance of Dr Peter Ditchfield at the RLAHA, University of Oxford. The methodologies employed within the isotopic investigation of this thesis are summarised within figure 4.2 and will be discussed sequential through 4.6.1 – 4.6.5

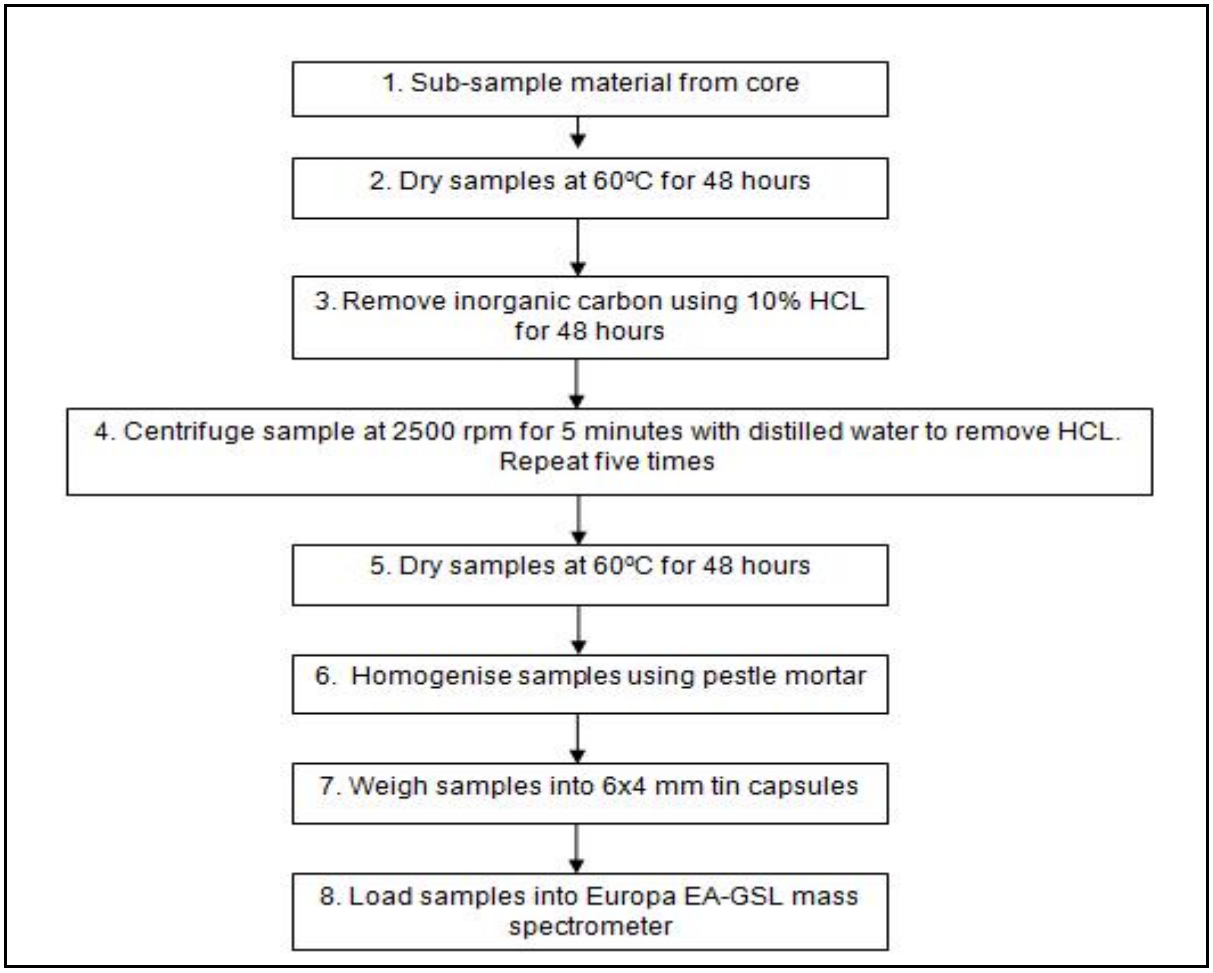


Figure 4.2 – Schematic representation of field and laboratory methodological approaches employed within the isotopic investigation of this thesis.

4.6.1 Sediment sampling

Sediment samples of 1 cm^3 were dried at 60°C in a drying cabinet before being weighed to determine dry weight and bulk density. Inorganic carbon was then removed from samples with 1 M HCl after being left to react for 48 hours in a fume cupboard. Sediment samples were then rinsed four times with de-ionised water and left to dry at 60°C before being re-weighed to determine total inorganic carbon content. Dried samples were homogenised using a pestle and mortar and appropriately sized sub-samples (< 10 mg) placed into 6 x 4 mm tin capsules and loaded into an auto sampler.

4.6.2 Mass spectrometry

Sedimentary carbon and nitrogen analysis was performed on a Ser-Con 20-22 carbon and nitrogen elemental analyser coupled to a Europa EA-GSL mass spectrometer set to operate in a continuous flow mode, with a He carrier gas and a flow rate of 70 ml per min (RLAHA, Oxford University). The tin capsules were dropped individually and combusted at temperatures exceeding 1000°C in an atmosphere of $O_{2,}$ with carbon converted to CO_2 and nitrogen converted to nitrogen gas. Gases were separated by gas chromatography and analysed individually. Values of organic ^{13}C expressed in conventional δ notation as the per mill deviation (‰) from the Vienna PeeDee Belemnite (VPDB) standard and organic ^{15}N expressed in conventional δ notation as per mill relative to atmospheric N_2. In order to ensure precision and accuracy within the data sets, samples were run against in house duplicate alanine standards ($\delta^{13}C$ = -26.91, $\delta^{15}N$ = -2.03) performed every six samples.

Site	Standard deviation: $\delta^{13}C_{org}$ (1σ)	Standard deviation: $\delta^{15}N_{org}$ (1σ)
Slotseng	<0.1 ‰	<0.05 ‰
Endinger Bruch	<0.1 ‰	<0.1 ‰
Potremser Moor	<0.1 ‰	<0.1 ‰
Kieshofer Moor	<0.1 ‰	<0.1 ‰
Daschower Moor	<0.1 ‰	<0.1 ‰

Table 4.1 – Error ranges for in-house alanine standards, based upon duplicate analyses performed every six samples.

4.6.3 Total organic carbon

TOC is expressed as the total amount of organic carbon by weight present within the total carbon fraction of a sediment sample and is thus given as:

$TOC = W_{tc} – W_{ic}$

Where: W_{tc} = weight of total carbon

W_{ic} = weight of inorganic carbon

4.6.4 Total nitrogen

TN is expressed as the total amount of nitrogen by weight present within the sediment sample and is thus given as:

$TN = (W_n / W_{dry}) * 100$

Where: W_n = weight of nitrogen in sample

W_{dry} = dry weight of sediment

Total Nitrogen (TN) are used as a proxy for the total amount of organic nitrogen within sediments as the total amount of inorganic nitrogen is usually low compared to organic nitrogen (Meyers, 1997). In organic-poor sediments (TOC <0.3) however, inorganic nitrogen can comprise a significant portion of the TN record, thus lowering C:N ratios (Rau *et* al., 1987; Calvert, 2004; Hyodo and Longstaffe, 2011). To test for this TN is plotted against TOC (Figure 4.3). The intercept of the TN –TOC regression on the TN axis is a measure of the sedimentary inorganic nitrogen content (Nijenhuis and de Lange, 2000). This procedure gives extremely low (<0.1 %) inorganic nitrogen contents for Endinger Bruch and Daschower Moor (Figure 4.3A and B). The relationship of TN and TOC however breaks down within Slotseng, Kieshofer Moor and Potremser Moor (Figure 4.3 B, C and E). The causes of this breakdown will be discussed further within sections 6.1.2; 6.3.2 and 6.4.2 Chapter 6.

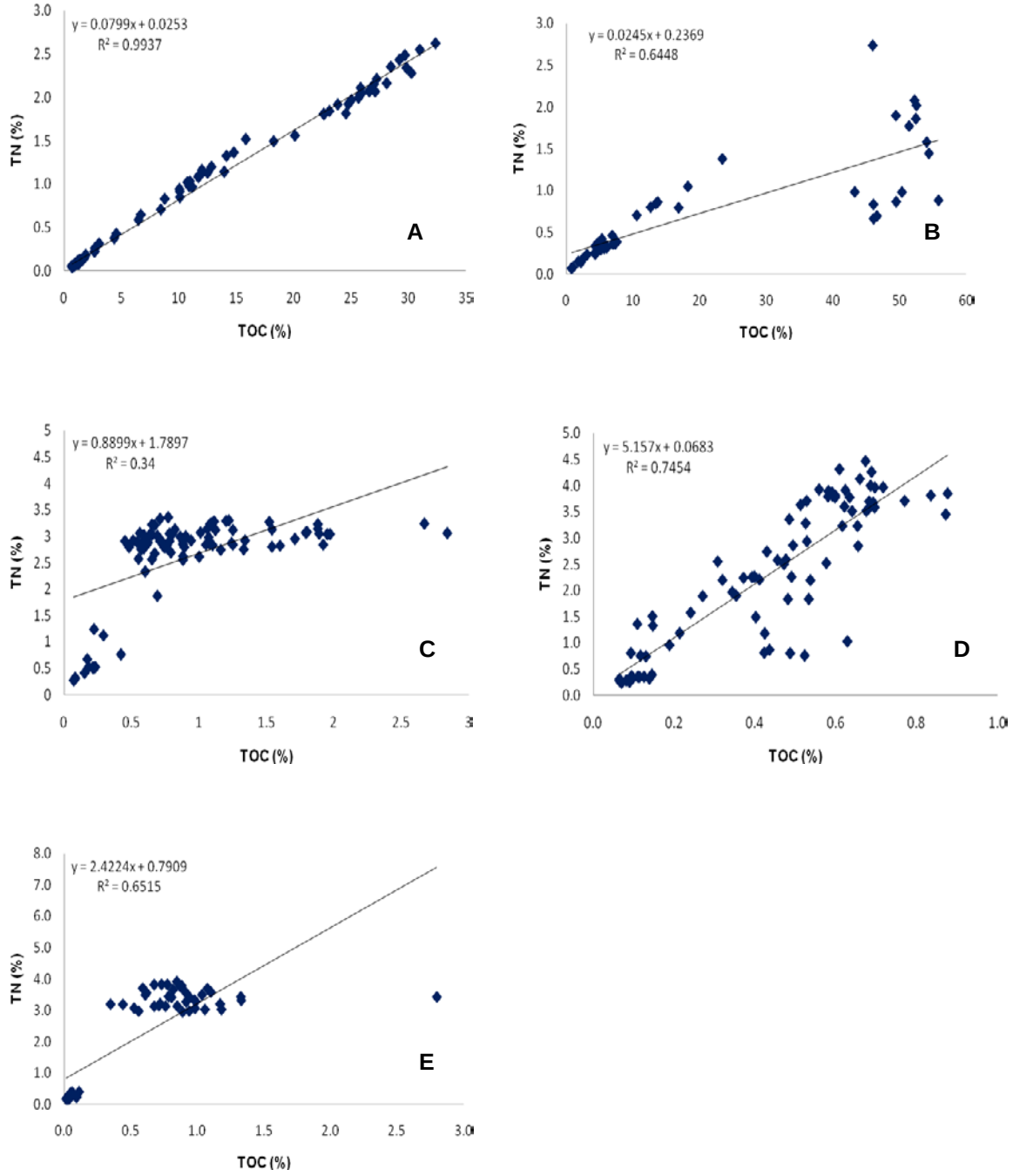


Figure 4.3 – Bi-plots of the realtionship between TOC (%) and TN (%). Data presented is the complete core record. Linear regression parameters given are according to the equation y = a·x+b. A – Endinger Bruch, B – Slotseng, Kieshofer Moor – C, Daschower Moor – D and Potremser Moor – E.

4.6.5 C:N ratios

C:N ratios are expressed as the molar ratio of carbon and nitrogen and are thus given as:

$C:N = (W_{carb} / 12) / (W_{nitro} / 14)$

Where: W_{carb} = total weight of carbon

W_{nitro} = total weight of nitrogen

An important issue to consider is diagenesis within the TOC record affecting C:N values. If organic matter losses related to post-depositional diagenesis dominated the TOC record within the five sites presented within this thesis, then one would expect a monotonic down-core trend of decreasing TOC values. While TOC (and TN) both decrease down-core (see Chapter 6) these decreases are discontinuous, and are associated in cases in sudden rises in TOC values. Its is therefore unlikely that organic matter diagenesis is affecting the TOC record. A high correlation between C:N and $\delta^{13}C_{org}$ may further indicate if digenesis has significantly altered the sedimentary record (Herczeg, 1988; Meyers, 1997; Sharma *et al*., 2005). Microbial degradation acts predominantly on the nitrogen-bearing compounds in lacustrine sediments leading to the preferential removal of ^{12}C to ^{13}C, resulting in lower $\delta^{13}C_{org}$ values (Herczeg, 1988; Meyers, 1997). There are three organic matter zones within the studied sites that show a strong correlation between C:N and $\delta^{13}C_{org}$. Two of these however (DOZ IV – r^2 0.708; SOZ III – r^2 0.728) are located in areas where the TOC – TN record has deviated, with high C:N and depleted $\delta^{13}C_{org}$ values serving to skew this relationship. The third isotopic zone (POZ I – r^2 0.795) is based upon a fragmentary data set of only five values, therefore making any relationships difficult to ascertain.

4.7 Laboratory methods: cladoceran analysis

Cladoceran sub-fossil analysis was performed at 5 cm intervals within the sites of Slotseng and Endinger Bruch and at 2.5 cm intervals within the sites of Potremser Moor, Kieshoffer Moor and Daschower Moor due to varying core lengths. All cladoceran analysis presented in this thesis was conducted by the author. Sample preparation was conducted at the RLAHA, University of Oxford; cladoceran counting and analysis was conducted at the Department of Zoology, University of Oxford.

The methodologies employed within the cladoceran investigation of this thesis are summarised within figure 4.4 and will be discussed sequentially through 4.7.1 – 4.7.2

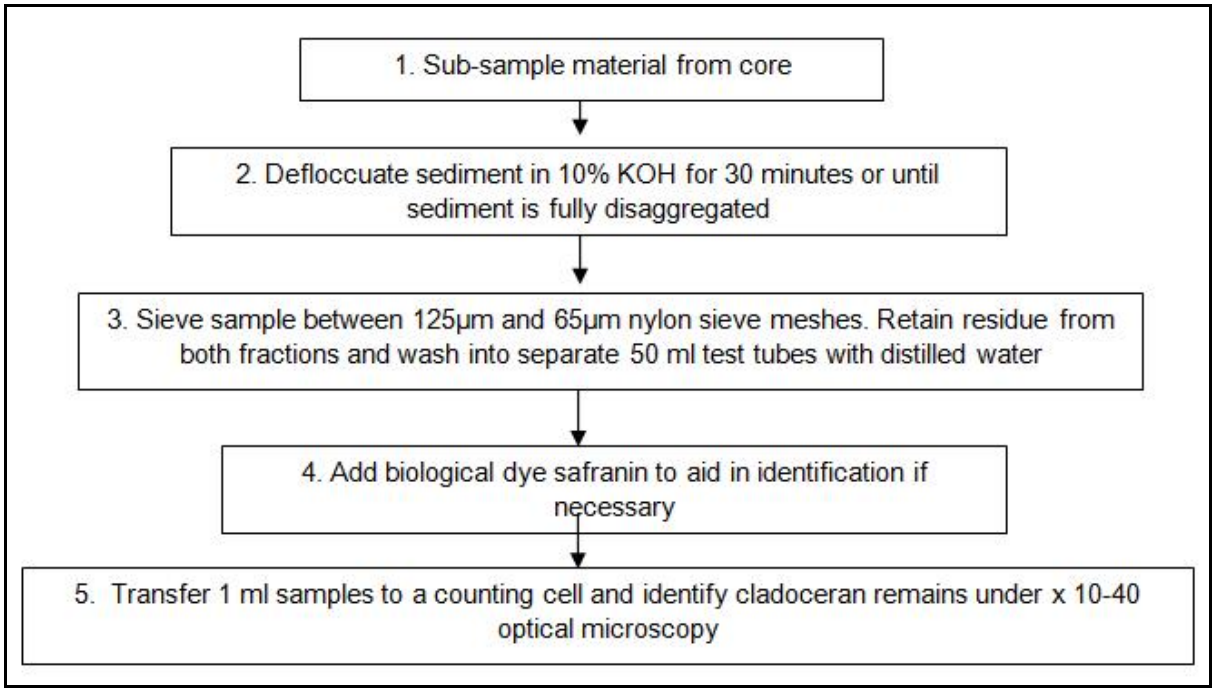


Figure 4.4 – Schematic representation of field and laboratory methodological approaches employed within the cladoceran investigation of this thesis.

4.7.1 Sediment sampling

Sediment samples of 2 cm^3 were disaggregated using 10 % KOH for 40 minutes then carefully washed through 125 and 65 µm nylon sieve meshes. The remaining residue from both fractions was retained and washed into separate 50 ml test tubes using distilled water. In order to aid in identification, the biological dye safranin was added to the 50 ml samples where necessary

4.7.2 Identification

Well mixed 1 ml samples were transferred to a Sedgewick Rafter© counting cell slide (50 mm x 20 mm x 1 mm) using disposable plastic pipettes and distilled water. Both the 125 and 65 µm fraction were analysed separately. Mucro length was recorded and measured within the species *Bosmina longirostris* and ephippia length within *Daphnia pulex* from a minimum of 20 individuals per sample. In order to ensure accurate representation of cladoceran sub-fossils, a minimum number of 100

individuals were recorded for the 125 µm fraction and 20 individuals for the 65 µm fraction following that of (Kurek *et al*., 2010). All cladoceran remains for the two fractions were tabulated separately, however only the most numerous parts were used for estimating taxon abundance. For instance, one half of a carapace would be counted as half an individual, while a headshield would count as a single individual. Cladoceran abundance was calculated to the total number of individuals per 50 ml sample.

Identification of cladoceran sub-fossils was made to species level with reference to Frey (1960; 1962) and Scourfield and Harding, (1966). The nomenclature follows that of Scourfield and Harding (1966).

4.8 Laboratory methods: radiocarbon dating

25 plant macrofossil samples were handpicked from Kieshoffer Moor, Daschower Moor, Potremser Moor and Gorinsee; whilst a further four bulk sediment samples were selected from Schunsmoor. Samples selected for AMS radiocarbon dating followed the standard ABA protocol of the ORAU, University of Oxford. The standard ABA protocol is intended to remove inorganic carbon, organic acid (humic and fulvic) contaminates and dissolved atmospheric CO_2 prior to combustion (Brock *et al*., 2010). For full ORAU pre-treatment, target preparation and AMS measurement see Bronk Ramsey *et al*., (2004) and Brock *et al*., (2010).

4.9 Laboratory methods: additional sedimentary analysis

4.9.1 Loss on ignition

Loss on ignition was performed at 1 cm intervals within the sites of Slotseng and at 5 cm intervals within Endinger Bruch. The sites of Potremser Moor, Kieshoffer Moor and Daschower Moor where all sampled at 2.5 cm intervals. The loss on ignition method is given below.

1 cm^3 of sediment was dried at 60°C in a drying cabinet before being weighed to determine dry weight. Samples were then placed in porcelain crucibles and ashed at 550°C for two hours to remove organics. The total LOI value is thus given as:

LOI 550°C = $(W_{dry} – W_{ash}) / (W_{dry}) * 100$

Where: W_{dry} = dry weight of sediment

W_{ash} = ashed weight of sediment

4.9.2 $CaCO_3$ content

$CaCO_3$ content analysis was performed at 5 cm intervals within the sites of Slotseng and Endinger Bruch and at 2.5 cm intervals within the sites of Potremser Moor, Kieshoffer Moor and Daschower Moor. The method for $CaCO_3$ content analysis is given below

Sediment samples of 1 cm^3 were dried at 60°C in a drying cabinet before being weighed to determine dry weight. $CaCO_3$ was removed from samples with 1 M HCl after being left to react for 48 hours in a fume cupboard. Sediment samples were then rinsed four times with de-ionised water and left to dry at 60°C before being re-weighed. The total $CaCO_3$ value is thus given as:

$CaCO_3 = (W_{dry} – W_{HCl}) / (W_{dry}) * 100$

Where: W_{dry} = dry weight of sediment

W_{HCl} = weight of sediment following HCl

4.9.3 Dry bulk density

Wet sediment samples of 1 cm^3 were dried at 60°C in a drying cabinet before being weighed to determine dry weight. Dry bulk density is thus given as:

Dry bulk density = (W_{dry}/V_{wet})

Where: W_{dry} = dry weight of sediment

V_{wet} = volume of wet sample

Dry bulk density was performed on material from the sites of Potremser Moor, Kieshofer Moor and Daschower Moor. This is due to drying out of sample material from Slotseng and Endinger Bruch, which prevented a wet sediment weight being recorded.

4.10 Chapter summary

The field and laboratory methods highlighted in Chapter 4 provide robust proxies for reconstructing Lateglacial aquatic system development. The further addition of microtephra analysis and ^{14}C dates allows this thesis to make chronological inferences based upon age models for each site.

Chapter 5: Results I Chronology

5.1 Potremser Moor tephrochronology

Primary 10 cm scans showed the presence of glass shards at 440 - 460 cm within Potremser Moor (OxT_7416 - OxT_7418). Further 1 cm contiguous scans showed that this concentration was formed of two discrete peaks of 1033 sg^{-1} recorded at 455 - 456 cm (POT- 455) and 325 sg^{-1} (absolute count 12) recorded at 446 - 447 cm (POT- 446) that appear midway through the main expansion of *Corylus* and a drop in *Pinus* (Theuerkauf and Joosten, unpublished data).

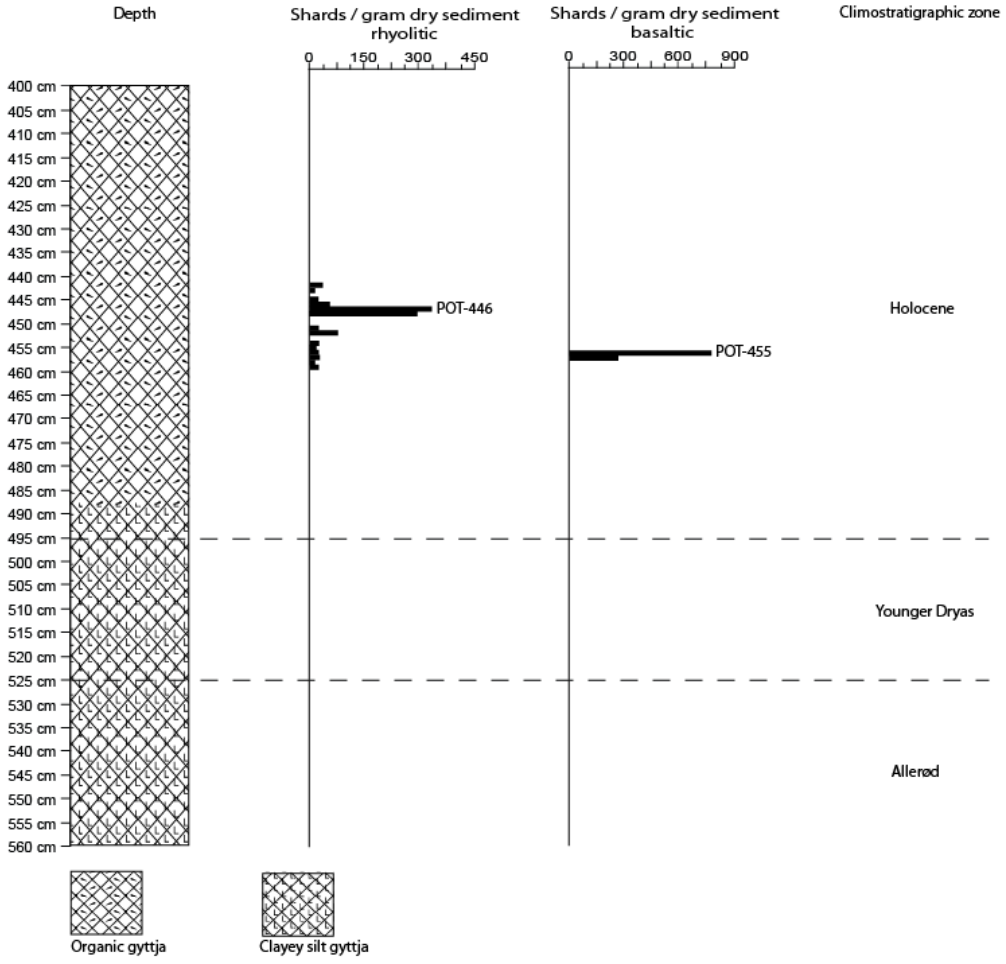


Figure 5.1 – Composite diagram showing shard counts (per gram dry sediment) from this study with lithology and relative chronozones within Potremser Moor (Theuerkauf, pers. comm.)

5.1.1 POT-455

Glass shards from the peak at 455 cm were almost exclusively brown in colour, with platey through to curvilinear morphologies and a maximum long axis length of 110 µm. A small number (absolute count 3) of colourless shards were also identified within the large peak in brown shards (Figure 5.1). An area of sediment, sterile of tephra, between 448 - 450 cm indicates therefore that the colourless shards within POT-455 are unlikely to be the product of down-core reworking from the peak at 446 cm and most likely to represent sporadic colourless shards amounts the brown shards. Geochemical analysis indicates that POT-455 is a tholeiitic basalt with glass compositional ranges of 49.12 - 50.49 wt% SiO_2, 1.72 - 2.63 wt% Na_2O, 0.33 - 0.56 wt% K_2O, 12.75 - 13.53 wt% Al_2O_3 and 12.52 - 14.55 wt% FeO, 9 ppm Rb, 170 - 180 ppm Zr and 17 - 18 ppm Nb (Table 5.1 and 5.2).

WDS-EPMA results: Tephra and secondary standards for POT-455

		SiO2	TiO2	Al2O3	FeO	MnO	MgO	CaO	Na2O	K2O	P2O5	Total
Tephra analysis												
POT-455 - (a)		50.36	2.99	13.16	14.24	0.24	5.30	10.05	2.37	0.43	0.34	99.48
		49.46	3.00	13.05	13.55	0.22	5.14	9.87	2.10	0.56	0.34	97.29
		50.49	2.85	13.53	12.52	0.17	5.01	9.62	2.24	0.30	0.34	97.07
		49.98	3.13	13.44	13.17	0.24	4.92	9.54	2.63	0.55	0.36	97.96
		49.71	3.14	12.98	14.26	0.28	5.59	10.06	2.11	0.47	0.34	98.93
		48.28	2.84	12.75	13.62	0.27	5.02	9.62	1.72	0.45	0.36	94.93
		49.58	2.79	13.09	14.08	0.28	5.77	8.78	2.32	0.33	0.38	97.42
		49.91	2.69	12.92	13.51	0.24	5.77	8.89	2.38	0.41	0.37	97.11
	average	49.72	2.93	13.11	13.62	0.24	5.32	9.55	2.23	0.44	0.36	97.52
	2 σ	1.37	0.32	0.52	1.18	0.07	0.70	0.97	0.53	0.18	0.03	
Secondary standards												
ATHO-G	average	75.37	0.25	12.26	3.28	0.11	0.10	1.68	4.22	2.76	0.03	100.06
	2 σ	0.21	0.02	0.09	0.12	0.02	0.02	0.05	0.22	0.03	0.01	
StHs6/80-G	average	63.32	0.72	17.59	4.31	0.10	1.99	5.32	4.67	1.32	0.15	99.49
	2 σ	0.33	0.03	0.17	0.15	0.03	0.04	0.04	0.10	0.02	0.01	
GOR132-G	average	45.50	0.32	10.96	10.15	0.16	22.53	8.42	0.84	0.03	0.03	98.94
	2 σ	0.14	0.04	0.05	0.11	0.03	0.14	0.09	0.04	0.01	0.02	
Tephra analysis												
POT-455 - (b)		49.81	2.91	13.18	14.13	0.27	5.72	10.08	2.58	0.45	0.25	99.38
		49.24	3.09	12.82	14.55	0.24	5.74	10.22	2.49	0.45	0.24	99.08
		49.12	3.05	12.87	14.38	0.26	5.75	9.99	2.50	0.43	0.24	98.60
	average	49.39	3.02	12.95	14.36	0.25	5.74	10.10	2.52	0.44	0.24	99.02
	2 σ	0.74	0.18	0.39	0.43	0.03	0.04	0.22	0.09	0.02	0.01	
Secondary standards												
ATHO-G	average	75.41	0.25	12.30	3.33	0.12	0.09	1.67	4.05	2.76	0.01	99.99
	2 σ	0.41	0.06	0.30	0.25	0.05	0.03	0.07	0.47	0.18	0.02	
StHs6/80-G	average	63.09	0.69	17.35	4.39	0.08	1.97	5.31	4.56	1.29	0.10	98.83
	2 σ	0.46	0.09	0.35	0.23	0.08	0.05	0.18	0.16	0.10	0.07	
GOR132-G	average	45.56	0.29	10.88	10.21	0.14	22.19	8.43	0.80	0.04	0.03	98.57
	2 σ	0.66	0.05	0.23	0.25	0.04	0.32	0.17	0.14	0.05	0.03	
GeoRem prefered value												
ATHO-G		75.60	0.26	12.20	3.27	0.11	0.10	1.70	3.75	2.64		99.62
	Uncertainty (95%)	0.70	0.02	0.20	0.10	0.01	0.01	0.03	0.31	0.09		
GeoRem prefered value												
StHs6/80-G		63.70	0.70	17.80	4.37	0.08	1.97	5.28	4.44	1.29		99.63
	Uncertainty (95%)	0.50	0.02	0.20	0.07	0.00	0.04	0.09	0.14	0.02		
GeoRem prefered value												
GOR132-G		45.50	0.31	11.00	10.10	0.15	22.40	8.45	0.83	0.03		98.77
	Uncertainty (95%)	0.40	0.01	0.20	0.10	0.01	0.20	0.12	0.04	0.00		
GeoRem prefered value												
GOR128-G												
	Uncertainty (95%)	46.10	0.29	9.91	9.81	0.18	26.00	6.24	0.57	0.04		99.13
		0.40	0.01	0.17	0.12	0.01	0.30	0.12	0.03	0.01		

Table 5.1 – Non-normalised major and minor elemental oxide compositions for POT-455 from two EPMA runs (a and b; Bramham-Law *et al*., 2013). Intermittent analysis of MPI-DING volcanic glass standards ATHO-G and StHs6/80-G (Jochum *et al*., 2005; 2006; http://georem.mpch-mainz.gwdg.de/) were used as secondary standards to check for accuracy and measure precision during EPMA analysis.

LA-ICP-MS results: Tephra and secondary standards for POT-455

		Rb	Sr	Y	Zr	Nb	Ba	La	Ce	Pr	Nd	Sm	Eu	Gd	Dy	Er	Yb	Ta	Th	U	Spot size (μ)
Tephra anlysis																					
POT-455																					
		9	182	37	171	18	83	13	34	5	22	6	2	6	7	4	4	1	1	<LOD	25
		9	186	38	175	17	83	14	35	4	23	6	2	6	7	4	4	1	1	<LOD	25
		9	182	36	180	18	82	14	33	4	21	6	2	7	7	4	3	1	1	<LOD	25
		9	184	35	170	17	80	12	33	4	22	7	2	6	7	4	4	1	1	<LOD	25
Secondary standards																					
ATHO-G	**Obeserved**	66	91	89	482	57	541	54	118	14	61	14	2	14	16	10	10	4	7	2	25
	Certified	65	94	95	512	62	547	56	121	15	61	14	3	15	16	10	11	4	7	2	25
StHs6/80-G	**Obeserved**	30	469	11	110	6	293	11	25	3	11	<LOD	1	<LOD	2	1	<LOD	<LOD	2	1	25
	Certified	31	482	11	118	7	298	12	26	3	13	3	1	3	2	1	1	0	2	1	25

Table 5.2 – LA-ICP-MS results for POT-455 from Potremser Moor (Bramham-Law *et al*., 2013). <LOD indicates samples below 6σ of the background. Intermittent analysis of MPI-DING volcanic glass standards ATHO-G and StHs6/80-G (Jochum *et al*., 2005; 2006; http://georem.mpch-mainz.gwdg.de/) were used as secondary standards to check for accuracy and measure precision during LA-ICP-MS.

5.1.2 POT-446

A peak in shard concentration of 325 sg^{-1} (absolute count 12) was recorded at 446 - 447 cm (Figure 5.1). Glass shards were colourless, showing irregular and fluted morphologies with occasional closed vesicles and a maximum long axis length of 30 μm. Following repeated efforts to chemically characterise POT-446 using WDS-EMPA, only a single geochemical analysis was produced. Whilst indicating a glass shard of rhyolitic composition, the total single grain glass total was 91.45% and therefore had to be rejected. The sediment from which tephra was extracted was a fine algal/detrital gyttja with a high water content. Approximately 2 cm^3 of sediment was sampled for each tephra layer, but when dried this yielded dry weights of < 0.1 g, therefore giving artificially high shard g^{-1} counts. Repeated efforts to produce more shards for WDS-EPMA were not possible, due to the limited core material available and low absolute shard counts.

5.1.3 Geochemical comparison of POT-455

The major and minor elemental glass composition POT-455 is indistinguishable from the Saksunarvatn Ash recognised from the type site on the Faroe Islands (see Bramham-Law *et al*., 2013), GRIP 1528.61 m and LINK 15:185 (Figure 5.2A, B and C). However through the comparison of single-grain glass trace element ratios Davies *et al*., (2012) show a compositional distinction (based

on Zr/Ce – Y/Ce ratios, Figure 5.3C) between two tephra layers correlated to the Saksunarvatn Ash from the Greenland ice core GRIP 1528.61 m (Grönvold *et al*., 1995) and North Atlantic marine core LINK 14:185 (Rasmussen *et al*., 2011).

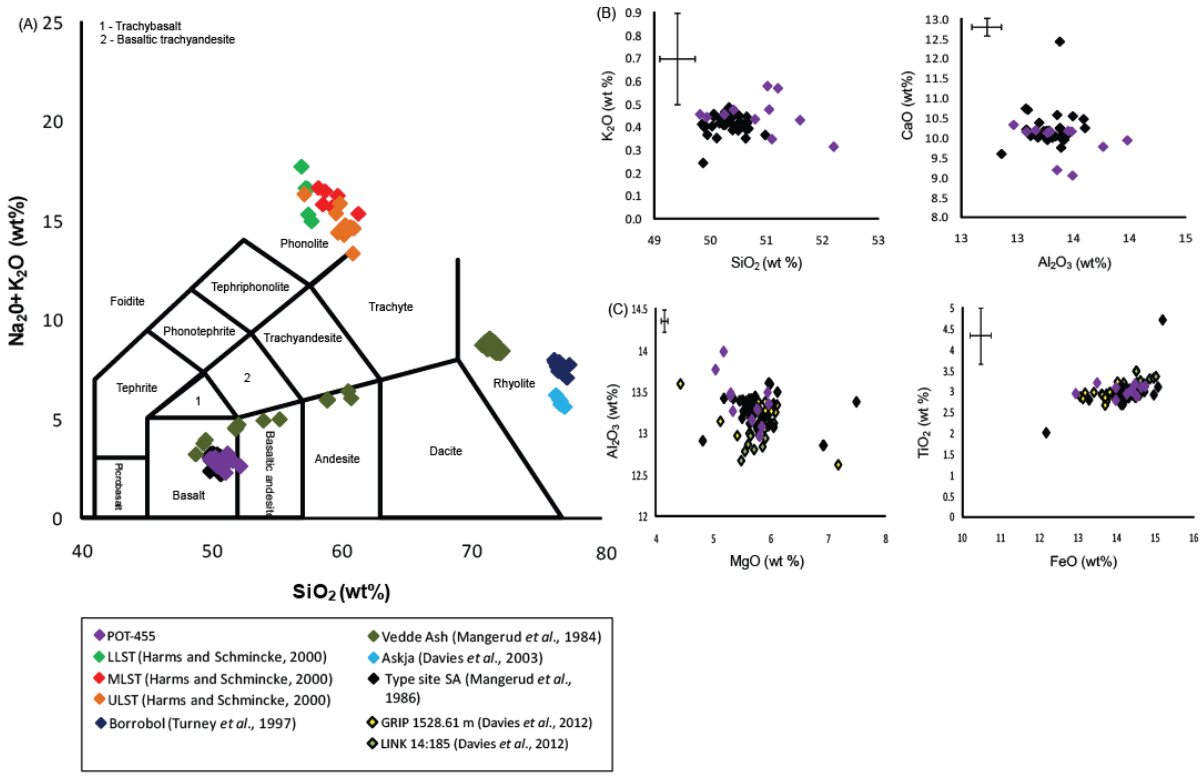


Figure 5.2 – Major and minor element plots of POT-455 with selected major northern European Lateglacial tephras. All major and minor data plotted as normalised values. (A) Total-alkali-silica (after Le Bas *et al*., 1986) plot of POT-455 and selected Lateglacial and early Holocene European tephras. (B) Selected bi-plots of POT-455 with type site Saksunarvatn Ash as reported by Mangerud *et al*., (1986). (C) Selected bi-plots of POT-455 with comparison of Saksunarvatn Ash type site (Bramham-Law *et al*., 2013), GRIP 1528.61 m and LINK 15:185 (Davies *et al*., 2012). Representative 2σ are indicated for each bi-plot within B (upper left) based upon precision established from secondary standard analysis (Table 5.1). Figure adapted from Bramham-Law *et al*., (2013).

The composition of POT-455 and data from the type site Saksunarvatn Ash is more consistent with the data from LINK 14:185, than GRIP 1528.61 m, (Figure 5.3C). It is therefore likely that the Saksunarvatn Ash found within Potremser Moor was produced by the same eruption that formed the

ash layer within the type site and within LINK 14:185, but separate from the eruption that produced the Saksunarvatn Ash layer within GRIP 1528.61 m (Bramham-Law *et al*., 2013).

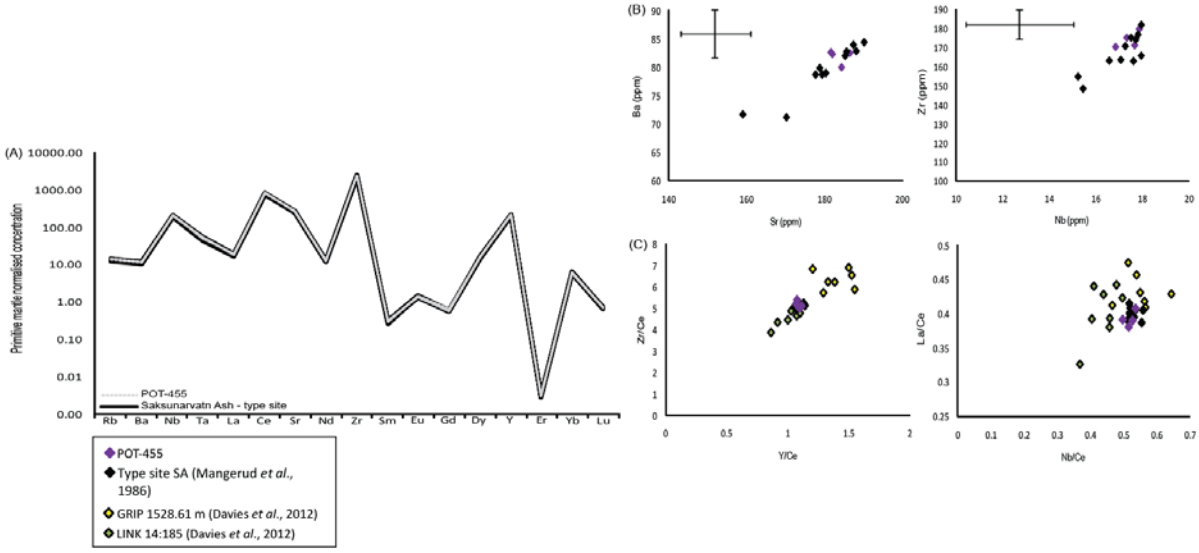


Figure 5.3 – POT-455, Saksunarvatn Ash, GRIP 1528.61 m and LINK 14:185 trace element plots. (A) Primitive mantle normalised trace element composition profile (after Sun and McDonough 1989) of POT-455 and type site Saksunarvatn Ash. (B) Selected bi-plots of trace element concentrations showing comparison of POT-455 with type site Saksunarvatn Ash (Mangerud *et al*., 1986). Representative 2σ uncertainties are indicated for each bi-plot (upper left) based upon precision established from secondary standard analysis (Table 5.2). (C) Selected trace element ratio bi-plots for comparison of POT-455 and type site Saksunarvatn Ash with Saksunarvatn Ash reported from GRIP 1528.61 m (Grönvold et al., 1995; Davies et al., 2012) and LINK 14:185 (Davies et al., 2012, Rasmussen et al., 2011). Figure adapted from Bramham-Law *et al*., (2013).

Comparison of age estimates for the Saksunarvatn Ash from Greenland (10,297 ± 45 GICC05 a BP; Rasmussen *et al*., 2006) and Norway (10,210 ± 35 cal yr BP; Lohne *et al*., 2013) also are consistent with the hypothesis of separate eruptions, with an initial, older eruption with a northwest dispersal axis followed by the Saksunarvatn eruption, which was dispersed to the southeast towards the Faroe Islands and continental Europe, forming the Saksunarvatn Ash type ash (Bramham-Law *et al*., 2013; Figure 5.4). Based upon this, this thesis will utilise the age of 10,210 ± 35 cal yr BP; Lohne *et al*., 2013) for the Saksunarvatn Ash within Potremser Moor which is consistent with the age of the younger eruption dispersed to the southeast. Positive correlation of POT-455 with the Saksunarvatn

Ash provides the first *in-situ* calendrical age estimate for the Potremser Moor chronology and allows the tephra isochrone to be correlated with the Saksunarvatn Ash present in Kråkenes, Norway with an age of 10,210 ± 35 cal yr BP (Bramham-Law *et* al., 2013; Lohne *et al*., 2013).

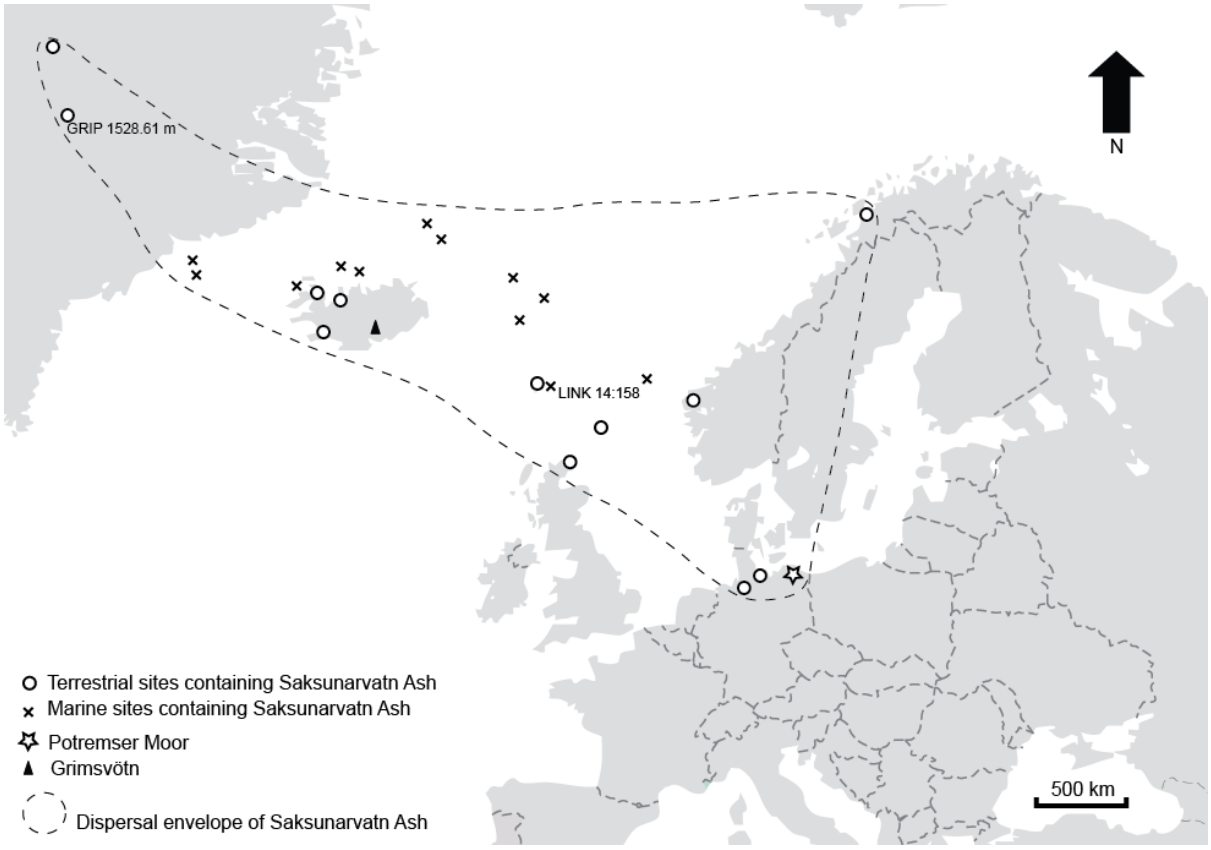


Figure 5.4 – Distribution envelope of the Saksunarvatn Ash identified within terrestrial and marine records as primary air-fall deposits based upon published data (Jóhansen, 1977; Mangerud *et al*., 1986; Haflidason *et al*., 1990; Sjøholm *et al*., 1991; Bennet *et al*., 1992; Björck *et al*., 1992; Koç and Jansen, 1992; Merkt *et al*., 1993; Sigurgeirsson and Leosson, 1993; Bunting, 1994; Grönvold *et al*., 1995; Haflidason *et al*., 1995; Ingólfsson *et al*., 1995; Birks *et al*., 1996; Dugmore and Newton, 1998; Eiríksson *et al*., 2000; Haflidason *et al*., 2000; Wastegård *et al*., 2001; Geirsdóttir *et al*., 2002; Jennings *et al*., 2002; Caseldine *et al*., 2003; Bondevik et al*.,* 2005 Mortensen *et al*., 2005; Lind and Wastegård, 2011; Rasmussen et al., 2011; Aarnes *et al*., 2012). Adapted from Bramham-Law *et al*., (2013).

5.1.4 Potremser Moor radiocarbon dates

A total of five macrofossil samples were submitted for radiocarbon analysis at the ORAU, of these three yielded suitable ^{14}C dates, while the other two (408 and 410 cm) yielded modern ages and consequently were not used (Table 5.3). An issue with dating Potremser Moor was the availability of suitably large plant macrofossils (Theuerkauf *pers. comm.*). A consequence of this was the reliance on small sample sizes producing low carbon yields (0.5 - 1.2 mg) therefore increasing the age uncertainties of the samples. The addition of the Saksunarvatn Ash (Bramham-Law *et al*., 2013) has been used to refine the subsequent age model for the site; however the uncertainties coupled with 447 cm, 471 cm and 482 cm serves to reduce the models precision. The large age uncertainties are due to scatter in the standards caused by small carbon yields.

Depth (cm)	Lab Code	Material	$\delta^{13}C$ (‰ VPDB)	^{14}C age (yr BP)	Model age	A
447	OxA - 2495-48	Assorted plant macrofossils	-25.13	8610 ± 230	10251 - 9491	70%
471	OxA - 2495-40	Assorted plant macrofossils	-20.85	8880 ± 160	10487 - 10197	29%
482	OxA - 2495-38	Assorted plant macrofossils	-25.94	9330 ± 100	10666 - 10227	90%
408	OxA - 2495-18	Assorted plant macrofossils	-25.13	modern	n/a	n/a
410	OxA - 2496-39	Assorted plant macrofossils	-24.25	modern	n/a	n/a

Table 5.3 – ^{14}C dates and modelled ages for samples from Potremser Moor. Dates calibrated using OxCal 4.2.2 (Bronk Ramsey, 2009a) and IntCal 09 (Reimer *et al*., 2009). Column A refers to the model agreement index.

5.1.5 An age model for Potremser Moor

Using the Saksunarvatn Ash and the three available ^{14}C dates a Bayesian depositional model (following Bronk Ramsey, 2008) was constructed using OxCal 4.2.2 and IntCal 09 (Reimer *et al*., 2013) for the Potremser Moor core between 495 - 440 cm (Figure 5.5). The P_Sequence model has been used to reflect variable sedimentation rates with depth coupled with an outlier probability of 0.05 in a *General* outlier model and a *k* value = 1. Sedimentation rates between 495 - 440 cm are in the order of 1.7 mm y^{-1} and are generally consistent; however with only four dates to constrain the model,

minor sedimentary fluctuations may be missed. The basin during this time was characterised by shallow water conditions that were dominated by aquatic macrophytes (see section 6.3.6, Chapter 6) and coupled with landscape stabilisation during the early Holocene it is likely that sedimentation is being driven by the deposition of aquatic macrophyte derived organic material. The ^{14}C dates from Potremser Moor are largely indistinguishable within errors (Table 5.3). It is only through the use of the Saksunarvatn Ash isochrone that the age model is able to find an accurate solution for the Potremser Moor age model (Figure 5.5).

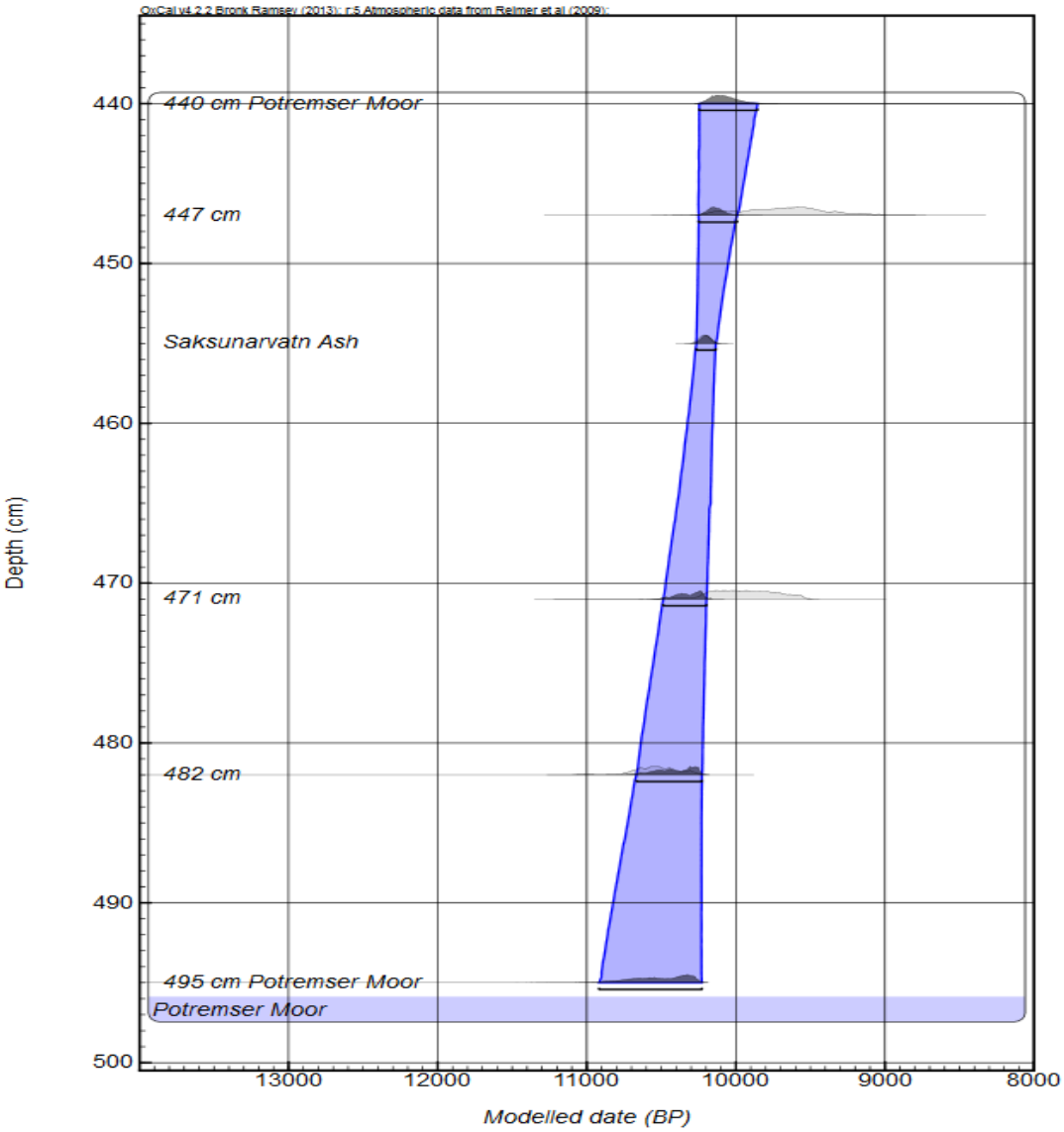


Figure 5.5 – Bayesian P_Sequence depositional model for Potremser Moor, based upon three ^{14}C dates and the Saksunarvatn Ash. Model was constructed following Bronk Ramsey, (2008) using

OxCal 4.2.2 and IntCal 09 (Reimer *et al*., 2009). An outlier probability of 0.05 was used within a *General* outlier model coupled with a *k* value = 1 to allow for variations in sedimentation rates.

5.2 Kieshofer Moor tephrochronology

Visual inspection indicated presence of a visible ash layer between 795.5 – 797 cm (OxT_7267), while additional 10 cm scans throughout the rest of the core indicate the presence of glass shards between 620 – 630 cm (OxT_7250) and 740 – 750 cm (OxT_7262). Further 1 cm contiguous scans showed the presence of two peaks in glass shard concentration of 50 shards g^{-1} (absolute count 3) between 622 – 623 cm (KHM-622) and 30 shards g^{-1} (absolute count 3) at 749 – 750 cm (KHM-749).1 cm contiguous samples taken between 790 – 800 cm showed a peak in shard concentration of > 500,000 shards g^{-1} (KHM-796) coinciding with the visible ash layer.

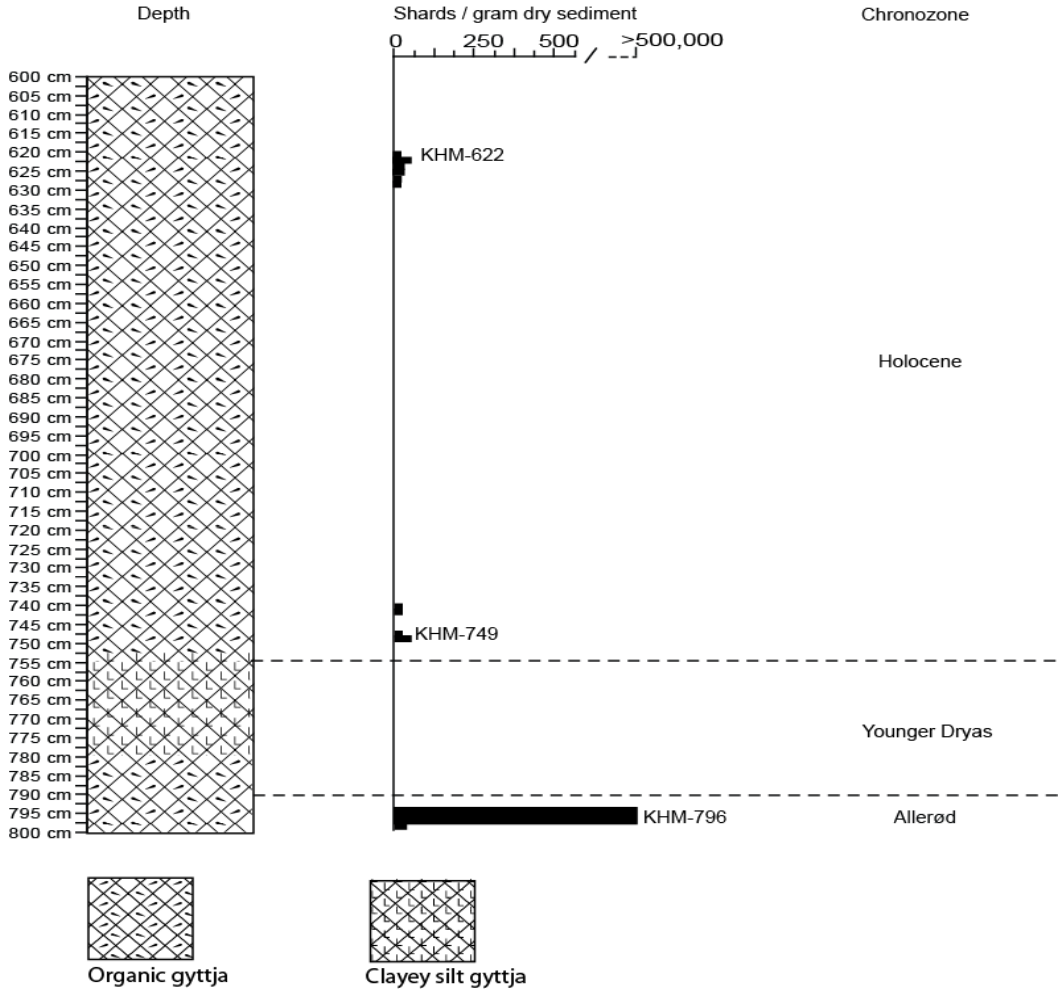


Figure 5.6 – Composite diagram showing shard counts (per gram dry sediment) from this study with lithology and relative chronozones (Theuerkauf, pers. comm.) within Kieshofer Moor.

5.2.1 KHM-796

The oldest tephra layer with Kieshofer Moor is located within late Allerød organic gyttja just prior to the onset of Younger Dryas (Figure 5.6). KHM-796 is contained within 6 cm of sediment between 794 – 800 cm with geochemical analysis carried out on the peak in shard concentration located at 796 cm. Glass shards are all highly vesicular with closed vesicle forms with a maximum long axis of 90 µm. Geochemical analysis indicates that KHM-796 is a phonolite with a K-rich profile. Major element glass composition gives ranges of 57.34 - 58.66 wt% SiO_2, 10.02 - 11.77 wt% Na_2O, 4.92 - 5.34 wt% K_2O, 21.61 - 22.27 wt% Al_2O_3 and 1.48 - 1.6 wt% FeO (Table 5.4).

WDS-EPMA results: Tephra and secondary standards for KHM-796

		SiO_2	TiO_2	Al_2O_3	MgO	CaO	MnO	FeO	Na_2O	K_2O	*Total*
Tephra analysis											
KHM-796 - (a)		54.92	0.09	22.27	0.02	0.36	0.11	1.49	11.25	4.78	95.60
		53.38	0.13	21.61	0.04	0.38	0.15	1.38	10.63	4.64	92.73
	average	54.15	0.11	21.94	0.03	0.37	0.13	1.43	10.94	4.71	94.16
	2 σ	2.17	0.05	0.92	0.03	0.03	0.05	0.16	0.88	0.19	
Secondary standards											
ATHO-G	**average**	75.06	0.26	12.38	0.10	1.67	0.04	3.32	4.14	2.75	99.75
	2 σ	0.27	0.03	0.08	0.02	0.06	0.04	0.15	0.13	0.04	
StHs6/80-G	**average**	63.55	0.72	17.83	1.95	5.31	0.03	4.43	4.50	1.34	99.83
	2 σ	0.18	0.03	0.15	0.04	0.06	0.02	0.16	0.17	0.03	
KHM-796 - (b)		52.17	0.15	21.89	0.01	0.37	0.39	1.30	14.34	4.18	95.39
		56.18	0.14	22.94	0.01	0.38	0.49	1.53	11.76	4.78	98.56
		54.87	0.15	22.78	0.02	0.41	0.51	1.62	13.49	4.75	98.93
		53.20	0.13	21.92	0.03	0.37	0.48	1.57	10.76	4.51	93.28
		56.88	0.15	22.67	0.01	0.43	0.49	1.61	11.35	4.66	98.60
		55.12	0.11	22.11	0.04	0.43	0.52	1.57	11.03	4.60	95.88
		56.37	0.14	23.08	0.03	0.49	0.54	1.51	11.30	4.74	98.52
		56.92	0.12	23.68	0.02	0.40	0.56	1.41	11.67	4.87	99.96
		53.73	0.11	21.83	0.05	0.36	0.50	1.55	10.99	4.33	93.81
		54.98	0.09	22.11	0.03	0.39	0.48	1.65	12.83	4.88	97.71
		56.85	0.13	23.03	0.02	0.35	0.52	1.45	12.03	4.74	99.46
		55.88	0.13	22.72	0.04	0.36	0.50	1.48	10.53	4.76	96.74
		52.28	0.10	22.33	0.03	0.35	0.36	1.37	12.29	4.07	94.29
		54.20	0.12	21.07	0.07	0.40	0.44	1.56	10.81	4.61	93.54
		53.54	0.13	20.51	0.03	0.39	0.43	1.53	11.08	4.59	92.52
	average	54.88	0.13	22.31	0.03	0.39	0.48	1.51	11.75	4.60	96.48
	2 σ	3.27	0.04	1.63	0.03	0.08	0.11	0.20	2.17	0.48	
Secondary standards											
ATHO-G	**average**	75.31	0.22	12.43	0.10	1.63	0.09	3.27	3.98	2.72	99.75
	2 σ	0.71	0.16	0.28	0.05	0.08	0.05	0.39	0.46	0.06	
StHs6/80-G	**average**	63.65	0.70	17.78	1.97	5.15	0.10	4.38	4.36	1.30	99.40
	2 σ	0.52	0.11	0.50	0.09	0.21	0.02	0.39	0.44	0.14	
GeoRem prefered value											
StHs6/80-G		63.70	0.70	17.80	1.97	5.28	0.08	4.37	4.44	1.29	99.63
	Uncertainty (95%)	0.50	0.02	0.20	0.04	0.09	0.00	0.07	0.14	0.02	
GeoRem prefered value											
ATHO-G		75.60	0.26	12.20	0.10	1.70	0.11	3.27	3.75	2.64	99.62
	Uncertainty (95%)	0.70	0.02	0.20	0.01	0.03	0.01	0.10	0.31	0.09	

Table 5.4 – Non-normalised major and minor elemental oxide compositions for KHM-796 from two EPMA runs (a and b). Intermittent analysis of MPI-DING volcanic glass standards ATHO-G and StHs6/80-G (Jochum *et al*., 2005; 2006; http://georem.mpch-mainz.gwdg.de/) were used as secondary standards to check accuracy and measure precision during analysis.

5.2.2 KHM-749

The peak of 30 g^{-1} was located within organic algal gyttja coinciding with the early Holocene (Figure 5.6). Glass shards were non-vesicular, platey (with some bi-cuspate and fluted features) and colourless, with maximum long axis lengths of 50 µm. Following glass shard separation it was not possible to extract any shards for EPMA. As with POT-446 (section 5.1.2) the limited amounts of core material and low absolute counts made further sampling for WDS-EPMA impossible.

5.2.3 KHM-622

The peak of 50 g^{-1} was located within Holocene organic algal gyttja (Figure 5.6). Glass shards were non-vesicular, platey and colourless with a maximum long axis of 55 µm. Following glass shard separation it was not possible to extract any shards for WDS-EPMA due to the same conditions experienced with KHM-749.

5.2.4 Geochemical comparison of KHM-796

The results of WDS-EPMA are presented in Table 5.4 and elemental plots (Figure 5.7) where they are compared to the three phases of the Laacher See Eruption. The Laacher See Tephra (LST) is represented by three main phases within the northern European record based on the dispersal of an evolving magma by varying wind directions in the troposphere, with the upper phase generally constrained to the south of the Eifel region, while the middle and lower phases are distributed to the North-East throughout Germany, Poland, Denmark and Sweden. Major element glass composition of the lower, middle and upper phases of the LST is plotted in Figure 5.7. The closest compositional match based on major elements is to the lower phase of the LST. This is entirely consistent with reported distal LST major elemental chemistry reported from northern Germany (Lane *et al*., 2011b; Riede *et al*., 2011). The eruption of the LST has been dated by varve counting within Eifel lakes to 12,880 ± 40 (Brauer et al., 1999) which phases it firmly within the later stages of the Allerød, approximately 200 years before the onset of the Younger Dryas.

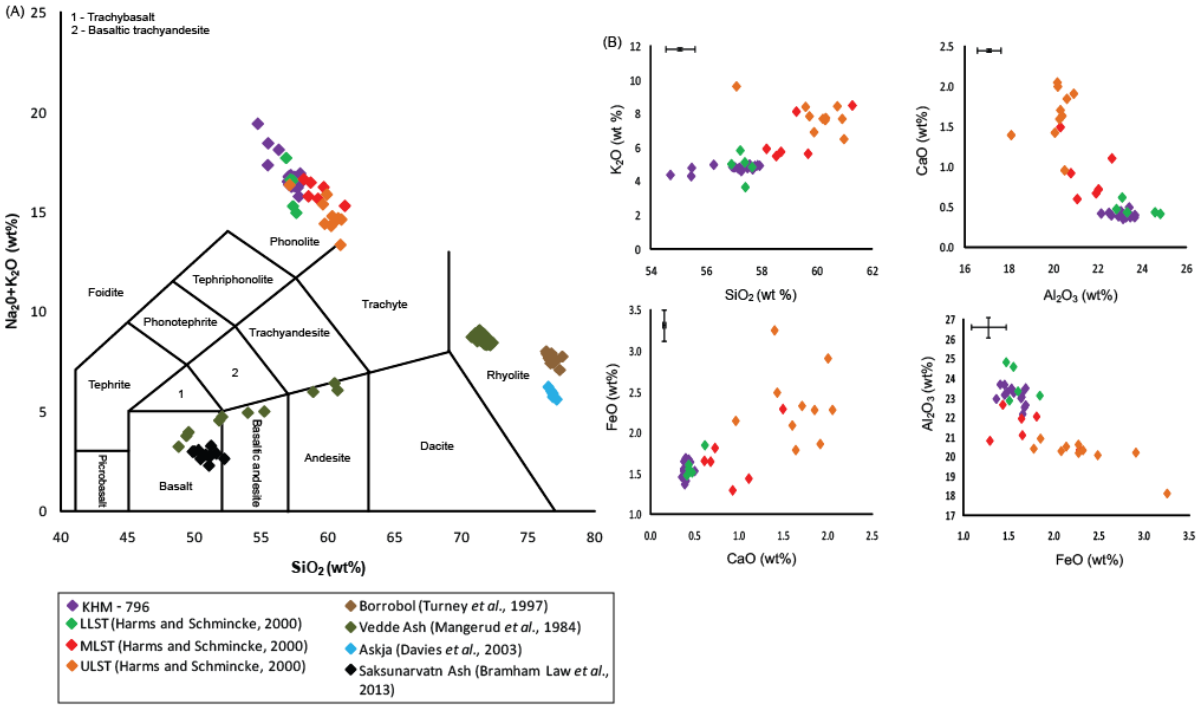


Figure 5.7 – Major and minor element plots of KHM-796 with selected major northern European Lateglacial tephras (A) Total-alkali-silica (after Le Bas *et al*., 1986) plot of KHM-796 and selected Lateglacial and early Holocene European tephras. (B) Selected bi-plots of KHM-796 with the three phase of the Laacher See eruption as reported by Harms and Schmincke, (2000). Representative 2σ are indicated for each bi-plot within B (*upper left*) based upon precision established from secondary standard analysis (Table 5.4). All major and minor data plotted as normalised values.

5.2.5 Kieshofer Moor radiocarbon dates

A total of 10 plant macrofossil samples were submitted for radiocarbon analysis at the ORAU, of these nine yielded ^{14}C ages and a single sample giving a modern age (Table 5.5). As with Potremser Moor, there was significant difficulty in obtaining sufficient material for ^{14}C dating and with those age estimates gained represented by low carbon yields (<1.2 mg); a consequence of this therefore is larger age uncertainties associated with the un-modelled dates in the order of 110 – 290 cal yr BP. In order to address this issue and evaluate the accuracy of the age model, a series of seven ^{14}C dates have also been calibrated from a neighbouring core located ~10 m from the original within the same basin, with the LST used as link between the two records (Figure 5.8).

Depth (cm)	Lab Code	Material	$\delta^{13}C$ (‰ VPDB)	^{14}C age (yr BP)	Model age	A
676	OxA - 2495-31	Assorted plant macrofossils	-27.137	2820 ± 210	10533-1937	32%
688	OxA - 2495-45	Assorted plant macrofossils	-24.015	2310 ± 140	10533-2121	26%
690	OxA - 2495-32	Assorted plant macrofossils	-23.938	9140 ± 170	10559-2204	33%
716	OxA - 2495-46	Assorted plant macrofossils	-26.464	8780 ± 270	10999-9303	58%
730	OxA - 2495-35	Assorted plant macrofossils	-24.267	9650 ± 100	11247-10674	102%
770	OxA - 2495-47	Assorted plant macrofossils	-24.233	3040 ± 260	12554-11673	6%
772	OxA - 2495-36	Assorted plant macrofossils	-27.022	7320 ± 290	12569-11983	7%
774	OxA - 2495-37	Assorted plant macrofossils	-26.239	10400 ± 110	12566-12799	115%
714	OxA - 2495-33	Assorted plant macrofossils	-25.78	modern	n/a	n/a
Neighbouring core						
141	Poz-35882	Assorted plant macrofossils	n/a	290 ± 30	modern	6%
224	Poz-35883	Assorted plant macrofossils	n/a	645 ± 30	670-556	103%
245	Poz-35884	Assorted plant macrofossils	n/a	1160 ± 30	1144-977	107%
335	Poz-35885	Assorted plant macrofossils	n/a	2635 ± 30	2841-2724	101%
436	Poz-35887	Assorted plant macrofossils	n/a	4300 ± 35	4965-4829	99%
566	Poz-35888	Assorted plant macrofossils	n/a	8170 ± 50	8313-7152	6%
651	Poz-35889	Assorted plant macrofossils	n/a	8900 ± 50	10176-8717	58%

Table 5.5 – ^{14}C dates and modelled ages for samples from Kieshofer Moor and the neighbouring core (Theuerkauf, pers. comm.). Dates calibrated using OxCal 4.2.2 (Bronk Ramsey, 2009a) and IntCal 09 (Reimer *et al*., 2009). Column A refers to the model agreement index.

5.2.6 An age model for Kieshofer Moor

The age model produced for Kieshofer Moor was hampered by ^{14}C ages with large uncertainties as well as two major outliers located at 772 and 770 cm (Figure 5.8). The model diverges significantly within the Holocene above 716 cm, with the model predicting two possible scenarios; an 'older' scenario that conforms to the model and a 'younger' scenario that follows the uncalibrated ^{14}C dates. It is possible to constrain the model to give it a more precise outcome by either stating a *priori* that certain samples are outliers or by giving an age distribution to the upper boundary (670 cm) thus preventing younger ages from being possible. While improving the precision of the model it would sacrifice scientific accuracy leading to erroneous age estimates. An alternative approach is to validate the model with a comparison from the same site. Seven separate dates were taken from a neighbouring core which have much smaller uncertainties and as such are more accurate. The

position of the LST (visible) in both cores can be used as an isochronous link between the records, therefore allowing the modelled dates to be evaluated against those from the neighbouring core. The LST is recorded at 796 cm within Kieshofer Moor while it is located at 820 cm in the neighbouring core, leading to an offset of 24 cm. Using this offset, the model from the neighbouring core can be used between 830 - 694 cm to evaluated whether the 'older' or 'younger' scenario is most accurate. The timing of the onset and termination of the Younger Dryas agree within multi-centennial errors between both cores suggesting that the records are in good agreement (Table 5.6).

Core	Onset Younger Dryas cal yr BP	End Younger Dryas cal yr BP	End of age model cal yr BP
Kieshofer Moor	12,930 – 12,161	12,394 – 10,924	11,051 – 8490 (670 cm)
Kieshofer Moor sister core	12,961 – 12,101	12,898 – 11,352	11,100 – 9,610 (694 cm)

Table 5.6 – Modelled age comparisons for the Kieshofer Moor and neighbouring core. Based on a 24 cm offset between the cores, the modelled ages for the onset and termination of the Younger Dryas agree within errors.

The results from Table 5.6 and Figure 5.8 strongly suggest that the 'older' scenario is the most likely possibility for the dates within Kieshofer Moor. Based upon this upper boundary of the age model at 670 cm in the Kieshofer Moor core can be dated to 11,051 – 8490 cal yr BP which agrees with the date suggested by the neighbouring core.

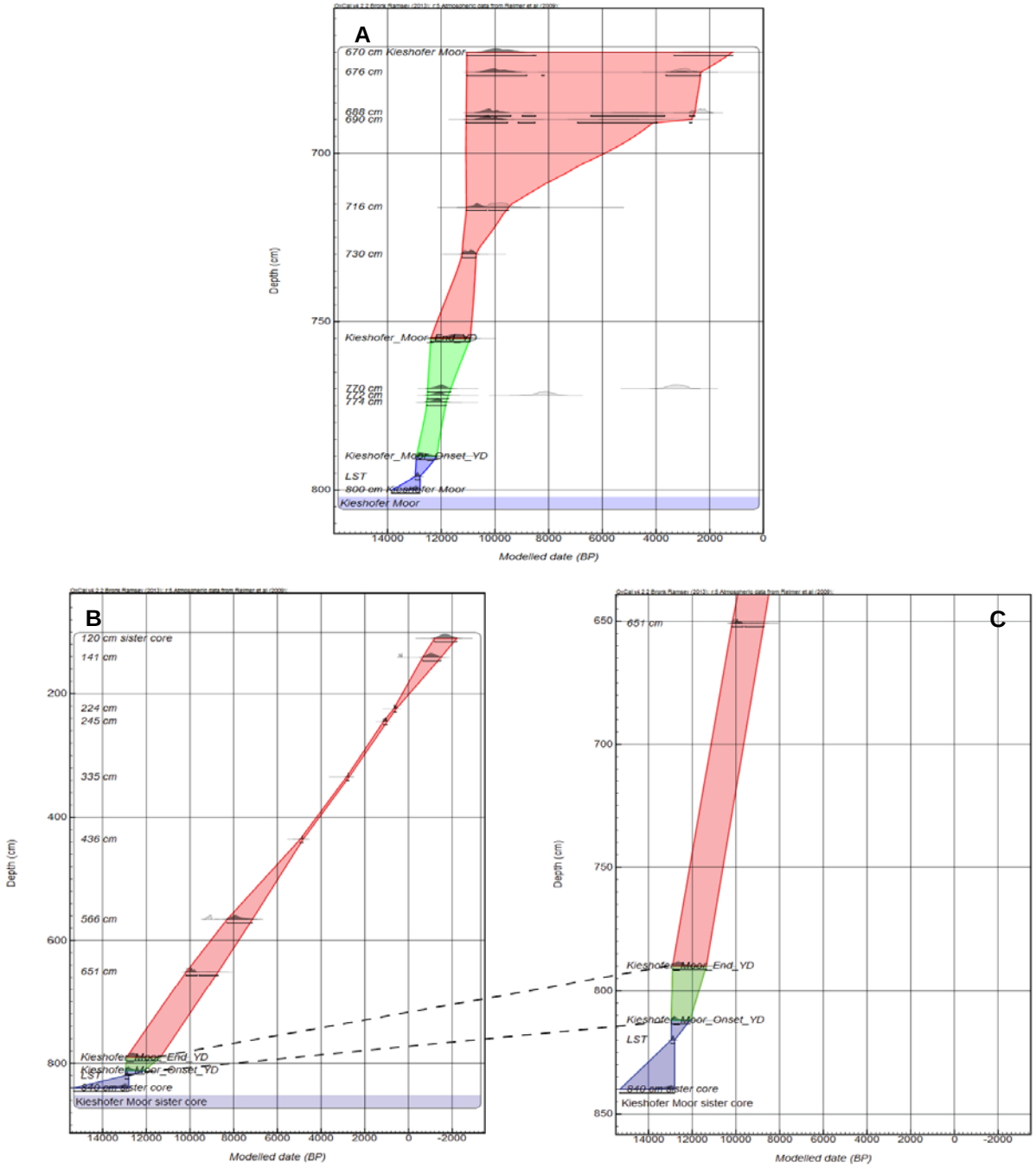


Figure 5.8 – Bayesian P_Sequence depositional model for Kieshofer Moor (A) and the neighbouring core (B). An enlarged section of the Younger Dryas portion of the neighbouring core is presented in (C) to allow comparison with the model from Kieshofer Moor presented in (A). Both models were constructed following Bronk Ramsey, (2008) using OxCal 4.2.2 and IntCal 09 (Reimer *et al*., 2009). An outlier probability of 0.05 was used within a *General* outlier model coupled with a *k* value = 1 to reflect variations in sedimentation rates.

5.3 Daschower Moor tephrochronology

Visual inspection showed the presence of a visible ash layer between 263 – 263.5 cm (OxT_7287). Further 10 cm scans revealed a small peak of 13 g^{-1} (absolute count 3) between 190 – 200 cm (OxT_7280), however based upon the limited volume of sediment and the low absolute shard counts, this was not investigated at 1 cm resolution. 1 cm contiguous samples between 260 – 280 cm showed a clear peak in shard concentration of > 500,000 shards g^{-1} (DAM-263) coinciding with the visible ash layer (Figure 5.9).

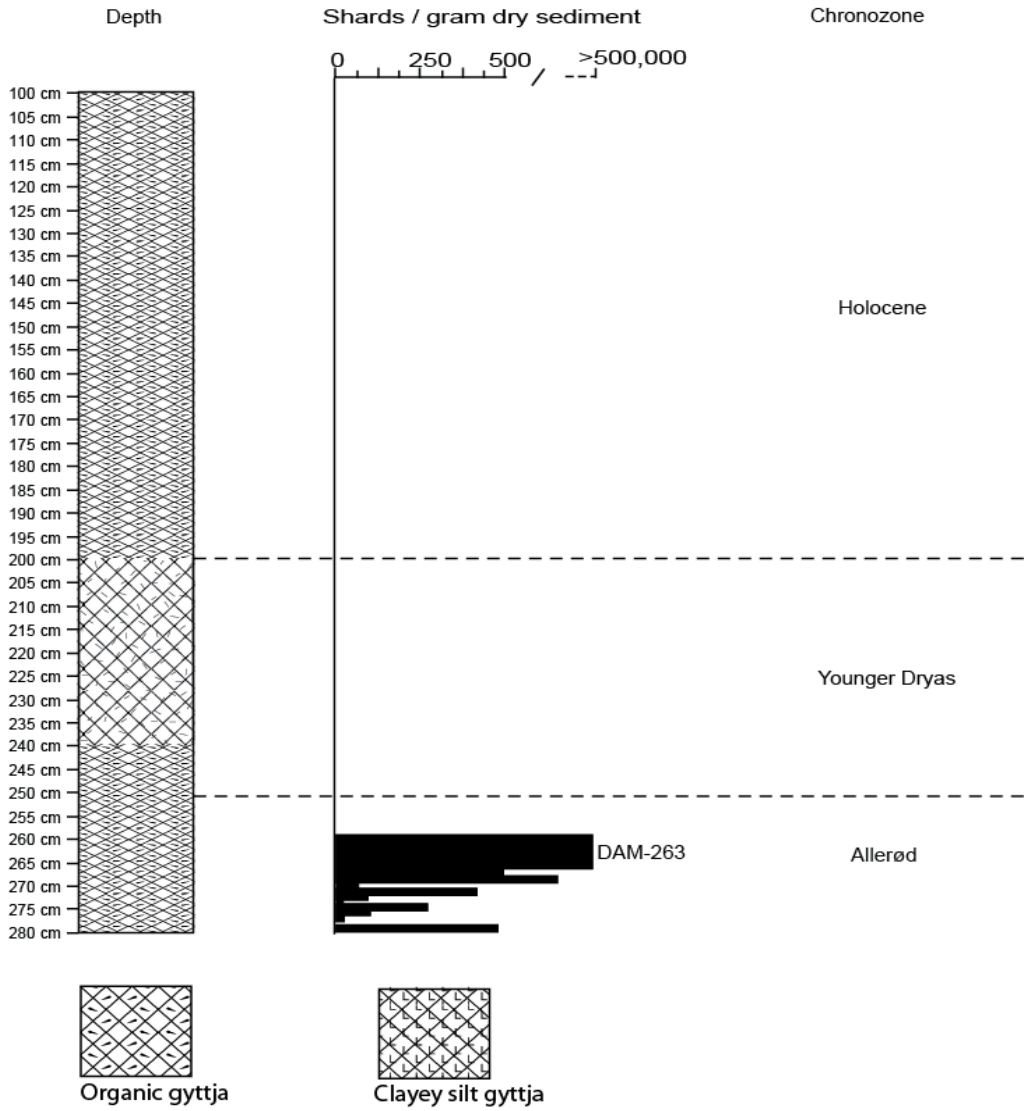


Figure 5.9– Composite diagram showing shard counts (per gram dry sediment) from this study with lithology and relative chronozones (Theuerkauf, pers. comm.) within Daschower Moor.

5.3.1 DAM-263

The large ash layer within Daschower Moor is located within late Allerød organic gyttja just prior to the onset of Younger Dryas (Figure 5.9). Glass shards are all highly vesicular with closed vesicle forms with a maximum long axis of 80 µm. Geochemical analysis indicates that DAM-263 is a phonolite with a K-rich profile. Major element glass composition gives ranges of 54.44 - 58.08 wt% SiO_2, 7.17 - 11.90 wt% Na_2O, 4.63 - 7.24 wt% K_2O, 19.93 - 22.14 wt% Al_2O_3 and 1.37 - 2.29 wt% FeO (Table 5.7).

WDS-EPMA results: Tephra and secondary standards for DAM-263

		SiO_2	TiO_2	Al_2O_3	MgO	CaO	MnO	FeO	Na_2O	K_2O	*Total*
Tephra analysis											
DAM-263		55.16	0.11	22.03	0.02	0.39	0.52	1.56	11.90	4.77	96.47
		54.44	0.14	21.93	0.03	0.55	0.49	1.37	10.52	4.63	94.10
		58.08	0.49	19.93	0.24	1.54	0.30	2.29	7.17	7.24	97.28
		54.73	0.10	22.14	0.03	0.37	0.46	1.64	11.53	4.81	95.81
	average	55.60	0.21	21.51	0.08	0.71	0.44	1.72	10.28	5.36	95.91
	2 σ	3.35	0.38	2.11	0.21	1.12	0.20	0.81	4.30	2.51	
Secondary standards											
ATHO-G	**average**	75.31	0.22	12.43	0.10	1.63	0.09	3.27	3.98	2.72	99.75
	2 σ	0.71	0.16	0.28	0.05	0.08	0.05	0.39	0.46	0.06	
StHs6/80-G	**average**	63.65	0.70	17.78	1.97	5.15	0.10	4.38	4.36	1.30	99.40
	2 σ	0.52	0.11	0.50	0.09	0.21	0.02	0.39	0.44	0.14	
GeoRem prefered value											
StHs6/80-G		63.70	0.70	17.80	1.97	5.28	0.08	4.37	4.44	1.29	99.63
	Uncertainty (95%)	0.50	0.02	0.20	0.04	0.09	0.00	0.07	0.14	0.02	
GeoRem prefered value											
ATHO-G		75.60	0.26	12.20	0.10	1.70	0.11	3.27	3.75	2.64	99.62
	Uncertainty (95%)	0.70	0.02	0.20	0.01	0.03	0.01	0.10	0.31	0.09	

Table 5.7 – Non-normalised major and minor elemental oxide compositions for DAM-263. Intermittent analysis of MPI-DING volcanic glass standards ATHO-G and StHs6/80-G (Jochum *et al*., 2005; 2006; http://georem.mpch-mainz.gwdg.de/) were used as secondary standards to check for accuracy and measure precision during EPMA analysis.

5.3.2 Geochemical comparison of DAM-263

A single chemical analysis for the LST from Daschower Moor was previously published by Riede *et* al., (2011). To augment this and to strengthen the tephrochronological and tephrostratigraphic record for Daschower Moor and to allow the direct correlation of the organic matter and cladoceran record

with other sites, a further series of analysis has been conducted as part of this study. The results of WDS-EPMA are presented in Table 5.8 and elemental plots (Figure 5.10) where they are compared to the three phases of the Laacher See eruption. Based on major and minor elements, DAM-263 is closely correlated to the lower phase of the LST. However a single data point overlaps with the upper phase of the LST eruption, which is particularly evident on CaO - Al_2O_3 and Al_2O_3 - FeO bi-plots (Figure 5.10B). It is well known that proximal LST deposits show a degree of scatter in glass chemistry between phases, and in particular the middle and upper phases (Harms and Schmincke, 2000). Riede *et al*., (2011) found a similar pattern, with a single data point from Daschower Moor, closely corresponding with the middle phase (MLST-C) of the LST eruption. Analysis of two pumice samples from ULST XIX-B16 (upper phase) in the Mendig Facies (Harms and Schmincke, 2000) show a glass composition that is closely aligned with the middle phase of the LST (Riede *et al*., 2011). Whether the variation in glass chemistry within DAM-263 and also that within the data reported by Riede *et al*., (2011) is representative of the evident proximal variation is impossible to say without further analysis of the compositional range of the middle phase of the LST and further geochemical data from Daschower Moor. However they do serve to highlight the complex pattern of stratification or mixing of phonolite melt in the Laacher See magma chamber prior to and during the eruption (Riede *et al*., 2011).

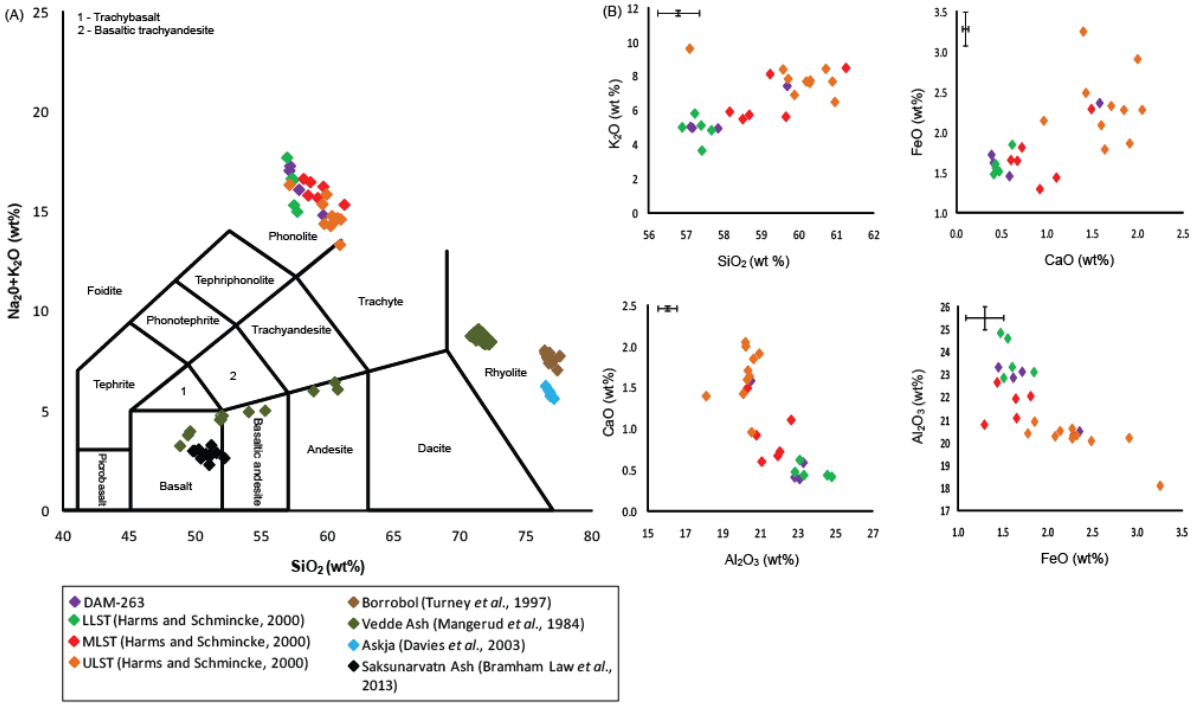


Figure 5.10 – Major and minor element plots of DAM-263 with selected major northern European Lateglacial tephras. (A) Total-alkali-silica (after Le Bas *et al*., 1986) plot of DAM-263 and selected Lateglacial and early Holocene European tephras. (B) Selected bi-plots of DAM-263 with the three phase of the Laacher See eruption as reported by Harms and Schmincke, 2000). Representative 2σ are indicated for each bi-plot within B (*upper left*) based upon precision established from secondary standard analysis (Table 5.7). All major and minor data plotted as normalised values.

5.3.3 Daschower Moor radiocarbon dates

A total of seven plant macrofossil samples were submitted for radiocarbon analysis at the ORAU, of these six yielded ^{14}C ages and a single sample giving a modern age (Table 5.8). As with the previous sites, there was significant difficulty in obtaining sufficient material for ^{14}C dating and with those age estimates gained represented by low carbon yields (<1.2 mg); causing larger age uncertainties associated with the dates in the range of 90 – 220 cal yr BP.

Depth (cm)	Lab Code	Material	$\delta^{13}C$ (‰ VPDB)	^{14}C age (yr BP)	Model age	A
118	OxA - 2495-16	Assorted plant macrofossils	-24.83	7550 ± 90	8433-7778	56%
128	OxA - 2495-17	Assorted plant macrofossils	-26.24	7490 ± 90	8697-8189	61%
154	OxA - 2495-42	Assorted plant macrofossils	-20.82	8550 ± 250	9774-9024	116%
174	OxA - 2495-43	Assorted plant macrofossils	-26.94	8860 ± 140	10641-9561	73%
193	OxA - 2495-29	Assorted plant macrofossils	-11.24	10150 ± 100	11836-10057	39%
273	OxA - 2495-44	Assorted plant macrofossils	-25.73	11750 ± 220	13951-13104	99%
257	OxA - 2495-30	Assorted plant macrofossils	-25.5	modern	n/a	n/a

Table 5.8 – ^{14}C dates and modelled ages for samples from Daschower Moor. Dates calibrated using OxCal 4.2.2 (Bronk Ramsey, 2009a) and IntCal 09 (Reimer *et al*., 2013). Column A refers to the model agreement index.

5.3.4 An age model for Daschower Moor

A Bayesian depositional model (following Bronk Ramsey, 2008) was constructed using OxCal 4.2.2 and IntCal 09 (Reimer *et al*., 2013) for the Daschower Moor core between 280 - 110 cm. The P_Sequence model has been used to reflect variable sedimentation rates with depth coupled with an outlier probability of 0.05 in a *General* outlier model and a *k* value = 1. The base of the Daschower Moor sequence (280 cm) has a modelled age range of 14,854 - 13,194 cal yr BP, which agrees with the premise that organic sedimentation began within the Daschower Moor basin during the Allerød period (Figure 5.11). A ^{14}C date of 13,951 – 13,104 cal yr BP at 273 cm, may suggest that the basal sediments in Daschower Moor (including 20 cm of disturbed sediment not sampled; see section 3.5.5) were deposited during the earliest stages of the Allerød. Unfortunately, due to the large age uncertainties associated with the dates, it is impossible to narrow date of organic sedimentation down further. Due to the relatively long Younger Dryas period, as represented in Daschower Moor, a separate boundary was introduced into the model to account for any changes in sedimentation associated with reduced landscape instability. The lack of dateable material during the Younger Dryas period unfortunately led to large modelled age ranges for the boundaries associated with the onset and termination of the Younger Dryas.

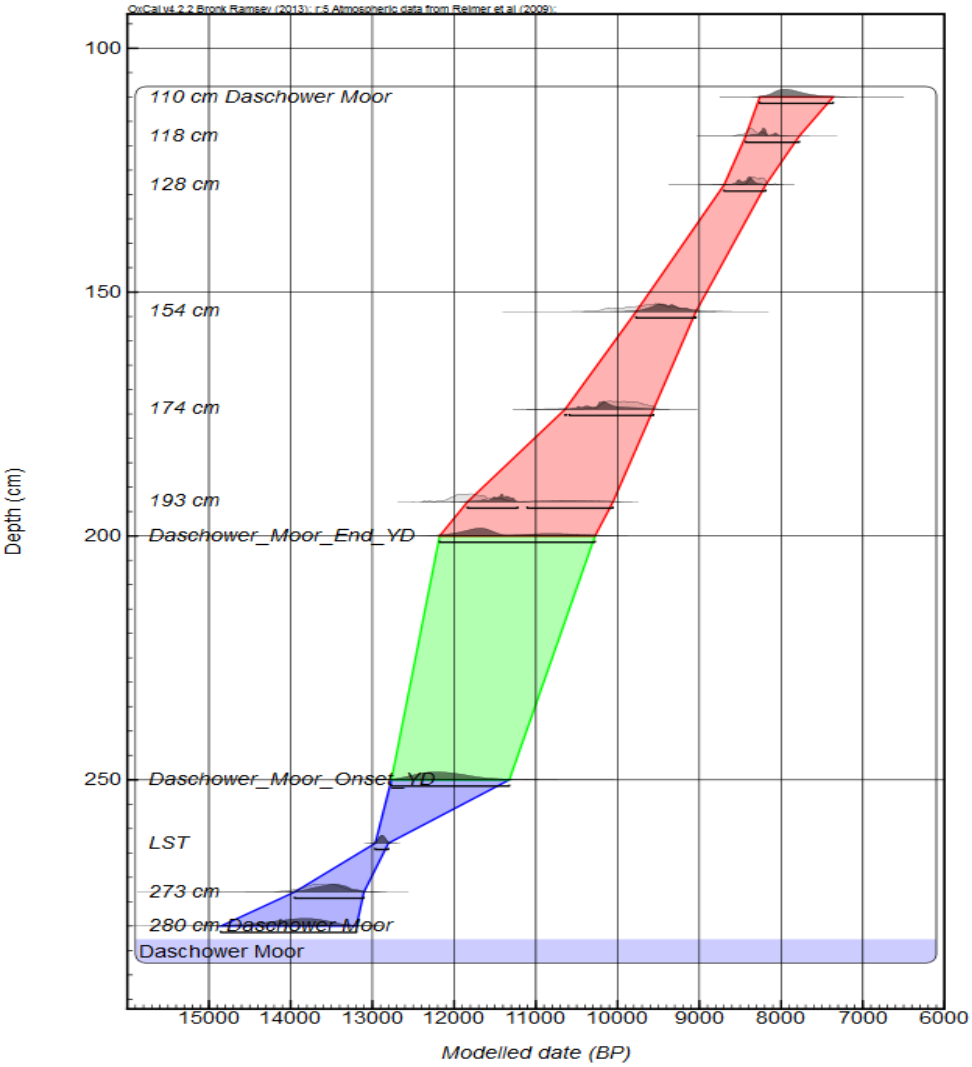


Figure 5.11 – Bayesian P_Sequence depositional model for Daschower Moor based upon six ^{14}C dates and the LST, constructed following Bronk Ramsey, (2008) using OxCal 4.2.2 and IntCal 09 (Reimer *et al*., 2009). An outlier probability of 0.05 was used within a *General* outlier model coupled with a *k* value = 1 to reflect variations in sedimentation rates.

5.4 Chapter summary

A total of two Lateglacial – early Holocene tephras have been identified within the sites of Potremser Moor, Kieshofer Moor and Daschower Moor, thus augmenting the previously identified tephras present in Slotseng and Endinger Bruch (see section 3.5.1.2 and 3.5.2.2).The presence of discrete tephra layers within the sites presented in this thesis allows high resolution isochronous links to be made between sites thus allowing comparisons to be made in the organic matter and cladoceran records. The ^{14}C chronologies produced for Potremser Moor, Kieshofer Moor and Daschower Moor are inhibited by large age uncertainties leading to a reduction in the precision of subsequently produced age models. However, the addition of known ages provided by the tephra layers allows the models to be refined, and in the case of Potremser Moor it is only through the use of the Saksunarvatn Ash that the age model is able to find an accurate solution.

Chapter 6: Results II Isotopes and Cladocera

The following chapter will discuss in turn the organic matter and cladoceran records from the five sites presented in this thesis. Following the description of the results in both records, each site will be summarised in a chronological discussion of the palaeoevolution of each site. The palaeoevolution of each site will be discussed in the context of each site with comparisons made between sites discussed fully in Chapter 7.

6.1 Slotseng, Denmark

6.1.1 Isotope and organic content record

Large changes in the amount and composition of organic matter (OM) accumulation in Slotseng sediments occurred during the Lateglacial – Holocene transition, signalling rearrangements of the aquatic system and the surrounding environment. Organic content (TOC and TN) of the Slotseng sediments varies largely throughout the length of core, with minimum values recorded during the "pre-Bølling" (0.78 wt% TOC, 0.07 wt% TN) and maximum values in the Holocene (55.88 wt% TOC, 1.44 wt% TN). Patterns of TOC and TN accumulation are highly correlated through a large portion of the record (r2 = 0.978, n = 26), however this correlation breaks down in places. The implications of this breakdown in correlation for basin development will be further discussed in section 6.1.2. Superimposed on the variable long term trend is variability on multiple scales, which is reflected in the $\delta^{13}C_{org}$ (-21.5‰ to -31.15‰), $\delta^{15}N_{org}$ (-5.5‰ to 2.33‰) and C:N (13.42 to 81.5) of sediments. Major breaks in the sedimentary organic record were used to define five separate OM zones (SOZ I – SOZ V) which will be discussed sequentially below and are presented in Figures 6.1 and 6.2. Extremely low organic content was recorded between 0 - 5 cm, making analysis of this section unfeasible, therefore the OM record begins at 5 cm (Figure 6.1).

SOZ I: 5 – 40 cm (15,430 ± 515 – 14,006 ± 98 cal yr BP)

Initial sedimentation within Slotseng is characterised by enriched $\delta^{13}C_{org}$ values which remain relatively stable until ~30 cm before gradually decreasing to -26.69‰ at the boundary between SOZ I and SOZ II. The $\delta^{15}N_{org}$ record is punctuated by a large decrease in $\delta^{15}N_{org}$ values to a profile minimum of -5.5‰ located at 20 cm, coinciding with a transition from clayey silt to silty gyttjas (Figure

6.1). Following this sharp decrease, $\delta^{15}N_{org}$ values rise rapidly throughout 25 - 40 cm, reaching -0.81‰ at the SOZ I/II boundary. The lowest recorded TN values are recorded within SOZ I (0.07 wt%, 5 cm) they are however followed by a rising trend in concentration throughout SOZ I, peaking at 0.42 wt% at the boundary of SOZ I/II. C:N values fluctuate between 13.42 - 15.77, however a slight increase is observable throughout the zone. TOC values climb steadily throughout SOZ I, rising from 0.78 wt% at 5 cm to 4.69 wt% at the boundary with SOZ II.

SOZ II: 40 – 85 cm (14,006 ± 98 – 13,365 ± 155 cal yr BP)

$\delta^{13}C_{org}$ continues to fall towards more depleted values, this however is punctuated by a series of two sharp increases located at 55 cm (-25.58‰) and 70 cm (-26.75‰). The downward trend reaches a profile minimum of -31.2‰ at 85 cm, marking the OM boundary between SOZ II/III (Figure 6.1). The $\delta^{15}N_{org}$ record following the period of enrichment during SOZ I, levels off between 45 - 55 cm before rapidly decreasing to -2.84‰. Values rise again to 0.14‰ before gradually decreasing towards the SOZ II/III boundary. After an initial drop in TN at 45 cm (0.14 wt%), an observed gradual increase in values is observed throughout the zone, with values rising to 1.38 wt% at the boundary between SOZ II/III. The C:N record continues to increase, with a progressive rise in values towards the SOZ II/III boundary. TOC is positively correlated with $\delta^{13}C_{org}$ ($r2 = 0.725$, $n = 10$; Figure 6.2B) with values rising within the early stages of SOZ II before dropping to 2.21 wt% at 45 cm. Following this drop, TOC rises continuously to a maximum of 23.43 wt% at 85 cm.

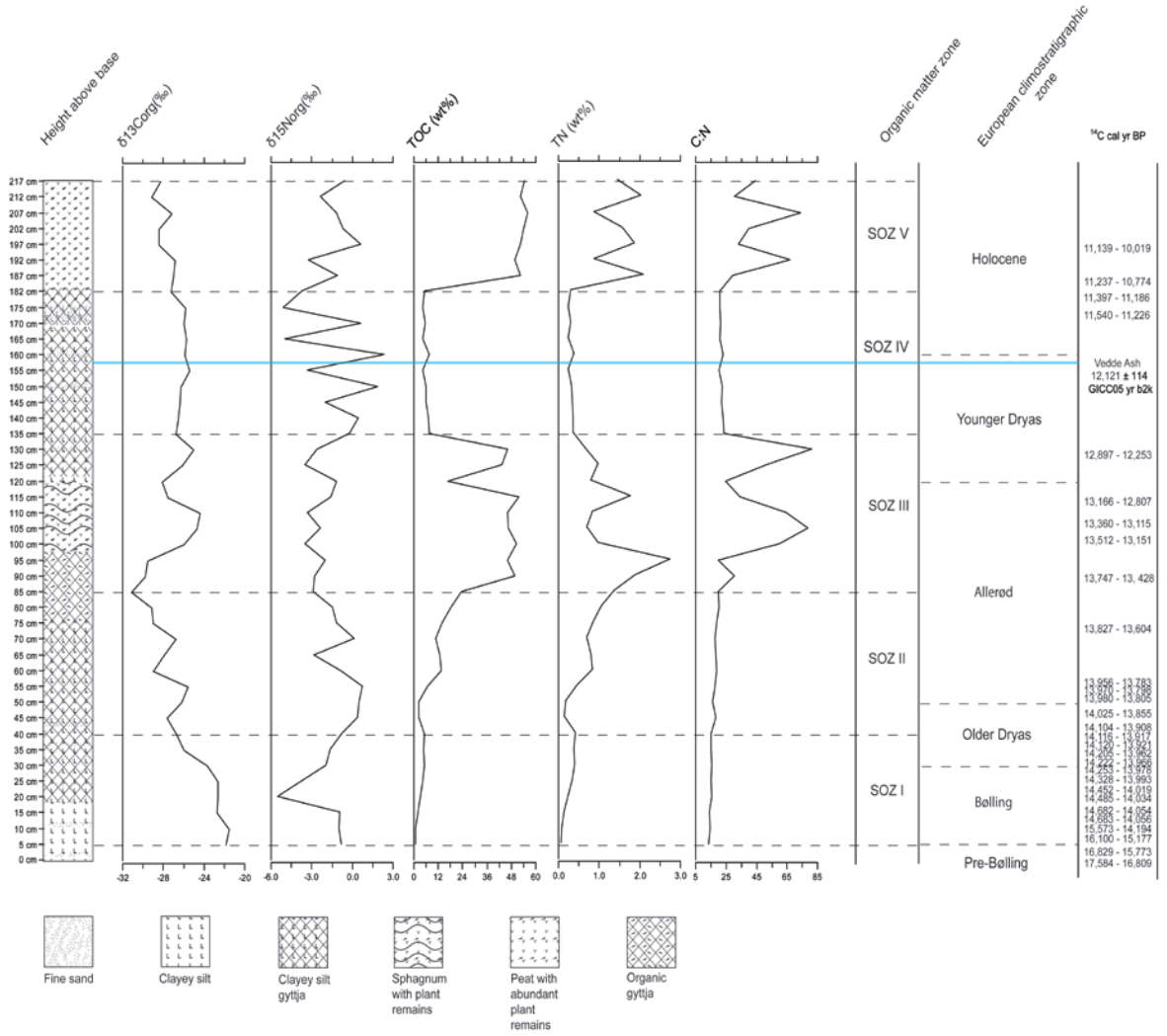


Figure 6.1 – Stable isotope profiles and selected organic properties, showing lithology, $\delta^{13}C_{org}$, $\delta^{15}N_{org}$, TOC, TN and C:N, major European climostratigraphic zones, calibrated radiocarbon dates and tephra layers for Slotseng (after Mortensen *et al.*, 2011). The five OM zones are listed as SOZ I – SOZ V.

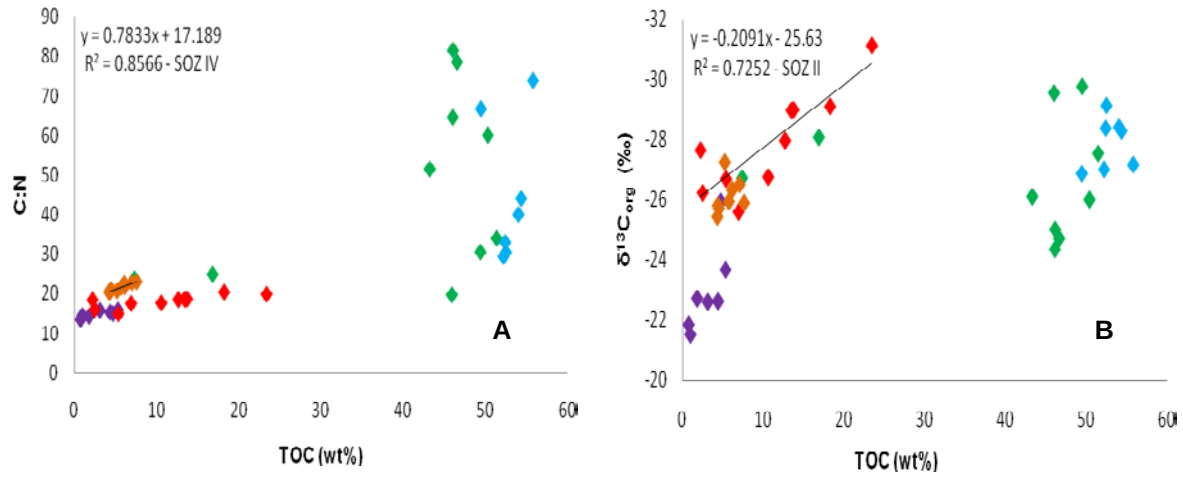
SOZ III: 85 – 135 cm (13,365 ± 155 – 12,408 ± 292 cal yr BP)

SOZ III is characterised by two pronounced peaks in the C:N ratio, occurring in both instances concurrently with peaks in the $\delta^{13}C_{org}$ record, but after peaks in the TN record (Figure 6.1). $\delta^{13}C_{org}$ values show two peaks of 24.34‰ and -25.0‰ located at 110 cm and 130 cm respectively, interspaced by more depleted values of -28.08‰ at 120 cm. $\delta^{13}C_{org}$ is inversely related to C:N within SOZ III ($r = 0.728$, $n = 11$; Figure 6.2F) with C:N values increasing to around 78.5 at 105 cm, before declining to 24.8 at 120 cm. Like the $\delta^{13}C_{org}$ record, C:N values peak a second time at 130 cm where

values rise to 81.5. The $\delta^{15}N_{org}$ record during SOZ III shows no obvious increase or decrease in values; instead the $\delta^{15}N_{org}$ record fluctuates between -2.01‰ and -3.5‰ throughout the duration of the zone. Like the C:N record, TOC values are represented by two peaks in values located at 95 cm and 115 cm with values of 2.74% and 1.77% respectively. TOC values rise to 46 - 51.46 wt% during 90 - 115 cm, before dropping to 16.86 wt% at 120 cm. Following this dip, values rise again to 46.13 wt%, before again dropping to 7.36 wt% at 135 cm.

SOZ IV: 135 – 182 cm (12,408 ± 292 – 11,200 ± 120 cal yr BP)

The $\delta^{13}C_{org}$ record during SOZ IV varies within a relatively small range from -25.43‰ to -26.72‰ between 135 - 175 cm, before declining slightly to -27.24‰ at 182 cm. $\delta^{15}N_{org}$ values fluctuate sharply and rapidly over a large range between 2.33‰ to -5.09‰. TN values remain more or less constant between 0.24 - 0.38 wt%, whilst C:N values fluctuate between 20.20 and 23.71 and are positively correlated with TOC (r = 0.856, n = 9; Figure 6.2A).The TOC record drops sharply just below the onset of SOZ IV, falling to values between 7.36 - 4.26 wt% throughout the entirety of the zone.



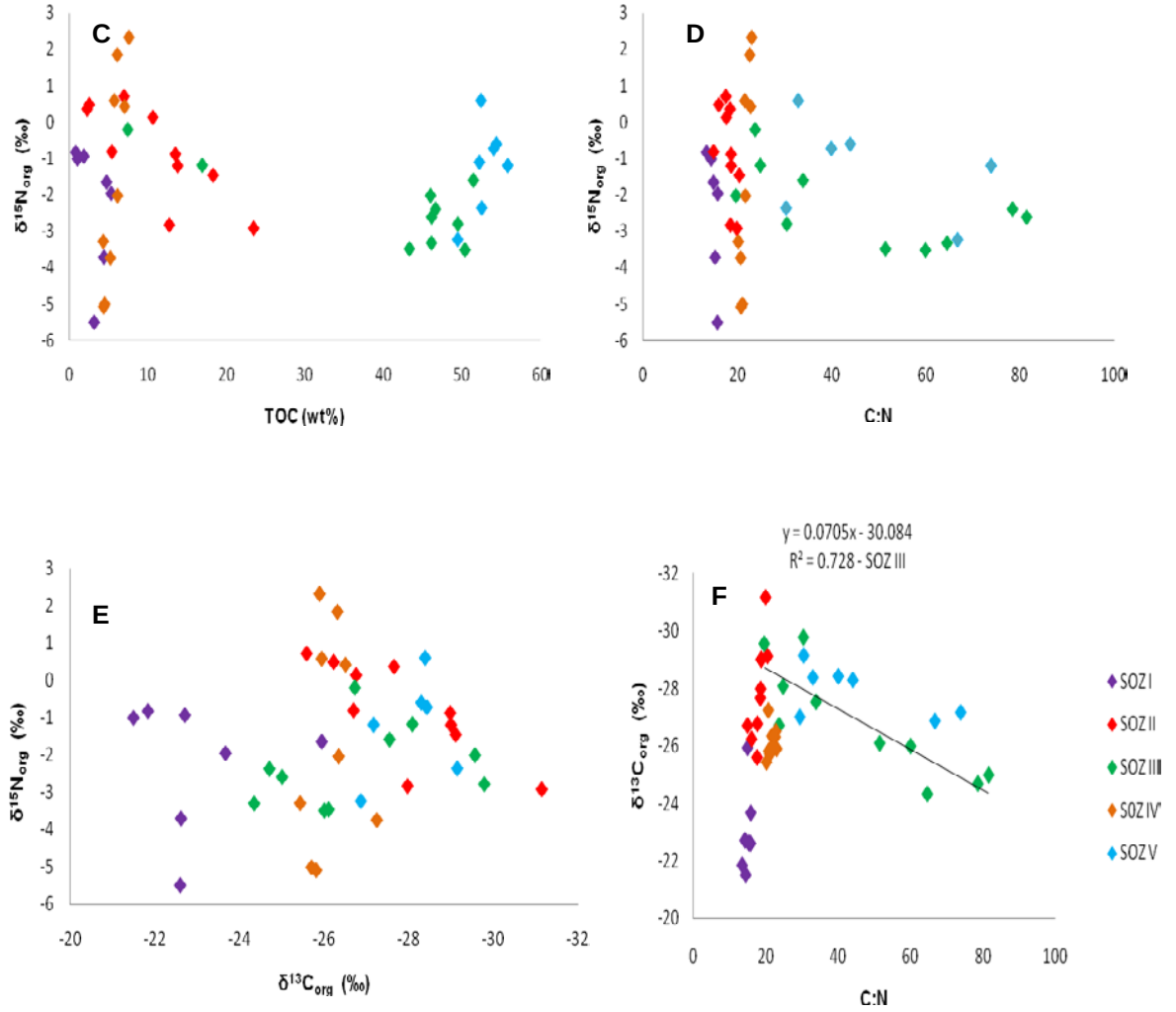


Figure 6.2 – Bi-plots of stable isotope values and selected organic properties for Slotseng. Figures A – F are plotted as OM zones (SOZ I – SOZ V). Significant relationships between parameters discussed in the text are marked by linear regression parameters in Figure 6.2A, B and F and are according to the equation y = a·x + b.

SOZ V: 182 – 217 cm (11,200 ± 120 – 10,506 ± 487 cal yr BP)

The final zone within Slotseng is characterised by decreasing $\delta^{13}C_{org}$ values with some minor fluctuations. $\delta^{13}C_{org}$ values fall from -27.24‰ on the SOZ IV boundary to -28.3‰ at 217 cm, with a range between -26.87‰ to -29.15‰ (Figure 6.1). $\delta^{15}N_{org}$ values become more enriched, reaching a peak of 0.6 wt‰ at 197 cm. Following this early rise, values begin a transition into more depleted values reaching -2.36‰ at 212 cm before finally rising slightly to -0.6‰ at 217 cm. TN values rise sharply from the preceding OM zone, reaching 2.08 wt% at 187 cm, before fluctuating throughout the

remainder of SOZ V over a range of 0.87 wt% to 2.08 wt%. C:N values also rise sharply within SOZ V to form two distinct peaks located at 192 cm and 207 cm with values of 66.76 and 73.89 respectively.TOC values increase from the preceding zone (5.18 wt%,182 cm; 52.28 wt%,187 cm). Following this rise, TOC generally increases throughout the zone, with values of 54.43 wt% at 217 cm.

6.1.2 Deviation of TN record

As discussed with section 4.6.5 (Chapter 4) the relationship between TN and TOC within Slotseng breaks down within the profile. SOZ I, II and IV all have strong TN – TOC relationships; however SOZ III and SOZ V are represented by deviations in the record (Figure 6.3),

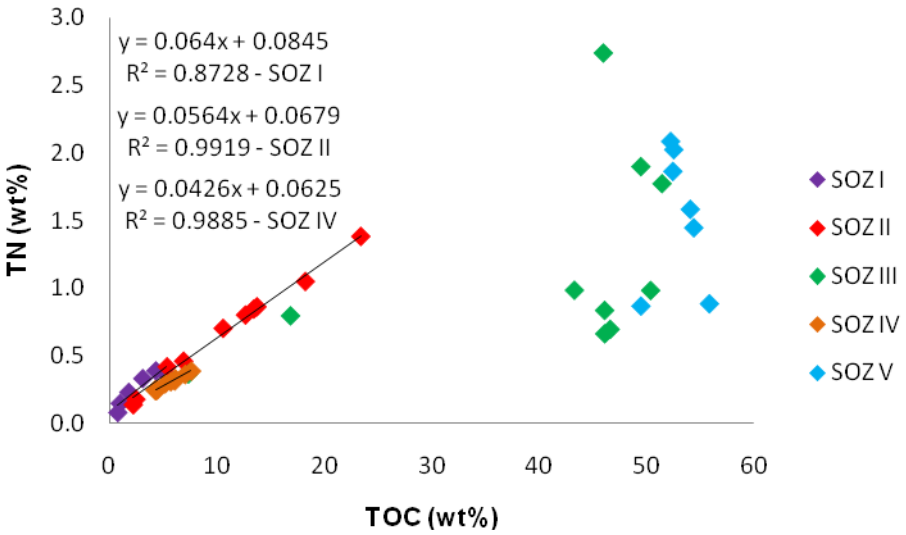


Figure 6.3 – Bi-plot of TN – TOC for SOZ I – SOZ V. OM zones SOZ I, SOZ II and SOZ IV all show strong linear relationships, indicating low inorganic nitrogen within these OM zones. SOZ III and SOZ V, however show no such relationship, indicating the relationship between TN – TOC has broken down during these zones. Linear regression parameters given in SOZ I, SOZ II and SOZ IV according to the equation $y = a \cdot x + b$.

SOZ III and SOZ V are characterised by the development of *Sphagnum* peat during the Allerød (SOZ III; 100-120 cm) and *Sphagnum*/*moss* peat during the Holocene (SOZ V; see section 3.5.1.1, Chapter 3). The effect of the terrestrialisation of the Slotseng basin during these periods leads to the breakdown of the relationship between TN – TOC thus leading to an elevation in inorganic nitrogen

within the system. The development and response of *Sphagnum* and moss peats to enhanced atmospheric nitrogen deposition is triphasic. Therefore with increasing atmospheric nitrogen deposition: (1) nitrogen limits *Sphagnum* production such that increased nitrogen deposition leads to increasing moss growth. (2) nitrogen is no longer limiting, but increases in nitrogen deposition are transferred to increases in the organic nitrogen concentration in living *Sphagnum* tissues. (3) the *Sphagnum* layer becomes nitrogen-saturated so that inorganic nitrogen bypasses the living *Sphagnum* layer and is transferred downward in to the sediment layer (Lamers *et al*., 2000; Berendse *et al*., 2001; Limpens and Berendse, 2003; Bragazza *et al*., 2004). The high C:N ratios of SOZ III and SOZ V (Figure 6.1) are insufficient to sequester all nitrogen deposition, therefore leading to a failure in the natural nitrogen filter causing a strong increase in available inorganic nitrogen (Lamers *et al*., 2000). This process has been linked to the expansion of birch over raised bogs due to high nitrogen availability, a process which occurs during SOZ V.

6.1.3 Distinction of OM zones

Principle Component Analysis (PCA) was used to evaluate whether the 'grouping' of the OM zones in Slotseng was significant. Figure 6.4A and B indicates that there is a deal of scatter and overlap between all OM zones. This scatter is due to the presence of a number of OM zones (SOZ II and SOZ IV; SOZ III and SOZ V) which although stratigraphically separate, record similar OM conditions. This leads to a situation whereby there is a clear shift in the pattern of OM accumulation (e.g. the transition from SOZ II to SOZ III) that by definition requires a new OM zone, leading to stratigraphically and chronologically separate OM zones, but when plotted overlap with one another. It is clear however in Figure 6.4A, that each OM zone is distinct from the preceding OM zone, therefore validating the distinction of the zones presented in Figure 6.1.

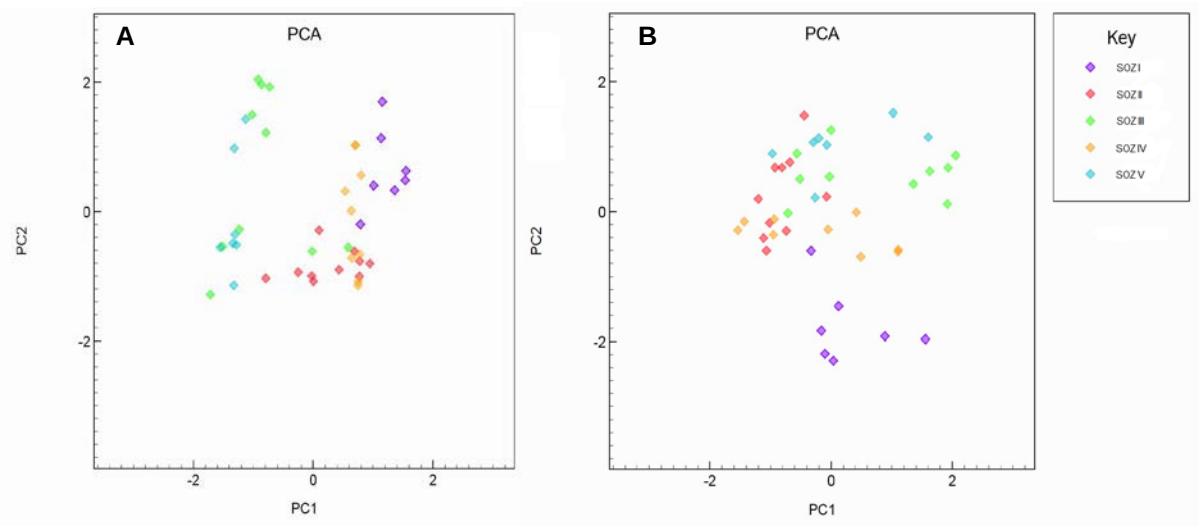


Figure 6.4 – PCA bi-plots of selected isotopic and organic properties for Slotseng plotted by: A = $\delta^{13}C_{org}$, $\delta^{15}N_{org}$, TOC, TN and C:N. B = $\delta^{13}C_{org}$, $\delta^{15}N_{org}$ and C:N.

6.1.4 Chronozone distinction

The degree of separation between the OM profiles of each chronozone within Slotseng is not particularly clear with only the Pre-Bølling and Bølling showing any signs of separation from the main cluster of data points associated with the Holocene, Younger Dryas, Allerød and Older Dryas (Figure 6.5A and B).

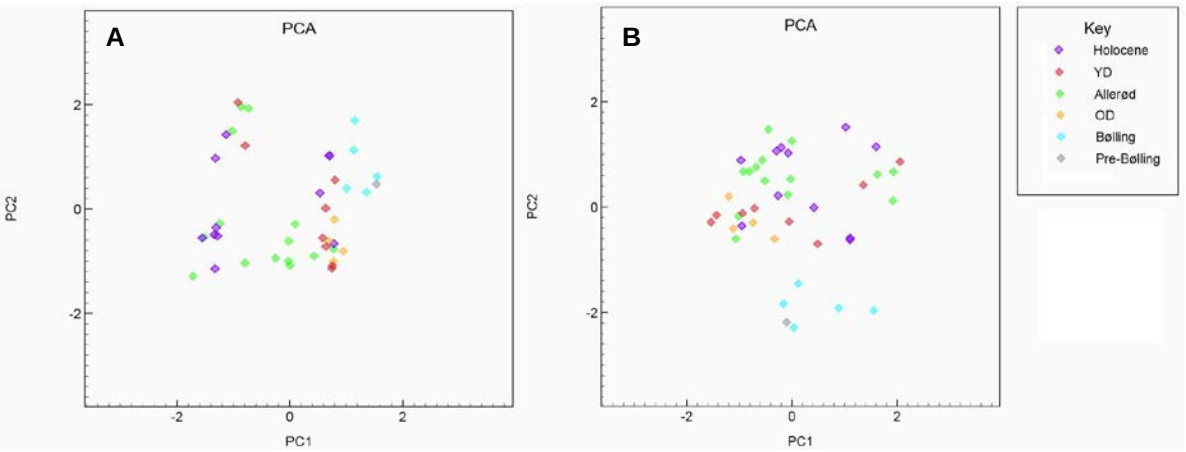


Figure 6.5 – PCA bi-plots of selected isotopic and organic properties for Slotseng plotted by: A = $\delta^{13}C_{org}$, $\delta^{15}N_{org}$, TOC, TN and C:N. B = $\delta^{13}C_{org}$, $\delta^{15}N_{org}$ and C:N.

PCA axis scores for $\delta^{13}C_{org}$ (PC1 – 0.40047) shows that variations in the $\delta^{13}C_{org}$ record are primarily driving the variability in chronozone data with only $\delta^{15}N_{org}$ contributing further (PC1 – 0.08426). In order to try and refine this pattern, $\delta^{13}C_{org}$, $\delta^{15}N_{org}$ and C:N ($\delta^{13}C_{org}$, PC1 – 0.33611; $\delta^{15}N_{org}$, PC1 – -0.72488; C:N, PC1 – 0.60132) were plotted in Figure 6.5B. Whilst further separating the Pre-Bølling and Bølling, there was however no further significant isolation of the remaining chronozones.

The wide scatter of data points attributed to the Holocene, Younger Dryas, Allerød and Older Dryas is largely due to the overlap of major OM events with chronozone boundaries. For instance, there is a significant shift in the $\delta^{13}C_{org}$, TOC, TN and C:N record between 85 - 135 cm and again between 182 - 217 cm which is separated by a period of consistent values (Figure 6.1). This process causes similar isotope values to occur within the Holocene, Younger Dryas and Allerød, with peaks in the $\delta^{13}C_{org}$, TOC, TN and C:N record occurring in the aforementioned chronozones, as well as consistent isotopes values occurring in the Holocene and Younger Dryas (Figure 6.1). Within the Slotseng basin therefore, there is not a pattern of abrupt OM response to external climatic and environmental changes, but a gradual evolution, interspersed by abrupt authochronous developments that occur within chronozone boundaries.

6.1.5 Cladoceran record

A total of 33 cladoceran species were identified from chitinous remains including, ephippia, headshields, carapaces and post abdomen claws (Table 6.1). The maximum number of species recorded from a single sample was 17 occurring within organic gyttja at 40 cm. Figure 6.6 shows that cladoceran community structure underwent several rapid changes throughout the length of the core. The cladoceran assemblage at Slotseng is essentially split into two; SCZ I, II and III; and SCZ IV, V and VI. SCZ I, II and III are represented by open water pelagic species *B. longirostris* and *D. pulex* with cladoceran concentrations between 11,000 and 57,000 individuals / 50 ml. With the transition into SCZ IV and V, there is a reduction in total cladocerans and a rapid shift to the benthic species *A. excise* and *A. nana*.

Chydorids	Non-chydorids
Chydoridae	Bosminidae
Acroperos harpae Baird	*Bosmina coregoni* Baird
A. elongates Sars	*B. longirostris* O.F. Muller
Alona affinis Leydig	
A. costata Baird	Daphniidae
A. guttata/ rectangula Sars	*Daphnia longispina* O.F. Muller
A. guttata var tub Sars	*D. pulex* Leydig
A. intermedia Sars	*Ceriodaphnia* O.F. Muller
A. quadrangularis O.F. Muller	
A. rustica Scott	Sididae
Alonella excise Fischer	*Sida crystallina* O.F. Muller
A. exigua Stebbing	
A. nana Baird	
Camptocercus rectirostris Schödler	
Chydorus sphaericus O.F. Muller	
C. piger Sars	
Eurycercus lamellatus O.F. Muller	
Graptoleberis testudinaria Fischer	
Kurzia latissima Kurz	
Monospilus dispar Stebbing	
Pleroxus aduncus Baird	
P. laevis Sars	
P. trigonellus Baird	
P. procurvatus Birge	
P. uncinatus Stebbing	
Leydigi acanthocercoides Fischer	
L. leydigi Schödler	
Rhynchotalona falcate Stebbing	

Table 6.1 – List of cladoceran species recorded for Slotseng. The nomenclature follows Scourfield and Harding (1966).

SCZ I: 0 – 30 cm (17,784 ± 923 – 14,116 ± 137 cal yr BP)

The cladoceran record during this period is dominated by the pelagic species *B. longirostris* (mean - 5856 / 50 ml), with smaller concentrations of the benthic species *A. affinis* (mean – 2541 ± 4787 / 50 ml), *A. guttata/ rectangular* (mean – 1365 ± 1837 / 50 ml), *A. quadrangularis* (mean – 787 ± 552 / 50 ml) and *C. sphaericus* (mean – 716 ± 507 / 50 ml). The interaction of *B. longirostris* with the benthic species gives a high pelagic: benthic ratio of 5.3 at 0 cm, followed by a reduction in this figure to 0.5 at 30 cm (Figure 6.6). *B. longirostris* mucro length within SCZ I varies between 35 - 48 µm (Figure 6.7A).

SCZ II: 30 – 45 cm (14,116 ± 137 – 13,940 ± 85 cal yr BP)

SCZ II records the highest taxonomic diversity with 17 separate species recorded at 40 cm (Figure 6.6), however there is a reduction in total cladoceran abundance, with total counts falling to 21,702 / 50 ml (Figure 6.6). *B. longirostris* abundance is reduced, coinciding with the first appearance of *D. pulex* (mean – 196 ± 174 / 50 ml) in the Slotseng core. Following a drop in lengths from SCZ I *B. longirostris* mucro length gradually increases during SCZ II with lengths between 36 - 44 µm (Figure 6.6A). The appearance of *D. pulex* within SCZ II prompts the first appearance of resting ephippia, with a maximum size during SCZ II of 1100 µm and a range between 745 - 1100 µm (Figure 6.7B).The benthic record during SCZ II is still largely composed of *A. affinis* which decreases slightly in abundance to a mean value of 1516 ± 1507 / 50 ml, as does *A. guttata/ rectangular* which declines to a mean of 1049 / 50 ml. *A. quadrangularis* in contrast, increases during SCZ II, rising to a maximum abundance of 2300 / 50 ml at 45 cm. The increase in benthic species during SCZ II therefore causes a decline in the pelagic: benthic ratio, with values falling to between 0.2 - 0.5.

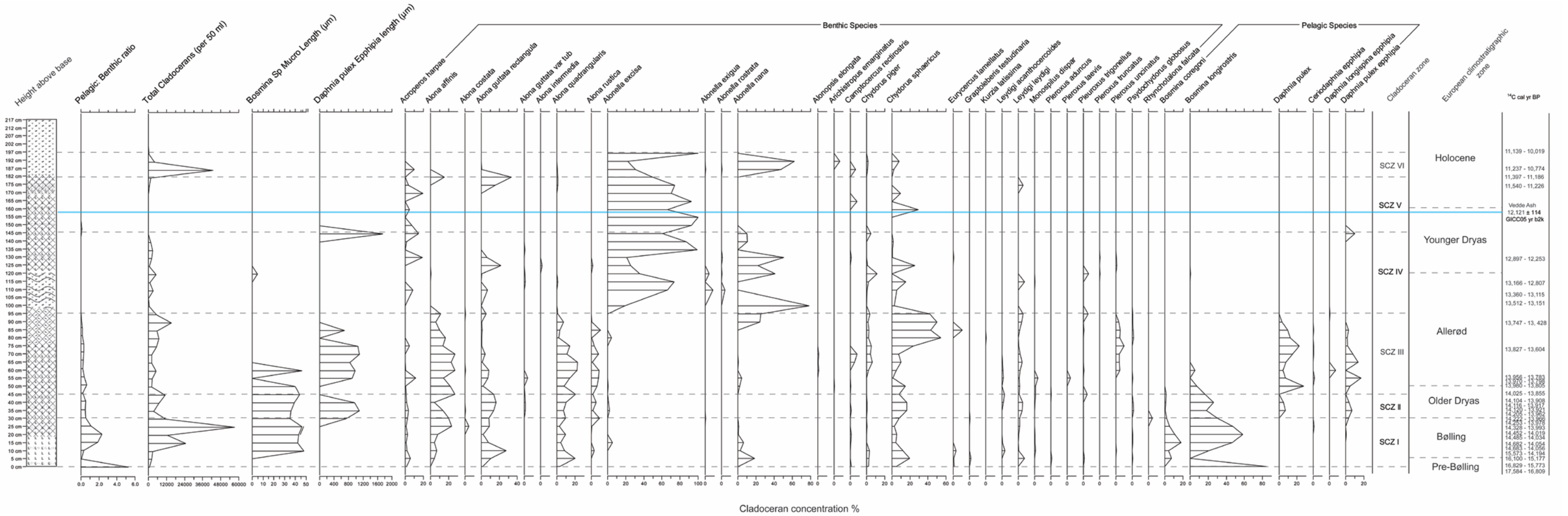
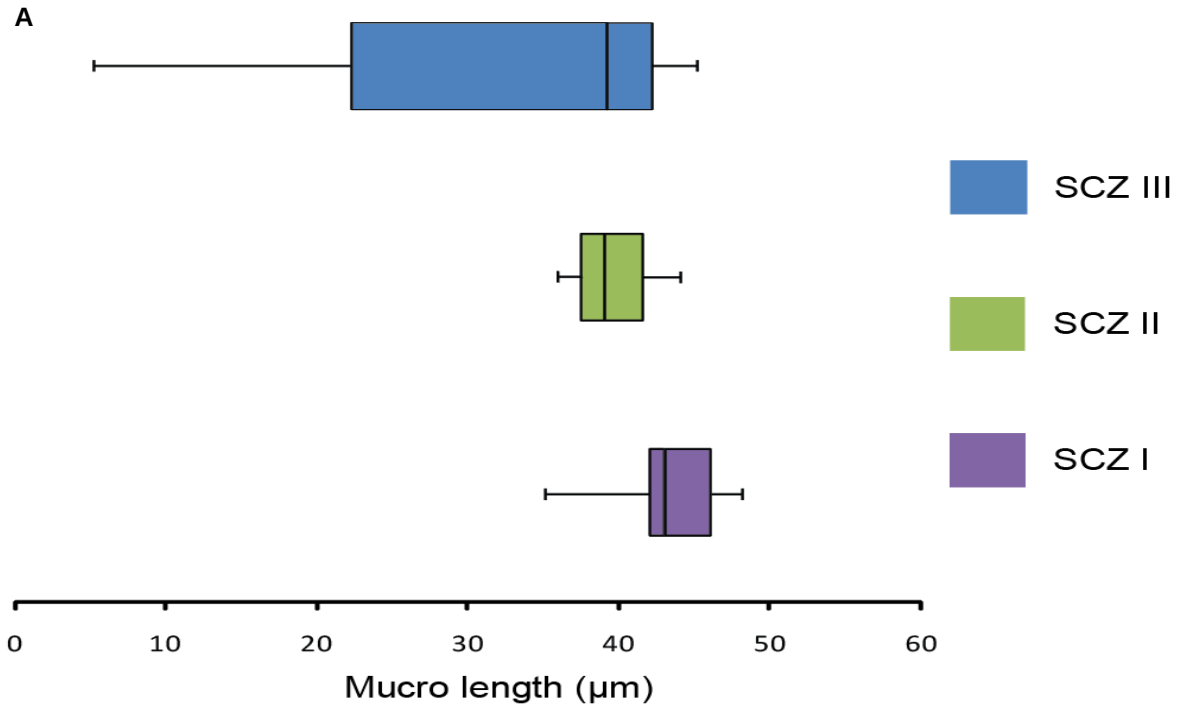


Figure 6.6 – Composite diagram of lithology, relative abundance of cladoceran species (this thesis), major European climostratigraphic zones, radiocarbon dates and tephra layers for Slotseng (Mortensen et al., 2011). Species are expressed as percentages of the total cladoceran count for each level. Bosmina mucro length and total cladoceran counts (expressed as absolute) are also shown.

SCZ III: 45 – 95 cm (13,940 ± 85 – 13,485 ± 195 cal yr BP)

The cladoceran record within SCZ III is characterised by increases in benthic species such as *A. affinis* (mean – 921 ± 362 / 50 ml), *A. guttata/ rectangular* (mean – 260 ± 135 / 50 ml), *A. quadrangularis* (mean – 627 ± 401 / 50 ml) and *C. sphaericus* (mean – 1738 ± 2329 / 50 ml). Total cladoceran numbers decline between 45 - 70 cm, falling from 11,225 / 50 ml to 2310 / 50 ml. This trend is reversed at 75 cm when total abundance increases to 5256 / 50 ml before continuing to rise to 15,185 / 50 ml at 90 cm. The pelagic record is characterised by the emergence of *D. pulex* (mean – 538 ± 364 / 50 ml), which is largely represented by resting ephippia (Figure 6.6). Increasing benthic concentrations during SCZ III thus causes a significant depression in the pelagic: benthic ratio, with values fluctuating between 0.2 - 0.3 for the majority of the zone. The gradual replacement of *B. longirostris* (mean – 339 ± 90 / 50 ml) by *D. pulex* shows a complete reversal from SCZ II, with a 94% reduction in *B. longirostris* remains between SCZ II and III. Median mucro length are largely similar from that recorded in SCZ II however with greater variability (Figure 6.7A), before *B. longirostris* completely disappears from Slotseng. Ephippia size remains relatively constant from the preceding cladoceran zone with only a slight increase in size variability recorded (Figure 6.7B).



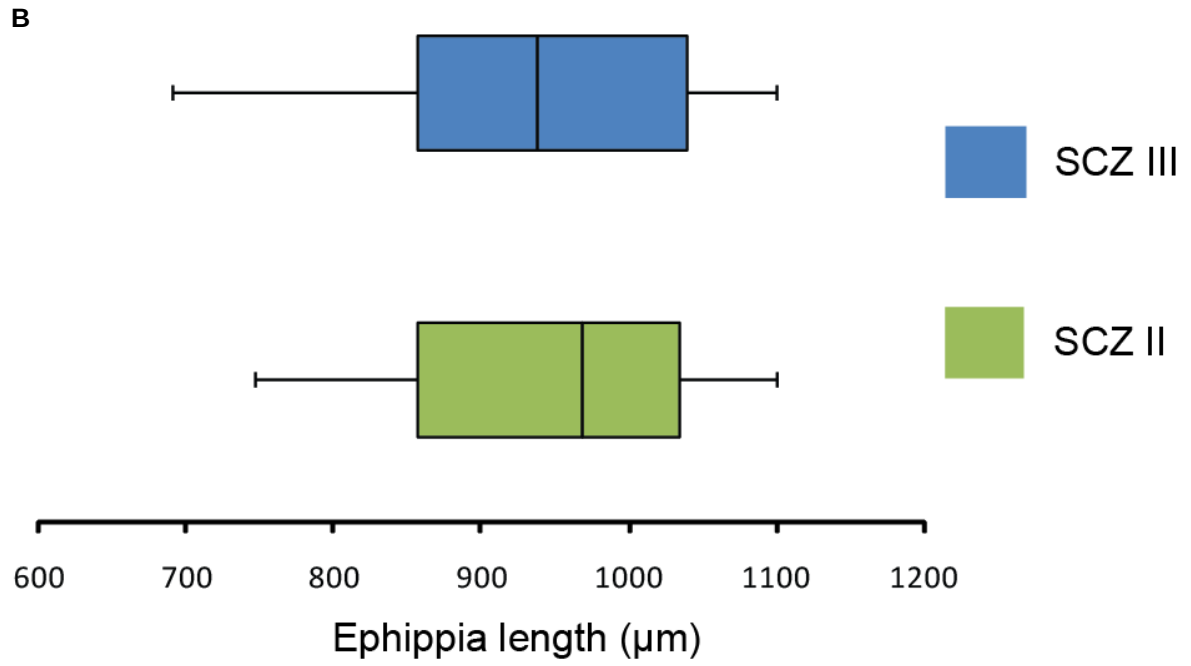


Figure 6.7 – (A) box plots of *B. longirostris* mucro length plotted by cladoceran zone. (B) box plots of *D. pulex* ephippia length plotted by cladoceran zone for Slotseng.

SCZ IV: 95 – 145 cm (13,485 ± 195 – 12,198 ± 257 cal yr BP)

The emergence of a *Sphagnum* mat within the Slotseng basin between 97 - 120 cm coincides with the complete loss of pelagic species as indicated by Figure 6.6 and a sharp rise in *A. excisa* (mean – 866 ± 1018 / 50 ml) and *A. nana* (mean ± 733 - 483 / 50 ml). Total cladoceran numbers fluctuate over a relatively wide range during SCZ IV, with total abundances of 102 - 5092 / 50 ml, coupled with no cladocerans recorded at 105 cm. As a result of the loss of all pelagic species during SCZ IV, the pelagic: benthic ratio remains at 0, and does so for the remainder of the cladoceran zones recorded in Slotseng.

SCZ V: 145 – 182 cm (12,198 ± 257 – 11,200 ± 120 cal yr BP)

The onset of SCZ V is characterised by extremely low cladoceran numbers; with total numbers of <140 / 50 ml between 145 - 165 cm. Benthic species again dominate SCZ V and only *A. excisa* (mean – 232 ± 289 / 50 ml) and *A. harpae* (mean – 9 ± 11 / 50 ml) are recorded in any appreciable numbers.

SCZ VI: 182 – 197 cm (11,200 ± 120 – 10,957 ± 182 cal yr BP)

SCZ VI is characterised by a sudden rise in cladoceran abundance, with a value of 42,750 individuals / 50 ml recorded at 187 cm (Figure 6.6). Species diversity is poor within SCZ VI with only *A. excisa* (mean – 3777 ± 4914 / 50 ml), *A. harpae* (mean – 4333 ± 1637 / 50 ml) and *A. nana* (mean – 5729 ± 7583 / 50 ml) recorded in great numbers.

6.1.6 Palaeoevolution of Slotseng

Pre-Bølling – Bølling: SOZ I and SCZ I

The onset of sedimentation in the Slotseng basin is characterised by clayey silts and gyttja with fine sands, which covers the Pre-Bølling and Bølling periods (0 - 30 cm). The Pre-Bølling – Bølling period is represented by the lowest C:N ratios (~14). Whilst these ratios span a range higher than that typical for lacustrine algae (<10), they are however lower than expected for terrestrial vegetation (>20). Values of $\delta^{13}C_{org}$ (-21‰ to -24‰) suggest that terrestrial vegetation is an unlikely source for the OM present during this period (Figure 6.1). There are therefore two possible mechanisms contributing to OM production during the onset of basin development. Firstly, algal growth under conditions of nitrogen deficiency can produce OM with C:N ratios of 13 -10 (Hecky *et al*., 1993; Talbot and Lærdal, 2000). It is possible therefore that during the Pre-Bølling – Bølling period, nutrient deficiency within the basin caused a slight elevation in the C:N record. Alternatively and although on larger scale, it has been observed within the Lateglacial sediments of Lake Superior, North America, that microbial soil OM absorbed onto clay minerals can elevate C:N ratios when washed into a basin (Hyodo and Longstaffe, 2011). With the lowermost portions of the core (0 - 19 cm) composed of clayey silt, and evidence of inwash events as shown by sand horizons, this mechanism is also possible. The overwhelming abundance of *B. longirostris* during this initial phase, which is associated with nutrient and electrolyte rich environments, appears to rule out algal productivity under nutrient deficient conditions. This suggests therefore, that during Slotseng's early development, algal productivity was the dominant source of organic carbon, however due to the input of organic matter bound to clay minerals, C:N ratios were elevated to those slightly above the threshold for lacustrine algae. The benthic cladoceran community during the Pre-Bølling – Bølling period, is primarily composed of those

species from the “arctic to sub-arctic” group, most notably *A. affinis* and *A. guttata/ rectangular*, *A. Harpae* (Harmsworth, 1968). The presence of *B. coregoni* within the earliest sediments suggests that at the inception of sedimentation within Slotseng, conditions were most likely oligotrophic. This brief, nutrient poor environment, is further confirmed by low (<1 wt%) TOC content during the first 10 cm of the core, suggesting low autochthonous or allochthonous organic deposition in the basin during this early period (Figure 6.1). The replacement of *B. coregoni* by *B. longirostris* after ~10 cm is consistent with increasing levels of lacustrine productivity and a decrease in lake depth. The absence of *D. pulex* and dominance of *B. longirostris* during the Pre-Bølling – Bølling period is highly suggestive of the presence of planktivorous fish, with the larger bodied *D. pulex* preyed upon, the smaller *B. longirostris* is able to flourish when predation pressure by fish is high (Frey, 1986; Jeppesen *et al*., 1996; Alexander and Hotchiss, 2010). The sharp reduction in *B. longirostris*, and subsequent increase in generalist / tolerant species such *A. nana*, *C. piger* and *C. sphaericus* at ~5 cm, may possibly indicate dead-ice melt events within the basin which formed the slumping features discussed within section 3.5.1 (Chapter 3).

Older Dryas: SOZ I, SOZ II, SCZ II and SCZ III

The Older Dryas, as shown in Figure 6.5 A and B, is subtly different from the preceding Pre-Bølling – Bølling period. Decreasing $\delta^{13}C_{org}$ values (-25.94‰ to -27.65‰) are coupled with slight increases in the TOC, TN and C:N, which all indicate a greater input of terrestrial material, especially after ~45 cm when scattered twigs, possibly from birch are found within the core (Mortensen *et al*., 2011). The cladoceran fauna during the Older Dryas is still represented by cold tolerant species such as *A. affinis*, *A. guttata/ rectangular*, *A. Harpae*, and *C. sphaericus*, which all show an overall increase in abundance during this period. *B. longirostris* by contrast declines steadily during the Older Dryas, with an observed replacement by *D. pulex*, occurring by at least the earliest stages of the Older Dryas (Figure 6.6). The gradual replacement of *B. longirostris* by *D. pulex* indicates that predation pressure from planktivorous fish is reduced during the Older Dryas, most likely as a result of increased water turbidity caused by erosional input.

Allerød: SOZ II, SOZ III, SCZ III and SCZ IV

The Allerød period is effectively characterised by two, largely different regimes. The first, between 50 - 85 cm, is similar to that during the Older Dryas. However, there is a progression towards more depleted $\delta^{13}C_{org}$ values, which fall from -25.58‰ to -31.15‰ (Figure 6.1). Conversely TOC, TN and C:N all gradually increase during this period suggesting increased erosional input into the basin, however remaining below that expected for pure allochthonous input and deposition (C:N <18). During this first phase of the Allerød, algal productivity is still relatively high; however its signal is reduced by further increases in allochthonous input. The $\delta^{13}C_{org}$ record drops to its lowest value at 85 cm (-31.15‰.), which forms part of large negative excursion in values between 75 - 95 cm. Low $\delta^{13}C_{org}$ values within lake sediments are often observed where algal productivity is supported to some degree by the uptake of ^{13}C-depleted, respired carbon produced by organic matter regeneration in the water column or methogenesis in anoxic sediments (Rau, 1978; Meyers and Ishiwatari, 1993; Hollander and Smith, 2001; Bastviken *et al*., 2003; Teranes and Bernasconi, 2005; Li *et al*., 2008). The presence of laminated sediments during this period may indicate seasonal anoxia within the surface sediment, which would promote microbial respiration and oxygen depletion, leading to depleted $\delta^{13}C_{org}$ values (Street *et al*., 2012). Persistent open water, with high nutrient levels is confirmed by the presence of *D*. *pulex* during this first phase. *D*. *pulex* dominance, coupled with the complete loss of *B. longirostris* by 70 cm, is indicative of fishless conditions, which is to be expected in oxygen poor conditions after this point.

The second phase of the Allerød is represented by the development of a *Sphagnum* mat across the Slotseng basin. This development coincides with an increase in $\delta^{13}C_{org}$, TOC and C:N (Figure 6.1). $\delta^{13}C_{org}$ increases relatively rapidly to -24.34‰ which is consistent with emergent aquatic vegetation. Although C:N values increase dramatically, conditions within the basin are not yet fully terrestrial as indicated by continued cladoceran deposition during this period. The cladoceran community undergoes a dramatic transformation during the later stages of the Allerød. *D*. *pulex*, the remaining pelagic species, become locally extinct from this point forward (apart from at 150 cm, where a small number of *D. pulex* ephippia were found), indicating a loss of open water and a decrease in water depth. Similarly, *A. affinis*, *A. quadrangularis*, *A. rustica* and *C. sphaericus* all decrease significantly at

100 cm. Conversely, *A. excisa* and *A. nana* both increase dramatically from this point forward. Both species are acid tolerant, with *A. excisa* in particular found at its greatest abundance at pH <5.0 (Kulesza *et al*., 2011). The acidification of the Slotseng basin during this period coincides with the absence of $CaCO_3$ within the sedimentary record, due to its dissolution by the acidic waters.

Younger Dryas: SOZ III, SOZ IV, SCZ IV and SCZ V

The early Younger Drays is characterised by a clayey silt gyttja, with well defined fine sand horizons, as well as evenly dispersed sand and numerous small twigs and scattered organic material throughout the section. The increase in C:N and TOC values to 81.5 wt% and 46.13 wt% respectively is likely due to an increase in water depth, leading to open water lake type conditions once again. The reduction in acid tolerant *A. excisa* is evident of an increase in water depth, leading to the submergence, and subsequent burial of the acidic *Sphagnum* layer. Coupled with this is the increase in the generalist species *A. nana*, *C. piger* and *C. sphaericus*, which are able to rapidly colonise new, unstable substrates (Grabowska *et al.,* 2009).

The latter half of the Younger Dryas, from 135 cm onwards, shows more or less consistent, stable values across all OM proxies. The only exception to this is the $\delta^{15}N_{org}$ record which fluctuates erratically between 2.33‰ and -3.29‰. During this period of fluctuation, high $\delta^{15}N_{org}$ (>0‰) values are always associated with subtle increases in the TOC, C:N and LOI record, while the $\delta^{13}C_{org}$ record remained apparently unaffected. The development of fen/marsh vegetation around the Slotseng basin during this period (Mortensen *et al*., 2011) is likely the source of this fluctuating signal. The contribution of partially-degraded, marsh plant organic matter, which is ^{15}N enriched relative to fresh plant litter, can serve to elevate $\delta^{15}N_{org}$ values above the base line for surface sediments (Kendall, 1998; Street *et al*., 2012). The cladoceran record during this phase is characterised by extremely low total abundances (2946 – 67 / 50 ml), which is typical of many Younger Dryas cladoceran sequences (e.g. Duigan and Birks, 2000; Kulesza *et al*., 2011). *A. excisa* is the dominant cladocera during this phase, accounting for almost the total cladoceran count. Its elevation at this point is likely to be the product of its association with slightly acidic waters within the marsh and fen land surrounding the site. Due to the lack of other cladoceran remains, *A. excisa* therefore appears to dominate the record.

Holocene: SOZ IV, SOZ V, SCZ V and SCZ VI

The early Holocene, between 160 - 182 cm roughly follows the same pattern witnessed during the latter stages of the Younger Dryas (Figure 6.1) the one exception to this is the significant rise in LOI which precedes the rise in all other values by 22 cm (a duration of ~500 cal yr BP). The slight decrease in $\delta^{13}C_{org}$ values between 160 - 182 cm from -25.89‰ to -27.24‰, coupled with C:N values >20 indicates that input into the basin is now largely composed of terrestrial organic matter, most likely from the fen type vegetation surrounding the basin. The emergence of moss/birch peat from 182 cm, coincides with elevated TOC, TN and C:N. The values, similar to those experienced at the end of the Allerød – early Younger Dryas, mark the onset of complete terrestrialisation of the site. The cladoceran fauna, confirm this process, however they also indicate a brief period of increased water depth at the site. Total cladoceran numbers rapidly increase to >47,000 at 187 cm, this rise is almost exclusively composed of *A. excisa and A. nana*, thus indicating acidic waters <pH 5.0. Following this brief inundation, the site is covered by light birch forest, and ceases to exist as a water body.

6.2 Endinger Bruch, Germany

6.2.1 Isotope and organic content record

The organic content record from Endinger Bruch is characterised by large variability. Minimum values are recorded during the Bølling (0.69 wt% TOC, 0.06 wt% TN) while maximum values are located during the Holocene (31 wt% TOC, 2.55 wt% TN). The accumulation of TOC and TN is highly correlated throughout Endinger Bruch ($r = 0.993$, $n = 119$) thus indicating the TN record can be interpreted as that of organic nitrogen deposition (Nijenhuis and de Lange, 2000; Calvert, 2004). Alongside the trend in TOC and TN accumulation, there is variability in the $\delta^{13}C_{org}$ (-18.22‰ to -31.96‰), $\delta^{15}N_{org}$ (-1.36‰ to 2.08‰) and C:N (11.77 to 17.80) of sediments. Major breaks in the sedimentary organic record were used to define seven separate OM zones which will be discussed sequentially below and presented in Figures 6.8 and 6.9.

EOZ I: 1461 – 1391 cm (14,577 ± 653 – 13,925 ± 325 cal yr BP)

Recordable levels of organic carbon are first detected at 1461 cm with $\delta^{13}C_{org}$ values of ~ -23‰ (Figure 6.8). Centred at 1446 cm, there is enrichment in $\delta^{13}C_{org}$ values to a maximum of -19.39‰. Above this values drop to between -25‰ and -24.58‰ throughout the rest of the zone. The C:N profile follows that of $\delta^{13}C_{org}$, with a general increase in values between 1461 - 1421 cm. This pattern however is reversed from 1421 - 1386 cm, with C:N values falling away with proximity to EOZ II. The $\delta^{15}N_{org}$ record between 1461 - 1416 cm shows depleted values, falling to -1.36‰ at 1426 cm. Above this $\delta^{15}N_{org}$ values increase to 0.76‰ at 1391 cm. Between 1461 - 1391 cm there is very little variation in the TN record, with values fluctuating between 0.06 - 0.09 wt%. TOC values are low within EOZ I, fluctuating between 0.69 - 1.15 wt% with a maximum value of 1.15 wt% at 1401 cm.

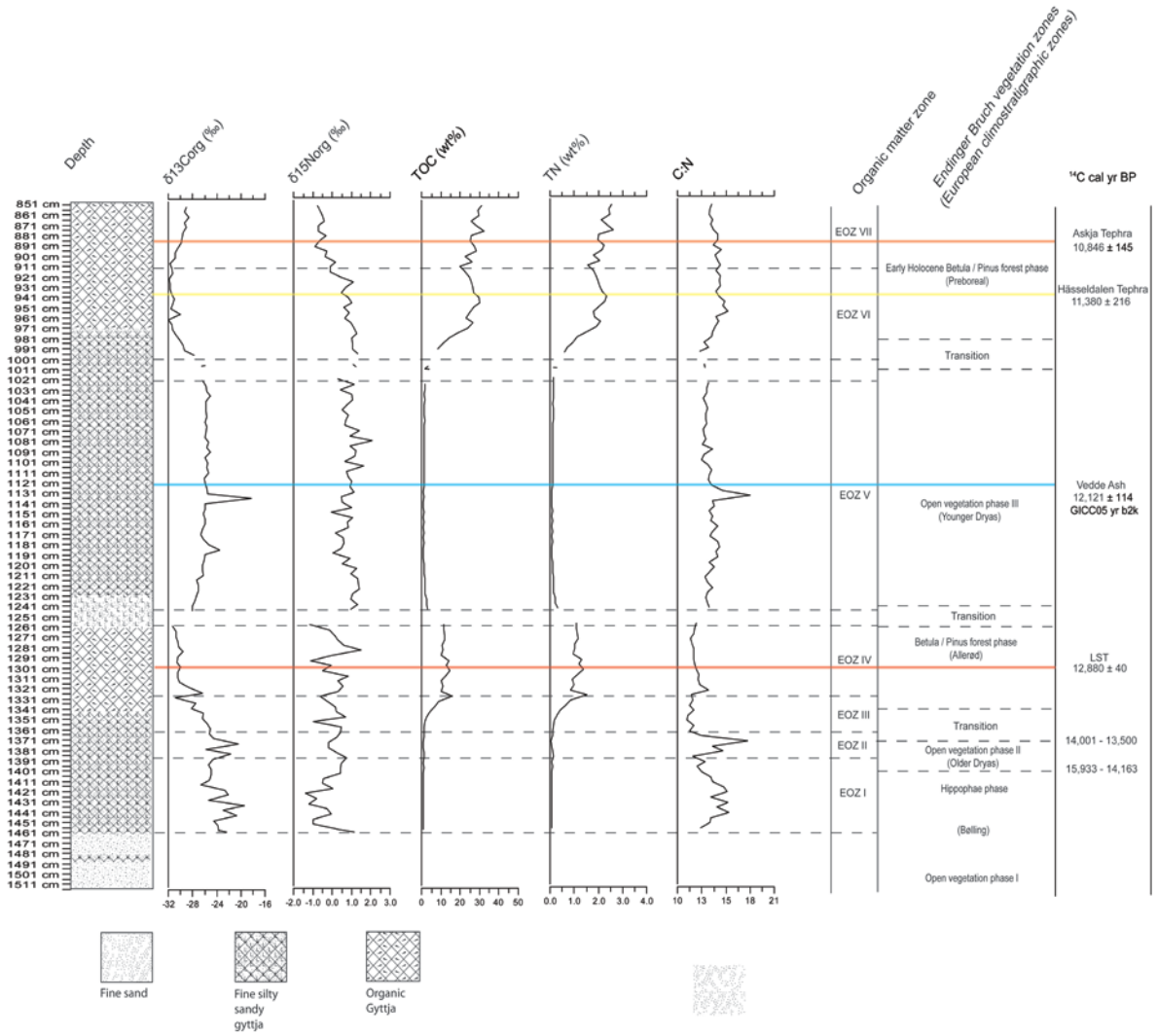
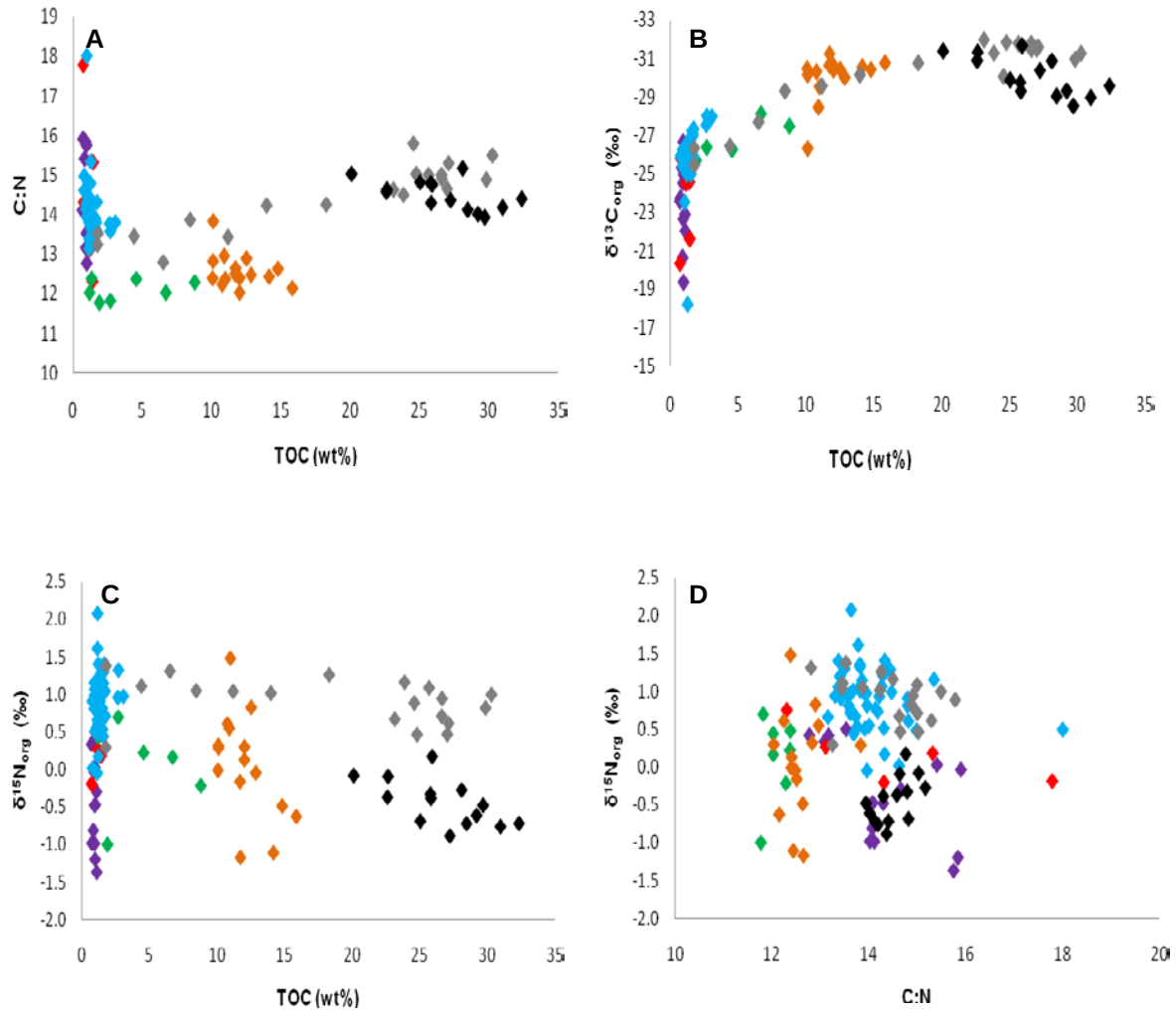


Figure 6.8 – Stable isotope profiles and selected organic properties, showing lithology, $\delta^{13}C_{org}$, $\delta^{15}N_{org}$, TOC, TN, C:N, major European climostratigraphic zones, modelled age for date KZA (see section 3.5.2.3, Chapter 3) and tephra layers for Endinger Bruch. The seven separate zones are displayed as EOZ I – EOZ VII. It was not possible to record $\delta^{13}C_{org}$ and $\delta^{15}N_{org}$ values between 1256 - 1241 and 1021 - 981 cm, this is shown as a blank space between EOZ IV and EOZ V and EOZ V and VI.

EOZ II: 1391 – 1366 cm (13,925 ± 325 – 13,688 ± 237 cal yr BP)

The $\delta^{13}C_{org}$ record sharply falls to -25.79‰, this however is immediately followed by an enrichment in values to -20.36‰ at 1376 cm. $\delta^{15}N_{org}$ values fall mid way through EOZ II to a minimum of -0.2‰ before gradually increasing to 0.48‰ at 1361 cm. The C:N record is characterised by an abrupt

increase in values to a maximum of 17.80 during EOZ II. Following on from EOZ I, TN values remain very low and continue to fluctuate over a small range. There is however a small but perceptible rise in TN towards the end of EOZ II (1371 - 1356 cm) with values reaching 0.19 wt%. TOC values remain low within EOZ II, they do however increase slightly with values reaching 1.42 wt% at 1386 cm (Figure 6.8).



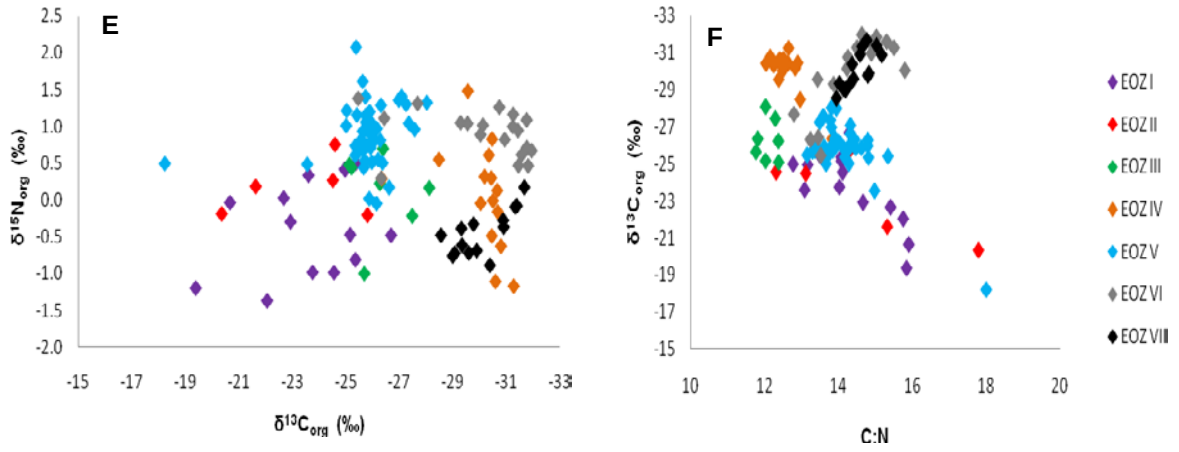


Figure 6.9 – Bi-plots of stable isotope values and selected organic properties for Endinger Bruch. Figures A – F are plotted as OM zones (EOZ I – EOZ VII).

EOZ III: 1366– 1331 cm (13,688 ± 237 – 13,380 ± 250 cal yr BP)

EOZ III is characterised by a gradual depletion in $\delta^{13}C_{org}$ values, falling from -25.20‰ at 1366 cm to -30.8‰ at 1331 cm (Figure 6.8). The $\delta^{15}N_{org}$ record also shows a gradual reduction in values which is punctuated by a sudden drop in values to -0.99‰ at 1356 cm. TN values rise gradually from 0.19 wt% at 1356 cm to 1.52 wt% at 1331 cm. The gradual rise in TN values is accompanied by relatively stable C:N values, fluctuating over a small range between 11.77 and 12.38. TOC values climb steadily within EOZ III, reaching 15.85 wt% at the boundary with EOZ IV.

EOZ IV: 1331 – 1261 cm (13,380 ± 250 – 12,700 ± 190 cal yr BP)

The $\delta^{13}C_{org}$ record increases during the first 10 cm of EOZ IV from -30.80‰ at 1331 cm to -28.48‰ at 1321 cm. Following this the $\delta^{13}C_{org}$ record remains relatively stable, fluctuating between -31.28‰ and -29.56‰ throughout the remainder of the zone (Figure 6.8). $\delta^{15}N_{org}$ increases to 0.83‰ at 1311 cm, before dropping away to -1.11‰ at 1296 cm, this drop is followed by an increase in values to 1.48‰ at 1286 cm. The TN record is generally stable during EOZ IV except for a rise in values between 1296 - 1306 cm which coincides with the reduction in $\delta^{15}N_{org}$ values. As with EOZ III, the C:N record is relatively stable fluctuating between 12.15 - 13.84 over the entirety of the zone. TOC values initially fall within EOZ IV to 10.10 wt% before levelling off between 10.90 - 12.85 wt% throughout the

remainder of the zone. Two smaller peaks in TOC are observed at 1306 cm and 1296 cm, where values reach 14.80 wt% and 14.16 wt% respectively.

EOZ V: 1246 – 1021 cm (12,598 ± 227 – 11,780 ± 410 cal yr BP)

Following the sedimentary hiatus between 1261 – 1246 cm, $\delta^{13}C_{org}$ values become gradually enriched from 1246 - 1141 cm, however following the major positive excursion of -18.22‰ at 1136 cm, this increase appears to plateaux, with values remaining relatively consistent at approximately -26‰ (Figure 6.8).The $\delta^{15}N_{org}$ record shows a general drop in values between 1246 - 1141 cm, however following the spike in $\delta^{13}C_{org}$ values, the $\delta^{15}N_{org}$ record increases for a period between 1121 - 1066 cm, whereby following this, values again decline. During this period of enrichment and depletion the $\delta^{15}N_{org}$ fluctuates rapidly with a range between -0.05‰ and 2.08‰. TN remains extremely low within EOZ V; however a small but perceptible rise in values from 0.06 wt% to 0.15 wt% is observed. C:N values fluctuate over a range of 13.15 - 15.35. A sharp rise in C:N to 18.01 is witnessed at 1136 cm, and is the only major deviation in the C:N record. TOC values decline during the early stages of EOZ V, with values reaching 0.77 wt% at 1196 cm, throughout the remainder of the zone values remain low between 0.79 - 1.73 wt%.

EOZ VI: 1021 – 916 cm (11,780 ± 410 – 11,118 ± 247 cal yr BP)

There is a gradual reduction in $\delta^{13}C_{org}$ throughout EOZ VI. Values fall from -26.33‰ at 1021 cm to -31.34‰ at 916 cm. $\delta^{15}N_{org}$ fluctuates over a relatively broad range during EOZ VI, with values between -0.09‰ and 1.31‰ recorded (Figure 6.8). TN values rise from 0.15 wt% at 1021 cm before peaking at 941 cm with values of 2.34 wt%, above this TN drops away to 1.81 wt% at 916 cm. The C:N record shows an overall increasing trend, with values increasing from 13.25 at 1021 cm to 15.03 at 921 cm. The onset of EOZ VI coincides with an increase in TOC values, with values rising from 1.75 wt% at 1021 cm before peaking at 30.28 wt% at 946 cm. TOC then declines throughout the remainder of the zone reaching 24.78 wt% at the boundary with EOZ VII.

EOZ VII: 916 – 851 cm (11,118 ± 247 – 10,654 ± 444 cal yr BP)

The last zone of the Endinger Bruch profile shows a gradual and steady increase in the $\delta^{13}C_{org}$ record. Values increase from -31.34‰ at the EOZ VI/VII boundary to -28.99‰ at 851 cm (Figure 6.8). The rate of change in $\delta^{13}C_{org}$ is constant, with no reversals in values witnessed. $\delta^{15}N_{org}$ declines within EOZ VII, with values approaching -0.80‰ recorded at 851 cm. TN continues to increase from EOZ VI, and displays a relatively steady rate of change. An increase in TN is however witnessed at 876 cm, when values rapidly rise to 2.62 wt%. This is then followed by a return to a more gradual change, with values of 2.55 wt% located at 851 cm. The C:N record is relatively stable within EOZ VII, with values fluctuating between 14.02 and 15.17. TOC increases from 22.67 wt% at 916 cm to 31 wt% at the 851 cm. This rise is however not steady, and is composed of a series of TOC fluctuations between 20.12 - 31 wt% (Figure 6.8).

6.2.2 Distinction of OM zones

The OM record in Endinger Bruch is characterised by variations throughout the profile (Figure 6.9). In order to validate the separation of OM zones EOZ I – EOZ VII, PCA analysis was used to determine the individuality of these groups. As observed in Slotseng there is a degree of overlap between the groups caused by similar conditions at different times in the basins development. When plotted however, OM zones EOZ I - EOZ VII can be largely separated based upon their different OM properties. Zones EOZ I and EOZ II show the greatest degree of overlap and are to a large extent similar. They have been separated in Figure 6.8 due to the large spike in C:N values. This spike is most likely representative of increased allochthonous input into the basin during the Older Dryas. This event represents a distinct phase in Endinger Bruch's development and therefore is treated as a separate OM zone. EOZ VI and EOZ VII also show some overlap, especially in Figure 6.11A and B. Figure 6.8 shows that there is a clear difference in the $\delta^{13}C_{org}$ and $\delta^{15}N_{org}$ record in EOZ VII, with $\delta^{13}C_{org}$ enriched and $\delta^{15}N_{org}$ depleted. This difference is reflected in Figure 6.10C with the variations in the $\delta^{13}C_{org}$ and $\delta^{15}N_{org}$ record used to separate the OM zones.

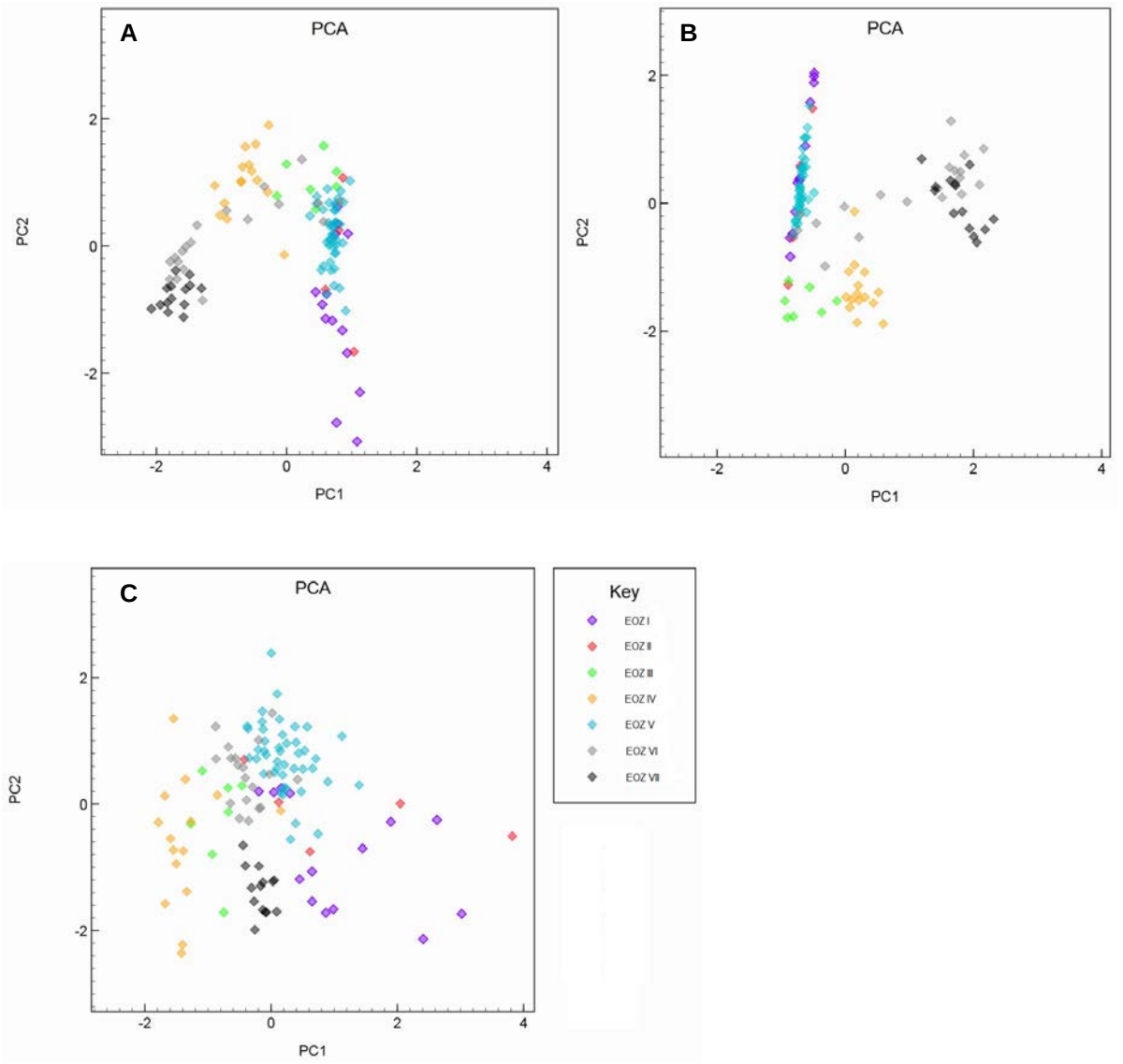


Figure 6.10 – PCA bi-plots of selected isotopic and organic properties for Endinger Bruch plotted by: A = $\delta^{13}C_{org}$, $\delta^{15}N_{org}$, TOC, TN and C:N. B = $\delta^{13}C_{org}$, TOC and TN. C = $\delta^{13}C_{org}$, $\delta^{15}N_{org}$ And C:N.

6.2.3 Chronozone distinction

The chronozones represented in Endinger Bruch can be largely separated based upon their respective OM profiles (Figure 6.11).

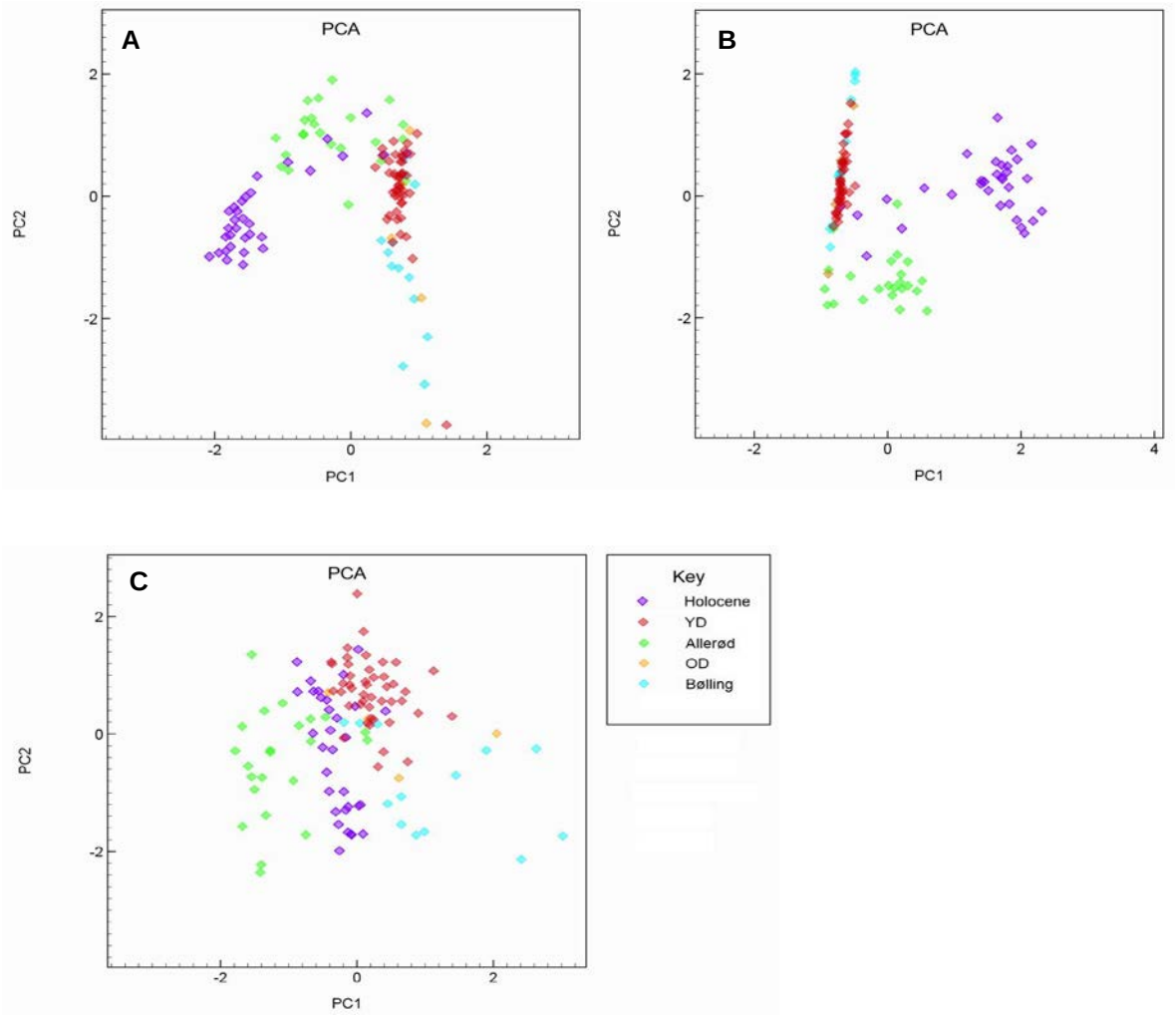


Figure 6.11 – PCA bi-plots of selected isotopic and organic properties for Endinger Bruch plotted by: A = $\delta^{13}C_{org}$, $\delta^{15}N_{org}$, TOC, TN and C:N. B = $\delta^{13}C_{org}$, TOC and TN. C = $\delta^{13}C_{org}$, $\delta^{15}N_{org}$ and C:N.

PCA axis scores for TOC (PC1 – 0.58707) and TN (PC1 – 0.58821) indicate that the separation of chronozones within Figure 6.11A is primarily driven by these parameters. When plotted by TOC and TN however, the record for Endinger Bruch becomes increasingly clustered with the Younger Dryas, Older Dryas and Bølling all overlapping (Figure 6.11B). By plotting the chronozones by their respective $\delta^{13}C_{org}$, $\delta^{15}N_{org}$ and C:N values it is possible to broadly separate out each chronozone,

albeit with a higher degree of scatter, especially within the Holocene, Younger Dryas and Allerød (Figure 6.11C).

The data within Figure 6.11A and B indicate that the most distinct chronozones in Endinger Bruch are the Holocene and Allerød. There is a degree of overlap between chronozones, especially between the Younger Dryas, Older Dryas and Bølling but also with Late Allerød and Early Holocene. The separation of different OM parameters, but also close association of certain chronozones strongly indicates that Endinger Bruch did not respond in a monotonic fashion to climatic and environmental changes but that productivity rates and authochronous and allochthonous processes fluctuated in response to these forcing mechanisms.

6.2.4 Cladoceran record

A total of 34 cladoceran species were identified from chitinous remains including, ephippia, headshields, carapaces and post abdomen claws (Table 6.2). The maximum number of species recorded from a single sample is 17 which occur within Holocene gyttja at 941 cm. Seven distinct cladoceran assemblage zones (ECZ I – VII) were recorded within Endinger Bruch as shown in Figure 6.13.

Chydorids	Non-chydorids
Chydoridae	Bosminidae
Acroperos harpae Baird	*Bosmina coregoni* Baird
A. elongates Sars	*B. longirostris* O.F. Muller
Alona affinis Leydig	
A. costata Baird	Daphniidae
A. guttata/ rectangula Sars	*Daphnia longispina* O.F. Muller
A. guttata var tub Sars	*D. pulex* Leydig
A. intermedia Sars	
A. quadrangularis O.F. Muller	
A. rustica Scott	Sididae
Alonella excisa Fischer	*Sida crystallina* O.F. Muller
A. nana Baird	*Latona setifer* O.F. Muller
A. rostrata	
Alonopsis elongate	
Camptocercus rectirostris Schödler	
Chydorus sphaericus O.F. Muller	
C. piger Sars	
Eurycercus lamellatus O.F. Muller	
Graptoleberis testudinaria Fischer	
Kurzia latissima Kurz	
Monospilus dispar Stebbing	
P. trigonellus Baird	
P. truncates	
P. uncinatus Stebbing	
Psydochydorus globosus	
Leydigi acanthocercoides Fischer	
L. leydigi Schödler	
Rhynchotalona falcate Stebbing	

Table 6.2 – List of cladoceran species recorded from Endinger Bruch. The nomenclature follows Scourfield and Harding (1966).

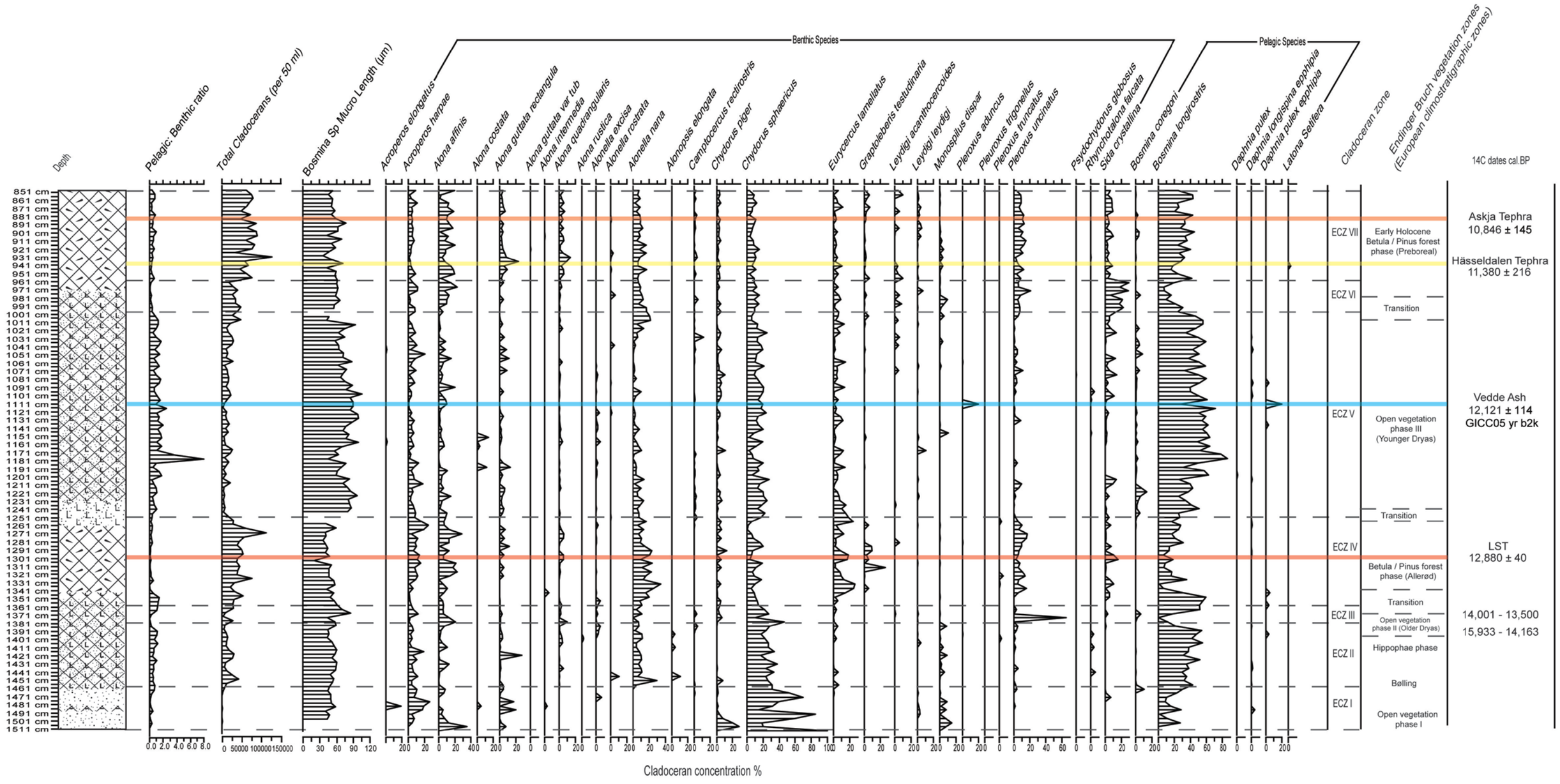


Figure 6.12 – Composite diagram of lithology, relative abundance of cladoceran species, major European climostratigraphic zones, the modelled age for date KZA (see section 3.5.2.3, Chapter 3) and tephra layers for Endinger Bruch. Species are expressed as percentages of the total cladoceran count for each level. Bosmina mucro length and total cladoceran counts (expressed as absolute) are also show.

The cladoceran assemblage within Endinger Bruch is dominated by pelagic *B. longirostris* which are ubiquitous throughout the cores entirety. Concentrations are highest within ECZ V (mean - 17935 / 50 ml) and lowest within ECZ I (mean - 292 / 50 ml).

ECZ I: 1511 – 1461 cm (15,048 ± 885 – 14,577 ± 653 cal yr BP)

Cladoceran concentrations are low (mean – 1128 ± 1968 / 50 ml) within ECZ I and are characterised by the benthic species *A. affinis* (mean – 82 ± 156 / 50 ml), *A. harpae* (mean ± 208 - 120 / 50 ml), *C. piger* (mean – 34 ± 56 / 50 ml), *C. sphaericus* (mean – 403 ± 665 / 50 ml) and *M. dispar* (mean - 24 ± 41/ 50 ml), as well as pelagic *B. longirostris* (mean – 292 ± 595 / 50 ml). The lowest total cladoceran count is located at 1511 cm with only eight individuals recorded (*C. sphaericus*) this also represents the lowest total number of species (n = 1). Total cladoceran values increase steadily throughout ECZ I, however towards the end of ECZ I there is a rapid increase in total cladocerans from 150 / 50 ml at 1471 cm to 2471 / 50 ml at 1466 cm. Mucro lengths of *B. longirostris* vary over a relatively small range of 40 - 58 µm (Figure 6.13). The dominance of benthic species within ECZ I depresses the pelagic: benthic ratio to <0.5, there is however a slight rise in values with progression towards ECZ II (Figure 6.13).

ECZ II: 1461 – 1381 cm (14,577 ± 653 – 13,848 ± 287 cal yr BP)

ECZ II is begins with a rapid rise in cladoceran concentrations (mean – 19439 ± 6388 / 50 ml). *A. affinis* (mean – 670 ± 1394 / 50 ml), *A. harpae* (mean – 1056 ± 1104 / 50 ml) and *C. sphaericus* (mean – 4573 ± 3272 / 50 ml) still dominate the assemblage; however there is a sudden appearance of *A. nana* (mean – 1822 ± 2935 / 50 ml) and *P. uncinatus* (mean – 125 ± 134 / 50 ml) within ECZ II. The pelagic component with ECZ II is represented by a sharp rise in *B. longirostris* (mean – 5889 ± 3733 / 50 ml) which in turn is accompanied by a rise in the pelagic: benthic ratio, before it again returns to low values (<0.5) at 1386 cm. There is an increase in median mucro lengths within ECZ II with the range of values decreasing slightly to 44 - 60 µm (Figure 6.13). Again no ephippia were recorded within ECZ II.

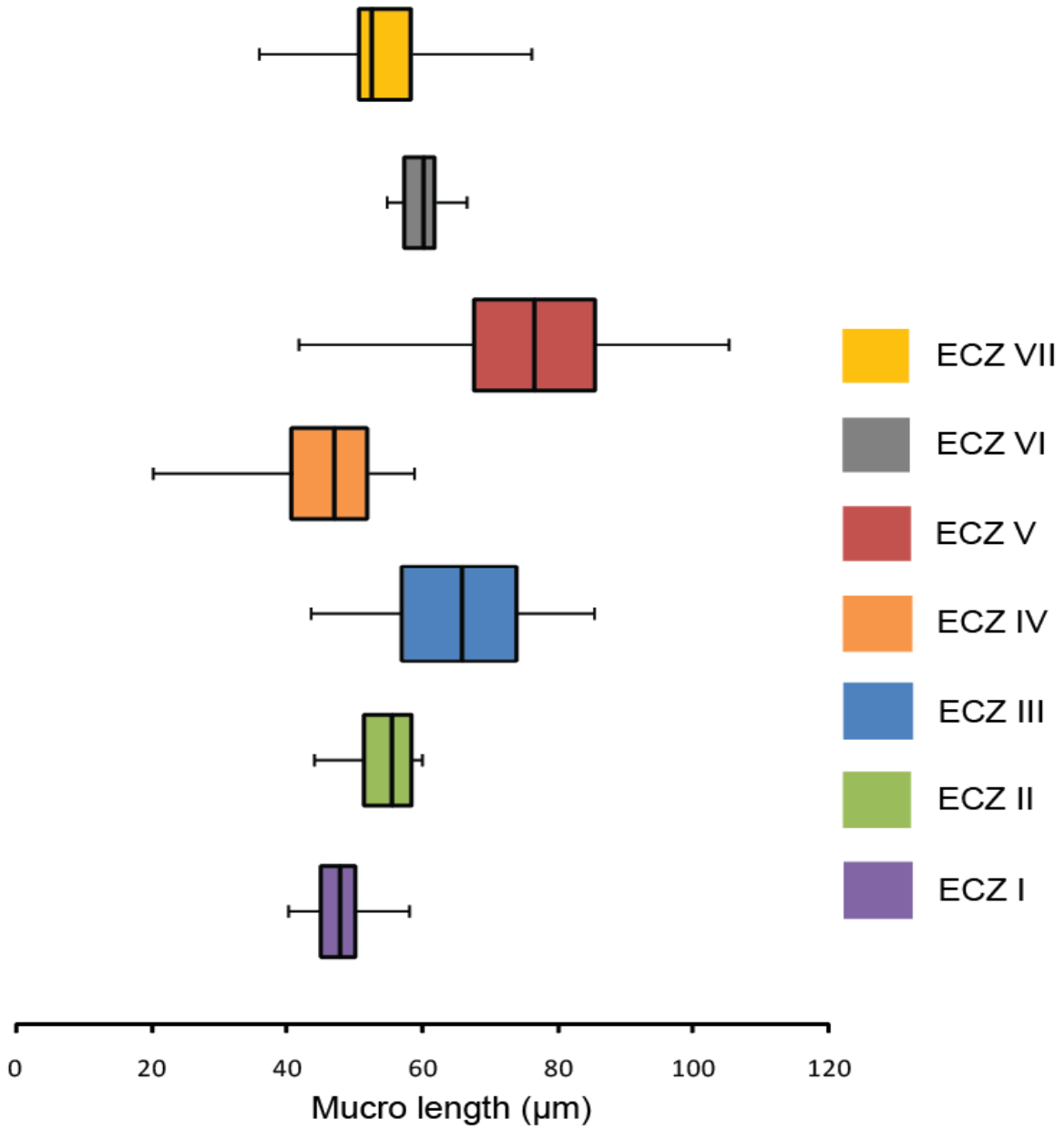


Figure 6.13 – Box plots of *B. longirostris* mucro length plotted by cladoceran zone for Endinger Bruch.

ECZ III 1381 – 1361 cm (13,848 ± 287 – 13,675 ± 200 cal yr BP)

ECZ III is characterised by a sudden and short lived reduction in total cladoceran species. Values fall from 27819 / 50 ml at 1381 cm to 2122 / 50 ml at 1376 cm. This is followed by a rapid rise in total cladoceran abundance, with values of 29228 / 50 ml recorded at 1366 cm. The response of cladoceran species is equally as dramatic with *B. longirostris* absent from the record at 1376 cm.

Accompanying this drop in *B. longirostris* is a sudden increase in *P. uncinatus* concentration, which, at 1376 cm account for over 80% of the total cladoceran count (1390 / 50 ml). Also recorded is a rise, albeit small, in *C. piger* (mean – 429 ± 405 / 50 ml). The pelagic: benthic ratio rises gradually during ECZ III, with values increasing from 0.1 - 1.2 during the duration of the zone. *B. longirostris* mucro length varies over a large range during ECZ III, with lengths ranging from 44 - 86 µm recorded (Figure 6.13).

ECZ IV: 1361 – 1251 cm (13,675 ± 200 – 12,618 ± 227 cal yr BP)

ECZ IV is accompanied by a large increase in total cladoceran abundance (mean – 44080 ± 20581 / 50 ml) which comprises a large increase in total *A. nana* (mean – 6463 ± 2985 / 50 ml), *E. lamellatus* (mean – 4233 ± 3793 / 50 ml), *Graptoleberis testudinaria* (mean – 1208 ± 2808 / 50 ml), *P. uncinatus* (mean – 3550 ± 4180 / 50 ml) and *Sida crystalline* (mean – 1507 ± 2005 / 50 ml). *B. longirostris* increases rapidly between 1356 - 1351 cm (mean – 24772 ± 8562 / 50 ml) before falling away to 333 / 50 ml at 1336 cm coinciding with a sharp rise in *A. nana* and *E. lamellatus*. Following this *B. longirostris* numbers again increase to 27338 / 50 ml before falling and becoming more constant (3095 - 6938 / 50 ml) between 1326 - 1291 cm. Following this *B. longirostris* once again increases between 1286 - 1271 cm (12098 - 19181 / 50 ml), before finally dropping back to between 4282 - 7893 / 50 ml at the boundary with ECZ V. Resting *D. longispina* ephippia are also recorded within ECZ IV (mean – 55 ± 101 / 50 ml), always coinciding with low numbers of *B. longirostris*, particularly between 1326 - 1291 cm. There is a gradual reduction in *B. longirostris* mucro length within ECZ IV and an associated increase in total range (20 - 59 µm; Figure 6.13). The pelagic: benthic ratio likewise decreases during ECZ IV, declining from 1.2 - 0.2 throughout the duration of the zone.

ECZ V: 1251 – 1001 cm (12,618 ± 227 – 11,676 ± 405 cal yr BP)

The cladoceran record during ECZ V is characterised by a reduction in total cladocerans (mean – 13,870 ± 8918 / 50 ml). *B. longirostris* dominates this zone (mean – 7037 ± 5148 / 50 ml) with values remaining stable between 1251 - 1041 cm before increasing rapidly in the last 40 cm of ECZ V. This pattern is also witnessed amongst the small concentrations of *A. nana* (mean – 803 ± 1657 / 50 ml), and *E. lamellatus* (mean – 722 ± 901 / 50 ml) while *C. sphaericus* (mean – 1848 ± 1086 / 50 ml) is

relatively constant throughout ECZ V. *D. longispina* ephippia are recorded in small numbers (mean – 23 ± 79 / 50 ml) as are *D. pulex* (mean – 49 ± 14 / 50 ml). As is seen in ECZ IV resting ephippia are only recorded injunction with low numbers of *B. longirostris*. The reduction in total cladocerans is rapid; the recovery however is far more gradual and numbers slowly begin to rise after 1101 cm. *B. longirostris* mucro length increases from ECZ IV with a large range from 42 - 106 µm (Figure 6.13) while *D. pulex* ephippia length is relatively stable at ~790 µm. The pelagic: benthic ratio shows a small increase during ECZ V, with an increase from 0.4 - 0.9. This gradual rise is punctuated by several large increases in this ratio, most notably at 1176 cm (8), 1171 am (3.7), 1136 cm (2) and 1116 cm (2.5) (Figure 6.13).

ECZ VI: 1001 – 961 cm (11,676 ± 405 – 11,421 ± 299 cal yr BP)

A rise in total cladocerans (mean – 32,707 ± 9565 / 50 ml) is marked by a rapid increase in *A. affinis* (mean – 3056 ± 1707 / 50 ml), *A. nana* (mean – 3929 ± 2257 / 50 ml), *E. Lamellatus* (mean – 1312 ± 1078 / 50 ml), *P. uncinatus* (mean – 2936 ± 2334 / 50 ml) and *S. crystallina* (mean – 6636 ± 3259 / 50 ml), whilst. *B. longirostris* numbers however decease during ECZ VI (mean – 5950 ± 4372 / 50 ml). *B. longirostris* mucro length also decreases and remains relatively stable between 55 - 67 µm (Figure 6.13). The reduction in total *B. longirostris* and subsequent rise in benthic species reduces the pelagic: benthic ratio between 0.1 - 0.3 throughout ECZ VI.

ECZ VII: 961 – 851 cm (11,421 ± 299 – 10,654 ± 444 cal yr BP)

A sharp rise in total cladocerans (mean – 70,086 ± 19,604 / 50 ml) is accompanied by a rise in *B. longirostris* (mean – 22,551 ± 10,330/ 50 ml) as well as *A. affinis* (mean – 7304 ± 4191 / 50 ml) and *A. quadrangularis* (mean – 3093 ± 3518 / 50 ml). *S. crystalline* however is seen to markedly decrease during ECZ VII (mean – 3511 ± 2263 / 50 ml), whilst *A. nana*, *C. sphaericus* and *P. uncinatus* populations remain relatively stable. *B. longirostris* mucro lengths remain stable between 961 - 921 cm, however there is a marked period of fluctuation between 916 - 891 cm with lengths varying between 77 - 42 µm (6.13). The pelagic: benthic ratio during this final zone shows greater variation than the previous zone, however with no observable increase or decrease values.

6.2.5 Palaeoevolution of Endinger Bruch

Bølling: EOZ I, ECZ I and ECZ II

The base of the Endinger Bruch core is represented by fine sands which yielded no OM data. The cladoceran fauna, between 1511 - 1461 cm conform to an oligotrophic – mesotrophic type environment, which is generally unstable and prone to inwash/aeolian events and disturbances. *B. longirostris*, which is indicative of high nutrient conditions (Alhonen, 1970), increases between 1511 - 1461 cm, however the species undergoes two rapid phase of decline occurring at 1486 and 1466 cm, which in both instances, coincides with a sharp rise in *A. harpae* and *C. sphaericus*, with both species indicative of disturbed benthic substrates (Figure 6.12). The cladoceran community composition from 1511 - 1461 cm is characterised by species from "arctic to sub-arctic" groups (Harmsworth, 1968), with *A. affinis*, *A. harpae* and *C. sphaericus* all present. The development of silty gyttjas after 1461 cm, coincides with an increase C:N values, which coupled with a reduction in $\delta^{15}N_{org}$, is consistent with allochthonous input as the primary source of organic carbon input into the basin. Abundant *Pediastrum sp* (see de Klerk 2002) throughout this phase (and into the Older Dryas) indicates high levels of aquatic, algal productivity. It is likely that unstable conditions surrounding the basin, led to high nutrient input into the lake. These input events are picked out by the fluctuating C:N profile. The situation during the Bølling therefore is a lake system that is relatively nutrient rich but prone to instability and rapid fluctuations in primary productivity. The decrease in *A. harpae* and *C. sphaericus* and subsequent increase in *B. longirostris* suggests authochronous productivity and nutrient levels are sufficient to support a substantial in *B. longirostris* population. The rise in *A. quadrangularis* within Endinger Bruch is also consistent with increasing water temperatures, during the latter Bølling period as reported by Grabowska *et al*., (2009) in lakes from central Poland. The absence of *D. pulex* throughout most of the core, and in particular, during the Bølling – Older Dryas period, is suggestive of a lacustrine system with a stable planktivorous fish population (after Jeppesen *et al*., 2002). Lower variability and reduced length in mucro morphology (when compared to Younger Dryas) further strengthens this assumption, as uniform predation by fish will produce smaller mucro lengths with lower variability as opposed to a system where predation pressure is driven by fish and aquatic invertebrates (Sweetman and Finney, 2003; Alexander and Hotchkiss, 2010).

Older Dryas: EOZ I, EOZ II, ECZ II and ECZ III

The general increase in $\delta^{13}C_{org}$ and C:N values, from the preceding Bølling period continues within the Older Dryas. The sharp increase in C:N (>15) between 1386 - 1366 cm, coinciding with more enriched $\delta^{13}C_{org}$ values is consistent with an episode of allochthonous inwash into the basin. There is little impact on the TOC, TN or LOI record, and therefore may relate to inwash of soil organic matter bound onto clay minerals, thus serving to elevate the $\delta^{13}C_{org}$ and C:N record (Hyodo and Longstaffe, 2011). This similar pattern was also observed within the Pre- Bølling – Bølling phase of Slotseng. The cladoceran record supports the notion of unstable basin sediments with inwash events. Abundances of the nutrient dependent *B. longirostris* are significantly reduced in the latter half of the Older Dryas, coinciding with small increases in cold tolerant species such as *A. harpae* and *C. sphaericus* (Figure 6.12). The increase in *B. longirostris* mucro length at 1371 cm, coincides with the sharp rise in C:N. The inwash event triggering this rise may have significantly increased turbidity in the system, leading to reduced predation pressure by fish, and aligning the trophic web with a system more heavily influenced by predation by aquatic invertebrates (after Schulze, 2011).

Allerød: EOZ II, EOZ III, EOZ IV, ECZ III, and ECZ IV

The early Allerød period, which forms part of the transition from the Older Dryas, shows the highest levels of aquatic, autochthonous productivity, during the evolution of the Endinger Bruch basin. Between 1371 - 1346 cm, $\delta^{13}C_{org}$ values decrease steadily, coinciding with the lowest consistent C:N values throughout the entire core (<12). While slightly above the threshold for pure algal derived organic matter (<10) the values during this phase indicate a significant contribution of algal derived organic matter to the Endinger Bruch basin during the Allerød. This is supported by the continuation of high concentrations of *Pediastrum sp* (de Klerk, 2002). After 1326 cm however, the level of aquatic productivity begins to decline within Endinger Bruch, as indicated by the slight rise in C:N (Figure 6. 8). The sudden drop in $CaCO_3$ between 1296 - 1271 cm is most likely due to the deposition of the LST recorded over 1300 – 1260 cm. The deposition of the LST likely reduced $CaCO_3$ levels through acidification caused by the ash entering a water body (Terberger *et al*., 2004; de Klerk *et al*., 2008). Evidence of acidification at this point is supported by the reduction of acid intolerant species such as *A. quadrangularis* and a rise in acid tolerant species such as *S. crystallina* (Kulesza *et al*., 2011). *B.*

longirostris also increases in abundance during this period, however due to the rise in other species such as *A. nana*. *E. Lamellatus* and *P. uncinatus*, its relative percentage decreases. A significant rise in *B. longirostris* mucro lengths (ANOVA p = 0.003971) at ~1266 cm may also be the product of acidification within the Endinger Bruch basin. The impact of volcanic ash upon lake systems may have two detrimental effects on fish populations. Firstly, studies have shown that at pH <5.0, malformations and death among fish populations are extremely common, especially during periods of spawning. The eruption of the Laacher See is believed to have occurred during late spring/early summer (Schmincke *et al*., 1999) which coincides with the spawning periods of most northern European freshwater fish. Whether acidification of Endinger Bruch caused pH to fall as low as this is difficult to judge, however in studies of lakes much closer to the Laacher See volcano it was found that the modelled drop in pH was not much more than the error range for the model (Birks and Lotter, 1994). Secondly, volcanic ash at quantities ~6.1 g/litre is fatal to fish. Data gathered following the eruption of Mt St Helens showed ash covers fish gills, leading to impaired respiration and subsequent death (Newcomb and Flagg, 1982).The acidification and direct ash fall within Endinger Bruch during this period may well have led to the temporary reduction of fish, leading to greater predation pressure by aquatic invertebrates, which have greater tolerances to such events, thus causing the observed increase in *B. longirostris* mucro length (Sweetman and Finney, 2003).

Younger Dryas: EOZ V, ECZ IV and ECZ V

The transition into the Younger Dryas is clear in the Endinger Bruch profile. The reduction in TN and TOC are indicative of reduced deposition of OM within the basin. Because the cooling of the Younger Dryas should lead to more depleted $\delta^{13}C_{org}$ values; the enrichment of $\delta^{13}C_{org}$ relative to depleted $\delta^{15}N_{org}$ values between 1246 - 1131 cm is consistent with increased algal productivity, most probably triggered by nutrient loading of the basin caused by a higher degree of erosive input (Street *et al.,* 2012*)*. By 1131 cm, $\delta^{13}C_{org}$ values plateau and remain stable, this couple with relatively enriched $\delta^{15}N_{org}$ values, suggests a slight increase in the trophic state of Endinger Bruch and thus algal productivity (Lücke *et al*., 2003). The C:N record during this phase drops slightly in response to the $\delta^{13}C_{org}$ and $\delta^{15}N_{org}$ record, but however remains ~14, likely due to the steady input of terrestrial material from the surrounding catchment. A similar pattern of $\delta^{13}C_{org}$ and $\delta^{15}N_{org}$ response during the

Younger Dryas was observed at both Meerfelder Maar and Lake Holzmaar, which are both situated in the Eifel region of Germany (see Lücke *et al*., 2003; Lücke and Brauer *et al*., 2004) as well as Lake Kråkenes in Norway (Birks *et al*., 2000). While the early Younger Dryas shows elevated levels of primary production, it is most likely that the entire Younger Dryas period was characterised by an oligotrophic type environment with relatively low nutrient levels compared to the previous Allerød period. The possible bipartite feature of the Younger Dryas will be discussed further in Chapter 7 (section 7.2.3.2).

Cladoceran numbers drop significantly at the onset of the Younger Dryas with only *C. sphaericus* and *B. longirostris* recorded in any abundance. The increase in the pelagic: benthic ratio throughout the Younger Dryas is consistent with increased water depth and therefore open water within the Endinger Bruch Basin. For most of the Younger Dryas, *B. longirostris* contributes >50 % of the total cladoceran assemblage, however only in low abundances of typically <5000 50 / ml. The clear increase in *B. longirostris* mucro length (Figure 6.12) during the Younger Dryas suggests a significant shift in the ecosystem of Endinger Bruch. Studies have highlighted the effect winter ice cover can have lake ecosystems, with winter fish kills well documented (see Sin and Chiu, 1982). The primary cause of fish deaths within ice covered lakes is oxygen depletion (see Meding and Jackson, 2003). The cascading effect of fish kills on the cladoceran community has recently been investigated by Balayla *et al*., (2010). Their studies showed that during periods of ice cover, and thus reduced fish populations, cladocerans increased in size with the mucro lengths of *B. longirostris* also exhibiting an increase in length. The loss of fish therefore shifts predation pressure towards aquatic invertebrates, which causes the increase in mucro length. The increase in mucro length during the Younger Dryas of Endinger Bruch therefore shows that during this time, fish populations were significantly reduced. The subsequent rapid reduction in mucro lengths at the onset of the Holocene, suggests however that fish remained present within Endinger Bruch albeit, at lower abundances.

Holocene: EOZ VI, EOZ VII, ECZ VI, ECZ VII

The Endinger Bruch Holocene can be seen as a bipartite sequence, with changing sources of organic matter input. Between 1001 - 911 cm the synchronous increase in TOC, TN and C:N coupled with

depleted $\delta^{13}C_{org}$ and $\delta^{15}N_{org}$ values is interpreted as a mixed algal and terrestrial/semi aquatic signal. The $\delta^{13}C_{org}$ values are in line with the range of lacustrine algae utilizing CO_2 in equilibrium with the atmosphere (Meyers, 1993, 2003) this is further supported by the increases in *Pediastrum* sp. during the early Holocene (de Klerk, 2002). The elevated C:N values are unlikely to be caused by algal productivity under nutrient limited conditions due to the high TOC and TN values (see Street *et al*., 2012), and therefore represent allochthonous input into the basin. A reduction in water depth during this phase is supported by the decrease in *B. longirostris* abundance and subsequent rise in *P. uncinatus* and *S. crystallina*, both of which inhabit shallow muddy/weedy type environments (Kattle and Sirocko, 2011). The exposure of a larger littoral zone would also increase allochthonous input into the basin, thus contributing to the rise in C:N. From 911 cm onwards, the $\delta^{13}C_{org}$ record becomes increasingly enriched while $\delta^{15}N_{org}$ continues to become more depleted. This is coupled with increasing TOC and TN values and falling C:N values (Figure 6.8). *B. longirostris* abundances increase above 911 cm at the expense of *S. Crystallina* and *P. uncinatus*, which although still present, are reduced in concentration. This is interpreted as increasing autochthonous productivity coupled with reduced input from the surrounding basin. Interestingly, the concentration of *Pediastrum sp* falls, from this point onwards. This however may be a consequence of a reduced littoral zone due to reduced water depth in Endinger Bruch and the stabilising of surrounding landscape (as witnessed during the Allerød), thus reducing nutrient input into the basin relative to the interval 1001 - 911 cm.

6.3 Potremser Moor, Germany

6.3.1 Isotope and organic content record

Potremser Moor is represented by a fragmentary OM record (representing variations in the aquatic system and terrestrial conditions surrounding the basin during the Lateglacial – Holocene) due to extremely low organic carbon weights (<0.2 mg). This problem is particularly evident between 560 - 540 cm, where only a small number of samples with sufficient organic carbon weights (>0.2 mg) where recorded. The other depths at which Potremser Moor has an incomplete OM record are: 522 - 518 cm, 514 - 510 cm, 506 - 502 cm, 494 - 484 cm, 474 - 462 cm, 444 - 440 cm and 432 - 424 cm (Figure 6.14). There is a stepwise increase in the organic content record located at 484 cm with TOC and TN both increasing from 0.11 wt% TOC, 0.40 wt% TN to 0.78 wt% TOC, 3.44 wt% TN.TOC and

TN are highly correlated between 560 - 484 cm (POZ I and POZ II; r = 0.805, n = 26). The agreement between TOC and TN breaks down above 484 cm (POZ III; ~10,666 – 10,227 cal yr BP), the causes of this will be discussed further in section 6.3.2. Alongside the shifting relationship between TOC and TN is variability reflected in the $\delta^{13}C_{org}$ (-10.17‰ to -29.74‰), $\delta^{15}N_{org}$ (-3.57‰ to 3.21‰) and C:N (12.45 to 31.88) of sediments. Major changes in the sedimentary organic record were used to define three separate OM zones which are presented in Figures 6.14 and 6.15 and will be discussed sequentially below.

POZ I: 560 – 540 cm (no age estimate)

The first OM zone within Potremser Moor is characterised by low amounts of organic carbon leading to an incomplete OM record between 560 - 540 cm. The recordable values of $\delta^{13}C_{org}$ show extremely high values of -12.71‰ to -10.17‰ between 556 - 550 cm (Figure 6.16) which are negatively correlated with C:N (r = -0.795, n = 5; Figure 6.15F). Following these high values, the remaining $\delta^{13}C_{org}$ samples appear to indicate a decline in values dropping to -29.74‰ at 544 cm. $\delta^{15}N_{org}$ values show a relatively enriched $\delta^{15}N_{org}$ values of 0.34‰ to 2.05‰ during POZ I, these however are punctured by a significant reduction in values at 552 cm ($\delta^{15}N_{org,}$ -3.57‰). As discussed the TOC record is extremely low within POZ I with values recorded of 0.03 wt% to 0.06 wt%. The TN record is likewise low within POZ I there is however an slight increase in values within the zone from 0.17 wt% at 552 cm to 0.38 wt% at 540 cm. The C:N record appears to be high within the early stages of POZ I, with values peaking at 31.88 at 552 cm. Following this peak the C:N record declines throughout the zone, dropping to 17.39 at the boundary with POZ II. Whilst the available data points give an impression of the likely OM conditions during POZ I, one must be careful as they may miss smaller variations in the OM record.

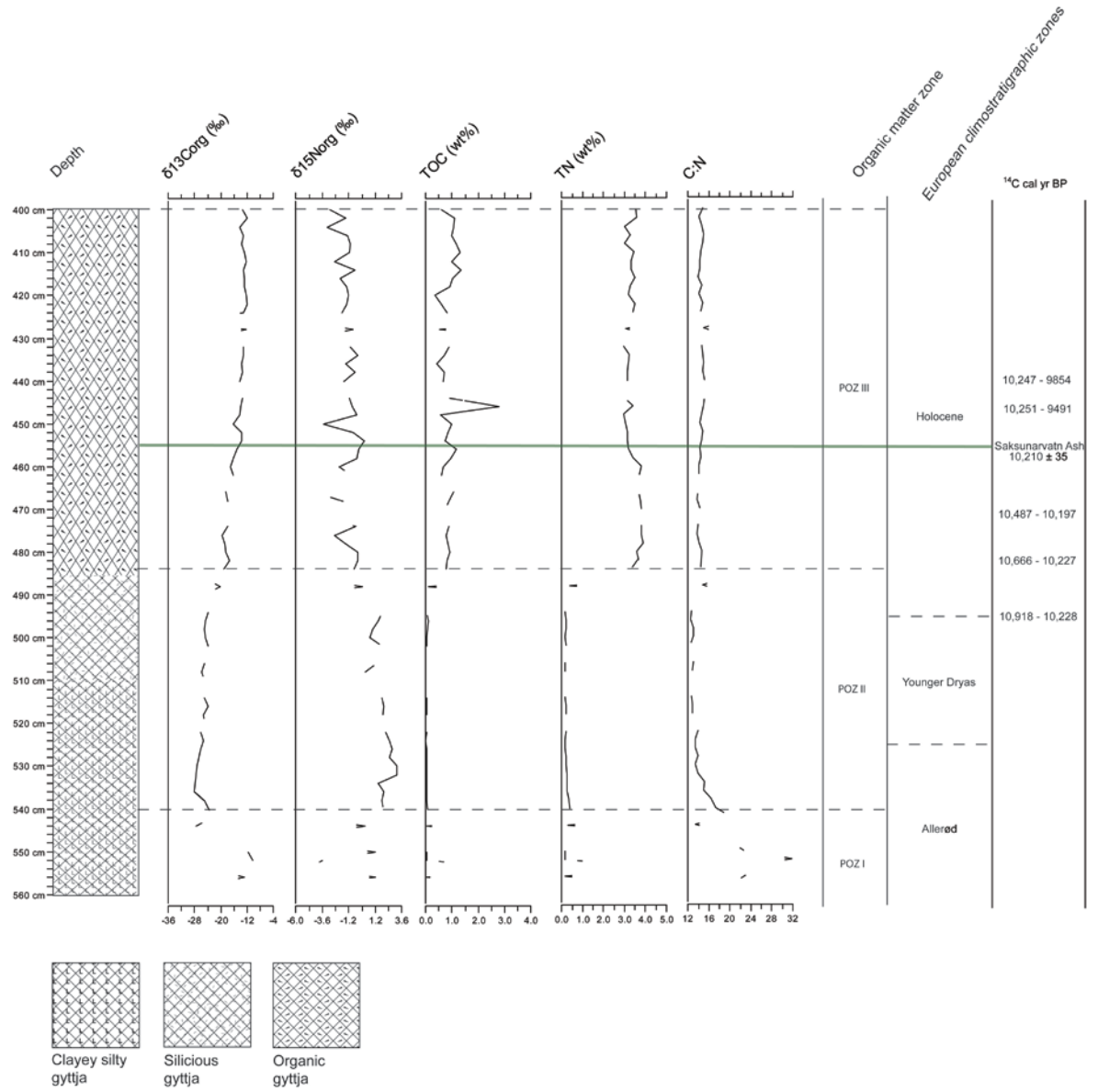
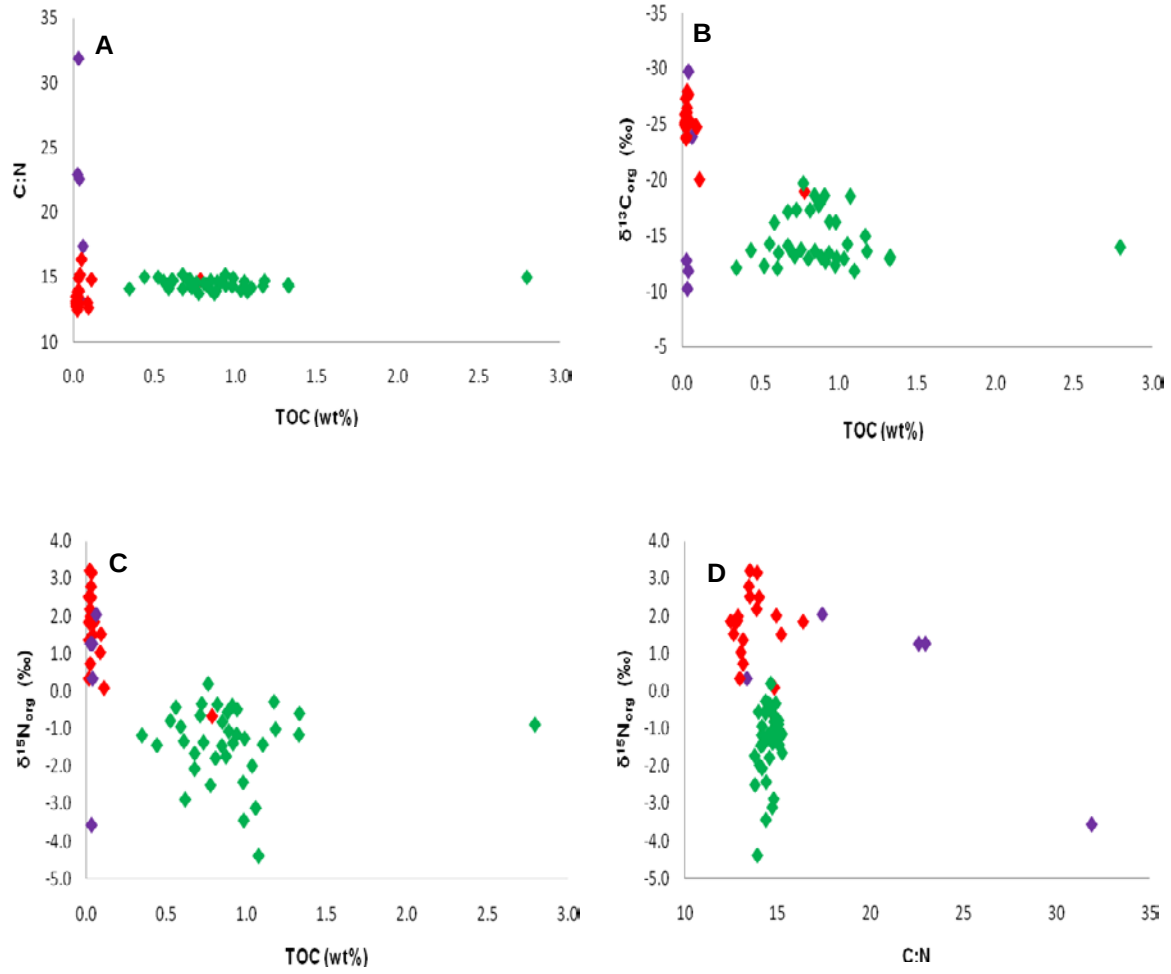


Figure 6.14 – Stable isotope profiles and selected organic properties, showing lithology, $\delta^{13}C_{org}$, $\delta^{15}N_{org}$, TOC, TN, C:N, major European climostratigraphic zones, radiocarbon dates and the Saksunarvatn Ash in Potremser Moor. The three OM zones for the profile are listed as POZ I – POZ III.

POZ II: 540 – 484 cm (no age estimate – 10,463 ± 237 cal yr BP)

The decline in $\delta^{13}C_{org}$ values suggested within POZ I appears to be reversed within the early stages of POZ II with values of -23.85‰ at 540 cm. The $\delta^{13}C_{org}$ record drops slightly at 520 cm (-27.36‰) before increasing steadily throughout the remainder of the zone culminating in values of -18.95‰ at

the boundary with POZ III. The $\delta^{15}N_{org}$ record decreases throughout POZ II. Maximum values of 3.21‰ are recorded at 530 cm, this peak however is followed by a gradual decline in values before reaching -0.68‰ at 484 cm. As with the previous zone, the TOC and TN record remains extremely low. TOC values remain <0.1 wt% throughout much of the zone with a small rise to 0.78 wt% recorded at 484 cm. TN values also record an increase in values at 484 cm, rising from 0.19 wt% - 0.40 wt% to 3.44 wt%. As with the $\delta^{15}N_{org}$ record, the C:N record decreases throughout POZ II. Values decrease from 16.37 at the onset of the zone to 14.81 at its boundary with POZ III.



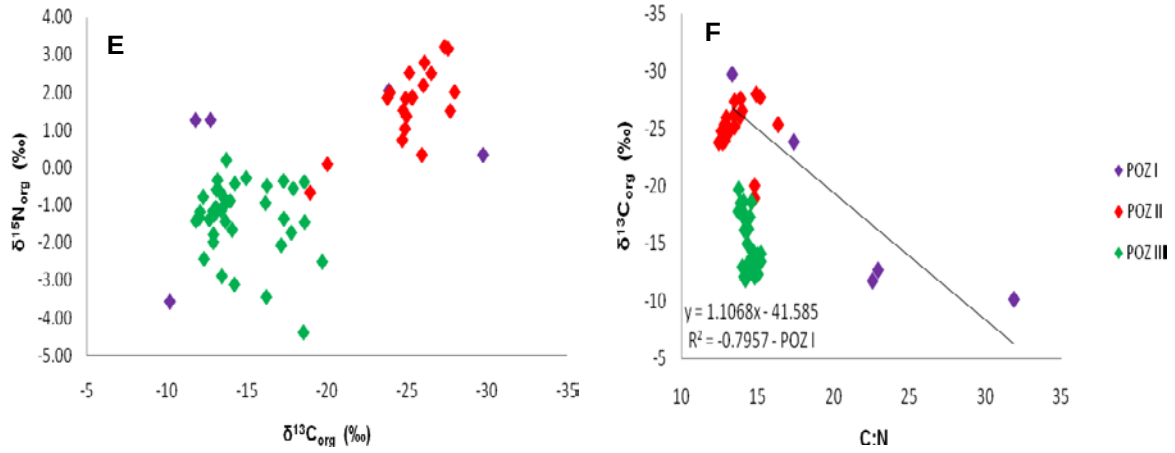


Figure 6.15 – Bi-plots of stable isotope values and selected organic properties for Potremser Moor. Figures A – F are plotted as OM zones (POZ I – POZ III). Significant relationships between parameters discussed in the text are marked by linear regression parameters in Figure 6.15F and are according to the equation y = a·x +b.

POZ III: 484 – 400 cm (10,463 ± 237 – no age estimate)

The onset of POZ III is characterised by increasing $\delta^{13}C_{org}$ values of -19.69‰ to -16.15‰. At 456 cm however there is a jump in values of 1.3‰, rising from -16.25‰ at 458 cm to -14.95‰. This is then followed by a steady enrichment in values, culminating in extremely high values of -11.82‰ close to the top of the core. The $\delta^{15}N_{org}$ record declines throughout POZ III, this however is not gradual with more depleted values recorded at 450 cm (-3.44‰) and at 404 cm (-3.11‰). As with TOC throughout the entire core, values are low within POZ III, however there is a slight increase in values from 0.82 wt% at the start of the zone to 1.10 wt% at 402 cm. There are several abrupt increases in TOC within POZ III, most notably at 446 cm (2.80 wt% TOC), 414 cm (1.33 wt% TOC) and 402 cm (1.10 wt% TOC). The TN record experiences the largest shift across all parameters within the Potremser Moor core. Throughout POZ I and POZ II, TN remains low, however the POZ II/III transition is characterised by 760% increase in TN values over the space of 2 cm (Figure 6.14). Following this large and rapid increase, TN values become relatively stable from 2.95 wt% to 3.91 wt% for the remainder of POZ III. C:N values show a small rise in values between 484 - 428 cm, with values peaking at 15.23 (440 cm). This rise however then gives way to falling values which drop to 14.77 at the top of the core.

6.3.2 Deviation of TN record

As discussed within section 4.6.4 (Chapter 4) the correlation of TOC – TN within Potremser Moor breaks down. POZ I and POZ II both show extremely strong correlations between TOC – TN, this however then collapses with progression into POZ III (Figure 6.16A). The cause of this breakdown during POZ III is likely due to a weakening in the uptake of Dissolved Inorganic Nitrogen (DIN; NO_3^-, NO_2^-, NH_4^+) by algae within Potremser Moor. DIN is the primary source of nitrogen for lacustrine, non-nitrogen fixing algae, and during periods of high productivity a higher proportion of the DIN reservoir is consumed. This process increases the $\delta^{15}N$ values of the remaining reservoir, thus producing an increase in the $\delta^{15}N_{org}$ values of subsequently produced organic matter (Hyodo and Longstaffe, 2011). Conversely when productivity is low, a lower proportion of the DIN reservoir is utilised by algae, thus producing organic matter with depressed $\delta^{15}N_{org}$ values. Figure 6.16B shows a bi-modal relationship between TN and $\delta^{15}N_{org}$ in the Potremser Moor core suggesting that algal productivity within the system is low during POZ III (Holocene) and that the Allerød and Younger Dryas were influenced by separate basin processes than the Holocene.

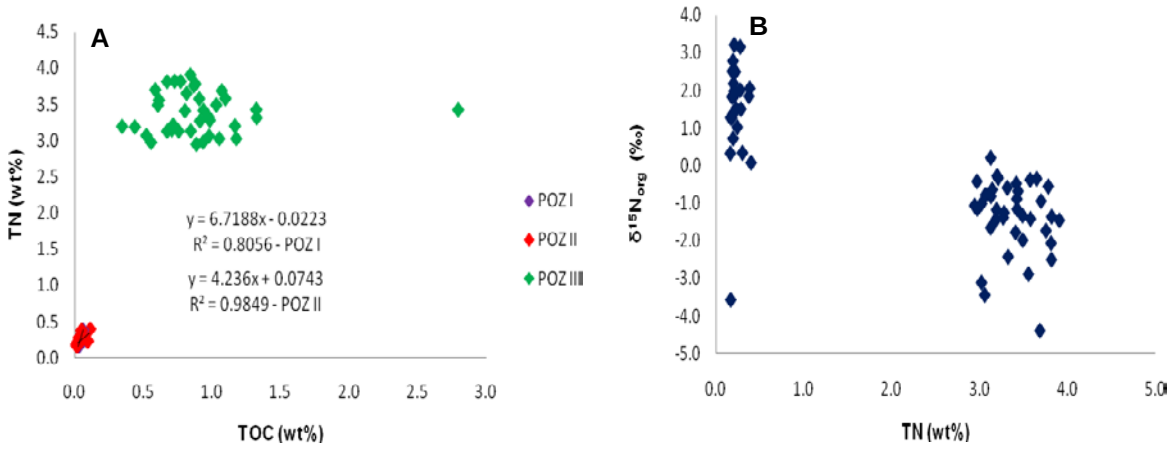
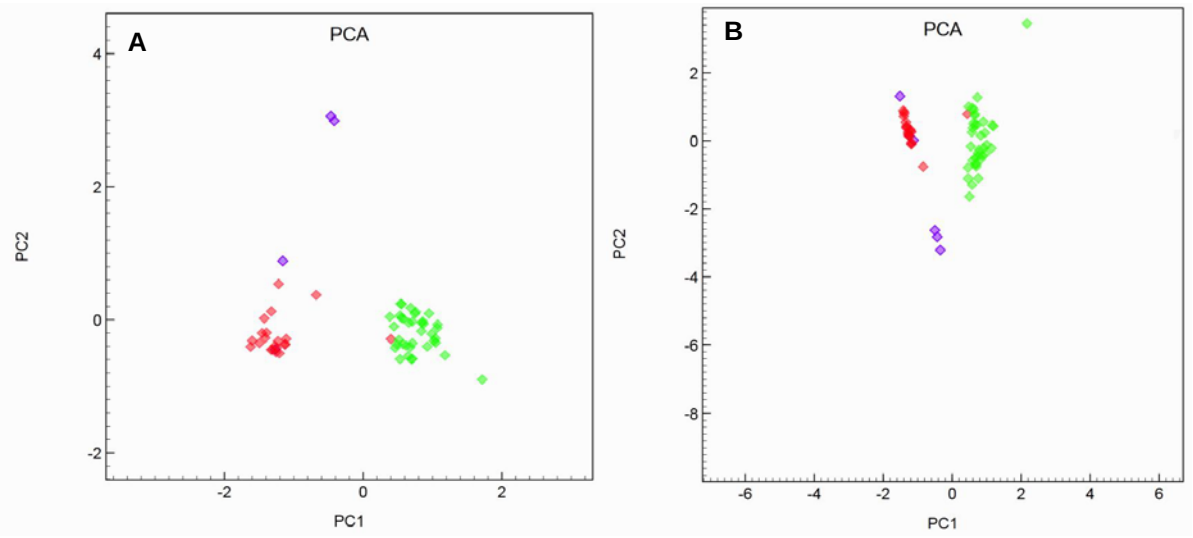


Figure 6.16 – Bi-plots of TN – TOC for POZ I – POZ III and TN – $\delta^{15}N_{org}$ for all OM zones in Potremser Moor. A – OM zones POZ I and POZ II show a strong linear relationship, indicating low inorganic nitrogen within these OM zones. POZ III however, shows no such relationship, indicating the relationship between TN – TOC has broken down during these zones. B - The bi-modal

relationship between TN – $\delta^{15}N_{org}$ within the Potremser Moor core. Linear regression parameters given in POZ I and POZ II according to the equation y = a·x + b.

6.3.3 Distinction of OM zones

PCA analysis of the Potremser Moor OM zones indicate they can be distinguished based upon organic content parameters. Figure 6.17A gives the clearest separation based upon $\delta^{13}C_{org}$, $\delta^{15}N_{org}$, TOC, TN and C:N data, with POZ I, POZ II and POZ III forming distinct groups. There is a degree of overlap between POZ I and POZ II which is highlighted in Figure 6.17B and C. Due to the fragmentary record present in POZ I it is not possible to determine the extent of this overlap, however based upon Figure 6.14 it is possible to interpret this overlap as a result of similar TOC and TN values within each zone.



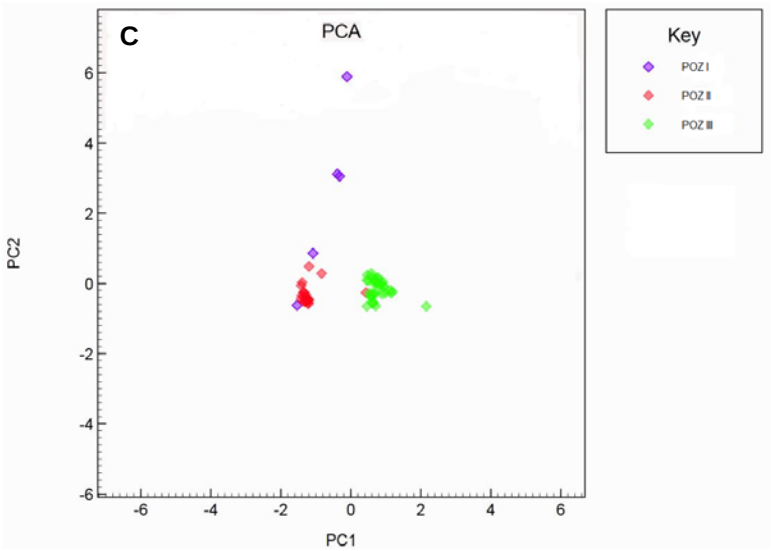


Figure 6.17 – PCA bi-plots of selected isotopic and organic properties for Potremser Moor plotted by: A = $\delta^{13}C_{org}$, $\delta^{15}N_{org}$, TOC, TN and C:N. B = $\delta^{13}C_{org}$, TOC and TN. C = $\delta^{13}C_{org}$, TOC, TN and C:N.

6.3.4 Chronozone distinction

The chronozones within Potremser Moor show relatively distinct OM profiles (Figure 6.18A, B and C. The Holocene is the most clearly defined chronozone, with good sepertaion from the Allerød and Younger Dryas. The Younger Dryas is also tightly clustered showing vary little variation in values. The Allerød by contrast, shows some overlap with the Younger Dryas, with a trend in values towards the Younger Dryas (Figure 6.18A, B and C). Unlike the Holocene and Younger Dryas, the Allerød is characterised by a wide scatter of data due to the large variability in the $\delta^{13}C_{org}$ and C:N record.

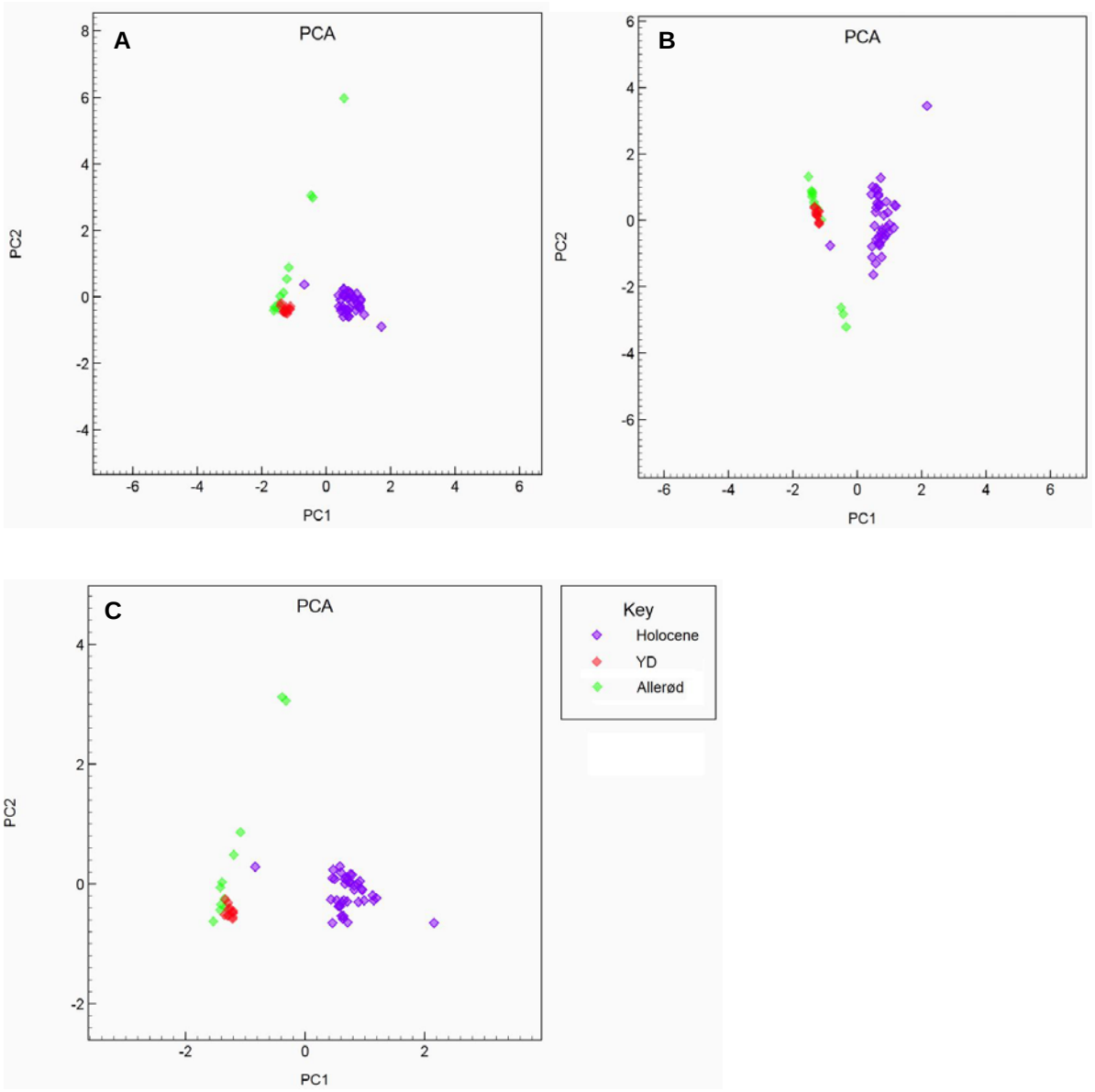


Figure 6.18 – PCA bi-plots of selected isotopic and organic properties for Potremser Moor plotted by: A = $\delta^{13}C_{org}$, $\delta^{15}N_{org}$, TOC, TN and C:N. B = $\delta^{13}C_{org}$, TOC and TN. C = $\delta^{13}C_{org}$, TOC, TN and C:N.

The data presented in Figure 6.18A, B and C indicates that the chronozones within Potremser Moor are represented by different OM regimes. The tight clustering of data attributed to the Holocene and Younger Dryas suggests that there was little OM variation during these intervals, with autochthonous and allochthonous processes consistent. The Allerød by contrast shows values associated with the early Younger Dryas and is represented by a widely varying OM profile. Due to the incomplete record,

it is difficult to fully ascertain OM response during the Allerød, however from the data available it is possible to see a general pattern of $\delta^{13}C_{org}$ depletion coupled with decreasing C:N values.

6.3.5 Cladoceran record

A total of 22 cladoceran species were identified from chitinous remains including, ephippia, headshields, carapaces and post abdomen claws (Table 6.3). The greatest number of species recorded from a single sample is 14 which occur within Holocene gyttja at 450 cm while the maximum total cladoceran count comes from 400 cm, with counts of 39,211 individual cladocerans per 50 ml. Six distinct cladoceran assemblage zones (PCZ I – VI) were defined within Potremser Moor as shown in Figure 6.19.

Chydorids	Non-chydorids
Chydoridae	Bosminidae
Acroperos harpae Baird	*Bosmina coregoni* Baird
Alona affinis Leydig	*B. longirostris* O.F. Muller
A. costata Baird	
A. guttata/ rectangula Sars	Daphniidae
A. guttata var tub Sars	*D. pulex* Leydig
A. quadrangularis O.F. Muller	
Alonella excisa Fischer	Sididae
A. nana Baird	*Sida crystallina* O.F. Muller
Camptocercus rectirostris Schödler	
Chydorus sphaericus O.F. Muller	
C. piger Sars	
Eurycercus lamellatus O.F. Muller	
Graptoleberis testudinaria Fischer	
Leydigi acanthocercoides Fischer	
L. leydigi Schödler	
Monospilus dispar Stebbing	
P. truncates	
P. uncinatus Stebbing	

Table 6.3 – List of cladoceran species recorded for Potremser Moor. The nomenclature follows Scourfield and Harding (1966).

PCZ I: 560 – 540 cm (no age estimate)

PCZ I is dominated by four benthic species, *A. harpae* (mean – 870 ± 404 / 50 ml), *A. nana* (mean – 841 ± 672 / 50 ml), *C. sphaericus* (mean – 1586 ± 807 / 50 ml) and *E. lamellatus* (mean – 581 ± 474 /

50 ml). Total cladoceran counts within PCZ I remain low, reaching a maximum of 8650 ± 1931 / 50 ml at 552.5 cm. *B. longirostris* numbers climb steadily within PCZ I, peaking at 555 cm, with counts of 825 ± 329 / 50 ml, following this rise however, their abundance tails off to 91 / 50 ml at 550 cm before climbing again at the boundary with PCZ II. *A. harpae* and *A. nana* decrease throughout PCZ I, dropping from 1263 to 278 / 50 ml and 2017 to 306 / 50 ml respectively. In contrast, *C. sphaericus* abundance remains relatively stable between 560 - 545 cm, before dropping to 389 / 50 ml at 540 cm. *B. longirostris* mucro length during PCZ I, varies from 39 - 55 µm (Figure 6.20). An apparent drop in mucro values at 550 cm is attributed to no fully intact mucrone being recorded.

PCZ II: 540 – 530 cm (no age estimate)

Total cladoceran numbers decline within PCZ II, falling to a minimum of 2378 ± 377 / 50 ml at 530 cm. Coupled with this reduction is a rise in the pelagic: benthic ratio to 0.95 at 532.5 cm, an increase of ~500% from the previous zone. This is driven by the overall reduction in total benthic species during this zone, falling from a mean value of 4726 / 50 ml within PCZ I to 1725 / 50 ml coinciding with the small increase in *B. longirostris* abundance (mean – 656 ± 249 / 50 ml). The appearance of *D. pulex* at 537.5 – 532.5 cm (mean – 556 ± 358 / 50 ml) coincides with a reduction in *B. longirostris* and *C. sphaericus*, with *E. lamellatus* abundances also significantly reduced coinciding with peak *D. pulex* numbers at 532.5 cm (Figure 6.19). There is no significant change in *B. longirostris* mucro length or size variability within PCZ II, with a median length of 47 µm recorded (Figure 6.20).

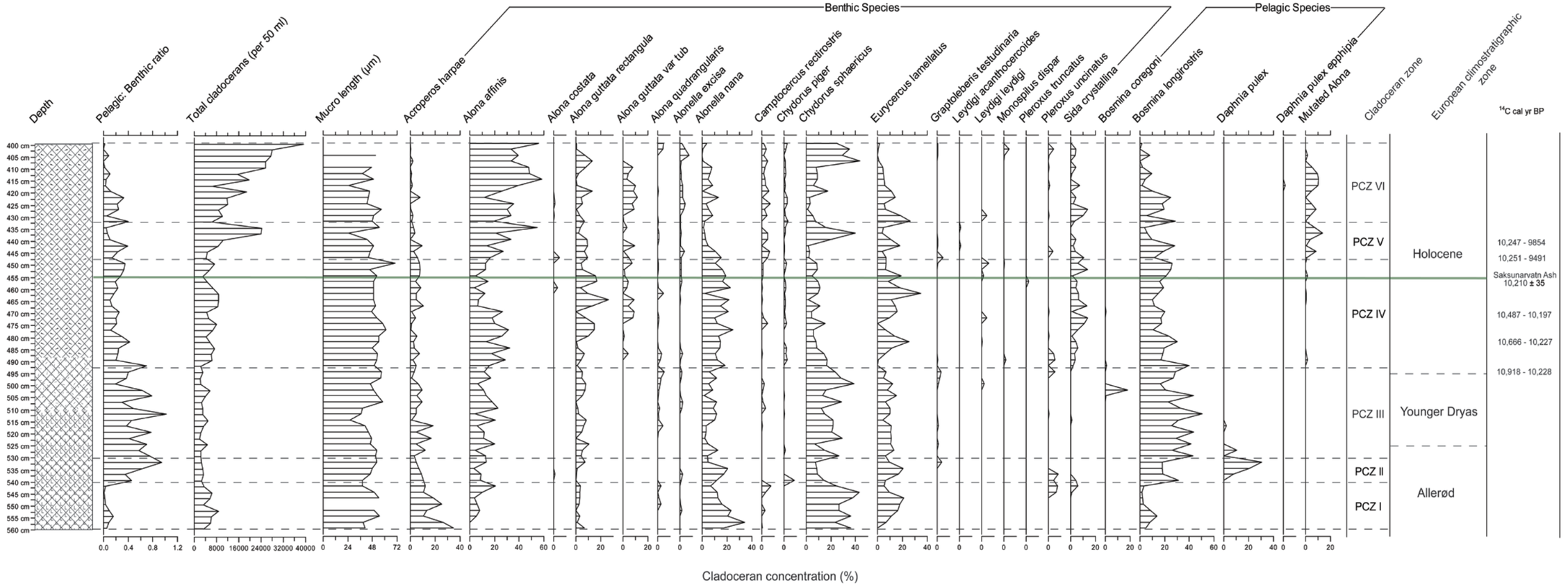


Figure 6.19 – Composite diagram of lithology, relative abundance of cladoceran species, major European climostratigraphic zones, radiocarbon dates and the Saksunarvatn Ash in Potremser Moor. Species are expressed as percentages of the total cladoceran count for each level. Bosmina mucro length and total cladoceran counts (expressed as absolute) are also shown.

PCZ III: 530 – 492.5 cm (no age estimate – 10,550 ± 310 cal yr BP)

Total cladoceran numbers remain low within PCZ III ranging from a minimum of 1991 / 50 ml at 522.5 cm to a maximum of 5754 / 50 ml at 502.5 cm. The pelagic: benthic ratio fluctuates widely within PCZ III, with values ranging from 0.2 - 1.02. This variability in the pelagic: benthic ratio is characterised by five distinct peaks in the pelagic: benthic ratio located at 525 cm, 520 cm, 512.5 cm, 505 cm and 492.5 cm. PCZ III is largely dominated by the pelagic community of cladocerans, with *B. longirostris* prevalent throughout the entire zone (mean – 1023 ± 483 / 50 ml). The benthic record is again characterised by *A. harpae* (mean – 219 ± 168 / 50 ml), *A. nana* (mean – 245 ± 148 / 50 ml), *C. sphaericus* (mean – 609 ± 229 / 50 ml) and *E. lamellatus* (mean – 284 ± 156 / 50 ml). In addition *A. affinis* abundance increases by ~50% within PCZ III, with mean values of 432 / 50 ml recorded. As with the previous two cladoceran zones, *B. longirostris* mucro length remains at ~47 µm (Figure 6.20) however a significant reduction is recorded between 515 cm and 517.5 cm where lengths drop by ~26 (ANOVA p = 0.045364).

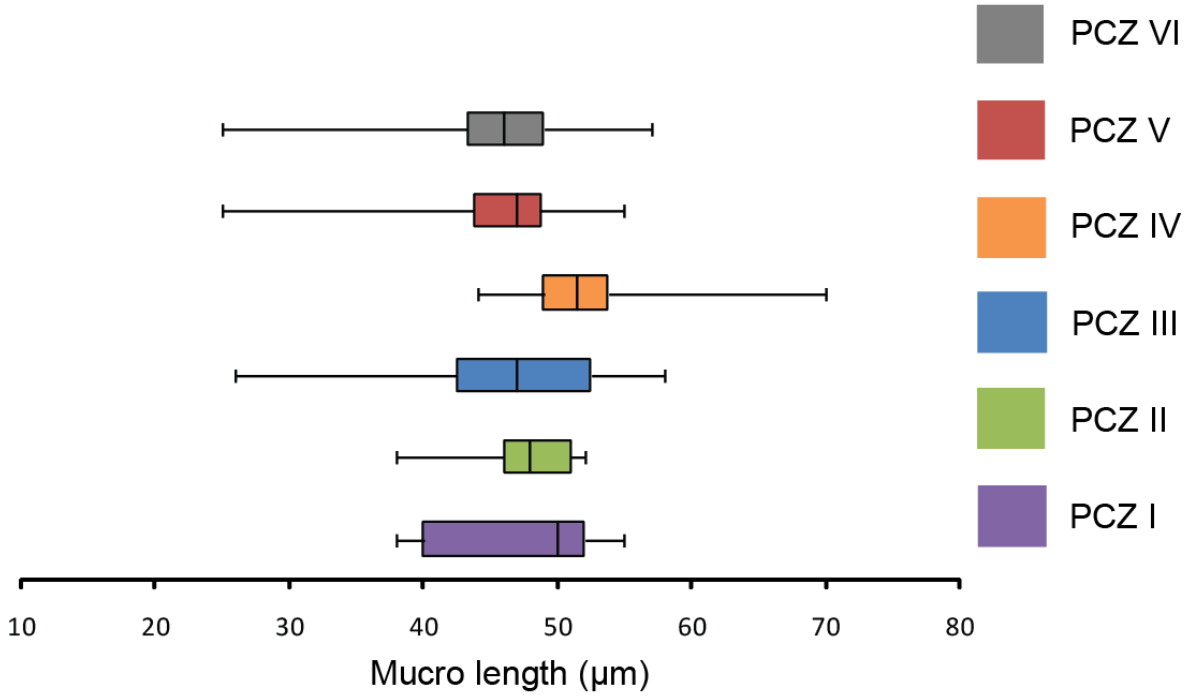


Figure 6.20 – Box plots of *B. longirostris* mucro length plotted by cladoceran zone for Potremser Moor.

PCZ IV: 492.5 – 447.5 cm (*10,550 ± 310 – 10,125 ± 125 cal yr BP)*

Total cladoceran numbers show an overall increase between 492.5 - 465 cm, rising from 2268 / 50 ml to 8688 / 50 ml before declining towards the boundary with PCZ V (Figure 6.19). The pelagic: benthic ratio decreases throughout PCZ, falling to 0.13 at the boundary with PCZ V. The drop in the pelagic: benthic ratio is evidence of an overwhelming dominance of benthic species within this portion of the Potremser Moor core. The benthic record is still characterised by *A. affinis* (mean – 1029 ± 591 / 50 ml), *A. nana* (mean – 910 ± 418 / 50 ml) and *E. lamellatus* (mean – 747 ± 688 50 / ml). Coupled with this, abundances of *A. guttata/ rectangula* (mean – 588 ± 553 / 50 ml) and *S. crystallina* (mean – 417 ± 294 / 50 ml) increase during PCZ IV; the first consistent expansion of the species in Potremser Moor. Mean numbers of *B. longirostris* remain consistent from the preceding zone at 1102 / 50 ml, with their overall percentage dropping due to the increase in benthic species. *B. longirostris* mucro length increases during PCZ IV to a median length to 52 µm, this is associated with the longest mucro lengths recorded during the entire core (~70 µm) located at 450 cm.

PCZ V: 447.5 – 432.5 cm (10,125 ± 125 cal yr BP – no age estimate)

The penultimate zone in Potremser Moor is characterised by a large increase in total cladocerans, rising to peak at 24,139 / 50 ml at 435 cm (Figure 6.19). This large increase in total cladocerans is accompanied by a drop in the pelagic: benthic ratio, falling to a zone low of 0.04 at 335 cm. The increase in benthic species is driven by a large peak at 435 cm in *A. affinis*, rising to 13,263 (mean – 3750 ± 4976 / 50 ml) and *C. sphaericus*, rising to 9574 (mean – 2340 ± 3836 / 50 ml) at 237.5 cm while numbers of *A. nana* (mean – 390 ± 143 / 50 ml) and *S. Crystallina* (mean – 212 ± 187 / 50 ml) fall within PCZ V. Mean values of *B. longirostris* increase during PCZ V and are characterised by three small peaks in total abundance at 442.5 cm, 437.5 cm and 432.5 cm. *B. longirostris* mucro length decreases within PCZ V, falling to 44 µm (Figure 6.20). Mutated forms of *A. affinis*, characterised by head pore anomalies, are also present within PCZ V, with peak values of 3235 / 50 ml at 437.5 cm (Figure 6.19).

PCZ VI: 432.5 – 400 cm (no age estimate)

Total cladoceran values increase throughout PCZ VI, with an initial peak of 13,956 / 50 ml, followed by a drop, and a second increase to 18,477 / 50 ml at 402.5 cm. The pelagic: benthic ratio increases within the early stages of PCZ VI, rising to 0.33 at 422.5 cm, before declining throughout the remainder of the zone (Figure 6.19). The dominance of the benthic record is again driven by *A*. *affinis* (mean – 7295 ± 5585 / 50 ml) and *C. sphaericus*, which increases to a peak value of 11,250 / 50 ml at 407.5 cm. Mean values of *B. longirostris* remain close to those of the previous zone, however there is decline in abundance throughout PCZ VI, with no individuals recorded at 407.5 cm and 402.5 cm. Mucro length shows little variation from the previous zone, with median values of 45 µm (Figure 6.20).

6.3.6 Palaeoevolution of Potremser Moor

Allerød: POZ I, POZ II, PCZ I, PCZ II and PCZ III

As discussed in section 6.3.1, there are only a few data points attributed to the Allerød period in Potremser Moor. Whilst caution must be used in over-interpreting the data, the following conditions can be suggested as likely to have occurred in the basin during the Allerød. The Allerød, as represented in Potremser Moor, is characterised by enriched $\delta^{13}C_{org}$ values which are consistent with those exhibited by aquatic plants such as *Potamogeton* which would have thrived in the shallow conditions experienced at the site during this period (Osmond *et* al., 1981; Meyers and Ishiwatari, 1995; Lücke *et al*., 2003). The high (>16) C:N values, particularly between 560 - 540 cm are interpreted as representing periods of terrestrial input into the basin, coupled with low algal productivity (Lamb *et al*., 2004). The cladoceran community between 560 - 540 cm confirms the interpretation of a shallow lake system with low algal primary productivity, coupled with unstable input events. Abundances of *A. harpae*, *A. nana* and *C. sphaericus*, coupled with low *B. longirostris* is indicative of unstable substrates, with shallow water (Figure 6.19). After 540 cm, conditions within Potremser Moor generally improve, with higher levels of primary algal productivity. $\delta^{13}C_{org}$ values become more depleted and fall to a range typical of lacustrine algae (< -26‰), supporting this is the reduction in C:N values, which gradually decline from >31 to 13 and the enrichment of $\delta^{15}N_{org}$ values during the duration of the Allerød (Olsen *et al*., 2010). This second phase of the Allerød is

characterised by a shift in the dominant cladoceran fauna. Abundances of *A. harpae*, *A. nana* and *C. sphaericus* all decline, whilst *B. longirostris* and *D. pulex* both increase. The relationship between *B. longirostris* and *D. pulex*, during 540 - 530 cm suggests a shift in predation pressure in the Potremser Moor basin. As discussed previously, the presence of *D. pulex* and reduction in *B. longirostris* is consistent with an absence of fish predation. This interpretation is supported by changes in *B. longirostris* mucro length during this period. There is a significant increase in mucro length between 540 - 530 cm (ANOVA p = 0.000304), which suggests that with an absence of fish, predation pressure is primarily driven by aquatic invertebrates (Sweetman and Finney, 2003). Following the loss of *D. pulex* and renewed dominance of *B. longirostris* after 530 cm, mucro lengths decline steadily towards the Younger Dryas boundary.

Younger Dryas: POZ II and PCZ III

The Younger Dryas is characterised by stability throughout much of the OM record (Figure 6.14). OM conditions are interpreted as reflecting the primary deposition of algal derived organic material. Low TOC, TN, C:N and LOI values indicate a loss of aquatic macrophyte derived material, and a greater abundance of primary algal deposition (Janbu *et al*., 2011). This is supported by consistent $\delta^{13}C_{org}$ values which remain at approximately -26‰ and elevated $\delta^{15}N_{org}$ values. While algal productivity is the primary driving force behind the observed OM signal, autochthonous productivity is still low, which like the Younger Dryas of Endinger Bruch, is likely to be typified by an oligotrophic type environment. Total cladoceran numbers do not undergo a rapid decline, as is witnessed within some of the other sites in this study, with numbers already low from the previous Allerød period. Community structure is also relatively consistent with *A. harpae*, *A. nana*, *C. sphaericus* and *E. lamellatus* all present. The abundance of *B. longirostris* increases during the Younger Dryas, increasing pelagic: benthic values, thus indicating expanding open water conditions (Duigan and Birks, 1995). Mucro length continues to decline during the Younger Dryas, however at 515 cm there is a sudden increase, which remains high well into the Holocene. This change, as seen during the previous Allerød period, indicates a change in predation pressure. A similar pattern is witnessed during the Younger Dryas of Endinger Bruch, whereby a likely loss of fish populations led to an elevation in mucro lengths. The rise in mucro lengths during the second half of the Younger Dryas in Potremser Moor may therefore indicate a

change in predation pressure, with the presence of planktivorous fish unlikely at this point. The possible reasons for this will be further addressed in section 7.2.1 (Chapter 7).

Holocene: POZ II, POZ III, PCZ III, PCZ IV, PCZ V and PCZ VI

The Holocene shows abrupt increases in the TOC and TN records (Figure 6.14) The C:N record shows a slight increase during the Holocene, with values approaching 15. The $\delta^{13}C_{org}$ record becomes progressively enriched during the Holocene, whilst $\delta^{15}N_{org}$ values by contrast become progressively depleted. The enriched $\delta^{13}C_{org}$ values are consistent with those produced by aquatic macrophytes (Aichner *et al*., 2010). As discussed within section 6.3.2, the non-linear relationship between TOC – TN during this period is characteristic of reduced DIN uptake by algae during the Holocene. The weakening of primary algal driven productivity therefore coincides with the expanse of aquatic macrophytes across the Potremser Moor basin. This interpretation is supported by changes in cladoceran community structure. Abundances of *B. longirostris* decline throughout the Holocene, with shallow water, benthic species increasing. The emergence of *S. crystallina* at the onset of the Holocene confirms the presence of abundant vegetation, with the species strongly associated with *Potamogeton* (Scourfield and Harding, 1966). The gradual reduction in the pelagic: benthic record during the Holocene indicates that this period was characterised by decreasing water depths, with limited open water type conditions.

6.4 Kieshofer Moor

6.4.1 Isotope and organic content record

At Kieshofer Moor extremely low amounts of organic carbon (<0.2 mg) were present between 782 – 754 cm making it impossible to accurately quantify OM values between these depths (blank space between KOZ I and KOZ II Figure 6.21). Values of TOC and TN increase from the Lateglacial into the Holocene, with the TOC record showing multiple variations during the late Allerød - Holocene. Minimum TOC and TN values are recorded during the Younger Dryas (0.07 wt% TOC, 0.30 wt% TN) while maximum values are recorded during the Holocene (2.67 wt% TOC, 3.24 wt% TN). Variability in the origin of OM in Kieshofer Moor is reflected in the $\delta^{13}C_{org}$ (-13.48‰ to -26.38‰), $\delta^{15}N_{org}$ (-1.71‰ to 1.28‰) and C:N (13.79 to 17.49) of sediments. Major changes in the sedimentary organic record

were used to define two OM zones which are presented in Figures 6.21 and 6.22 and will be discussed sequentially below.

KOZ I: 800 – 782 cm (13,340 ± 545 – 12,355 ± 355 cal yr BP)

The $\delta^{13}C_{org}$ record is relatively stable during the early stages of KOZ I fluctuating between -23.41‰ and -24.38‰ (Figure 6.21). Above 792 cm $\delta^{13}C_{org}$ values decline to a zone low of -26.38‰ at 786 cm, before rising slightly to -25.80‰ at the boundary with the zone with no data (782-754 cm). $\delta^{15}N_{org}$ values rise steadily from -0.51‰ to 1.26‰ between 800 - 790 cm. Maximum zone values of $\delta^{15}N_{org}$ is followed by decreasing values throughout the remainder of the zone, reaching 0.67‰ at 782 cm. The TOC and TN record are closely aligned within KOZ I. TOC and TN values both rise steadily, with TOC peaking at 792 cm (0.42 wt%) and TN peaking at 794 cm (1.12 wt%). A decline in values reaches its minimum at 786 cm, with both TOC and TN falling to 0.08 wt% and 0.30 wt% respectively. The C:N record is characterised by a sharp drop in values between 798 - 794 cm, with values reaching as low as 13.79 at 794 cm. Values subsequently increase at 792 cm, and remain consistent throughout the remainder of the zone fluctuating between 16.05 - 16.97.

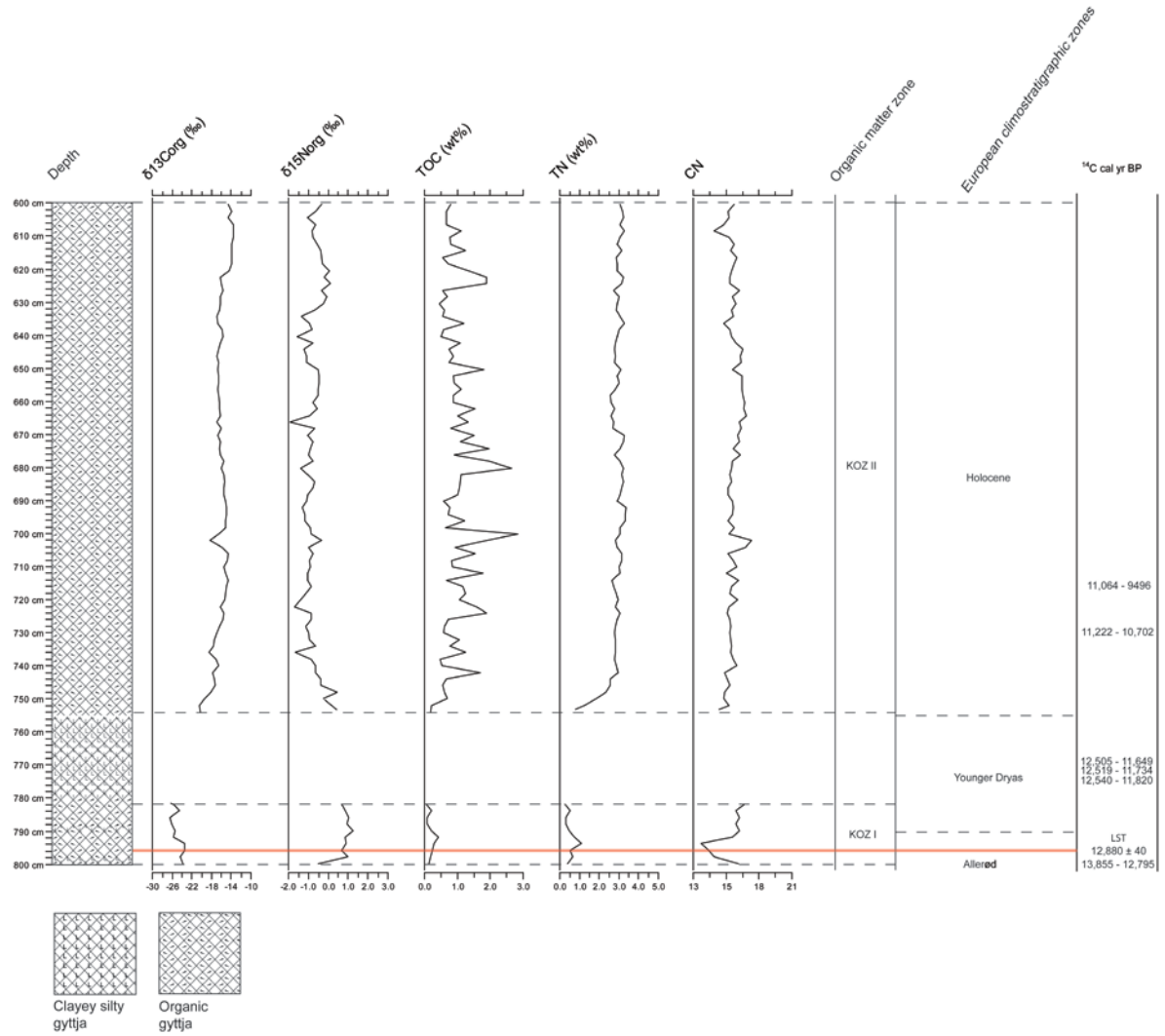
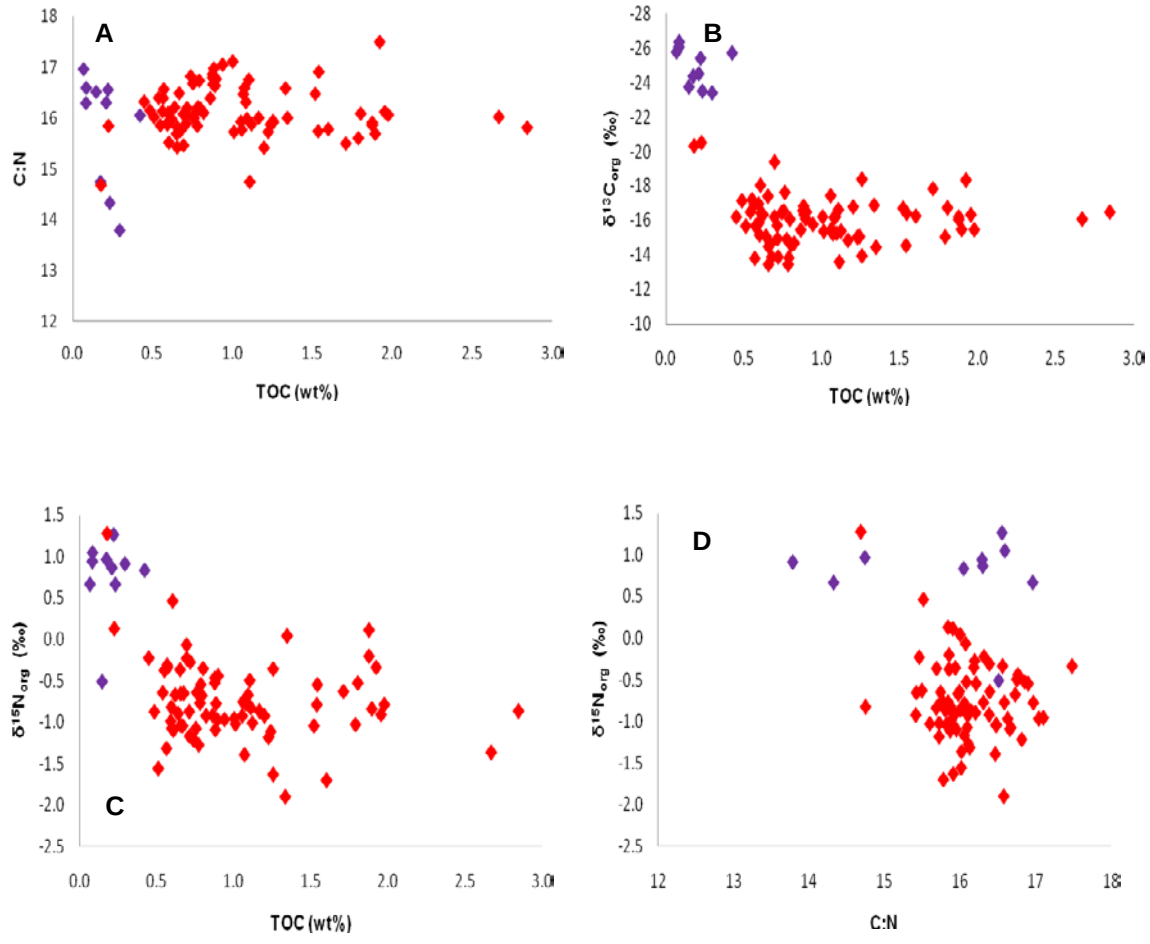


Figure 6.21 – Stable isotope profiles and selected organic properties, showing lithology, $\delta^{13}C_{org}$, $\delta^{15}N_{org}$, TOC, TN, C:N, major European climostratigraphic zones, radiocarbon dates and the LST in Kieshofer Moor. The two main OM zones are listed as KOZ I – KOZ II

KOZ II: 754 – 600 cm (11,618 ± 707 – 8925 ± 675* cal yr BP) *based upon modelled age from sister core

KOZ II is characterised by homogeneity in the OM record with values showing no observable trend during this period. KOZ II is characterised by a significant rise in $\delta^{13}C_{org}$ values from the preceding OM zone (KOZ I) with values of -20.34‰ recorded at 754 cm. Following this the $\delta^{13}C_{org}$ record continues to become increasingly enriched through the zone reaching -14.60‰ at 600 cm. The $\delta^{15}N_{org}$ record initially drops between 754 - 734 cm with values falling by ~0.80‰. Above 754 cm however the record

shows no observable increase or decrease until 632 cm when values rise by ~0.30 - 1‰ until 600 cm. The TOC record is characterised by an erratic profile, which like the TN and C:N record, shows no observable trend with values fluctuating between 0.18 – 2.84% for the duration of the zone. There are no large deviations in the TN record, with values climbing steadily. TN values of 0.52 wt% are recorded at 754 cm, above this values continue to climb steadily throughout the remainder of KOZ II, reaching 3.04% at 600 cm. The onset of the C:N record in KOZ II shows slightly lower values than the proceeding KOZ I with values of 14.69 recorded at 754 cm. Above this C:N values rise progressively throughout the remainder of KOZ II, reaching 16.18 at the top of the core at 600 cm.



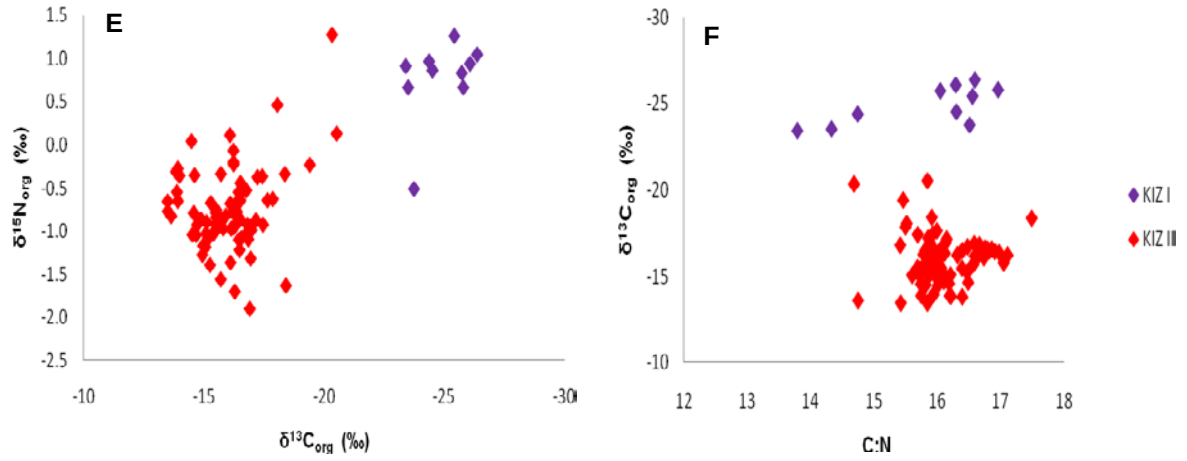


Figure 6.22 – Bi-plots of stable isotope values and selected organic properties for Kieshofer Moor. Figures A – F are plotted as isotope zones (KOZ I – KOZ II).

6.4.2 Deviation of TN record

As with Potremser Moor (section 6.3.2) the TOC – TN record also breaks down within Kieshofer Moor. The lack of correlation between the two proxies is evident from during KOZ II (Figure 6.23A). As discussed within section 6.3.2, the cause of this breakdown within Kieshofer Moor is likely due to a reduced uptake in the DIN reservoir, caused by reduced algal productivity. This conclusion is further supported by the bi-modal relationship between TN and $\delta^{15}N_{org}$ throughout the core (Figure 6.23B).

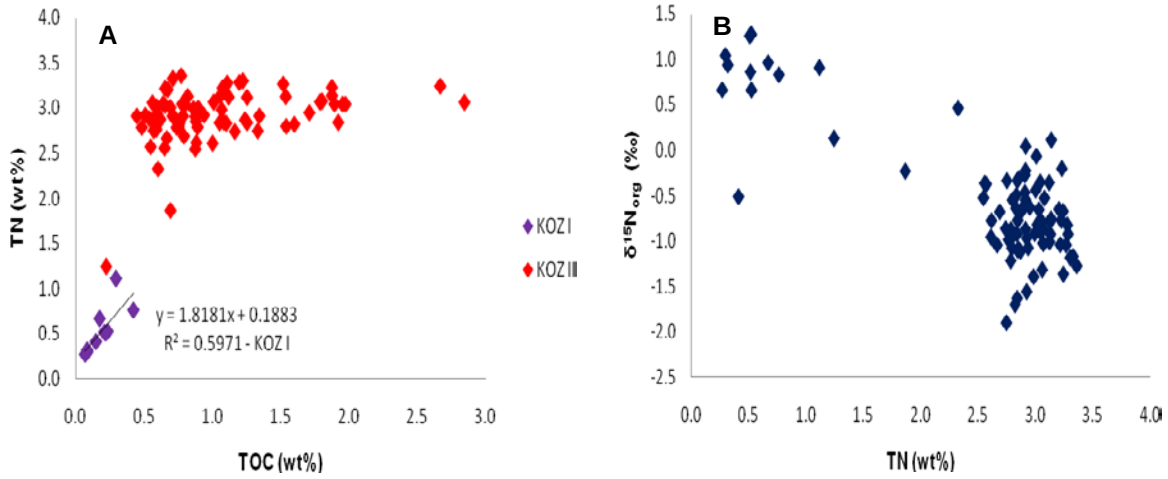


Figure 6.23 – Bi-plots of TN – TOC for KOZ I – KOZ II and TN – $\delta^{15}N_{org}$ for all OM zones in Kieshofer Moor. A – Although relatively weak, OM zone KOZ I shows a linear relationship, indicating low inorganic nitrogen within these OM zones. KOZ II however shows no such relationship, indicating the relationship between TN – TOC has broken down during this zone. B - The bi-modal relationship between TN – $\delta^{15}N_{org}$ in Kieshofer Moor core. Linear regression parameters given in KOZ I according to the equation $y = a \cdot x + b$.

6.4.3 Distinction of OM zones

PCA analysis of OM zones KOZ I – KOZ II indicates that both OM zones are distinct, and can be clearly separated. This separation indicates that both zones have different OM parameters suggesting that organic deposition was forced by different mechanisms during each zone.

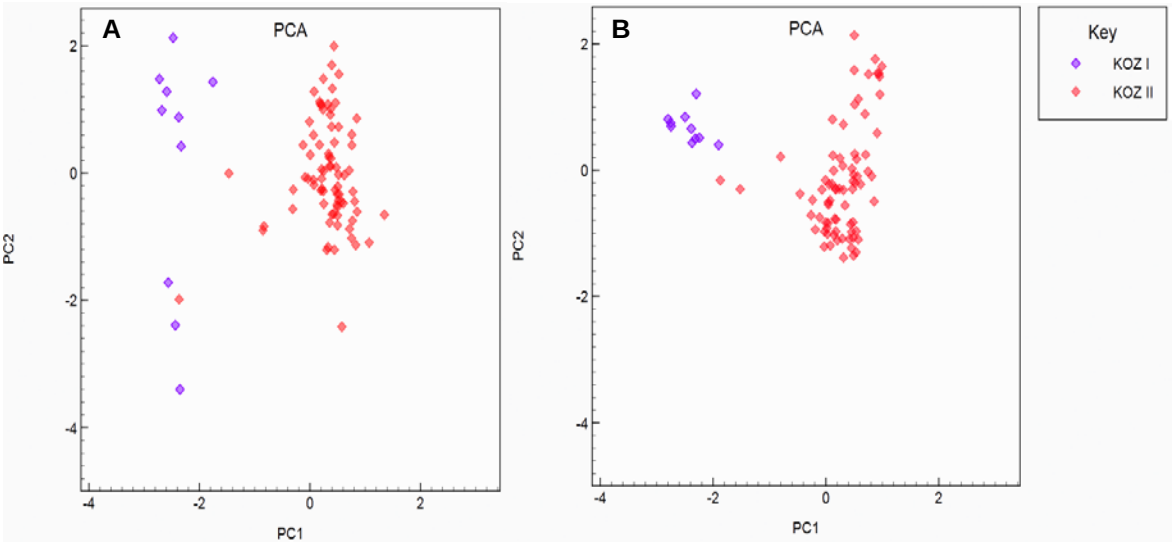


Figure 6.24 – PCA bi-plots of selected isotopic and organic properties for Kieshofer Moor plotted by: A = $\delta^{13}C_{org}$, $\delta^{15}N_{org}$, TOC, TN and C:N. B = $\delta^{13}C_{org}$, TOC and TN.

6.4.4 Chronozone distinction

The data presented within Figure 6.25A, B and C clearly show distinction between data points from the Holocene, Younger Dryas and Allerød chronozones. PCA axis scores for and TN (PC1 – 0.55272), $\delta^{13}C_{org}$ (PC1 – 0.52327) and TOC (PC1 – 0.38951) indicate that the separation of these data points within Figure 6.25A is primarily driven by these parameters, which when plotted in Figure 6.25B show tighter clustering of the Younger Dryas and Allerød chronozones. Due to the limited amount of data for the Allerød and Younger Dryas it is impossible to say if the OM data for these chronozones is representative of the entire chronozone, however as will be further discussed in section 7.2.3.1 (Chapter 7), it is possible to assess lake productivity during the timing of the LST deposition based on this fixed isochrone. While the data from the Younger Dryas and Allerød have an OM profile that is clearly distinct from the Holocene, they do share a small degree of overlap between samples from the lower most part of the Allerød within the core and the early Younger Dryas (Figure 6.25A and C).

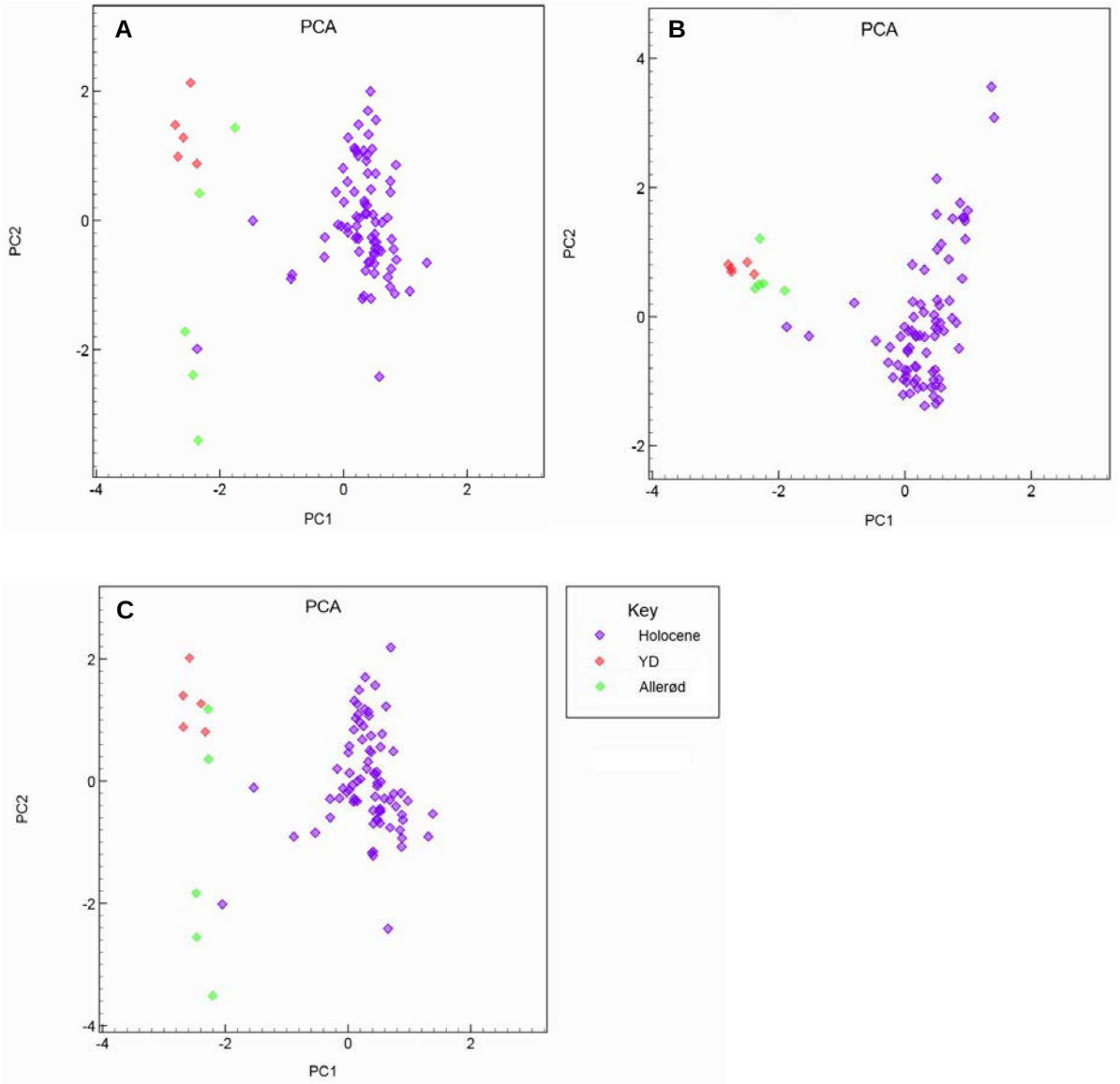


Figure 6.25 – PCA bi-plots of selected isotopic and organic properties for Kieshofer Moor plotted by: A = $\delta^{13}C_{org}$, $\delta^{15}N_{org}$, TOC, TN and C:N. B = $\delta^{13}C_{org}$, TOC and TN. C = $\delta^{13}C_{org}$, TOC, TN and C:N.

Apart from the small overlap between the first Allerød samples and the early Younger Dryas, both zones and the Holocene show distinct OM profiles within Kieshofer Moor. The OM trends within the core may therefore be seen as representative of the influence of climatic and environmental instability on the autochthonous and allochthonous processes within the Kieshofer Moor basin.

6.4.5 Cladoceran record

A total of 25 cladoceran species were identified from chitinous remains including, ephippia, headshields, carapaces and post abdomen claws (Table 6.4). The greatest number of species recorded from a single sample is 14 which occur at 627.5 cm and 712.5 cm while the maximum total cladoceran count comes from 742.5 cm, with counts of 20,240 individual cladocerans per 50 ml. Five distinct cladoceran assemblage zones (KCZ I – V) were recorded within Kieshofer Moor as shown in Figure 6.26.

Chydorids	Non-chydorids
Chydoridae	Bosminidae
Acroperos harpae Baird	*Bosmina coregoni* Baird
Alona affinis Leydig	*B. longirostris* O.F. Muller
A. costata Baird	
A. guttata/ rectangula Sars	Daphniidae
A. guttata var tub Sars	*D. pulex* Leydig
A. intermedia Sars	
A. quadrangularis O.F. Muller	Sididae
Alonella excise Fischer	*Sida crystallina* O.F. Muller
A. nana Baird	
A. rostrata	
Camptocercus rectirostris Schödler	
Chydorus sphaericus O.F. Muller	
C. piger Sars	
Eurycercus lamellatus O.F. Muller	
Graptoleberis testudinaria Fischer	
L. leydigi Schödler	
Monospilus dispar Stebbing	
Pleroxus aduncus Baird	
P. trigonellus Baird	
P. uncinatus Stebbing	
Psydochydorus globosus	

Table 6.4 – List of cladoceran species recorded for Kieshofer Moor. The nomenclature follows Scourfield and Harding (1966).

KCZ I: 800 – 752.5 cm (13,340 ± 545 – 11,538 ± 662 cal yr BP)

The first cladoceran zone within Kieshofer Moor is dominated by the benthic species *A.affinis* (mean – 922 ± 993 / 50 ml), *A. guttata/ rectangula* (mean – 462 ± 550 / 50 ml), *A. harpae* (mean – 839 ± 1021 / 50 ml), *A. nana* (mean – 810 ± 799 / 50 ml) and *C. sphaericus* (mean – 1218 ± 729 / 50 ml). Total

cladocerans rise to form an early peak of 9846 / 50 ml at 795 cm before subsequently declining to 1261 / 50 ml at 765 cm. Total cladoceran abundance lastly rises a second time to form a peak at 752.5 cm of 18,150 / 50 ml. The pelagic record is characterised by a dominance of *B. longirostris* which, like the total cladoceran record, forms two peaks separated by a reduction in values. *B. longirostris* abundance rises to 1937 / 50 ml at 795 cm before declining to 75 / 50 ml at 777.5 cm (Figure 6.26). The second peak in *B. longirostris* occurs at 757.5 cm where values rise to 799 / 50 ml. As such, the pelagic: benthic ratio is low (0.04 - 0.14) between 787.5 - 762.5 cm. The mucro length of *B. longirostris* fluctuates between 29 - 57 µm (Figure 6.27) with a median value of 42 µm. An apparent sharp reduction in mucro lengths at 770 cm is attributed to no fully intact mucrone being recorded.

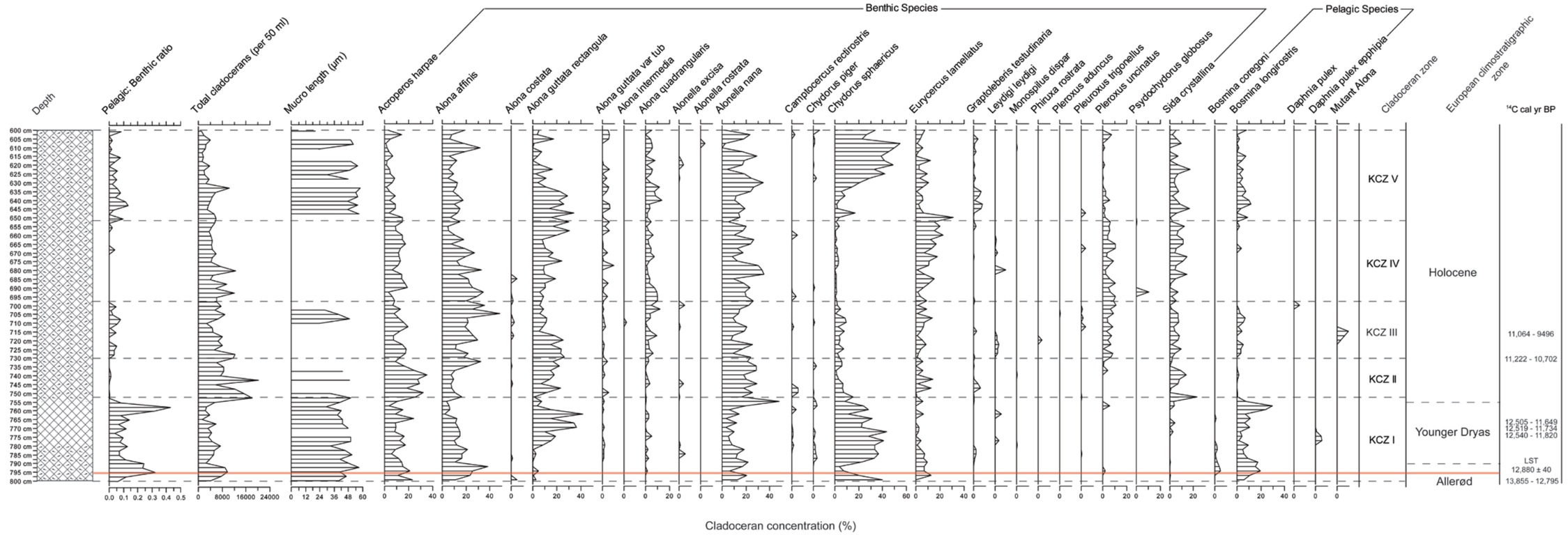


Figure 6.26 – Composite diagram of lithology, relative abundance of cladoceran species, major European climostratigraphic zones, radiocarbon dates and LST in Kieshofer Moor. Species are expressed as percentages of the total cladoceran count for each level. Bosmina mucro length and total cladoceran counts (expressed as absolute) are also shown.

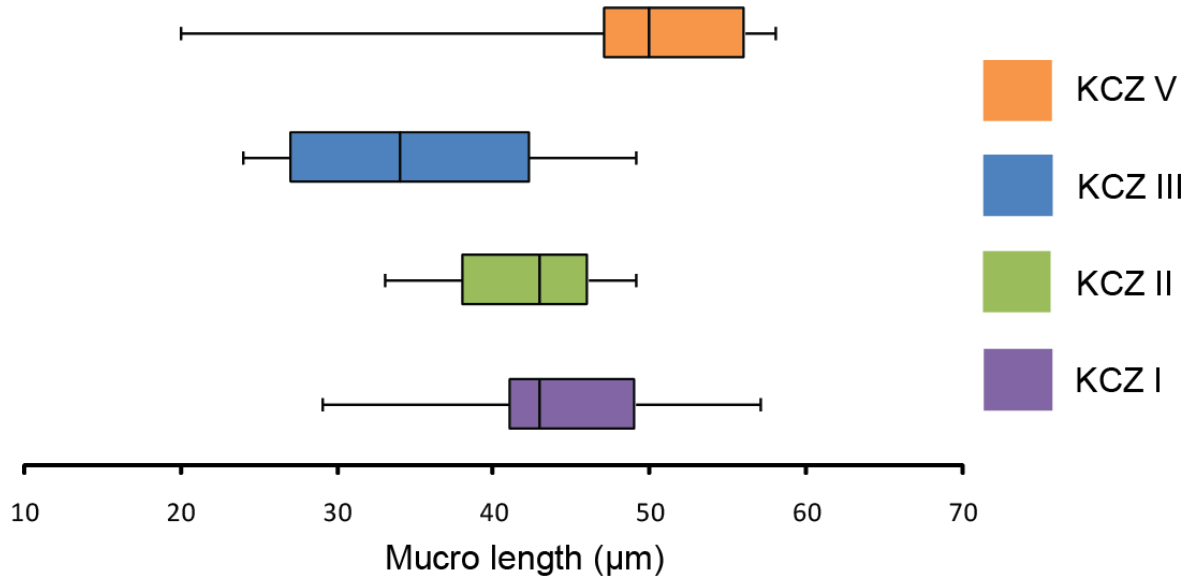


Figure 6.27 – (A – D) box plots of *B. longirostris* mucro length plotted by cladoceran zone for Kieshofer Moor. No recordable mucrones were recovered from KCZ IV.

KCZ II: 752.5 – 730 cm (11,538 ± 662 – 10,962 ± 260 cal yr BP)

Total cladoceran numbers remain high during the early portions of KCZ II with counts of 15,292 / 50 ml. A large drop in values at 745 cm is immediately followed by the maximum cladoceran counts for Kieshofer Moor of 20,240 / 50 ml at 742.5 cm (Figure 6.26). The most striking feature of KCZ II is the complete dominance of the benthic record at the expense of pelagic species causing the pelagic: benthic ratio for KCZ II to remain <0.01 throughout the entirety of the zone. *A.affinis* (mean – 1385 ± 704 / 50 ml), *A. guttata/ rectangula* (mean – 1835 ± 1015 / 50 ml), *A. harpae* (mean – 2511 ± 1484 / 50 ml) and *A. nana* (mean – 2473 ± 903 / 50 ml) all increase from the previous cladoceran zone, while *C. sphaericus* (mean – 502 ± 245 / 50 ml) decreases. There is an almost complete loss of *B. longirostris* during KCZ II, with only 750 cm, 742.5 cm, 740 cm and 737.5 cm recording *B. longirostris* (<150 / 50 ml). The recordable mucro lengths during KCZ II show a smaller range from those in KCZ I, median lengths however remain consistent at 42 µm recorded (Figure 6.27).

KCZ III: 730 – 697.5 cm (10,962 ± 260 – 10,840 ± 760* cal yr BP)*based upon modelled age from sister core

Total cladoceran values are initially high in KCZ III with counts of 12,335 / 50 ml at 727.5 cm recorded (Figure 6.26). This is followed by a reduction in values to 2724 / 50 ml at 710 cm before a final rise to 6252 / 50 ml at the boundary with KCZ IV. The onset of KCZ III coincides with the return of *B. longirostris*, which although low (<500 / 50 ml), returns in two intervals, the first between 727.5 - 722.5 cm and the second from 715 - 702.5 cm. Mucro lengths during this period are lower than those recorded during KCZ II, with median values of 35 µm during KCZ III (Figure 6.27). *A.affinis* (mean – 1691 ± 1060 / 50 ml) increases during KCZ III, while *A. guttata/ rectangula* (mean - 905 ± 751/ 50 ml), *A*. *harpae* (mean – 779 ± 450 / 50 ml) and *A. nana* (mean -1050 ± 512 / 50 ml) all decrease. KCZ III also witnesses the increase of *A. quadrangularis* (mean – 368 ± 260 / 50 ml) and *P. uncinatus* (mean – 471 ± 311 / 50 ml). The dominance of benthic species over the pelagic causes the pelagic: benthic ratio to remain low (<0.1).

KCZ IV: 697.5 – 652.5 cm (10,840 ± 760* – 9875 ± 725* cal yr BP)

Total cladoceran numbers show a small overall decline during KCZ IV, decreasing from 6100 / 50 ml at 695 cm to 5620 / 50 ml at 652.5 cm (Figure 6.26). This decline is punctuated by three larger peaks in total values located at 692.5 cm (12,130 / 50 ml), 687.5 cm (9468 / 50 ml) and 680 cm (12,437 / 50 ml). As with KCZ II, there is an almost complete loss of *B. longirostris* during KCZ IV with values of <180 / 50 ml recorded only at 667.5 cm and 655 cm, as a result the pelagic: benthic ratio again remains <0.05. Overall the benthic record shows a small reduction from the previous cladoceran zone, decreasing from a mean of 6868 / 50 ml to 6042 / 50 ml. Coupled with this is a reduction in *A.affinis* (mean – 1286 ± 1175 / 50 ml), *A. guttata/ rectangula* (mean – 770 ± 321 / 50 ml), *A*. *harpae* (mean – 684 ± 295 / 50 ml) and *C. sphaericus* (mean – 83 ± 54 / 50 ml). Conversely there is an increase in *A. nana* (mean – 1260 ± 968 / 50 ml) and *E*. *lamellatus* (mean – 586 ± 272 / 50 ml). There is no recordable mucro length during KCZ IV as no fully intact *B. longirostris* mucrone was recorded***KCZ V: 652.5 – 600 cm (9875 ± 725* – 8925 ± 675* cal yr BP) *based upon modelled age from sister core***

The final cladoceran zone in Kieshofer Moor is characterised by decreasing total counts during the zone. The exception to this declining trend is punctuated at 632.5 cm when values rise abruptly from 5810 / 50 ml to 10,353 / 50 ml (Figure 6.26). *B. longirostris* returns during KCZ V (mean – 154 ± 185 / 50 ml) and although represented by low numbers, this return prompts an increase in pelagic: benthic ratio, which peaks at 0.13 at 642.5 cm. The mucro length of *B. longirostris* are higher than those recorded within KCZ III, with a median of 47 µm, there is however large variation in mucro length during KCZ V, with a range of 20 - 58 µm (Figure 6.27). The benthic record shows an overall reduction in cladocerans, with only *C. sphaericus* (mean – 670 ± 490 / 50 ml) increasing during this final zone. *E. lamellatus* shows a sharp reduction at the onset of KCZ V, falling from 1832/ 50 ml at 650 cm to 327 / 50 ml at 647.5 cm. Coupled with this decrease in *E. lamellatus* is a decline in *A.affinis* (mean – 419 ± 273 / 50 ml), *A. guttata/ rectangula* (mean – 572 ± 549 / 50 ml), *A. harpae* (mean – 225 ± 187 / 50 ml) and *A. nana* (mean – 601 ± 599 / 50 ml).

6.4.6 Palaeoevolution of Kieshofer Moor

Allerød: KOZ I and KCZ I

The sediments attributed to the Allerød chronozone within Kieshofer Moor most likely represent the final Allerød as the LST is found only 4 cm above the cores base (LST, 12,880 ± 40 cal yr BP located at 796 cm). The short record indicates that between 798 - 794 cm the C:N ratio falls to the lowest values throughout the entire core (13 - 14). This is matched by enriched $\delta^{15}N_{org}$ values and a moderate $\delta^{13}C_{org}$ record, with values of approximately -23 ‰ (Figure 6.21). The relatively elevated TOC and TN record coupled with $\delta^{13}C_{org}$ values that are higher than those of lacustrine algae, suggesting that the final stages of the Allerød within Kieshofer Moor are represented by moderate levels of primary algal productivity, with the OM signal closely aligned with that of aquatic macrophytes (Aichner *et al*., 2010). The deposition of the LST at 796 cm, appears to have had little effect on the pH of the basin, with $CaCO_3$ actually peaking at the time of its deposition. *B. longirostris* mucro length decreases slightly following the deposition of the LST (46 µm, 797.5 cm; 41 µm, 795 cm). However at 792.5 cm there is a sharp rise in mucro length to 57 µm, possibly indicating a delayed biological response to this event in the order of ~230 years (based upon modelled ages) this point will be further discussed in Chapter 7. Total cladoceran concentrations decrease during the

Allerød, falling to <2500 at 790 cm which is coupled by low pelagic: benthic ratios which remain <0.35. Although open water indicator species such as *B. longirostris* are present during the Allerød, they are low in abundance compared to benthic, shallow water indicators. The relatively high pelagic: benthic ratio during this zone therefore is not necessarily representative of open water conditions. Instead, due to the extremely low concentrations of pelagic species throughout the rest of the core, the pelagic: benthic ratio appears high when compared to the rest of the record. The majority of cladoceran species during the Allerød are attributed to generalist species such as *A. affinis* and *A. harpae*, which are indicative of shallow, nutrient poor conditions while the presence of *E. lamellatus* during the final Allerød confirms the presence of aquatic macrophytes (Grabowska *et al*., 2009; Kattle and Sirocko, 2011).

Younger Dryas: KOZ I and KCZ I

Due to the gaps in the OM record, it is difficult to make any interpretations about the condition of the basin during the Younger Dryas. In the early part of the Younger Dryas, $\delta^{13}C_{org}$, $\delta^{15}N_{org}$ and C:N record is much the same as that recorded during the preceding Allerød (Figure 6.21). The decrease in the TOC and TN record, suggests the start of the Younger Dryas is similar to that recorded within the previous sites, with low levels of primary algal productivity and high inorganic input from the surrounding basin. The cladoceran record shows a rise in generalist species *A. affinis*, *A. harpae* and *C. sphaericus,* with *A. harpae* and *C. sphaericus* considered “arctic species” (Harmsworth, 1968). Abundances of *A. guttata*/*rectangular* also increase during the latter Younger Dryas. The species, characteristic of acidic waters may indicate a rise in water levels leading to an inundation of the surrounding lake margins (e.g. Kulesza *et al*., 2011). A rise in water levels is also supported by a subsequent rise in *B. longirostris* (Figure 6.26)

Holocene: KOZ II, KCZ I, KCZ II, KCZ III, KCZ IV and KCZ V

The OM profile during the Holocene is very similar to that witnessed within the Holocene of Potremser Moor. The progressive enrichment of the $\delta^{13}C_{org}$ record, coupled with the depletion of $\delta^{15}N_{org}$ values and C:N values of ~16 at the start of the Holocene are consistent with the development of a substantial aquatic macrophyte population within the basin (Aichner *et al*., 2010). The reduction in

primary algal productivity is confirmed by the non-linear relationship between TOC – TN, with the uptake of DIN reduced during the Holocene (Figure 6.23A). The appearance of *P. uncinatus* and *S. crystallina* at the onset of the Holocene supports the interpretation of aquatic macrophyte dominance within the basin (Frey, 1988; Grabowska *et al*., 2009). A reduction in *B. longirostris* indicates that water depths had decreased during the Holocene, with shallow water conditions predominating. A large increase in *C. sphaericus* coupled with a small rise in *B. longirostris* after 650 cm, suggests an increase in water depth, with the reduction in *E. lamellatus* and *P. unicinatus* suggesting that this increase flooded the littoral zones (Kulesza *et al*., 2011).

6.5 Daschower Moor, Germany

6.5.1 Isotope and organic content record

The Lateglacial – Holocene OM and organic content record is represented by varying accumulations of autochthonous and allochthonous material. No or extremely low amounts of organic carbon (<0.2 mg) where present between 244 - 206 cm, therefore DOZ II is represented by an incomplete OM record (Figure 6.28). The values within DOZ II do however appear to be consistent suggesting that the few values recorded within this zone may be an accurate representation of the entire zone. The organic content record of Daschower Moor is variable with minimum values recorded during the Younger Dryas (0.07 wt% TOC, 0.24 wt% TN) and maximum values recorded during the Holocene (0.87 wt% TOC, 4.46 wt% TN). TOC and TN accumulation are highly correlated throughout the record ($r = 0.745$, $n = 82$) indicating TN content represents organic nitrogen (Nijenhuis and de Lange, 2000; Calvert, 2004). Further variability in depositional sources is reflected in the $\delta^{13}C_{org}$ (-11.16‰ to -26.39‰), $\delta^{15}N_{org}$ (-3.57‰ to 1.40‰) and C:N (12.73 to 75.11) of sediments. Major changes in the sedimentary organic record were used to define five separate OM zones which are presented in Figures 6.28 and 6.29 and will be discussed sequentially below.***DOZ I: 280 – 244 cm (14,024 ± 830 – 11,880 ± 770 cal yr BP)***

$\delta^{13}C_{org}$ values steadily decline between 280 - 276 cm from -18.63‰ to -20.13‰, above 280 - 276 cm values rise to the DOZ I maximum of -16.53‰ at 266 cm before declining towards the end of the zone (Figure 6.28). The $\delta^{15}N_{org}$ record shows a general enrichment in values punctuated by larger short-

lived increase with values rising to 0.07‰ at 270 cm. Both TN and TOC show similar responses during DOZ I, increasing to 2.93 wt% and 0.53 wt% respectively, at 272 cm. Both records show stability between 272 – 264 cm before declining to 0.76 wt% and 0.12 wt% respectively at the DOZ II boundary. The C:N trend follows those of the TN and TOC records between 280 - 266 cm with values rising from 14.50 to 17.03, before falling away to 12.41 at 258 cm. A second steady rise in values, peaking at 16.95, is seen in the upper part of DOZ I.

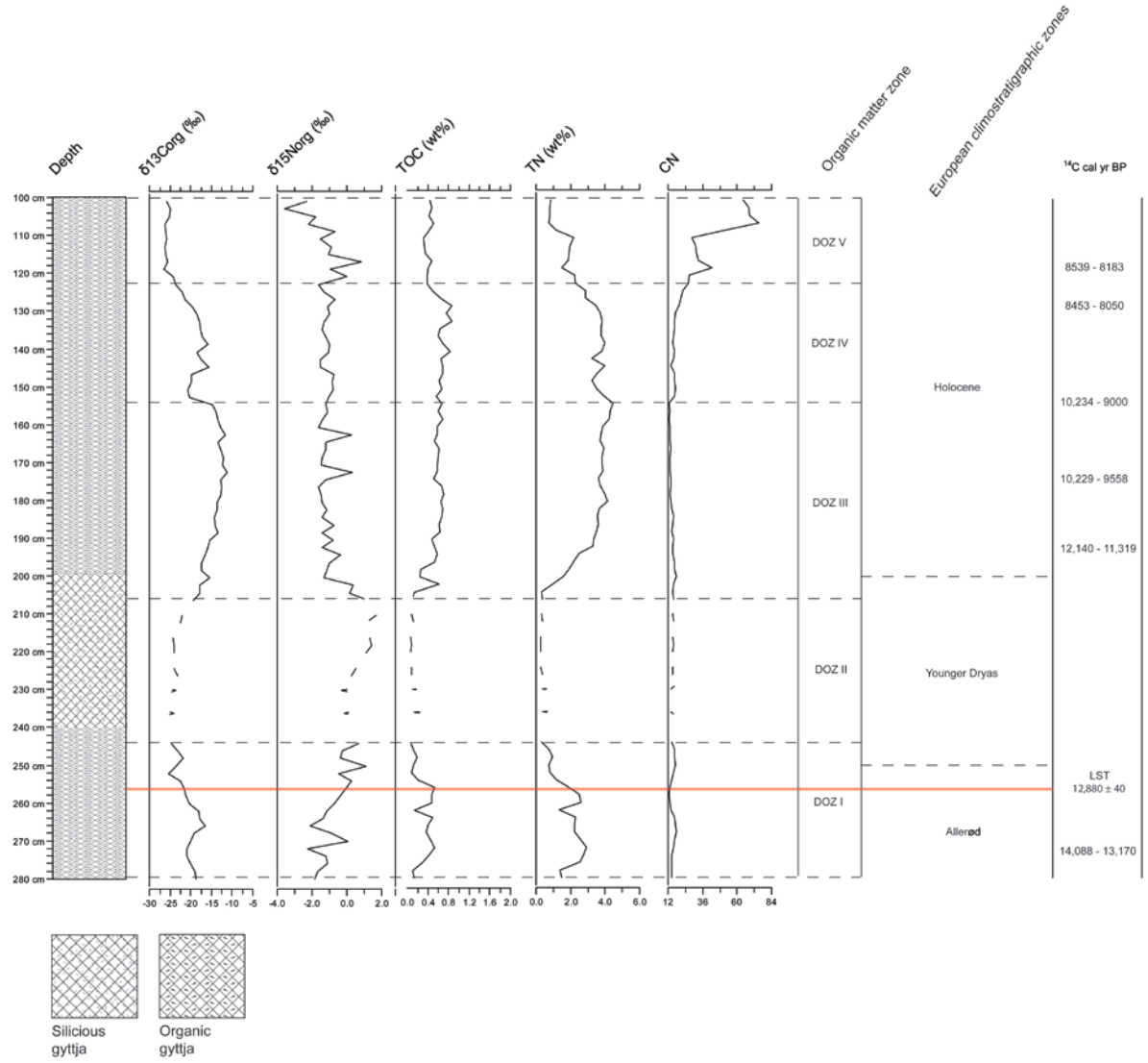
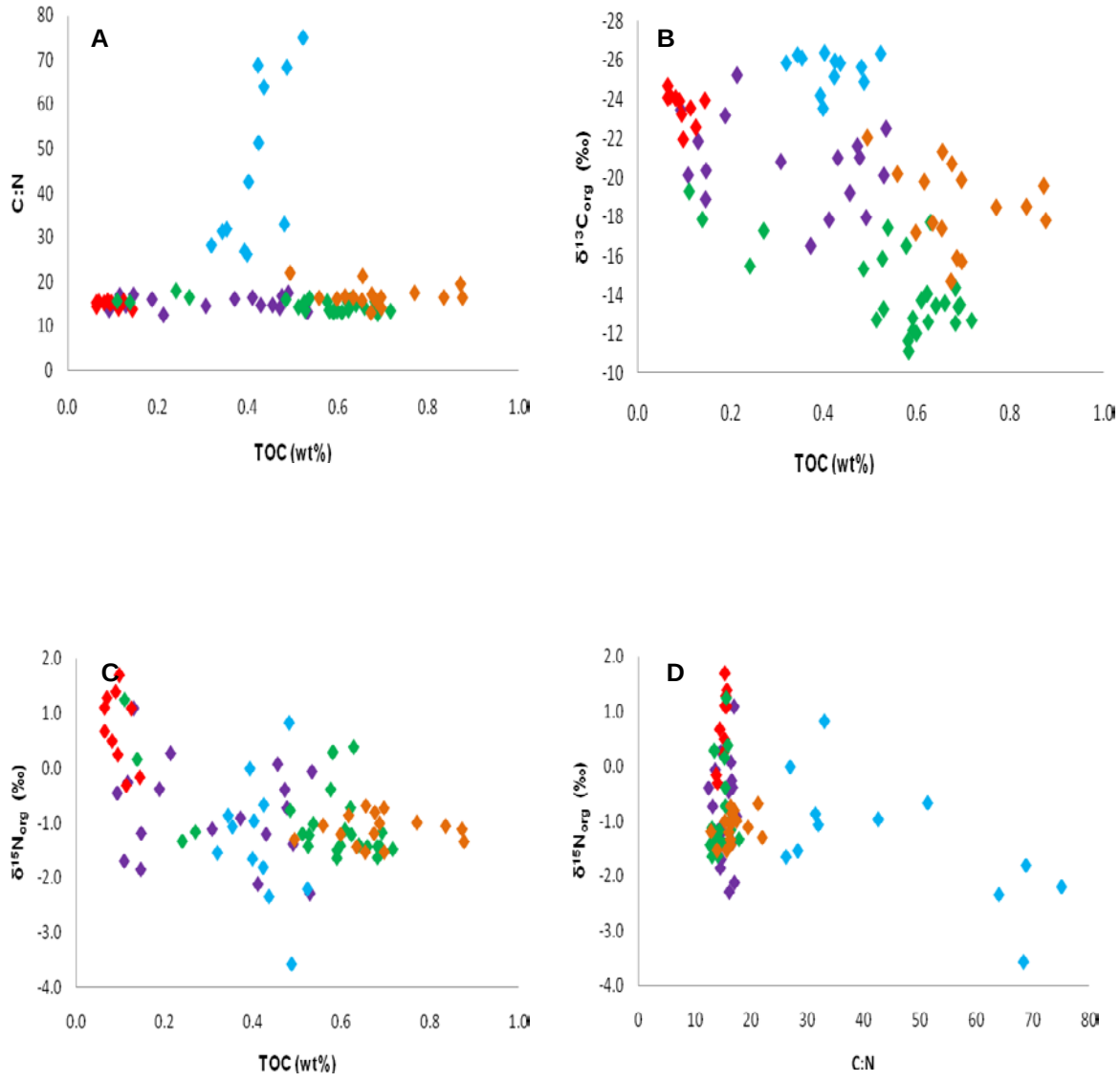


Figure 6.28 – Stable isotope profiles and selected organic properties, showing lithology, $\delta^{13}C_{org}$, $\delta^{15}N_{org}$, TOC, TN, C:N, major European climostratigraphic zones, radiocarbon dates and the LST in Daschower Moor. The five OM zones are listed as DOZ I – DOZ V.

DOZ II: 244 – 206 cm (11,880 ± 770 – 11,325 ± 925 cal yr BP)

DOZ II is characterised by a fragmentary OM record, with extremely low carbon values making analysis of a number of points impossible. Recordable values indicate that the $\delta^{13}C_{org}$ record gradually becomes more enriched, with values rising from -23.97‰ at 236 cm to -21.95‰ at 210 cm. The $\delta^{15}N_{org}$ record is characterised by a rise in values, however this is more pronounced than that witnessed in the $\delta^{13}C_{org}$ record with values increasing from -0.16‰ to 1.71‰ at the boundary with DOZ II. The TOC, TN and C:N records are all stable showing very little variation (Figure 6.28).



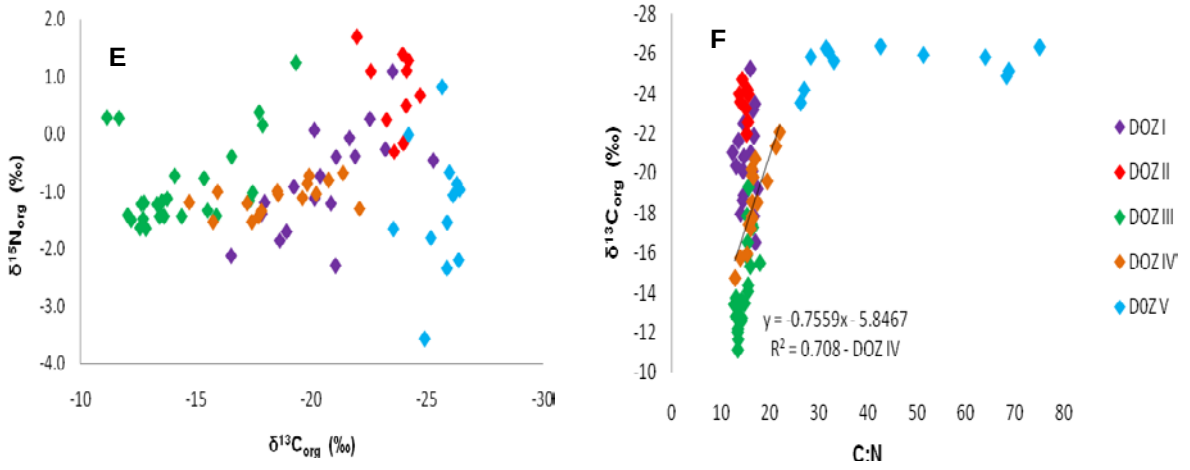


Figure 6.29 – Bi-plots of stable isotope values and selected organic properties for Daschower Moor. Figures A – F are plotted as OM zones (DOZ I – DOZ V). Significant relationship between $\delta^{13}C_{org}$ and C:N shown in F. Linear regression parameters given in DOZ IV (Figure F) according to the equation y = a·x + b.

DOZ III: 206 – 154 cm (11,325 ± 925 – 9475 ± 375 cal yr BP)

$\delta^{13}C_{org}$ values rise during DOZ II with values becoming increasingly enriched from -19.33‰ to -13.76‰ at the boundary with DOZ IV. Two small peaks in $\delta^{13}C_{org}$ values are observed at 172 cm and 162 cm, coinciding with two pronounced peaks in the $\delta^{15}N_{org}$ record. $\delta^{15}N_{org}$ values fall from 1.24‰ to -1.63‰ between 206 - 176 cm. Following this decrease in values, there are two pronounced peaks, with values rising to 0.29 at 172 cm and 0.28 at 162 cm. The TN record shows a steady rise in values from the onset of DOZ III until its boundary with DOZ IV, with values increasing from 0.36 wt% to 4.31 wt%. The TOC record also shows an increase in values with two small peaks, occurring at 178 cm (0.72 wt% TOC) and 158 cm (0.69 wt% TOC). The C:N record shows a slight increase in values of 15.61 - 17.90 between 206 - 200 cm. Following this rise, values gradually fall away to 12.73 at 158 cm.

DOZ IV: 154 – 122 cm (9475 ± 375 – 8310 ± 290 cal yr BP)

The onset of DOZ IV coincides with an overall depletion in $\delta^{13}C_{org}$ values throughout the zone punctuated by a short lived, large negative excursion as values drop from -14.70‰ to -20.72‰ at 150

cm. C:N values vary between 152 - 132 cm (15.34 - 17.02) before gradually climbing to 21.96 at the boundary with DOZ V. The $\delta^{15}N_{org}$ record in contrast shows no overall trend to more enriched or depleted values, with values fluctuating between -0.72‰ and -1.53‰. A small rise in $\delta^{15}N_{org}$ is observed between 134 - 128 cm, however this is short lived and values only increase by 0.35‰. Between 154 - 148 cm TN values fall to 3.23 wt%, before rising to a maximum of 3.99 wt% at 138 cm. Following this rise, values gradually decline to 2.86 wt% at 124 cm. The TOC record within DOZ IV shows very little variation from the preceding OM zone, excepting a small drop in values to 0.60 wt% between 134 - 136 cm. Values rise slightly between 132 - 128 cm, however this is followed by a drop in values to 0.49 wt% at 124 cm.

DOZ V: 122 – 100 cm (8310 ± 290 – 7448 ± 590 cal yr BP)

The $\delta^{13}C_{org}$ record continues to decline within DOZ V, falling to -26.39‰ at 118 cm. Following this drop, values stabilise between -25.15‰ and -26.39‰ for the rest of the zone. In contrast, $\delta^{15}N_{org}$ values vary largely between 0.82‰ and -3.57‰. The $\delta^{15}N_{org}$ record, between 124 - 118 cm is characterised by two peaks in $\delta^{15}N_{org}$, the first at 120 cm of 0.01‰, and the larger second peak at 116 cm of 0.82‰ (Figure 6.28). The TN record continues the general downward trend in values from DOZ IV; however this pattern is briefly reversed at 110 cm, where values rise to 2.20 wt%. This positive shift however gives way to lower values, and by 104 cm, TN values are <0.5 wt%. The C:N record in contrast is characterised by a large rise in values. C:N initially rises to 42.55 at 118 cm, before gradually dropping back down to 28.28 at 110 cm. Values however rapidly rise to 75.11 at 106 cm and level off at ~68 for the remainder of the zone. The TOC record of DOZ V shows no such increases and remains low between 0.32 - 0.52 wt%.

6.5.2 Distinction of OM record

PCA analysis of the OM zones presented in Figure 6.28 show they can be largely separated based upon their $\delta^{13}C_{org}$, $\delta^{15}N_{org}$, TOC, TN and C:N profiles. As experienced in a number of sites within this thesis, there is some overlap of OM zones. This overlap however occurs between zones which are stratigraphically separate therefore indicating similar basin conditions recur over varying timescales. The only zones that are stratigraphically linked are DOZ I and II with Figure 6.28 and 6.30A indicating

some overlap between the end members of DOZ I and DOZ II. The separation of the remaining OM zones therefore allows them to be considered as separate events indicating changing autochthonous and allochthonous conditions at Daschower Moor.

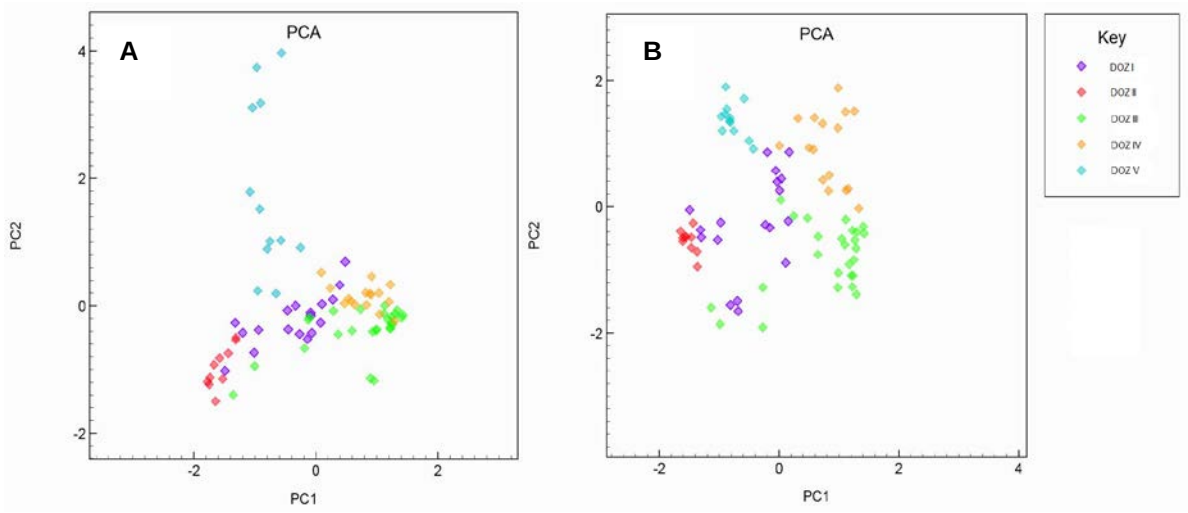


Figure 6.30 – PCA bi-plots of selected isotopic and organic properties for Daschower Moor plotted by: A = $\delta^{13}C_{org}$, $\delta^{15}N_{org}$, TOC, TN and C:N. B = $\delta^{13}C_{org}$, TOC and TN.

6.5.3 Distinction of chronozones

The OM data when plotted by chronozone shows that there is relatively close overlap of the Holocene, Allerød and Younger Dryas within Daschower Moor. Despite this association it is possible separate out the three chronozones based upon their OM profiles (Figure 6.31).

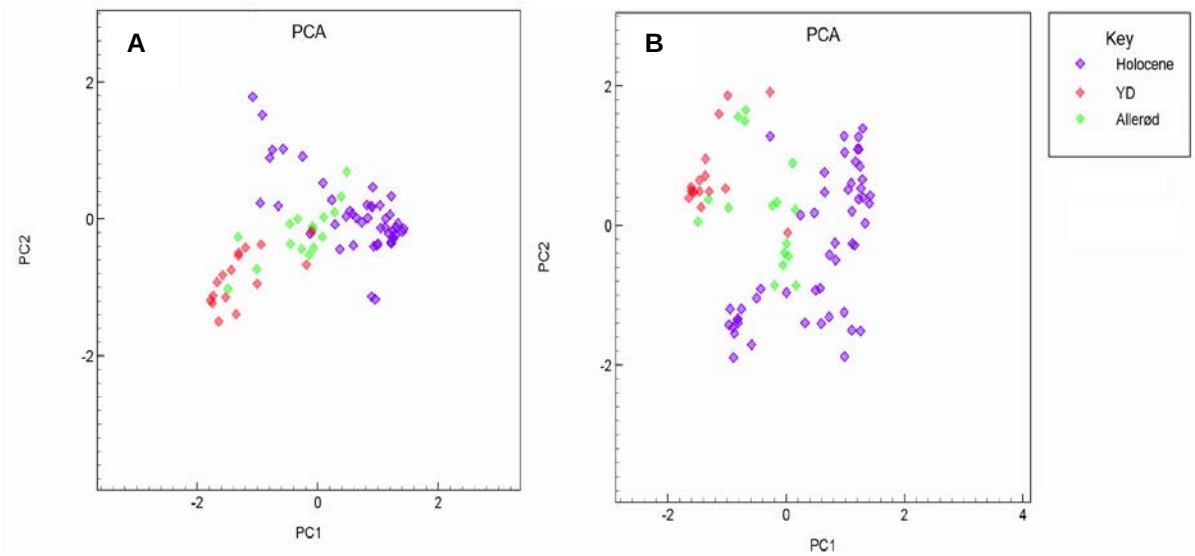


Figure 6.31 - PCA bi-plots of selected isotopic and organic properties for Daschower Moor plotted by: A = $\delta^{13}C_{org}$, $\delta^{15}N_{org}$, TOC, TN and C:N. B = $\delta^{13}C_{org}$, TOC and TN.

The greatest separation is between the Holocene and Younger Dryas, primarily driven by differences in the $\delta^{13}C_{org}$ (PC1 – 0.49927), TOC (PC1 – 0.52289) and TN (PC1 – 0.57512) record (Figure 6.31A). The Allerød OM profile sits between the Holocene and Younger Dryas, with a small number of samples overlapping towards the onset and termination of the chronozone (Figure 6.31A and B). Aside from this small overlap, the separation of the chronozones within Daschower Moor allows this thesis to infer that each chronozone is represented by varying and different OM regimes. Therefore the evolution of the system was not isotopically homogenous and that productivity rates and autochthonous and allochthonous processes varied throughout time. The separation of chronozones strongly suggests that climatic and environmental change had some influence on the OM regime of Daschower Moor. However as the Daschower Moor system does not respond rapidly at the established chronozone boundaries also suggests that external climate change was not the sole forcing mechanism.

6.5.4 Cladoceran record

A total of 23 cladoceran species were identified from chitinous remains including, ephippia, headshields, carapaces and post abdomen claws (Table 6.5). The greatest number of species recorded from a single sample is 15 which occurs at 157.5 cm while the maximum total cladoceran count comes from 277.5 cm, with counts of 11,785 individual cladocerans per 50 ml. Five distinct cladoceran assemblage zones (DCZ I – V) were recorded within Daschower Moor as shown in Figure 6.32.

Chydorids	Non-chydorids
Chydoridae	Bosminidae
Acroperos harpae Baird	*Bosmina coregoni* Baird
Alona affinis Leydig	*B. longirostris* O.F. Muller
A. costata Baird	
A. guttata/ rectangula Sars	Daphniidae
A. guttata var tub Sars	*D. pulex* Leydig
A. quadrangularis O.F. Muller	
Alonella excisa Fischer	Sididae
A. nana Baird	*Sida crystallina* O.F. Muller
A. rostrata Koch	
Camptocercus rectirostris Schödler	
Chydorus sphaericus O.F. Muller	
C. piger Sars	
Eurycercus lamellatus O.F. Muller	
Graptoleberis testudinaria Fischer	
L. leydigi Schödler	
Monospilus dispar Stebbing	
Pleroxus truncates Mueller	
P. uncinatus Stebbing	
Psydochydorus globosus	

Table 6.5 – List of cladoceran species recorded for Daschower Moor. The nomenclature follows Scourfield and Harding (1966).

DCZ I: 280 – 250 cm (14,024 ± 830 –12,046 ± 721 cal yr BP)

DCZ I is characterised by tripartite pattern of cladoceran deposition. Between 280 - 270 cm total cladoceran numbers are high and rise from 8552 / 50 ml at the onset of the zone to 11,111 at 270 cm (Figure 6.32). This large rise in cladoceran abundance is largely driven by increases in *B. longirostris*, which during this phase records a mean value of 3912 / 50 ml. The benthic record by contrast is represented by relatively low numbers of *A.affinis* (mean – 537 ± 267 / 50 ml), *A*. *harpae* (mean – 1495 ± 613 / 50 ml), *A. nana* (mean – 1070 ± 585 / 50 ml), *C. sphaericus* (mean – 917 ± 357 / 50 ml) and *E*. l*amellatus* (mean - 883 ± 471/ 50 ml). As a consequence the pelagic: benthic ratio is high, peaking at 1.15 at 275 cm. This initial peak in cladoceran abundance is immediately followed by a sharp drop in total numbers, falling to 3025 / 50 ml at 262.5 cm. This drop is accompanied by a dramatic fall in *B. longirostris* abundance, falling to 952 / 50 ml at 265 cm with *A.affinis* (mean – 262 ± 251 / 50 ml) and *A*. *harpae* (mean – 563 ± 279 / 50 ml) similarly affected. In contrast numbers of

Alonella excisa increase by 140% from 272.5 - 267.5 cm, while *S. crystalline* also shows an increase of >900 % during the same period. The pelagic: benthic ratio falls during this phase, with a value of 0.19 recorded at 267.5 cm. The final stage of DCZ I, is characterised by a rapid return to greater cladoceran abundance. From 262.5 - 250 cm, cladoceran numbers peak at 11,766 (257.5 cm), before gradually declining towards DCZ II. Like the initial stage of DCZ I, this increase in total cladocerans is largely driven by an increase in *B. longirostris*, rising to a mean value of 2541 ± 2248 / 50 ml and a maximum count of 6772 / 50 ml at 257.5 cm. *A. nana* (mean – 1229 ± 826 / 50 ml) and *E*. l*amellatus* (mean – 394 ± 247 / 50 ml) likewise increase. The dominance of *B. longirostris* during this final phase of DCZ I initiates a rise in the pelagic: benthic ratio, with values peaking at 1.36 at 257.5 cm. *B. longirostris* mucro lengths during DCZ I appear to be inversely related to total *B. longirostris* numbers. Mucro length increases from 46 µm to 67 µm during the first two phases of DCZ I, before lengths drop slightly to 60 µm during the final phase. There is large variability in mucro length during DCZ I, with lengths of 40 - 74 µm recorded (Figure 6.33).

Figure 6.32 – Composite diagram of lithology, relative abundance of cladoceran species, major European climostratigraphic zones, radiocarbon dates and LST in Daschower Moor. Species are expressed as percentages of the total cladoceran count for each level. Bosmina mucro length and total cladoceran counts (expressed as absolute) are also shown.

DCZ II: 250 – 225 cm (12,046 ± 721 – 11,320 ± 920 cal yr BP)

Total cladoceran numbers are variable within DCZ II, however they show an overall decline from the onset of the zone to the boundary with DCZ III, falling from 3529 / 50 ml at 250 cm to 1666 / 50 ml at 225 cm (Figure 6.32). This decline is punctuated briefly at 235 cm, when total cladoceran abundance increases to 9447 / 50 ml. Numbers of *B. longirostris* also decrease during DCZ II, falling to 214 / 50 ml at 225 cm. Likewise *A. harpae* decreases from 1024 / 50 ml at 242.5 cm to just 214 / 50 ml at 225 cm, while *A.affinis* shows a similar reduction falling to 265 / 50 ml. In contrast, benthic species generally increase during this second zone, and in particular *A. nana* and *C. sphaericus*, show large increases from DCZ I. The dominance of the benthic community during DCZ II is evident in the low pelagic: benthic ratio, with values ranging between 0.07 - 0.31 throughout the zones entirety. As with total *B. longirostris* during DCZ II, mucro length also decreases. This drop is relatively gradual, falling from 55 µm to 40 µm at 225 cm (Figure 6.33). This gradual reduction is however punctuated at 240 cm and 235 cm where total lengths sharply drop to 29 µm and 30 µm respectively.

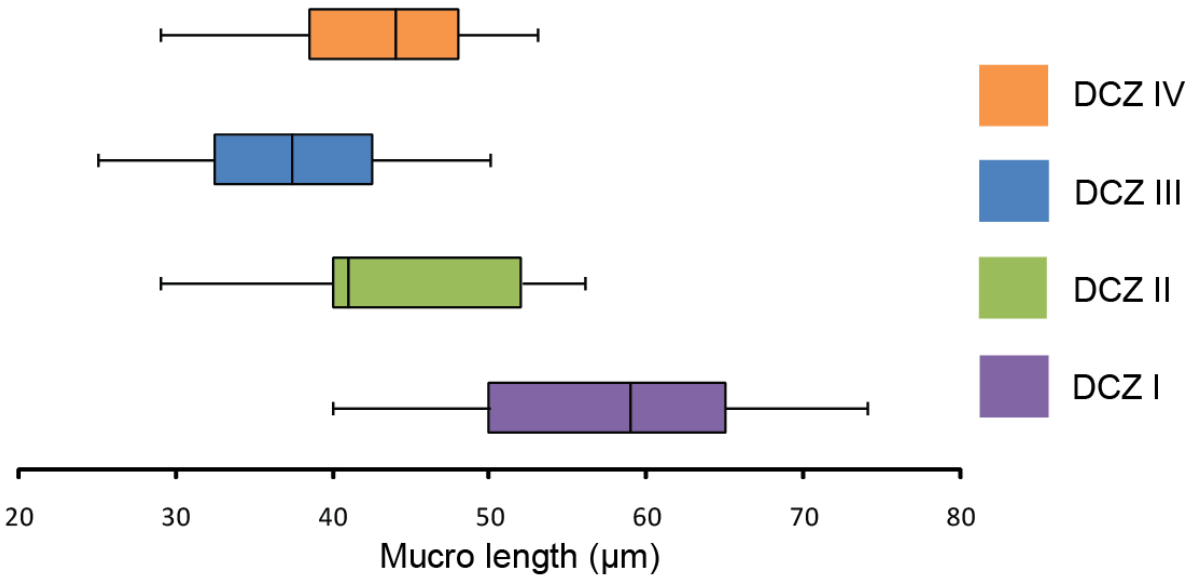


Figure 6.33 – (A – D) box plots of *B. longirostris* mucro length plotted by cladoceran zone for Daschower Moor.

DCZ III: 225 – 202.5 cm (11,320 ± 920 – 11,285 ± 945 cal yr BP)

Total cladoceran abundance decreases dramatically during DCZ III, falling to 755 / 50 ml at 210 cm (Figure 6.32). This drop in total cladocerans is matched by a decline in *B. longirostris*, which apart from a small rise (246 / 50 ml) at 212.5 cm decreases throughout DCZ III, with no individuals recorded at 205 - 202.5 cm. *A. nana*, shows the greatest abundance during DCZ III, while mean counts are lower than those of the previous zone (mean – 789 ± 441 / 50 ml), *A. nana* comprises >80 % of the cladoceran community during the early stages of DCZ III. *C. sphaericus* likewise shows an increase in abundance during DCZ III, this is characterised by increasing abundance from 220 - 202.5 cm. Due to the continued dominance of the benthic record during DCZ III, the pelagic: benthic ratio remains <0.2 for the zones entirety, apart from a spike of 0.38 that coincides with the increase in *B. longirostris* at 212.5 cm. The mucro length record during DCZ III is fragmentary due to ephemeral *B. longirostris* abundance. The values recorded show a range from 25 - 50 µm, with median values of 38 µm (Figure 6.33).

DCZ IV: 202.5 – 122.5 cm (11,285 ± 945 – 8250 ± 300 cal yr BP)

The penultimate cladoceran zone is characterised by fluctuating total cladoceran abundance with a gradual replacement of pelagic species by members of the benthic community. Total cladoceran abundance during DCZ IV generally increases throughout the zone, rising from 1775 / 50 ml at 202.5 cm to 3089 / 50 ml at the zones boundary with DCZ V (Figure 6.32). This rise is punctuated by several abrupt increases, most notable that at 162.5 cm, where total cladoceran counts increase to 10,839 / 50 ml. The abundance of *B. longirostris*, following an initial peak between 192.5 - 182.5 cm (mean – 1144 ± 528 / 50 ml), declines gradually throughout the remainder of DCZ IV, falling to 185 / 50 ml at 122.5 cm. Similarly the abundance of *A. harpae* and *A. nana* also decrease during DCZ IV with *A. harpae* disappearing from the cladoceran record by 122.5 cm and *A. nana* soon after. DCZ IV is dominated by *A. excisa* which increases rapidly between 182.5 - 155 cm. Following a small drop in abundance at 147.5 cm, *A. excisa* numbers increase again to 4636 / 50 ml at 135 cm. Coupled with the increase in *A. excisa*, is the rise of *A. affinis*, which increases by 900% between 197.5 - 135 cm. *A. guttata var tub* is also consistently present with DCZ IV, with its abundance increasing between 132.5 - 122.5 cm. The pelagic: benthic ratio is characterised by a steady decline in values throughout

DCZ IV, due to the replacement of the pelagic community by the benthic, with values falling from 0.18 - 0.06. Mucro length of *B. longirostris* shows a slight increase during DCZ IV, values however fluctuate over a broad range of 29 - 53 µm (Figure 6.33).

DCZ V: 122.5 – 100 cm (8250 ± 300 – 7448 ± 590 cal yr BP)

Total cladoceran abundance continues to fall during DCZ V and apart from a rise at 112.5 cm of 6664 / 50 ml, declines relatively rapidly, falling to 150 / 50 ml at 100 cm. The onset of DCZ V coincides with an almost complete disappearance of many of the cladoceran species within Daschower Moor (Figure 6.32). *A. affinis* and *A. guttata var tub* both disappear at 120 cm and 110 cm respectively, while *A. nana* is lost at 115 cm. Only *A. excisa* is represented throughout the zones entirety and after a peak in abundance of 5239 / 50 ml at 112.5 cm, numbers decline to 50 / 50 ml at 100 cm. Lastly, *C. piger* shows a small increase during DCZ V, increasing by ~50% between 107.5 - 100 cm. The loss of all pelagic species during DCZ V causes the pelagic: benthic ratio to remain at 0.

6.5.5 Palaeoevolution of Daschower Moor

Allerød: DOZ I and DCZ I

OM data indicates that algal primary productivity increased during the Allerød period in Daschower Moor, before decreasing during the Younger Dryas. Below 266 cm, an enriched $\delta^{13}C_{org}$ and a depleted $\delta^{15}N_{org}$ record is encountered (Figure 6.28). This, coupled with elevated C:N and LOI values during this phase, indicate a greater contribution of terrestrial organic matter into the basin and lower primary algal productivity, most likely representative of shallow water conditions with aquatic macrophytes (after Street *et al*., 2012). Above 266 cm however, the gradual depletion of the $\delta^{13}C_{org}$ record and subsequent enrichment of $\delta^{15}N_{org}$ values is consistent with increasing algal derived organic material, thus indicating greater autochthonous productivity and a reduction in terrestrial input (after Cook *et* al., 2012; Street *et al*., 2012). As observed within Endinger Bruch, the deposition of the LST (263 cm) appears to have caused a reduction in $CaCO_3$. The cladoceran record during the Allerød conforms to the bipartite OM signal. Below 266 cm, numbers of the nutrient dependent *B. longirostris* fall steadily, coinciding with small increases in *A. affinis* and *A. harpae* coupled with a decline in the pelagic: benthic ratio indicates a reduction in water depths and an expanse of the littoral

zone (after Frey, 1988; Kattel and Sirocko, 2011). This further supports the OM indication of high allochthonous terrestrial input into a shallow basin. Above 266 cm however a shift in the cladoceran community supports the interpretation of changing basin conditions. Numbers of *B. longirostris* increase relative to benthic species, raising the pelagic: benthic ratio thus indicating an increase in lake levels coupled with improved algal productivity. The acidification of Daschower Moor, as indicated by the $CaCO_3$ record, appears to have impacted on the trophic structure of the lake with mucro lengths increasing immediately (ANOVA p = 0.016616) after the deposition of the ash, suggesting a re-ordering of the trophic structure with fish likely lost after the deposition of the ash (see section 7.2.2, Chapter 7).

Younger Dryas: DOZ I, DOZ II, DOZ III, DCZ II and DCZ III

The Younger Dryas is characterised by general stability across all OM and sedimentary proxies, however due to an incomplete record during this period, caution must be used when interpreting this chronozone (Figure 6.28). The Younger Dryas up until 216 cm follows this pattern of stability with $\delta^{13}C_{org}$ values ~ -24 ‰ and a gradual enrichment of the $\delta^{15}N_{org}$ record coupled with C:N values of ~14 - 15. *B. longirostris* mucro lengths decrease during this early part of the Younger Dryas, suggesting that predation pressure is driven by fish as opposed to aquatic invertebrates. The reduction in *B. longirostris* and the increase in *A*. *harpae*, A*. nana* and *C. sphaericus* after this point indicate further reduction in lake levels and an expanse of the littoral zone (after Kulesza *et al*., 2011). Combining the OM and cladocera data indicates that below 216 cm, algal productivity was stable coupled with greater water depths, but with increasing levels of allochthonous input from the surrounding basin. At 216 cm, an enrichment of $\delta^{13}C_{org}$ values coinciding with depletion in the $\delta^{15}N_{org}$ record and elevated TOC, TN all indicate the development of an aquatic macrophyte population and a lowering of primary algal productivity (after Håkansson, 1985; Aichner *et al*., 2010). The reduction in *B. longirostris* abundance supports this interpretation; however the rise in other species associated with these conditions is delayed until the onset of the Holocene, suggesting aquatic macrophyte coverage was still limited at the termination of the Younger Dryas.

Holocene: DOZ III, DOZ IV, DOZ V, DCZ IV and DCZ V

The Holocene OM record is characterised by a continuation of the trend seen in the latter stages of the Younger Dryas. The expansion of aquatic macrophytes continues as indicated by the enrichment of $\delta^{13}C_{org}$ values coinciding with depletion in the $\delta^{15}N_{org}$ record and elevated TOC and TN values. An increase in lake depth between 195 - 185 cm is indicated by an increase in *B. longirostris* triggering a rise in the pelagic: benthic ratio (Figure 6.32). Mucro lengths increase sharply just prior to the onset of the Holocene which is consistent with a switch in predation pressure from fish to aquatic invertebrates. The continued rise in *A. excisa* and drop in *B. longirostris* above 185 cm suggests shallow, acidic (pH <5) conditions are present in the lake (Kulesza *et al*., 2011) which further supports this interpretation of fishless environment from the late Younger Dryas – early Holocene onwards. At 126 cm there is a significant rise in the C:N record coinciding with depleted $\delta^{15}N_{org}$ values. Such high (>50) CN values indicate a significant input of terrestrial material into the basin. The cladoceran response suggests that Daschower Moor became significantly shallower at this point, with most cladoceran species becoming locally extinct. The dominance of *A. excisa* indicates continued acidic conditions, within a very shallow, boggy type environment.

6.6 Chapter summary

The OM and cladoceran records presented in Chapter 6 suggest that there was significant variability in aquatic system development during the Lateglacial – Holocene period. The relatively good separation of chronozone OM records from Endinger Bruch, Potremser Moor, Kieshofer Moor and Daschower Moor strongly suggests that climatic and environmental change had some influence on the OM regimes of these basins during the Lateglacial – Holocene. Slotseng by contrast shows no clear separation in the OM record of the chronozones recorded in its basin. Within Slotseng, therefore there is not a pattern of abrupt OM response to external climatic and environmental changes, but a gradual evolution, interspersed by abrupt authochronous developments that occur within chronozone boundaries. What is also clear across a number of sites is that the OM and cladoceran record does not respond rapidly at the established chronozone boundaries therefore suggesting that external climate change was not the sole forcing mechanism in driving these records.

Chapter 7: Discussion

The following chapter will interpret and discuss the results presented in Chapters 5 and 6 and their relevance to Lateglacial aquatic system development. In order to address the aims and objectives highlighted in section 1.7 (Chapter 10), Chapter 7 will evaluate the Lateglacial aquatic record on the following three discussion points and questions (section 7.1, 7.2 and 7.3):

1) Comparison and agreement of site chronologies

2) Were variations in aquatic system development consistent across the NEP, or did they develop independently?

3) What was the potential contribution of aquatic systems to the subsistence strategies of hunter-gatherer societies during the Lateglacial on the NEP?

7.1 Site chronologies

The earliest Lateglacial (pre-Allerød), in many north European palaeoenvironmental records, poses the greatest difficulty in terms of correlation and interpretation (Kulesza *et al*., 2011). The stages of climate change, distinguished as the Oldest Dryas, Bølling, and Older Dryas have various unique features and different durations, depending largely on local conditions (Ammann and Lotter, 1989; Stuiver *et al*., 1998; Litt and Stebich, 1999; Litt *et al*., 2001; see section 1.1.1, Chapter 1). Coupled with this is the limited availability of former basins with a continuous record of lacustrine processes spanning the Bølling-Preboreal period, with basin size appearing to have influenced the onset of lacustrine sedimentation in many NEP basins (Figure 7.1).

Site	Size (hectares)	Start of record	End of record
Slotseng	~0.5	18,707 – 16,860 cal yr BP	10,993 – 10,019 cal yr BP
Endinger Bruch	~0.4	15,933-14,163 cal yr BP	11,098-10,210 cal yr BP
Potremser Moor	15	10,918-10,228 cal yr BP	*1 Holocene
Kieshofer Moor	40	13,885-12,795 cal yr BP	*2 Holocene
Daschower Moor	2	14,854-13,194 cal yr BP	8038-6858 cal yr BP

Table 7.1 – Summary of the age ranges for the basins presented in this thesis. *1 – no precise estimate for the age of the top of the Potremser Moor record. *2 – no precise estimate for the age of the top of the Kieshofer Moor record.

Aquatic system development in smaller basins (kettle holes <0.3 km^2) largely precedes that witnessed in larger and medium sized basins (0.3-100 km^2), primarily due to faster dead-ice melt in smaller systems (Kaiser *et al.*, 2012). A consequence of smaller basin size however is increased sedimentation and peat formation, with the majority of small basins becoming telmatic or fully terrestrialised during the Allerød or Preboreal. The five sites presented in this thesis cover the Bølling-Preboreal period (Table 7.1). The smaller basins of Slotseng and Endinger Bruch both contain a full range of sediments from the Bølling-Preboreal period. The larger basins of Potremser Moor, Kieshofer Moor and Daschower Moor are represented by mid to late Allerød-Preboreal age sediments.

The accepted chronozone boundaries presented within the sites used by this thesis are often defined differently (often by fluctuations in different pollen taxa). An example of this is the accepted date for the onset of the Older Dryas in Slotseng, with changes in the pollen record preceding that witnessed in the macrofossil record by ~100 years. Therefore one must explore the level of synchronicity between sites with caution. Furthermore chronological uncertainties are multi-centennial (Table 7.2), therefore synchronising the records to compare the timing in the response of the aquatic record to AETs between sites is only possible at a low resolution (multi-centennial). Consequently, the timing of

response in the aquatic record discussed in section 7.2 will be done so at an intra-site level only. As an exception to this, records can be synchronised at discrete stratigraphic positions using tephra as isochrones, and this will be discussed further in sections 7.2.3.1 and 7.2.3.2. Additionally, it is possible to compare the *level* of response in aquatic systems to AETs, with the aquatic record of each site compared on a chronozone level.

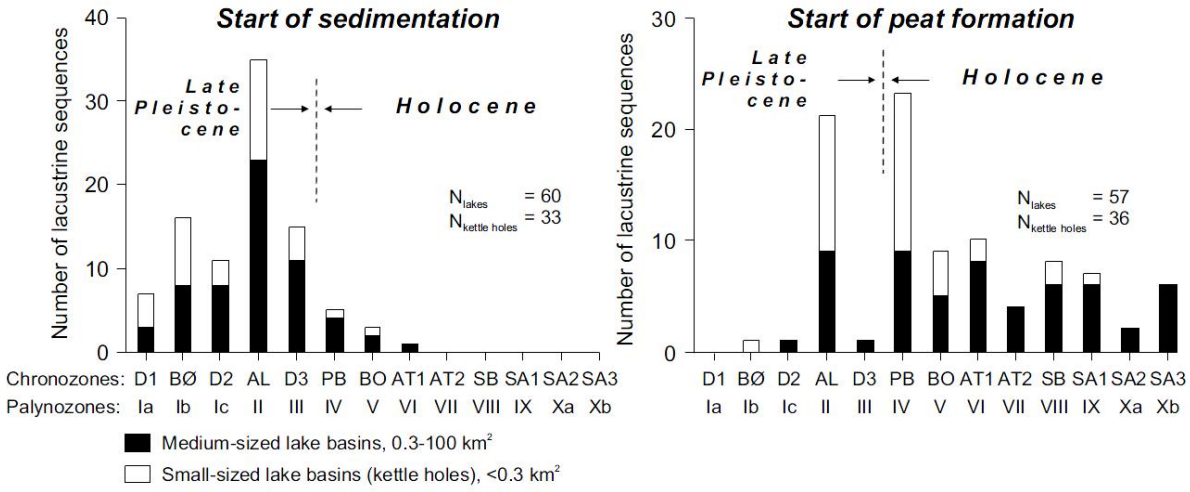


Figure 7.1 – Onset of lacustrine sedimentation (left) and peat formation (right) in lake basins of northeast Germany. Modified from (Kaiser *et al*., 2012).

Pre-Bølling

The oldest sediments of all the sites in this thesis come from Slotseng. Believed to represent the Oldest Dryas, these "*Pre-Bølling*" sediments record the onset of sedimentation in the Slotseng basin. No available ^{14}C dates are available for this portion of the core; therefore the exact timing of the onset of lacustrine deposition is unknown. The extrapolation of the age model produced by Mortenson *et al*., (2011) for the sequence provides an estimated age of 22,200 ± 1160 cal yr. BP for the onset of sedimentation. This is considerably older than the suggested period of deglaciation for the area which is believed to be ~19,000 cal yr. BP (Houmark-Nielsen and Kjær, 2003). It is likely therefore that the oldest ^{14}C date overestimates the age of the deposit or that sedimentation rates were not constant below this point (Mortenson *et al*., 2011).

Bølling

Classically the Bølling period has been correlated with the expansion of *Hippophaë* and *Betula nana*, *Dryas octopetela* and *Salix* sp (see section 1.3, Chapter 1). The general agreement of vegetation records from across northwestern Europe suggests that the expansion of *Hippophaë* in particular was relatively synchronous and has been dated to ~ 14,600 cal yr BP (Hoek, 2001; de Klerk, 2002; Bos *et al*., 2006; Veski *et al*., 2012). The onset of the Bølling period within Slotseng is dated to ~16,600 - 15,500 cal yr BP which is considerably older than the generally accepted date of ~14,600 cal yr BP. Mortensen *et al*., (2011) give an age of ~14,700 cal yr BP, however this is based upon assumed linear sedimentation rates (k = 100) and therefore may be unrepresentative. The radiocarbon samples for this period are all associated with multi-centennial errors which reduce the model's precision making it difficult to accurately estimate the true age of the onset of Bølling. The vegetation response is nevertheless consistent with the classic Bølling vegetation record, with increases in *Betula nana*, *Dryas octopetela* and *Salix* sp recorded (Mortensen *et al*., 2011), suggesting the position of the onset of the Bølling defined in the Slotseng core by Mortensen *et al*., (2011) is accurate. The expansion of *Hippophaë* in Endinger Bruch occurs at ~1450 cm, strongly suggesting that the onset of sedimentation may well stretch back into the Oldest Dryas/ earliest part of the Bølling dated to 15,933 -14,163 cal yr BP.

Older Dryas

The transition from the Bølling to the Older Dryas is dated at 14,222 - 13,966 cal yr BP in Slotseng based upon terrestrial pollen records. The responses to climate change associated with the onset of the Older Dryas in Slotseng are however slight and not synchronous across the records of different environmental proxies (Mortensen *et al*., 2011). The terrestrial pollen record at 14,222 - 13,966 cal yr BP is marked by continued deposition of *B. nana* (but with a percentage reduction caused by increased deposition of other pollen species) and a marked increase of *Helianthemum oelandicum*, while changes in the macrofossil assemblage, characterised by increases in drought tolerant species (e.g. *Rumex acetosella* and *Lychnis alpine*) occur at ~14,000 cal yr BP. If the responses are representative of the same climatic event then there appears to be a lagged response of ~100 years within the terrestrial proxies and as such the accepted date of the Older Dryas in Slotseng, which

although within dating errors, is represented by a stratigraphic difference in the Slotseng core. The age given 14,222 - 13,966 cal yr BP for the onset of the Older Dryas does however appear to agree well with other generally accepted dates for this event, with a decline in *Betula* pollen in northern Germany dated to ~14,000 cal yr BP (de Klerk, 2004) and to ~14,100 cal yr BP in the Netherlands (Hoek, 2001). The increase in *Juniperus* associated with the Older Dryas in the Endinger Bruch core occurs at ~1400 cm (de Klerk, 2002) and has a modelled age of 14,397 - 13,671 cal yr BP which appears to lag slightly behind the Slotseng record, however with an error range of 363 cal yr BP it is difficult to determine the exact level of offset.

Site	Bølling	Older Dryas	Allerød	Younger Dryas	Holocene
Slotseng	~16,600-15,500	14,222-13,966	14,190-13,940	13,120-12,500	11,900-11,290
Endinger Bruch	15,933-14,163	14,397-13,671	14,001-13,500	12,886-12,416	12,174-11,307
Potremser Moor			*[1]	*[2]	10,918-10,228
Kieshofer Moor			13,885-12,795	12,930-12,161	12,394-10,924
Daschower Moor			14,854-13,194	12,767-11,324	12,177-10,276

Table 7.2 – Modelled ^{14}C ages for the Lateglacial chronozones represented in this thesis. Chronozone boundaries are derived from vegetation records; Slotseng – Mortensen *et al*., (2011); Endinger Bruch – de Klerk *et al*., (2002); Potremser Moor, Kieshofer Moor and Daschower Moor – Theuerkauf (pers, comm.). *[1] and *[2] no age estimate as all ^{14}C dates and tephra layers for Potremser Moor are located above the onset of the Holocene.

Allerød

The termination of the Older Dryas and the onset of the Allerød is represented by an abrupt decrease in *Dryas octopetala* coupled with a gradual decline in *B. nana* and *H. oelandicum* pollen dated to

14,190 - 13,940 cal yr BP in the Slotseng record. The decline in non-arboreal pollen is used to define the onset of the Allerød in Endinger Bruch and was initially assigned a tentative age of 13,900 - 13,800 cal yr BP, which agreed well with the suggested age of the 'classical' Allerød, as reported from numerous Danish records (e.g. Hoek, 1997). The radiocarbon date from core KZA (section 3.5.2.3, Chapter 3), which can be correlated to Endinger Bruch, on the basis of its stratigraphic position and the almost complete loss of *Hippophaë* pollen in both cores, is located at the transition from the Older Dryas to the Allerød. The date gives a modelled age of 14,001 - 13,500 cal yr BP which agrees with previously published age ranges for this transition (de Klerk, 2002; Lane *et al*., 2011b). The presence of the LST in Endinger Bruch, Kieshofer Moor and Daschower Moor, allows not only modelled age ranges for the onset of sedimentation in Kieshofer Moor and Daschower Moor, but also age estimates for the Allerød – Younger Dryas transition across all three sites. The stratigraphic position of the LST in Kieshofer Moor (796 cm) suggests that the sediments studied as part of this thesis are from the late Allerød, and are likely ~13,000 cal yr BP in age. However the extrapolated age for the basal sediments within the basin gives an age of 13,885 - 12,795 cal yr BP, and as discussed in section 5.2.6 (Chapter 5), this must be treated with caution due to the large uncertainties in the model. It was not possible to accurately define an age for the onset of sedimentation in Daschower Moor due to disturbances in the lower 20 cm (300 - 280 cm) of sediment (see section 3.5.5, Chapter 3). The LST at 263 cm and a further ^{14}C date at 273 cm (13,951 - 13,104 cal yr BP) enables a modelled age of 14,854 - 13,194 cal yr BP to be given for the sediments at 280 cm, with a likely age towards the younger most age estimate based upon the stratigraphic gap of 17 cm between the LST (12,880 ± 40) and the sediments at 280 cm. It was not possible to accurately model the age of the lower most sediments in Potremser Moor as the only modelled ages all fell above the Younger Dryas (see section 5.1.5, Chapter 5).

Younger Dryas

The onset of the Younger Dryas at Slotseng was originally given as ~12,800 cal yr BP by Mortensen *et al*., (2011) based upon changes in the LOI and vegetation record. Re-modelling of this transition within a Bayesian P-Sequence model as part of this thesis gives a revised age of 13,120 - 12,500 cal yr BP, which utilises a lower *k* value, allowing for greater variation in sedimentation rates (Bronk

Ramsey, 2008). This agrees well with the age for the onset of the Younger Dryas from Endinger Bruch (12,886 - 12,416 cal yr BP); Herthamoor, northeast Rügen (13,315 - 12,412 cal yr BP; Schamacher and Endtmann, 1998) and Kolczewo, northwest Poland (13,118 - 12,631 cal yr BP; Latalowa, 1992). Modelled ages for the onset of the Younger Dryas from Kieshofer Moor (12,930 - 12,161 cal yr BP) and Daschower Moor (12,767 - 11,324 cal yr BP) are associated with large age uncertainties, however Kieshofer Moor broadly agrees with the other environmental records, including Slotseng and Endinger Bruch.

Holocene

The end of the Younger Dryas and the transition to the Holocene at Slotseng is given as 11,500 cal yr BP by Mortensen *et al.,* (2011). Increased sedimentation during the Younger Dryas is evident from the buried *Sphagnum* mat (see section 6.1.6, Chapter 6) and, as such, the previously modelled dates, using a high *k* value, may be unrealistic. The re-modelled age produced by this thesis for the onset of the Holocene is given as 11,900 - 11,290 cal yr BP. This agrees reasonably well with Endinger Bruch (12,174 - 11,307 cal yr BP). Modelled ages for the onset of the Holocene from Kieshofer Moor (12,394 - 10,924 cal yr BP) and Daschower Moor (12,177 - 10,276 cal yr BP) show overlap with Slotseng and Endinger Bruch, but again are associated with centennial errors. The dates for the onset of the Holocene appear to agree relatively well with other northern European records such as Herthamoor, northeast Rügen (11,975 - 11,140 cal yr BP; Schamacher and Endtmann, 1998); Kolczewo, northwest Poland (12,376 - 11,271 cal yr BP; Latalowa, 1992) and Lake Lielais, eastern Latvia (11,650 - 11,390 cal yr BP; Veski *et al*., 2012). Potremser Moor by contrast shows a younger modelled age for the onset of the Holocene (10,918 - 10,228 cal yr BP). This is most probably due to the model underestimating the true age of the boundary at 495 cm due to the rapid sedimentation rates throughout the model.

7.2 Comparison of OM and cladoceran response to climatic boundaries across study sites

The impact AETs had on intra-site development has been confidently reconstructed within this thesis (Chapter 6). The next step is to elucidate whether variability in the palaeoenvironmental record (Chapter 6) is unique within each site, or whether AETs influenced aquatic system development at a

regional scale This variability (or lack of) is crucial in beginning to assess the likely potential aquatic systems had in supporting hunter-gatherer societies. As discussed in section 3.1.1 (Chapter 3) the attractiveness of aquatic and fish resources lies in the lower risk of failure they pose in any one given hunting/gathering expedition (Kelly, 1995). The environment of the NEP during the Lateglacial would have made it economically unfeasible for a hunter-gatherer society to base their subsistence strategy around an unpredictable and spatially variable resource base. If aquatic resources formed a major and spatially widespread part of Lateglacial subsistence strategies, they would have needed to be predictable in terms of their development and productivity.

The following sections will address this issue of predictability and whether levels of productivity within studied sites were comparable, or whether they varied over a local scale. Coupled with this, section 7.2.2 will also evaluate how unique environmental events impacted aquatic system development. The presence of the LST in three of the study sites, allows the response of these systems to the Laacher See eruption to be discussed and comparisons made with other previously published sites containing the LST.

7.2.1 Variability between study sites

Bølling

The inception of Lateglacial aquatic system development, demonstrated in the sites of Slotseng and Endinger Bruch, occurred at the onset of the Bølling (~14,600 - 14,100 cal yr BP). Both sites during this time are represented by similar levels of aquatic productivity in an oligotrophic type environment. The $\delta^{13}C_{org}$ record of both sites during the Bølling is relatively high (~ -21 to -25 ‰) and it is likely that during this time aquatic primary productivity was influenced by cold water temperatures and low organic matter regeneration. This combination would have exacerbated carbon limitation thus causing the production of aquatic algae with high $\delta^{13}C_{org}$ values (Street *et al*., 2012). These cold water conditions are confirmed in both sites by the presence of “arctic to sub-arctic” cladoceran species, with *A. harpae*, *A. affinis* and *C. sphaericus* present during the Bølling in both cores. Similar ecological conditions have been observed in modern “cold water” lakes from Finland and Greenland with *A. harpae*, *A. affinis* and *C. sphaericus* predominating these oligtrophic type environments (Brancelj *et*

al., 2009). However one must treat such comparisons carefully due to the no-analogue environment of the North European Lateglacial.

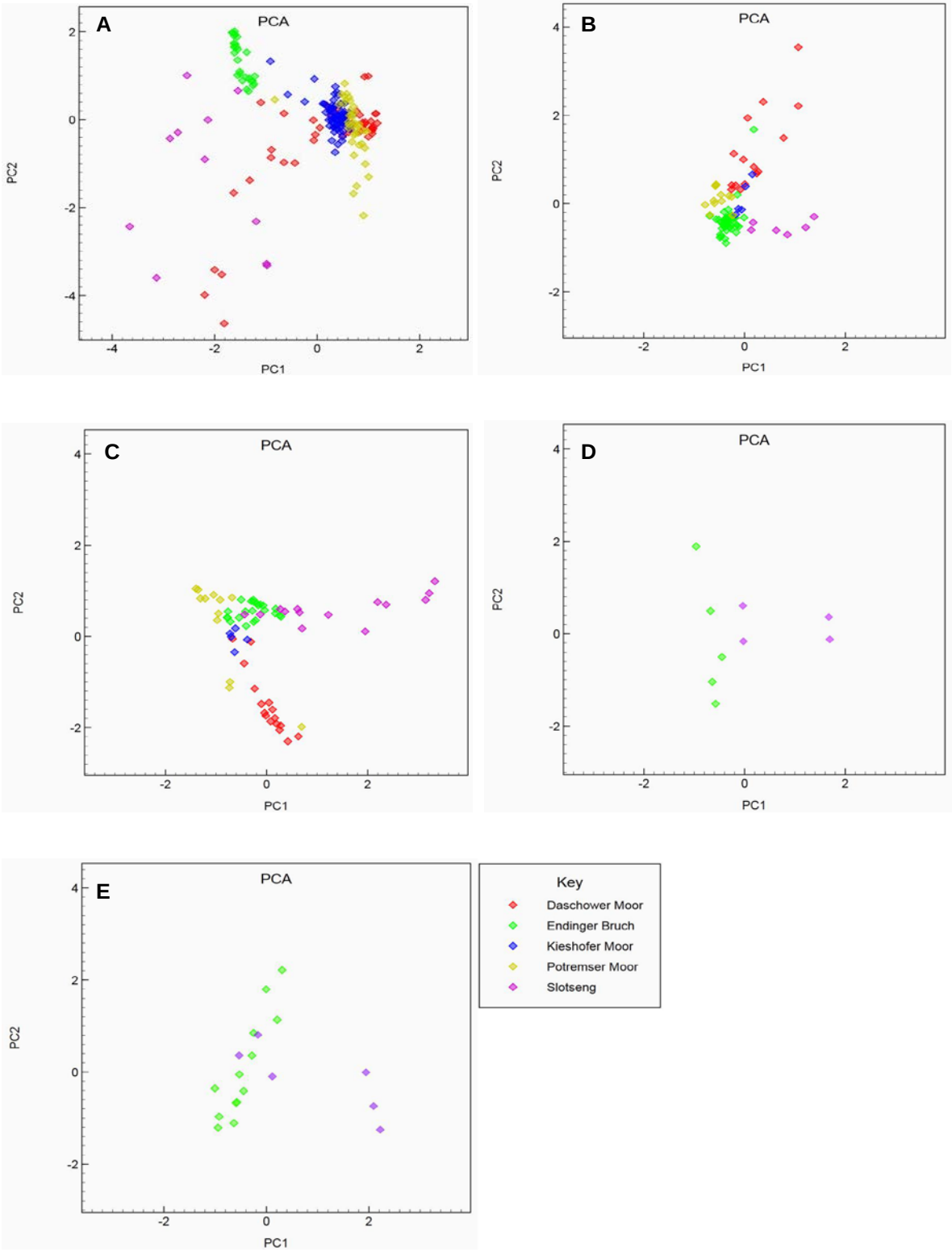


Figure 7.2 – PCA bi-plots of $\delta^{13}C_{org}$, $\delta^{15}N_{org}$, TOC, TN and C:N plotted by chronozones for the five sites presented in this thesis. Holocene (A); Younger Dryas (B); Allerød (C); Older Dryas (D); Bølling (E).

There are however some major isotopic and sedimentary differences during the Bølling leading to differences in the OM record which are likely the result of inwash or slumping events in Slotseng (Figure 7.2). Increases in the Slotseng C:N, TOC and TN record during the Bølling, are most likely driven by the slumping of organic material, including aquatic macrophytes, within the basin. This is confirmed by Mortensen *et al*., (2011) who observed that several of the submerged aquatic macrophyte species disappeared by the end of the Bølling due to water turbidity caused by these slumping events. Due to the limited disturbance of the Endinger Bruch basin during the Bølling, its OM signal may provide a "signature" for cold-water, oligotrophic type conditions during the earliest phases of its development. The cladoceran communities of Slotseng and Endinger Bruch are largely similar based upon concentrations of major species. Both basins during the Bølling are represented largely by arctic and generalist type species such as *A. harpae*, *A. affinis* and *C. sphaericus* (Harmsworth, 1968) as well as *B. longirostris*. The presence of *B. longirostris* in both basins, coupled with an absence of *D. pulex*, strongly suggests that during the Bølling the pelagic communities of both basins were subject to the same dominant predation pressure, which in this case is driven by planktivorous fish. The major difference between the two basins during this period is in the concentration of individual species from the benthic cladoceran community, with Endinger Bruch having far higher concentrations of individual benthic cladoceran species, thus driving the difference between the two basins during the Bølling. The likely cause of this difference can again be attributed to basin instability within the Slotseng basin. As discussed in section 6.1.6 (Chapter 6), these slumping events led to a reduction in *B. longirostris* at 14,104 - 13,908 cal yr BP caused by basin turbidity, which in turn is likely to have impacted on fish populations in the basin at this time. The instability of littoral sediments during this phase, whilst initiating a rise in species associated with disturbed sediments such as *A. nana*, *C. piger* and *C. sphaericus* (Harmsworth, 1968), at the same time resulted in an overall reduced concentration of a large number of littoral species.

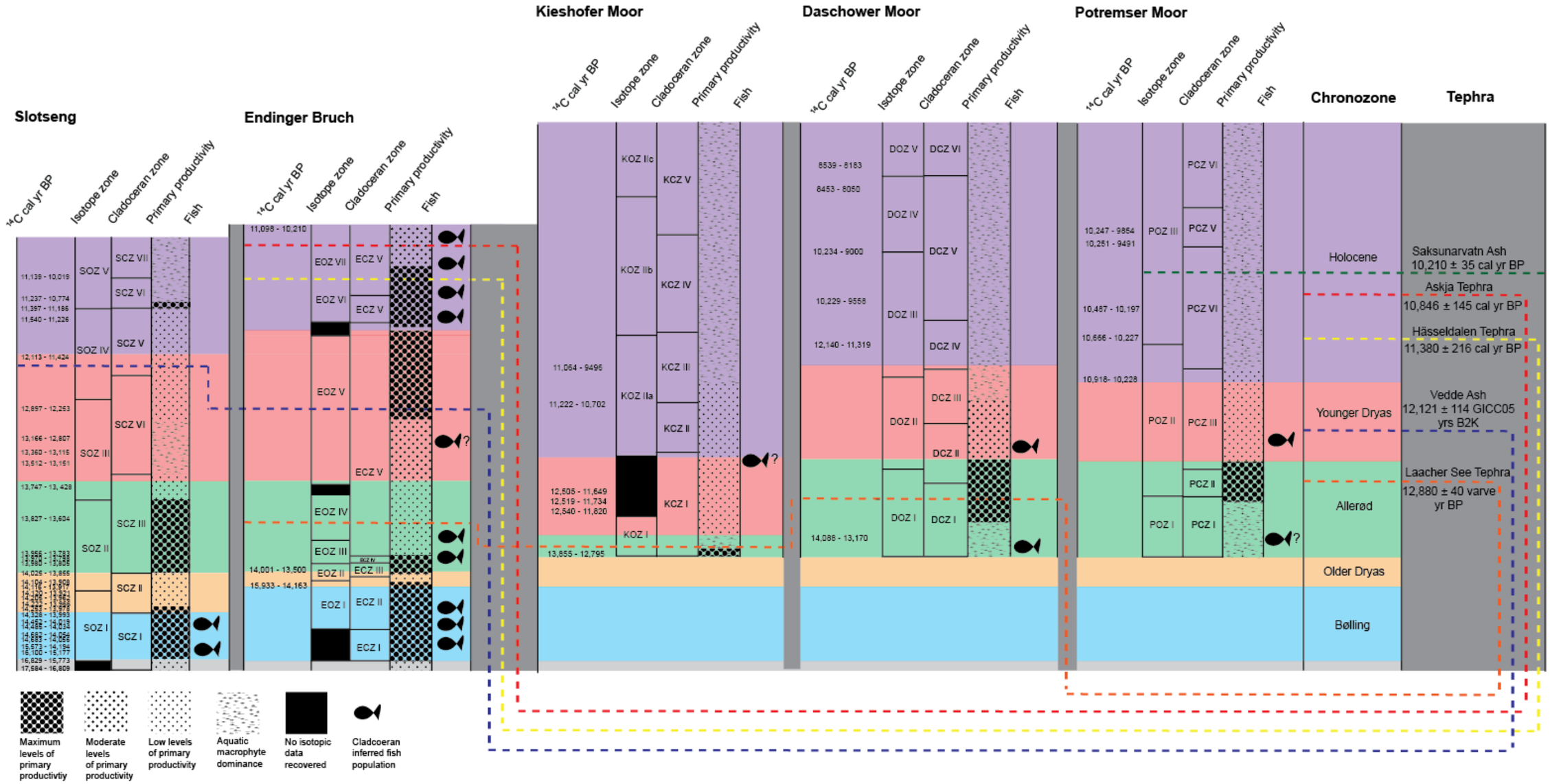


Figure 7.3 – Composite diagram showing the five sites presented in this thesis plotted with OM derived productivity levels and cladoceran inferred fish populations. The ^{14}C dates and tephra layers for each site are also shown. Chronozone position within each site is denoted by colour: purple – Holocene; red – Younger Dryas; green – Allerød; yellow – Older Dryas; blue – Bølling and light grey – pre-Bølling. Site logs not to scale.

Older Dryas

The onset of the Older Dryas in Slotseng and Endinger Bruch appears to be asynchronous, with the onset of the Older Dryas in Endinger Bruch potentially lagging behind the Slotseng record by ~100 years based on modelled age ranges. Within both basins however the impact of Older Dryas conditions on the OM record is relatively muted, with changes appearing after the onset of the Older Dryas (Figure 7.3). The lag present in both basins is evident by the change in OM zone during the Older Dryas with a shift from SOZ I to SOZ II in Slotseng and EOZ I to EOZ II in Endinger Bruch. As discussed in sections 6.1.1 and 6.2.1 (Chapter 6), these new OM zones differ from the preceding zone, suggesting that at this point basin conditions changed which is dated to 14,104 - 13,908 cal yr BP in Slotseng and to 14,250 - 13,600 cal yr BP in Endinger Bruch based upon modelled ages. The response of the OM and sedimentary record is similar in both basins. Increased $\delta^{13}C_{org}$ and C:N is coupled with a reduction or continued low amounts of TOC and TN. In both cases erosion in the surrounding catchment, linked to more open conditions, is likely to have caused increased allochtonous deposition. The time-trangressive response of the terrestrial vegetation record and the aquatic records of Slotseng and Endinger Bruch raises two possible scenarios for the response of aquatic systems to the Older Dryas. The lag in response of the aquatic record behind the pollen inferred Older Dryas boundary may on the one hand indicate that the Slotseng and Endinger Bruch basins were initially buffered to the effects of the reversal in climate, with conditions in the lake deteriorating ~ 100 years (based on modelled ages) after the onset of the Older Dryas. Alternatively, and in particular in Slotseng, the response of the macrofossil record coincides with changes in the OM record, this may therefore suggest that the local and therefore aquatic response to the Older Dryas came after the more regional signal as interpreted by the pollen record. This problem is further compounded by the observation that vegetation is known to lag behind climate, often by as much as 300 years (Wright, 1984) and the variability in the pollen derived position of the chronozone boundary reported by the Mortensen *et al*., (2011) and de Klerk (2002). The cladoceran record offers no clear answer to these scenarios, with records from Slotseng and Endinger Bruch giving conflicting views. The Slotseng cladoceran record responds in time with the inferred pollen chronozone boundary for the Older Dryas (Figure 6.6; Chapter 6). This response is driven primarily by a large reduction in total cladoceran individuals, coupled with the emergence of *D. pulex* ephippia and a reduction in *B.*

longirostris. As discussed in section 6.1.6 (Chapter 6), this indicates unfavourable basin conditions as a result of increased erosional input which is suggestive of the Older Dryas. In Endinger Bruch the cladoceran record sees a similar reduction in total individuals and *B. longirostris* (ECZ III, 14,135 - 13,561 cal yr BP). This however occurs above the Older Dryas boundary as defined by changes in the pollen record and ~10 cm above the change in the OM record. Evidence from Soppensee, Switzerland and Meerfelder Maar, Germany suggests that changes in the aquatic record were penecontemporaneous with the onset of the Older Dryas (Brauer *et al*., 1999; Lotter, 1999). The cooling associated with the onset of the Older Dryas is recorded in Greenland ice records at 13,954 ± 165 GICC05 yr b2k (Rasmussen *et al*., 2006) which would appear to agree with the delayed response in aquatic systems as suggested by the OM and cladoceran record. However as discussed in section 1.1.2 (Chapter 1) one must treat chronological comparisons between Greenland and northern European records with caution so as to avoid any assumption of synchronicity. Based on the available data and the centennial age errors associated with the modelled dates for Slotseng and Endinger Bruch it is not possible at present to conclude whether the lag in the OM and cladoceran record within Slotseng and Endinger Bruch is truly a delayed response to climate deterioration or a factor of an overriding and at times muted regional pollen signal.

While it is impossible to say if the aquatic systems of Slotseng and Endinger Bruch were synchronous in their response to the cooling at the start of the Older Dryas, we can evaluate the level of their response, and whether the changes in aquatic development were similar between both basins. What is perhaps most striking about the aquatic record of both basins during the Older Dryas is the response of the cladoceran community. Total cladoceran abundance is severally reduced during the Older Dryas, with a sharp downturn associated with the onset of cooler conditions at Slotseng. Total cladoceran numbers also fall within Endinger Bruch, however unlike Slotseng, there is a gradual fall throughout the chronozone. The response of the pelagic *B. longirostris* during this phase is the same across both sites, with a reduction in numbers. The turbidity of the systems during the Older Dryas would have likely rendered them fishless due to reduced oxygen content of the water. This is supported by the emergence of *D. pulex* in Slotseng and the increase in *B. longirostris* mucro length in Endinger Bruch during the Older Dryas. While the pelagic record indicates a loss of fish and a reduction in algal productivity, the benthic record from Slotseng and Endinger Bruch remain more or

less consistent within each basin, at least from the Bølling into the Older Dryas. Both basins are still represented by arctic and generalist type species such as *A. harpae*, *A. affinis* and *A. guttata/ rectangular* and *C. sphaericus*. The uniformity of this benthic composition during the Bølling and Older Dryas suggests that while levels of aquatic productivity decreased, the basins themselves remained relatively uniform with generally unstable conditions prone to disturbances. The uniformity shown in the benthic cladoceran response is not particularly evident in the OM record (Figure 7.2D). While both sites are influenced by inwash processes during the Older Dryas, the effect of this process on both basins is different. During the Older Dryas, Slotseng likely became shallower; with inwash from the surrounding catchment and littoral zone contributing to the OM record. In Endinger Bruch, by contrast, the same inwash events led to very little change in the record, with only C:N affected, likely caused by the inwash of soil organic matter bound onto clay and silt minerals (after Hyodo and Longstaffe, 2011). While the cladoceran fauna of both basins is similarly affected and fish are likely to have disappeared during the Older Dryas (Figure 7.3), the primary difference between Slotseng and Endinger Bruch is the composition of material delivered into the basins, with Slotseng characterised by large amounts of organic material and Endinger Bruch by microbial organic matter bound to clays and silts.

Allerød

Unlike the transition to the Older Dryas, the response of the OM record to the climate amelioration of the Allerød coincides with the vegetation response from both sites (see de Klerk, 2002; Mortenson *et al*., 2011). As discussed in section 6.1.6 (Chapter 6) the development of the Allerød in the Slotseng basin is characterised by two different regimes. Figure 7.2C shows that within Slotseng there is a trend away from the central cluster of data points as a result of the development of a *Sphagnum* mat over the site. Due to this telmatic phase of the late Allerød in Slotseng, this period will be discussed as two separate periods, that below 85 cm (Allerød I) and that above 85 cm (Allerød II), therefore allowing comparison with the more open water type conditions present in Endinger Bruch, Potremser Moor and Kieshofer Moor. Daschower Moor also shows the same bi-partite pattern in the OM record during the Allerød, however unlike Slotseng this is not due to telmatic development and therefore has not been divided. Both Slotseng and Endinger Bruch during the early Allerød are characterised by

high levels of aquatic authochronous productivity as indicated by the OM record immediately following the termination of the Older Dryas (Figure 7.3). During this phase allochthonous input into the Slotseng basin increases prior to the telmatic phase of Allerød II. This pattern of increasing allochthonous terrestrial input is also witnessed in Endinger Bruch, where at 13,550 - 13,060 cal yr BP drops in aquatic authochronous productivity coincided with increased input from the surrounding basin. This pattern in both basins, suggests that primary production reaches a maximum immediately after the Older Dryas before decreasing during the mid to late Allerød. A similar pattern of increasing primary production following the Older Dryas was observed in the early Allerød sediments of Lake Steisslingen, southwest Germany (Mayer and Schwark, 1999). While the OM regimes of Slotseng and Endinger Bruch during this phase are similar, the pelagic component of the cladoceran community highlights that the basins were completely different in terms of their trophic web structure (Figure 7.3). The transition from *B. longirostris* to *D. pulex* at 14,050 - 13,850 cal yr BP confirms that Slotseng was highly likely to be fishless from this point onwards. In the four other sites presented in this study, all have a population of *B. longirostris* during the Allerød, Younger Dryas and Holocene, while at Slotseng *B. longirostris* becomes locally extinct during the Allerød. In contrast, the pelagic cladoceran record of Endinger Bruch indicates an aquatic system with a fish population which remains stable until the deposition of the LST at 12,880 ± 40 cal yr BP (Brauer *et al*., 1999). The recolonisation of Potremser Moor and Daschower Moor by fish is likely due to the passive dispersal of fish eggs by wading birds entering from lakes containing fish (see Bassett Maguirc 1963).

The OM record of Potremser Moor and Kieshofer Moor during the Allerød are closely associated with both basins characterised by a bipartite OM signal (Figure 7.3). This is manifested in Kieshofer Moor by the highest levels of aquatic productivity from 13,328 - 12,690 cal yr BP, followed by the increasing dominance of aquatic macrophyte cover and lower levels of productivity until 12,932 - 12,158 cal yr BP and the onset of the Younger Dryas. Potremser Moor is also characterised by this bipartite signal, however unlike Kieshofer Moor, aquatic productivity increases towards the Younger Dryas boundary. As previously mentioned Daschower Moor also exhibits this bipartite signal; however it is far more pronounced than at either Potremser Moor or Kieshofer Moor, with a period of aquatic macrophyte cover from 14,024 ± 830 to 13,050 ± 200 cal yr BP giving OM conditions similar to those experienced in all three basins during the Holocene. In contrast to the OM record, the cladoceran record of

Kieshofer Moor and Daschower Moor is largely the same. This is driven by the relative abundances of the species such as *A. harpae* and *A. affinis*, which are indicative of shallow, nutrient poor conditions. Each is characterised by variations in aquatic productivity during the Allerød. This is characterised at Kieshofer Moor by maximum levels of aquatic productivity, followed by a decline, whilst at Daschower Moor the reverse is true. This variability in the OM record however produces a strikingly similar cladoceran response, suggesting that cladoceran record is varying independently of the OM record during the Allerød. The cladoceran response in Potremser Moor during the Allerød is actually most similar to the Younger Dryas record from all sites apart from Endinger Bruch. The reason for this is most likely due to the response of pelagic species to this phase, most notably *B. longirostris*. In Potremser Moor the cladoceran record during the Allerød is characterised by low numbers of *B. longirostris* and elevated numbers of benthic species such as *A. harpae*, *A. nana* and *C. sphaericus* for much of the duration of the Allerød. This type of cladoceran community structure is found within all basins (apart from Endinger Bruch) during the Younger Dryas. Evidence for changing patterns in predation pressure is however clear in the cladoceran record from Potremser Moor. Like that witnessed in Slotseng, there is a transition from *D. pulex* to *B. longirostris* between 540 - 530 cm, which is consistent with an absence of fish predation during this period. Coupled with this is a significant increase in mucro length between 540 - 530 cm (*t* test – 0.0039), which suggests that with an absence of fish, predation pressure is primarily driven by aquatic invertebrates (after Sweetman and Finney, 2003). It was not possible to date this phase but based on its stratigraphic distance below the Younger Dryas boundary at 525 cm it is likely that it occurred during the latter phase of the Allerød.

The evidence for fish populations in Kieshofer Moor and Daschower Moor is not as clear cut as at Slotseng, Endinger Bruch and Potremser Moor. The deposition of the LST and subsequent morphological changes in *B. longirostris* mucro length however allow robust inferences to be made on the likelihood of fish presence during the later Allerød period. In Kieshofer Moor immediately following the deposition of the LST, there is no observable increase in *B. longirostris* mucro length which would otherwise suggest a re-ordering of the pelagic food web. Instead what is witnessed is an initial decrease in mucro length followed by a sharp length increase dated at 12,920 - 12,380 cal yr BP (12,650 ± 270 cal yr BP) ~230 years (based on modelled ages) after the deposition of the ash. The

lack of response to this event is suggestive of two possible scenarios in Kieshofer Moor. Firstly, the reduction in *B. longirostris* mucro length immediately following the deposition of the LST may suggest that there were simply no fish present within the basin during this period, and that invertebrate predation was driving the variability in mucro length. Secondly, it is possible that the sharp increase in mucro length dated at 12,920 - 12,380 cal yr BP represents a delayed biological response to this event, with the loss of fish only manifested within the *B. longirostris* mucro record long after the ash event. Of the two scenarios the former is the most likely. In studies on the effects of volcanic ash on lake systems Eicher and Rounsefell (1957) discovered that in all studied lakes, the maximum recovery time of the system was <12 years. What the authors witnessed was a catastrophic reduction in fish populations followed by a swift recovery to pre-ash conditions in less than 12 years. The delay of ~230 years witnessed in Kieshofer Moor would seem far too long to be representative of a lag in the biological system to LST deposition. This thesis therefore argues that the Allerød period in Kieshofer Moor was most likely fishless. In contrast there is an immediate increase in the mucro length of *B. longirostris* following the deposition of the LST within Daschower Moor.

Younger Dryas

Prior to the onset of the Younger Dryas $\delta^{13}C_{org}$ varied considerably in response to changes in primary algal productivity and terrestrial inwash. However, during the Younger Dryas the records presented in this thesis became far more consistent and stable, with values of -24‰ to -26‰. The relative enrichment of the $\delta^{13}C_{org}$ record during the Younger Dryas is interpreted as a change in discrimination by the algal community (e.g. Brenner *et al*., 1999; Gu *et al*., 1999). It is possible that resuspended littoral material is contributing to this enrichment during the Younger Dryas. If resuspended littoral OM is contributing to the $\delta^{13}C_{org}$ record during the Younger Dryas, one would expect a more depleted signal coming from the Allerød – Younger Dryas boundary in Endinger Bruch, Potremser Moor and Daschower Moor (Lücke and Brauer, 2004). The fact that $\delta^{13}C_{org}$ values are enriched during the Younger Dryas relative to the Allerød would therefore suggest that resuspended OM contributing to the enrichment of the $\delta^{13}C_{org}$ record during the Younger Dryas is not the case; and as greater changes in atmospheric carbon dioxide (pCO_2, $\delta^{13}CO_2$) and the photosynthetically used dissolved inorganic carbon source are also unlikely to have influenced this process, the observed enrichment of

the $\delta^{13}C_{org}$ record of ~3 - 4‰ is therefore a record of increased carbon demand generated by algal photosynthesising cells (Lücke and Brauer, 2004). Such conditions coupled with a generally enriched $\delta^{15}N_{org}$ profile and low TOC and TN values are highly suggestive of low to moderate levels of primary productivity, and can be correlated with an oligotrophic type environment across all sites (apart from Slotseng) during the Younger Dryas. In studies of varved sequences from Germany (e.g. Meerfelder Maar), it was observed that the lacustrine palaeoproductivity increased rapidly at the start of the Younger Dryas (Lücke and Brauer, 2004). The cause of this rise in productivity is likely the result of a number of processes leading to:

- Landscape instability associated with a more open environment would have caused nutrients bound within soil organic material to be transported and deposited within lake basins leading to higher nutrient loading of the water columns during this phase.

- The drop in winter temperatures coupled with extended ice cover during the winter months would have caused the build up of an undiminished nutrient pool.

- The shorter summer season and reduced strength in stagnation of littoral OM, would have further increased nutrient availability (Salmaso, 2002).

- Algal photosynthetic activity, supported by improved nutrient abundance and development, was likely enhanced and expressed as strongly reduced discrimination against ^{13}C, leading to $\delta^{13}C_{org}$ enrichment (after Goericke *et al*., 1994; Riebesell *et al*., 1993).

These processes therefore effectively led to a concentration of primary algal productivity during the warmer summer months, relative to the colder winter months. The OM record during the Younger Dryas period is the most closely correlated period across all study sites with the exception of Slotseng, which remains distinct (Figure 7.2).The close association of Endinger Bruch, Potremser Moor, Kieshofer Moor and Daschower Moor strongly suggests that authochronous and allochthonous processes were in equilibrium during the cold reversal of the Younger Dryas and that these spatially disparate basins responded to this event in a similar fashion. However the timing of changes witnessed in the OM record appear to differ across the sites studied. The response of the OM record to the Younger Dryas in Endinger Bruch coincides with increases in the *Betula* and *Juniperus* record

(de Klerk, 2002) indicating at least a local response to the Younger Dryas, and strongly suggests that the deterioration in climate and temperature had an influence on the development of Endinger Bruch during this phase. The lack of data for the Younger Dryas period in Kieshofer Moor makes comparison with Endinger Bruch impossible; however the records from Potremser Moor and Daschower Moor do allow such comparisons. What is observed in these two records is a lag between the onset of the Younger Dryas and the response of the OM record. Firstly, the enrichment and subsequent stability of the $\delta^{13}C_{org}$ record in Potremser Moor falls 8 cm above the Younger Dryas transition as recorded in the sediment and pollen profile (Theuerkauf pers. comm.). The lack of ^{14}C dates for this period makes it impossible to determine the age of this offset and extrapolating sediment accumulation rates from the Holocene is likely to give spurious results. However it is possible that the algal response of the basin, as manifested in the OM record, lags behind the onset of the Younger Drays on at least a decadal timescale. The OM record of Daschower Moor likewise lags behind the onset of the Younger Dryas by an order of 4 cm. The modelled ages for this lag suggest a period of ~70 years between the onset of the Younger Dryas and the OM response (onset of Younger Dryas, 12767 - 11324 cal yr BP; response of OM record, 12,700 - 11,250 cal yr BP). This however must be treated with caution, as both periods overlap within standard errors. While the sites of Endinger Bruch, Potremser Moor, Kieshofer Moor and Daschower Moor suggest that the OM response to the Younger Dryas can be correlated spatially, the timing of these basin developments cannot. This may be indicate a true chronological difference between sites in the response of the aquatic record to the Younger Dryas or be a factor of variability in the pollen derived chronozone boundaries for the sites.

The response of Slotseng to the Younger Dryas is completely different to that experienced at the other sites in this study. The early Younger Dryas (120 - 135 cm) in Slotseng is characterised by elevated C:N values (>40) that coincide with the burial of the *Sphagnum* mat. The burial and subsequent remobilisation of this Allerød age feature during the early Younger Dryas produces an OM record that is incomparable with any of the other sites during this time and serves to mask any response in the OM record to the onset of the Younger Dryas. Analysis of the second half of the Younger Dryas above 135 cm shows stability in the OM record, like that recorded from the other study sites, but characterised by different basin conditions. As previously discussed, the second half of the

Allerød in Endinger Bruch and Slotseng is characterised by increasing levels of allochthonous input coupled with a reduction in primary algal productivity. This scenario is present in Slotseng from 13,750 - 13,310 cal yr BP however with C:N values >20 this strongly suggests that deposition during this phase was controlled by allochthonous input and that lake productivity was low. OM deposition in Slotseng is defined by sharply contrasting regimes, the magnitude of which are not present in any of the other sites studied here. The OM deposition and productivity fluxes during the Younger Dryas are representative of the basins evolution as a whole during the Lateglacial – Holocene with rapid transitions from aquatic to telmatic sedimentation and *vice-versa*. The cladoceran response in the Younger Dryas is remarkably similar, with all sites characterised by a total reduction in cladoceran abundance coupled with relatively higher numbers of pelagic species serving to elevate the pelagic: benthic ratio. The relative consistency in the OM record, and thus basin conditions would appear to have generated a cladoceran profile that is responsive to the aquatic environment.

The presence of *B. longirostris* and variability in mucro length during the Younger Dryas suggests that fish were likely present in Endinger Bruch, Potremser Moor and Daschower Moor. The Endinger Bruch record shows a marked *B. longirostris* response to the Younger Dryas, with mucro lengths increasing significantly, coinciding with the onset of the chronozone. This thesis suggests that extended ice cover during the Younger Dryas led to significant winter fish kills, resulting in a re-ordering of the trophic web, with aquatic invertebrates becoming increasing prevalent leading to the morphological response in *B. longirostris* (see Sin and Chiu, 1982; Meding and Jackson, 2003; Balaya *et al*., 2010). The sharp decrease in mucro lengths at the onset of Holocene suggests, that while fish populations were heavily impacted by this cooling event they remained throughout this cold period. With the onset of increased summer temperatures, fish once again became the dominant source of predation pressure in the basin. The *B. longirostris* record for Potremser Moor and Daschower Moor by contrast suggests that fish populations were only present during the first half of the chronozone. This occurs between 525 - 515 cm in Potremser Moor and from 12,046 ± 721 to 11,320 ± 920 cal yr BP in Daschower Moor. The cause of this bi-partite *B. longirostris* signal in Daschower Moor is most likely due to a reduction in lake depth and the expansion of the littoral zone coinciding with increasing aquatic macrophyte abundance. This interpretation is supported by a decrease in *B. longirostris* coupled with an increase of *A.* harpae, A*. nana* and *C. sphaericus* which

are associated with shallow muddy/weedy type conditions (Kulesza *et al*., 2011). Increasing shallowness coupled with a probable increase in water turbidity would have rendered Daschower Moor increasingly unsuitable for fish, during the second phase of the Younger Dryas. The increase in *B. longirostris* mucro lengths in Potremser Moor during the second half of the Younger Dryas is more difficult to interpret. Unlike Daschower Moor there is no recognisable change in the OM record that would indicate a shift in basin conditions during the Younger Dryas. Instead the record shows relatively consistent values allied with algal productivity under oligotrophic type conditions. It is possible that increased winter ice cover during the second phase of the Younger Dryas led to increased fish mortality. This scenario is however unlikely as it is recognised that the latter half of the Younger Dryas was in fact warmer than the early half of the chronozone (von Grafenstein *et al*., 1999; Schwark *et al*., 2002). It is most likely that the fish population in Potremser Moor declined of its own accord through natural processes. The lack of dating in this portion of the core frustrates any attempt to quantify the duration of fish presence; however the response of the record does provide valuable clues as to the productivity of the basin during the coldest part of the Younger Dryas.

Holocene

The OM record of the Holocene in Potremser Moor, Kieshofer Moor and Daschower Moor are all characterised by similar basin conditions, with extensive aquatic macrophyte cover coupled with prevailing shallow water conditions (Figure 7.2 and 7.3). This transition occurs above the onset of the Holocene in Potremser Moor, dated to 10,710 - 10,230 cal yr BP. As previously discussed, the modelled age ranges for the Holocene period in Potremser Moor may underestimate the true age of the sediments. In comparison with the modelled age for the onset of the Holocene (10,918 - 10,228 cal yr BP) in Potremser Moor it is difficult to accurately quantify the duration of the lag between climatic amelioration and aquatic response due to the large centennial errors associated with the dates. There is however an appreciable stratigraphic difference between these two events (~9 cm) suggesting that there is a genuine lag in the aquatic record behind the terrestrial response to this event. Daschower Moor by contrast sees the reduction in algal productivity and the development of shallow, acidic and macrophyte dominant conditions prior to the termination of the Younger Dryas and onset of the Holocene which is dated at 12,350 - 10,600 cal yr BP. This suggests the response seen

at Daschower Moor may have pre-dated the onset of the Holocene by ~250 years (based on modelled ages). Unlike Potremser Moor and Daschower Moor, Kieshofer Moor shows no apparent lead or lag in the OM response to the warming associated with the onset of the Holocene. The development of conditions comparable with those at Potremser Moor and Daschower Moor, occur at the onset of the Holocene, dated at 12,394 - 10,924 cal yr BP. The OM record from the remaining sites of Slotseng and Endinger Bruch cannot be closely correlated with the Holocene in Potremser Moor, Kieshofer Moor and Daschower Moor (Figure 7.2). Instead both basins are unique in their development. The Holocene record from Slotseng is similar to that witnessed in the late Allerød and early Younger Dryas, with all three periods associated with *Sphagnum* development and a significant drop in algal productivity. The timing of the response in the OM record in the Slotseng basin appears to lag behind the onset of the Holocene as given by the pollen record for the site (Mortensen *et al*., 2011). The transition from the Younger Dryas to the Holocene within Endinger Bruch is obscured by a lack of OM data between 1021 - 981 cm. The incomplete record during this time suggests however that the depletion in the $\delta^{13}C_{org}$ record and subsequent rise in the TOC and TN coincided approximately with the onset of the Holocene as indicated by the pollen record (de Klerk, 2002). The bipartite Holocene sequence in Endinger Bruch shares some similarities with the other four sites, in that there is an increase in allochthonous deposition during the early phases of the Holocene. However unlike the other sites this does not manifest itself in the development of the shallow, macrophyte rich conditions of Potremser Moor, Kieshofer Moor or Daschower Moor and neither does the site become telmatic as seen in Slotseng. What is witnessed, however, is a mixed algal and terrestrial/semi aquatic signal, that is more allied with increased algal productivity. In the other four sites, the deposition of allochthonous material or the development of macrophyte cover increases during the Holocene. The reverse however is true in Endinger Bruch, with increasing aquatic productivity after 11,905 - 11,200 cal yr BP.

The similarity of the Slotseng cladoceran record during the Holocene with the Younger Dryas period represented in its own basin as well as that within Potremser Moor, Kieshofer Moor and Daschower Moor is primarily driven by a large reduction in total cladocerans coupled with reduced species richness caused by the terrestrialisation of the site. Terrestrialisation and lack of a pelagic record from Slotseng make it extremely unlikely that fish were present during this phase. As with Potremser Moor,

Kieshofer Moor and Daschower Moor, the dominance of aquatic macrophytes coupled with shallow water and in cases acidic water conditions also make the presence of fish unlikely during the Holocene. This is further supported by the relative stability in *B. longirostris* mucro length throughout much of this period across all three sites. It is only from Endinger Bruch that the likely presence of fish can be detected in the *B. longirostris* record. This interpretation is based on the rapid decline in mucro lengths at the start of the Holocene. As discussed, such a morphological response is most likely associated with a switch from aquatic invertebrate predation to that driven by planktivorous fish (Sweetman and Finney, 2003).

7.2.2 The impact of the Laacher See eruption on Lateglacial aquatic systems

Volcanism has always played an important role in Earth's history, with volcanic eruptions both destroying and creating new habitats (Birks and Lotter, 1994). The direct impacts include lava-flows, ash fall, pyroclastic flows and landslides, while indirect impacts may consist of short-term climate changes caused by stratospheric sulphuric aerosols and fine ash particles that inhibit solar radiation (Birks and Lotter, 1994). The eruption of the Laacher See volcano during the late Allerød spread ash over a large area of north-central Europe (~700,000 km^2 at depths >1 mm and 225, 000 km^2 at depths >5 mm; Bogaard, 1983; Bogaard and Schmincke, 1985). The Laacher See eruption is considered one of the major Plinian eruptions of the Late Quaternary period (Schmincke *et al*., 1999) and must have had an impact on the environment far beyond its immediate surroundings. It has been estimated that at least 2 Mt, but possibly as high as 150 Mt of sulphur was ejected during the eruption (Schmincke *et al*., 1999). This, coupled with widespread ash deposition (Figure 7.4), increased precipitation, acid rain, increased atmospheric albedo and a consequent decrease in average temperatures in the Northern Hemisphere, are likely to have played a role in shaping the hemispheric and local environment following the eruption (Schmincke *et al*., 1999; Graf and Timmreck, 2001; Baales *et al*., 2002; de Klerk *et al*., 2008). Supporting the notion of reduced annual temperatures, Kaiser (1993) inferred a reduction in temperatures for a period of six years from tree rings in fossil pine trunks dating from the time of the eruption, it is however possible that acidification, not reduced temperatures led to the thinner rings (Highwood and Stevenson, 2003).

Several studies have addressed the environmental impact of the eruption of the Laacher See volcano (e.g. Lotter and Birks, 1993; Birks and Lotter, 1994; Schmincke *et* al., 1999; Baales *et al*., 2002) these however all focussed on sites at relatively close distances to the volcano. A recent study by de Klerk *et al*., (2008) addressed the impact of the eruption the Laacher See volcano in a more distal location, Mecklenburg-Vorpommern, Germany, where four sites from this thesis are located. The authors noted an increase in limnic diatom populations following the deposition of the LST, due to abundant silica supplied by the ash which acted as a nutrient source for the construction of frustules. They also noted acidification coupled with an increase in the conductivity of the former lakes.

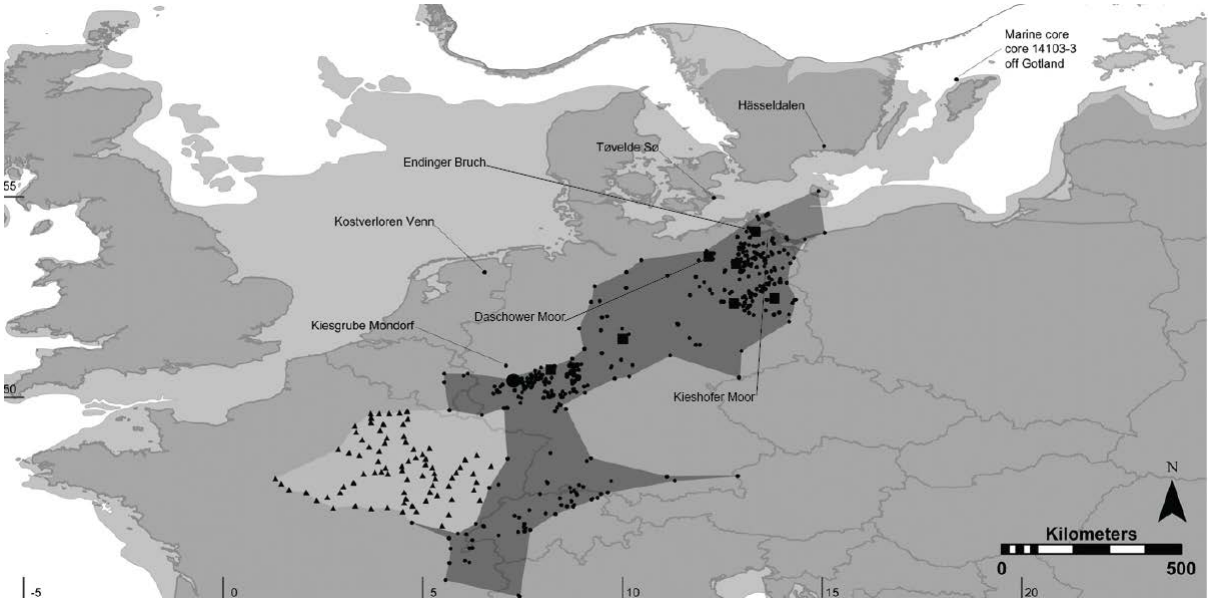


Figure 7.4 - Distribution of the LST following the eruption of the Laacher See volcano. The sites presented in this thesis containing the LST are located in the northeast region of the fallout lobe shown in grey. Adapted from Riede *et al*., (2011).

The impact the LST had on cultural and material change across the NEP has been previously studied in a number of papers (e.g. Riede, 2008; Riede and Edinborough, 2012), which consider the relationship between the Lateglacial hunter-gatherer and the environment of the NEP. Specifically in the case of the Laacher See eruption, the question of whether the aquatic systems would have provided a more stable resource base to hunter-gatherers than the surrounding terrestrial landscape. The emergence of the Bromme technocomplex and the loss of bow and arrow technology at the end

of the Allerød are seen by some authors as a direct result of the Laacher See eruption, with this technocomplex postdating the Laacher See eruption (e.g. Riede, 2008). Henrich (2004) presented a formal demographic model that relates perceived maladaptive adaptations (in this cases the loss of bow and arrow technology) to parameters such as population size, density and connectedness. The Laacher See eruption is suggested to have led to a significant and sudden reduction in at least one of these parameters, connectedness (Riede, 2008), thus giving rise to the Bromme (Riede and Edinborough, 2012). While the Laacher See eruption is argued to have led to material and cultural change across the NEP, the precise way in which the eruption achieved this and how local environments responded is still not clear. This paradox is further complicated by why and how the impact of the Laacher See eruption on the archaeological record appears to change along a proximal-to-distal transect, and why even relatively small amounts of ash could have had such pronounced effects (especially in distal environments such as the Mecklenburg-Vorpommern region). In studies on landscapes close to the Laacher See, it has been demonstrated that despite the evident destruction of proximal environments, hunter-gatherers moved back into the those affected areas after a relatively short (but difficult to estimate) settlement hiatus (Baales *et al*., 2002; Grimm, 2004). Ecosystem recovery studies on recent eruptions suggest that the re-colonisation of areas affected by volcanic eruptions can be rapid (see Dale *et al*., 2005). They do however serve to highlight two key questions regarding this event and the relationship between hunter-gatherers and the environmental and ecological response: (1) are certain ecosystems predisposed to the effects of ash fallout on the landscape? (2) did certain ecosystems offer more favourable resources during this event? In reference to the sites of Endinger Bruch, Kieshofer Moor and Daschower Moor presented in this thesis, as well as through other previously published work, it is possible to begin to address the effect the Laacher See eruption had on the aquatic record, how this compares with the terrestrial record and the implications it would have had for Lateglacial hunter-gatherer groups.

The distal aquatic record

The response of the aquatic environment to the deposition of the LST differs across Endinger Bruch, Kieshofer Moor and Daschower Moor. Both Endinger Bruch and Daschower Moor show a marked response to the deposition of the ash in the cladoceran record. Theoretically, the deposition of the

LST should mostly affect the habitat of benthic organisms by completely covering the lakes substrate (Figure 7.5), leading to turbidity which would severely impact upon any fish populations present within a lake during this time. While the complete recovery time to such events are shown to be <12 years (Eicher and Rounsefell, 1957), its deposition during the spawning season could have magnified the effect of even small volumes of the LST leading to a complete re-ordering of the pelagic food web. Littoral species may have also been affected by ash deposition, with turbid water leading to significantly reduced light penetration through the water, which in turn can affect feeding rates of both planktonic and littoral cladocerans (Hart, 1988). The effect of these processes should therefore lead to an increase in the pelagic cladoceran record. This very response is witnessed in both Endinger Bruch and Daschower Moor, with *B. longirostris* increasing after the deposition of the LST. Coupled with this pelagic response is a reduction in certain benthic species, most notable *A. affinis*, *A. guttata rectangular*, *C. sphaericus* and *P. unicinatus* in Endinger Bruch and *A. nana* in Daschower Moor. These species are to varying degrees, tolerant of increased water conductivity and acidity (Birks and Lotter, 1994; Heinrichs *et al*., 1999). The decline of these benthic species after the deposition of the LST suggests that it was the act of ash covering the lakes substrate that lead to the loss of these species, rather than increased water conductivity or acidity. Comparison of cladoceran response to the LST is found at the site of Soppensee, Switzerland, with a switch from *B. longispina* to *B. longirostris* in the pelagic record (Figure 7.10) with *B. longispina* well known to be more tolerant of acidic conditions than *B. longirostris* (Flöβner, 1972). This suggests therefore, that Soppensee did not likely acidify following the Laacher See eruption, as was indicated at Endinger Bruch and Daschower Moor. This interpretation is supported by the presence of calcite summer layers throughout the Allerød (Lotter, 1999). In further contrast to Endinger Bruch and Daschower Moor is the shift in total cladocerans and the concentration of pelagic species during the latter stages of the Allerød, post LST in Soppensee. Firstly, in Endinger Bruch and Daschower Moor, there is an increase in the total cladoceran concentration during the later stages of the Allerød period. At the time of the deposition of the LST, total cladoceran concentrations fall within Soppensee. This shift is likely driven in part by decreasing pelagic concentrations and a general switch from “turbid” to “clear water” species. Interestingly, in the sample located immediately above the LST in Soppensee, there is a small but noticeable increase in “turbid” species coupled with a decrease in “clear water” species (Figure 7.10).

Whether this represents a trophic response to the deposition of the LST and increase in water turbidity as seen in Endinger Bruch and Daschower Moor is impossible to say without higher resolution sampling at this point. However it does hint at potentially similar responses in certain basins to this event over large areas of Europe.

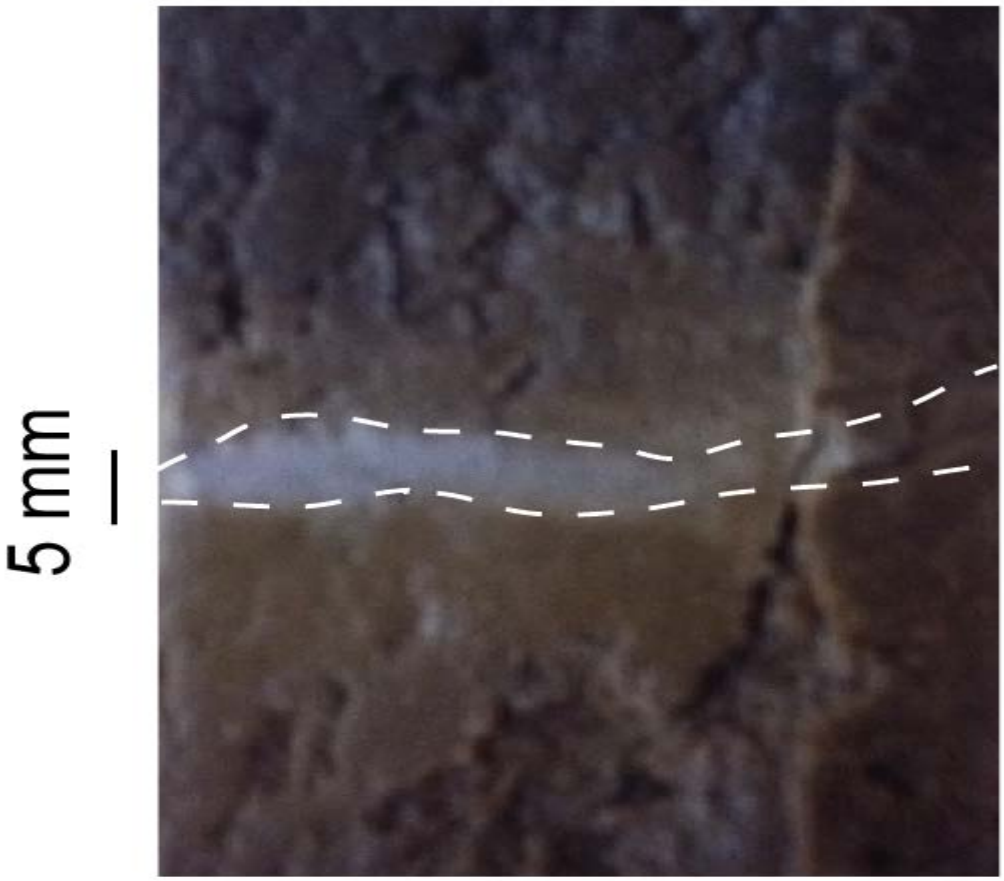


Figure 7.5 – The visible LST layer recorded in Daschower Moor. The combination of primary air-fall and inwash from the surrounding landscape would have blanketed the benthic environment of affected lakes.

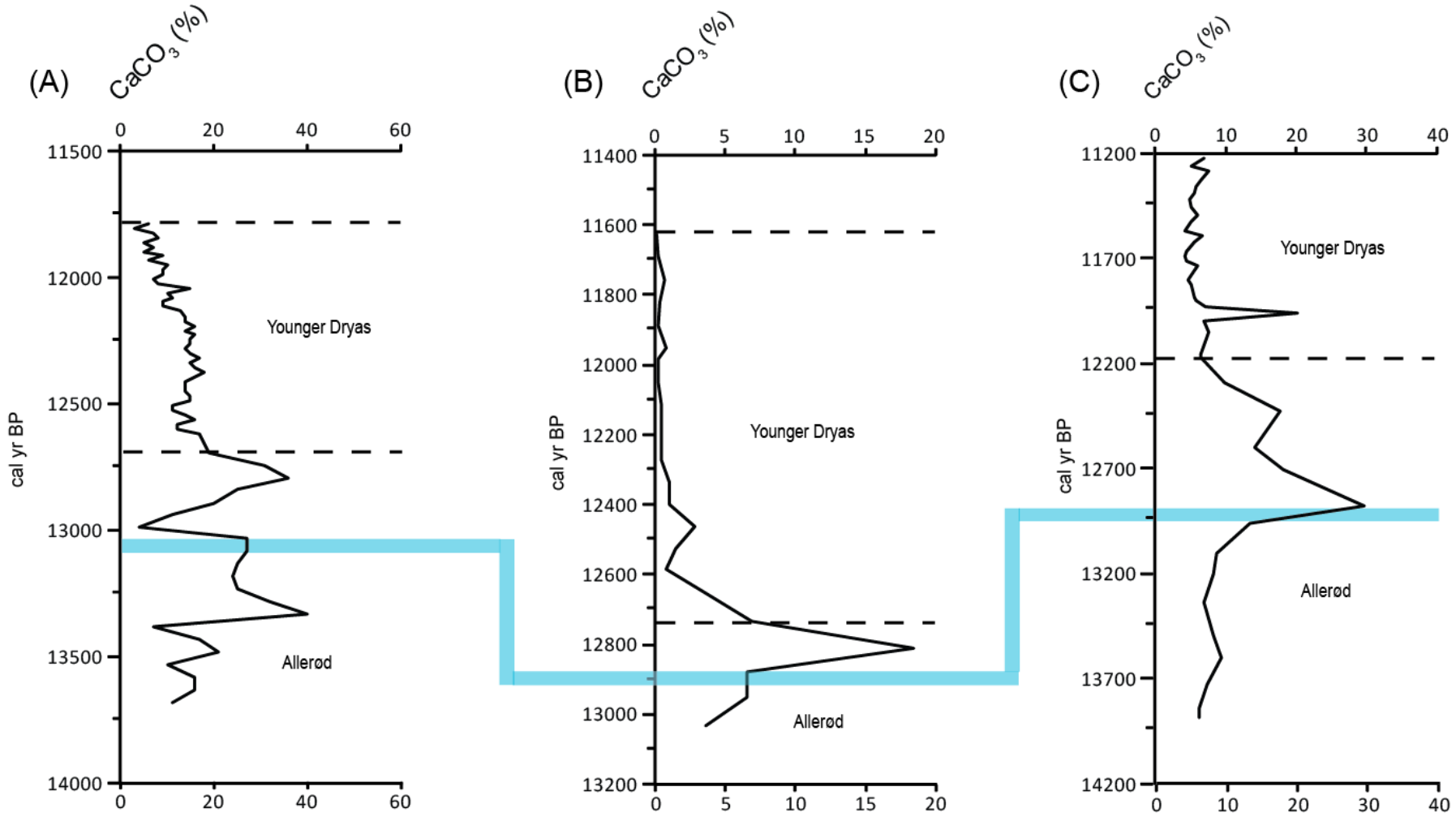


Figure 7.6 – $CaCO_3$ response to the deposition of the LST (shown in blue) from Endinger Bruch (A), Kieshofer Moor (B) and Daschower Moor (C).

As previously discussed the *B. longirostris* mucro record suggests that in Endinger Bruch and Daschower Moor, the impact of the LST's deposition may have led to the loss or reduction in fish populations of both lakes, due to lake acidity and turbidity, increased conductivity or a combination of both; Kieshofer Moor in contrast shows a subtly different response to the deposition of the LST. Like Endinger Bruch and Daschower Moor, the pelagic record of Kieshofer Moor does in fact increase following the event. This however forms part of an increasing trend that was already underway prior to the deposition of the LST, and as explained in section 6.4.5 (Chapter 6), this elevation in the pelagic record is more of an artefact due to the extremely low concentrations of pelagic species throughout the rest of the core. Interestingly the benthic record in Kieshofer Moor appears to follow that of Daschower Moor, with a relatively muted response to ash deposition with only *C. sphaericus* showing any real decline in values. Where the basins do differ is in the morphological response of *B. longirostris*. The lack of a response in the *B. longirostris* mucro record suggests that there was no change in the pelagic food web of Kieshofer Moor following the deposition of the LST. The OM record of Kieshofer Moor supports the interpretation of a muted response to the deposition of the LST with no apparent acidification of the basin as shown by the $CaCO_3$ record (Figure 7.6). The spatially variable response in pH across sites containing the LST, suggests that lake acidification may have been locally variable and not regionally controlled. It is possible that basin size may have influenced the level of lake acidification associated with the LST, with smaller basins such as Endinger Bruch and Daschower Moor more susceptible to lake acidification, while in larger basins such as Kieshofer Moor (40 hectares) the larger volumes of water may have buffered the acidic affects of the LST. While plausible, the comparison of other previously published data does not seem to support this interpretation. Although situated closer to the Laacher See the sites of Hirschenmoor (12 ha), Rotsee (48 ha) and Rotmeer (19 ha) all show the effects of basin acidification after the input of <10 mm of LST (Lotter and Birks, 1993; Birks and Lotter, 1994). It has also been suggested that in regions with acidic bedrock (e.g. granite and gneiss) the acidification of lakes may be intensified following an eruption (Lotter and Birks, 1993). However the basins in this study all overlay glacial till (Kaiser *et al*., 2009) and are therefore better buffered to the effects of ash deposition. While currently it is not possible to conclusively suggest why some basins are affected by LST induced acidity, it does serve to highlight the inconsistency in response to this event across these basins.

The distal terrestrial record

In the distal environment, the Laacher See eruption appears to have had a variable impact on the terrestrial vegetation record. Small pollen fluctuations occur in many pollen records from northeastern Germany, with increasing *Betula* and decreasing *Pinus* a general phenomenon around the time of the Laacher See eruption (Müller, 1961a; 1965; 1967; Lange *et al*., 1986; Wolters, 1999; 2002; Mathews, 2000; Theuerkauf, 2002, 2003; de Klerk and Helbig, 2006). The majority of these records however do not show changes in other pollen types, and if changes do occur with a peak, these are generally formed of different pollen types from different locations (de Klerk *et al*., 2008). In a number of the records from northeast Germany it is difficult to correlate these fluctuations to the Laacher See eruption or the deposition of the LST, since many of them begin prior to the deposition of the ash (de Klerk *et al*., 2008). If the fluctuations in the pollen record were independent of the Laacher See eruption they would exhibit an uninterrupted trend during the event, this however is not the case with a number of records showing an interruption above the LST caused by smaller fluctuations in certain pollen types superimposed on the pre-LST trend (de Klerk *et al*, 2008). These fluctuations are mainly recorded from smaller basins and are driven by pollen deposition from plants directly surrounding the basin, which may in turn explain why these fluctuations are primarily absent from larger basin records (e.g. Kloss, 1980; Zerbe *et al,* 2000). To complicate this picture further, a number of smaller basins record no fluctuations in the pollen record at the time of the Laacher See eruption. This therefore indicates that an opening of the vegetation during this time was not a regional feature, but highly variable at a local level (Kloss, 1994). There are several possible mechanisms that could have led to the small, variable fluctuations in the pollen record at the time of the Laacher See eruption, a decrease in northern Hemisphere temperatures is however unlikely to affected the vegetation record as its relative magnitude and duration would have been too small (de Klerk *et al*., 2008). Equally unlikely is that dryland tree vegetation suffered from ashfall thus allowing open vegetation taxa to flourish (Müller, 1961b; Lotter, 1999) as, following the eruption of Mt St Helens, pine trees were observed to show no effect from 15 cm of direct ash fall (Mack, 1981; Zobel and Antos, 1997). More likely causes for the variability in the pollen record are:

- The possible dying of trees due to acidification of the environment (e.g. Kaiser, 1993).

- The response of vegetation, particularly wetland vegetation, to increased water-levels as a result of increased precipitation following the Laacher See eruption. While there is no evidence of such an event occurring in the sites within this thesis, a number of studies from the Mecklenburg-Vorpommern region have shown evidence of increased soil erosion and overflow of lakes (Schmincke *et al*., 1999; Timmermann, 1999; Baales *et al*., 2002; Theuerkauf, 2003).

- Increased frequency of vegetation fires as indicated by the increase in charcoal particles above the LST in a number of sites (Theuerkauf, 2003). In environments that are distal from the Laacher See volcano, these fires can only be explained by an increase in thunderstorm-frequency (e.g. Anderson *et al*., 1965; Christiansen, 1980) which probably relates to the increased conductivity of volcanic ash (Kenedi *et al*., 2000). While these observations were made at relatively short distances to the volcano and not in the distal realm, it is however known, that following the AD 1783 eruption of Laki, intense thunderstorms swept across northern Europe, causing fires to buildings and agricultural fields (Grattan and Brayshay, 1995; Brayshay and Grattan, 1999).

Another potential influence the Laacher See eruption could have had on the terrestrial environment is the effect of the ashfall itself on grazing animals across the NEP. It has been demonstrated that inhaled ash can lead to chronic irritation of the lungs and in some cases death (Riede and Bazerley, 2009). Coupled with this is the effect of the ash on the teeth of grazing herbivores, with the fine ash particles leading to serious tooth wear during grazing (Riede and Wheeler, 2009; Figure 7.7) and also possible acute fluoride poisoning (Kierdorf and Kierdorf, 1997; Appleton *et al*., 2000; Cronin *et al*., 2000). These factors may therefore have rendered large areas of the terrestrial environment unsuitable for hunter-gatherer occupation following the Laacher See eruption.

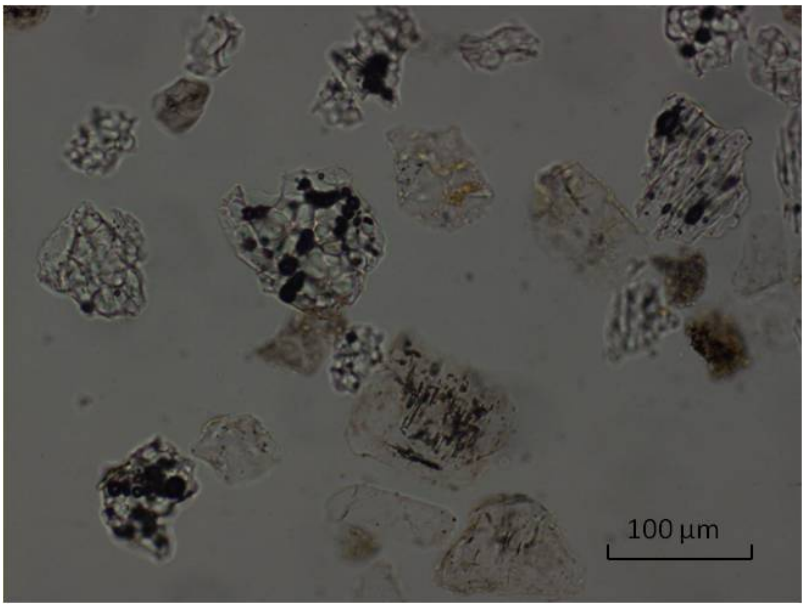


Figure 7.7 – Single grain glass shards from the LST recorded in Kieshofer Moor which have been demonstrated to significantly wear away tooth enamel.

Both aquatic and terrestrial ecosystems would have undoubtedly have been affected by the eruption of the Laacher See volcano, however to what degree varied over a local scale. The acidification of lake systems was not ubiquitous across the NEP, with some sites showing no reaction to the event (e.g. Kieshofer Moor) and in those basins where water acidification is evident the drop in pH was probably not significant enough to affect the trophic structure of the lake (Birks and Lotter, 1994). The direct effect of ash input into the basin is likely to have had a larger impact on lake systems and in the sites of Endinger Bruch and Daschower Moor ash fall has been shown to impact the benthic cladoceran community and also fish populations. These effects are however offset by the sporadic nature of LST deposition across the NEP, with some basins showing no signs of LST deposition or the associated effects such as in Potremser Moor. The impact of the Laacher See eruption on aquatic systems in the distal realm appears therefore to vary over local scales. This largely corresponds with the impact of eruptions on the terrestrial record as given by de Klerk *et al*., (2008), with the effects of increased water-levels, dying of trees due to acidification and fires very much localised in their occurrence. The direct effect of ash fallout on grazing herbivores is also likely to have been temporally and spatially variable. A number of investigations into open air sites across the NEP (e.g. Housley *et al*., 2012; Tolksdorf *et al*., 2013) within the dispersal area of the LST have all yielded no

trace of ash. This suggests that once deposited across the landscape it was quickly eroded away, either through aeolian or fluvial processes before it could be incorporated into land surface. One is therefore left with the impression that the deposition of the LST was highly variable at a local level and that in those open areas where the ash was deposited; it was very quickly eroded away into rivers and lakes.

Aquatic systems as a resource after the Laacher See eruption

Returning to the two questions posed earlier in this section: (1) are certain ecosystems predisposed to the effects of ash fallout on the landscape? (2) did certain ecosystems offer more favourable resources during this event? It is possibly to draw some key conclusions over the position of aquatic systems within the landscape of the NEP during the eruption of the Laacher See volcano. Turning to the first question, it appears the effect of the Laacher See eruption was variable in both aquatic systems and the surrounding landscape. In those areas where the LST was deposited, this thesis suggests that aquatic systems were more vulnerable to the effects of this process. Undoubtedly, fires caused by thunderstorms following the eruption would have caused local destruction; however as is shown in a number of ethnographical studies, burning of the landscape can greatly improve its diversity and foraging potential (e.g. Bird *et al*., 2008). Likewise an increase in water-levels may have served to promote a greater diversity of prey animals such as elk, which are known to have been exploited by Federmesser populations and are closely associated with aquatic systems (Geist, 1999). Lastly direct ash fall on the landscape is likely to have been eroded away relatively quickly, and would not likely have formed extensive deposits in the distal environment. Lakes and aquatic systems in areas where the LST was deposited, would not only receive ashfall directly from the air, but also as ash was eroded off the surrounding landscape, it became focussed within these basins. The result of this therefore is a greater volume of ash deposited in the aquatic environment than the surrounding terrestrial landscape. As aeolian and fluvial processes continued to erode and deposit ash into affected basins, the impact this had on aquatic ecosystems could have continued for months or possibly years. With this in mind, and the likely affect of ash deposition of fish populations (e.g. Newcomb and Flagg, 1982) it is suggested here, and in answer to the second question, that effected

lakes would have offered less favourable conditions and resources for hunter-gatherer groups than the surrounding terrestrial landscape.

7.2.3 Inter-site correlation and wider implications

The application of tephrochronology and tephrostratigraphy presented in this thesis not only provides independent age estimates, thus helping to refine individual age models (see sections 5.1.5, 5.2.6 and 5.3.4, Chapter 5) but also allows the direct correlation, at discrete points, between the sites studied as well as to other palaeoenvironmental records across northern Europe. A total of five tephra layers have been documented at the sites described in this thesis (Table 7.3).

Ash	**Source**	**Date**	**Site/s**	**Reference for age estimate**
Saksunarvatn Ash	Iceland	10,297 ± 45 GICC05 yr b2k' [1] 10,210 ± 35 cal yr BP[2]	Potremser Moor	Rasmussen *et al*., 2006[1] Lohne *et al*., 2013[2]
Askja	Iceland	10,570 – 11,050 cal yr BP	Endinger Bruch	Wohlfahrt *et al*., 2006
Hasseldalen	Iceland	11,543 – 11,232 cal yr BP[3] 11,596 – 11,164 cal yr BP[4]	Endinger Bruch	Wohlfahrt *et al*., 2006
Vedde Ash	Iceland	12,121 ± 114 GICCO5 yr BP	Endinger Bruch Slotseng	Rasmussen *et al* 2006
LST	Eifel Region, Germany	12,880 varve yr BP	Endinger Bruch Kieshofer Moor Daschower Moor	Brauer *et al*., 1999

Table 7.3 – Summary table showing the tephra layers found at the five sites studied in this thesis. [1] and [2] the two ages given for the Saksunarvatn Ash. Based on trace element analysis the Saksunarvatn Ash is argued to be represented by two separate eruptions dispersing tephra to the NW

and SE (see Bramham Law *et al*., 2013). [3] and [4] the two age models constructed for the Hasseldalen tephra (Wohlfarth *et al*., 2006).

All the tephras shown in Table 7.3 are known from various Lateglacial to Holocene palaeoenvironmental records found elsewhere in northern Europe. These tephras provide widespread isochronous marker horizons, allowing temporal and spatial variations in lake development to be assessed. The LST and Vedde Ash are the most crucial tephra layers studied here, as they are present in two or more study sites, therefore allowing isochronous comparison between these records and area also widely distributed throughout northwestern Europe (Figure 7.8). The presence of the LST and/or Vedde Ash in Endinger Bruch, Slotseng, Kieshofer Moor and Daschower Moor allows this thesis to use the tephra isochrones to assess the variability in aquatic productivity between disparate sites in order to help determine how aquatic productivity varied over a regional and local scale.

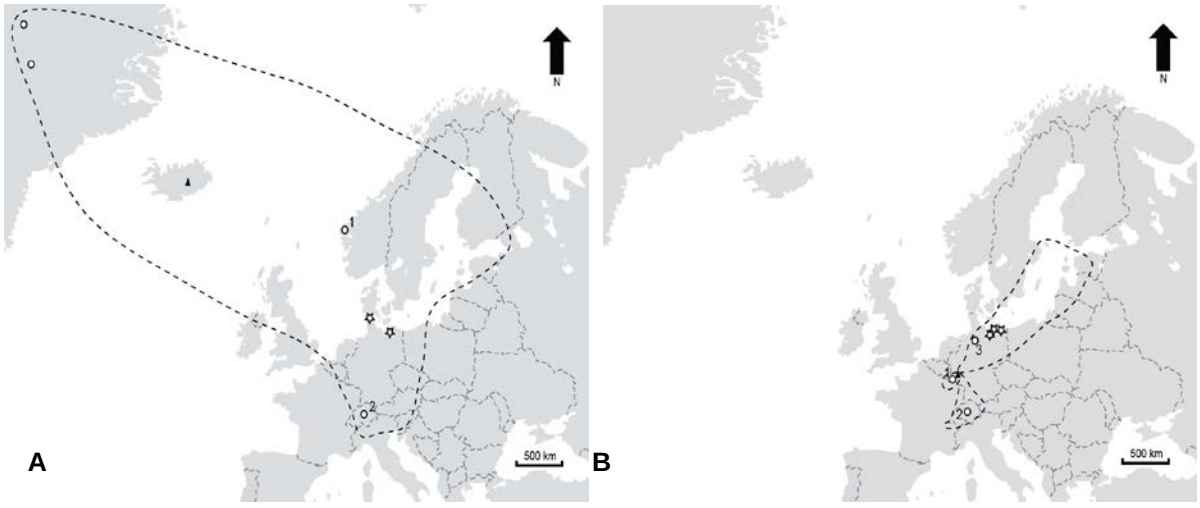


Figure 7.8 – Distribution envelopes of key tephras discussed in section 7.2.3.1. A – Vedde Ash, 1 – Kråkenes (Mangerud *et al*., 1984); 2 – Soppensee (Blockley *et al*., 2007). B – LST, 1 – Meerfelder Maar (Brauer *et al*., 1999); 2 – Soppensee (Hajdas *et al*., 1993); 3 – Hämelsee (Merkt and Müller, 1999)

Section 7.2.3.1 and 7.2.3.2 will compare OM and cladoceran results from sites studied in this thesis with previously published data from the following sites:

Meerfelder Maar - LST

Meerfelder Maar (6° 52' 50" E, 50° 07' 05" N) is a medium sized lake (38 ha) located in the West Eifel region of Germany ~70 km southwest of the Laacher See volcano. Unlike the sites presented in this thesis, Meerfelder Maar was not formed by dead-ice melt, but by volcanic activity, with the lake itself positioned within a former crater (Lücke and Brauer, 2004). A 2.05 m varved sediment section was investigated by Lücke and Brauer (2004) to evaluate changes in palaeoproductivity from the Older Dryas to the Preboreal using changes in $\delta^{13}C$ and $\delta^{15}N$ values of the varved sediments. The extant lake at Meerfelder offers a different system to that which likely controlled the relatively shallow lakes of the NEP. However as demonstrated by Lücke and Brauer (2004) the OM record is largely controlled by autochthonous processes and thus offers a good standard by which the sites of Endinger Bruch, Kieshofer Moor and Daschower Moor can be compared using the LST as an isochrone.

Soppensee - LST

Soppensee (8° 05' E, 47° 05' 30" N) is a medium sized lake (23 ha) with a maximum depth of 27 m, located in the alpine foreland region, 17 km northeast of Lucerne, Switzerland (Hoffmann, 2001). The lake has been extensively studied (e.g. Züllig, 1989, Lotter, 1997, Lotter, 1999; Lotter, 2001; Hoffmann, 2001; Lane *et al*., 2011c) and offers a good comparison of autochthonous processes during the latter Allerød period. Two separate cores (SO89-23 and SO86-14) were investigated in a number of studies for changes in lake productivity using fossil pigments (see Züllig, 1989; Lotter, 2001) and cladocera (Hoffmann, 2001). The presence of the LST in both cores allows the findings of these studies to be compared directly with the cladoceran results reported in the sites of Endinger Bruch, Kieshofer Moor and Daschower Moor. Lake Soppensee also contains the Vedde Ash; however the cladoceran sampling resolution is too coarse to allow meaningful comparison with the cladoceran records from Endinger Bruch, Kieshofer Moor and Daschower Moor during the Younger Drays.

Hämelsee - LST

Hämelsee (9° 19' E, 52° 46' N) is a medium sized lake with laminated deposits (7.3 hectares) located in northwestern Germany (Figure 7.8) and was formed by the development of a sinkhole over

Permian salt deposits (Merkt and Müller, 1999). The basin records sediments of Oldest Dryas age, and due its position on the NEP offers a good correlative to the other sites presented in this thesis using the LST as an isochrone. The Saksunarvatn Ash has also been discovered in the Hämelsee basin (Merkt *et al*., 1993) however the cladoceran record produced by Merkt and Müller (1999) does not extend this far into the Holocene so unfortunately the Saksunarvatn Ash cannot be used to link records between Potremser Moor and Hämelsee.

Kråkenes lake – Vedde Ash

Kråkenes lake (5° 00' E, 62° 02' N) is situated on an exposed peninsula on Vågsøy island south of Stad on the west coast of Norway (Birks and Wright, 2000). A number of multidisciplinary studies (see Jonsgard and Birks, 1995; Birks *et al*., 1996; Birks and Wright, 2000; Bakke *et al*., 2009) have provided a detailed picture of the aquatic evolution of the basin, thus allowing comparison within Endinger Bruch and Slotseng using the Vedde Ash.

7.2.3.1 Lake productivity at 12,880 ± 40 cal yr BP: The LST

Comparison of the sites containing the LST presented here with records from Meerfelder Maar and Hämelsee, Germany and Lake Soppensee, Switzerland (Figure 7.8), allow the record of aquatic productivity to be compared on the NEP, the central German-uplands and the Alpine foreland during the late Allerød. By linking aquatic records over largely varying environments it is possible to address whether variations in aquatic productivity at the end of the Allerød were regionally homogenous or more variable. Figure 7.9 shows the comparison of $\delta^{13}C$ and $\delta^{15}N$ values from Endinger Bruch, Kieshofer Moor and Daschower Moor, with the $\delta^{13}C$ and $\delta^{15}N$ record from Meerfelder Maar. Allerød age sediments in Meerfelder Maar show relatively large $\delta^{13}C$ fluctuations prior to the deposition of the LST (Lücke and Brauer, 2004). However following tephra deposition, the last ~200 years of the Allerød prior to the onset of the Younger Dryas, shows biogenic silica accumulation reaching its absolute minimum coupled with both $\delta^{13}C$ and $\delta^{15}N$ values decreasing by 2‰ (see Lücke and Brauer, 2004). Evidence from the adjacent Lake Holzmaar demonstrated that tephra deposition had no significant impact on diatom (biogenic silica) accumulation (Birks and Lotter, 1994). The reduction in biogenic silica accumulation and subsequent decline in $\delta^{13}C$ and $\delta^{15}N$ values within Meerfelder Maar

was therefore suggested to represent reduced nutrient input into the lake leading to a diminished utilization of the silica and inorganic carbon and nitrogen pools during the last 200-300 years of the Allerød (Lücke and Brauer, 2004). The $\delta^{13}C$ record from Endinger Bruch corresponds well with the pattern witnessed in Meerfelder Maar, with $\delta^{13}C$ values falling by 0.60‰ following the deposition of the LST and subsequently remaining low until the transition to the Younger Dryas. $\delta^{15}N$ values also record a dip following this event, falling by 1.7‰. This negative excursion is however short lived with values increasing by 2.59‰ in the space of 10 cm (~108 yrs based on modelled ages). While subtle similarities existed between both basins following the deposition of the LST, they were in fact characterised by different levels of aquatic productivity. Prior to the deposition of the LST there is far less variability in the $\delta^{13}C$ record during the Allerød, than that seen in Meerfelder Maar. Rather than an abrupt decrease in aquatic productivity following the LST seen in Meerfelder Maar, there is a more gradual reduction in productivity that begins at 13,550 - 13,060 cal yr BP and continues until the onset of the Younger Dryas. The $\delta^{13}C$ record from Kieshofer Moor and Daschower Moor also looks similar to Meerfelder Maar. The final stages of the Allerød, following the deposition of the LST are characterised by a drop of ~2‰ in the $\delta^{13}C$ record from both Kieshofer Moor and Daschower Moor. There is no decline in $\delta^{15}N$ values at Kieshofer Moor while Daschower Moor records a brief negative excursion, with values falling by ~0.60‰ (Figure 7.9). Due to the short sediment record from Kieshofer Moor it is difficult to assess whether basin conditions were already changing prior to the deposition of the LST. The longer record from Daschower Moor however allows better comparison with Meerfelder Maar. As with Endinger Bruch, the change in aquatic productivity precedes that witnessed in Meerfelder Maar, however aquatic productivity increases from 13,050 ± 200 cal yr BP onwards, prior the deposition of the LST. As discussed previously, before 13,050 ± 200 cal yr BP, Daschower Moor was characterised by high a C:N and enriched $\delta^{13}C$ values indicative of aquatic macrophytes and allochthonous deposition. The decline in $\delta^{13}C$ values, unlike Endinger Bruch and Meerfelder Maar, does not represent a reduction in aquatic productivity, but rather a gradual transition to conditions associated with autochthonous, algal productivity in the latter stages of the Allerød.

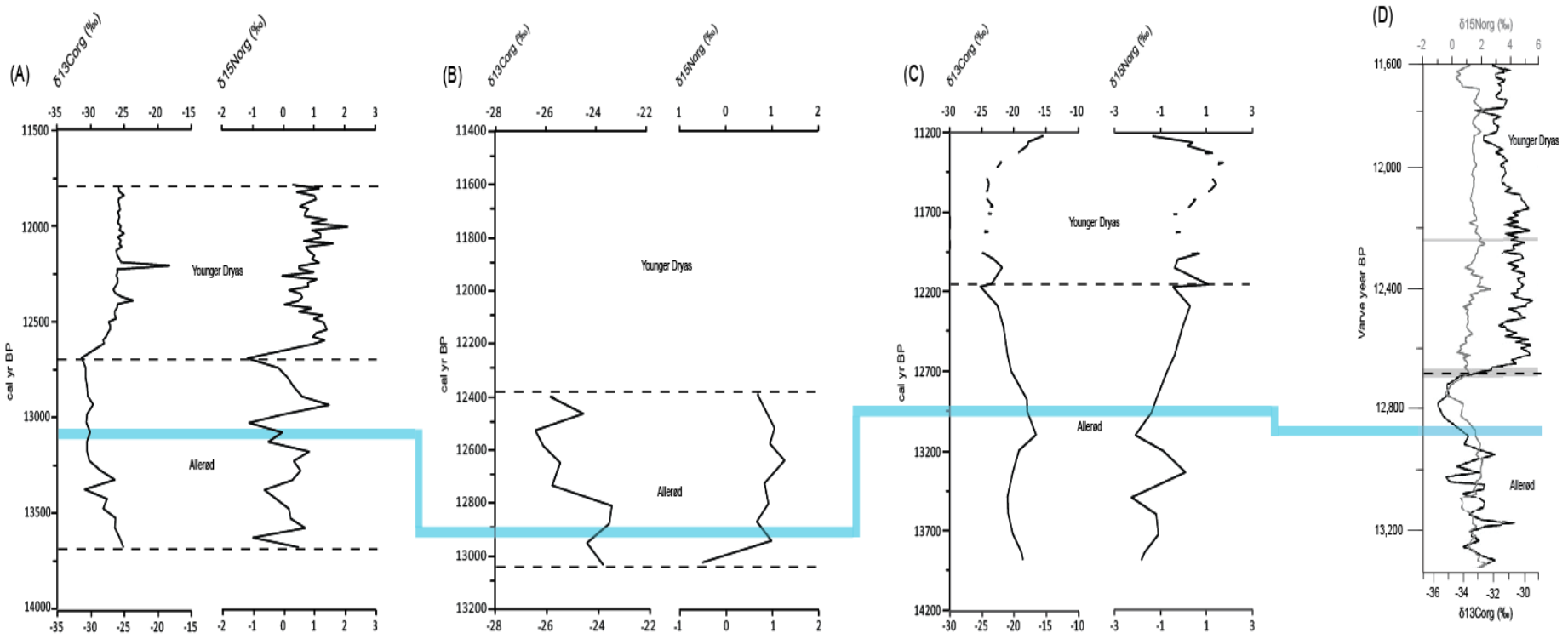


Figure 7.9 – $\delta^{13}C$ and $\delta^{15}N$ records from (A) Endinger Bruch, (B) Kieshofer Moor, (C) Daschower Moor and (D) Meerfelder Maar. The sites are linked by the LST, shown in blue.

The Soppensee cladoceran record is dominated by pelagic species, with over 90% of identified specimens coming from the *Daphnia* spp. and *Bosmina* spp. groups (Hofmann, 2001). Such a community structure reflects constant deep water conditions in the basin during the Lateglacial – Holocene period. The only exception to this is in the Older Dryas where <5% pelagic cladocera were recorded (Hofmann, 2001). The sampling resolution of Hofmann (2001) makes it challenging to accurately correlate changes in the cladoceran record between Soppensee and the sites in this thesis (Figure 7.10C, D and E) with cladoceran samples only taken every 10 - 20 cm until the upper 40 cm of the Soppensee record (Hofmann, 2001; Figure 7.10A and B). What is witnessed in Soppensee during the late Allerød is a reduction in total cladocerans coupled with a switch from *B. longispina* to *B. longirostris* in the pelagic record. This response in Soppensee may relate to the effect of the deposition of the LST itself (see section 7.2.2) or form part of a more general cladoceran trend during the late Allerød. It is likely that during this period, prior to the onset of the Younger Dryas, the pelagic record was more susceptible to environmental transitions / events (Laacher See eruption) due to the larger open water zone relative to the benthic zone. The speed of change in the pelagic community is not known with certainty due to the coarse sampling resolution of Soppensee. It is however possible to say that at the time of the LST, the cladoceran community of Soppensee was largely different to that present in the shallower sites of Endinger Bruch, Kieshofer Moor and Daschower Moor. Even with the relative drop in pelagic concentration during the later Allerød, the Soppensee basin was still more productive in terms of its cladoceran community than any of the other sites considered in this thesis during this time.

In comparison with the *Daphnidae* sp. and *Bosminidae* sp records from Endinger Bruch, Kieshofer Moor and Daschower Moor (Figure 7.11) pelagic community structure in Hämelsee during the late Allerød was very different. The record from Hämelsee suggests that during this period, prior to the deposition of the LST, Hämelsee was a moderately productive system, with sufficient nutrient concentrations to support pelagic species in both the *Daphnidae* and *Bosminidae* groups. This is supported by the presence of siderite in the varved layers from this period, which requires at least moderate production of autochthonous material (Merkt and Müller, 1999). Unlike the shallower basins of Endinger Bruch and Kieshofer Moor over this period, which show declining autochthonous

production, the record from Hämelsee shows increased aquatic productivity in response to the warming climate of the later Allerød.

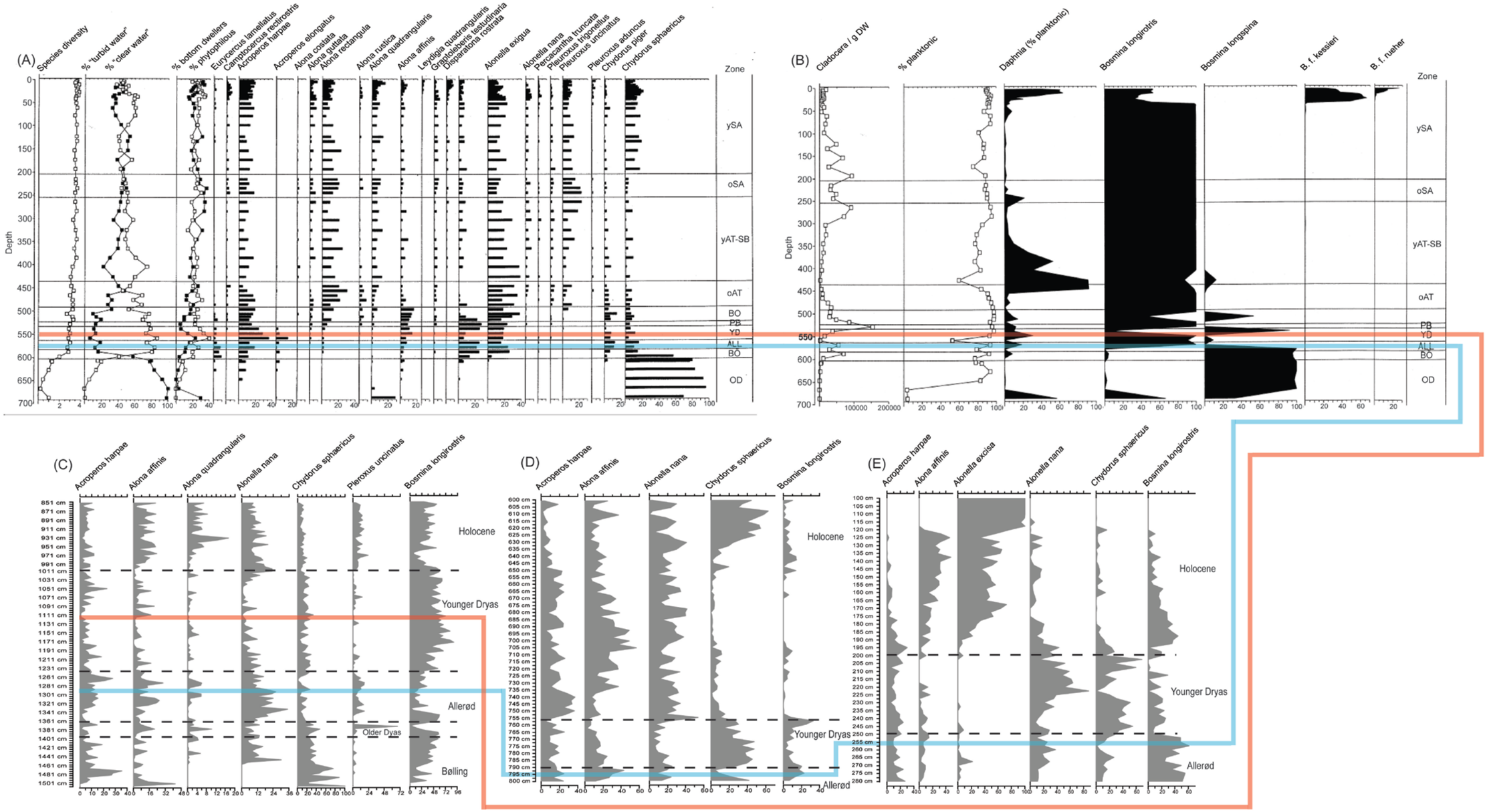


Figure 7.10– Composite diagram showing the comparison of cladoceran records from Soppensee (A – benthic species, B – pelagic species), Endinger Bruch (C), Kieshofer Moor (D) and Daschower Moor (E). The sites are linked through the position of the LST located in late Allerød sediments.

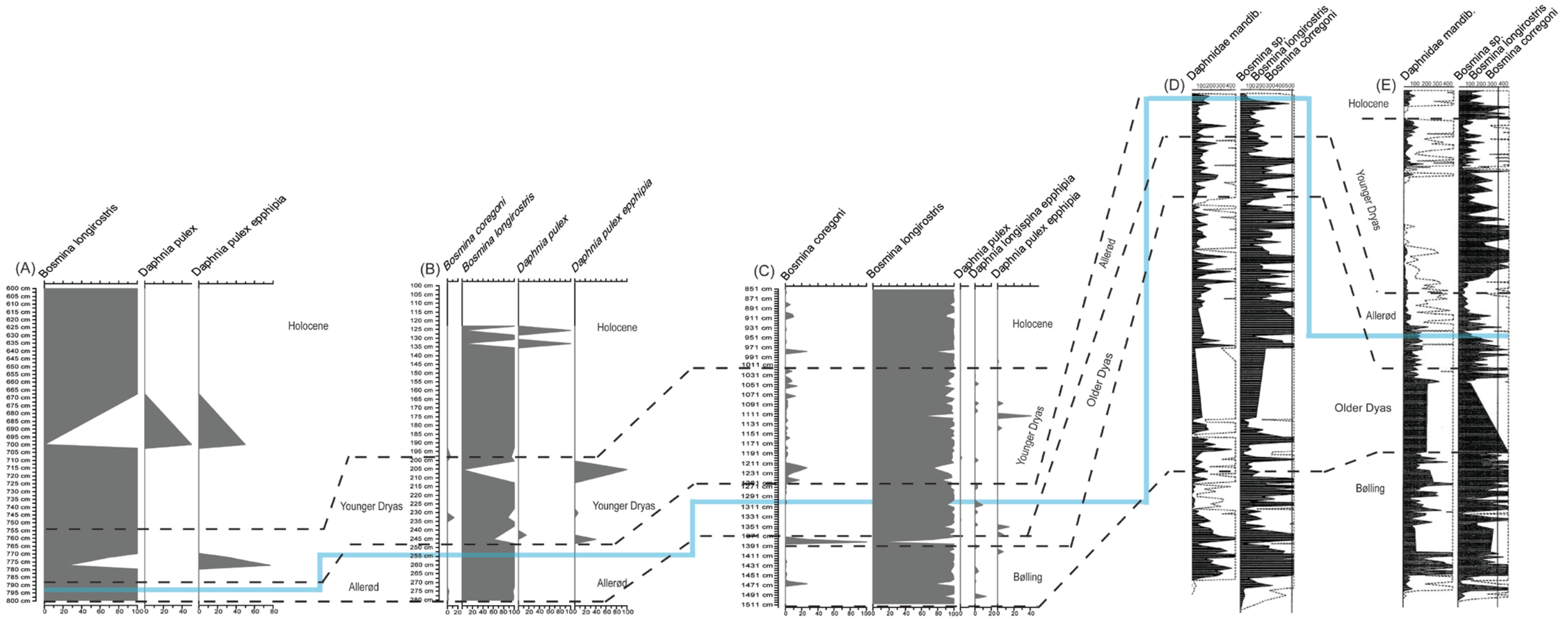


Figure 7.11 – Composite diagram showing the comparison of pelagic cladoceran records from Kieshofer Moor (A), Daschower Moor (B), Endinger Bruch (C) with the pelagic cladoceran record from Hämelsee (Hä9 D and Hä6 E).The sites are linked through the position of the LST located in late Allerød sediments (shown by a blue connecting line).

7.2.3.2 Lake productivity at 12,121 ± 114 GICCO5 yr BP: The Vedde Ash

As discussed in section 7.2.1, the Younger Dryas is characterised by a pattern of general stability in all sites apart from Slotseng. With the Vedde Ash it is however possible to address whether this same pattern is evident in areas north and south of the NEP; from Kråkenes, Norway and Soppensee. Following Birks *et al* (2000) it was noted that the Younger Dryas period was represented by a bipartite productivity signal. The first half of the Younger Dryas is characterised by cold and turbid water conditions which would have been extremely unfavourable for aquatic life, with the Kråkenes sediments yielding very few aquatic flora and fauna sub-fossils, and cladocerans being particularly rare (Birks *et al*., 2000). Just above the Vedde Ash, dated in Kråkenes to 12,066 ± 42 cal yr BP (Lohne *et al*., 2013) and approximately half way through the Younger Dryas, the sediments deposited in the basin record a change towards higher aquatic productivity (Stalsberg, 1995; Birks *et al*., 1996; Baake *et al*., 2009). This change is interpreted as a shift towards a slightly warmer climate, which is supported by a higher concentration of plant macrofossils and an increase in *Capsella*-type and *Sedum* pollen spores (Solhøy and Solhøy, 2000). As discussed in section 6.2.4 (Chapter 6) a similar bipartite feature to the Younger Dryas is also represented in Endinger Bruch, however unlike Kråkenes, aquatic productivity does not shut down during the early part of the Younger Dryas; it may have actually increased during the earliest stages of this period, with enriched $\delta^{15}N_{org}$ values recorded in the core prior to falling away above 1205 cm (Figure 7.12). This shift to more stable and higher levels of autochthonous productivity appears to occur just below the deposition of the Vedde Ash located at 1118 cm (Lane *et al*., 2011b). At 1131 cm the $\delta^{13}C_{org}$ and C:N record became more stable, following a period of greater variation in values, also while variable, the $\delta^{15}N_{org}$ record becomes more enriched after 1131 cm. The cladoceran record likewise shows signs of improvement after 1131 cm, again while variable, total cladoceran counts increase from a mean of 10,321/ 50 ml below 1131 cm to 15,051 / 50 ml above 1131 cm. This change in the productivity prior to the deposition of the Vedde Ash is further supported by an increase in *Pediastrum* sp. above 1130 cm reported by de Klerk (2002).

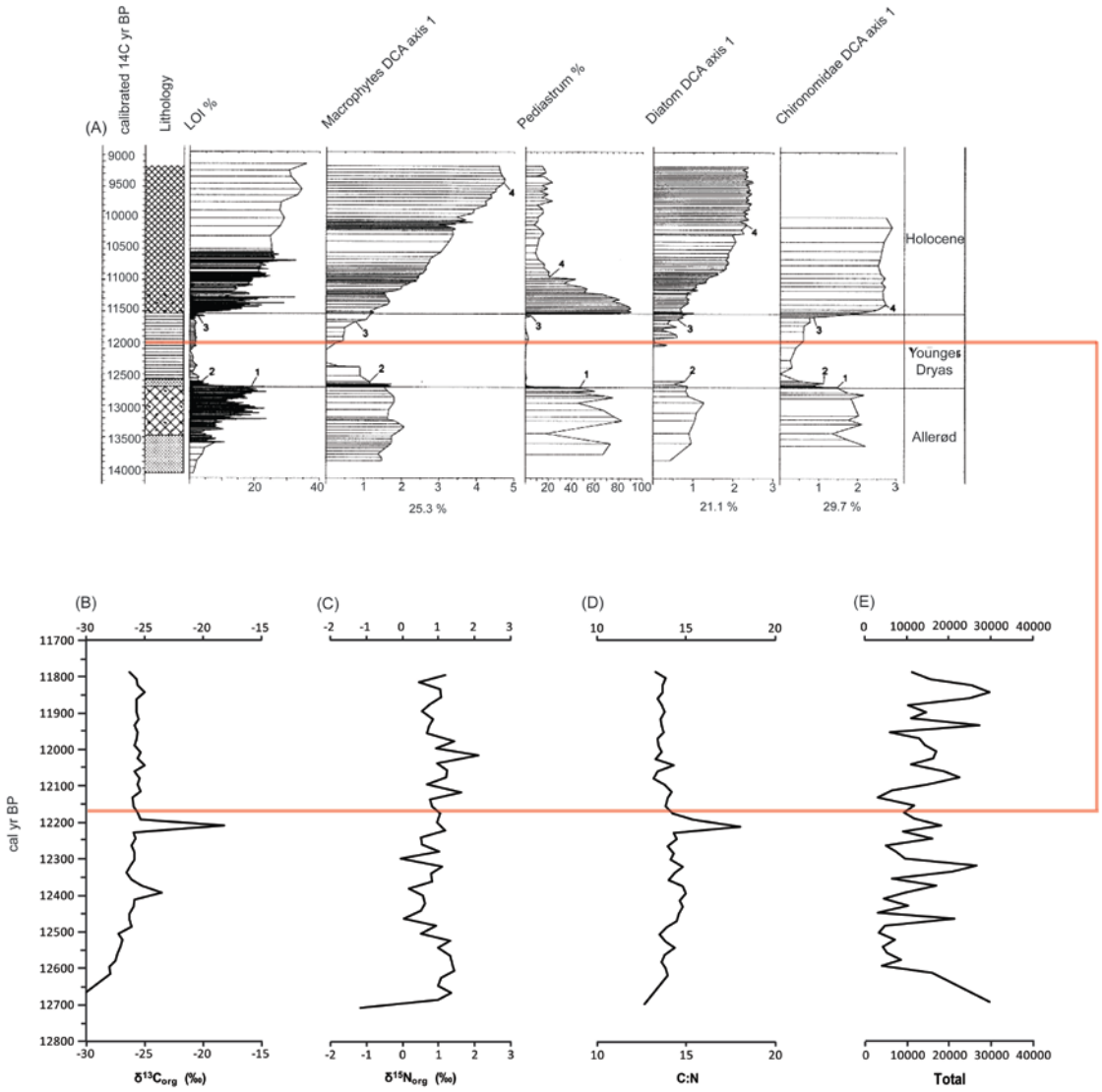


Figure 7.12 – Composite diagram showing the Younger Dryas in Kråkenes (A), compared with the $\delta^{13}C_{org}$ (B), $\delta^{15}N_{org}$ (C), C:N (D) and total cladoceran (E) records from Endinger Bruch. The change in autochthonous productivity in both basins appears to occur just below the deposition of the Vedde Ash, shown in red.

The cladoceran record for the Younger Dryas from Soppensee is relatively short due to the coarse sampling resolution (Figure 7.10) and as such only tentative comparisons can be made. As with most Younger Dryas cladoceran sequences there is a reduction in the total number of individuals, coupled with a slight increase in “arctic type” species such as *A. harpae* similar to the pattern recorded at Endinger Bruch, Kieshofer Moor and Daschower Moor. A more detailed comparison can however be made with the cladoceran record from Kråkenes (see Duigan and Birks, 2000; Figure 7.13). Comparison of cladoceran records from Kråkenes, Slotseng and Endinger Bruch indicates that the cladoceran community structure of all three basins during the Younger Dryas was completely different. During the Younger Dryas period in Kråkenes, only *A. harpae*, *A. excisa* and *C. sphaericus* are recorded. Such low species diversity and total cladoceran concentration indicates that the increase in autochthonous productivity just prior to the Vedde Ash was not manifest in the cladoceran record. In comparison, Endinger Bruch and Slotseng shows that although total cladoceran dropped during the Younger Dryas (Figure 6.6 and 6.13; Chapter 6) both basins maintained populations of a number of species including *A. excisa*, *A. harpae*, *C. sphaericus* and *B. longirostris* (Figure 7.13).

What is clear in the case of Kråkenes, Slotseng and Endinger Bruch is that the three spatially disparate basins located in different environments, can respond in a similar fashion to the Younger Dryas. Furthermore at a primary level the relationship between the OM record from Endinger Bruch and the Ti and diatom record from Kråkenes show a similar response to changing environmental conditions, located around the time of the deposition of the Vedde Ash. How this change in autochthonous productivity is manifest further up the trophic web however appears to deviate between both sites, with Endinger Bruch maintaining higher levels of secondary consumers which increases the potential of the site in supporting populations of fish.

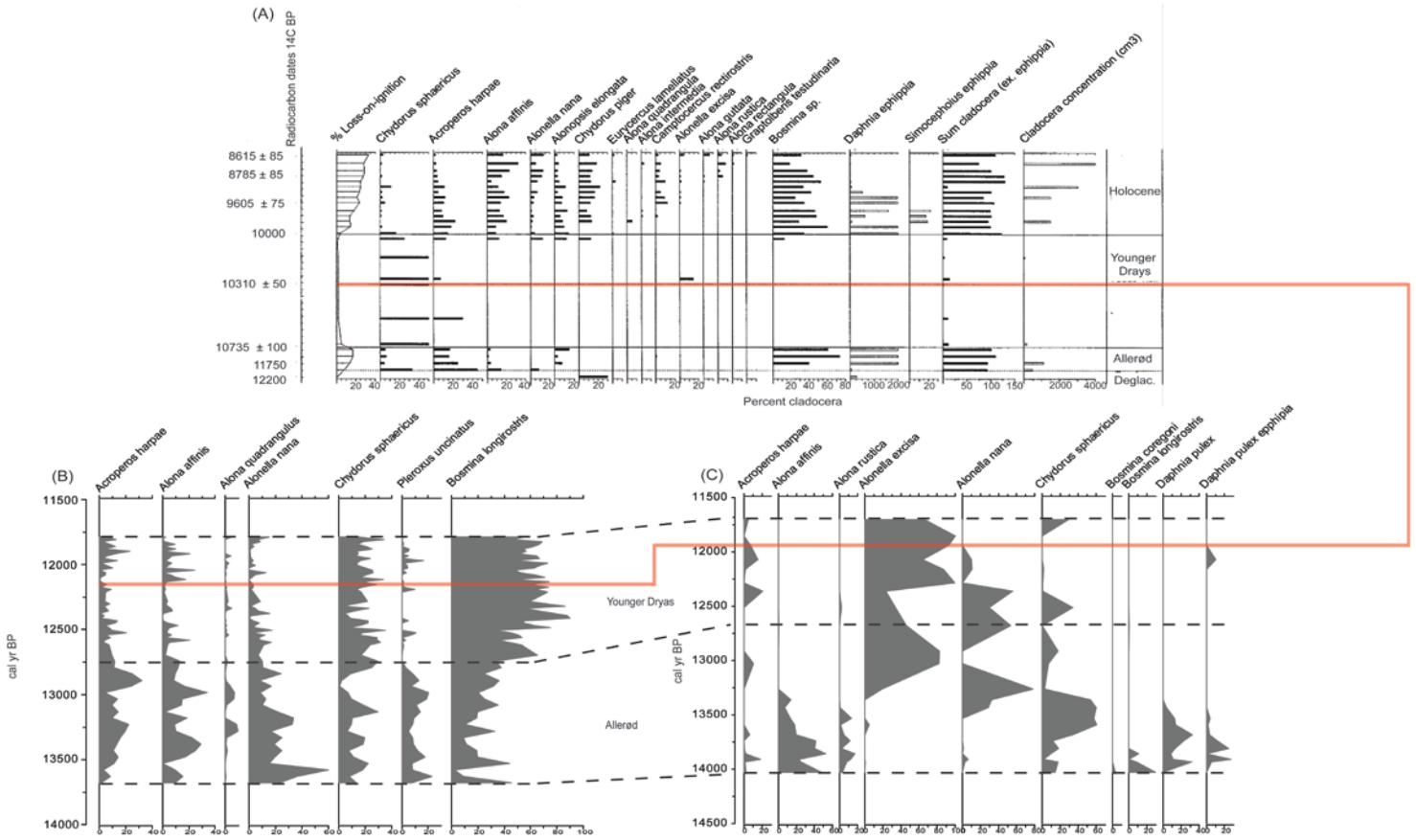


Figure 7.13 - Composite diagram showing the comparison of cladoceran records from Kråkenes (A) with Endinger Bruch (B) and Slotseng (C). The records are linked through the Vedde Ash, shown in red, deposition during the Younger Dryas. Comparison of the records shows the large difference in cladoceran concentration during this cold phase between Kråkenes and the sites of Endinger Bruch and Slotseng.

7.3 What potential did the Lateglacial lakes of the NEP have of supporting hunter gatherer groups?

The key in evaluating section 7.3 is the need to address local ecological and environmental factors, outside the realm of regional climate change, which would have shaped the behaviour of hunter-gatherer groups. While anthropologists often presume an unspecified association between various "limiting factors" (e.g. low temperature, rainfall and primary productivity) and the human carrying capacity of an environment, an understanding of the actual mechanisms that relate these limiting factors to humans is needed (Mandryk, 1993).

According to Dincauze (1987: 319)

Investigators must scrupulously define the mechanisms that link phenomena to processes if they are to illuminate the relationships between phenomena... the observation of a correlation in the beginning of the search for mechanism; the end is explanation of a relationship... the successful resolution of a research problem requires the demonstration, not of correlations, but of mechanisms that link observed data with formulated processes.

With this in mind therefore, successful explanation requires the use of more closely reasoned arguments than are generally utilised in anthropological explanations of environment/hunter-gatherer interactions. This successful explanation and understanding of the dynamic relationship between the physical and biotic environment and the associated hunter-gather systems embedded within it can be attained through what Binford (1991) referred to as "theory building" i.e. "the intellectual ability to explain the observed variability in terms of general conditions". Following the general discussion of aquatic exploitation in Chapter 3, this section accordingly aims to explain the potential of aquatic systems in supporting the general requirements of hunter-gatherer groups across the NEP during the Lateglacial. In Chapter 3, this thesis proposed a model for aquatic exploitation across the NEP, with three testable hypothesises:

1. That aquatic systems within the NEP during the Lateglacial responded synchronously to AETs making them a predictable resource base.

2. Levels of productivity within aquatic systems are consistent across all systems regardless of the surrounding terrestrial environment.

3. Aquatic systems contained fish populations necessary to support hunter-gatherers during the Lateglacial of the NEP.

These three hypothesises are characterised by a number of interconnected factors, that individually or combined serve to influence the potential aquatic systems had in supporting hunter-gather groups. Based upon the results presented in Chapters 5 and 6, as well as the discussion points highlighted earlier in this chapter, the following sections will discuss each of these hypothesises in turn.

7.3.1 Hypothesis 1: aquatic systems within the NEP during the Lateglacial responded synchronously to AETs making them a predictable resource base

The aquatic response to AETs varied at both intra and inter site levels, with the aquatic response in some sites apparently synchronous to some AETs and not others, while other sites were never in phase. This level of variability suggests that basin sensitivity to the onset of AETs was controlled at a local level, with catchment conditions likely influencing basin response. The chronological uncertainties associated with the Lateglacial period in some of the sites, particularly Potremser Moor and Kieshofer Moor hampers attempts to correlate the aquatic response with AETs. The application of tephrostratigraphy and tephrochronology in this thesis has demonstrated the techniques' value, not only in refining age models, but also in linking sites together at fixed isochrons. By evaluating basin conditions at a number of sites during the late Allerød and Younger Dryas this thesis has demonstrated that while some basins show similarities (e.g. the response to the Younger Dryas) other sites show altogether different responses, as is the case during the late Allerød in Endinger Bruch, Kieshofer Moor and Daschower Moor when compared to Meerfelder Maar. The chronological resolution of the Lateglacial – Holocene period in this thesis is insufficient to allow direct comparison of the timing of aquatic system response to AETs between the five sites presented in this thesis. Using isochronous tephra horizons it is however possible to compare changes in aquatic system development at discrete levels between sites. At these discrete levels there appears to be variability

in aquatic system development between sites not only located across the NEP but also in regions outside of this zone.

In summary therefore, it appears that aquatic systems were not always synchronous in their response to AETS. The greatest similarity between sites in response to an AETs is found during the transition from the Allerød to the Younger Dryas, with Endinger Bruch, Daschower Moor and Potremser Moor, all indicating abrupt changes in productivity, both negatively and positively. Likewise the Older Dryas – Allerød transition in Slotseng and Endinger Bruch is also synchronous with changes in the terrestrial record. Apart from this, all other aquatic responses are non-synchronous, suggesting therefore that a regional model for aquatic response to AETs is not valid for all AETs during the Lateglacial.

7.3.2 Hypothesis 2: levels of productivity within aquatic systems are consistent across all systems regardless of the surrounding terrestrial environment

Figure 7.6 clearly demonstrates that there is a large amount of variability in the levels of productivity across the five sites presented in this thesis. However, whilst there is variability in the *timing* of the response of aquatic systems to AETs, this thesis has demonstrated that the *type* of aquatic response (OM and cladoceran record) of all sites (with the exception of Slotseng) can be correlated at a number of points. Figures 7.3 and 4.4 demonstrate that the onset of the Younger Dryas, produced a similar response in the OM record of Endinger Bruch, Potremser Moor, Kieshofer Moor and Daschower Moor. Likewise the consistency between Slotseng and Endinger Bruch, particularly in the cladoceran record, during the Bølling – early Allerød and the Holocene period in Potremser Moor, Kieshofer Moor and Daschower Moor, does demonstrate some regional connectedness in how these basins responded to AETs during the Lateglacial regardless of the timing. The data presented in Chapter 6 indicates that there is far lower variability in aquatic development during colder periods as opposed to warmer conditions. During colder phases the consistent C:N record suggests that the aquatic system is in equilibrium with the surrounding terrestrial environment and lower total cladocerans indicate a reduction in the potential of the system for supporting larger animals such as fish. Warmer conditions allow the development of aquatic vegetation which generally coincides with decreasing water depths. However this is manifested differently across the sites of this study, e.g. the response in Potremser Moor, Kieshofer Moor and Daschower Moor is the development of shallow weedy conditions, while in

Endinger Bruch aquatic productivity increases before stabilising during the early Holocene. Slotseng, in contrast to all other sites, rapidly becomes telmatic followed by a brief period of increased depth before finally becoming terrestrial during the early Holocene. This level of local variability in aquatic development is further highlighted by the Laacher See eruption, with some sites showing a reaction to the event and deposition of the LST, and others apparently remaining unaffected. If the Younger Dryas is considered in isolation, then it appears that basin size may have influenced how aquatic systems responded to AETs during the Lateglacial. Figure 7.3 suggests that the smaller basins of Endinger Bruch and Slotseng were more variable in their responses than the larger basins of Potremser Moor, Kieshofer Moor and Daschower Moor.

In summary therefore, this thesis suggests that during the relatively cooler Bølling – early Allerød periods and the cold reversal of the Younger Dryas, the sites presented in thesis can be correlated in terms of their OM and cladoceran response. The warmer Holocene does also show some consistency in OM and cladoceran response, this however is not applicable to all sites, with higher variability in the smaller basins. The significance of this variability in the OM and cladoceran record to hunter-gatherer groups will be summarised in section 7.3.3.

7.3.3 Hypothesis 3: Aquatic systems contained fish populations necessary to support hunter-gatherers during the Lateglacial of the NEP

This final hypothesis ultimately brings one back to the “push” and “pull” models of human dispersal during the Lateglacial and whether the “local resources” of the NEP, in this case aquatic (fish), were sufficient to support hunter-gatherer groups. It is one thing to view ecologically productive places in the landscape as “attractors” and another to suggest that aquatic systems made all things possible for hunter-gatherer groups on the NEP. In his study of hunter-gatherer mobility in the Great Lakes region of North America Hemphill (1999) noted that the relationship between mobility and wetlands can be interpreted in very different ways: on the one hand it can be suggested that aquatic systems supported a semisedentary or sedentary lifestyle in this region, while others have suggested that aquatic environments only represented a secondary resource base. The presence of freshwater aquatic systems across the NEP during the Lateglacial is significant, as the daily need for drinking water would have effectively “tethered” hunter-gatherer groups to these aquatic environments.

Through the constant association with aquatic environments it seems unlikely that hunter-gatherers would not have utilised these systems as a resource base if they contained populations of fish (Erlandson and Moss, 2001). As previously discussed, the NEP during the Lateglacial had a significantly large mammal population, most notably reindeer and elk. Therefore the crucial question to a Lateglacial hunter-gatherer is whether the advantages offered by aquatic exploitation such as lower energy consumption in resource procurement and social sedentism outweighed the advantages offered by large mammal hunting. The key to this is, as explained, is the implication of the OM and cladoceran records, and what these records would have meant to hunter-gatherers across the NEP. Studies have indicated that major population expansions occurred in eastern Fennoscandia from 7500-5700 cal yr BP, directly coinciding with large increases in terrestrial and aquatic productivity (Tallavaara and Seppä, 2011). Could the aquatic systems of the NEP during the Lateglacial have offered a similar stimulus for population expansion by providing a stable, readily exploitable resource base?

The aquatic systems studied as part of this thesis do show that at certain times during their development they were significantly productive in terms of primary productivity and fish populations to support groups of hunter-gatherers. However, this thesis suggests that aquatic systems are unlikely to have played a significant role in firstly enticing and subsequently supporting hunter-gatherer groups across the NEP during the Lateglacial for the following reasons:

1. While smaller lakes (< 3 hectares) formed earlier than larger basins (3-10,000 hectares) and in the case of Slotseng and Endinger Bruch did support fish populations, these basins were also more prone to instability and variations in productivity. It is highly unlikely that these smaller basins would have had the capacity to contain the necessary stocks of fish to support groups of hunter-gatherers for long periods of time during population dispersal events in the Bølling. The period of population consolidation of the NEP during the Allerød coincides with highly variable aquatic conditions, which would have offered at best ephemeral resource availability. The deposition of volcanic ash would have seriously impacted the trophic structure of numerous aquatic systems within the dispersal envelope of the LST (e.g. Newcomb and Flagg, 1982), with the three sites described here as containing this tephra

showing either a likely loss of fish or in the case of Kieshofer Moor, the indication of no fish in the lake prior to the ash fall event. Such variability within aquatic systems is unlikely to have provided the necessary platform for widespread consolidation of the NEP.

2. The influence of AETS on the resource capacity of Lateglacial aquatic systems varied significantly between sites, causing the resource availability of these sites to become unpredictable, not only at a regional level but also locally. As discussed in Chapter 3, the main advantage for gathering smaller resources like fish is the lower chance of failure (Hawkes *et al*., 1991). However as demonstrated by this thesis there is variability across all sites when fish were present, and unlike larger terrestrial mammals which can be spotted from distance, determining whether fish are present within a lake can require significant time investment. In variable and unpredictable lakes therefore the risk of failure is significantly raised when compared to hunting larger mammals, with the likely calorific return potentially too low to warrant extensive, time consuming exploitation.

3. The impact of the Laacher See eruption on lakes across the NEP brings into focus the potential vulnerability of aquatic systems to the affect of environmental events such as the Laacher See eruption. The same can be said of the Older Dryas, with the fish populations in both Slotseng and Endinger Bruch lost during this period, probably as the result of basin turbidity. The terrestrial environment during these period offers far higher resource potential, as prey animals have the ability to migrate to more productive areas, allowing hunter-gatherers to follow. Aquatic systems and associated resources such as fish on the other hand cannot move away with their potential as a resource base controlled by the impact of these events.

7.8 Chapter summary

Chapter 7 has drawn together the three hypothesises presented in Chapter 3 that form the model for aquatic exploitation on the NEP during the Lateglacial – Holocene. Chapter 7 has interpreted and answered each of these in turn with reference to the data presented in Chapters 5 and 6, before summarising the findings in sections 7.3.1, 7.3.2 and 7.3.3. This thesis will now conclude the main outcomes and highlights of this thesis in Chapter 8.

Chapter 8: Conclusions

Using both palaeoecological and chronological methods, this thesis has reconstructed the aquatic development of a number of Lateglacial lake basins on the NEP. As discussed in chapter 7, this study has been able to evaluate the temporal and spatial variation in basin response to the abrupt climatic changes of the Lateglacial as well as assess the potential of these small lacustrine systems to support hunter gatherer populations re-occupying the NEP following the deglaciation. Following chapter 7, five important conclusions have been reached:

- The OM and cladoceran records presented as part of this thesis suggest that there was significant variability in aquatic system development during the Lateglacial – Holocene period. The chronostratigraphic separation of the OM record, in the case of Endinger Bruch, Potremser Moor, Kieshofer Moor and Daschower Moor, suggests that climatic and environmental change had some influence on the OM regimes of these basins during the Lateglacial – Holocene. However as highlighted in Slotseng there is no pattern of abrupt OM response to external climatic and environmental changes, but rather a gradual evolution interspersed by abrupt autochthonous developments that occur within chronozone boundaries. A similar situation is observed in the cladoceran records from all sites that appear, at times, not to respond rapidly at the established chronozone boundaries, but fluctuate independently of external climate change. These two points suggest therefore that the Lateglacial – Holocene development of aquatic systems across the NEP cannot be solely explained by external climate change, and that local environmental and ecological factors are likely to have played a major part in driving the variability seen in the OM and cladoceran records presented by this thesis.

- Variability in the definition of chronostratigraphic boundaries coupled with large modelled error ranges, makes testing synchronicity in aquatic response to AETs between sites challenging. Based upon the current chronologies for each site it is only possible to test for synchronicity between records at low (multi-centennial) resolution. Where synchronicity can be tested at high resolution however is through the use of discrete tephra layers. This thesis has

demonstrated the using such isochrons, particularly the LST and Vedde Ash, it is possible to assess variability in aquatic development over large geographic areas at fixed points in time.

- Like the terrestrial record, aquatic systems were variable in their response to the Laacher See eruption, with some basins recording changes in aquatic development following the event, while others appeared unaffected. This thesis however suggests that in those areas where the LST was deposited, aquatic systems were more vulnerable to the effects of this process than the terrestrial realm. The morphological changes recorded in *B. longirostris* immediately after the deposition of the LST in Endinger Bruch and Daschower Moor strongly suggests that fish were significantly affected by this event. This thesis therefore suggests that lakes affected by the Laacher See eruption would have offered far less favourable conditions and resources for hunter-gatherer groups than the surrounding terrestrial landscape.

- The aquatic systems studied as part of this thesis do show that at certain times during their development they were significantly productive, in terms of primary productivity and fish populations, and would have been able to support groups of hunter-gatherers. However aquatic systems are unlikely to have played a significant role in firstly enticing and subsequently supporting hunter-gatherer groups across the NEP during the Lateglacial. While the smaller basins of Slotseng and Endinger Bruch likely supported fish populations during the Bølling period, these basins show higher levels of instability and were prone to basin disturbances and fluctuations in primary productivity. It is highly unlikely therefore that these smaller basins would have had the capacity to contain the necessary stocks of fish to support groups of hunter-gatherers for long periods of time during population dispersal events in the Bølling. Furthermore the period of population consolidation of the NEP during the Allerød coincides with highly variable aquatic conditions and fish populations, which would have offered at best ephemeral resource availability therefore making it highly unlikely that these systems played a major role in supporting this period of population consolidation. It must however be considered that the lakes studied in this thesis could have played a small role in a wider network of aquatic resources, such as rivers, streams and possibly marine. Within the scope of this thesis it is only possible to fully consider the contribution of lake systems to

hunter-gatherer subsistence strategies. Therefore to further our understanding of the potential contribution of all aquatic systems to Lateglacial Hunter-gatherers, further study is needed into these other aquatic environments.

- The local variability in resource capacity and vulnerability to environmental events such as the Laacher See eruption strongly suggests that lakes were unlikely to have formed a major resource base for hunter-gatherer groups across the NEP. It is more likely that lakes were exploited opportunistically and as such formed only a minor component of a subsistence strategy more focussed on large mammal hunting.

Bibliography

Aaris-Sørensen, K. 1992, Deglaciation Chronology and Re-Immigration of Large Mammals. A South Scandinavian Example from Late Weichselian – Early Flandrian. In: W, von Koenigswald., and L, Werdelin (eds.): Mammalian Migration and Dispersal Events in the European Quaternary. *Courier Forschungsinstitut Senckenberg*. **153**: 143 - 49. Frankfurt am Main

Aaris-Sørensen, K., Mühldorff., and Petersen, E.B. 2007. The Scandinavian reindeer (*Rangifer tarandus* L.) after the last glacial maximum: time, seasonality and human exploitation. *Journal of Archaeological Science*. **34**: 914 - 923

Aarnes, I., Bjune, A.E., Birks, H.H., Balascio, N.L., Bakke, J., and Blaauwj, M. 2012. Vegetation responses to rapid climatic changes during the last deglaciation 13, 500 – 8, 000 years ago on southwest Andøya, artic Norway. *Vegetation History and Archaeobotany.* **21**: 17 - 35

Abbott, P.M., Davies, S.M., Steffensen, J-P., Pearce, N.J.G., Bigler, M., Johnsen, S.J., Seierstad, I., Svensson, A., Wastegård, S. 2012. A detailed framework of Marine Isotope Stages 4 and 5 volcanic events recorded in two Greenland Ice-cores. *Quaternary Science Reviews.* **36**: 59 - 77

Achilli, A.C., Rengo, C., Magri, V., Battaglia, S., Olivieri, R., Scozzari, F., Cruciani, M., Zeviani, E., Briem, V., Carelli, P., Moral, J.M., Dugoujon, U., Roostalu, E.L., Loogväli, T., Kivisild, H.J., Bandelt, M., Richards, R., Villems, A.S., Santachiara-Benerecetti, O., Semino and A. Torroni, A. 2004. The molecular dissection of mtDNA haplogroup H confirms that the Franco-Cantabrian glacial refuge was a major source for the European gene pool. *American Journal of Human Genetics*. **75**: 910 - 18

Aichner, B., Wilkes, H., Herzschuh, U., Mischke, S., and Zhang, C. 2010. Biomarker and compound-specific $\delta^{13}C$ evidence for changing environmental conditions and carbon limitation at Lake Koucha, eastern Tibetan Plateau. *Journal of Paleolimnology*. **43**: 873 - 899

Alhonen, P. 1970. On the significance of the planktonic/littoral ratio in the cladoceran stratigraphy. *Commentationes Biologicae*. **35**: 1 - 9

Alley, R.B., Meese, D.A., Shuman, C.A., Gow, A.J., Taylor, K.C., Grootes, P.M., White, J.W.C., Ram, M., Waddington, E.D., Mayewski, P.A., Zielinski, G.A. 1993. Abrupt increase in Greenland snow accumulation at the end of the Younger Dryas event. *Nature*. **362**: 527 - 529

Allen, J.R.M., Huntley, B., and Watts, W.A. 1996. The vegetation and climate of northwest Iberia over the last 14,000 yr. *Journal of Quaternary Science*. **11**: 125 - 147

Alonso, D.A. 2007. El Magdaleniense inferior cantábrico. Contexto cronológico y estructuración = Cantabrian Lower Magdalenian. Chronology context and structure. *Munibe. Antropologia-arkeologia*. **58**: 127 - 142

Alexander, M.L., and Hotchkiss. 2010. *Bosmina* remains in lake sediment as indicators of zooplankton community composition. *Journal of Paleolimnology*. **43**: 51 - 59

Ammann, B., and Lotter, A.F. 1989. Lateglacial radiocarbon and palynostratigraphy on the Swiss Plateau. *Boreas*. **18**: 109 - 126

Amsinck, S.L., Jeppesen, E., and Ryves, D. 2003. Cladoceran stratigraphy in two shallow brackish lakes with special reference to changes in salinity, macrophyte abundance and fish predation. *Journal or Paleolimnology*. **29**: 495 - 507

Amundsen, P.A., Siwertsson, A., Primicerio, R., and Bøhn, T. 2009. Long-term response of zooplankton to invasion by a planktivorous fish in a subarctic watercourse. *Freshwater Biology*. **54**: 24 - 34

Anderson, R., Björnsson, S., Blanchard, D.C., Gathman, S., Hughes, J., Jónasson, S., Moore, C.B., Survilas, H.J., and Vonnegut, B. 1965. Electricity in volcanic clouds. *Science*. **148**: 1179 - 1189

Appleton, J., Chesters, J., Kierdorf, U., and Kierdorf, H. 2000. Changes in the structure of dentine from cheek teeth of deer chronically exposed to high levels of environmental fluoride*. Cells Tissues Organs*. **167**: 266 - 272

Aura, J.E., and Pérez, M. 1992. Tardiglacier y Postglacier en la region mediterránea de la Peninsula Ibérica (13.500-8.500 BP): transforaciones industrials y económicas. *Sagumtum*. **25**: 25 - 47

Aura, J.E., Villaverde, V., González Morales, M., González Sainz, C., Zilhão, J., and Straus, L.G. 1998. The Pleistocene-Holocene transition in the Iberian peninsula: continuity and change in human adaptations. *Quaternary International*. **49/50**: 87 - 103

Baales, M. 1992. ‘‘Head’em-off-at-the-pass’’ - Ökologie und Ökonomie der Ahrensburger Rentierjäger im Mittelgebirge. *Archäologische Informationen*. **16:** 116 - 119

Baales, M., 2002. Der spätpalaölithische Fundplatz Kettig. Untersuchungen zur Siedlungsarchäologie der Federmesser-Gruppen am Mittelrhein. *Monographien des Römisch-Germanischen Zentralmuseums*. Mainz 51

Baales, M., Jöris, O., Street, M., Bittmann, F., Weninger, B., and Wiethold, J. 2002. Impact of the Late Glacial Eruption of the Laacher See Volcano, Central Rhineland, Germany. *Quaternary Research*. **58:** 273 - 288

Bagniewski, Z. 1999. Tanged-points and the problem of Palaeolithic settlement in Pomerania. In: Kozlowski, S.K., Gurba, J., and Zaliznyak, L.L. (eds.) Tanged Point Cultures in Europe. Read at the International Archaeological Symposium, Lublin, September 13-16, 1993. Maria Curie-Sklodowska University Press, Lublin, pp. 131-145

Bailey, H. 1960. A method of determining warmth and temperatures of climate. *Geografiska Annaler*. **43**: 1 - 16

Bailey, G., and Milner, N. 2003. Coastal hunter-gatherers and social evolution: marginal or social? *Before Farming*. **4**: 1 - 15

Bakke, J., Lie, Ø., Heegaard, E., Dokken, T., Haug, G.H., Birks, H.H., Dulski, P., and Nilsen, T. 2009. Rapid oceanic and atmospheric changes during the Younger Dryas cold period. *Nature Geoscience*. **2**: 202 - 205. doi:10.1038/NGEO439

Balayla, D., Lauridsen, T.L., Søndergaard, M., and Jeppesen, E. 2010. Larger zooplankton in Danish lakes after cold winters: are winter fish kills of importance? *Hydrobiologia*. **646**: 159 - 172

Barker, D. S. 1983. Igneous rocks. Englewood Cliffs, NJ: Prentice-Hall

Barton, R.N.E., and Froom, F.R. 1986. The long blade assemblage from Avington VI, Berkshire. In: Collcutt, S.N. (ed.) The Palaeolithic of Britain and its Nearest Neighbours: Recent Trends (Sheffield, University of Sheffield Department of Archaeology and Prehistory), 80 - 4

Barton, R.N.E. 1992. Hengistbury Head, Dorset. Volume 2: The Late Upper Palaeolithic and Early Mesolithic Sites. Oxford Committee for Archaeology, Oxford

Barton, R.N.E., Jacobi, R.M., Stapert, D., and Street, M.J. 2003. The Late-glacial reoccupation of the British Isles and the Creswellian. *Journal of Quaternary Science*. **18**: 631 – 643

Bassett Maguric, J.R. 1963. The passive dispersal of small aquatic organisms and their colonization of isolated bodies of water. *Ecological Monographs*. **33**: 161 – 185

Bastviken, D., Ejlertsson, J., Sundh, I., and Tranvik, L. 2003. Methane as a source of carbon and energy for lake pelagic food webs. *Ecology*. **84**: 969 - 981

Bat, S., Otschirbat, G., and Ligaa, U.1988. Natürliche Vorkommen von Sanddorn in der Mongolischen Volksrepublik. *Gartenbau*. **35**: 85 - 86

Baugh, R.A. 1998. Atlatl dynamics. *Lithic Technology*. **23**: 31 - 41

Bennett, K.D., Boreham, S., Sharp, M.J., and Switsur, V.R. 1992. Holocene history of environment, vegetation and human settlement on Catta Ness, Lunnasting, Shetland. *Journal of Ecology*. **80**: 241 - 273

Bennike, O., Sarmaja-Korjonen, K., Seppänen, A. 2004. Reinvestigation of the classic late-glacial Bølling Sø sequence, Denmark: chronology, macrofossils, Cladocera and chydorid ephippia. *Journal of Quaternary Science*. **19**: 465 - 478

Beran, J. 2001. Spätpaläolithische und Mesolithsche Funde der Rettungsgrabung Wustermark 22 im Havelland. *Die Kunde N.F.* **52**: 1 - 16

Berendse, F., Van Breemen, N., Rydin, H., Buttler, A., Heijmans, M.M.P.D., Hoosbeek, M.R., Lee, J.A., Mitchell, E., Saarinen, T., Vasander, H., and Wallén, B. 2001. Raised atmospheric CO_2 levels and increased N deposition cause shifts in plant species composition and production in *Sphagnum* bogs. *Global Change Biolology*. **7**: 591 – 598

Berglund, B.E. 1979. The deglaciation of southern Sweden 13,500-10,000 B.P. *Boreas*. **8**: 89-117

Binford, L. 1980. Willow smoke and dogs' tails: Hunter-gatherer settlement systems and archaeological site formation. *American Antiquity*. **45**: 4 - 20

Binford, L. 1990. Mobility, housing, and environment: A comparative study. *Journal of Anthropological Research*. **46**: 119 - 152

Binford, L.R. 1991. There is always more we need to know. In: Dillehay, T.D., and Meltzer, D.J. (eds.) The first Americans: search and research. Boca Raton, Fla, CRC Press. pp 275 – 286

Bird, R.B., Bird, D.W., Codding, B.F., Parker, C.H., and Jones, J.H. 2008. The "fire stick farming" hypothesis: Australian Aboriginal foraging strategies, biodiversity, and anthropogenic fire mosaics. *Proceedings of the National Academy of Sciences*. **105**: 14796 - 14801

Birks, H.J.B., and Lotter, A.F. 1994. The impact of the Laacher See Volcano (11 000 yr B.P.) on terrestrial vegetation and diatoms. *Journal of Palaeolimnology*. **11**: 313 - 322

Birks, H.H., Gulliksen, S., Halflidason, H., Mangerud, J., and Possnert, G. 1996. New radiocarbon dates for the Vedde Ash and the Saksunarvatn Ash from Norway. *Quaternary Research*. **45:** 119 - 127

Birks, H.H., and Wright, H.E. 2000. Introduction to the reconstruction of the late-glacial and early-Holocene aquatic ecosystems at Kråkenes Lake, Norway. *Journal of Paleolimnology*. **23**: 1 - 5

Birks, H.H., Battarbee, R.W., Birks, H.J.B., (with contributions from) Bradshaw, E.G., Brooks, S.J., Duigan, C.A., Jones, V.J., Lemdahl, G., Peglar, S.M., Solem, J.O., Solhøy, I., Solhøy, T., and Stalsberg, M.K. 2000. The development of the aquatic ecosystem at Kråkenes Lake, western Norway, during the late-glacial and early Holocene - a synthesis. *Journal of Paleolimnology.* **23**: 91 - 114

Björck, S., Ingólfsson, O., Haflidason, H., Hallsdóttir, M., and Anderson, N.J.1992. Lake Torfadalsvatn: a high resolution record of the North Atlantic ash zone I and the last glacial-Interglacial environmental changes in Iceland. *Boreas*. **21**: 15 - 22

Björck, S., Walker, M.J.C., Cwynar, L.C., Johnsen, S., Knudsen, K.L., Lowe, J.J., Wohlfarth, B., and INTIMATE Members. 1998. An event stratigraphy for the Last Termination in the North Atlantic Region based on the Greenland ice-core record: a proposal by the INTIMATE group. *Journal of Quaternary Science*. **13**: 283 - 292

Błaszkiewicz, M. 2010. Development of fluvio-lacustrine systems in the young glacial area in Poland based on the research in the valleys of the rivers Wierzyca and Wda. *Questiones Geographicae*. **29**: 13 - 19

Błaszkiewicz, M. 2011. Timing of the final disappearance of permafrost in the central European Lowland, as reconstructed from the evolution of lakes in N Poland. *Geological Quarterly*. **55**: 361 - 374

Blockley, S.P.E., Lowe, J.J., Walker, M.J.C., Asioli, A., Trincardi, F., Coope, G.R., Donahue, R.E., and Pollard, A.M. 2004. Bayesian analysis of radiocarbon chronologies: examples from the European Late-glacial. *Journal of Quaternary Science*. **19**: 159 - 175

Blockley, S.P.E., Pyne-O'Donnell, S.D.F., Lowe, J.J., Matthews, I.P., Stone, A., Pollard, A.M., Turney, C.S.M., and Molyneux, E.G. 2005. A new and less destructive laboratory procedure for the physical separation of distal glass tephra shards from sediments. *Quaternary Science Reviews*. **24**: 1952 - 1960

Blockley, S.P.E., Blockley, S.M., Donahue, R.E., Lane, C.S., Lowe, J.J., and Pollard, A.M. 2006. The chronology of abrupt climate change and Late Upper Palaeolithic human adaption in Europe. *Journal of Quaternary Science*. **21**: 575 - 584

Blockley, S.P.E., Lane, C.S., Lotter, A.F., and Pollard, A.M. 2007. Evidence for the presence of the Vedde Ash in Central Europe. *Quaternary Science Reviews*. **26**: 3030 - 3036

Blockley, S.P.E., Bronk Ramsey, C., Lane, C.S., and Lotter, A.F. 2008. Improved age modelling approaches as exemplified by the revised chronology for the Central European varved lake Soppensee. *Quaternary Science Reviews*. **27**: 61 - 71

Bobrowski, P., and Sobkowiak-Tabaka, I. 2006. How far east did the Hamburgian reach? *Arcaeologia Baltica*. **7**: 11 - 20

Bodu, P. 1998. Magdalenians-Early Azilians in the centre of the Paris Basin: a filiation? The example of Le Closeau (Rueil-Malmaison, France). In: Milliken, S. (ed.) The Organization of Lithic Technology in Late Glacial and Early Postglacial of Europe. BAR(IS) 700, Oxbow, Oxford, pp. 131 - 147

Boessenkool, K.P. 2002. Environmental changes in the North Atlantic region during the last deglaciation. LPP Contributions Series No. **15**: 128 pp

Bogaard, P. 1983. Die Eruption des Laacher See Vulkans. Unpublished Ph.D. thesis. Ruhr-Universität, Bochum

Bogaard, P., and Schmincke, H.U. 1985. Laacher See tephra: a widespread isochronous late Quaternary tephra layer in Central and Northern Europe. *Geological Society of America Bulletin*. **96**: 1554 - 1571

Bogaard, C.V.D., and Schmincke, H.U. 2002. Linking the North Atlantic to central Europe: a high resolution Holocene tephrochronological record from northern Germany. *Journal of Quaternary Science*. **17**. 3 - 20

Bogucki, P. 1996. The spread of early farming in Europe. *American Scientist*. **84**: 242 - 253

Böhme G.1997. Fossile Fischfaunen aus dem jüngeren Känozoikum Deutschlands. *Quartär*. **47/48**: 113 - 138

Bohmers, A. 1947. Jong-Palaeolithicum en Vroeg-Mesolithicum. In: van Gelder, H.E., Glazema, P., Bontekoe, G.A., Halbertsma, H., and Glasbergen, W. (eds.) Oudheidkundig bodemonderzoek in Nederland; Gedenkboek van Giffen, A.E. J.A. Boom and Zoon: Meppel. 129 - 201

Bokelmann, K. 1978. Ein Federmesserfundplatz bei Schalkholz, Kreis Dithmarschen. *Offa*. **35**: 36 - 54

Bokelmann, K. 1979. Rentierjäger am Gletscherrand in Schleswig-Holstein? *Offa*. **36**: 12 - 22

Bokelmann, K., Heinrich, D., and Menke, B. 1983. Fundplätze des Spätglazials am Hainholz-Esinger Moor. Kreis Pinneberg. *Offa*. **40**: 199 - 240

Bokelmann, K. 1991. Some new thoughts on old data on humans and reindeer in the Ahrensburgian Tunnel Valley in Schleswig-Holstein, Germany. In: Barton, R. N. E., Roberts, A. J., and Roe, D. A. (eds.) The Lateglacial in north-west Europe: Human adaptation and environmental change at the end of the Pleistocene. *CBA Research Report*. **77**: 72 - 81

Bokelmann, K. 1999. Eine Stielspitze mit Schäftungspech der Ahrensburger Kultur aus Stellmoor. In: Cziesla, E., Kersting, T., and Pratsch, S. (eds.) Den Bogen spannen. Festschrift für Bernhard Gramsch. Beier and Beran, Weißbach, pp. 77 - 79

Bondevik, S., Mangerud, J., Dawson, S., Dawson, A., and Lohne, Ø. 2005. Evidence for three North Sea tsunamis at the Shetland Islands between 8000 and 1500 years ago. *Quaternary Science Reviews*. **24**: 1757 - 1775

Bosinski, G. 1984. Paläolithische Funde in den Höhlen Nordrhein-Westfalens. *Kölner Geographische Arbeiten*. **45**: 371 - 398

Bos, J.A.A. 2001. Lateglacial and early Holocene vegetation history of the northern Wetterau and the Amöneburger basin (Hessen), central-west Germany. *Review of Palaeobotany and Palynology*. **115**: 117 - 212

Bos, J.A.A., Bohncke, S.J.P., and Janssen, C.R. 2006. Lake-level fluctuations and small-scale vegetation patterns during the late glacial in the Netherlands. *Journal of Paleolimnology*. **35**: 211 - 238

Bouchud, J. 1966. *Essai sur le renne et la climatologie du Paléolithique moyen et supérieur*. Périgueux: Impremerie Magne

Bousman, C.B. 1993. Hunter-gatherer adaptations, economic risk and tool design. *Lithic Technology*. **18**: 59 – 86

Bragazza, L., Tahvanainen, T., Kutnar, L., Rydin, H., Limpens, J., Hajek, M., Grosvernier, P., Hajek, T., Hajkova, P., Hansen, I., Iacumin, P., and Gerdol, R. 2004. Nutritional constraints in ombrotrophic *Sphagnum* plants under increasing atmospheric nitrogen deposition in Europe. *New Phytologist*. **163**: 609 - 616

Bramham-Law, C.W.F., Theuerkauf, M., Lane, C.S., and Mangerud, J. 2013. New findings regarding the Saksunarvatn Ash in Germany. *Journal of Quaternary Science*. **28**: 248 - 257

Brande, A. 1980. Pollenanalytische Untersuchungen im Spätglazial und fruühen Postglazial Berlins. Verh. Bot. Ver. Prov. Brandenburg. **115**: 21 - 72

Brande, A. 2003. Late Pleistocene and Holocene pollen stratigraphy of Lake Stechlin. *Archiv fur Hydrobiologie, Special. Issues: Advances in Limnology*. **58**: 281 - 311

Bratlund, B. 1990. Rentierjagd im Spätgazial. Eine Untersuchung der Jagdfrakturen an Rentierknochen von Meiendorf und Stellmoor, Kreis Stormarn. *Offa*. **47**: 7 - 34

Bratlund, B. 1991. A study of hunting lesions containing flint fragments on reindeer bones at Stellmoor, Schleswig-Holstein, Germany. In: Barton, N., Roberts, A.J., and Roe, D.A. (eds.) *The Late Glacial in north-west Europe: human adaptation and environmental change at the end of the Pleistocene*. Oxford: Alden Press, pp. 193 - 207

Bratlund, B. 1996. Hunting strategies in the Lateglacial of northern Europe: a survey of the faunal evidence. *Journal of World Prehistory*. **10**: 1 - 48

Brauer, A., Endres, C., Negendank, J.F.W. 1999. Lateglacial calendar year chronology based on annually laminated sediments from Lake Meerfelder Maar, Germany. *Quaternary International*. **61**: 17 - 25

Brauer, A., Haug, G.H., Dulski, P., Sigman, D.M., and Negendank, J.F.W. 2008. An abrupt wind shift in western Europe at the onset of the Younger Dryas cold period. *Nature Geoscience*. **1**: 520 - 523

Brayshay, M., and Grattan, J. 1999. Environmental and social response in Europe to the 1783 eruption of the Laki fissure volcano in Iceland: a consideration of contemporary documentary evidence. In: Firth,C.R., and McGuire,W.J. (eds.) Volcanoes in the Quaternary. *Geological Society of London Special Publications*. **161**: London. pp 173 - 187

Breest, K. 1999. Der spätpaläolithische Oberflächenfundplatz mit Rücken-und Bromme-Spitzen bei Dohnsen-Bratzloh, Ldkr. Celle (Niedersachsen). In: Cziesla, E., Kersting, and T., Pratsch, S. (eds.) Den Bogen spannen. Festschrift für Bernhard Gramsch. Beier & Beran, Weissbach, pp. 67 - 75

Breest, K. 2000. Spätglaziale Fundstellen im Landkreis Celle. *Die Kunde N.F*. **51**: 151 - 178

Brenner, M., Whitmore, T.J., Curtis, J.H., Hodell, D.A., and Schelske, C.L. 1999. Stable isotope ($\delta^{13}C$ and $\delta^{15}N$) signatures of sedimented organic matter as indicators of historic lake trophic state. *Journal of Paleolimnology*. **22**: 205 - 221

Brinch Petersen, E. 2009. The human settlement of southern Scandinavia 12500-8700 cal BC. In: Street, M., Barton, R.N.E., and Terberger, T. (eds.) Humans, environment and chronology of the late glacial of the North European Plain. RGZM – Tagungen, Band 6. Verlag des Römisch-Germanischen Zentralmuseums, Mainz, pp. 89 - 129

Brock, F., Higham, T.F.G, Ditchfield, P., and Bronk Ramsey, C. 2010. Current pre-treatment methods for AMS radiocarbon dating at the Oxford Radiocarbon Accelerator Unit (ORAU).*Radiocarbon*. **52**: 103 - 112

Bronk Ramsey, C. 2001. Development of the radiocarbon calibration program OxCal. *Radiocarbon*. **43**: 355 - 363

Bronk Ramsey, C., Higham, T.F.G., Bowles, A., and Hedges, R.E.M. 2004. Improvements to the pre-treatment of bone at Oxford. *Radiocarbon*. **46**: 155 - 163

Bronk Ramsey, C. 2008. Deposition models for chronological records. *Quaternary Science Reviews*. **27**: 42 - 60

Bronk Ramsey, C. 2009a. Bayesian analysis of radiocarbon dates. *Radiocarbon*. **51**: 337 - 360

Brooks, S.J., Matthews, I.P., Birks, H.H., and Birks, H.J.B. 2012. High resolution Lateglacial and early-Holocene summer air temperature records from Scotland inferred from chironomid assemblages. *Quaternary Science Reviews*. **41**: 67 - 82

Bunting, M.J.1994. Vegetation history of Orkney, Scotland: pollen records from two small basins in West Mainland. *New Phytologist*. **128**: 771 - 792

Burdukiewicz, J.M. 1986. The Late Pleistocene shouldered point assemblages in western Europe. E.J. Leiden: Netherlands, pp. 10 - 20

Burdukiewicz, J. M. 1987. Zum Forschungsstand der Hamburger Kultur. *Jahrbuch des Romisch-Germanischen Zentralmuseums Mainz 34*. **1**: 143 - 167

Burdukiewicz, J. M. 1989. Le Hambourgien: origine, evolution dans un contexte stratigraphique, paleoclimatique et paleogeographique. *L'Anthropologie*. **93**: 189 - 218

Burdukiewicz, J.M. 2011. Late Glacial hunter-gatherer reactions to the Younger Dryas cooling event in the southern and eastern Baltic regions of Europe. *Quaternary International*. **242**: 302 - 312

Calvert, S.E. 2004. Beware intercepts: interpreting compositional ratios in multicomponent sediments and sedimentary rocks. *Organic Geochemistry*. **35**: 981 - 987

Caseldine, C., Geirsdóttir, A., and Langdon, P. 2003. Efstadalsvatn - a multi-proxy study of a Holocene lacustrine sequence from NW Iceland. *Journal of Paleolimnology*. **30**: 55 - 73

Cavalli-Sforza, L.L., Menozzi, P., and Piazza, A. 1994. The History and Geography of Human Genes. *Princeton University Press*, Princeton, USA

Chollet, A., Boutin, P., and Célérier, G. 1980. Crochets en bois de cerf de l'azilien du sud-Ouest de la France. *Bulletin de la Societé Préhistorique Francaise*. **77**: 11 - 16

Christiansen, R.L. 1980. Eruption of Mt. St. Helens: volcanology. *Nature.* **285**: 531 - 533

Churchill, S.E. 1993. Weapon technology, prey size selection, and hunting methods in modern hunter-gatherers: implications for hunting in the Palaeolithic and Mesolithic. In: Peterkin, G.L., Bricker, H.M., and Mellars, P. (eds.) Hunting and Animal Exploitation in the Later Palaeolithic and Mesolithic of Eurasia. Archeological Papers of the American Anthropological Association, Nr.4. American Anthropological Association, Washington, DC, pp. 11 - 24

Clark, J.G.D. 1936. The Mesolithic Settlement of northern Europe. Cambridge University Press, Cambridge

Clark, J.G.D. 1938. The reindeer hunting tribes of northern Europe. *Antiquity*. **12**: 154 - 172

Clark, J.G.D. 1952. Prehistoric Europe, the economic basis. Methuen, London

Clausen, I. 1997. Neue Untersuchungen an späteiszeitlichen Fundplätzen der Hamburger Kultur bei Ahrenshöft, Kr. Nordfriesland (ein Vorbericht). *Archäologische Nachrichten aus Schleswig-Holstein*. **8**: 8 - 49

Clausen, I. 2004. The reindeer antler axe of the Allerød period from Klappholz LA 63, Kreis Schleswig-Flensburg/Germany. Is it a relict of the Federmesser, Bromme or Ahrensburgian culture. In: Terberger, T., and Eriksen, B.V. (eds.) Hunters in a Changing World. Environment and Archaeology of the Pleistocene - Holocene Transition (Ca. 11000-9000 B.C.) in Northern Central Europe, Workshop of the U.I.S.P.P.- Commission XXXII at Greifswald in September2002, Internationale Archäologie, 5. Verlag Marie Leidorf, Rahden/Westfalen, pp. 141 - 164

Cook, C.G., Leng, M.J., Jones, R.T., Langdon, P.G., and Zhang, E. 2012. Lake ecosystem dynamics and links to climate change inferred from a stable isotope and organic palaeorecord from a mountain lake in southwestern China (ca. 22.6 – 10.5 cal ka BP). *Quaternary Research*. **77**: 132 - 137

Coope, G. R., Lemdahl, G., Lowe, J. J. and Walking, A. 1998. Temperature gradients in northern Europe during the last interglacial–glacial transition (14–9 14C kyr BP) interpreted from coleopteran assemblages. *Journal of Quaternary Science.* **13**: 419 - 433

Cronin, S.J., Manoharan, V., Hedley, M.J., and Loganathan, P. 2000. Fluoride: a review of its fate, bioavailability, and risks of fluorosis in grazed-pasture systems in New Zealand. *New Zealand Journal of Agricultural Research*. **43**: 295 - 321

Cziesla, E. 2000. Späpaläolithische Widerhakenspitzen aus Brandenburg. Eine Forschungsgeschichte. *Archäologisches Korrespondenzblatt.* **30**: 173 - 186

Cziesla, E. 2001. Feine Spitzen. Neufunde aus dem Bützee bei Altfriesack, Landkreis Ostprignitz – Ruppin*. Archäologie in Berlin und Brandenburg*. 30 - 32

Cziesla, E. 2004. Late Upper Palaeolithic and Mesolithic cultural continuity – or: bone and antler objects from the Havelland. In: Terberger, T., and Eriksen, V.B. (eds.) Hunters in a changing world. Environment and archaeology of the Pleistocene – Holocene transition (ca. 11000 – 9000 B.C.) in northern central Europe. Workshop of the U.I.S.P.P. commission XXXII at Greifswald. 2002. 165 - 182

Dale, V.H., Swanson, F.J., and Crisafulli, C.M. 2005. Disturbance, survival, and succession: Understanding ecological responses to the 1980 eruption of Mount St. Helens. In: Dale, V.H., Swanson, F.J., and Crisafulli, C.M (eds.) Ecological responses to the 1980 eruption of Mount St. Helens Springer, New York, pp 3 - 11

Dansgaard, W., Johnsen, S.J., Clausen, H.B., Dahl-Jensen, D., Gundestrup, N.S., Hammer, C.U., Hvidberg, C.S., Steffensen, J.P., Sveinbjörnsdottir, A.E., Jouzel, J., and Bond, G. 1993. Evidence for general instability of past climate from a 250-kyr ice-core record. *Nature*. **364**: 218 - 220

Darwin, C. 1839. Journal of researches into the geology and natural history of the various countries visited by H.M.S. Beagle, under the command of Captain Fitzroy, R.N. from 1832-1836. London, Henry Colbum

Davidson, I. 1989. La economia del Final del Paleolitico en la España oriental. *Servei d'Investigación Prehistórica, Trabajos Varios*. **85**: Valencia

Davies, S.M., Branch, N.P., Lowe, J.J., and Turney, C.S.M. 2002. Towards a European tephrochonological framework for Termination 1 and the Early Holocene. *Philosophical Transactions: Mathematical, Physical and Engineering Sciences*. **360**: 76 - 802

Davies, S.M., Wohlfarth, B., Wastegard, S., Andersson, M., Blockley, S.P.E., and Possnert, G. 2004. Were there two Borrobol Tephras during the early Late Glacial period: implications for tephrochronology. *Quaternary Science Reviews*. **23**: 581 - 589

Davies, S.M., Abbott, P.M., Pearce, N.J.G., Wastegård, S., and Blockley, S.P.E. 2012. Integrating the INTIMATE records using tephrochronology: rising to the challenge. *Quaternary Science Reviews.* **36**: 11 - 27

De Bie, M., and Caspar, J.P. 2000. Rekem. A Federmesser Camp on the Meuse River Bank. Leuven University Press, Leuven

Deecke, W. 1900. Vorkommen von bearbeiteten Riesenhirschknochen bei Endingen (Kreis Franzburg) in Vorpommern. *Globus*. **78**: 13 - 15

Degerbøl, M., and Krog, H. 1959. The Reindeer (*Rangifer tarandus* L.) in Denmark. *Biologiske Skrifter udgivet af Det Kongelige Danske Videnskabernes Selskab.* **10**: 1 - 165

Dewez, M., Francis, A. and Teheux, E., 2008. Le Paléolithique supérieur final de la grotte Walou (Province de Liège, Belgique). Second rapport de fouille. In: Dewez, M. (ed.) Recherches à la grotte Walou à Trooz (Belgique), British Archaeological Reports, International Series, 1789. Archaeopress, Oxford, pp. 29 - 36

Dincauze,D .F. 1987. Strategies for Paleoenvironmental Reconstruction in Archaeology. *Advances in Archaeological Method and Theory*. **11**: 255 - 336

Drucker, D.G., Kind, C.J., and Stephan, E. 2011. Chronological and ecological information on Late-Glacial and early Holocene reindeer from northwest Europe using radiocarbon (^{14}C) and stable isotope ^{13}C, ^{15}N) analysis of bone collagen: Case study in southwestern Germany. *Quaternary International*. **245**: 218 - 224

Dugmore, A.J., and Newton, A.J. 1998. Holocene Tephra layers in the Faroe Islands. *Fróðskaparrit*. **46**: 191 - 204

Duigan, C.A., and Birks, H.H. 2000. The Late-glacial and early-Holocene palaeoecology of cladoceran microfossil assemblages at Kråkenes, western Norway, with a quantitative reconstruction of temperature changes. *Journal of Paleolimnology*. **23**: 67 - 76

Dupuy, B.M., Stenersen, M., Lou, T.T., and Olaisen, B. 2006. Geographical heterogeneity of Y-chromosomal lineages in Norway. *Forensic Science International*. **164**: 10 - 19

Eicher, G.J., and Rounsefell, G.A. 1957. Effects of lake fertilisation by volcanic activity on abundance of salmon. *Limnology and Oceanography*. **2**: 70 - 76

Eiríksson, J., Knudsen, K.L., Haflidason, H., and Henriksen, P. 2000. Lateglacial and Holocene palaeoceanography of the North Icelandic shelf. *Journal of Quaternary Science*. **15**: 23 - 42

Enloe, J. G. 1991. Subsistence organization in the Upper Paleolithic: Carcass refitting and food sharing at Pincevent. *Unpublished Ph.D*. *thesis*. University of New Mexico

Eriksen, V.B. 1999. Late Palaeolithic settlement in Denmark – how do we read the record? *Folia Quaternaria* **70**: 157 - 173

Eriksen, V.B. 2002. Reconsidering the geochronological framework of Lateglacial hunter-gather colonization of southern Scandinavia. *Jutland Archaeological Society Publications* **39**: 25 - 41

Erlandson, J.M., and Moss, M.L. 2001. Shellfish feeders, carrion eaters, and the archaeology of aquatic adaptations. *America Antiquity*. **66**: 413 - 432

Evans, H.M. 1932. The Maglemose harpoon. *Proceedings of Prehistoric Society East Anglia*. **7**: 131 - 132

Evans, J.G. 1969. The exploitation of molluscs. In: P.J. Ucko and G.W. Dimbleby (eds.) The Domestication and Exploitation of Plants and Animals. Duckworth, London. pp. 479 - 84

Fagnart, J.P., and Coudret, P. 2000. Le Tardiglaciaire dans le Nord de la France. In Valentin, B., Bodu, P., and Christensen, M. (eds.) L'Europe central et septentrionale au Tardglaciaire. Confrontation des modèles régionaux de peuplement. *Mémoires du Musée Préhistoire d'Ile de France.* **7**: 111 - 128

Fischer, A., and Nielsen, F.O.S. 1986. Senistidens bopladser ved Bromme. En genbearbejdning af Westerby's og Mathiassen's fund. *Aarbøger for nordisk Oldkyndighed og Historie*. **1986**: 5 - 42

Fischer, A., and Tauber, H. 1986. New 14C-datings of the late Palaeolithic cultures from northwestern Europe. *Journal of Danish Archaeology*. **5**: 7 - 13

Fischer, A. 1988. A Late Palaeolithic Flint Workshop at Egtved, East Jutland. *Journal of Danish Archaeology*. **7**: 7 - 23

Fischer, A. 1991. Pioneers in deglaciated landscapes: The expansion and adaptation of Late Palaeolithic societies in Southern Scandinavia. In: Barton, R.N.E., Roberts, A.J., and Roe, D.A. (eds.) Late Glacial in north-west Europe: human adaptation and environmental change at the end of the Pleistocene. CBA, Oxford, pp. 100 - 122

Flößner, D. 1972. Kiemen- und Blattfüßler; Branchiopoda, Fischläuse,Branchiura. In Fischer, G. (ed.) Die Tierwelt Deutschlands **6**: Jena. pp 1 - 501

Fogel, M.L., and Cifuentes, L.A. 1993. Isotope fractionation during primary production. In: Engel, M.H., and Macho, S.A. (eds.) Organic Geochemistry. Plenum Press, New York, pp 73 - 98

Frey, D.G. 1960. The ecological significance of cladocera remains in lake sediments. *Ecology*. **41**: 684 - 699

Frey, D.G. 1962. Cladocera from the Eemian Interglacial of Denmark. *Journal of Palaeontology*. **36**: 1133 - 1154

Frey, D.G. 1986. Cladoceran analysis. In: Berglund, B.E. (ed.) Handbook of Holocene palaeoecology and palaeohydrology. John Wiley and Sons: New York

Frey, D.G. 1988. Are there tropicopolitan Macrothricid Cladocera? *Acta Limnologica Brasiliensia*. **2**: 513 - 525

Friedrich, M., van der Kroft, P., Renno, A., Schmidt, S., Ullrich, O., and Vollbrecht, J. 2001. Ein Wald am Ende der letzten Eiszeit. Untersuchungen zur Besiedlungs, Landschafts und Vegetationsentwicklung an einem verlandeten See im Tagebau Reichwalde, Niederschlesischer Oberlausitzkreis. *Arbeits- und Forschungsberichte zur sächsischen Bodendenkmalpflege*. **43**: 21 - 9

Froom, R. 2005. Late Glacial Long Blade sites in the Kennet Valley. Fieldwork at Avington VI, Wawcott XII and Crown Acres. London

Gamble, C.S. 1982. Interaction and alliance in Palaeolithic society. *Man*. **17**: 92 - 107

Gamble, C.S. 1986. *The Palaeolithic Settlement of Europe*. Cambridge: Cambridge University Press

Gamble, C., Davies, W., Pettitt, P., and Richards, M. 2004. Climate change and evolving human diversity in Europe during the last glacial. *Philosophical Transactions of the Royal Society Biological Sciences*. **359**: 243 - 254

Gamble, C., Davies, W., Pettitt, P., Hazelwood, L., and Richards, M. 2005. The archaeological and genetic foundations of the European population during the Late Glacial: implications for 'agricultural thinking'. *Cambridge Archaeological Journal*. **15**: 193 - 223

Gamble, C., Davies, W., Pettitt, P., Hazelwood, L., and Richards, M. 2006. The Late Glacial ancestry of Europeans: Combining genetic and archaeological evidence. *Documenta Praehistorica XXXIII*. 1 - 10

Garcia, O., Fregel, R., Larruga, J. M., Alvarez, V., Yurrebaso, I., Cabrera, V.M., and González, A.M. 2011.Using mitochondrial DNA to test the hypothesis of a European post-glacial human recolonization from the Franco-Cantabrian refuge. *Heredity*. **106**: 37 - 45

Garzón, M.B., Sánchez de Dios, R., and Ollero, H.S. 2007. Predictive modelling of tree species distributions on the Iberian Peninsula during the Last Glacial Maximum and Mid-Holocene. *Ecography*. **30**: 120 - 134

Geirsdóttir, Á., Andrews, J.T., Ólafsdóttir, S., Helgadóttir, G., and Hardardóttir, J. 2002. A 36 Ky record of iceberg rafting and sedimentation from north-west Iceland. *Polar Research*. **21**: 291 - 298

Geist, V. 1999. Deer of the World. Their Evolution, Behaviour, and Ecology. Swan Hill Press, Shrewsbury

Gerken, K., 2001. Studien zur jung- und spätpaläolithischen sowie mesolithischen Besiedlung im Gebiet zwischen Wümme und Oste. Isensee Verlag, Oldenburg

Godwin, H., and Godwin, M.E. 1933. British Maglemosian harpoon sites. *Antiquity*. **7**: 36 - 48

Goericke, R., Montoya, J.P., and Fry, B. 1994. Physiology of isotopic fractionation in algae and cyanobacteria. In: Lajtha, K., Michener, R.H. (eds.) Stable Isotopes in Ecology and Environmental Science. Blackwell, Oxford, pp 187 - 221

Gordon, B.C. 1988. Of men and reindeer herds in French Magdalenian prehistory. BAR International Series 390

Grabowska, J.M., Niska, M., and Sienkiewicz, E. 2009. Evolution of the palaeolake at Ruszkówek (central Poland) during the Eemian Interglacial based on isotope, cladoceran and diatom data. *Journal of Palaeolimnology*. **42**: 467 - 481

Graf, H.F., and Timmreck, C. 2001. A general climate model simulation of the aerosol radiative effects of the Laacher See eruption (10,900 B.C.). *Journal of Geophysical Research*. **106**: 14747 - 14756

Gramsch, B. 1973. Das Mesolithikum im Flachland zwischen Elbe und Oder, Teil 1.*Veröffentlichungen des Museums für Ur und Frühgeschichte Postdam*. **7**

Gramsch, B. 2004. From the Late Palaeolithic to the early Mesolithic in northeastern Germany. In: Terberger, T., and Eriksen, V.B. (eds.) Hunters in a changing world. Environment and archaeology of the Pleistocene – Holocene transition (ca. 11000 – 9000 B.C.) in northern central Europe. Workshop of the U.I.S.P.P. commission XXXII at Greifswald. 2002. **5**: 183 - 201

Gramsch, B., Beran, J., Hanik, S., and Sommer, R.S. 2013. A Palaeolithic fishhook made of ivory and the earliest fishhook tradition in Europe. *Journal of Archaeological Science*. **40**: 2458 - 2463

Grattan, J., and Brayshay, M. 1995. An amazing and portentous summer: environmental and social responses in Britain to the 1783 eruption of an Iceland volcano. *The Geographical Journal*. **161**: 125 - 134

Grimm, S.B., 2004. Ein spätallerödzeitlicher Fundplatz bei Bad Breisig, Kreis Ahrweiler. *Berichte zur Archäologie an Mittelrhein und Mosel*. **9**: 11 - 32

Grimm, S.B., and Weber, M-J. 2008. The chronological framework of the Hamburgian in the light of old and new ^{14}C dates. *Quartär*. **55**: 17 - 40

Gripp, K. 1937. Die Rengeweihstangen von Meiendorf. In: Rust, A. (ed.) Das altsteinzeitlichen Rentierjägerlager Meiendorf. *Wachholtz Verlag, Neumünster*, pp. 62 - 72

Gripp, K. 1943. Die Rengeweihen von Stellmoor. In: Rust, A. (ed.) Die alt-und mittelsteinzeitlichen Funde von Stellmoor. *Wachholtz Verlag, Neumünster*, pp. 106 - 122

Grønnow, B. 1985. Meiendorf and Stellmoor revisited. An analysis of Late Palaeolithic reindeer exploitation. *Acta Archaeologica*. **56**: 131 - 156

Grönvold, K., Oskarsson, N., Johnsen, S.J., Clausen, H.B., Hammer, C.U., Bond, G., and Bard, E.1995. Ash layers from Iceland in the GRIP ice core correlated with oceanic and land sediments. *Earth and Planetary Science Letters*. **135**: 149 - 155

Grote, K., 1993. Die Abris im südlichen Leinebergland bei Göttingen. Archäologische Befunde zum Leben unter Felsschutzdächern in urgeschichtlicher Zeit I. *Archäologischer Teil*. Veröffentlichungen der urgeschichtlichen Sammlungen des Landesmuseums Hannover. **43**

Gu, B., Alexander, V., and Schell, D.M. 1999. Seasonal and interannual variability of plankton carbon isotope ratios in a subarctic lake. *Freshwater Biology*. **42**: 417 - 426

Håkansson, S.1985. A review of various factors influencing the stable carbon isotope ratio of organic lake sediments by the change from glacial to post-glacial environmental conditions. *Quaternary Science Reviews*. **4**: 135 - 146

Haflidason, H., Sejrup, H.P., and Jones, G.A.1990. Tephra, bio, and lithostratigraphy of an AMS dated core from the Norway basin, southern Norwegian Sea. *Geonytt*. **17**: 52

Haflidason, H., Sejrup, H.P., Johannesson, H., and Jones, G.1995. The southern Norwegian Greenland Sea through the last 20 Ka: sedimentation, tephra layers and palaeoceanography. In: Abstract, *The Lateglacial Palaeoceanography of the North Atlantic Margins*. Quaternary Research Association, Edinburgh, UK Annual Discussion Meeting

Haflidason, H., Eiríksson, J., and van Kreveld, S. 2000. The tephrochronology of Iceland and the North Atlantic region during the Middle and Late Quaternary: a review. *Journal of Quaternary Science*. **15**: 3 - 22

Hanik, S., Jahns, S. 2010. Untersuchungen zur Pflanzen- und Tierwelt am Fundplatz Wustermark 22. In: Gramsch, B., Beran, J.: Spätaltsteinzeitliche Funde von Wustermark, Fundplatz 22, Lkr. Havelland. *Veröffentlichungen zur brandenburgischen Landesarchäologie*. **41**: 132 - 137

Hajdas, I., Ivy, S.D., Beer, J., Bonani, G., Imboden, D., Lotter, A.F., Sturm, M., and Suter, M. 1993. AMS radiocarbon dating and varve chronology of Lake Soppensee: 6000 to 12 000 14C years BP. *Climate Dynamics*. **9**: 107 - 116

Hann, B.J. 1988. Methods in Quaternary ecology #6. Cladocera. *Geoscience Canada*. **16**: 17 - 26

Hansen, K. M. 2003. Pre-Boreal elk bones from Lundby Mose. In: Larsson, L., Kindgren, H., Hansen, K.M., and Pedersen, K.B. 2006. With or without bones – Late Palaeolithic hunters in South Zealand. In: Hansen, K.M., and Pedersen, K.B. (eds.) Across the western Baltic. Proceedings from an archaeological conference in Vordinborg. Sydsjællands Museums Publikationer I. 93 - 110

Knutsson, K., Loeffler, D., and Åkerlund, A. (eds.) Mesolithic on the Move. Oxford: Oxbow Books Harms, E., and Schmincke, H.U. 2000. Volatile composition of the phonolitic Laacher See magma (12,900 yr BP): implications for syn-eruptive degassing of S, F, Cl and H_2O. *Contributions to Mineralogy and Petrology*. **138**: 84 - 98

Harmsworth, R.V. 1968. The development history of Blelham Tarn (England) as shown by animal microfossils, with special reference to Cladocera. *Ecological Monographs*. **38**: 223 - 241

Hart, R.C. 1988. Zooplankton feeding rates in relation to suspended sediment content: potential influences on community structure in a turbid reservoir. *Freshwater Biology*. **19**: 123 - 139

Hartz, N., and Milthers, V. 1901. Det senglaciale Ler i Allerød Teglværksgrav. *Meddelelser Dansk Geologisk Foreningen*, **8**: 31 - 60

Hartz, S. 1987. Neue spätpaläolithische Fundplätze bei Ahrenshöft, Kreis Nordfriesland. *Offa*. **44**: 5 - 52

Hawkes, K., O'Connell, J., and Blurton Jones, N. 1989. Hardworking Hadza grandmothers. In: Standen, V., and Foley, R. (eds.) Comparative Socioecology: The behavioural ecology of humans and other mammals. Blackwell Scientific, Oxford. pp 341 - 366

Hawkes, K., O'Connell, J., and Blurton Jones, N. 1991. Hunting income patterns among the Hadza: Big game, common goods, foraging goals and the evolution of the human diet. In: Whiten, A., and Widdowson (eds.) Foraging stratagies and the natural diet of monkeys, apes and humans. *Proceedings of the Royal Society of London*. **334**. Clarendon Press, Oxford

Hecky, R.E., Campbell, P., and Hendzel, L.L. 1993. The stoichiometry of carbon, nitrogen, and phosphorus in particulate matter of lakes and oceans. *Limnology and Oceanography*. **38**: 709 - 724

Hedges, R.E.M., Housley, R.A., Bronk Ramsey, C., and Van Klinken, G.J. 1993. Radiocarbon dates from the Oxford AMS system: Archaeometry datelist 17. *Archaeometry*. **35**: 305 - 326

Henrich, J. 2004. Demography and Cultural Evolution: How Adaptive Cultural Processes Can Produce Maladaptive Losses – the Tasmanian Case. *American Antiquity*. **69:** 197 - 214

Heinrichs, M.L., Walker, I.R., Mathewes, R.W., and Hebda, R.J. 1999. Holocene chironomid-inferred salinity and paleovegetation reconstruction from Kipoola Lake, British Columbia. *Geographie physique et Quaternaire*. **53**: 211 - 221

Hemphill, B. E. 1999, Wear and Tear: Osteoarthritis as an Indicator of Mobility among Great Basin Hunter-Gatherers. In: Hemphill, B.E., and Larsen, C.S (eds.) Prehistoric Lifeways in the Great Basin Wetlands: Bioarchaeological Reconstruction and Interpretation. University of Utah Press, Salt Lake City, pp 241 - 289

Herczeg, A.L. 1988. Early diagenesis of organic matter in lake sediments - a stable carbon isotope study of pore waters. *Chemical Geology*. **72**: 199 - 209

Herre, W., and Requate, H. 1958. Die Tierreste der paläolithischen Siedlungen Poggenwisch, Hasewisch, Borneck und Hopfenbach bei Ahrensburg. In: Rust, A. (ed.) Die jungpaläolithischen Zeltanlagen von Ahrensburg, pp. 23 - 27

Higham, T.F.G., Jacobi, R.M., Bronk Ramsey, C. 2006. AMS radiocarbon dating of ancient bone using ultrafiltration. *Radiocarbon*. **48**: 179 - 195

Highwood, E.J., and Stevenson, D.S. 2003. Atmospheric impact of the 1783–1784 Laki eruption: part II climatic effect of sulphate aerosol. *Atmospheric Chemistry and Physics Discussions*. **3**: 1599 - 1629

Hoek, W.Z., 1997. Palaeogeography of Lateglacial vegetations. Aspects of Lateglacial and Early Holocene vegetation, abiotic landscape, and climate in The Netherlands. *Netherlands Geographic Studies*. **230**: 1 - 147

Hoek, W.Z. 2001. Vegetation response to the ~14.7 and ~11.5 ka cal. BP climate transitions: is vegetation lagging climate? *Global and Planetary Change*. **30**: 103 - 115

Hofmann, W. 1987. Cladocera in space and time: Analysis of lake sediments. *Hydrobiologia*. **145**: 315 - 321

Hofmann, W. 2001. Late-Glacial/Holocene succession of the chironomid and cladoceran fauna of the Soppensee (Central Switzerland). *Journal of Paleolimnology*. **25**: 411 - 420

Hofmann, W. 2003. The long-term succession of high-altitude cladoceran assemblages: a 9000-year record from Sägistalsee (Swiss Alps). *Journal of Paleolimnology*. **30**: 291 - 296

Hollander, D.J., and Smith, M.A. 2001. Microbially mediated carbon cycling as a control on the $\delta^{13}C$ of sedimentary carbon in eutrophic Lake Mendota (USA): new models for interpreting isotopic excursions in the sedimentary record. *Geochimica. Cosmochimica. Acta*. **65**: 4321 - 4337

Holm, J., Christensen, C., and Aaris-Sørensen, K. 2002. Istidsjægerne i Sønderjylland. *Nyt fra Nationalmuseet*. **94**: 10 - 13

Holm, J. 2003. Rentierjäger im norden. *Archäologie in Deutschland*. **3**: 54 - 56

Houmark-Nielsen, M., and Kjaer, K.H. 2003. Southwest Scandinavia, 40-15 kyr BP: palaeogeography and environmental change. *Journal of Quaternary Science*. **18**: 769 - 786

Housley, R.A., Gamble, C.S., Street, M., and Pettitt, P. 1997. Radiocarbon evidence for the Late Glacial human recolonisation of Northern Europe. *Proceedings of the Prehistoric Society*. **63**: 25 - 54

Housley, R.A., Lane, C.S., Cullen, V.L., Weber, M-J., Riede, F., Gamble, C.S., and Brock F. 2012. Icelandic volcanic ash from the Late-glacial open-air archaeological site of Ahrenshöft LA58 D, North Germany. *Journal of Archaeological Science*. **39**: 708 - 716

Houtsma, P., Roodenberg, J. J. and Schilstra, J. 1981: A Site of the Tjonger Tradition along the Schipsloot at Een (Gemeente of Norg, Province of Drenthe, the Netherlands). *Palaeohistoria*. **23**: 45-74

Hunt, J. B., and Hill, P. G. 1993. Tephra geochemistry: a discussion of some persistent analytical problems. *Holocene*. **3**: 271 - 278

Hyodo, A., and Longstaffe, F.J. 2011. The palaeoproductivity of ancient Lake Superior. *Quaternary Science Reviews*. **30**: 2988 - 3000

Ikinger, E.M. 1998. Der endeiszeitliche Rückenspitzen-Kreis Mitteleuropas. LIT, Münster

Ingólfsson, Ó., Norddahl, H., and Haflidason, H.1995. Rapid isostatic rebound in southwestern Iceland at the end of the last glaciation. *Boreas*. **24**: 245 - 259

Isarin, R.F.B. 1997. Permafrost distribution and temperatures in Europe during the Younger Dryas. *Permafrost and Periglacial Processes*. **8**: 313 - 333

Isarin, R.F.B., and Bohncke, S.J.P. 1999. Mean July temperatures during the Younger Dryas in northwestern and Central Europe as inferred from climate indicator plant species. *Quaternary Research*. **51**: 158 - 173

Iversen, J. 1942. En pollenanalytisk tidsfæstelse af Ferskvandslagene ved Nørre Lyngby. *Meddelelser fra Dansk Geologisk Forening*. **10/2**: 130 - 151

Iversen, J. 1954. The Late Glacial flora of Denmark and its relation to climate and soil. *Danmarks Geologiske Undersøgelse II.* Rk. Nr. **80**: 87 - 119

Iversen, J., 1973. The development of Denmark's nature since the last glacial. Translated by M. Robson. *Danmarks Geologiske Undersøgelser*. Række V **7C**: 1 - 126

Jacobi, R.M., and Higham, T.F.G. 2009. The early Lateglacial re-colonization of Britain: new radiocarbon evidence from Gough's Cave, southwest England. **28**: 1895 - 1913

Janbu, A.D., Paasche, Ø., and Talbot, M.R. 2011. Paleoclimate changes inferred from stable isotopes and magnetic properties of organic-rich lake sediments in Arctic Norway. *Journal of Paleolimnology*. **46**: 29 - 44

Jennings, A.E., Grönvold, K., Hilberman, R., Smith, M., and Hald, M. 2002. High-resolution study of Icelandic tephras in the Kangerlussuaq Trough, southeast Greenland, during the last deglaciation. *Journal of Quaternary Science*. **17**: 747 - 757

Jeppesen, E., Agerbo Madsen, E., Jensen, J.P., and Anderson, N.J. 1996. Reconstructing the past density of planktivorous fish and trophic structure from sedimentary zooplankton fossils: a surface sediment calibration data set from 30 predominantly shallow lakes. *Freshwater Biology*. **36**: 115 - 127

Jeppesen, E., Jensen, J.P., Amsinck, S., Landkildehus, F., Lauridsen, T., and Mitchell, S.F. 2002. Reconstructing the historical changes in *Daphnia* mean size and planktivorous fish abundances in lakes from the size of *Daphnia* ephippia in the sediment. *Journal of Paleolimnology*. **27**: 133 - 143

Jochum, K.P., Nohl, U., Herwig, K., Lammel, E., Stoll, B. and Hofmann, A.W. 2005. GeoReM: A new geochemical database for reference materials and isotopic standards. *Geostandards and Geoanalytical Research*. **29**: 333 - 338.

Jochum, K.P., Stoll, B., Herwig, K., Willbold, M., Hofmann, A.W., Amini, M., Aarburg, S., Abouchami, W., Hellebrand, E., Mocek, B., Raczek, I., Stracke, A., Alard, O., Bouman, C., Becker, S., Ducking, M., Bratz, H., Klemd, R., de Bruin, D., Canil, D., Cornell, D., de Hoog, C.J., Dalpe, C., Danyushevsky, L., Eisenhauer, A., Gao, Y.J., Snow, J.E., Goschopf, N., Gunther, D., Latkoczy, C., Guillong, M., Hauri, E.H., Hofer, H.E., Lahaye, Y., Horz, K., Jacob, D.E., Kassemann, S.A., Kent, A.J.R., Ludwig, T., Zack, T., Mason, P.R.D., Meixner, A., Rosner, M., Misawa, K.J., Nash, B.P., Pfander, J., Premo, W.R., Sun, W.D.D., Tiepolo, M., Vannucci, R., Vennemann, T., Wayne, D. and Woodhead, J.D., 2006. MPI-DING reference glasses for in situ microanalysis: new reference values for element concentrations and isotope ratios. *Geochemistry Geophysics Geosystems*. **7**: doi:10.1029/2005GC001060

Jóhansen, J. 1975. Pollen diagrams from the Shetland and Faroe islands. *New phytologist*. **75**: 369 - 387

Jóhansen, J.1977. Outwash of terrestric soils into Lake Saksunarvatn, Faroe Islands. *Danmarks Geologiske Undersøgelse*. **1977**: 31 - 37

Johansen, L. 2000. The Late Palaeolithic in Denmark. In: Valentin, B., Bodu, P., Christensen, M. (eds.) L'Europe Centrale et Septentrionale au Tardiglaciaire. Confrontation des modéles régionaux de peuplement. Mémoires du Museé de Préhistoire d'Ile-de-France. **7**: pp 197 - 215

Johannsson, O.E., Leggett, M.F., Rudstam, L.G., Servos, M.R., Mohammadian, M.A., Gal, G., Dermott, R.M., and Hesslein, R.H. 2001. Diet of *Mysis relicta* in Lake Ontario as revealed by stable isotope and gut content analysis. *Canadian Journal of Fish and Aquatic Science*. **58**: 1975 - 1986

Jonsgard, B., and Birks, H.H. 1995. Late-glacial mosses and environmental reconstructions at Kråkenes, western Norway. *Lindbergia*. **20**: 64 - 82

Joosten, H. 2008. What are peatlands? – In: Parish, F., Sirin, A., Charman, D., Joosten, H., Minaeva, T., and Silvius, M. (eds.) Assessment on peatlands, biodiversity and climate change: 8–19. Kuala Lumpur, Wageningen (Global Environment Centre, Wetlands International)

Julien, M. 1982. Les harpons Magdaléniens, Supplément á Gallia Préhistoire. **17**

Kabaciński, J., Bratlund, B., Kubiak, L., Makowiecki, D., Schild, R., and Tobolski, K. 1999. The Hamburgian settlement at Mirkowice: recent results and research perspectives. *Folia Quaternaria*. **70**: 211 - 238

Kabaciński, J., and Sobkowiak-Tabaka, I. 2009. Big game versus small game hunting – subsistence strategies of the Hamburgian culture. In: Street, M., Barton, N., and Terberger, T. (eds.). Humans environment and chronology of the Late Glacial of the North European Plain. Proceedings of Workshop 14. The final Palaeolithic of the great European Plain, Lisbon, 2006. 67 - 75

Kaiser, K.F. 1993. Klimageschichte vom späten Hochglazial bis ins frühe Holozän, rekonstruiert mit Jahrringen und Molluskenschalen aus verschiedene Vereisungsgebieten. Eidgenössische Forschungsanstalt für Wald, Schnee und Landschaft, Zürich

Kaiser, K., and Terberger, T. 1996. Archäologisch-geowissenschaftliche Untersuchungen am spätpaläolithischen Fundplatz Nienhagen, Lkr. Nordvorpommern. Bodendenkmalpege in Mecklenburg-Vorpommern Jahrbuch 1995. pp 7 - 48

Kaiser, K., de Klerk, P., and Terberger, T. 1999. Die ”Riesenhirschfundstelle” von Endingen: geowissenschaftliche und archäologische Untersuchungen an einem spätglazialen Fundplatz in Vorpommern. *Eiszeitalter und Gegenwart*. **49**: 102 – 123

Kaiser, K. 2001. Die spätpleistozane bis frühholozäne Beckenentwicklung in Mecklenburg-Vorpommern – Untersuchungen zur Stratigraphie, *Geomorphologie und Geoarchäologie. – Greifswalder Geographische Arbeiten*, **24**: 1 - 259

Kaiser, K. 2004. Lake basin development in the Endinger Bruch area (Vorpommern, NE Germany) during the Late Pleistocene and Early Holocene. *Zeitschrift fur Geomorphologie*. **48**: 461 - 480

Kaiser, K., Lorenz, S., Germer, S., Juschus, O., Küster, M., Libra, J., Bens, O., and Hütti. 2012. Late Quaternary evolution of rivers, lakes and peatlands in northeast Germany reflecting past climatic and human impacts – an overview. *Quaternary Science Journal*. **61**: 103 - 132

Kanwiszer, A., and Trzeciak, P. 1984. Lodz Radiocarbon Dates I. *Radiocarbon*. **26**: 111 - 126

Kapsner, W. R., Alley, R. B., Shuman, C. A., Anandakrishnan, S., and Grootes, P. M. 1995. Dominant influence of atmospheric circulation on snow accumulation in Greenland over the past 18,000 years. *Nature*. **373**: 52 - 54.

Kattel, G., and Sirocko, F. 2011. Palaeocladocerans as indicators of environmental, cultural and archaeological developments in Eifel maar lakes region (West Germany) during the Lateglacial and Holocene periods. *Hydrobiologia*. **676**: 203 - 221

Keeley, L. 1988. Hunter-gather economic complexity and "Population Pressure": A cross-cultural analysis. *Journal of Anthropological Archaeology*. **7**: 373 - 411

Kelly, R.L. 1995. The foraging spectrum: Diversity in hunter-gatherer lifeways. Smithsonian Institution Press, Washington and London, pp. 65 - 111

Kendall, C. 1998. Tracing nitrogen sources and cycling in catchments. In: Kendall, C., and McDonnell, J.J. (eds.) Isotope Tracers in Catchment Hydrology. Elsevier Science B.V., Amsterdam. pp 519 - 576

Kenedi, C.A., Brantley, S.R., Hendley II, J.W., and Stauffer, P.H. 2000. Volcanic ash fall — a "hard rain" of abrasive particles. USGS Fact Sheet 027-00

Kerfoot, W. C.1974. Net accumulation rates and the history of cladoceran communities. *Ecology*. **55**: 51 - 61

Kerfoot, W. C. 1977. Competition in cladoceran communities: the cost of evolving defences against copepod predation. *Ecology*. **58**: 303 - 313

Kerfoot, W.C. 1981. Long-term replacement cycles in cladoceran communities: A history of predation. *Ecology*. **62**: 216-233

Kierdorf, H., and Kierdorf, U. 1997. Disturbances of the secretory stage of amelogenesis in fluorosed deer teeth: a scanning electron-microscopic study. *Cell Tissue Research*. **289**: 125 - 135

Kitagawa, H., and van der Plicht, J.1998. Atmospheric radiocarbon calibration to 45,000 yr B.P: Late Glacial fluctuations and cosmogenic isotope production. *Science*. **279**. 1187 - 1190

de Klerk, P., Helbig, H., Helms, S., Janke, W., Krügel, K., Kühn, P., Michaelis, D. and Stolze, S. 2001. The Reinberg Researches: palaeoecological and geomorphological studies of a kettle hole in Vorpommern (NE Germany), with special emphasis on a local vegetation during the Weichselian Pleniglacial/Lateglacial transition. *Greifswalder Geographische Arbeiten.* **23**: 43 - 131

de Klerk, P. 2002. Changing vegetation patterns in the Endinger Bruch area (Vorpommern, NE Germany) during the Weichselian Late Glacial and Early Holocene. *Review of Palaeobotony and Palynology*. **119**: 275 - 309

de Klerk, P., and Helbig, H. 2006. A pollen diagram from a kettle-hole near Horst (Vorpommern, NE Germany) covering the later part of the Weichselian Lateglacial. *Zeitschrift für Geologische Wissenschaften*. **34**: 379 - 387

de Klerk, P. 2008. Patterns in vegetation and sedimentation during the Weichselian Late-glacial in north-eastern Germany. *Journal of Biogeography*. **35**: 1308 - 1322

Kloss, K. 1980. Pollenanalysen zur Vegetations, Siedlungs und Moorgeschichte am Südrand der ostmecklenburgischen-brandenburgischen Seenplatte (Kreis Gransee). *Archiv für Naturschutz und Landschaftsforschung*. **20**: 203 - 212

Kloss, K. 1994. Das Pollendiagramm vom Schlangenpfuhl in Eberswalde, Kr. Barnim. Vegetations- und Siedlungsgeschichte am Südrand des Urstromstals - Materialvorlage. *Veröffentlichungen des Brandenburgischen Landesmuseums für Ur- und Frühgeschichte*. **28**: 99 - 104

Koç, N., and Jansen, E. 1992. A high resolution diatom record of the last deglaciation from the SE Norwegian Sea: documentation of rapid climatic changes. *Palaeoceanography*. **7**: 499 - 520

Kollau, W. 1943. Zur Osteologie des Rentiers (nach den Funden von Stellmoor in Holstein). In: Rust, A. (ed.) Die alt- und mittelsteinzeitlichen Funde von Stellmoor. *Wachholtz Verlag, Neumünster*: pp. 60 - 105

Kolstrup, E. 1982. Late-glacial pollen diagrams from Hjelm and Draved Mose (Denmark) with a suggestion of the possibility of drought during the Earlier Dryas. Review Palaebotony and Palynology. **36**: 35 - 63

Kolstrup, E. 1991. Palaeoenvironmental developments during the Late Glacial of the Weichselian. In: Barton, N., Roberts, A.J.., and Roe, D.A. (eds.) The Late Glacial in north-west Europe: human adaption and environmental change at the end of the Pleistocene. *Council for British Archaeology Research Report*. **77**: 1 - 6

Kolstrup, E. 1999. Some classical methods used for reconstruction of Lateglacial environments in the European plain: potentials and limitations. In: Bratlund, B., Eriksen, B.V. (eds.) Recent Studies in the Final Palaeolithic of the European Plain. Jutland Archaeological Society, Aarhus

Korhola, A. 1999. Distribution patterns of Cladocera in subarctic Fennoscandian lakes and their potential in environmental reconstruction. *Ecography*. **22**: 357 - 373

Korhola, A., and Rautio, M. 2001. Cladocera and other branchiopod crustaceans. In: Smol, J.P., Birks H.J.B and Last, W.M. (eds.) Tracking Environmental Change Using Lake Sediments Volume 4: Zoological Indicators. Kluwer Academic Publishers, Dordrecht, the Netherlands, pp 5 - 41

Korhola, A., Tikkanen, M., and Weckström, J. 2005. Quantification of Holocene lake-level changes in Finnish Lapland using a cladocera – lake depth transfer model. *Journal of Paleolimnology*. **34**: 175 - 190

Korponai, J., Magyari, E.K., Buczkó, K., Iepure, S., Namiotko, T., Czakó, D., Kövér, C., and Braun, M. 2011. Cladocera response to Late Glacial to Early Holocene climate change in a south Carpathian mountain lake. *Hydrobiologia*. **676**: 223 - 235

Kozłowski, S.K., Połtowicz-Bobak, M., Bobak, D., and Terberger, T. 2012. New information from Maszycka Cave and the Late Glacial recolonisation of Central Europe. *Quaternary International*. **272-273**: 288 - 296

Krause, W. 1937. Die eiszeitlichen Knochenfunde yon Meiendorf. In: Rust, A. (ed.) Das altsteinzeitliche Rentierjagderlager Meiendorf. Karl Wachholtz Verlag: Neumünster, pp 48 - 61

Kroeber, A. 1939. Cultural and Natural areas of Native North America. University of California Publications in American Archaeology and Ethnology 38. Berkley

Krzywicki, L. 1934 Primitive Society and Its Vital Statistics. London: Macmillan and Co Kuehn, S.C., Froese, D.G., Shane, P.A.R., and INTAV intercomparison participants 1. 2011. The INTAV intercomparison of electron-beam microanalysis of glass by tephrochronology laboratories: Results and recommendations. *Quaternary International*. **246**: 19 - 47

Kulesza, P., Suchora, M., Pidek, I.A., and Alexandrowicz, W.P. 2011. Chronology and directions of Late Glacial palaeoenvironmental changes: A multi-proxy study on sediments of Lake Słone (SE Poland). *Quaternary International*. **238**: 89 - 106

Kurek, J., Korosi, J.B., Jeziorski, A., and Smol, J.P. 2010. Establishing reliable minimum count sizes for cladoceran subfossils sampled from lake sediments. *Journal of Paleolimnology*. **44**: 603 - 612

Lagerlund, E., and Houmark-Nielsen M. 1993. Timing and pattern of the last deglaciation in the Kattegat region, southwest Scandinavia. *Boreas*. **22**: 337 - 347

Lamb, A.L., Leng, M.J., Mohammed, M.U., and Lamb, H.F. 2004. Holocene climate and vegetation change in the Main Ethiopian Rift Valley, inferred from the composition (C/N and $\delta^{13}C$) of lacustrine organic matter. *Quaternary Science Reviews*. **23**: 881 - 891

Lamers, L.P.M., Bobbink, R., and Roelofs, JG.M. 2000. Natural nitrogen filter fails in polluted raised bogs. *Global Change Biology*. **6**: 583 - 586

Lane, C.S., Andric, M., Cullen, V.L., and Blockley, S.P.E. 2011a. The occurrence of distal Icelandic and Italian tephra in the Lateglacial of Lake Bled, Slovenia. *Quaternary Science Reviews.* **30**: 1013 - 1018

Lane, C.S., De Klerk, P., Cullen, V.L. 2011b. A tephrochronology for the Lateglacial palynological record of the Endinger Bruch (Vorpommern, north-east Germany). *Journal of Quaternary Science* **27**: 141 - 149

Lane, C.S., Blockley, S.P.E., Mangerud, J., Smith, V.C., Lohne, Ø.S., Tomlinson, E.L., Matthews, I.P., and Lotter, A.F. 2011c. Was the 12.1 ka Icelandic Vedde Ash one of a kind? *Quaternary Science Reviews*. **33**: 87 - 99

Lange, E., Jeschke, L., and Knapp, H.D. 1986. Ralswiek und Rügen. Landschaftsentwicklung und Siedlungsgeschichte der Ostseeinsel. Teil I: Die Landschaftsgeschichte der Insel Rügen seit dem Spätglazial. Akademie Verlag, Berlin

Lanting, J.N., and Van der Plicht, J. 1996. De ^{14}C chronology van de Nederlandser pre en protohistorie I: Laat-Paleolithicum. *Palaeohistoria*. Netherlands, pp. 71 - 127

Larsen, G., Newton, A.J., Dugmore, A.J., Vilmundardóttir, E.G. 2001. Geochemistry, dispersal, volumes and chronology of Holocene silicic tephra layers from the Katla volcanic system, Iceland. *Journal of Quaternary Science*. **16**: 119 - 132

Latałowa, M. 1992. Man and vegetation in the Pollen diagrams from Wolin Island (NW Poland). *Acta Palaeobotanica*. **32**: 123 - 249

Le Bas, M.J., Le Maitre, R.W., Streckeisen, A., and Zanettin, B. 1986. A chemical classification of volcanic rocks based on the total alkali-silica diagram. *Journal of Petrology* **27**: 745 - 750

Lee, R.B. 1968. What hunters do for a living, or, how to make out on scarce resources. In: Lee, R.B., and Devore, I. (eds.) Man the Hunter. Aldine, Chicago. pp 30 - 48

Leesch, D., Müller, W., Nielsen, E., and Bullinger, J. 2012. The Magdalenian in Switzerland: re-colonization of a newly accessible landscape. *Quaternary International*. **272-273**: 191 - 208

Li, L., Yu, Z., Moeller, R.E., and Bebout, G.E. 2008. Complex trajectories of aquatic and terrestrial ecosystem shifts caused by multiple human-induced environmental stresses. Geochimica. Cosmochimica. Acta. **72**: 4338 - 4351

Liljegren, R. 1994. Late Glacial fauna in South Sweden. Paper presented at the conference: *Earliest Settlement of Scandinavia*. Ystad

Liljegren, R., and Ekström, J. 1996. The terrestrial Late Glacial fauna in South Sweden. *Acta Archaeologica Lundensia Series in 8°*. **24**: 135 - 139

Limpens, J., and Berendse, F. 2003. Growth reduction of *Sphagnum magellanicum* subjected to high nitrogen deposition: the role of amino acid nitrogen concentration. *Oecologia*. **135**: 339 - 345

Lind, E.M., and Wastegård, S. 2011. Tephra horizons contemporary with short early Holocene climate fluctuations: New results from the Faroe Islands. *Quaternary International*. **24:** 157 - 167

Litt, T., and Stebich, M. 1999. Bio and chronostratigraphy of the Lateglacial in the Eifel region. *Quaternary International*. **61**: 5 - 16

Litt, T., Brauer, A., Goslar, T., Merkt, J., Balaga, K., Müller, H., Ralska-Jasiewiczowa, M., Stebich, M., and Negendank, J.F.W. 2001. Correlation and synchronisation of Lateglacial continental sequences in northern central Europe based on annually laminated lacustrine sediments. *Quaternary Science Reviews*. **20**: 1233 - 1249

Loewe, G. 1998. Kreis Schleswig. Text - und Kartenband. *Archäologische Denkmäler Schleswig-Holsteins*. **8**

Lohne, Ø.S., Mangerud, J., Birks,. H.H. 2013. Precise 14C ages of the Vedde and Saksunarvatn ashes and the Younger Dryas boundaries from western Norway and their comparison with the Greenland Ice Core (GICC05) chronology. *Journal of Quaternary Science*. **28**: 490 - 500

Lotter, A.F., and Birks, H.J.B. 1993. The impact of the Laacher See Tephra on terrestrial and aquatic ecosystems in the Black Forest, southern Germany. *Journal of Quaternary Science*. **8**: 263 - 276

Lotter, A.F., Merkt, J., and Strum, M. 1997. Differential sedimentation *versus* coring artifacts: a comparison of two widely used piston-coring methods. *Journal of Paleolimnology*. **18**: 75 - 85

Lotter, A.F., Walker, I.R., Brooks, S.J., and Hofmann, W. 1999. An international comparison of chironomid palaeotemperature inference models: Europe vs. North America. *Quaternary Science Reviews*. **18**: 717 - 735

Lotter, A.F. 2001. The palaeolimnology of Soppensee (Central Switzerland), as evidenced by diatom, pollen, and fossil-pigment analyses. *Journal of Paleolimnology*. **25**: 65 - 79

Lowe, J.J. and Gray, J.M. 1980. The stratigraphic subdivision of the Late Glacial of NW Europe: a discussion. In: Lowe, J.J., Gray, J.M., Robinson, J.E. (eds.) Studies in the Late Glacial of north-west Europe. Including papers presented at a symposium of the Quaternary Research Association held at University College London, January 1979, pp 157 - 175

Lowe, J.J., Ammann, B., Birks, H.H., Björck, S., Coope, G.R., Cwynar, L.C., de Beaulieu, J. L., Mott, R.J., Peteet, D.M., and Walker, M.J.C. 1994. Climatic changes in areas adjacent to the North Atlantic during the last glacial–interglacial transition (14–9 ka BP) a contribution to IGCP-253. *Journal of Quaternary Science*. **9**: 185 - 198

Lowe, J.J., and Turney, C.S.M. 1997. Vedde Ash layer discovered in a small lake basin on the Scottish mainland. *Journal of the Geological Society of London*. **154**: 605 - 612

Lowe, J. J., Hoek, W. Z., and INTIMATE group. 2001. Inter-regional correlation of palaeoclimatic records for the Last Glacial-Interglacial transition: a protocol for improved precision recommended by the INTIMATE project group. *Quaternary Science Reviews*. **20**: 1175 - 1187

Lowe, J.J., Blockley, S., Trincardi, F., Asioli, A., Cattaneo, A., Matthews, I.P., Pollard, M., and Wulf, S. 2007. Age modelling of late Quaternary marine sequences in the Adriatic: Towards improved precision and accuracy using volcanic event stratigraphy. *Continental Shelf Research*. **27**: 560 - 582

Lowe, J. J., Rasmussen, S.O., Björck, S., Hoek, W.Z., Steffensen, J.P., Walker, M.J.C., Yu, Z.C., and INTIMATE group. 2008. Synchronisation of palaeoenvironmental events in the North Atlantic region during the Last Termination: a revised protocol recommended by the INTIMATE group. *Quaternary Science Reviews*. **27**: 6 - 17

Lücke, A., Schleser, G.H., Zolitschka, B., and Negendank, J.F.W. 2003. A Lateglacial and Holocene organic carbon isotope record of lacustrine palaeoproductivity and climatic change derived from varved lake sediments of Lake Holzmaar, Germany. *Quaternary Science Reviews*. **22**: 569 - 580

Lücke, A., and Brauer, A. 2004. Biogeochemical and micro-facial fingerprints of ecosystem response to rapid Late Glacial climatic changes in varved sediments of Meerfelder Maar (Germany). *Palaeogeography, Palaeoclimatology, Palaeocology*. **211**: 139 - 155

Lücke, A. 2007. Abrupt climate changes of the Late Glacial and seasonality: Evidences from varved lake sediments of Western Europe. *Geophysical Research Abstracts*. **9**

Mace, A. 1959. An Upper Palaeolithic open-site at Hengistbury Head, Christchurch, Hants. *Proceedings of the Prehistoric Society*. **25**: 233 - 259

Mack, R.N. 1981. Initial effects of ashfall from Mount St. Helens on vegetation in eastern Washington and adjacent Idaho. *Science*. **213**: 537 - 539

Madsen, B. 1996. Late Palaeolithic cultures of south Scandinavia: tools, traditions and technology. In: Larsson, L. (ed.) The Earliest Settlement of Scandinavia and Its Relationship with Neighbouring Areas. Almqvist & Wiksell, Stockholm, pp. 61 - 73

Malyarchuk, B., Derenko, M., Grzybowski, T., Perkova, M., Rogalla, U., Vanecek, T., and Tsybovsky, I. 2010. The peopling of Europe from the mitochondrial haplogroup U5 perspective*. PLoS ONE* **5**: e10285

Mandryk, S.A. 1993. Hunter-gatherer social costs and the nonviability of submarginal environments. *Journal of Anthropological Research*. **49**: 39 - 71

Mangerud, J., Andersen, S.T., Berglund, B.E., and Donner, J.J. 1974. Quaternary stratigraphy of Norden, a proposal for terminology and classification. *Boreas*. **3**: 109 - 128

Mangerud, J., Lie, S.E., Furnes, H., Kristiansen, I.L., and Lømo, L. 1984. A Younger Dryas ash bed in western Norway and its possible correlations with tephra in cores from the Norwegian Sea and the North Atlantic. *Quaternary Research*. **21**: 85 - 104

Mangerud, J., Furnes, H., and Johansen, J. 1986. A 9,000 year old ash bed on the Faroe Islands. *Quaternary Research*. **26**: 262 - 265

Manne, T., Cascalheira, J., Évora, M., Marreiros, J., and Bicho. 2012. Intensive subsistence practices at Vale Boi, an Upper Palaeolithic site in southwestern Portugal. *Quaternary International*. **264**: 83 - 99

Mark, D.F., Petraglia, M., Smith, V.C., Morgan, L.E., Barfod, D.N., Ellis, B.S., Pearce, N.J., Pal, J.N., and Korisettar, R. 2013. A high-precision $^{40}Ar/^{39}Ar$ age for the Young Toba Tuff and dating of ultra-distal tephra: Forcing of Quaternary climate and implications for hominin occupation of India. *Quaternary Geochronology*. In press.

Mathiassen, T.1946. En senglacial Boplads ved Bromme. *Aarbøger for nordisk Oldkyndighed og Historie*. **1946**: 121 - 197

Mathews, A. 2000. Palynologische Untersuchungen zur Vegetationsentwicklung im Mittelelbegebiet. *Telma*. **30**: 9 - 42

Mayer, B., and Schwark, L. 1999. A 15,000-year stable isotope record from sediments of Lake Steisslingen, Southwest Germany. *Chemical Geology*. **161**: 315 - 337

Meding, M.E., and Jackson, L.J. 2003. Biotic, chemical and morphological factors contributing to winter anoxia in prairie lakes. *Limnology and Oceanography*. **48**: 1633 - 1642

Mellars, P.1996. *The Neanderthal legacy*. Princeton: Princeton University Press

Menke, B. 1983. Palynologische Befunde. In: Bokelmann, K., Heinrich, D., and Menke, B. (eds.) Fundplätze der spätglazials am Hainholz-Esinger Moor, Kreis Pinneberg. *Offa*. **40**: 199 - 239

Merkt, J., Muller, H., Knabe, W., Muller, P., and Weiser, T. 1993. The early Holocene Saksunarvatn Tephra found in lake sediments in N.W. Germany. *Boreas*. **22**: 93 - 100

Merkt, J., and Muller, H. 1999. Varve chronology and palynology of the Lateglacial in northwest Germany from lacustrine sediments of Hämelsee in Lower Saxony. *Quaternary International*. **61**: 41 - 59

Meyers, P.A., and Ishiwatari, R. 1993. The early diagenesis of organic matter in lacustrine sediments. In: Engel, M.H., and Macko, S.A. (eds.) Organic Geochemistry. Principles and Applications. Plenum Press, New York, pp 185 - 209

Meyers, P.A. 1997. Organic geochemical proxies of paleoceanographic, paleolimnologic, and paleoclimatic processes.*Organic Geochemistry*. **27**: 213 - 250.

Meyers, P.A. 2003. Application of organic geochemistry to palaeolimnological reconstructions: a summary of examples from the Laurentian Great Lakes. *Organic Geochemistry*. **34**: 261 - 289

Miller, R. 2012. Mapping the expansion of the Northwest Magdalenian. *Quaternary International*. **272-273**: 209 - 230

Möller, C. 1975. Ein Rentierwirbel mit eingeschossener Feuersteinpfeilspitze aus der Ahrensburger Fundschicht von Stellmoor. *Hammaburg neue Folge*. **2**: 93 - 94

Morin, E. 2008. Evidence for declines in human population densities during the early Upper Palaeolithic in western Europe. *Proceedings of the National Academy of Science*. **105**: 48 - 53

Mortensen, A.K., Bigler, M., Gronvold, K., Steffensen, J.P., and Johnsen, S.J. 2005. Volcanic ash layers from the Last Glacial termination in the NGRIP ice core. *Journal of Quaternary Science*. **20**: 209 - 219

Mortensen, M.F. 2007. Biostratigraphy and chronology of the terrestrial late Weichselian in Denmark - New investigations of the vegetation development based on pollen and plant macrofossils in the Slotseng basin. *Ph.D. thesis, Aarhus University, Denmark*. **30**: 1396 - 5263

Mortensen, M.F., Birks, H.H., Christensen, C., Holm, J., Noe-Nygaard, N., Odgaard, B.V., Olsen, J., and Rasmussen, K.L. 2011. Lateglacial vegetation development in Denmark – New evidence based on macrofossils and pollen from Slotseng, a small-scale site in southern Jutland. *Quaternary Science Reviews*. **30**: 2534 - 2550

Müller, H.M.1961a. Ein Pollendiagramm aus dem Äppelbruch bei Eberswalde (Ein Beitrag Zur Waldentwicklung). *Archiv für Forstwesen.* **10**: 809 - 816

Müller, H.M. 1961b. Pollenanalytische Untersuchungen im Bereich des Meßtischblattes Thurow/Südostmecklenburg. PhD-thesis, Halle University, Germany

Müller, H.M. 1965. Vorkommen spätglazialer Tuffe in Nordostdeutschland. *Geologie*. **14**: 1118 - 1123

Müller, H.M. 1967. Das Pollendiagramm “Serwest”, ein Beitrag zur Wechselwirkung natürlicher und anthropogener Faktoren in der Vegetationsentwicklung. *Feddes Repertorium*. **74**: 123 - 137

Müller, U.C., Pross, J., and Bibus, E. 2003. Vegetation response to rapid climate change in Central Europe during the past 140,000 yr based on evidence from the Füramoos pollen record. *Quaternary Research*. **59**: 235 - 245

Müller, W., Shelley, M., Miller, P., and Broude S. 2009. Initial performance metrics of a new custom-designed ArF excimer LA-ICP-MS system coupled to a two-volume laser-ablation cell. *Journal of Analytical Atomic Spectrometry*. **24**: 209 - 214

Naughton, F., Sanchez Goñi, M.F., Desprat, S., Turon, J.L., Duprat, J., Malaize, B., Joli, C., Cortijo, E., Drago, T., and Freitas, M.C. 2007. Present-day and past (last 25 000 years) marine pollen signal off western Iberia. *Marine Micropaleontology*. **62**: 91 - 114

Nakagawa, T., Gotanda, K., Haraguchi, T., Danhara, T., Yonenobu, H., Brauer, A., Yokoyama, Y., Tada, R., Takemura, K., Staff, R., Payne, R., Bronk Ramsey, C., Bryant, C., Brock, F., Schlolaut, G., Marshall, M, Tarasov, P, Lamb, H., and Suigetsu 2006 Project Members 1. SG06, a fully continuous and varved sediment core from Lake Suigetsu, Japan: Stratigraphy and potential for improving the radiocarbon calibration model and understanding of late Quaternary climate changes. *Quaternary Science Reviews*. **36**: 164 - 176

Newcomb, T.W., and Flagg, T.A. 1982. Some effects of Mount St. Helens volcanic ash on juvenile salmon smolts. *Northwest and Alaska Fisheries Center National Marine Fisheries Service National Oceanic and Atmospheric Administration 2725 Montlake Boulevard East Seattle, Washington 98112*

Nichols, S.J., and Garling, D. 2000. Food-web dynamics and trophic-level interactions in a multispecies community of freshwater unionids. *Canadian Journal of Zoology*. **78**: 871 - 882

Nijenhuis, I.A., and de Lange, G.J. 2000. Geochemical constraints on Pliocene sapropel formation in the eastern Mediterranean. *Marine Geology*. **163**: 41 - 63

Nilsson, T. 1961. Ein neues Standardpollendiagramm aus Bjärsjö holmssjön in Schonen. *Lunds Universitet Årskr N.F*. **2**: pp. 80

Nitz, B., Schirrmeister, L., and Klessen, L. 1995. Spatglazial-altholozane Landschaftsgeschichte auf dem nordlichen Barnim – zur Beckenentwicklung im nordostdeutschen Tiefland. *Petermanns Geographische Mitteilungen*. **139**: 143 - 158

Noe-Nygaard, N., Knudsen, K.L., Houmark-Nielsen, M. 2006. Fra istid til og med Jægerstenalder. In: Larsen, G. (ed.) Naturen I Danmark. Geologien, first ed. Gyldendal, Copenhagen.

Olsen, J., Björck, S., Leng, M.L., Gudmundsdóttir, E.R., Odgaard, B.V., Lutz, C.M., Kendrick, C.P., Andersen, T.J., and Seidenkrantz, M.S. 2010. Lacustrine evidence of Holocene environmental change from three Faroese lakes: a multiproxy XRF and stable isotope study. *Quaternary Science Reviews*. **29**: 2764 - 2780

Osmond, C.B., Valaane, N., Haslam, S.M., Uotila, P., and Roksandic, Z.1981. Comparisons of $\delta^{13}C$ values in leaves of aquatic macrophytes from different habitats in Britain and Finland; some implications for photosynthetic processes in aquatic plants. *Oecologia*. **1981**:117 - 124

Pala, M., Achilli, A., Olivieri, A., Kashani, B. H., Perego, U. A., Sanna, D., Metspalu, E., Tambets, K., Tamm, E., Accetturo, M., Carossa, V., Lancioni, H., Panara, F., Zimmermann, B, Huber, G., Al-Zahery, N., Brisighelli, F., Woodward, S.R., Francalacci, P., Parson, W., Salas, A., Behar, D.M., Villems, R., Semino, O., Bandelt, H.J. and Torroni, A. 2009. Mitochondrial haplogroup U5b3: a distant echo of the Epipaleolithic in Italy and the legacy of the early Sardinians. *American Journal of Human Genetics*. **84**: 814 - 821

Pardiñas, A.F., Roca, A., Garcia-Vazquez, E., and Lopez, B. 2012. Mitochondrial diversity patterns and the Magdalenian resettlement of Europe: new insights from the edge of the Franco-Cantabrian refuge. *Journal of Human Genetics*. **57**: 717 - 726

Parplies, J., Lücke, A., Vos, H., Mingram, J., Stebich, M., Radtke, U., Han., and Schleser, G.H. 2008. Late Glacial environmental and climate development in northeastern China derived from geochemical

and isotopic investigations of the varved sediment record from Lake Sihailongwan (Jilin Province). *Journal of Palaeolimnology*. **40**: 471 - 487

Pasda, C. 2001. Das Knochengerät vom spätpaläolithischen Fundplatz Kleinlieskow in der Niederlausitz. In: Gehlen, B., Heinen, M., and Tillmann, A. (eds.) Zeit-Räume. Gedenkschrift für Wolfgang Taute. *Archäologische Berichte.* **14/2**: 397 - 408

Passarino, G., Cavalleri, G.L., Lin, A.A., Cavalli-Sforza, L.L., Borresen-Dale, A.L., and Underhill, P.A. 2002. Different genetic components in the Norwegian population revealed by the analysis of mtDNA and Y chromosome polymorphisms. *European Journal of Human Genetics*. **10**: 521 - 529

Pearson, M.C., and Rodgers, J.A. 1962*. Hippophaë rhamnoides* L. *Journal of Ecology*. **50**: 501 - 513

Pedersen, K.B. 2009. Stederne Og Menneskene. Istidsjægere omkring Knudshoved Odde. Forlaget Museerne.dk, Vordingborg

Pelegrin, L.J. 2000. Les techniques de débitage laminaire au Tardiglaciaire: critères de diagnose et quelques reflexions. In: Valentin, B., Bodu, P., and Christensen, M. (eds.) L'Europe central et septentrionale au Tardiglaciaire. Confrontation des modèles régionaux de peuplement. *Mémoires du Musée Préhistoire d'Ile de France.* **7**: 73 - 86

Pennington, W. (Mrs T.G. Tutin). 1986. Lags in adjustment of vegetation to climate caused by the pace of soil development. Vegetation. **67**: 105 - 118

Petersen, P.V., and Johansen, L. 1993. Sølbjerg I - an Ahrensburgian site on a reindeer migration route through eastern Denmark. *Journal of Danish Archaeology*. **10**: 20 - 37

Petersen, P.V. 2006. White flint and hilltops – Late Palaeolithic finds in southern Denmark. In: Hansen, K.M., and Pedersen, K.B. (eds.) Across the western Baltic. Proceedings from an archaeological conference in Vordinborg. Sydsjællands Museums Publikationer I. 57 - 74

Pettitt, P.B., Davies, W., Gamble, C.S., and Richards, M.B. 2003. Palaeolithic radiocarbon chronology: quantifying our confidence beyond two half-lives. *Journal of Archaeological Science*. **30**: 1685 - 1693

Pittioni, R., 1955. Die Funde aus der Zigeunerhöhle im Hausberg bei Gratkorn, Steiermark. **5**: 12 - 24

Pokines, J. T., and Krupa, M. 1997. Self-barbed antler spear-points and evidence of fishing in the Late Upper Paleolithic of Cantabrian Spain. In: Knecht, H. (ed.) Projectile Technology. New York: Plenum Publishing, pp. 241 - 262

Pons, A., and Reille, M. 1986. Nouvelles recherches pollenanalytiques à Padul (Granada): La fin du dernier glaciaire et l'Holocène. In: López-Vera, E (ed.) Quaternary Climate in Western Mediterranean. University Autónoma de Madrid. 405 - 420

Rasmussen, S.O., Andersen, K.K., Svensson, A.M., Steffensen ,J.P., Vinther, B.M., Clausen, H.B., Siggaard-Andersen, M.L., Johnsen, S.J., Larsen, L.B., Bigler, M., Röthlisberger, R., Fischer, H., Goto-Azuma, K., Hansson, M.E., Ruth, U. 2006. A new Greenland ice core chronology for the last glacial termination. *Journal of Geophysical Research*. **111**: (D06102, doi: 10.1029/2005JD006079)

Rasmussen, T.L., Thomsen, E., Nielsen, T., and Wastegård, S. 2011. Atlantic surface water inflow to the Nordic seas during the Pleistocene-Holocene transition (mid-late Younger Dryas and Pre-Boreal periods, 12 450-10 000 a BP). *Journal of Quaternary Science*. **26**: 723 - 733

Rau, G.H. 1978. Carbon-13 depletion in a subalpine lake: carbon flow implication. *Science*. **201**: 901 - 902

Rau, G.H., Arthur, M.A., and Dean, W.E. 1987. $^{15}N/^{14}N$ variations in Cretaceous Atlantic sedimentary sequences: implication for past changes in marine nitrogen biogeochemistry. *Earth and Planetary Science Letters*. **82**: 269 - 279

Reimer, P.J., Baille, M.G.L., Bard, E., Bayliss, A., Beck, W.J., Blaauw, M., Blackwell, P.G., Bronk Ramsey, C., Buck, C.E., Burr, G.S., Edwards, R.L., Friedrich, M., Grootes, P.M., Guilderson, T.P., Hajdas, I., Heaton, T.J., Hogg, A.G., Hughen, K.A., Kaiser, K.F., Kromer, B., McCormac, F.G., Manning, S.W., Reimer, R.W., Richards, D.A., Southon, J.R., Talamo, S., Taylor, F.W., Turney, C.S.M., van der Plicht, J., and Weyhenmeyer, C.E. 2009. Progress in the extension and update of the IntCal04, and SHCal04 radiocarbon calibration curves. *Oral presentation, 20th International Radiocarbon Conference*. Big Island, Hawaii, USA, 31st May – 5th June 2009

Renssen, H., and Isarin, R.F.B. 2001. The two major warming phases of the last deglaciation at ~14.7 and ~11.5 ka cal BP in Europe: climate reconstructions and AGCM experiments. *Global and Planetary Change*. **30**: 117 - 153

Richard, C., Pennarun, E., Kivisild, T., Tambets, K., Tolk, H.V., Metspalu, E., Reidla, M., Chevalier, S., Giraudet, S., Barać Lauc, L., Peričić, M., Rudan, P., Claustres, M., Journel, H., Dorval, I., Müller, C., Villems, R., Chaventre, A., and Moisan, J.P. 2007. An mtDNA perspective of French genetic variation.*Annuals of Human Biology*. **34**: 68 - 79

Richards, M.P., and Trinkaus, E. 2009. Isotopic evidence for the diets of European Neanderthals and early modern humans. *Proceedings of the National Academy of Sciences*. **106**: 16034 - 16039

Riebesell, U., Wolf-Gladrow, D.A., and Smetacek, V. 1993. Carbon dioxide limitation of marine phytoplankton growth rates. *Nature*. **361**: 249 - 251

Riede, F. 2008. The Laacher See-eruption (12,920 BP) and the material culture change at the end of the Allerød in Northern Europe. *Journal of Archaeological Science*. **35**: 591 - 599

Riede, F., and Wheeler, J.M. 2009. Testing the 'Laacher See Hypothesis': tephra as a dental abrasive. *Journal of Archaeological Science*. **36**: 2384 - 2391

Riede, F., Grimm, S.B., Weber, M.J., and Fahlke, J.M. 2010. Neue Daten für alte Grabungen. Ein Beitrag zur spätglazialen Archäologie und Faunengeschichte Norddeutschlands. *Archäologisches Korrespondenzblatt*. **40:** 297 - 316

Riede, F., Bazely, O., Newton, A.J., and Lane, C.S. 2011. A Laacher See-eruption supplement to Tephrabase: Investigating distal tephra fallout dynamics. *Quaternary International*. **246**: 134 - 144

Riede, F., and Edinborough, K. 2012. Bayesian radiocarbon models for the cultural transition during the Allerød in southern Scandinavia. *Journal of Archaeological Science*. **39**: 744 - 756

Roucoux, K.H., Abreu, de. L., Shackelton, N.J., Tzedakis, P.C. 2005. The response of NW Iberian vegetation to North Atlantic climate oscillations during the last 65 kyr. *Quaternary Science Reviews*. **24**: 1637 - 1653

Rust, A. 1937. Das altsteinzeitliche Renntierjägerlager Meiendorf. *Krl Wachholtz Verlag*. pp. 146

Rust, A. 1941-42. Ueber die endglaziale Kulturentwicklung im rechtselbischen nordwesteuropa, unter Berücksichtigung der geologischen und siedlungsarchäologischen Verhältnisse. *Offa*. **6/7**: 52 - 75

Rust, A. 1943. Die alt und mittelsteinzeitlichen Funde von Stellmoor. *Karl Wachholtz Verlag*. pp. 240

Salmaso, N. 2002. Ecological patterns of phytoplankton assemblages in Lake Garda: seasonal, spatial and historical features. *Journal of Limnology*. **61**: 95 - 115

Salo, J., Walls, M., Rajasilta, M., Sarvala, J., Räsänen, M., and Salonen, V.P. 1989. Fish predation and reduction in body size in a cladoceran population: palaeoecological evidence. *Freshwater Biology*. **21**: 217 - 221

Sarmaja-Korjonen, K., and Alhonen, P. 1999. Cladoceran and diatom evidence of lake-level fluctuations from a Finnish lake and the effect of aquatic-moss layers on microfossil assemblages. *Journal of Paleolimnology*. **22**: 277 - 290

Sarmaja-Korjonen, K. 2001. Correlation of fluctuations in cladoceran planktonic: littoral ratio between three cores from a small lake in southern Finland: Holocene water-level changes. *The Holocene*. **11**: 53 - 63

Šatavičius, E. 2004. Bromės (liungbiu) kultūra Lietuvoje. *Lietuvos Archeologija*. **25:** 17 - 44

Schumacher, W., and Endtmann, E. 1998. Umweltreflexionen eines soligenen Kesselmoores auf Rügen. Project report, Greifswald University

Schaub, M., Kaiser, K.F., Frank, D.C., Büntgen, U., Kromer, B., and Talamo, S. 2008. Environmental change during the Allerød and Younger Dryas reconstructed from Swiss tree-ring data. *Boreas*. **37**: 74 - 86

Scheer, A. 1993. The organization of lithic resource use during the Gravettian in Germany. In: Knecht, H., Pike-Tay, A., and White, R. (eds.) Before Lascaux. The Complex Record of the Early Upper Palaeolithic. Boca Raton, pp. 193 - 210

Schild, R. 1975. Terminal Palaeolithic, in Prahistoria ziem polskich I (Ossolineum, Wroctaw Warsaw-Cracow-Gdadsk). 159 - 338

Schild, R. 1984. Terminal Palaeolithic of the North European Plain: A review of lost chances, potential, and hopes. *Advances in World Archaeology*. **3**: 193 - 274

Schmincke, H.U., Park, C., and Harms, E. 1999. Evolution and environmental impacts of the eruption of Laacher See Volcano (Germany) 12,900 a BP. *Quaternary International*. **61**: 61 - 72

Schuler, A. 1994. Die Schussenquelle-Eine Freilandstation des Magdalénien in Oberschwaben. *Materialhefte zur Archäologie in Baden-Württemberg*. **27**: Stuttgart

Schulz, W. 1998. Streifzüge durch die Geologie des Landes Mecklenburg-Vorpommern. cw Verlagsgruppe, Schwerin

Schulze, P.C. 2011. Evidence that fish structure the zooplankton communities of turbid lakes and reservoirs. *Freshwater Biology*. **56**: 352 - 365

Schwabedissen, H. 1937. Die Hamburger Stufe im nordwestlichen Deutschland. *Offa*. **2**: 1 - 30

Schwabedissen, H. 1954. Die Federmessergruppen des nordwesteuropäischen Flachlandes. Zur Ausbreitung des Spät-Magdalénien. Neumünster: Karl Wachholtz Verlag

Schwantes, G. 1932. Eine neue jungpaläolithische Zivilisation in Holstein. *Nachrichtenblatt für deutsche Vorzeit*. **8**: 183 - 187

Schwark, L., Zink, K., and Lechterbeck, J. 2002. Reconstruction of postglacial to early Holocene vegetation history in terrestrial Central Europe via cuticular lipid biomarkers and pollen records from lake sediments. *Geology*. **30**: 463 - 466

Schwendler, R.H. 2012. Diversity in social organization across Magdalenian Western Europe ca. 17-12,000 BP. *Quaternary International*. **272-273**: 333 - 353

Scourfield, D. J., and Harding, J.P. 1966. A key to the British species of freshwater Cladocera. Freshwater Biological Association. Scientific Publication. 5, 3rd ed. pp. 55

Sharma, S., Mora, G., Johnston, J.W., and Thompson, T.A. 2005. Stable isotope ratios in swale sequences of Lake Superior as indicators of climate and lake level fluctuations during the Late Holocene. *Quaternary Science Reviews*. **24**: 1941 - 1951

Shen, J., Liu, X., Matsumoto, R., Wang, S., and Yang, X. 2005. A high-resolution climatic change since the Late Glacial Age inferred from multi-proxy of sediments in Qinghai Lake. *Science in China series*. **48**: 742 - 751

Sigurgeirsson, M.A., and Leosson, M.A.1993. Two early Holocene tephra layers in the Sogamyri peat deposit. Reykjavik. *Nátturufrædingurinn*. **62**: 129 - 137

Simoneit, B., and Veil, S. 1999. Gadenstedt FStNr.121, Gde Lahstedt, Ldkr. Peine, Reg. Bez. BS. Nachrichten aus Niedersachsens Urgeschichte. *Beiheft*. **2**: 10 - 12

Sin, A.W.C., and Chiu, T.L. 1982. Summer and winter kills in fish ponds of Hong Kong and their possible prediction. *Aquaculture*. **29**: 125 - 135

Sinitsyna, G. 2002. Lyngby points in Eastern Europe. *Archaeologia Baltica*. **5**: 83 - 94

Sjøholm, J., Sejrup, H.P., and Furnes, H. 1991. Quaternary volcanic ash zones on the Iceland Plateau, southern Norwegian Sea. *Journal of Quaternary Science*. **6**: 159 - 173

Skogen, A.1972. The *Hippophaë rhamnoides* alluvial for est at Leinöra, central Norway. A phytosociological and ecological study. *K. Norske Vidensk. Selsk*. *Skr*. **4**: 1 - 115

Smith, C.H. 1992. Late Stone Age hunters of the British Isles. London

Soares, P., Achill, A., Semino, O., Davies, W., Macaulay, V., Bandelt, H.J., Torroni, A., and Richards, M.B. 2010.The Archaeogenetics of Europe. *Current Biology*. **20**: 174 - 183

Aaris Sørensen, K. 1988. Danmarks Forhistoriske Dyreverden. Frasidste Istid til vikingetid: Copenhagen. Gyldendal

Solhøy, I. W., and Solhøy, T. 2000. The fossil oribatid mite fauna (Acari: Oribatida) in late-glacial and early-Holocene sediments in Kråkenes Lake, western Norway. *Journal of Paleolimnology*. **23**: 35 - 47

Stalsberg, M.K. 1995. Seinglasial sedimentasjon i Kråkenesvatnet, Vågsøy, Sogn og Fjordane. Cand. Scient. thesis, University of Tromsø

Stapert, D., and Street, M. 1997. High resolution or optimum resolution? Spatial analysis of the *Federmesser* site at Andernach, Germany. *World Archaeology*. **29**: 172 - 194

Starkel, L. 2003. Palaeohydrology of Central Europe. – In: Gregory, K.J., and Benito, G. (eds.) *Paleohydrology, understanding global change*. Chichester, Wiley. pp. 77 - 104

Steffensen, J.P., Andersen, K.K., Bigler, M., Clausen, H.B., Dahl-Jensen, D., Fischer, H., Goto-Azuma, K., Hansson, M., Johnsen, S.J., Jouzel, J., Masson-Delmotte, V., Popp, T., Rasmussen, S.O., Röthlisberger., Ruth, U., Stauffer, B., Siggard-Andersen, M.L., Sveinbjörnsdóttir., Svensson, A., and White, J.W.C. 2008. High-resolution Greenland ice core data show abrupt climate change happens in few years. *Science*. **321**: 680 - 684

Straus, L.G. 1991. The Mesolithic-Neolithic transition in Portugal. *Antiquity*. **65**: 899 - 903

Straus, L.G. 1992. Iberia before the Iberians. *University of New Mexico Press*: Albuquerque

Straus, L. G. 1996. The archaeology of the Pleistocene – Holocene transition in southwest Europe. In: Straus, L., Eriksen, V.B., Erlandson, J.M., and Yesner, D.R. (eds.) Humans at the end of the ice age. The archaeology of the Pleistocene – Holocene transition. New York

Street, J.H., Anderson, R.S., and Paytan, A. 2012. An organic geochemical record of Sierra Nevada climate since the LGM from Swamp Lake, Yosemite. *Quaternary Science Reviews*. **40**: 89 - 106

Street, M., Baales, M., and Weninger, B. 1994. Absolute chronologie des späten Paläolithikums und des Frühmesolithikums im nördlichen Rheinland. *Archäologisches Korrespondenzblatt*. **24**: 1 - 28

Street, M. 1996. The Late Glacial Faunal Assemblage from Endingen, Lkr. Nordvorpommern. *Archäologisches Korrespondenzblatt*. **26**: 33 - 42

Street, M. 1998. The archaeology of the Pleistocene-Holocene transition in the northern Rhineland, Germany. *Quaternary International*. **49/50**: 45 - 67

Street, M. 2000. Aspects of Late Upper Palaeolithic Settlement and Chronology in Northern Central Europe. In: *Mémoires du Musée de Préhistoire d'Ile de France*. **7**: pp. 55 - 71

Street, M., Baales, M., Cziesla, E., Hartz, S., Heinen, M., Jöris, O., Koch, I., Pasda, C., Terberger, T., and Vollbrecht, J. 2001. Final Palaeolithic and Mesolithic research in reunified Germany. *Journal of World Prehistory*. **15**: 365 - 453

Street, M., Jöris, O., and Turner, E. 2012. Magdalenian settlement in the German Rhineland - an update. *Quaternary International*. **272-273**: 231 - 250

Stuiver, M., Reimer, P.J., Bard, E., Beck, J.W., Burr, G.S., Hughen, K.A., Kromer, B., McCormac, G., van der Plicht, J., and Spurk, M. 1998. INTCAL98 radiocarbon age calibration, 24,000-0 cal BP. *Radiocarbon*. **40**. 1041 - 1083

Sturdy, D. 1975. Some reindeer economies in prehistoric Europe. In: Higgs, E.S. (ed.) Palaeoeconomy. Cambridge: Cambridge University Press

Sweetman, J.N., and Finney, B.P. 2003. Differential responses of zooplankton populations (*Bosmina longirostris*) to fish predation and nutrient-loading in an introduced and a natural sockeye salmon nursery lake on Kodiak Island, Alaska, USA. *Journal of Paleolimnology*. **30**: 183 - 193

Talbot, M.R., and Lærdal, T. 2000. The Late Pleistocene - Holocene palaeolimnology of Lake Victoria, East Africa, based upon elemental and isotopic analyses of sedimentary organic matter. *Journal of Palaeolimnology*. **23**: 141 - 164

Tallavaara, M., and Seppä, H. 2011. Did the mid-Holocene environmental changes cause the boom and bust of hunter-gatherer population size in eastern Fennoscandia? *The Holocene*. **22**: 215 **-** 225

Taute, W. 1968. Die Stielspitzen-gruppen im nördlichen Mitteleuropa. *Fundamenta*. **A5**: Köln, Graz

Teranes, J.L., and Bernasconi, S.M. 2005. Factors controlling ^{13}C values of sedimentary carbon in hypertrophic Baldeggersee, Switzerland, and implications for interpreting isotope excursions in lake sedimentary records. *Limnology and Oceanography*. **50**: 914 - 922

Terberger, T. 1996. Die ”Riesenhirschfundstelle” von Endingen, Lkr. Nordvorpommern. Spätglaziale Besiedlungsspuren in Nordostdeutschland. *Archäologisches Korrespondenzblatt*. **26**: 13 - 32

Terberger, T. 1998. Grundwasserstände und spätpaläolithische-mesolithische Besiedlung im Endinger Bruch. *Urgesch.Mater*. **12**: 89 - 102

Terberger, T., and Lübke, H. 2004. Hamburger Kultur in Mecklenburg-Vorpommern? *Jahrbuch Bodendenkmalpflege Mecklenburg-Vorpommern*. **52**: 15 - 34

Terberger, T., De Klerk, P., Helbig, H., Kaiser, K. and Kühn, P. 2004. Late Weichselian landscape development and human settlement in Mecklenburg-Vorpommern (NE Germany). *Eiszeitalter und Gegenwart*. **54**: 138 - 175

Terberger, T. 2006. From the first humans to the Mesolithic hunters in the northern German lowlands – current results and trends. In: Hansen, K.M., and Pedersen, K.B. (eds.) Across the western Baltic. **1**: pp. 23 - 56

Terberger, T., Barton, N., and Street, M. 2009. The Late Glacial reconsidered – recent progress and interpretations. In: Street, M., Barton, N., and Terberger, T. (eds.) Humans, environment and chronology of the Late Glacial of the North European Plain. Proceedings of Workshop 14, The Final Palaeolithic of the great European Plain, Lisbon, 2006. 189 - 207

Theuerkauf, M. 2002. Die Laacher See-Tephra in Nordostdeutschland: Paläoökologische Untersuchungen mit hoher zeitlicher und räumlicher Auflösung. *Greifswalder Geographische Arbeiten.* **26**: 171 - 174

Theuerkauf, M. 2003. Die Vegetation NO-Deutschlands vor und nach dem Ausbruch des Laacher See-Vulkans (12880 cal. BP). *Greifswalder Geographische Arbeiten.* **29**: 143 - 18

Timmermann, T. 1999. Sphagnum-Moore in Nordostbrandenburg: stratigraphischhydrodynamische Typisierung und Vegetationswandel seit 1923. *Dissertationes Botanicae.* **305**: 1 - 175

Tolksdorf, J.F., Turner, F., Kaiser, K., Eckmeier, E., Stahlschmidt, M., Housley, R.A.., Breest, K., and Veil, S. 2013. Multiproxy Analyses of Stratigraphy and Palaeoenvironment of the Late Palaeolithic Grabow Floodplain Site, Northern Germany. *Geoarcheology*. **28**: 50 - 65

Torke, W. 1998. Fische aus jungpleistozänen und holozänen siedlungsplätzen in Baden Württemberg. *Naturkunde Württemberg*. **154**: 231 – 259

Torroni, A., Bandelt, H.J., d'Urbano, L., Lahermo, P., Moral, P., Selitto, D., Reengo, C., Forster, P., Savontaus, M.L., Bonné-Tamir, B., and Scozzari, R. 1998. MtDNA analysis reveals a major late Paleolithic population expansion from southwestern to northeastern Europe. *American Journal of Human Genetics*. **62**: 1137 - 1152

Tromnau, G. 1975. Die Fundplätze der Hamburger Kultur von Heber und Deimern, Kreis Soltau. *Materialhefte zur Ur und Frühgeschichte Niedersachsens*. **9**: pp. 46

Tromnau, G. 1976. Rentierjäger der Späteiszeit in Norddeutschland. Hildesheim

Turner, C., and Hannon, G.E. 1988. Vegetational evidence for late Quaternary climatic changes in southwest Europe in relation to the influence of the North Atlantic Ocean. *Philosophical Transactions of the Royal Society of London B*. **318**: 451 - 485

Turney, C.S.M., Harkness, D. D. and Lowe, J. J. 1997. The use of microtephra horizons to correlate Lateglacial lake sediments successions in Scotland. *Journal of Quaternary Science*. **12**: 525 - 531

Turney, C.S.M. 1998. Extraction of rhyolitic ash from minerogenic lake sediments. *Journal of Palaeoliminology*. **19**: 199 - 206

Turney, C.S.M., Coope, G.R., Harkness, D.D., Lowe, J.J., Walker, M.J.C. 2000. Implications for the dating of Wisconsinan (Weichselian) Lateglacial events of systematic radiocarbon age differences between terrestrial plant macrofossils from a site in SW Ireland. *Quaternary Research* **53**: 114 - 121

Turney, C.S.M., Lowe. J.J., Davies, S.W., Hall. V., Lowe, D.J., Wastegård, S., Hoek, W.Z., Alloway, B., and SOTAV and INTIMATE members. 2004. Tephrochronology of Last Termination sequences in Europe: a protocol for improved analytical precision and robust correlation procedures (a joint SOTAV-INTIMATE proposal). *Journal of Quaternary Science*. **19**: 111 – 120

Turney, C.S.M., Van Den Burg, K., Wastegård, S., Davies, S.M., Whitehouse, N.J., Pilcher, J.R., and Callaghan, C. 2006. North European last glacial-interglacial transition (LGIT; 15-9ka) tephrochronology: extending limits and new events. *Journal of Quaternary Science*. **21**: 335 - 345

Usinger, H. 1997. Pollenanalytische Datierung spätpaläolithischer Fundschichten bei Ahrenshöft, Kr Nordfriesland. *Archäologische Nachrichten aus Schleswig-Holstein.* **8**: 50 - 73

Usinger, H. 1998. Pollenanalytische Datierung spätpaläolitischer Fundschichten bei Ahrenshöft, Kr. Nordfriesland. Archäologische bNachrichten aus Schleswig-Holstein; Mitteilungen der Archäologischen Gesellschaft Schleswig-Holstein e.v. *und des Archäologischen Landesamtes Schleswig-Holstein*. **8**: 50 - 73

Usinger, H. 2004. Vegetation and climate of the lowlands of northern Central Europe and adjacent areas around the Younger Dryas – Preboreal transition with special emphasis on the Preboreal oscillation. In: Terberger, T., Eriksen, B.V. (eds.) Hunters in a changing world. Environment and Archaeology of the Pleistocene – Holocene Transition (ca. 11000–9000 B.C.) in Northern Central Europe. Internationale Archaologie – Arbeitsgemeinschaft, Tagung, Kongress 5. Leidorf, Rahden, pp 1 - 26

Valentin, B., and Pigeot, N. 2000. Eléments pour une chronologie des occupations magdaléniennes dans le Bassin parisien. In: *Mémoires du Musée de Préhistoire d'Ile de France*. **7**: pp. 129 - 138

Van der Hammen, T. 1957. The stratigraphy of the Late Glacial. *Geologie en Mijnbouw*. **19**: 250 - 254

Van Geel, B., Kolstrup, E. 1978. Tentative explanation of the Lateglacial and Early Holocene climatic changes in northwestern Europe. *Geology Mijnbouw*. **57**: 87 - 89

Van Geel, B., Coope, G.R., Van der Hammen, T. 1989. Palaeoecology and stratigraphy of the Lateglacial type section at Usselo (The Netherlands). *Review of Palaeobotany and Palynology*. **60**: 25 - 129

Veil, S., Geyh, M.A., Merkt, J., Müller, U., and Staesche, U. 1991. Eine Widerhakenspitze aus Lemförde am Dümmer, Landkreis Diepholz. *Neue Ausgrabungen und Forschungen in Niedersachsen*. **19**: 1 - 19

Veil, S., and Breest., K. 1995. Figurenfragmente aus Bernstein vom Federmesser Fundplatz Weitsche bei Lüchow, Lkr. Lüchow-Dannenberg (Niedersachsen). *Archäologisches Korrespondenzblatt*. **25**: 29 47

Veil, S., and Breest, K. 2000. Der archäologische Befund der Kunstgegenstände aus Bernstein auf dem Federmesser-Fundplatz Weitsche. Die Grabungen 1994-1998. *Die Kunde N.F*. **51**: 179 - 202

Veil, S., Breest, K., Grootes, P., Nadeau, M., and Hüls, M. 2012. A 14 000-year-old amber elk and the origins of northern European art. *Antiquity*. **86**: 660 - 673

Verhart, L.B.M. 1988. Mesolithic barbed points and other implements from Europoort, The Netherlands. Oudheidkundige Mededelingen uit het Rijksmuseum van Oudheden te Leiden. **68**: 145 - 194

Veski, S., Amon, L., Heinsalu, A., Reitalu, T., Saarse, L., Stivrins, N., and Vassiljev. 2012. Lateglacial vegetation dynamics in the eastern Baltic region between 14,500 and 11,400 cal yr BP: A complete record since the Bølling (GI-1e) to the Holocene. *Quaternary Science Reviews*. **40**: 39 - 53

Villaverder, V., and Martinez, R. 1992. Economia y aprovechamiento del medio en el Paleolitico de la región central del Mediterráneo español. In: Moure, A. (ed.) Elefantes, civeros y ovicaprinos. Universidad de Cantabria: Santander Von Grafenstein, U., Erlenkeuser, H., Brauer, A., Jouzel, J., and

Johnsen, S.J. 1999. A Mid-European decadal isotope-climate record from 15,500 to 5000 years B.P. *Science*. **284**: 1654 - 1657

Vuorio, K., Meili, M. and, Sarvala, J. 2006. Taxon-specific variation in the stable isotopic signatures ($\delta^{13}C$ and $\delta^{15}N$) of lake phytoplankton. *Freshwater Biology*. **51**: 807 - 822

Waagstein, R., and Jóhansen, J. 1968. Tre vulkanske askelag fra Faeröerne. *Meddelelser fra Dansk Geologisk Forening.* **34**: 257 - 264

Waldmann, G., Jöris, O., and Baales, M. 2001. Nach der Flut - Ein spätallerødzeitlicher Rückenspitzen-Fundplatz bei Bad Breisig (Kr. Ahrweiler, Rheinland-Pfalz). *Archäologisches Korrespondenzblatt*. **31**: 173 - 184

Walker, M.J.C., Bohncke, S.J.P., Coope, G.R., O'Connell, M., Usinger, H., and Verbruggen, C. 1994. The Devensian (Weichselian) Late-glacial in northwest Europe (Ireland, Britain, northern Belgium, The Netherlands, northern Germany). *Journal of Quaternary Science*. **9**: 109 - 118

Walker, M.J.C., Björck, S., Lowe, J.J., Cwynar, L.C., Johnsen, S., Knudsen, K.L., Wohlfarth, B., and INTIMATE group. 1999. Isotopic 'events' in the GRIP ice core: a stratotype for the Late Pleistocene. *Quaternary Science Reviews*. **18**: 1143 - 1150

Walker, M.J.C., Coope, G.R., Sheldrick, C., Turney, C.S.M., Lowe, J.J., Blockley, S.P.E., and Harkness, D.D. 2003. Devensian Late Glacial environmental changes in Britain: a multi-proxy environmental record from Llanild, South Wales, UK. *Quaternary Science Reviews*. **22**: 475 - 520

Wastegård, S., Björck, S., Possnert, G., and Wohlfarth, B. 1998. Evidence for the occurrence of Vedde Ash in Sweden: radiocarbon and calendar age estimates. *Journal of Quaternary Science*. **13**: 271 - 274

Wastegård, S., Turney, C. S. M., Lowe, J. J., and Roberts, S. J. 2000. The Vedde Ash in NW Europe: distribution and geochemistry. *Boreas*. **29**: 72 - 78

Wastegård, S., Björck, S., Grauert, M., and Hannon, G.E. 2001. The Mjauvotn tephra and other Holocene tephra horizons from the Faroe Islands: a link between the Icelandic source region, the Nordic Seas, and the European continent. *The Holocene*. **11:** 101 - 109

Weber, M.J., Grimm, S.B., and Baales, M. 2011. Between warm and cold: Impact of the Younger Dryas on human behaviour in Central Europe. *Quaternary International*. **242**: 277 - 301

Weinstock, J. 2000. Osteometry as a source of refined demographic information: sex ratios of reindeer, hunting stratagies and herd control in the Late Glacial site of Stellmoor, Northern Germany. *Journal of Archaeological Science*. **27**: 1187 - 1195

Weniger, G. 1982. *Wildbeuter und ihre Umwelt. Ein Beitrag zum Magdalénien Südwestdeutschlands aus ökologischer und ethno-archäologischer Sicht*. Tübingen: Archaeologica Venatoria

Wennrich, V., Wagner, B., Melles, B., and Morgenstern, P. 2005. Late Glacial and Holocene history of former Salziger See, Central Germany, and its climatic and environmental implications. *International Journal of Earth Sciences*. **94**: 275 - 284

Westgate, J.A., and Gorton, M.P. 1981. Correlation techniques in tephra studies. In: Self, S., and Sparks, R.S.J. (eds.) Tephra Studies. Dordecht: Reidel

Wheeler, R.E.M. 1954. Archaeology from the Earth. Harmondsworth, Penguin

White, R. K. 1985. Upper Palaeolithic land-use in the Périgord. A topographic approach to subsistence. British Archaeological Reports International series. **253**: Oxford: B.A.R

Whiteside, M.C., Williams, J.B., and White, C.P. 1978. Seasonal abundance and pattern of chydorid, cladocera in mud and vegetative habitats. *Ecology*. **59**: 1177-1188

Wohlfahrt, B., Skog, G., Possnert, G. & Holmqvist, B. 1998. Pitfalls in the AMS radiocarbon-dating of terrestrial macrofossils. *Journal of Quaternary Science*. **13**: 137 - 146

Wohlfahrt, B., Blaauw, M., Davies, S.M., Andersson, M., Wastegård, S., Hormes, A., Possnert, G. 2006. Constraining the age of Lateglacial and early Holocene pollen zones and tephra horizons in southern Sweden with Bayesian probability methods. *Journal of Quaternary Science*. **21**: 321 - 334

Wolters, S.1999. Spät und postglaziale Vegetationsentwicklung im Bereich der Fercher Berge südwestlich von Potsdam. *Gleditschia*. **27**: 25 - 44

Wolters, S. 2002. Vegetationsgeschichtliche Untersuchungen zur spätglazialen und holozänen Landschaftsentwicklung in der Döberitzer Heide (Brandenburg). Dissertationes Botanicae **366**: 1 - 157

Wright, H.E. 1984. Sensitivity and response time of natural systems to climatic change in the late Quaternary. *Quaternary Science Reviews*. **3**: 91 - 131

Zerbe, S., Brande, A., and Gladitz, F. 2000. Kiefer, Eiche und Buche in der Menzer Heide (NBrandenburg). *Verhandlungen des Botanischen Vereins von Berlin und Brandenburg*. **133**: 45 - 86

Zobel, D.B., and Antos, J.A. 1997. A decade of recovery of understorey vegetation buried by volcanic tephra from Mount St. Helens. *Ecological Monographs*. **67**: 317 - 344

Züllig, H. 1989. Role of carotenoids in lake sediments for reconstructing trophic history during the late Quaternary. *Journal of Paleolimnology*. **2**: 23 - 40

Zvelebil, M., and Rowley-Conwy, P. 1984. Transition to farming in northern Europe: A hunter-gatherer perspective. **17**: 104 - 128

Appendix I: Additional study sites

One of the main objectives of this thesis was to establish a detailed tephrochronological and tephrostratigraphic record for sites within the NEP (section 1.7, Chapter 1). Not only does this improve site chronology, but essentially for this project, allows sites to be compared at fixed points, therefore allowing aquatic system evolution to be analysed across multiple sites. As discussed within sections 3.5.1.2 and 3.5.2.2, Slotseng and Endinger Bruch already have well established tephra records. In order to therefore augment these sites I analysed a further eight sites within the NEP (Figure I.1). As establishing a tephra record is crucial for this thesis, five of these sites were deemed unsuccessful as they failed to produce tephra records. These six sites therefore did not form a major part of this project. These sites will now be briefly described and their unsuitability to address the aims and objectives of this thesis discussed.

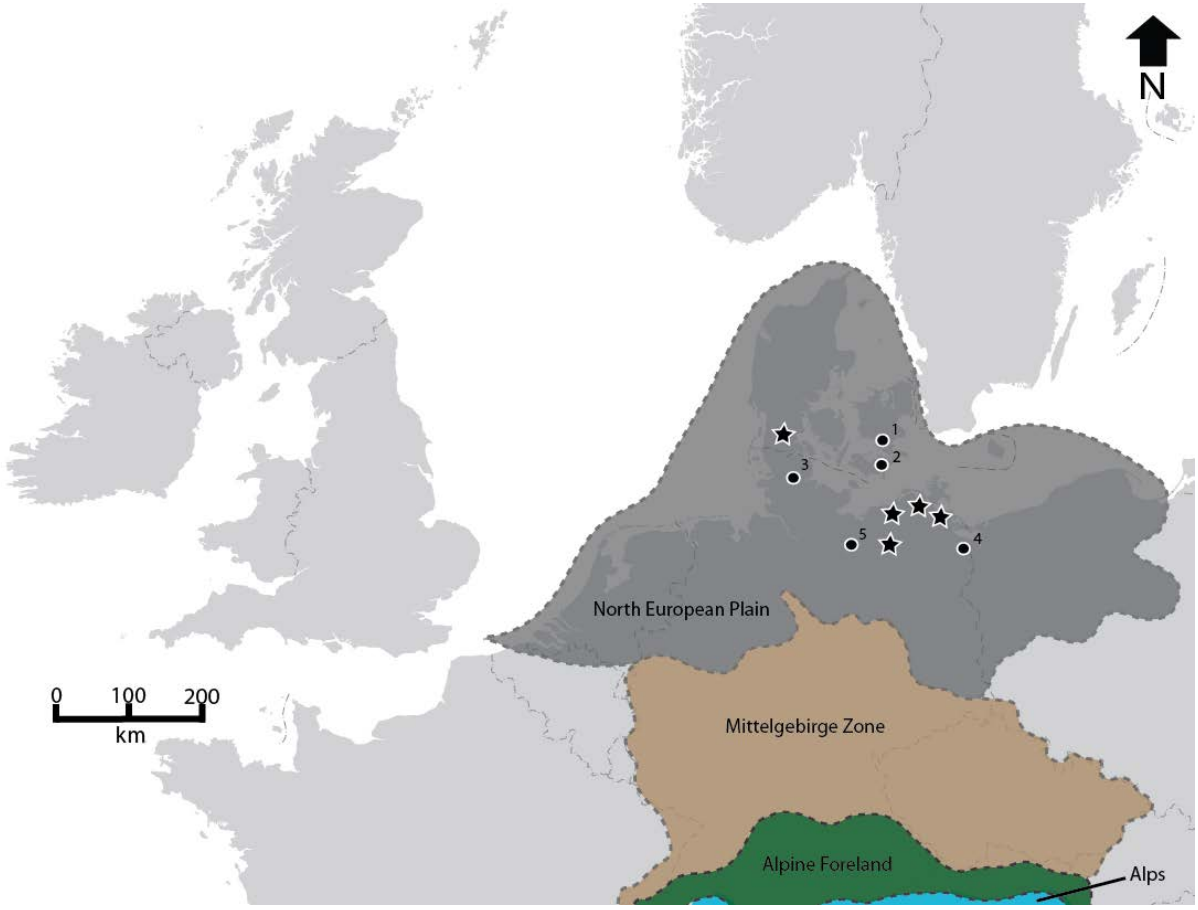


Figure I.1 – Sites 1- Lundby Mose; 2 – Gedser; 3 – Tolk, 4 – Gorinsee; 5 – Weitsche. The stars show the position of the sites used.

Lundby Mose

Lundby Mose is located on the southerly edge of the island of Zealand, Denmark (55° 6′ 29.6″ N, 11° 52′ 19″ E). The site comprises a small kettle hole (0.6 hectare) which in turn forms part of the Sværdborg-Lundby bog (Hansen and Pedersen, 2006). The site contains sediments with ages in excess of the Oldest Dryas as well as revealing evidence of a human presence at the site. Excavations at the site during 1999 and 2000 revealed the presence of at least six concentrations of marrow-split elk bones (Hansen, 2003). Subsequent dating of the elk remains places them within the Preboreal period giving the earliest firmed evidence for human occupation in Denmark during the early Holocene (Mortenson *pers comm*.). It is not however known if the elk deposits represent a single hunting evident, or deposition over time, as of yet no traces of human settlement have been located (Terberger, 2006).

In 2010 a 377 cm core was extracted from the western edge of the kettle hole by the author, Dr Rupert Housley and Dr Morten Mortensen. Initial 10 cm scans showed a large spread of microtephra between 134-377 cm, with the largest shard counts occurring between 144-154 cm, 304-314 cm and 364-377 cm, a small peak between 284-294 cm was also sampled due to its close association with the Allerød – Younger Dryas boundary. 1 cm contiguous samples indicated two small peaks in glass shard concentration. The first, located between 146-147 cm had a maximum shard count of 20 g^{-1} (absolute count 1) while the second peak located between 289-290 cm had a maximum shard count of 17 g^{-1} (absolute count 5; Figure I.2). The remaining peaks between 304-314 cm and 364-377 cm were not replicable at 1 cm resolution.

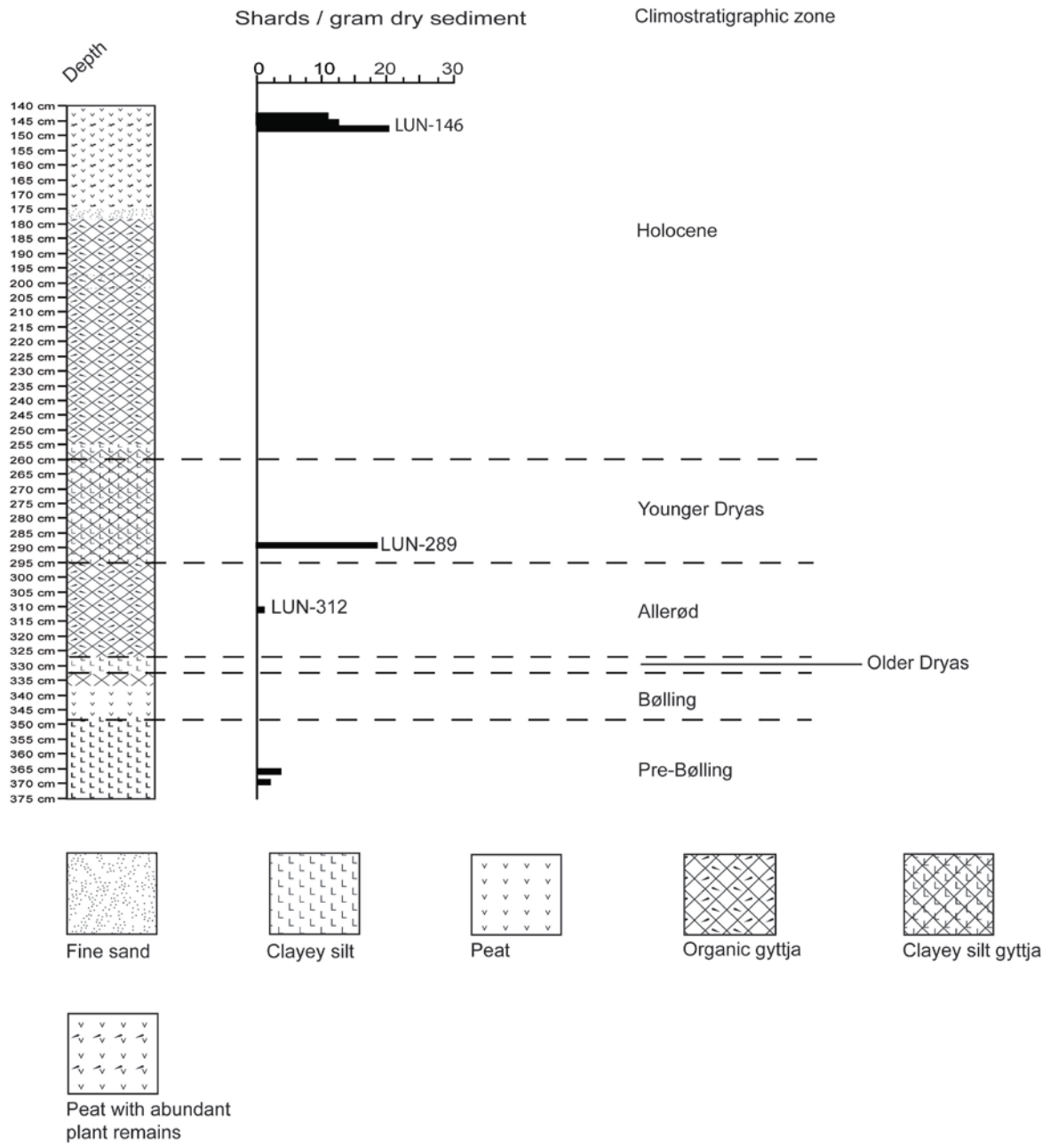


Figure I.2 - Composite diagram showing shard counts (per gram dry sediment) with lithology and relative climostratigraphic zones for Lundby Mose.

Due to the extremely low absolute shard counts, and limited volumes of sediment, it was not possible to extract any shards for EPMA. One of the shards from the peak at 289-290 cm was extremely vesicular and was morphologically consistent with the LST. However, without geochemical analysis it was not possible to identify any of the tephras within Lundby Mose. For this reason therefore no further analysis was taken on Lundby Mose.

Gedser

Gedser is located on the southern edge of the island of Falster, Denmark (54° 35′ 0″ N, 11° 56′ 0″ E). The site comprises a small kettle hole (<0.5 hectare) and an area of apparent occupation some 30 meters to the south of the kettle hole. The areas of occupation are associated with Federmesser and Bromme lithic assemblages after the Natural Museum of Denmark identified two surface concentrations during excavations in the 1990's (Mortenson, *pers comm*.). The kettle hole contains sediments of Bølling age, these are however sterile of any archaeology which may have tied this environmental sequence to the nearby occupation site. The area surrounding the former kettle hole has been extensively ploughed, and field levelling during the early 1900's has removed any trace of the former basin.

In 2010 a large trench was excavated by the author, Dr Rupert Housley and Dr Morten Mortensen across the kettle hole using a mechanical digger to expose the previous excavation trench. From this exposed section a series of five 50 cm monoliths were taken. Following initial 10 cm scans of the monolith material no glass shards were recorded at any level within the site. The lack of possible chronological tie points with other sites therefore precluded Gedser from any further work.

Tolk

Tolk is situated in the Schleswig-Holstein region of northern Germany (54° 34′ 0″ N, 9° 39′ 0″ E). The site comprises a palaeolake and contains sediments of Older Dryas age. Since the 1950's flint artefacts have been collected from the Tolk site in the vicinity of the Lobacker village (Taute, 1968). The artefacts collected at Tolk during this period were included in the archaeological register of the former district of Schleswig under the designation Tolk LA 8 (Loewe, 1998). Due to the association of Bromme type tanged points and backed points within this inventory, Taute (1968) defined the artefacts as '*Tolk-Sprenge-Gruppe*' located within the so-called Lyngby-Kreis, which correlates with the Allerød (Weber, *pers. comm*.). Initial coring at Tolk was undertaken in the hope to resolve the question of whether the '*Tolk-Sprenge-Gruppe*' represents a single tool typology or is evidence of admixing at the site.

This initial excavation at Tolk was carried out in 1959 and produced a 4 meter core with Older Dryas sediments at its base (Taute, 1968). Unfortunately, the sediments recovered where miss-interpreted

leading to incorrect sediment identification. In order to resolve these issues at second core was taken in 2009 using an Usinger corer (Weber, *pers. comm*.) A 496 cm core was excavated from the former lake shore. The resulting core form Tolk was sampled in 2010 at the Schleswig-Holstein State museum, Germany by the author. Initial 10 cm scans showed a small spread of glass shards between 361-369 cm. Further 1 cm contiguous samples showed two small peaks in glass shard concentration of 4 g^{-1} (absolute count 2) occurring between 361-362 cm and 5 g^{-1} (absolute count 3) occurring between 368-369 cm (Figure I.3). The highly vesicular shard morphologies displayed within the two small peaks and the subsequent stratigraphic position within ~ Late Allerød sediments is consistent with LST ash deposits and strongly suggests that both peaks form part of the same eruption. However due to the extremely low shard counts and limited core material, it was not possible to extract any further shards for EPMA regardless of multiple attempts. Despite the close physical and stratigraphic association to the LST, without geochemical analysis it was not possible to robustly identify any of the tephras within Tolk. For this reason therefore no further work was continued on the site.

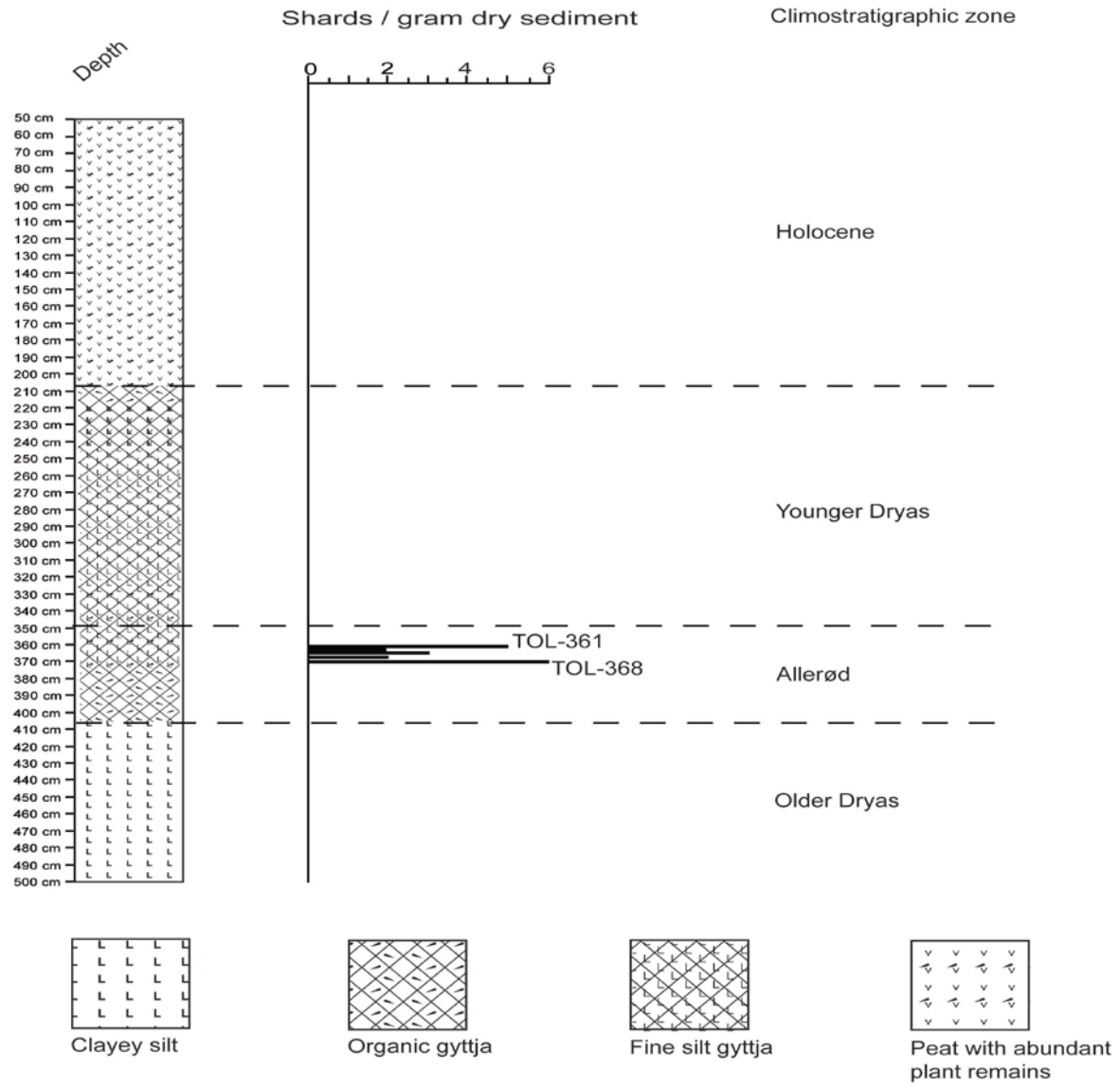


Figure I.3 - Composite diagram showing shard counts (per gram dry sediment) with lithology and relative climostratigraphic zones for Tolk.

Gorinsee

Gorinsee is located ~ 3 km west of the Polish border, in Mecklenburg-Vorpommern region of NE Germany (53°36'11" 14°14'41"). The site comprises a medium sized palaeolake of 10, hectares which became fully terrestrial only with the last century and is now covered by a reed bed with *sedges*, *Phragmites*, and *Equisetum* (Theuerkauf, *pers. comm.*). The area surrounding the site is primarily composed of pine woodlands with grassland towards the southwest. The kettle hole contains sediments of Allerød age, comprising calcareous gyttjas with clay at the base.

Gorinsee was cored in 2007 by Martin Theuerkauf, University of Greifswald, producing a core of 687 cm in length. A section of core from 500-640 cm, covering the Allerød – Holocene period was secured as part of this thesis. Initial 10 cm scans showed a concentration of tephra shards between 500-530 cm. Further 1 cm contiguous samples showed two small peaks in glass shard concentration of 20 g^{-1} (absolute count 2) occurring between 515-516 cm and 29 g^{-1} (absolute count 4) occurring between 523-524 cm (Figure I.4). The glass shards within both small peaks were composed of an almost equal split between brown and clear shards. As with previous sites, Gorinsee is hampered by extremely low absolute counts and limited core material, after repeated efforts it was not possible to extract any further shards for EPMA. For this reason therefore no further work was continued on the site.

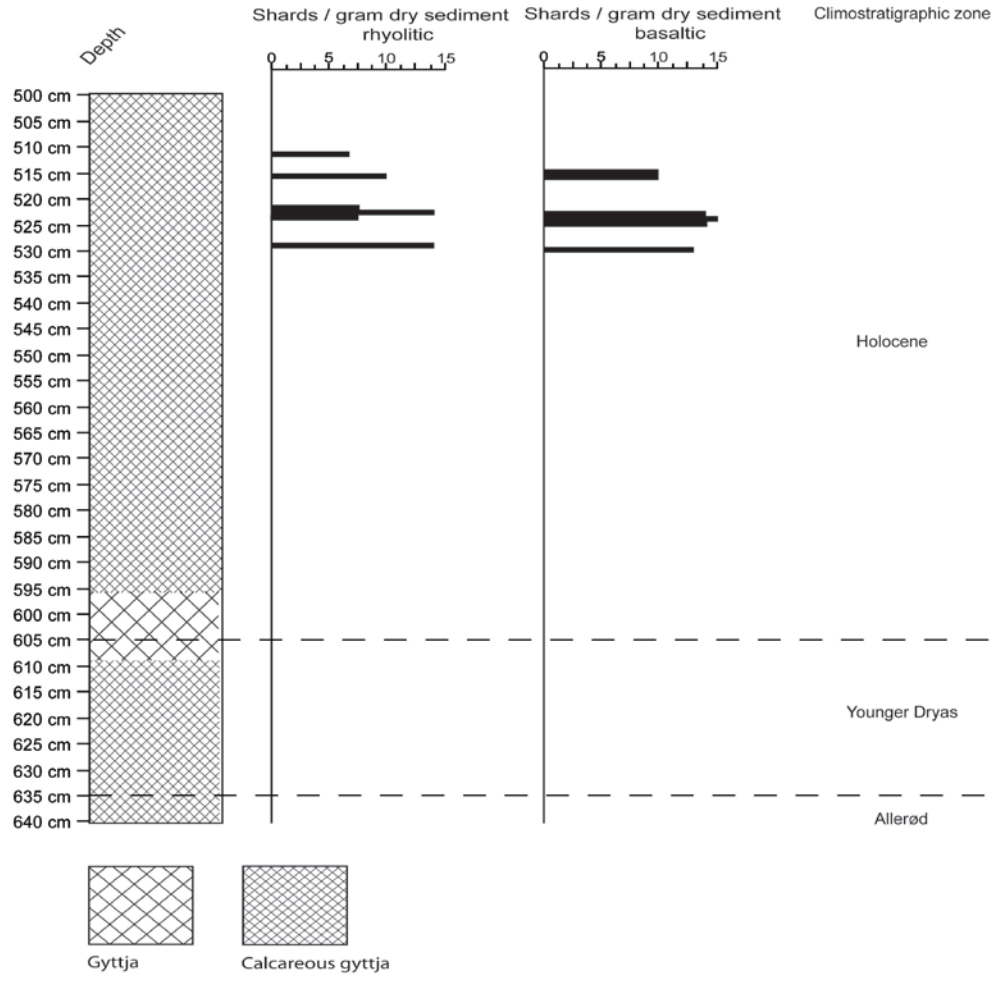


Figure I.4 - Composite diagram showing shard counts (per gram dry sediment) with lithology and relative climostratigraphic zones for Gorinsee.

Weitsche

Weitsche is situated in the Lower Saxony region of northern Germany (53° 1' 36'' N, 11° 7' 36''E) and is composed of an archaeological site (see Veil and Breest, 1995; Veil and Breest, 2000; Tolksdorf *et al*., 2012; Veil *et al.,* 2012) and an environmental site. The environmental site is composed of a series of abandoned river channels that formed during the Latglacial. The archaeological site is noted for its association with arch backed points of the Federmesser lithic industry in a series of surface scatters correlated to the Allerød. Excavations have also revealed significant evidence of amber working and associated waste, most notably, a worked amber elk head and numerous beads (Figure 2.12). The complete site has been heavily influenced by fluvial processes throughout its formation, with at least five different stages of channel formation during the Lateglacial (Turner, unpublished PhD thesis).

A series of two cores were recovered from the palaeochannels at Weitsche by Dr Falko Turner. Core W.VIII (50-148 cm) was taken from the oldest channel and covered the Bølling – Younger Dryas period, while core W.VI (121-390 cm), taken from a younger channel, covered the Allerød – Holocene period. Initial 10 cm scans showed a small spread of glass shards between 131-151 cm, 201-211 cm, 240-270 cm and 330-270 cm within W.VI. No glass shards were recorded in W.VIII. Further 1 cm contiguous samples within W.VI showed two extremely small peaks in glass shard concentration of 3 g^{-1} (absolute count 3) occurring between 240-241 cm and 1 g^{-1} (absolute count 1) occurring between 248-249 cm (Figure I.5). Several attempts were made to extract enough glass shards form the peak at 240-241 cm. Following this a single glass shard was picked for EPMA; however it was only possible to expose a shard surface area of 10 µm, therefore it was not possible to obtain any glass chemistry. Further material was sent by Dr Falko Turner, this however again produced extremely low shard counts of 1 g^{-1} and no shards for EPMA. Due to the extremely low shard counts and lack of chemical data within Weitsche, no further analysis was conducted on the site.

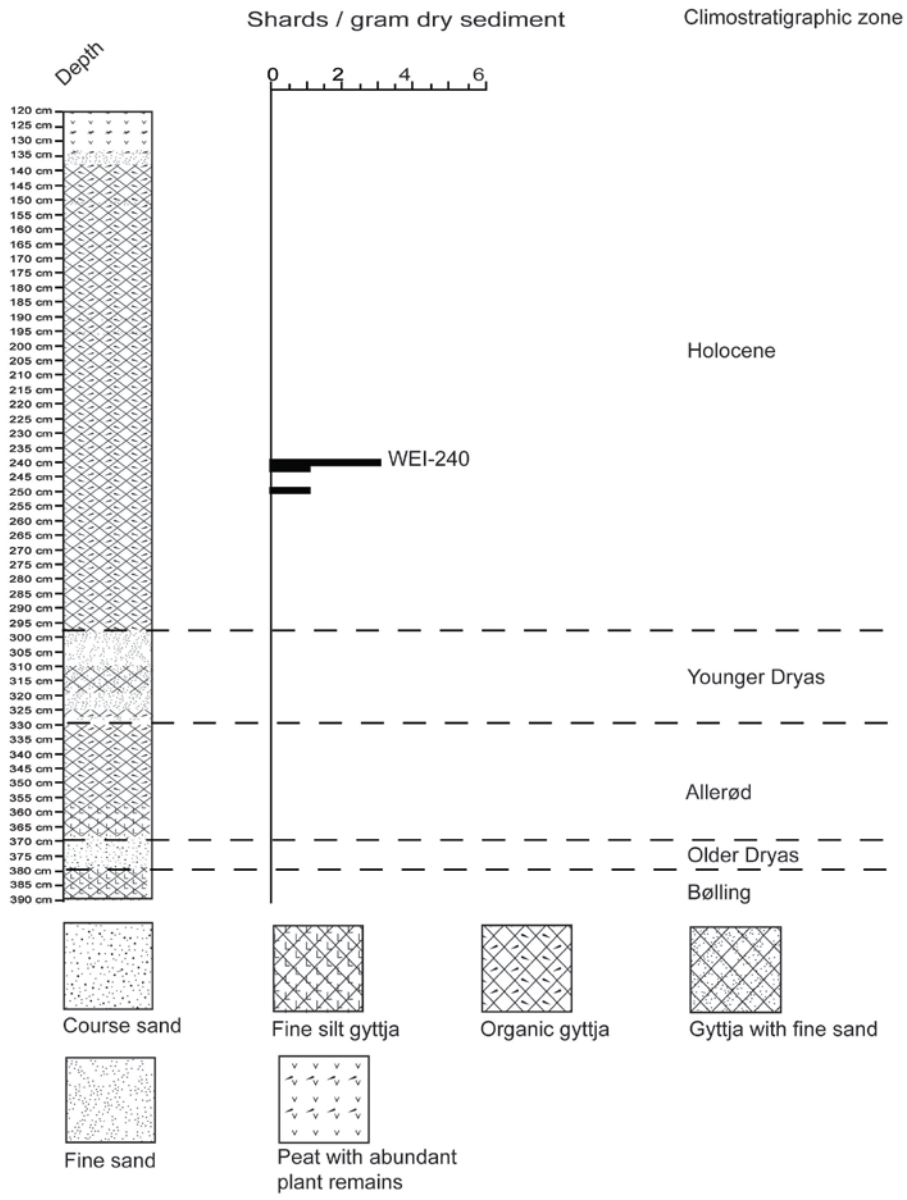


Figure I.5 - Composite diagram showing shard counts (per gram dry sediment) with lithology and relative climostratigraphic zones for Weitsche.

Appendix II: Stable isotope and selected organic matter data

$\delta^{13}C$ (‰)	$\delta^{15}N$ (‰)	TOC (wt%)	TN (wt%)	C:N	Depth (cm)	Sample	$\delta^{13}C$ (‰)	$\delta^{15}N$ (‰)	TOC (wt%)	TN (wt%)	C:N	Depth (cm)	Sample
-28.3	-0.6	54.43	1.44	44.00	217 cm	SIZ V	-24.7	-2.38	46.63	0.69	78.50	105 cm	SIZ III
-29.15	-2.36	52.57	2.02	30.39	212 cm	SIZ V	-26	-3.5	50.39	0.98	59.97	100 cm	SIZ III
-27.17	-1.19	55.88	0.88	73.89	207 cm	SIZ V	-29.56	-2.01	46.00	2.74	19.61	95 cm	SIZ III
-28.43	-0.72	54.11	1.58	39.98	202 cm	SIZ V	-29.78	-2.79	49.48	1.90	30.44	90 cm	SIZ III
-28.39	0.6	52.48	1.86	32.94	197 cm	SIZ V	-31.15	-2.93	23.43	1.38	19.83	85 cm	SIZ II
-26.87	-3.23	49.52	0.87	66.76	192 cm	SIZ V	-29.11	-1.46	18.26	1.05	20.35	80 cm	SIZ II
-27.01	-1.1	52.28	2.08	29.33	187 cm	SIZ V	-29	-1.2	13.74	0.86	18.63	75 cm	SIZ II
-27.24	-3.74	5.18	0.29	20.69	182 cm	SIZ IV	-26.75	0.14	10.58	0.70	17.60	70 cm	SIZ II
-25.81	-5.09	4.32	0.24	20.78	175 cm	SIZ IV	-27.97	-2.84	12.67	0.80	18.48	65 cm	SIZ II
-25.94	0.59	5.69	0.31	21.58	170 cm	SIZ IV	-28.98	-0.88	13.45	0.84	18.60	60 cm	SIZ II
-25.7	-5.01	4.45	0.25	21.07	165 cm	SIZ IV	-25.58	0.72	6.90	0.46	17.50	55 cm	SIZ II
-25.89	2.33	7.58	0.38	23.01	160 cm	SIZ IV	-26.22	0.49	2.46	0.18	16.01	50 cm	SIZ II
-25.43	-3.29	4.26	0.25	20.20	155 cm	SIZ IV	-27.65	0.37	2.21	0.14	18.39	45 cm	SIZ II
-26.31	1.85	6.07	0.31	22.61	150 cm	SIZ IV	-26.69	-0.81	5.35	0.42	14.90	40 cm	SIZ II
-26.34	-2.03	6.10	0.33	21.69	145 cm	SIZ IV	-25.94	-1.65	4.69	0.37	14.89	35 cm	SIZ I
-26.5	0.43	7.02	0.36	22.78	140 cm	SIZ IV	-23.67	-1.96	5.28	0.39	15.77	30 cm	SIZ I
-26.72	-0.2	7.36	0.36	23.71	135 cm	SIZ III	-22.62	-3.71	4.35	0.33	15.23	25 cm	SIZ I
-25	-2.6	46.13	0.66	81.50	130 cm	SIZ III	-22.6	-5.5	3.11	0.23	15.71	20 cm	SIZ I
-26.1	-3.47	43.30	0.98	51.44	125 cm	SIZ III	-22.71	-0.94	1.81	0.15	14.19	15 cm	SIZ I
-28.08	-1.18	16.86	0.79	24.80	120 cm	SIZ III	-21.5	-1.01	0.99	0.08	14.39	10 cm	SIZ I
-27.54	-1.59	51.46	1.77	33.90	115 cm	SIZ III	-21.84	-0.83	0.78	0.07	13.42	5 cm	SIZ I
-24.34	-3.31	46.11	0.83	64.56	110 cm	SIZ III							

Table II.1 – Stable isotope and selected organic properties for Slotseng

$\delta^{13}C$ (‰)	$\delta^{15}N$ (‰)	TOC (wt%)	TN (wt%)	C:N	Depth (cm)	Sample
-28.99	-0.76	31.00	2.55	14.19	851	EIZ VII
-29.34	-0.62	29.22	2.43	14.02	856	EIZ VII
-28.55	-0.48	29.71	2.49	13.94	861	EIZ VII
-29.31	-0.39	25.85	2.11	14.30	866	EIZ VII
-29.06	-0.73	28.48	2.35	14.13	871	EIZ VII
-29.59	-0.72	32.37	2.62	14.40	876	EIZ VII
-29.77	-0.33	25.81	2.04	14.79	881	EIZ VII
-29.89	-0.69	25.06	1.97	14.82	886	EIZ VII
-30.39	-0.89	27.25	2.21	14.37	891	EIZ VII
-30.88	-0.28	28.12	2.16	15.17	896	EIZ VII
-30.90	-0.37	22.62	1.81	14.58	901	EIZ VII
-31.68	0.17	25.93	2.05	14.76	906	EIZ VII
-31.40	-0.08	20.12	1.56	15.03	911	EIZ VII
-31.34	-0.09	22.67	1.81	14.64	916	EIZ VII
-31.83	0.47	24.78	1.92	15.03	921	EIZ VI
-31.77	1.09	25.67	2.00	15.00	926	EIZ VI
-31.78	0.71	26.60	2.07	15.01	931	EIZ VI
-31.47	0.47	27.01	2.15	14.65	936	EIZ VI
-30.95	0.82	29.84	2.34	14.89	941	EIZ VI
-31.25	1.00	30.28	2.28	15.50	946	EIZ VI
-31.58	0.62	27.11	2.07	15.30	951	EIZ VI
-30.04	0.89	24.57	1.81	15.79	956	EIZ VI
-31.96	0.67	23.13	1.84	14.63	961	EIZ VI
-31.45	0.95	26.62	2.08	14.91	966	EIZ VI
-31.27	1.16	23.85	1.92	14.50	971	EIZ VI
-30.75	1.26	18.27	1.49	14.26	976	EIZ VI
-30.14	1.02	13.97	1.14	14.24	981	EIZ VI
-29.56	1.04	11.17	0.97	13.44	986	EIZ VI
-29.30	1.05	8.44	0.71	13.87	991	EIZ VI
-27.69	1.31	6.49	0.59	12.80	996	EIZ VI
-26.44	1.11	4.39	0.38	13.46	1006	EIZ VI
-25.47	1.38	1.76	0.15	13.53	1011	EIZ VI
-26.33	0.30	1.75	0.15	13.25	1021	EIZ VI
-25.75	1.15	1.58	0.13	13.86	1026	EIZ V
-25.67	0.44	1.58	0.13	13.68	1031	EIZ V
-25.02	1.01	1.53	0.13	13.67	1036	EIZ V
-25.75	1.06	1.58	0.14	13.36	1041	EIZ V
-25.75	0.75	1.44	0.12	13.62	1046	EIZ V
-25.71	0.53	1.53	0.13	13.75	1051	EIZ V
-25.57	0.82	1.50	0.13	13.58	1056	EIZ V
-25.93	0.71	1.73	0.15	13.61	1061	EIZ V
-25.65	0.67	1.37	0.12	13.72	1066	EIZ V
-25.74	1.41	1.22	0.11	13.37	1071	EIZ V
-25.90	0.91	1.32	0.12	13.42	1076	EIZ V
-25.39	2.08	1.16	0.10	13.63	1081	EIZ V
-25.69	0.94	1.32	0.12	13.30	1086	EIZ V
-25.03	1.22	1.21	0.10	14.28	1091	EIZ V
-25.89	1.21	1.16	0.10	13.40	1096	EIZ V
-25.49	0.66	1.15	0.10	13.15	1101	EIZ V
-25.64	1.62	1.15	0.10	13.78	1106	EIZ V
-25.36	0.74	1.46	0.12	14.18	1111	EIZ V
-26.08	0.82	1.25	0.10	13.96	1116	EIZ V
-25.98	1.01	1.17	0.10	13.82	1121	EIZ V
-25.64	0.94	1.15	0.09	14.21	1126	EIZ V
-25.42	1.16	0.93	0.07	15.35	1131	EIZ V
-18.22	0.50	1.28	0.08	18.01	1136	EIZ V
-25.98	0.51	0.98	0.08	14.31	1141	EIZ V
-25.87	0.99	0.94	0.08	14.47	1146	EIZ V
-26.15	-0.05	1.13	0.09	13.96	1151	EIZ V
-25.91	1.08	0.95	0.08	14.27	1156	EIZ V
-25.89	0.77	1.19	0.10	14.14	1161	EIZ V
-26.29	0.81	0.92	0.07	14.80	1166	EIZ V
-26.62	0.17	1.21	0.10	14.32	1171	EIZ V
-26.21	0.55	1.06	0.09	14.00	1176	EIZ V
-25.35	0.61	1.17	0.09	14.82	1181	EIZ V
-23.56	0.49	1.06	0.08	14.98	1186	EIZ V
-25.88	0.02	0.79	0.06	14.62	1191	EIZ V
-25.99	0.91	0.77	0.06	14.80	1196	EIZ V
-26.38	0.51	1.25	0.10	13.91	1201	EIZ V
-26.32	1.29	1.41	0.11	14.44	1206	EIZ V
-26.16	0.98	1.15	0.10	13.91	1211	EIZ V
-27.26	1.31	1.60	0.14	13.50	1216	EIZ V
-26.99	1.36	1.62	0.14	13.81	1221	EIZ V
-27.09	1.41	1.66	0.14	14.33	1226	EIZ V
-27.37	1.05	1.72	0.15	13.78	1231	EIZ V
-27.58	0.96	2.65	0.23	13.59	1236	EIZ V
-28.04	1.33	2.69	0.23	13.81	1241	EIZ V
-28.01	0.98	3.06	0.32	13.95	1246	EIZ V
-31.28	-1.17	11.72	1.08	12.65	1261	EIZ IV
-30.68	-0.16	11.69	1.09	12.51	1266	EIZ IV
-30.66	0.13	12.01	1.13	12.41	1271	EIZ IV
-30.44	0.30	12.02	1.16	12.04	1276	EIZ IV
-30.35	0.61	10.75	1.02	12.25	1281	EIZ IV
-29.56	1.48	10.98	1.03	12.39	1286	EIZ IV
-30.50	-0.01	10.06	0.95	12.40	1291	EIZ IV
-30.60	-1.11	14.16	1.33	12.44	1296	EIZ IV
-30.04	-0.04	12.85	1.20	12.49	1301	EIZ IV
-30.46	-0.49	14.80	1.37	12.64	1306	EIZ IV
-30.47	0.83	12.51	1.13	12.90	1311	EIZ IV
-30.19	0.32	10.09	0.92	12.83	1316	EIZ IV
-28.48	0.55	10.90	0.98	12.97	1321	EIZ IV
-26.34	0.29	10.10	0.85	13.84	1326	EIZ IV
-30.80	-0.63	15.85	1.52	12.15	1331	EIZ IV
-27.47	-0.21	8.78	0.83	12.29	1336	EIZ III
-28.11	0.17	6.70	0.65	12.03	1341	EIZ III
-26.26	0.23	4.56	0.43	12.38	1346	EIZ III
-26.38	0.70	2.69	0.27	11.82	1351	EIZ III
-25.68	-0.99	1.90	0.19	11.77	1356	EIZ III
-25.11	0.48	1.33	0.13	12.38	1361	EIZ III
-25.20	0.45	1.19	0.12	12.03	1366	EIZ III
-24.51	0.28	1.15	0.10	13.11	1371	EIZ II
-20.36	-0.18	0.71	0.05	17.80	1376	EIZ II
-25.79	-0.20	0.75	0.06	14.32	1381	EIZ II
-21.63	0.19	1.42	0.11	15.32	1386	EIZ II
-24.58	0.76	1.38	0.13	12.31	1391	EIZ II
-25.36	0.50	0.95	0.08	13.54	1396	EIZ I
-24.99	0.42	1.15	0.10	12.78	1401	EIZ I
-24.95	0.42	0.97	0.09	13.17	1406	EIZ I
-25.15	-0.47	0.98	0.08	14.08	1411	EIZ I
-26.67	-0.48	0.92	0.08	14.30	1416	EIZ I
-22.67	0.03	0.94	0.07	15.41	1421	EIZ I
-22.05	-1.36	1.09	0.08	15.75	1426	EIZ I
-25.35	-0.81	0.83	0.07	14.08	1431	EIZ I
-19.39	-1.19	0.96	0.07	15.85	1436	EIZ I
-22.93	-0.29	1.07	0.09	14.67	1441	EIZ I
-20.67	-0.03	0.89	0.07	15.91	1446	EIZ I
-24.55	-0.98	0.92	0.08	14.12	1451	EIZ I
-23.75	-0.98	0.72	0.06	14.03	1456	EIZ I
-23.60	0.34	0.69	0.06	13.09	1461	EIZ I

Table II.2 – Stable isotope and selected organic properties for Endinger Bruch

$\delta^{13}C$ (‰)	$\delta^{15}N$ (‰)	TOC (wt%)	TN (wt%)	C:N	Depth (cm)	Sample
-13.44	-2.88	0.62	3.56	14.77	400	PIZ III
-11.82	-1.41	1.10	3.58	14.21	402	PIZ III
-14.22	-3.11	1.06	3.02	14.69	404	PIZ III
-12.97	-1.25	0.99	3.28	14.97	406	PIZ III
-13.58	-1.01	1.18	3.02	14.76	408	PIZ III
-12.89	-1.16	1.33	3.43	14.47	410	PIZ III
-12.33	-2.42	0.98	3.33	14.36	412	PIZ III
-13.10	-0.59	1.33	3.32	14.33	414	PIZ III
-12.91	-1.98	1.03	3.49	14.00	416	PIZ III
-12.66	-1.38	0.91	3.27	14.70	418	PIZ III
-12.09	-1.17	0.35	3.20	14.13	420	PIZ III
-12.05	-1.33	0.61	3.49	14.83	422	PIZ III
-12.92	-1.78	0.81	3.41	14.54	424	PIZ III
-12.28	-0.78	0.52	3.07	15.03	428	PIZ III
-13.06	-1.06	0.89	2.95	14.68	432	PIZ III
-13.17	-0.33	0.72	3.21	14.88	434	PIZ III
-13.66	-1.43	0.44	3.19	15.05	436	PIZ III
-13.33	-0.64	0.71	3.15	14.77	438	PIZ III
-14.08	-1.65	0.68	3.13	15.23	440	PIZ III
-13.40	-1.15	0.94	2.98	15.23	444	PIZ III
-13.96	-0.88	2.80	3.43	15.02	446	PIZ III
-14.25	-0.42	0.56	2.97	14.72	448	PIZ III
-16.21	-3.44	0.98	3.06	14.35	450	PIZ III
-13.60	-0.81	0.85	3.13	14.78	452	PIZ III
-13.72	0.21	0.76	3.13	14.62	454	PIZ III
-14.95	-0.27	1.17	3.20	14.33	456	PIZ III
-16.25	-0.48	0.94	3.42	14.40	458	PIZ III
-17.14	-2.06	0.68	3.82	14.14	460	PIZ III
-16.15	-0.94	0.59	3.70	14.14	462	PIZ III
-18.52	-4.39	1.07	3.69	13.89	466	PIZ III
-17.76	-1.73	0.87	3.76	13.74	468	PIZ III
-17.30	-1.36	0.73	3.82	14.22	470	PIZ III
-17.89	-0.55	0.88	3.78	13.95	474	PIZ III
-19.69	-2.50	0.77	3.82	13.76	476	PIZ III
-18.59	-1.45	0.85	3.91	14.09	478	PIZ III
-18.57	-0.38	0.91	3.58	14.61	480	PIZ III
-17.28	-0.35	0.82	3.65	14.50	482	PIZ II
-18.95	-0.68	0.78	3.44	14.81	484	PIZ II
-20.03	0.08	0.11	0.40	14.82	488	PIZ II
-23.79	1.85	0.03	0.19	12.70	494	PIZ II
-24.76	1.52	0.09	0.23	12.62	496	PIZ II
-24.88	1.03	0.09	0.24	13.01	498	PIZ II
-24.71	0.72	0.03	0.20	13.13	500	PIZ II
-23.78	1.85	0.02	0.20	12.45	502	PIZ II
-24.98	1.36	0.02	0.19	13.13	506	PIZ II
-25.94	0.33	0.02	0.16	12.95	508	PIZ II
-24.91	1.83	0.02	0.18	12.75	514	PIZ II
-23.94	1.98	0.03	0.21	12.85	516	PIZ II
-25.34	1.88	0.02	0.22	12.83	518	PIZ II
-26.03	2.18	0.02	0.20	13.86	522	PIZ II
-25.16	2.51	0.02	0.18	13.50	524	PIZ II
-26.10	2.79	0.03	0.19	13.44	526	PIZ II
-26.53	2.50	0.03	0.22	13.99	528	PIZ II
-27.36	3.21	0.02	0.21	13.50	530	PIZ II
-27.58	3.15	0.03	0.28	13.89	532	PIZ II
-27.72	1.50	0.04	0.28	15.19	534	PIZ II
-27.99	2.01	0.03	0.28	14.93	536	PIZ II
-25.33	1.84	0.05	0.38	16.37	538	PIZ I
-23.85	2.05	0.06	0.38	17.39	540	PIZ I
-29.74	0.34	0.04	0.30	13.34	544	PIZ I
-11.78	1.27	0.04	0.18	22.58	550	PIZ I
-10.17	-3.57	0.03	0.17	31.88	552	PIZ I
-12.71	1.27	0.03	0.17	22.94	556	PIZ I

Table II.3 – Stable isotope and selected organic properties for Potremser Moor

δ13C (‰)	δ15N (‰)	TOC (wt%)	TN (wt%)	C:N	Depth (cm)	Sample	δ13C (‰)	δ15N (‰)	TOC (wt%)	TN (wt%)	C:N	Depth (cm)	Sample
-14.60	-0.35	0.80	3.04	16.18	600	KOZ II	-16.58	-0.47	0.88	2.91	16.79	652	KOZ II
-13.91	-0.65	0.67	3.21	15.74	602	KOZ II	-16.51	-0.44	0.90	3.00	16.77	654	KOZ II
-14.51	-1.04	0.65	3.22	15.82	604	KOZ II	-16.64	-0.50	1.10	2.83	16.75	656	KOZ II
-13.48	-0.66	0.65	3.03	15.42	606	KOZ II	-16.60	-0.53	0.88	2.55	16.86	658	KOZ II
-13.63	-0.83	1.11	3.28	14.75	608	KOZ II	-16.37	-0.78	0.88	2.62	16.97	660	KOZ II
-13.48	-0.77	0.78	3.05	15.84	610	KOZ II	-16.44	-0.55	1.54	2.80	16.90	662	KOZ II
-13.87	-0.55	0.78	2.91	16.21	612	KOZ II	-16.23	-0.96	1.00	2.61	17.11	664	KOZ II
-13.98	-0.36	1.25	3.12	15.94	614	KOZ II	-16.90	-1.91	1.33	2.75	16.58	666	KOZ II
-13.83	-0.31	0.57	2.85	16.39	616	KOZ II	-16.09	-0.68	0.79	2.69	16.73	668	KOZ II
-13.91	-0.28	0.72	2.91	16.19	618	KOZ II	-16.73	-1.05	1.52	3.27	16.47	670	KOZ II
-14.47	0.04	1.34	2.92	16.00	620	KOZ II	-16.20	-0.78	1.08	3.23	16.59	672	KOZ II
-16.23	-0.20	1.88	3.23	15.86	622	KOZ II	-16.35	-0.91	1.95	3.04	16.12	674	KOZ II
-16.08	0.11	1.88	3.14	15.91	624	KOZ II	-16.13	-0.97	0.89	2.79	16.63	676	KOZ II
-15.70	-0.34	0.57	2.75	16.56	626	KOZ II	-15.49	-0.79	1.97	3.04	16.06	678	KOZ II
-16.22	-0.07	0.69	3.01	16.08	628	KOZ II	-16.10	-1.37	2.67	3.24	16.02	680	KOZ II
-16.23	-0.23	0.45	2.91	16.32	630	KOZ II	-15.41	-1.01	1.12	3.12	15.88	682	KOZ II
-16.36	-0.67	0.62	2.88	15.98	632	KOZ II	-15.28	-0.68	1.09	3.24	15.98	684	KOZ II
-16.94	-1.32	0.56	3.06	16.13	634	KOZ II	-15.51	-0.76	1.06	3.14	15.77	686	KOZ II
-16.81	-0.93	1.20	3.29	15.42	636	KOZ II	-15.40	-1.03	1.01	3.07	15.72	688	KOZ II
-15.90	-0.82	0.59	3.02	15.88	638	KOZ II	-15.18	-1.08	0.60	2.94	16.10	690	KOZ II
-15.69	-1.56	0.51	2.92	16.02	640	KOZ II	-14.93	-1.28	0.77	3.36	16.11	692	KOZ II
-16.23	-0.78	1.08	2.85	16.31	642	KOZ II	-14.96	-1.17	0.71	3.33	16.06	694	KOZ II
-16.48	-1.22	0.74	2.79	16.82	644	KOZ II	-15.06	-1.19	1.22	3.30	15.72	696	KOZ II
-16.84	-1.10	0.88	2.85	16.66	646	KOZ II	-15.10	-0.90	0.64	3.05	16.21	698	KOZ II
-16.55	-1.08	0.75	2.79	16.68	648	KOZ II	-16.51	-0.87	2.84	3.06	15.81	700	KOZ II
-16.76	-0.53	1.80	3.08	16.09	650	KOZ II	-18.37	-0.34	1.92	2.84	17.49	702	KOZ II

δ13C (‰)	δ15N (‰)	TOC (wt%)	TN (wt%)	C:N	Depth (cm)	Sample	δ13C (‰)	δ15N (‰)	TOC (wt%)	TN (wt%)	C:N	Depth (cm)	Sample
-15.79	-0.97	0.94	2.92	17.04	704	KOZ II	-25.80	0.67	0.07	0.27	16.97	782	KOZ I
-14.57	-0.79	1.54	3.13	15.74	706	KOZ II	-24.52	0.86	0.21	0.51	16.30	784	KOZ I
-14.71	-0.93	0.82	3.13	16.10	708	KOZ II	-26.38	1.05	0.08	0.30	16.60	786	KOZ I
-15.47	-0.92	0.86	2.99	16.39	710	KOZ II	-26.08	0.94	0.08	0.32	16.30	788	KOZ I
-15.08	-1.03	1.79	3.07	15.60	712	KOZ II	-25.43	1.26	0.22	0.51	16.56	790	KOZ I
-14.66	-1.05	0.67	2.67	16.49	714	KOZ II	-25.74	0.83	0.42	0.76	16.05	792	KOZ I
-14.88	-0.87	1.16	2.74	16.00	716	KOZ II	-23.41	0.91	0.29	1.12	13.79	794	KOZ I
-15.09	-1.12	1.24	2.87	15.87	718	KOZ II	-23.51	0.66	0.23	0.52	14.33	796	KOZ I
-15.25	-1.40	1.07	2.98	16.47	720	KOZ II	-24.38	0.97	0.17	0.67	14.74	798	KOZ I
-16.28	-1.71	1.60	2.82	15.78	722	KOZ II	-23.75	-0.51	0.15	0.41	16.52	800	KOZ I
-15.50	-0.84	1.89	3.05	15.69	724	KOZ II							
-15.74	-0.87	0.71	2.91	15.89	726	KOZ II							
-16.45	-1.10	0.61	2.84	15.95	728	KOZ II							
-16.97	-0.99	0.59	2.77	15.88	730	KOZ II							
-17.45	-0.93	1.05	2.84	15.93	732	KOZ II							
-17.64	-0.64	0.76	2.83	15.99	734	KOZ II							
-18.41	-1.64	1.25	2.84	15.91	736	KOZ II							
-17.16	-0.88	0.48	2.79	16.15	738	KOZ II							
-16.51	-0.65	0.54	2.89	16.39	740	KOZ II							
-17.86	-0.63	1.71	2.95	15.50	742	KOZ II							
-17.42	-0.37	0.65	2.56	15.69	744	KOZ II							
-17.22	-0.38	0.55	2.57	15.86	746	KOZ II							
-18.06	0.46	0.60	2.33	15.52	748	KOZ II							
-19.41	-0.23	0.69	1.87	15.46	750	KOZ II							
-20.53	0.13	0.22	1.24	15.84	752	KOZ II							
-20.34	1.28	0.18	0.52	14.69	754	KOZ II							

Table II.4 – Stable isotope and selected organic properties for Kieshofer Moor

$\delta^{13}C$ (‰)	$\delta^{15}N$ (‰)	TOC (wt%)	TN (wt%)	C:N	Depth (cm)	Sample
-25.84	-2.34	0.43	0.87	63.99	100 cm	DIZ V
-24.88	-3.57	0.49	0.80	68.36	102 cm	DIZ V
-25.15	-1.81	0.42	0.81	68.81	104 cm	DIZ V
-26.35	-2.20	0.52	0.76	75.11	106 cm	DIZ V
-25.95	-0.67	0.42	1.18	51.34	108 cm	DIZ V
-25.85	-1.54	0.32	2.20	28.28	110 cm	DIZ V
-26.27	-0.87	0.34	1.97	31.41	112 cm	DIZ V
-26.10	-1.07	0.35	1.90	31.93	114 cm	DIZ V
-25.63	0.82	0.48	1.84	33.02	116 cm	DIZ V
-26.39	-0.97	0.40	1.49	42.55	118 cm	DIZ V
-24.19	-0.01	0.39	2.25	26.93	120 cm	DIZ V
-23.53	-1.65	0.40	2.26	26.21	122 cm	DIZ V
-22.06	-1.30	0.49	2.86	21.96	124 cm	DIZ IV
-21.35	-0.68	0.65	2.85	21.21	126 cm	DIZ IV
-19.59	-1.11	0.87	3.45	19.44	128 cm	DIZ IV
-18.51	-0.99	0.77	3.70	17.41	130 cm	DIZ IV
-17.82	-1.34	0.88	3.85	16.32	132 cm	DIZ IV
-17.69	-1.44	0.63	3.77	16.41	134 cm	DIZ IV
-17.20	-1.21	0.60	3.77	16.04	136 cm	DIZ IV
-15.93	-1.00	0.68	3.99	15.34	138 cm	DIZ IV
-18.54	-1.05	0.83	3.81	16.38	140 cm	DIZ IV
-17.41	-1.53	0.65	3.23	15.67	142 cm	DIZ IV
-15.73	-1.53	0.70	3.96	13.97	144 cm	DIZ IV
-19.88	-0.72	0.70	3.58	16.38	146 cm	DIZ IV
-19.80	-0.86	0.62	3.23	16.59	148 cm	DIZ IV
-20.72	-0.80	0.67	3.51	17.02	150 cm	DIZ IV
-20.19	-1.04	0.56	3.92	16.28	152 cm	DIZ IV
-14.70	-1.19	0.67	4.46	12.89	154 cm	DIZ IV
-13.76	-1.12	0.61	4.31	13.07	156 cm	DIZ III
-13.43	-1.43	0.69	4.26	12.73	158 cm	DIZ III
-12.84	-1.64	0.59	3.86	13.08	160 cm	DIZ III
-11.68	0.28	0.58	3.79	13.52	162 cm	DIZ III
-13.32	-1.22	0.53	3.70	13.50	164 cm	DIZ III
-12.64	-1.21	0.62	3.91	13.62	166 cm	DIZ III
-12.05	-1.41	0.60	3.81	13.42	168 cm	DIZ III
-12.20	-1.49	0.59	3.81	13.45	170 cm	DIZ III
-11.16	0.29	0.58	3.89	13.43	172 cm	DIZ III
-12.76	-1.20	0.51	3.63	14.21	174 cm	DIZ III
-12.58	-1.63	0.68	3.69	14.12	176 cm	DIZ III
-12.72	-1.48	0.72	3.96	13.34	178 cm	DIZ III
-13.63	-1.43	0.66	4.12	14.15	180 cm	DIZ III
-13.53	-1.17	0.69	3.67	14.37	182 cm	DIZ III
-14.39	-1.43	0.68	3.57	15.52	184 cm	DIZ III
-14.09	-0.72	0.62	3.60	15.47	186 cm	DIZ III
-13.49	-1.40	0.64	3.51	14.82	188 cm	DIZ III
-15.36	-0.77	0.48	3.35	15.96	190 cm	DIZ III
-15.89	-1.42	0.52	3.28	15.23	192 cm	DIZ III
-16.55	-0.39	0.58	2.52	15.45	194 cm	DIZ III
-17.46	-1.02	0.54	2.19	16.25	196 cm	DIZ III
-17.31	-1.16	0.27	1.89	16.46	198 cm	DIZ III
-15.51	-1.33	0.24	1.58	17.90	200 cm	DIZ III
-17.74	0.38	0.63	1.03	15.91	202 cm	DIZ III
-17.89	0.16	0.14	0.32	15.30	204 cm	DIZ III
-19.33	1.24	0.11	0.36	15.61	206 cm	DIZ III
-21.95	1.71	0.10	0.33	15.27	210 cm	DIZ II
-22.56	1.10	0.12	0.36	15.55	212 cm	DIZ II
-24.19	1.29	0.07	0.24	15.45	216 cm	DIZ II
-23.94	1.40	0.09	0.26	15.64	218 cm	DIZ II
-24.11	1.11	0.06	0.28	15.30	220 cm	DIZ II
-24.09	0.50	0.08	0.29	15.20	224 cm	DIZ II
-23.24	0.25	0.09	0.37	15.09	226 cm	DIZ II
-23.57	-0.31	0.11	0.35	14.01	230 cm	DIZ II
-23.97	-0.16	0.14	0.39	13.78	236 cm	DIZ II
-24.70	0.68	0.06	0.31	14.40	244 cm	DIZ II
-23.19	-0.26	0.12	0.76	16.55	246 cm	DIZ I
-21.88	-0.38	0.19	0.96	16.71	248 cm	DIZ I
-23.50	1.09	0.13	0.74	16.95	250 cm	DIZ I
-25.26	-0.45	0.09	0.81	16.01	252 cm	DIZ I
-22.52	0.27	0.21	1.19	14.61	254 cm	DIZ I
-21.64	-0.06	0.53	1.84	13.58	256 cm	DIZ I
-21.06	-0.39	0.47	2.50	12.41	258 cm	DIZ I
-20.37	-0.72	0.48	2.59	13.13	260 cm	DIZ I
-17.97	-1.18	0.15	1.33	14.04	262 cm	DIZ I
-17.85	-1.38	0.49	2.26	16.73	264 cm	DIZ I
-16.53	-2.11	0.41	2.21	17.03	266 cm	DIZ I
-19.24	-0.91	0.37	2.24	17.46	268 cm	DIZ I
-20.12	0.07	0.45	2.58	16.41	270 cm	DIZ I
-21.04	-2.28	0.53	2.93	16.10	272 cm	DIZ I
-20.84	-1.20	0.43	2.74	14.69	274 cm	DIZ I
-20.13	-1.11	0.31	2.55	14.54	276 cm	DIZ I
-18.92	-1.69	0.11	1.36	14.66	278 cm	DIZ I
-18.63	-1.85	0.14	1.51	14.50	280 cm	DIZ I

Table II.5 – Stable isotope and selected organic properties for Daschower Moor

Appendix III: Cladoceran counts

Depth	Acroperos harpae	A. affinis	A. costata	A. guttata rectangula	A. guttata var tub	A. intermedia	A. quadrangularis	A. rustica	Alonella excisa	A. exigua	A. rostrata	A. nana	Alonopsis elongata	Arichistropus emarginatus	Camptocercus rectirostris	Chydorus piger	C. sphaericus	Eurycercus lamellatus
217 cm	0	0	0	0	0	0	0	0	0	0	0	0	0	0	0	0	0	0
212 cm	0	0	0	0	0	0	0	0	0	0	0	0	0	0	0	0	0	0
207 cm	0	0	0	0	0	0	0	0	0	0	0	0	0	0	0	0	0	0
202 cm	0	0	0	0	0	0	0	0	0	0	0	0	0	0	0	0	0	0
197 cm	0	0	0	0	0	0	0	0	255	0	0	0	0	0	0	0	0	0
192 cm	0	0	0	0	0	0	0	0	916	8	0	2584	0	263	0	69	325	0
187 cm	4333	0	0	333	0	0	167	0	13167	167	250	20333	0	0	2500	500	1000	0
182 cm	0	235	0	521	0	0	15	0	769	0	0	0	0	0	0	0	0	0
175 cm	30	0	0	120	0	0	10	0	570	0	0	0	0	0	0	0	0	0
170 cm	20	0	0	0	0	0	0	0	72	0	0	0	0	0	0	0	10	0
165 cm	0	0	0	0	0	0	0	0	125	0	0	0	0	0	10	0	0	0
160 cm	5	0	0	0	0	0	0	0	68	0	0	0	0	0	0	0	30	0
155 cm	0	0	0	0	0	0	0	0	125	0	0	0	0	0	0	0	0	0
150 cm	5	0	0	0	0	0	0	0	62.5	0	0	0	0	0	0	0	0	0
145 cm	15	0	0	0	0	0	0	0	62.5	0	0	10	0	0	0	5	0	0
140 cm	20	0	0	0	0	0	0	0	1284	0	0	153	0	0	0	0	20	0
135 cm	0	0	0	0	12	0	0	0	2911	0	0	0	0	0	0	0	23	0
130 cm	417	0	0	139	0	0	0	0	472	0	18	1119	0	0	18	0	9	9
125 cm	0	0	0	125	0	10	0	10	145	0	0	125	0	0	0	5	145	0
120 cm	0	14	0	14	14	0	0	0	1794	218	29	2092	0	0	0	588	0	0
115 cm	0	0	0	0	10	0	10	0	753	0	0	0	0	0	0	20	157	0
110 cm	259	3	0	217	0	0	0	6	2001	248	109	6	0	0	0	11	164	0
105 cm	0	0	0	0	0	0	0	0	0	0	0	0	0	0	0	0	0	0
100 cm	0	0	0	0	0	0	0	0	107	0	0	446	0	0	0	0	15	0
95 cm	0	588	21	294	0	0	52	0	0	0	0	1362	0	0	0	189	2249	0
90 cm	0	909	0	83	0	0	1106	83	0	0	0	3648	0	0	0	208	7617	0
85 cm	0	556	0	52	0	0	167	556	0	0	0	0	0	0	0	135	2438	556
80 cm	13	1111	0	39	0	0	132	52	278	13	0	0	0	0	0	158	3697	0
75 cm	238	714	0	38	0	0	752	173	0	0	0	0	0	0	0	269	1243	0
70 cm	0	617	0	100	0	0	259	176	0	0	0	0	27	0	172	101	174	0
65 cm	5	500	0	29	0	0	495	29	0	0	0	10	10	0	103	142	223	0
60 cm	38	1323	38	435	0	0	1106	429	0	0	0	0	58	0	0	96	236	0
55 cm	294	364	0	195	98	0	364	196	0	0	0	104	0	0	0	0	26	0
50 cm	15	449	0	49	0	0	163	137	10	0	0	49	0	10	10	0	312	5
45 cm	125	3000	0	1550	50	0	2300	200	0	0	0	0	0	0	0	0	900	0
40 cm	115	302	0	1154	58	0	679	371	77	0	0	0	0	0	0	38	1135	0
35 cm	135	485	10	493	31	0	253	63	73	0	0	0	0	0	42	21	577	0
30 cm	275	2275	0	1000	0	0	1104	1000	27	55	0	0	0	0	27	0	915	0
25 cm	750	13250	2500	5250	0	0	1500	250	0	0	0	500	0	0	0	250	1575	0
20 cm	357	982	0	286	0	0	1196	0	0	0	0	36	0	0	107	0	706	0
15 cm	313	1000	0	2000	0	0	1000	0	1313	0	0	1625	0	0	125	0	1000	0
10 cm	51	185	0	763	0	0	230	89	0	0	0	69	0	0	0	86	332	89
5 cm	133	95	0	243	0	0	458	0	0	0	0	421	0	0	0	63	454	13
0 cm	10	0	0	10	0	0	20	0	0	0	0	3	0	0	5	12	30	5

Table III.1 – Cladoceran counts for Slotseng.

Graptoleberis testudinaria	Kurzia latissima	Leydigi acanthocercoides	Leydigi leydigi	Monospilus dispar	Pleroxus aduncus	P. laevis	P. trigonellus	P. truncatus	P. uncinatus	Psydochydorus globosus	Rhynchotalona falcata	Bosmina coregoni	B. longirostris	Daphnia pulex	Ceriodaphnia epphipia	D. longispina epphipia	D. pulex epphipia
0	0	0	0	0	0	0	0	0	0	0	0	0	0	0	0	0	0
0	0	0	0	0	0	0	0	0	0	0	0	0	0	0	0	0	0
0	0	0	0	0	0	0	0	0	0	0	0	0	0	0	0	0	0
0	0	0	0	0	0	0	0	0	0	0	0	0	0	0	0	0	0
0	0	0	0	0	0	0	0	0	0	0	0	0	0	0	0	0	0
0	0	0	0	0	0	0	0	0	0	0	0	0	0	0	0	0	0
0	0	0	0	0	0	0	0	0	0	0	0	0	0	0	0	0	0
0	0	0	0	0	0	0	0	0	0	0	0	0	0	0	0	0	0
0	0	0	40	0	0	0	0	0	0	0	0	0	0	0	0	0	0
0	0	0	0	0	0	0	0	0	0	0	0	0	0	0	0	0	0
0	0	0	0	0	0	0	0	0	0	0	0	0	0	0	0	0	0
0	0	0	0	0	0	0	0	0	0	0	0	0	0	0	0	0	0
0	0	0	0	0	0	0	0	0	0	0	0	0	0	0	0	0	0
0	0	0	0	0	0	0	0	0	0	0	0	0	0	0	0	0	0
0	0	0	0	0	0	0	0	0	0	0	0	0	0	0	0	0	10
0	0	0	0	0	0	0	0	0	0	0	0	0	0	0	0	0	0
0	0	0	0	0	0	0	0	0	0	0	0	0	0	0	0	0	0
0	0	0	0	0	0	0	0	9	9	0	0	0	0	0	0	0	0
0	0	0	0	0	0	0	0	0	5	0	0	0	0	0	0	0	0
0	0	0	0	0	0	0	294	14	0	7	0	0	14	0	0	0	0
0	0	0	68	5	0	0	0	0	0	0	0	0	0	0	0	0	0
0	0	0	6	0	0	0	0	0	0	0	0	0	0	0	0	0	0
0	0	0	0	0	0	0	0	0	0	0	0	0	0	0	0	0	0
0	0	0	0	0	0	0	0	0	0	0	0	0	0	0	0	0	0
0	0	0	294	0	0	0	294	0	0	21	0	0	0	0	0	21	0
0	0	0	538	0	0	0	0	0	455	83	0	0	0	455	0	0	0
0	0	0	83	0	0	0	21	0	278	73	0	0	0	556	42	0	167
0	26	0	0	0	0	0	0	0	278	118	0	0	0	833	0	0	105
0	0	0	19	0	0	0	0	0	476	10	0	0	0	1190	19	0	115
0	0	0	54	0	0	0	0	0	86	0	0	0	0	345	14	0	176
0	0	15	93	0	0	0	0	0	83	0	0	0	0	167	0	0	303
0	0	48	96	0	0	0	19	0	217	0	0	0	275	217	0	327	0
0	0	39	26	91	0	91	0	0	0	7	0	0	0	182	40	0	434
0	0	5	29	20	0	0	0	0	0	0	0	0	153	571	0	0	98
0	0	300	100	100	50	0	500	0	0	0	0	200	1850	0	0	0	0
0	0	96	333	38	0	0	0	0	0	58	0	77	1795	333	0	0	269
0	0	0	146	0	0	0	0	0	0	52	0	21	641	256	0	0	250
55	0	0	165	0	0	0	0	0	0	0	500	220	3434	0	0	0	385
0	0	0	1000	0	0	0	0	0	0	0	0	3000	26750	0	500	0	0
0	0	0	71	36	0	0	0	0	0	36	0	1393	7393	0	0	0	72
0	0	125	0	125	0	0	0	0	0	125	0	4500	11625	0	0	0	0
0	0	89	17	34	0	0	0	0	17	0	0	112	567	0	0	0	0
37	0	0	158	0	25	0	25	0	0	12	0	167	0	0	0	0	0
0	0	0	0	0	0	0	0	0	0	0	0	0	500	0	0	0	0

Table III.1 continued – Cladoceran counts for Slotseng.

Depth	Acroperos elongatus	A. harpae	Alona affinis	A. costata	A. guttata rectangula	A. guttata var tub	A. intermedia	A. quadrangularis	A. rustica	Alonella excisa	A. rostrata	A. nana	Alonopsis elongata	Camptocercus rectirostris	C. piger	C. sphaericus	Eurycercus lamellatus
851 cm	0	5625	12250	0	2500	0	0	3750	0	0	0	4750	0	1250	2000	2125	3500
856 cm	0	1250	2083	0	1458	0	0	1250	0	0	0	4263	0	0	2965	6763	0
861 cm	0	2857	1389	0	2381	0	0	2381	0	0	0	7103	0	1667	1389	5913	2778
866 cm	0	7750	8500	0	2500	0	0	4000	0	0	0	2000	0	0	3250	8500	3500
871 cm	0	2500	6667	0	2833	0	0	667	0	0	0	5667	0	0	167	4167	7333
876 cm	0	2679	9048	0	3274	0	0	3333	0	0	0	2054	0	0	833	3214	417
881 cm	0	2750	8250	0	500	0	0	1500	0	0	0	6250	0	2500	500	2292	1500
886 cm	0	2610	4608	0	208	0	0	2304	0	0	417	4498	0	417	2083	5319	1667
891 cm	0	3833	11500	0	4333	0	0	1000	0	0	0	8000	0	1000	1750	7750	0
896 cm	0	3561	11136	0	1364	0	0	3333	0	0	0	7689	0	909	2121	4280	455
901 cm	0	4405	1250	0	3571	0	0	833	0	0	0	5863	0	417	2411	5119	3988
906 cm	0	4417	10500	0	1917	0	500	4333	0	0	0	8250	0	0	2000	3417	500
911 cm	0	4500	4500	0	1500	0	0	3500	0	0	0	3000	0	0	3000	5000	1500
916 cm	0	3333	16833	0	2417	0	0	1500	0	0	0	13667	0	500	1000	7000	3000
921 cm	0	2348	6742	0	3333	227	0	909	0	0	0	6136	0	0	1818	11742	1363
926 cm	0	1000	2909	0	2159	0	0	1591	0	0	1000	5318	0	682	568	2932	455
931 cm	0	1363	5455	0	10909	0	0	17727	0	0	455	10455	0	5000	682	14090	5909
936 cm	0	1667	4500	0	13500	0	0	5167	0	0	0	3833	0	0	1500	5250	1333
941 cm	0	2250	10167	0	3667	0	0	1667	0	0	0	4167	0	0	2917	4292	7250
946 cm	0	2308	8077	0	4231	0	0	2308	0	0	385	7692	0	0	769	5000	385
951 cm	0	5625	12250	0	2500	0	0	3750	0	0	0	4750	0	1250	2000	2125	3500
956 cm	0	1250	2083	0	1458	0	0	1250	0	0	0	4263	0	0	2965	6763	1250
961 cm	0	1005	2526	0	837	0	0	235	0	0	34	1165	0	34	134	1515	134
966 cm	0	3286	6429	0	36	0	0	960	0	0	36	2612	0	71	906	3482	1670
971 cm	0	4316	2778	0	99	0	0	0	0	0	0	3374	0	66	231	2778	298
976 cm	0	200	3330	0	50	0	0	350	0	0	1515	2973	0	50	125	4030	1665
981 cm	0	956	3526	0	1663	0	0	250	0	0	0	4400	0	1612	100	3019	3017
986 cm	0	588	3333	0	98	0	0	0	0	0	0	2402	0	98	1568	5049	686
991 cm	0	3914	294	0	0	0	0	392	0	0	0	7717	0	0	490	4453	490
996 cm	0	3395	2229	102	102	0	0	306	0	0	0	6789	0	204	2127	3701	2535
1006 cm	0	95	143	0	0	0	0	48	0	0	0	5467	0	0	48	1494	1541
1011 cm	0	250	375	0	500	0	0	750	0	0	0	10417	0	250	0	2833	1250
1016 cm	0	943	200	0	743	0	0	0	0	0	0	1000	0	0	0	2774	2774
1021 cm	0	659	227	0	0	0	0	454	0	0	0	1466	0	51	102	1373	408
1026 cm	0	1429	0	0	0	0	0	0	0	0	0	776	0	0	745	3915	1276
1031 cm	0	441	294	0	1515	0	0	0	0	0	0	1515	0	3030	758	3324	294
1036 cm	0	2088	2511	0	0	0	0	0	0	0	0	357	0	119	0	3755	476
1041 cm	0	2579	204	0	0	0	0	0	0	0	1136	823	0	153	102	4334	204
1046 cm	96	288	833	0	833	0	0	0	0	0	0	96	0	192	576	2019	192
1051 cm	0	2963	100	0	100	0	0	0	0	0	0	100	0	0	200	1800	0
1056 cm	0	967	1667	0	1250	0	0	0	0	0	0	67	0	33	100	1200	133
1061 cm	0	1243	1543	0	0	0	0	943	0	0	0	200	0	200	300	2758	4030
1066 cm	0	167	250	0	0	0	0	0	0	42	0	83	0	0	167	1272	250
1071 cm	0	1216	200	0	1149	0	0	0	0	0	0	267	0	0	367	1449	641
1076 cm	0	167	667	0	0	0	0	250	0	333	0	83	0	0	1500	1333	500
1081 cm	0	765	674	0	0	0	0	143	0	143	0	746	0	0	571	2135	817
1086 cm	0	1315	250	0	0	0	0	125	0	0	125	0	0	0	970	2646	125
1091 cm	0	28	2220	0	0	0	0	14	0	14	0	21	0	7	368	2277	1499
1096 cm	0	656	105	0	943	0	0	105	0	52	0	1887	0	0	1048	3776	158
1101 cm	0	819	1070	0	0	0	0	125	0	0	0	820	0	125	1195	3869	125

Table III.2 – Cladoceran counts for Endinger Bruch.

Graptoleberis testudinaria	Leydigi acanthocercoides	L. leydigi	Monospilus dispar	Pleroxus aduncus	P. trigonellus	P. truncatus	P. uncinatus	Psydochydorus globosus	Rhynchotalona falcata	Sida crystallina	Bosmina coregoni	B. longirostris	Daphnia pulex	D. longispina epphipia	D. pulex epphipia	Latona Setifera
750	2500	0	0	0	0	0	2000	0	0	4000	0	15500	0	0	0	0
4679	7692	833	417	0	0	0	6506	0	0	2500	417	32019	0	0	0	0
2302	0	1111	0	0	0	0	7143	0	0	6270	0	34603	0	0	0	0
500	0	0	500	0	0	0	6250	0	0	6000	0	16750	0	0	0	0
4250	0	2500	0	0	0	0	4000	0	0	5333	0	16000	0	0	0	0
1250	2857	833	0	0	0	0	4345	0	0	4524	0	9940	0	0	0	0
1250	0	2083	0	0	0	0	9000	0	0	1500	2000	31667	0	0	0	0
1042	0	0	0	0	0	0	5135	0	0	2083	0	15882	0	0	0	0
0	0	3333	0	0	0	0	11333	0	0	4333	0	29333	0	0	0	0
0	3333	3333	227	0	0	0	3333	0	0	909	0	17311	0	0	0	0
0	417	0	833	0	0	0	9643	0	0	6071	3571	39583	0	0	0	0
500	0	3833	0	0	0	0	7333	0	0	9167	3333	30333	0	0	0	0
500	0	0	1500	0	0	0	9500	0	0	1000	0	22000	0	0	0	0
0	0	500	500	0	0	0	10333	0	0	2500	0	20333	0	0	0	0
455	0	0	3788	0	0	0	5682	0	0	1818	0	31212	0	0	0	0
455	0	0	227	0	0	0	3614	0	0	1591	0	8573	0	0	0	0
2500	0	0	5000	0	0	0	2500	0	455	2727	455	41818	0	0	0	0
667	0	0	333	0	0	0	2250	0	0	2333	0	16417	0	0	0	0
833	2417	833	2417	208	0	0	4875	0	0	6083	0	12208	0	0	0	2000
0	769	0	385	0	0	0	5577	0	0	0	0	7115	0	0	0	0
750	2500	0	0	0	0	0	2000	0	0	4000	0	15500	0	0	0	0
4679	7692	833	417	0	0	0	6506	0	0	2500	417	32019	0	0	0	0
0	0	0	134	0	0	0	922	0	0	5065	0	3380	0	0	0	0
0	0	36	71	0	36	0	1581	0	0	5009	0	1992	0	0	0	0
0	0	2778	132	0	66	0	8333	0	33	11442	0	2927	0	0	0	0
758	1515	0	100	0	0	0	2273	0	0	1665	1515	4163	0	0	0	0
50	0	0	3226	0	0	0	1613	0	0	7452	0	3294	0	0	0	0
98	2941	0	1765	0	0	0	2206	0	0	5981	0	7549	0	0	0	0
98	0	294	686	0	0	0	3571	0	0	10995	0	14678	0	0	0	0
0	0	102	102	0	0	0	2986	0	0	5479	0	9615	0	0	102	0
1351	0	47	1351	0	0	0	1351	0	0	1399	0	12287	0	0	0	0
250	2083	0	0	0	0	0	0	0	0	2583	0	26750	0	0	0	0
200	0	200	0	0	0	0	0	0	0	543	0	11804	0	0	0	0
0	0	0	0	0	0	0	102	0	0	761	456	5264	0	0	0	0
0	0	0	0	0	0	0	0	31	0	2143	0	5357	0	0	0	0
0	1515	0	0	0	0	0	98	0	0	98	0	12478	0	98	0	0
0	0	0	1136	0	0	0	238	0	0	238	1136	17717	0	0	0	0
0	1136	0	102	0	0	0	0	0	0	0	1136	13056	0	0	0	0
96	0	0	0	0	0	0	416	0	0	0	0	4375	0	192	0	0
0	0	0	0	0	0	0	625	0	0	0	1250	7350	0	0	0	0
0	0	0	0	0	0	0	0	0	0	1383	0	4133	0	0	0	0
0	0	0	0	200	0	0	1043	0	0	943	0	13917	0	0	0	0
0	0	83	83	0	0	0	0	0	0	83	0	3542	0	0	0	0
67	575	0	0	0	0	0	1437	0	0	708	575	4191	0	0	0	0
0	0	0	0	0	0	0	167	83	0	2083	0	7250	0	0	0	0
0	0	0	0	0	0	0	532	0	0	0	286	10176	0	0	0	0
0	0	0	0	0	0	0	595	0	0	595	187	8321	0	375	595	0
0	0	0	0	0	0	0	14	0	0	0	121	4379	0	0	0	0
0	0	53	0	0	0	0	498	0	943	943	105	7608	0	53	0	0
0	0	0	0	0	0	0	0	0	0	2459	63	11488	0	375	0	0

Table III.2 continued – Cladoceran counts for Endinger Bruch.

Depth	Acroperos elongatus	A. harpae	Alona affinis	A. costata	A. guttata rectangula	A. guttata var tub	A. intermedia	A. quadrangularis	A. rustica	Alonella excisa	A. rostrata	A. nana	Alonopsis elongata	Camptocercus rectirostris	C. piger	C. sphaericus	Eurycercus lamellatus
1106 cm	0	167	1310	0	0	0	0	0	0	0	0	250	0	167	500	2059	833
1111 cm	0	28	653	0	0	0	0	0	0	0	0	7	0	0	0	1250	56
1116 cm	0	36	89	0	0	0	0	18	0	0	0	36	0	0	0	529	107
1121 cm	0	501	156	0	156	0	0	0	0	469	156	313	0	0	423	2798	156
1126 cm	0	125	125	0	458	0	0	63	0	0	0	250	0	0	375	1299	806
1131 cm	0	873	196	0	196	0	0	49	0	49	0	147	0	0	0	1373	1354
1136 cm	0	700	200	0	0	0	0	200	0	400	0	500	0	0	200	2600	1000
1141 cm	0	374	325	0	196	0	0	196	0	196	0	700	0	0	98	1840	98
1146 cm	0	1083	333	0	278	0	0	167	0	0	0	556	0	0	0	1444	167
1151 cm	0	133	133	714	133	0	0	67	0	0	0	33	0	0	67	133	133
1156 cm	98	343	392	0	98	0	0	294	0	392	0	288	0	0	0	1422	98
1161 cm	0	635	675	278	0	0	0	60	0	0	0	635	0	0	0	1111	0
1166 cm	0	137	137	0	0	0	0	0	0	68	0	2778	0	0	2778	753	3257
1171 cm	0	663	0	0	0	0	0	0	0	0	0	341	0	416	0	1307	1742
1176 cm	0	100	0	0	0	0	0	0	0	0	0	0	0	0	0	500	100
1181 cm	0	2174	102	0	725	0	0	102	0	362	0	510	0	102	0	3449	204
1186 cm	0	656	211	1154	1259	0	0	0	0	0	0	421	0	0	105	1209	1364
1191 cm	0	175	485	0	0	0	0	50	0	50	0	175	0	50	100	667	150
1196 cm	0	629	457	0	357	0	0	0	0	100	0	350	0	100	457	657	557
1201 cm	0	234	94	0	31	0	0	31	0	0	0	429	0	0	0	868	156
1206 cm	0	3846	600	0	0	0	0	100	0	50	0	400	0	0	100	3423	300
1211 cm	0	200	288	0	288	0	0	100	0	0	0	485	0	50	0	619	0
1216 cm	0	200	50	0	200	0	0	0	0	0	0	175	0	25	150	675	150
1221 cm	0	205	1039	0	207	0	0	0	0	0	0	410	0	207	207	1443	481
1226 cm	0	110	175	0	88	0	0	0	0	0	0	556	0	44	278	1038	322
1231 cm	0	292	143	0	143	0	0	0	0	0	0	448	0	71	0	948	794
1236 cm	0	646	125	0	458	0	0	0	0	63	0	444	0	125	125	1125	833
1241 cm	0	337	392	0	147	0	0	49	0	0	0	294	0	0	0	862	568
1246 cm	0	1282	1353	0	0	0	0	71	0	0	71	1212	0	641	71	2814	2912
1261 cm	0	4887	1903	0	0	0	0	32	0	0	0	4790	0	0	1613	1742	7194
1266 cm	0	7012	1923	0	0	0	0	83	0	714	0	1679	0	83	756	458	917
1271 cm	0	11909	8104	0	4148	0	0	1731	0	96	0	8283	0	0	3764	385	4341
1276 cm	0	4073	32629	0	1034	0	0	6595	0	0	0	7866	0	0	172	6422	14051
1281 cm	0	6632	7216	0	3275	0	0	2941	0	167	0	6024	0	0	2941	4525	1500
1286 cm	0	3774	5692	0	286	0	0	429	0	143	0	3887	0	0	71	7335	1286
1291 cm	0	3747	473	0	4613	0	0	68	0	68	0	5660	0	0	0	7764	743
1296 cm	0	3325	6500	0	100	25	0	0	50	25	0	11713	0	0	6250	3425	4225
1301 cm	0	7431	3125	0	2778	0	0	2778	0	0	0	11076	0	0	35	3194	10069
1306 cm	0	4342	2233	0	25	0	0	2083	0	0	0	3675	0	0	2083	1442	6700
1311 cm	0	5644	7927	0	98	0	0	392	0	0	0	8761	0	98	98	6982	686
1316 cm	0	3554	7959	0	2381	0	0	204	0	0	0	5153	0	0	2381	5000	918
1321 cm	0	3771	9208	0	375	0	0	625	0	125	0	9104	0	0	0	2729	3083
1326 cm	0	4385	5308	0	1923	0	0	167	0	0	0	6051	0	0	83	3423	3590
1331 cm	0	6970	130	0	22	0	0	22	0	0	0	9580	0	0	0	13810	9743
1336 cm	0	533	1695	0	67	0	0	0	0	0	0	10624	0	67	1429	3157	8276
1341 cm	0	1246	2326	0	0	0	0	42	0	0	0	5486	0	0	0	1162	5360
1346 cm	0	400	2067	0	0	0	1667	0	0	100	0	5100	0	0	100	2867	4833
1351 cm	0	978	217	0	0	0	0	0	0	0	0	10831	0	0	217	5933	1087
1356 cm	0	714	1515	0	102	0	0	102	0	1617	0	2587	0	0	1515	3956	1617

Table III.2 continued – Cladoceran counts for Endinger Bruch.

Graptoleberis testudinaria	Leydigi acanthocercoides	L. leydigi	Monospilus dispar	Pleroxus aduncus	P. trigonellus	P. truncatus	P. uncinatus	Psydochydorus globosus	Rhynchotalona falcata	Sida crystallina	Bosmina coregoni	B. longirostris	Daphnia pulex	D. longispina epphipia	D. pulex epphipia	Latona Setifera
0	0	0	0	0	0	0	0	0	167	333	83	9119	0	0	0	0
14	0	0	0	1250	0	0	0	0	0	0	14	1791	0	0	1250	0
18	0	0	0	0	0	0	36	0	0	0	18	2143	0	0	0	0
0	0	0	0	0	0	0	78	0	0	469	156	5938	0	0	0	0
0	0	0	0	0	0	0	125	0	0	222	0	5556	0	0	0	0
0	0	0	0	0	0	0	962	0	0	98	0	6335	0	0	0	0
0	0	0	100	0	0	0	0	0	0	200	300	11267	0	0	556	0
0	0	0	0	0	0	0	0	0	0	98	0	5026	0	0	0	0
0	0	0	1667	0	0	0	0	0	167	333	167	9722	0	0	0	0
100	0	67	0	0	0	0	0	0	0	67	0	3181	0	0	0	0
0	0	0	0	0	0	0	0	0	0	98	196	3529	0	0	0	0
0	0	0	0	0	0	0	0	0	0	0	0	6032	0	0	0	0
0	0	2778	0	0	0	0	0	0	0	0	34	13851	0	0	0	0
0	0	0	0	0	0	0	0	0	0	0	0	16326	0	0	0	0
0	0	0	0	0	0	0	0	0	0	0	150	5433	0	0	0	0
0	0	0	0	0	0	0	724	0	0	0	0	8644	0	0	0	0
53	0	0	0	0	0	0	0	0	0	0	79	2968	0	0	0	0
0	0	0	0	0	0	0	0	0	0	0	50	2619	0	0	0	0
0	0	0	0	0	0	0	0	0	0	0	50	6400	100	0	0	0
0	0	31	0	0	0	0	0	0	0	429	0	808	0	31	0	0
0	0	0	0	0	0	0	2023	0	0	2023	50	8469	0	0	0	0
0	0	0	0	0	0	0	288	0	0	50	350	2035	0	0	0	0
0	0	0	0	0	0	0	0	0	0	0	450	1250	0	0	0	0
0	0	139	0	0	0	0	139	0	0	346	411	1785	0	0	0	0
0	0	0	0	0	0	0	0	0	0	0	132	1433	0	0	0	0
0	71	0	0	0	0	0	36	0	0	0	71	2111	0	0	0	0
0	0	0	0	0	0	0	0	0	0	138	125	4326	0	0	0	0
0	0	0	0	0	0	0	0	0	0	49	196	980	0	0	0	0
0	0	0	0	0	0	0	321	0	0	784	143	4282	0	0	0	0
0	0	0	0	0	0	806	1613	0	0	97	32	4871	0	161	0	0
1429	0	83	83	0	0	0	2857	0	0	1929	83	7893	0	250	0	0
0	0	0	0	0	0	0	3571	0	0	192	0	15632	0	0	0	0
0	0	172	0	0	0	0	19440	0	0	1034	172	19181	0	0	0	0
0	0	0	167	0	0	0	8990	0	0	667	0	12098	0	0	0	0
143	2632	0	0	143	0	0	4305	0	0	143	0	13872	0	0	0	0
3409	0	0	0	0	0	0	3679	0	0	2746	0	5154	0	0	0	0
4688	0	0	0	0	0	0	3250	0	0	100	100	6600	0	200	0	0
1424	0	0	0	0	0	0	2778	0	0	5694	0	3403	0	347	0	0
2083	0	0	0	0	0	0	1092	0	0	6300	0	7342	0	0	0	0
98	0	98	98	0	0	0	2822	0	0	196	0	3165	0	0	0	0
11904	0	0	102	0	0	0	2381	0	0	408	0	3095	0	102	0	0
0	0	0	0	0	0	0	4292	0	0	125	0	6938	0	0	0	0
167	0	0	0	0	0	1923	5558	0	0	0	0	6103	0	0	0	0
0	0	0	0	0	0	11	4545	0	0	4611	0	27338	174	43	0	0
67	0	0	67	0	0	267	1429	0	0	3257	0	333	0	0	0	0
1163	0	0	0	0	0	0	3509	0	0	167	0	1371	0	42	0	0
0	0	0	0	0	0	0	1667	0	0	1767	0	10033	0	0	1667	0
0	0	0	217	0	0	0	0	0	0	2941	0	32455	0	0	0	0
0	0	0	0	0	0	0	0	0	0	0	0	17090	0	0	0	0

Table III.2 continued – Cladoceran counts for Endinger Bruch.

Depth	Acroperos elongatus	A. harpae	Alona affinis	A. costata	A. guttata rectangula	A. guttata var tub	A. intermedia	A. quadrangularis	A. rustica	Alonella excisa	A. rostrata	A. nana	Alonopsis elongata	Camptocercus rectirostris	C. piger	C. sphaericus	Eurycercus lamellatus
1361 cm	0	1064	1585	0	208	0	0	833	0	625	0	3054	0	0	1064	4002	0
1366 cm	0	1833	1500	0	208	0	0	417	0	0	0	1250	0	0	500	6354	1000
1371 cm	0	1096	551	0	273	0	0	182	0	182	0	1005	0	278	278	2429	91
1376 cm	0	49	275	0	21	0	0	0	0	0	0	0	0	0	138	210	0
1381 cm	0	250	5722	0	292	0	0	2778	0	83	0	1847	0	0	167	12944	250
1386 cm	0	375	539	0	21	0	0	42	0	414	0	560	0	331	0	2179	414
1391 cm	0	375	167	0	83	0	0	42	0	167	0	139	0	56	0	1361	83
1396 cm	0	294	205	0	342	0	0	205	0	274	0	1194	382	0	0	1864	0
1401 cm	0	650	125	0	500	0	0	525	400	0	0	1650	0	0	0	3188	525
1406 cm	0	208	542	0	0	0	0	521	0	0	0	521	0	0	0	3229	0
1411 cm	0	427	1109	0	100	0	0	0	0	0	0	455	455	0	0	2752	0
1416 cm	0	3472	63	0	0	0	0	0	0	0	0	1451	0	0	31	6306	0
1421 cm	0	1529	0	0	8380	0	0	0	0	0	0	3035	0	0	0	5218	0
1426 cm	0	2869	273	0	273	0	0	91	0	0	0	2778	0	0	0	6556	0
1431 cm	0	385	1245	0	91	0	0	0	0	0	0	682	0	0	0	3629	0
1436 cm	0	381	478	0	101	0	0	357	0	0	0	714	0	0	40	1624	40
1441 cm	0	784	120	0	40	0	0	0	0	0	0	1408	0	0	0	4157	704
1446 cm	0	3005	136	0	136	0	0	91	0	45	2778	1525	2778	0	45	6056	0
1451 cm	0	1731	68	0	0	0	0	0	0	68	0	12500	0	0	3125	10929	0
1456 cm	0	521	68	0	521	0	0	68	0	0	0	521	0	103	34	3679	726
1461 cm	0	704	526	0	311	0	0	0	0	0	0	0	0	0	71	2075	0
1466 cm	0	239	162	0	23	0	0	0	0	0	0	0	0	23	45	1312	23
1471 cm	0	10	0	0	0	0	0	0	0	10	0	0	0	0	0	105	0
1476 cm	0	30	0	0	20	0	0	0	0	0	0	0	0	0	0	45	0
1481 cm	125	125	0	32	0	0	21	0	0	0	0	0	0	0	11	209	0
1486 cm	0	141	43	0	161	0	0	0	0	0	0	0	0	0	0	114	0
1491 cm	0	15	10	0	0	0	0	0	0	0	0	0	0	0	10	288	0
1496 cm	0	10	10	0	0	0	0	0	0	0	0	0	0	0	10	80	0
1501 cm	0	44	113	0	19	0	0	0	0	0	0	0	0	0	188	175	0
1506 cm	0	0	43	0	10	0	0	0	0	0	0	0	0	0	35	25	0
1511 cm	0	0	0	0	0	0	0	0	0	0	0	0	0	0	0	8	0

Table III.2 continued – Cladoceran counts for Endinger Bruch.

Graptoleberis testudinaria	Leydigi acanthocercoides	L. leydigi	Monospilus dispar	Pleroxus aduncus	P. trigonellus	P. truncatus	P. uncinatus	Psydochydorus globosus	Rhynchotalona falcata	Sida crystallina	Bosmina coregoni	B. longirostris	Daphnia pulex	D. longispina epphipia	D. pulex epphipia	Latona Setifera
0	0	0	0	0	0	0	0	0	0	0	0	14135	0	0	1064	0
0	0	0	0	0	0	0	1000	0	0	0	0	15166	0	0	0	0
0	91	91	56	0	0	0	0	0	0	278	556	1551	0	0	0	0
0	0	0	0	0	0	0	1380	0	0	0	49	0	0	0	0	0
0	0	83	0	0	0	0	167	0	0	0	0	3236	0	0	0	0
0	0	0	662	0	0	0	373	0	0	83	0	1700	0	42	0	0
0	0	0	0	0	0	0	167	0	0	0	0	3083	0	0	0	0
0	0	68	0	68	0	0	0	0	382	0	0	5176	0	0	382	0
0	0	0	125	0	0	400	200	0	0	0	0	6000	0	0	0	0
0	0	521	0	0	0	0	0	0	0	0	0	6750	0	0	0	0
0	0	0	455	0	0	0	227	0	455	0	0	4006	0	0	0	0
0	0	0	0	0	0	0	63	0	0	0	125	6993	0	0	0	0
0	47	0	2778	0	0	0	0	0	0	0	23	9455	0	0	0	0
0	0	0	0	0	0	0	0	0	0	0	45	14020	0	0	0	0
0	0	0	182	0	0	0	0	0	0	0	0	3378	0	91	0	0
0	0	0	81	0	0	0	357	0	0	0	0	2667	0	121	0	0
0	0	0	744	0	0	0	40	0	704	0	60	3737	0	0	0	0
0	0	0	91	0	0	0	0	0	0	0	45	9288	0	0	0	0
0	0	0	68	0	0	0	0	0	0	0	0	13581	0	0	0	0
0	0	0	0	0	0	0	260	0	0	0	137	5043	0	68	0	0
0	0	0	0	0	0	0	263	0	0	0	717	2005	0	0	0	0
0	0	23	23	0	0	0	0	0	0	23	0	575	0	0	0	0
0	0	0	0	0	0	0	0	0	0	10	0	15	0	0	0	0
0	0	0	10	0	0	0	0	0	0	0	0	10	0	0	0	0
0	0	11	11	0	0	0	11	0	0	0	0	99	0	0	0	0
0	0	21	63	0	0	0	0	0	0	0	0	230	0	36	0	0
0	0	10	0	0	0	0	0	0	0	0	0	5	0	0	0	0
0	0	0	10	0	0	0	0	0	0	0	0	15	0	0	0	0
0	0	0	138	0	0	0	0	0	0	0	0	256	0	0	0	0
0	0	0	10	0	0	0	0	0	0	0	0	0	0	0	0	0
0	0	0	0	0	0	0	0	0	0	0	0	0	0	0	0	0

Table III.2 continued – Cladoceran counts for Endinger Bruch.

Depth	Acroperos harpae	Alona affinis	A. costata	A. guttata rectangula	A. guttata var tub	A. quadrangularis	Alonella excisa	A. nana	Camptocercus rectirostris	Chydorus piger	C. sphaericus	Eurycercus lamellatus
400 cm	0	21767	0	263	0	1955	658	1429	658	1053	9793	526
402.5 cm	217	9348	0	217	0	1250	1250	217	1087	435	9837	217
405 cm	0	10722	0	2041	0	0	2041	0	500	0	7951	0
407.5 cm	476	8571	0	3333	0	0	238	119	1190	238	11250	238
410 cm	0	12235	0	2000	2000	0	147	2088	735	221	2000	1147
412.5 cm	133	7448	0	332	633	0	133	1000	265	265	1362	765
415 cm	133	11500	0	0	602	0	200	936	467	133	1807	1002
417.5 cm	100	2625	0	57	659	0	142	572	201	85	402	398
420 cm	0	4954	0	2461	1604	111	389	56	1080	111	3270	2048
422.5 cm	909	1400	50	505	1364	0	225	1514	75	300	300	1655
425 cm	0	4295	119	638	919	0	519	400	800	298	400	655
427.5 cm	50	2623	0	25	769	0	267	460	200	50	100	535
430 cm	200	3400	50	325	0	0	50	850	400	100	550	1850
432.5 cm	60	1240	0	437	20	40	40	120	0	200	477	1667
435 cm	673	13263	0	946	746	0	100	300	0	200	3819	1146
437.5 cm	882	5059	0	500	0	294	250	500	1176	294	9574	882
440 cm	0	3488	0	909	0	109	54	254	509	0	2125	1126
442.5 cm	794	1197	0	794	794	0	50	397	0	50	150	1540
445 cm	133	1302	0	318	22	0	185	507	311	22	133	177
447.5 cm	250	701	201	402	201	0	50	651	201	0	99	300
450 cm	535	944	0	313	535	23	68	765	91	136	631	495
452.5 cm	447	690	0	294	51	26	51	901	51	51	485	345
455 cm	223	149	0	498	50	0	25	600	25	0	149	598
457.5 cm	200	700	0	800	200	0	75	775	0	50	450	400
460 cm	557	267	202	234	202	44	44	1509	22	89	767	1206
462.5 cm	394	1044	0	837	0	394	0	200	0	50	837	3006
465 cm	421	613	0	2308	769	0	29	1853	29	114	157	969
467.5 cm	916	543	0	1108	357	0	0	1271	0	72	968	1216
470 cm	47	1199	0	0	400	0	0	941	0	23	200	717
472.5 cm	217	920	0	412	412	57	0	506	86	57	231	486
475 cm	100	1625	0	1181	0	50	0	962	394	149	1235	0
477.5 cm	51	2028	0	938	0	0	0	1614	0	0	364	415
480 cm	217	1134	0	435	54	0	0	567	0	0	244	592

Table III.3 – Cladoceran counts for Potremser Moor.

Graptoleberis testudinaria	Leydigi acanthocercoides	L. leydigi	Monospilus dispar	Pleroxus truncatus	P. uncinatus	Sida crystallina	Bosmina coregoni	B. longirostris	Daphnia pulex	Mutated Alona
132	0	0	0	0	0	263	0	714	0	0
217	0	0	1250	0	1250	1250	0	0	0	0
200	0	0	200	0	200	1020	0	2141	0	400
0	0	0	0	0	0	0	0	0	0	0
0	0	0	0	0	147	1147	0	500	0	1324
0	0	0	0	0	0	133	0	1500	0	1459
0	0	0	0	0	0	0	0	835	0	2069
0	0	0	0	0	57	485	0	114	114	682
0	0	0	0	0	0	0	0	1937	0	889
0	0	0	0	0	0	505	0	2925	0	0
0	0	0	0	0	0	238	0	2179	0	595
0	0	0	0	0	0	1204	0	1688	0	735
0	0	400	0	0	50	1000	0	550	0	350
0	0	0	0	0	0	200	0	1830	0	0
0	200	0	0	0	0	0	0	946	0	1800
0	0	0	0	0	0	0	0	1441	0	3235
54	0	0	0	0	0	455	0	981	0	380
25	100	0	0	0	0	200	0	2412	0	50
0	0	0	0	0	185	177	0	918	0	399
201	0	0	0	0	0	451	0	501	0	50
23	0	404	45	0	0	404	0	1882	0	0
0	0	0	0	0	0	741	0	1381	0	0
0	0	50	0	0	0	50	0	670	0	50
0	0	0	0	100	0	250	0	750	0	0
0	0	0	0	0	0	291	0	1282	0	0
0	0	0	0	0	0	544	0	1262	0	50
0	0	0	0	0	0	527	0	870	0	29
0	0	0	0	0	0	1108	0	1007	0	0
0	0	0	0	0	23	47	12	905	0	0
0	0	206	0	0	0	703	0	872	0	0
0	0	0	0	0	0	887	0	1382	0	0
0	0	0	0	0	0	364	0	702	0	0
0	0	0	0	0	27	54	0	1000	0	0

Table III.3 continued – Cladoceran counts for Potremser Moor.

Depth	Acroperos harpae	Alona affinis	A. costata	A. guttata rectangula	A. guttata var tub	A. quadrangularis	Alonella excisa	A. nana	Camptocercus rectirostris	Chydorus piger	C. sphaericus	Eurycercus lamellatus
482.5 cm	148	746	0	44	0	0	0	850	0	0	461	1458
485 cm	234	2322	0	109	0	50	25	1018	0	150	617	835
487.5 cm	435	1042	0	403	246	177	133	624	44	88	853	379
490 cm	136	1860	0	273	0	136	45	784	0	182	1106	45
492.5 cm	105	360	0	25	0	0	0	415	0	0	380	0
495 cm	99	346	0	150	0	148	50	173	0	0	695	196
497.5 cm	25	341	0	95	0	50	25	236	0	0	564	91
500 cm	150	150	0	196	0	50	0	123	50	0	938	296
502.5 cm	556	648	0	417	0	46	0	475	46	0	903	440
505 cm	208	531	0	208	0	29	29	71	0	14	537	617
507.5 cm	258	488	0	0	0	0	61	305	25	0	766	172
510 cm	149	700	0	50	0	50	50	275	100	0	373	300
512.5 cm	155	137	0	59	0	20	0	360	0	10	468	309
515 cm	50	1016	0	408	0	50	0	504	0	0	1062	204
517.5 cm	600	188	0	200	0	141	0	109	16	0	700	356
520 cm	106	282	0	114	0	17	0	71	0	0	490	254
522.5 cm	333	222	0	0	0	0	0	46	0	0	584	222
525 cm	227	965	0	510	0	0	0	225	0	0	327	510
527.5 cm	278	99	0	125	0	0	0	287	0	27	350	304
530 cm	73	305	0	100	0	0	0	102	0	0	627	147
532.5 cm	124	351	0	200	0	0	0	127	0	0	198	247
535 cm	204	95	0	27	0	0	0	612	0	0	257	612
537.5 cm	292	298	42	21	0	0	73	571	0	0	293	548
540 cm	278	222	0	0	0	0	28	306	0	222	389	167
542.5 cm	443	748	0	133	0	95	0	248	267	0	890	190
545 cm	667	667	0	200	0	0	0	767	200	0	2800	600
547.5 cm	1056	222	0	172	0	50	0	731	0	0	2172	1212
550 cm	837	196	0	91	0	91	26	517	0	0	888	589
552.5 cm	1125	700	0	0	0	0	133	2017	250	0	2283	1417
555 cm	643	315	0	192	0	0	0	1261	0	0	2196	659
557.5 cm	1522	0	0	75	0	0	0	2000	0	0	1349	400
560 cm	1263	0	0	240	0	0	0	625	22	0	1306	0

Table III.3 continued – Cladoceran counts for Potremser Moor.

Graptoleberis testudinaria	Leydigi acanthocercoides	L. leydigi	Monospilus dispar	Pleroxus truncatus	P. uncinatus	Sida crystallina	Bosmina coregoni	B. longirostris	Daphnia pulex	Mutated Alona
0	0	44	0	0	0	252	0	1716	0	0
0	0	0	0	0	0	417	0	1418	0	0
0	0	0	0	0	246	177	0	1136	0	44
23	0	0	91	0	337	246	0	1093	0	91
0	0	0	0	0	0	50	25	908	0	0
98	0	0	0	0	150	0	0	844	0	0
45	0	0	0	0	0	0	0	545	0	0
25	0	50	0	0	0	0	0	396	0	0
0	0	0	0	0	0	0	1042	1181	0	0
0	0	0	0	0	0	0	29	1738	0	0
0	0	0	0	0	0	0	0	616	0	0
0	0	0	0	0	0	0	0	999	0	0
0	0	0	0	0	20	0	0	1572	0	0
25	0	0	0	0	0	50	0	1547	0	0
31	0	0	0	0	0	0	0	816	63	0
0	0	0	0	0	0	0	0	1030	0	0
0	0	0	0	0	0	0	0	584	0	0
56	0	0	0	0	0	0	0	1977	0	0
0	0	0	0	0	0	0	0	599	250	0
0	0	0	0	0	0	0	0	1024	0	0
100	0	0	0	0	0	0	0	478	800	0
0	0	0	0	0	0	0	0	528	612	0
0	0	0	0	0	256	0	0	595	256	0
0	0	0	0	0	111	111	0	833	0	0
0	0	0	0	0	267	214	0	114	0	0
0	0	0	0	0	400	67	0	100	0	0
0	0	0	0	0	0	0	0	136	0	0
0	0	0	0	0	0	0	0	91	0	0
0	0	0	0	0	0	0	0	725	0	0
0	0	0	0	0	0	0	0	829	0	0
0	0	0	0	0	0	0	0	475	0	0
0	0	0	0	0	0	0	0	177	0	0

Table III.3 continued – Cladoceran counts for Potremser Moor.

Depth	Acroperos harpae	Alona affinis	A. costata	A. guttata rectangula	A. guttata var tub	A. intermedia	A. quadrangularis	Alonella excisa	A. rostrata	A. nana	Camptocercus rectirostris	Chydorus piger	C. sphaericus	Eurycercus lamellatus
600 cm	28	198	0	53	50	0	55	0	0	28	0	55	350	77
602.5 cm	265	145	0	73	111	0	0	0	0	434	51	0	494	102
605 cm	196	255	0	710	204	0	175	0	0	738	0	36	924	145
607.5 cm	33	472	0	33	0	0	133	0	100	67	0	33	1430	33
610 cm	52	729	0	0	0	0	129	0	0	0	0	0	1136	129
612.5 cm	50	250	0	100	0	0	50	0	0	225	0	0	595	25
615 cm	120	100	0	75	0	0	0	0	0	500	0	0	660	0
617.5 cm	25	152	0	0	0	0	101	25	0	238	0	0	522	152
620 cm	63	327	0	245	31	0	31	132	0	649	0	16	1844	94
622.5 cm	75	100	0	300	102	0	104	0	0	75	0	0	602	50
625 cm	103	205	0	51	0	0	100	0	0	405	0	0	919	205
627.5 cm	307	171	0	405	135	0	29	29	0	915	0	100	1085	114
630 cm	160	320	0	107	0	0	107	0	0	857	0	0	509	254
632.5 cm	180	1191	0	1151	556	0	1191	0	0	2761	0	0	1495	596
635 cm	241	521	0	1317	213	0	413	0	0	1385	0	0	321	40
637.5 cm	425	662	0	1374	0	0	400	0	0	558	0	0	404	254
640 cm	171	714	0	890	0	0	551	0	0	431	0	0	157	237
642.5 cm	299	348	0	869	200	0	99	0	0	499	0	0	49	74
645 cm	278	457	0	413	192	0	114	0	0	582	0	0	57	114
647.5 cm	200	676	0	1834	0	0	96	0	0	741	0	0	899	327
650 cm	860	404	0	907	28	0	99	0	0	864	0	0	216	1832
652.5 cm	825	825	0	1677	313	0	256	0	0	286	0	0	71	854
655 cm	404	200	0	747	104	0	40	0	0	901	0	0	160	873
657.5 cm	350	200	0	1100	200	0	100	0	0	625	0	0	25	550
660 cm	625	450	0	833	0	0	258	0	0	417	208	0	25	950
662.5 cm	710	869	0	385	0	0	96	0	0	1262	0	0	75	585
665 cm	747	326	0	400	21	0	126	0	0	1037	0	0	0	726
667.5 cm	613	881	0	504	28	0	222	0	0	607	0	0	103	619
670 cm	700	1600	0	1000	250	0	250	0	0	1025	0	0	100	400
672.5 cm	545	909	0	582	0	0	345	0	0	400	0	0	127	818
675 cm	563	527	0	1040	36	0	145	0	0	554	0	0	127	473
677.5 cm	848	1108	0	714	714	0	73	0	0	2277	0	18	182	787
680 cm	756	4089	0	1111	0	0	200	0	0	4189	0	0	25	125
682.5 cm	713	667	0	483	0	0	104	0	0	1729	0	0	50	358
685 cm	563	856	185	741	0	0	150	0	0	370	0	0	50	606
687.5 cm	1611	2168	0	959	455	0	300	0	0	1711	0	0	100	1059
690 cm	1088	1490	0	626	50	0	425	0	0	1364	0	50	50	375
692.5 cm	400	4217	0	692	67	0	1158	0	0	2329	67	0	167	200
695 cm	400	1800	25	550	250	0	600	0	0	1225	250	0	25	225
697.5 cm	527	1250	100	477	50	0	627	0	0	1623	0	0	114	555
700 cm	534	2767	0	464	0	0	374	357	0	1720	0	0	160	133

Table III.4 – Cladoceran counts for Kieshofer Moor.

Graptoleberis testudinaria	Leydigi leydigi	Monospilus dispar	Phiruxa rostrata	P. aduncus	P. trigonellus	P. uncinatus	Psydochydorus globosus	Sida crystallina	Bosmina coregoni	B. longirostris	Daphnia pulex	Mutant Alona
0	0	0	0	0	0	0	0	55	0	81	0	0
0	0	0	0	0	0	132	0	44	0	0	0	0
142	0	0	0	0	0	175	0	240	0	87	0	0
33	0	0	0	0	0	0	0	247	0	0	0	0
13	0	13	0	0	0	39	0	0	0	39	0	0
25	0	0	0	0	0	0	0	0	0	0	0	0
0	0	0	0	0	0	0	0	120	0	125	0	0
0	0	0	0	0	0	0	0	0	0	51	0	0
31	0	0	0	0	0	51	0	265	0	0	0	0
0	0	0	0	0	0	0	0	313	0	102	0	0
0	0	0	0	0	0	0	0	154	0	51	0	0
57	0	0	0	0	0	14	0	164	0	182	0	0
0	0	0	0	0	0	0	0	94	0	53	0	0
40	0	0	0	0	0	80	0	556	0	556	0	0
361	0	0	0	0	0	146	0	426	0	426	0	0
227	0	0	0	0	0	100	0	100	0	204	0	0
43	0	0	0	0	0	237	0	237	0	423	0	0
249	0	0	0	0	0	0	0	299	0	400	0	0
192	0	0	0	0	0	57	0	499	0	96	0	0
18	0	0	0	0	192	55	0	301	0	0	0	0
0	0	0	0	0	0	113	0	28	0	526	0	0
29	0	0	0	0	0	341	29	114	0	0	0	0
104	0	0	0	0	0	238	0	537	0	104	0	0
0	0	0	0	0	0	200	0	250	0	0	0	0
0	0	0	0	0	0	175	0	242	0	0	0	0
0	50	0	0	0	0	200	0	542	0	0	0	0
11	21	0	0	0	0	468	0	484	0	0	0	0
0	0	0	0	0	179	490	0	262	0	179	0	0
0	125	0	0	0	0	225	0	250	0	0	0	0
18	0	0	0	0	0	155	0	673	0	0	0	0
0	0	0	0	0	0	381	0	490	0	0	0	0
0	0	0	0	0	0	394	0	394	0	0	0	0
0	1111	0	0	0	0	275	0	556	0	0	0	0
0	0	0	0	0	0	125	0	725	0	0	0	0
0	0	0	0	0	0	235	0	185	0	0	0	0
0	0	0	0	0	0	1005	0	100	0	0	0	0
0	0	0	0	0	0	288	0	0	0	0	0	0
0	0	0	0	0	0	758	1250	825	0	0	0	0
0	0	0	0	0	0	650	0	100	0	0	0	0
50	0	0	0	0	0	552	0	327	0	0	0	0
0	0	0	0	0	0	872	0	0	0	0	357	0

Table III.4 continued – Cladoceran counts for Kieshofer Moor.

Depth	Acroperos harpae	Alona affinis	A. costata	A. guttata rectangula	A. guttata var tub	A. intermedia	A. quadrangularis	Alonella excisa	A. rostrata	A. nana	Camptocercus rectirostris	Chydorus piger	C. sphaericus	Eurycercus lamellatus
702.5 cm	725	1400	0	500	50	0	650	0	0	800	0	0	250	500
705 cm	700	4300	0	500	0	0	350	0	0	1250	0	0	25	100
707.5 cm	787	1367	53	760	80	0	267	0	0	600	0	0	560	907
710 cm	423	587	73	302	36	55	0	0	0	319	0	36	255	182
712.5 cm	903	886	0	400	114	0	86	57	0	980	86	0	114	286
715 cm	611	1084	0	242	0	0	211	0	0	895	0	0	390	211
717.5 cm	583	2083	167	1500	0	0	750	0	0	708	0	0	292	83
720 cm	467	1933	0	1667	0	0	133	0	0	500	0	0	267	333
722.5 cm	1194	967	0	1200	133	0	200	0	0	2078	0	0	267	678
725 cm	932	587	0	1231	53	0	160	0	0	891	0	0	380	213
727.5 cm	2125	2667	0	2875	63	0	750	0	0	1104	0	0	250	250
730 cm	1556	2139	0	3104	125	0	250	0	0	2826	0	0	451	125
732.5 cm	550	2000	0	1025	250	0	150	0	0	1300	0	0	375	350
735 cm	1406	1851	62	1880	31	0	62	0	0	2467	0	216	493	0
737.5 cm	2114	900	0	1245	67	0	0	0	0	2440	0	0	100	490
740 cm	2587	538	0	1311	167	0	67	0	0	1345	0	0	100	102
742.5 cm	5544	1938	0	2872	0	0	400	0	0	4056	0	0	651	2841
745 cm	1650	425	50	375	0	0	200	200	0	1675	0	0	400	100
747.5 cm	2295	1005	0	2894	0	0	0	0	0	2229	714	18	812	1574
750 cm	4898	1667	29	1810	833	0	0	0	0	3917	833	71	1133	29
752.5 cm	4700	3000	0	150	0	0	50	50	0	3000	0	0	2750	150
755 cm	585	208	0	417	91	0	18	0	0	2638	0	127	481	317
757.5 cm	102	150	0	95	0	0	0	0	0	524	0	95	639	0
760 cm	370	150	0	373	25	0	0	0	0	141	91	0	682	0
762.5 cm	350	75	0	1600	0	0	100	0	0	550	0	0	425	250
765 cm	304	156	0	185	0	0	30	0	0	37	0	0	393	0
767.5 cm	525	650	0	2000	0	0	0	0	0	725	0	0	1350	0
770 cm	290	411	0	1148	42	0	0	0	0	105	21	0	705	84
772.5 cm	364	664	0	441	0	0	50	0	0	455	50	75	1925	100
775 cm	551	499	0	636	0	0	185	0	0	185	40	40	959	0
777.5 cm	579	471	0	721	50	0	0	0	0	286	0	0	1907	193
780 cm	1292	892	0	625	171	0	0	67	0	646	133	133	2479	67
782.5 cm	488	1137	0	25	50	0	101	0	0	986	25	75	1801	212
785 cm	296	826	0	135	57	0	0	270	0	649	0	114	1834	364
787.5 cm	450	650	50	50	50	0	100	0	0	450	0	125	1275	250
790 cm	367	269	0	0	0	0	0	0	0	560	0	17	576	242
792.5 cm	1357	3476	0	0	0	0	0	0	0	1524	0	0	333	619
795 cm	2068	2538	0	467	0	0	133	0	0	634	0	0	734	667
797.5 cm	828	1765	0	57	0	0	0	0	0	1595	0	0	1524	969
800 cm	923	445	200	109	0	0	0	0	0	518	0	0	1595	0

Table III.4 continued – Cladoceran counts for Kieshofer Moor.

Graptoleberis testudinaria	Leydigi leydigi	Monospilus dispar	Phiruxa rostrata	P. aduncus	P. trigonellus	P. uncinatus	Psydochydorus globosus	Sida crystallina	Bosmina coregoni	B. longirostris	Daphnia pulex	Mutant Alona
0	0	0	0	0	50	350	0	100	0	75	0	0
0	0	0	0	50	0	800	0	600	0	225	0	0
0	0	0	0	0	107	253	0	453	0	480	0	0
0	0	0	0	0	0	109	0	204	0	143	0	0
0	0	0	0	0	171	389	0	161	0	46	0	0
121	0	0	0	0	0	147	0	211	0	200	0	463
0	125	0	0	0	0	583	0	667	0	0	0	500
0	100	0	200	0	0	267	0	467	0	0	0	200
0	267	0	0	0	0	556	0	133	0	417	0	0
0	107	0	0	0	0	27	0	493	0	172	0	0
0	250	0	0	0	0	1042	0	542	0	417	0	0
125	0	0	0	0	0	826	0	250	0	0	0	0
0	0	0	0	0	0	75	0	100	0	0	0	0
31	0	0	0	0	0	62	0	0	0	0	0	0
0	0	0	0	0	0	357	0	781	0	67	0	0
0	0	33	0	0	0	0	0	1013	0	102	0	0
133	0	0	0	0	0	0	0	1672	0	133	0	0
200	0	0	0	0	0	0	0	400	0	0	0	0
714	0	0	0	0	0	0	0	145	0	0	0	0
29	0	0	0	0	0	0	0	0	0	43	0	0
50	0	0	0	0	50	0	0	4150	0	50	0	0
18	0	0	0	0	0	0	0	182	0	417	0	0
0	0	0	0	0	0	150	0	102	0	799	0	0
0	0	0	0	0	0	0	0	0	0	577	0	0
0	200	0	0	0	0	0	0	0	0	275	0	0
0	0	0	0	0	0	0	0	0	15	141	0	0
0	0	0	0	0	0	0	0	250	0	375	0	0
0	0	0	0	0	0	0	0	0	0	337	0	0
0	0	0	0	0	0	0	0	114	0	114	0	0
0	0	0	0	0	0	0	0	0	0	140	0	0
0	143	0	0	0	0	0	0	0	0	75	0	0
0	0	33	0	0	0	0	0	0	133	713	0	0
106	0	0	0	0	0	0	0	0	101	251	0	0
114	0	0	0	0	29	0	0	0	29	296	0	0
50	0	0	0	0	0	0	0	0	50	350	0	0
17	0	0	0	0	0	0	0	17	50	451	0	0
0	0	0	0	0	0	0	0	0	333	1381	0	0
0	0	0	0	0	0	201	0	0	467	1937	0	0
0	0	0	0	0	0	0	0	57	0	798	0	0
0	0	0	0	0	0	0	0	0	0	236	0	0

Table III.4 continued – Cladoceran counts for Kieshofer Moor.

Depth	Acroperos harpae	Alona affinis	A. costata	A. guttata rectangula	A. guttata var tub	A. quadrangularis	Alonella excisa	A. rostrata	A. nana	Camptocercus rectirostris	Chydorus piger	C. sphaericus	Eurycercus lamellatus
100 cm	0	0	0	0	0	0	50	0	0	0	100	0	0
102.5 cm	0	0	0	0	0	0	699	0	0	0	25	0	0
105 cm	0	0	0	0	0	0	450	0	0	0	75	0	0
107.5 cm	0	0	0	0	0	0	60	0	0	0	47	0	0
110 cm	0	0	0	0	1111	0	1562	0	0	0	0	0	0
112.5 cm	0	0	0	0	1401	0	5239	0	0	0	0	24	0
115 cm	0	0	0	100	432	0	3668	0	248	0	0	0	0
117.5 cm	0	0	0	0	0	0	1702	0	0	0	0	0	0
120 cm	0	108	0	54	980	0	1102	0	14	54	0	230	0
122.5 cm	0	610	0	0	556	54	1021	0	0	0	0	54	424
125 cm	43	691	0	152	266	0	481	0	273	0	0	22	43
127.5 cm	0	792	0	225	442	0	1565	0	0	100	196	50	196
130 cm	0	337	0	105	353	0	686	0	242	48	0	76	152
132.5 cm	0	867	0	244	217	54	1847	0	95	54	0	0	407
135 cm	50	2007	0	179	0	0	4636	0	179	0	0	125	275
137.5 cm	0	1812	0	803	141	81	1297	0	0	325	0	41	224
140 cm	36	1223	0	164	438	0	2281	0	73	402	0	18	109
142.5 cm	263	1464	0	0	263	0	2405	0	263	333	0	148	37
145 cm	116	1000	0	250	175	0	1107	0	538	375	0	150	232
147.5 cm	0	742	0	611	938	0	980	0	336	792	0	117	355
150 cm	0	880	0	250	790	0	1915	0	580	120	0	100	330
152.5 cm	42	958	241	507	21	0	1646	0	225	366	0	308	188
155 cm	150	2150	0	100	0	0	4050	0	225	550	0	100	200
157.5 cm	385	1269	385	485	192	75	2221	0	200	300	50	100	250
160 cm	270	548	0	104	0	52	1815	0	201	14	69	552	122
162.5 cm	505	1709	0	705	505	0	3489	0	505	0	0	35	1664
165 cm	172	1225	0	123	417	49	1863	74	380	0	0	0	343
167.5 cm	55	154	0	22	300	0	3655	0	278	0	0	0	110
170 cm	25	441	0	25	0	50	1583	0	0	0	0	25	50
172.5 cm	200	506	0	53	106	53	1506	0	0	0	0	0	600
175 cm	52	393	0	247	385	0	1195	0	0	0	26	0	481
177.5 cm	589	553	0	69	172	69	1384	0	345	0	0	0	242
180 cm	380	445	0	946	800	0	1600	0	1180	0	0	23	400
182.5 cm	100	300	0	0	100	0	475	0	350	0	0	125	50
185 cm	573	743	0	50	0	0	746	0	826	0	0	149	50
187.5 cm	244	44	0	44	0	0	341	0	143	0	0	99	44
190 cm	476	745	0	984	269	0	238	0	918	269	0	538	538

Table III.5 – Cladoceran counts for Daschower Moor.

Graptoleberis testudinaria	Leydigi leydigi	Monospilus dispar	Pleroxus truncatus	P. uncinatus	Psydochydorus globosus	Sida crystallina	Bosmina coregoni	B. longirostris	Daphnia pulex	D. pulex epphipia	Mutated Alona
0	0	0	0	0	0	0	0	0	0	0	0
0	0	0	0	0	0	0	0	0	0	0	0
0	0	0	0	0	0	0	0	0	0	0	0
0	0	0	0	0	0	0	0	0	0	0	0
0	0	0	0	0	0	0	0	0	0	0	0
0	0	0	0	0	0	0	0	0	0	0	0
0	0	0	0	0	0	0	0	0	0	0	0
0	0	0	0	0	0	0	0	0	0	0	0
301	0	0	27	304	0	0	0	0	0	0	0
0	0	0	0	0	0	185	0	185	0	0	0
0	0	0	0	0	0	0	0	0	222	0	0
0	196	0	0	0	0	0	0	123	0	0	0
0	0	0	0	0	0	57	0	95	0	0	0
0	0	0	0	0	0	0	0	0	217	0	54
25	0	0	0	0	0	0	0	357	0	0	100
141	0	0	0	0	0	0	0	684	0	0	0
0	0	0	0	36	0	201	0	237	0	0	0
56	0	0	0	0	0	263	0	206	0	0	0
300	0	0	50	0	0	313	0	313	0	0	0
217	0	0	39	59	0	0	0	117	0	0	0
635	0	0	0	20	0	0	0	495	0	0	0
0	0	0	83	83	0	0	0	125	0	0	0
0	0	50	0	0	0	150	0	550	0	0	0
192	0	0	0	0	0	50	0	1154	0	0	0
0	0	0	0	0	0	0	0	672	0	0	0
35	0	0	0	0	0	505	0	1132	0	0	50
0	0	0	0	49	0	0	0	809	0	0	0
0	0	0	0	0	0	0	0	906	0	0	0
0	0	0	50	0	0	0	0	398	0	0	0
0	0	0	0	0	0	0	0	872	0	0	0
0	0	0	0	0	0	0	0	648	0	0	0
0	0	0	0	0	0	0	0	1143	0	0	0
0	0	0	0	0	0	0	0	2050	0	0	0
0	0	0	0	0	0	0	0	525	0	0	0
0	0	0	0	0	50	403	0	1694	0	0	0
0	0	44	0	0	0	0	0	705	0	0	0
238	0	0	0	135	0	238	0	1722	0	0	0

Table III.5 continued – Cladoceran counts for Daschower Moor.

Depth	Acroperos harpae	Alona affinis	A. costata	A. guttata rectangula	A. guttata var tub	A. quadrangularis	Alonella excisa	A. rostrata	A. nana	Camptocercus rectirostris	Chydorus piger	C. sphaericus	Eurycercus lamellatus
192.5 cm	512	267	0	116	40	0	192	0	554	0	20	414	196
195 cm	700	50	0	750	0	0	50	0	1000	75	50	525	450
197.5 cm	450	50	0	200	0	0	25	0	575	0	0	550	150
200 cm	274	200	0	0	0	0	148	0	720	0	0	240	183
202.5 cm	300	0	0	0	100	0	0	0	200	50	50	1075	0
205 cm	233	0	0	0	0	0	0	0	523	0	0	248	279
207.5 cm	50	0	0	55	0	0	0	0	350	0	0	620	200
210 cm	134	0	0	0	0	0	0	0	441	0	0	180	0
212.5 cm	100	0	0	46	0	0	0	0	400	0	0	98	0
215 cm	77	0	0	0	0	0	0	0	501	0	0	247	0
217.5 cm	252	0	0	0	0	303	0	0	1536	0	0	477	202
220 cm	185	377	0	0	0	0	0	0	1491	0	0	359	333
222.5 cm	200	44	0	0	0	0	0	0	1661	0	0	0	0
225 cm	214	265	0	0	0	0	0	0	643	0	0	330	0
227.5 cm	304	0	0	405	0	0	0	0	834	0	202	732	0
230 cm	185	100	0	0	0	0	0	0	720	0	0	1823	470
232.5 cm	599	50	0	25	0	0	199	0	1821	0	50	2148	299
235 cm	1154	435	0	50	0	0	0	0	1887	0	0	3398	300
237.5 cm	817	255	0	333	0	36	0	0	723	0	0	1914	36
240 cm	652	435	0	217	0	0	0	0	417	0	0	1136	217
242.5 cm	1024	384	0	172	0	0	0	0	340	0	0	1512	169
245 cm	718	109	0	136	200	0	200	0	600	0	0	2491	182
247.5 cm	753	239	0	0	0	0	402	0	1354	0	0	1622	554
250 cm	610	400	0	50	0	0	50	0	752	175	0	852	410
252.5 cm	600	848	0	0	50	0	100	0	498	0	0	968	250
255 cm	377	238	0	200	200	113	0	0	1077	0	0	496	713
257.5 cm	1051	672	0	0	0	0	227	0	2273	0	0	109	435
260 cm	898	509	0	0	0	0	0	0	2251	0	0	326	163
262.5 cm	350	200	0	50	0	0	100	0	525	0	0	400	0
265 cm	694	109	0	167	0	0	167	0	741	0	0	959	276
267.5 cm	397	100	0	0	248	0	992	0	1315	0	0	646	546
270 cm	810	638	0	595	298	0	0	0	1491	0	0	726	1532
272.5 cm	2181	810	0	0	0	0	410	0	981	267	0	1481	1277
275 cm	774	414	0	0	0	0	102	0	750	0	0	687	168
277.5 cm	1803	667	0	0	0	0	403	0	1341	0	0	1072	333
280 cm	1905	158	0	0	0	53	0	0	787	197	53	617	1103

Table III.5 continued – Cladoceran counts for Daschower Moor.

Graptoleberis testudinaria	Leydigi leydigi	Monospilus dispar	Pleroxus truncatus	P. uncinatus	Psydochydorus globosus	Sida crystallina	Bosmina coregoni	B. longirostris	Daphnia pulex	D. pulex epphipia	Mutated Alona
238	0	0	0	0	0	76	0	1076	0	0	0
200	0	0	0	0	0	1275	0	0	0	0	0
300	100	0	0	0	0	0	25	400	0	0	0
357	23	0	0	0	0	23	0	385	0	0	0
0	0	0	0	0	0	0	0	0	0	0	0
0	0	0	0	0	0	46	0	0	0	161	0
0	0	0	0	0	0	0	0	28	0	55	0
0	0	0	0	0	0	0	0	0	0	0	0
0	0	0	0	0	0	0	0	246	0	0	0
0	0	0	0	0	0	0	0	0	0	0	0
0	0	0	0	0	0	0	0	152	0	0	0
0	0	0	0	0	0	0	0	544	0	0	0
0	0	0	0	0	0	0	0	0	0	0	0
0	0	0	0	0	0	0	0	214	0	0	0
0	0	0	0	0	202	0	0	505	0	0	0
0	0	0	0	0	0	0	0	741	0	50	0
0	0	0	0	50	0	50	50	349	0	0	0
0	0	0	0	0	0	50	0	2173	0	0	0
0	0	0	0	0	0	0	0	609	0	0	0
0	0	0	0	0	0	0	0	920	0	0	0
0	0	0	0	0	0	172	0	989	172	0	0
0	0	0	0	0	0	200	0	455	0	309	0
0	0	0	0	0	0	76	0	353	0	0	0
0	0	0	0	0	0	0	0	230	0	0	0
0	0	50	0	0	0	450	0	2836	0	0	0
0	0	0	0	0	0	438	0	2045	0	0	0
227	0	0	0	0	0	0	0	6772	0	0	0
27	0	0	0	0	0	54	0	2013	0	0	0
50	0	0	0	0	0	0	0	1350	0	0	0
203	0	0	0	167	0	239	0	952	0	0	0
298	0	0	0	0	0	1389	0	1117	0	0	0
595	0	0	0	0	0	852	0	3574	0	0	0
0	0	0	0	0	0	133	0	3116	0	0	0
0	0	0	0	42	0	42	84	3331	0	0	0
0	0	0	0	0	0	133	67	5966	0	0	0
0	0	53	0	0	0	0	53	3573	0	0	0

Table III.5 continued – Cladoceran counts for Daschower Moor.

Appendix IV: Additional sedimentary data

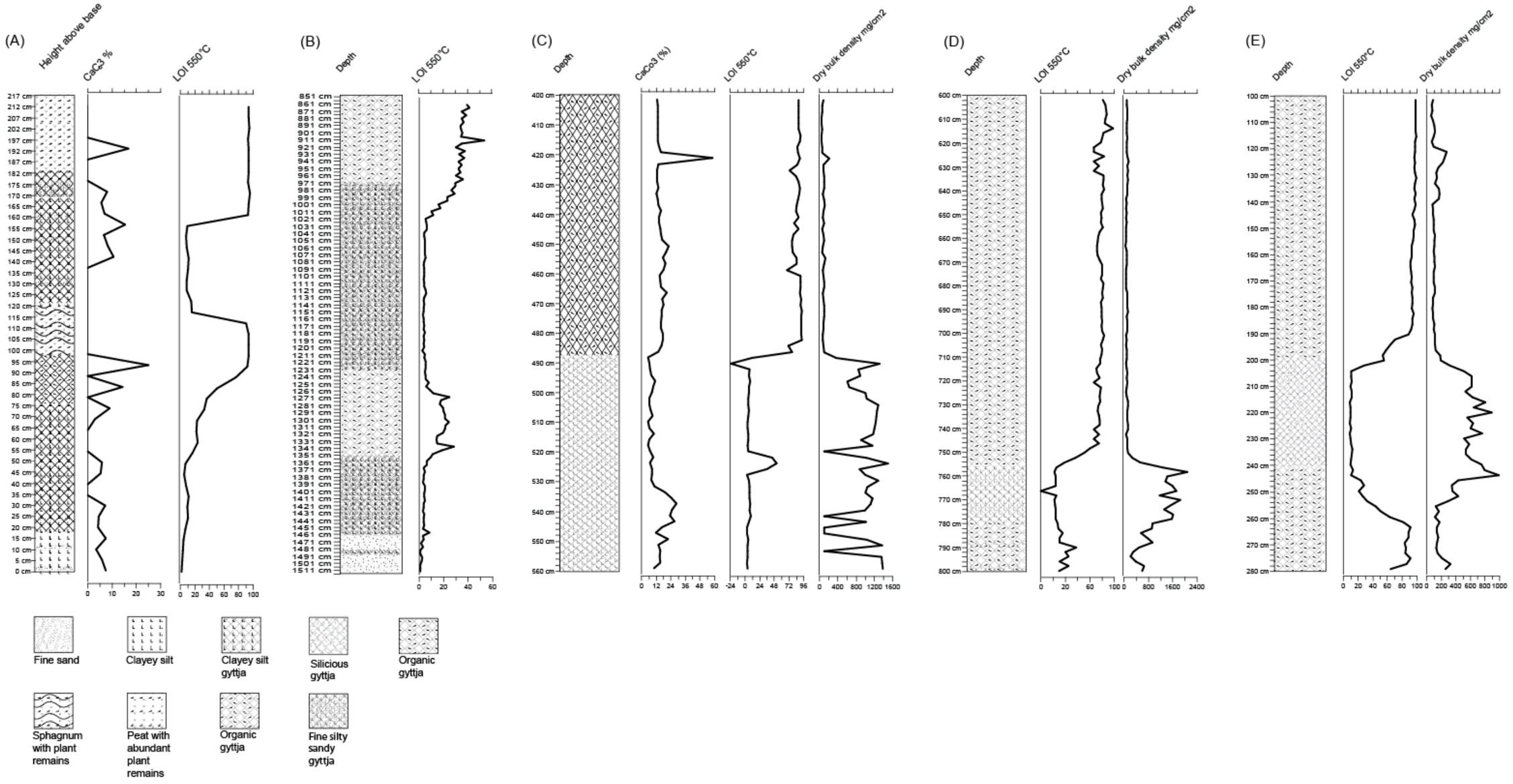
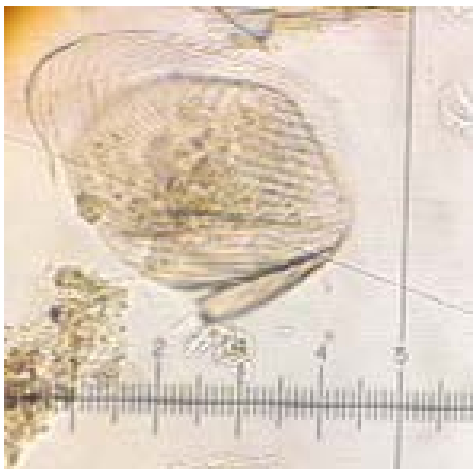
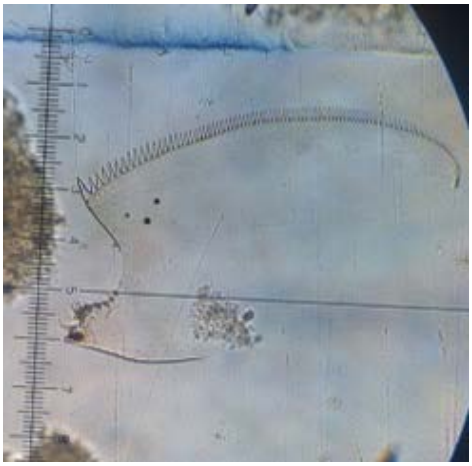


Figure IV.1 – Additional sedimentary data for Slotseng (A), Endinger Bruch (B), Potremser Moor (C), Kieshofer Moor (D) and Daschower Moor (E) that has not been referred to in Chapters 6 and 7.

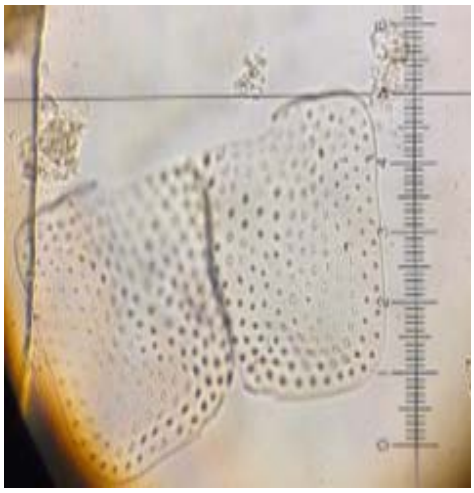
Appendix V: Selected cladoceran images



Alonella nana carapace



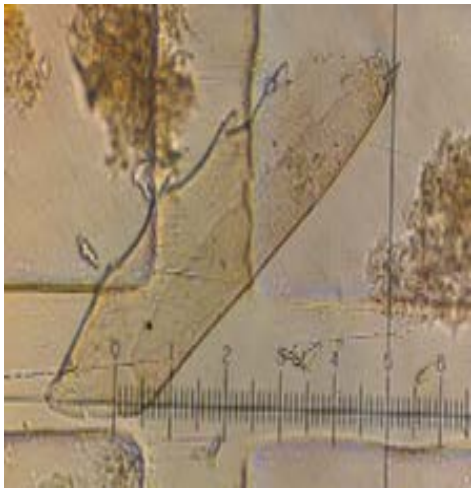
Eurycercus lamellatus post-abdominal claw



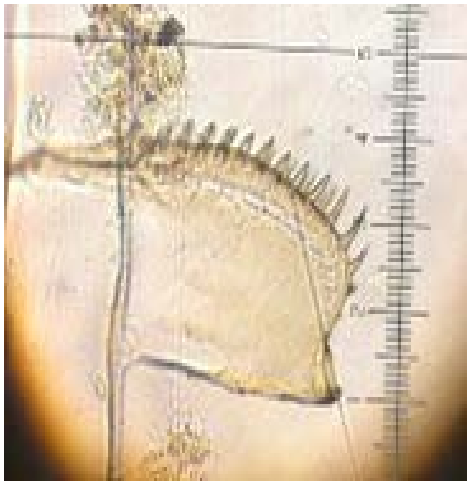
Alona guttata var tub carapace



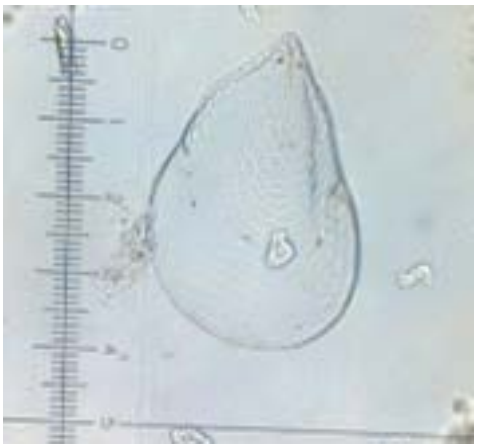
Pleroxus uncinatus headshield



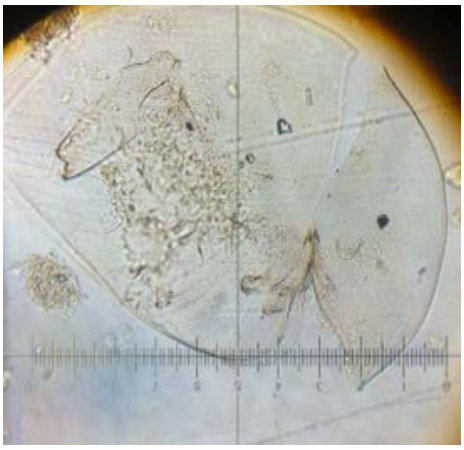
Sida crystallina post-abdominal claw



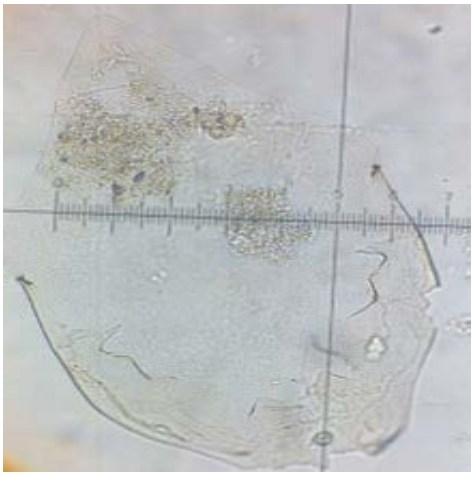
Alona affinis post-abdominal claw



Graptoleberis testudinaria head shield



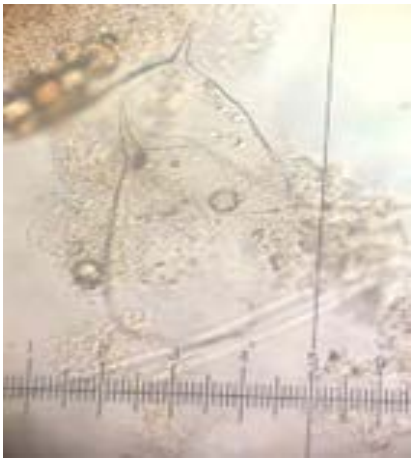
Sub-fossil *Acroperos harpae*



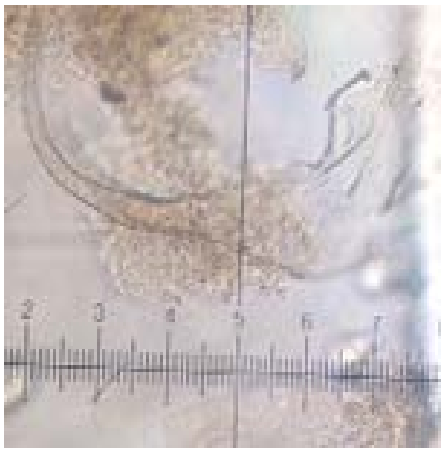
Mutated Alona affinis headshield



Eurycercus lamellatus headshield



Bosmina longirostris carapace



Bosmina longirostris headshield

Appendix VI: Bramham Law *et al*., 2013

JOURNAL OF QUATERNARY SCIENCE (2013) **28**(3) 248–257 ISSN 0267-8179. DOI: 10.1002/jqs.2615

New findings regarding the Saksunarvatn Ash in Germany

C. W. F. BRAMHAM-LAW,[1]* M. THEUERKAUF,[2] C. S. LANE[1] and J. MANGERUD[3]
[1]Research Laboratory for Archaeology and History of Art, University of Oxford, Dyson Perrins Building, South Parks Road, Oxford OX1 3QY, UK
[2]Institute for Geography and Geology, University of Greifswald, Germany
[3]Department of Earth Sciences & Bjerknes Centre for Climate Research, University of Bergen, Norway

ABSTRACT: The Saksunarvatn Ash is an important tephra layer for the correlation of Early Holocene environmental records in northern Europe, the North Atlantic and Greenland. The Saksunarvatn Ash is believed to have been produced by eruptions of the Grimsvötn volcanic system ~10.3 ka BP, which had two axes of dispersal, one plume in a north-west direction over northern Iceland and into Greenland, and a second southerly plume covering the Faroe Isles, Shetland Isles, western Norway and northern Germany. Here we present data from Potremser Moor, north-east Germany, extending the easterly margin of the ash fallout zone. We also present single grain trace element data from the type site at Saksunarvatn as well as from Potremser Moor. The Saksunarvatn Ash is indistinguishable between Potremser Moor and Saksunarvatn, suggesting the two tephras were produced by the same eruption. Trace element compositions from both sites are similar to data from the North Atlantic marine core (LINK 14:185), but different from the GRIP ice core (GRIP 1528.61 m), indicating that the south-east and north-west plumes may have arisen from separate eruption events. Copyright © 2013 John Wiley & Sons, Ltd.

KEYWORDS: cryptotephra; Holocene; Potremser Moor; Saksunarvatn Ash; tephrochronology.

Introduction

High-resolution palaeoclimate archives, such as the Greenland ice core records, have demonstrated that climatic oscillations during the Lateglacial–Holocene transition were both complex and abrupt, occurring over centennial and even decadal time frames (Alley *et al.*, 1993; Dansgaard *et al.*, 1993; Kapsner *et al.*, 1995; Rasmussen *et al.*, 2006; Steffensen *et al.*, 2008). This poses the challenge to scientists to determine the phasing of the palaeoenvironmental responses recognized across ice core, terrestrial and marine archives. Age models are most frequently generated by radiocarbon dating in the terrestrial and marine realms and these typically have centennial error ranges. A method that is increasingly employed in resolving these chronological issues is the use of, often invisible, volcanic ash layers (tephra, or cryptotephra). Tephra layers are deposited instantaneously, forming widespread isochrones that can be used to make correlations between sites, independent of other dating techniques (Mangerud *et al.*, 1984; Turney *et al.*, 2006; Brooks *et al.*, 2012). Whilst the most explosive eruptions disperse ash over thousands of kilometres (e.g. Lane *et al.*, 2011a), the distribution of tephra within sedimentary records is frequently discontinuous owing to atmospheric dynamics, sedimentation and preservation processes within varied landscapes (Boygle, 1999; Lawson *et al.*, 2012; Pyne O'Donnell, 2011).

The Icelandic Saksunarvatn Ash (SA) provides an example of the widespread but discontinuous nature of cryptotephra deposition. The SA was first described from the bog Hoydalar on the Faroe Islands (Jóhansen, 1975; Waagstein and Jóhansen, 1968). Subsequently, Jóhansen (1978, 1981, 1985) correlated an ash bed within Lake Saksunarvatn, also on the Faroe Islands, to the ash at Hoydalar. Further analysis, including microprobe analysis of the ash from Saksunarvatn by Mangerud *et al.* (1986), led to the ash being named the 'Saksunarvatn Ash', as the ash in Saksunarvatn was thicker, better dated and with existing samples, in contrast to the first finding at Hoydalar. Since then, tephra layers correlating with the SA have been identified within terrestrial, marine and ice core records across the North Atlantic region (Fig. 1) (Haflidason *et al.*, 1990; Sjøholm *et al.*, 1991; Merkt *et al.*, 1993; Birks *et al.*, 1996; Zielinski *et al.*, 1997; Andrews *et al.*, 2002; Lind and Wastegård, 2011). Whilst the SA is one of the most far-travelled Icelandic basaltic ash layers, being well represented in the Faroe Islands (Waagstein and Jóhansen, 1968; Jóhansen, 1981, 1985), the Shetland Islands (Bondevik *et al.*, 2005) and Norway (Birks *et al.*, 1996; Aarnes *et al.*, 2012), it is relatively under-represented on continental Europe, with only two sites in northern Germany to date having confirmed geochemical representation (Merkt *et al.*, 1993; Fig. 1). The SA has been dated using the GICCO5 timescale to $10\,297 \pm 45$ a BP (Rasmussen *et al.*, 2006) and to $10\,210 \pm 35$ cal a BP in Kråkenes, Norway (O. S. Lohne *et al.*, 2013).

Aims

1. To extend the known geographical ash footprint of the SA by documenting its presence in north-east Germany to the east of the last findings in central Europe by Merkt *et al.* (1993).
2. To fully chemically characterize the SA from the Saksunarvatn type site, using major, minor and trace element analysis.
3. To test chemical correlation of SA findings in Germany, the Faroe Islands and Greenland and re-evaluate the correlation of SA dispersal envelopes

Study site

Potremser Moor (53.991213°N, 12.275659°E) is an in-filled lake located in the Mecklenburg–Vorpommern region of Germany (Fig. 1). The former lake is located in an upland area surrounded by low hills and is ~15 ha in size. Today the site is covered by acidic, mesotrophic birch woodland with *Sphagnum* in the field layer. In September 2007 a 570-cm core was extracted from the site with a section from 410–530 cm analysed for pollen and cryptotephra analysis. The lower portion of the core from 486–530 cm is composed of a clayey

*Correspondence: C. W. F. Bramham-Law, as above
E-mail: cassian.bramhamlaw@rlaha.ox.ac.uk

Copyright © 2013 John Wiley & Sons, Ltd.

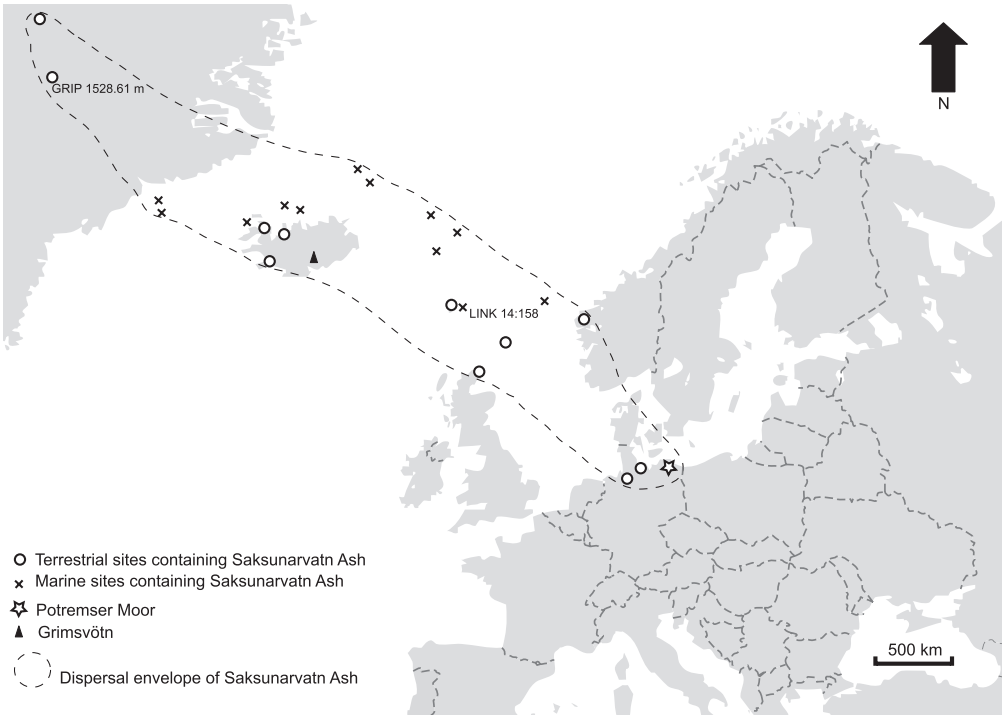


Fig. 1. Distribution envelope of the Saksunarvatn Ash identified within terrestrial and marine records as primary air-fall deposits based upon published data (Jóhansen, 1977; Mangerud *et al.*, 1986; Haflidason *et al.*, 1990; Haflidason *et al.*, 1995, 2000; Sjøholm *et al.*, 1991; Bennett *et al.*, 1992; Björck *et al.*, 1992; Koç and Jansen, 1992; Merkt *et al.*, 1993; Sigurgeirsson and Leosson, 1993; Bunting, 1994; Grönvold *et al.*, 1995; Ingólfsson *et al.*, 1995; Birks *et al.*, 1996; Dugmore and Newton, 1998; Eiríksson *et al.*, 2000; Wastegård *et al.*, 2001; Geirsdóttir *et al.*, 2002; Jennings *et al.*, 2002; Caseldine *et al.*, 2003; Bondevik *et al.*, 2005; Mortensen *et al.*, 2005; Lind and Wastegård, 2011; Rasmussen *et al.*, 2011; Aarnes *et al.*, 2012).

silty gyttja while the upper portion from 486–410 cm, containing the tephra layers, is composed of algal/detrital gyttja (Fig. 2).

Methods

Cryptotephra investigation

Samples for cryptotephra investigation were taken from the 2007 Potremser Moor core, thus allowing direct correlation of cryptotephra results with the high-resolution pollen record (M. Theuerkauf and H. Joosten, unpublished data). Contiguous 10-cm sediment samples were initially processed following the non-destructive, heavy liquid flotation method of Blockley *et al.* (2005). Tephra glass shards were counted using high-power optical microscopy under plane-polarized light. Where glass shards were detected, further contiguous 1-cm samples were taken at the corresponding depths of the greatest glass shard concentration to further refine the stratigraphic position of the cryptotephra. As glass shards were predominantly basaltic, only a cleaning float of 1.95 g cm^{-3} was employed at this stage, with the remaining dense residue mounted for optical microscopy. All samples were dried and weighed to provide an estimation of the total number of glass shards per gram of dry sediment. The sediment from which tephra was extracted was a fine algal/detrital gyttja with a high water content. Approximately 2 cm^3 of sediment was sampled for each tephra layer, but when dried this yielded dry weights of < 0.06 g, therefore giving artificially high shards g^{-1} counts.

Geochemical analysis

Further 1-cm depth samples were taken from where peaks in cryptotephra concentration were observed, and these were re-prepared for geochemical analysis following Blockley *et al.* (2005), with omission of ashing. To concentrate glass shards for analysis, shards were picked manually under high-power microscopy and mounted on epoxy resin stubs. Stubs were ground and polished to expose flat internal glass shard sections. Major element analysis was carried out using a JEOL JXA8600 electron microprobe, in wavelength-dispersive mode (WD-EMPA) at the Research Laboratory for Archaeology and the History of Art, University of Oxford. Ten major elements were analysed with varying analysis times (count times: Na, 10 s; Mg, Al, Si, K, Ca, Fe, 30 s; Ti, Mn, 40 s; P, 60 s) using an accelerating voltage of 15 kV, a beam current of 6 nA and a beam diameter of 10 μm. The MPI-DING secondary standards of fused volcanic glass, namely KL2-Basalt (basaltic), ATHO-G (rhyolite) and StHs6/80-G (andesite) (Jochum *et al.*, 2005, 2006) were used to monitor the precision of the data output and to ensure analytical accuracy (Table 1). All accepted data were normalized to 100% for comparative purposes. P_2O_5 was omitted in the normalization procedure for POT-455 to ensure comparability of all plotted datasets, as not all contain analysis of P_2O_5.

Trace element analysis was performed by laser ablation inductively coupled plasma mass spectrometry (LA-ICP-MS), using an Agilent 7500 ICP-MS coupled to a Resonetics 193-nm ArF eximer laser ablation system at the Department of Earth Sciences, Royal Holloway University of London (Müller *et al.*, 2009). For full details of LA-ICP-MS operating protocols and data quantification see Tomlinson *et al.* (2010). A 5-Hz repetition rate was used with a 40-s count time on the sample and the gas blank. NIST 612 was used as the standard for calibration and ^{29}Si as the internal standard element, having previously been measured by single-grain WD-EMPA. A laser spot size of 25 μm was used due to the relatively small size of the glass shards in the distal SA. As with WD-EMPA, the

Copyright © 2013 John Wiley & Sons, Ltd.

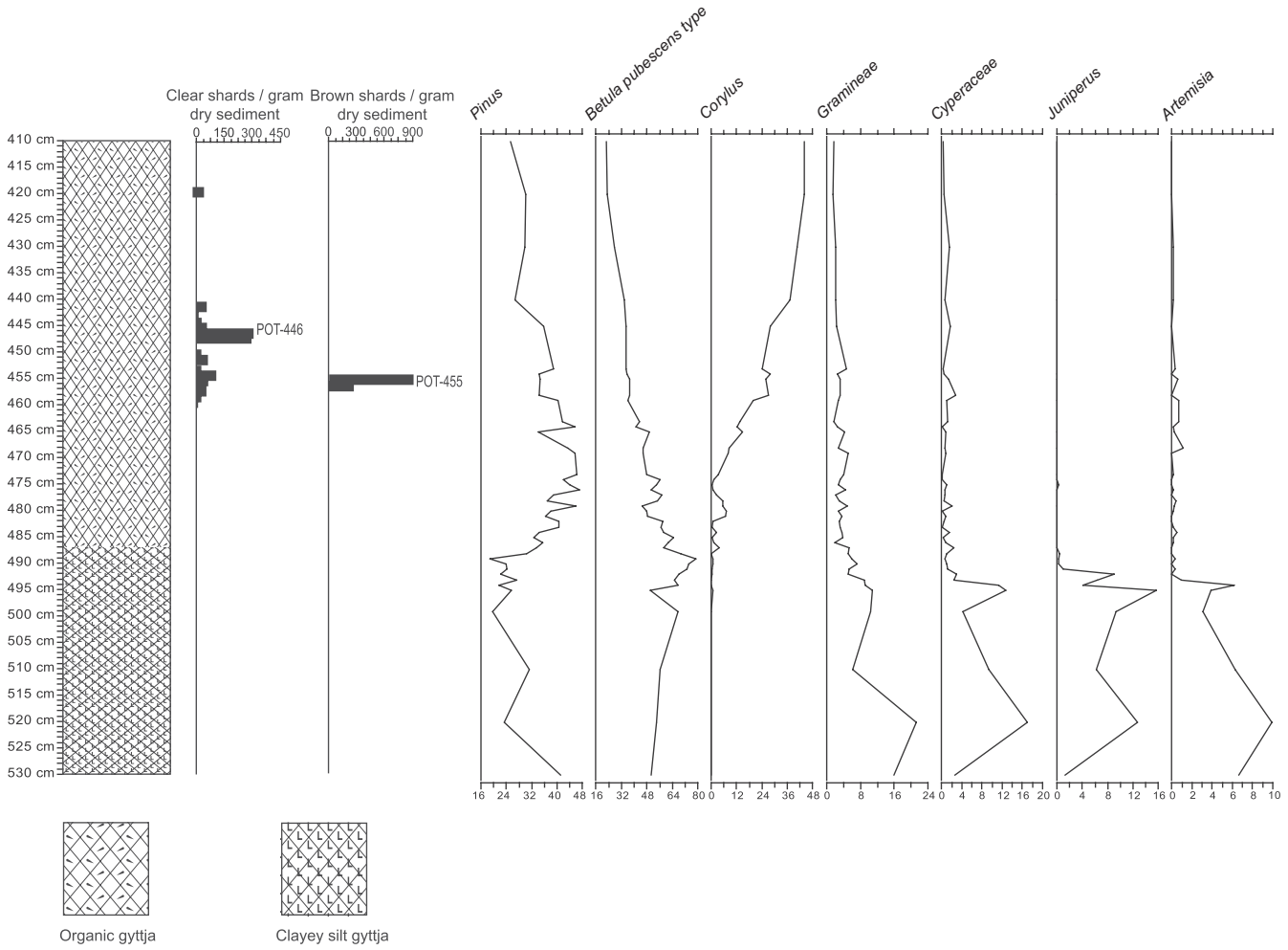


Fig. 2. Tephrostratigraphy and lithology of Potremser Moor with selected pollen curves (after M. Theuerkauf and H. Joosten, unpublished data). Tephra shards are plotted as the number of shards per gram of dry sediment. Tephra layers are named according to their depth within the Potremser Moor and are described in detail in the text.

ATHO-G and StHs6/80-G secondary standards were analysed to monitor instrumental accuracy and precision.

To validate the correlation to the SA, a sample from the type site at Saksunarvatn, as described by Mangerud *et al.* (1986), was also analysed by WD-EMPA and, for the first time, by LA-ICP-MS to determine the trace element composition of the volcanic glass. The SA, located at 29.85–30.30 m within Lake Saksunarvatn, was sieved to > 63 μm then prepared and analysed following the same methods outlined above (but with a larger LA-ICP-MS spot size of 34 μm).

Results

Position of tephra layers

Initial 10-cm scans showed the presence of cryptotephra at 440–460 cm within the Potremser Moor core. Further 1-cm contiguous scans showed that this concentration comprised two discrete peaks (Fig. 2). The older, larger peak was located at 455 cm (POT-455), within algal/detrital gyttja of the Early Holocene. The large peak of POT-455 appears midway through the main expansion of *Corylus* and decrease in *Pinus* (M. Theuerkauf and H. Joosten, unpublished data) with the main expansion of *Corylus* centring around 10 550 cal a BP within central Europe (Giesecke *et al.*, 2011). A peak in shard concentrations of 1033 g^{-1} was recorded at 455–456 cm where glass shards were almost exclusively brown in colour, with platy through to curvilinear morphologies and a maximum long axis length of 110 μm. A small number (absolute count of three) of colourless shards were also identified within the large peak in brown shards. An area of sediment, sterile of tephra, separating the two peaks between 448 and 450 cm indicates that these colourless shards are unlikely to be the product of down-core re-working of glass shards from the peak at 446 cm, and most likely represent sporadic colourless shards from within the basaltic peak. The second smaller, younger peak was located at 446 cm (POT-446) and is again located within Holocene algal/detrital gyttja and within the main expansion period of *Corylus*. A peak in shard concentration of 325 g^{-1} (absolute count 12) was recorded at 446–447 cm. Glass shards were colourless, showing irregular and fluted morphologies with occasional closed vesicles and a maximum long axis length of 30 μm.

Geochemical analysis

POT-455

Eleven major and minor element and four trace element analyses were produced for POT-455. As discussed above, the nature of the sediment served to inflate shard g^{-1} counts. Therefore, large amounts of sediment (2 cm^3) were required to produce enough shards for WD-EPMA. Due to the limited amount of core material available it was not possible to repeat this procedure. The geochemical analysis results presented in Figs. 3 and 4 and Tables 1 and 2 indicate that POT-455 is a tholeiitic basalt (Le Bas *et al.*, 1986). Figures 3 and 4, based

Copyright © 2013 John Wiley & Sons, Ltd.

Table 1. WDS-EPMA results for POT-455 from Potremser Moor and type site SA. Totals are un-normalized. Intermittent analysis of MPI-DING volcanic glass standards ATHO-G and STHS6/80-G was used as secondary standards to check for machine drift during EPMA analysis (Jochum *et al.*, 2005, 2006; http://georem.mpch-mainz.gwdg.de/).

	SiO_2	TiO_2	Al_2O_3	FeO	MnO	MgO	CaO	Na_2O	K_2O	P_2O_5	Total
Tephra analysis											
POT-455 - (a)											
	50.36	2.99	13.16	14.24	0.24	5.30	10.05	2.37	0.43	0.34	99.48
	49.46	3.00	13.05	13.55	0.22	5.14	9.87	2.10	0.56	0.34	97.29
	50.49	2.85	13.53	12.52	0.17	5.01	9.62	2.24	0.30	0.34	97.07
	49.98	3.13	13.44	13.17	0.24	4.92	9.54	2.63	0.55	0.36	97.96
	49.71	3.14	12.98	14.26	0.28	5.59	10.06	2.11	0.47	0.34	98.93
	48.28	2.84	12.75	13.62	0.27	5.02	9.62	1.72	0.45	0.36	94.93
	49.58	2.79	13.09	14.08	0.28	5.77	8.78	2.32	0.33	0.38	97.42
	49.91	2.69	12.92	13.51	0.24	5.77	8.89	2.38	0.41	0.37	97.11
Average	49.72	2.93	13.11	13.62	0.24	5.32	9.55	2.23	0.44	0.36	97.52
2σ	1.37	0.32	0.52	1.18	0.07	0.70	0.97	0.53	0.18	0.03	2.75
Secondary standards											
Atho-G											
Average	75.37	0.25	12.26	3.28	0.11	0.10	1.68	4.22	2.76	0.03	100.06
2σ	0.21	0.02	0.09	0.12	0.02	0.02	0.05	0.22	0.03	0.01	0.79
StHs6/80-G											
Average	63.32	0.72	17.59	4.31	0.10	1.99	5.32	4.67	1.32	0.15	99.49
2σ	0.33	0.03	0.17	0.15	0.03	0.04	0.04	0.10	0.02	0.01	0.92
GOR132-G											
Average	45.50	0.32	10.96	10.15	0.16	22.53	8.42	0.84	0.03	0.03	98.94
2σ	0.14	0.04	0.05	0.11	0.03	0.14	0.09	0.04	0.01	0.02	0.67
Tephra analysis											
POT-455 - (b)											
	49.81	2.91	13.18	14.13	0.27	5.72	10.08	2.58	0.45	0.25	99.38
	49.24	3.09	12.82	14.55	0.24	5.74	10.22	2.49	0.45	0.24	99.08
	49.12	3.05	12.87	14.38	0.26	5.75	9.99	2.50	0.43	0.24	98.60
Average	49.39	3.02	12.95	14.36	0.25	5.74	10.10	2.52	0.44	0.24	99.02
2σ	0.74	0.18	0.39	0.43	0.03	0.04	0.22	0.09	0.02	0.01	0.79
Secondary standards											
Atho-G											
Average	75.41	0.25	12.30	3.33	0.12	0.09	1.67	4.05	2.76	0.01	99.99
2σ	0.41	0.06	0.30	0.25	0.05	0.03	0.07	0.47	0.18	0.02	1.84
StHs6/80-G											
Average	63.09	0.69	17.35	4.39	0.08	1.97	5.31	4.56	1.29	0.10	98.83
2σ	0.46	0.09	0.35	0.23	0.08	0.05	0.18	0.16	0.10	0.07	1.77
GOR132-G											
Average	45.56	0.29	10.88	10.21	0.14	22.19	8.43	0.80	0.04	0.03	98.57
2σ	0.66	0.05	0.23	0.25	0.04	0.32	0.17	0.14	0.05	0.03	1.94
Tephra analysis											
Saksunarvatn Ash	49.59	2.94	13.09	14.44	0.32	5.45	9.81	2.55	0.46		98.64
	48.81	2.80	12.57	14.18	0.17	6.76	9.38	2.75	0.39		97.80
	49.33	2.81	12.88	14.03	0.22	5.86	10.53	2.39	0.35		98.41
	49.93	3.05	13.22	14.84	0.21	5.27	9.80	1.80	0.39		98.50
	49.58	2.88	13.01	14.08	0.38	5.54	9.88	2.49	0.45		98.30
	49.48	2.89	13.21	14.84	0.25	5.62	9.92	2.62	0.41		99.24
	49.51	2.89	12.97	14.10	0.18	6.00	10.65	2.48	0.40		99.17
	49.34	2.86	12.99	14.33	0.23	5.79	9.98	2.59	0.44		98.54
	49.34	2.99	13.17	14.07	0.25	5.56	9.82	2.54	0.44		98.17
	49.19	2.85	12.99	13.69	0.13	5.41	9.94	2.53	0.38		97.12
	49.48	3.05	13.09	13.91	0.19	5.69	9.94	2.65	0.40		98.41
	50.40	3.00	13.36	14.36	0.30	5.16	9.99	2.61	0.35		99.53
	49.47	2.95	13.01	13.91	0.19	5.58	9.97	2.49	0.38		97.93
	49.90	2.98	13.20	14.29	0.25	5.63	9.96	2.43	0.43		99.08
	49.55	2.89	13.13	13.91	0.32	5.46	10.05	2.39	0.41		98.10
	49.44	2.93	12.98	13.97	0.24	5.60	9.95	2.56	0.43		98.11
	49.14	2.94	12.97	14.07	0.24	5.58	9.93	2.53	0.40		97.80
	49.45	2.87	13.04	13.72	0.28	5.57	9.81	2.63	0.40		97.78
	49.14	2.96	12.94	14.31	0.17	5.55	9.88	2.75	0.45		98.14
	49.75	2.65	13.32	13.93	0.20	6.04	10.41	2.03	0.38		98.70
	50.60	3.14	13.44	14.56	0.30	5.48	9.78	2.65	0.41		100.36
	49.79	2.73	13.28	12.97	0.22	5.82	10.00	2.47	0.36		97.64
	49.56	2.94	13.11	14.17	0.20	5.67	9.95	2.54	0.42		98.57
	49.55	2.99	13.15	13.99	0.17	5.51	9.86	2.42	0.44		98.07
	49.26	2.95	13.03	14.16	0.25	5.47	9.97	2.54	0.44		98.07
	48.88	2.93	12.74	14.00	0.17	5.60	9.94	2.70	0.43		97.38

continued

Copyright © 2013 John Wiley & Sons, Ltd.

Table 1. (Continued)

	SiO_2	TiO_2	Al_2O_3	FeO	MnO	MgO	CaO	Na_2O	K_2O	P_2O_5	Total
	49.53	2.96	12.89	14.03	0.29	5.53	9.87	2.69	0.45		98.25
	49.56	3.01	12.95	13.90	0.23	5.59	9.95	2.21	0.43		97.83
	49.71	2.84	13.19	13.65	0.17	5.62	9.88	2.62	0.42		98.09
	49.30	2.76	13.35	13.72	0.19	5.88	10.29	2.35	0.41		98.26
	49.65	2.96	13.07	14.14	0.31	5.52	9.94	2.56	0.48		98.62
	49.45	2.86	13.20	14.20	0.26	5.61	9.94	2.55	0.43		98.50
	49.37	1.99	13.24	12.05	0.26	7.41	12.29	2.11	0.24		98.97
	49.51	2.93	12.92	14.27	0.23	5.39	9.81	2.53	0.44		98.03
	49.18	2.64	13.15	13.93	0.27	5.95	10.41	2.55	0.36		98.44
	49.45	2.96	13.17	14.33	0.21	5.42	9.80	2.54	0.45		98.33
	49.55	2.86	13.06	14.36	0.16	5.58	9.99	2.47	0.42		98.44
	49.44	2.82	13.04	14.31	0.26	5.77	10.26	2.52	0.40		98.81
	49.80	2.93	13.03	13.73	0.17	5.62	10.00	2.58	0.41		98.29
Average	49.51	2.88	13.08	14.04	0.23	5.68	10.04	2.50	0.41		98.37
2σ	0.67	0.36	0.34	0.93	0.11	0.77	0.87	0.38	0.08		1.18
Secondary standards											
StHs6/80-G											
Average	63.50	0.72	17.62	4.41	0.06	1.92	5.22	4.55	1.31		99.31
2σ	0.27	0.02	0.16	0.16	0.04	0.04	0.07	0.16	0.03		0.95
GOR128-G											
Average	45.98	0.29	9.94	9.87	0.17	25.59	6.24	0.55	0.04		98.67
2σ	0.26	0.03	0.09	0.14	0.08	0.21	0.09	0.05	0.02		0.97
GeoRem preferred value											
Atho-G	75.60	0.26	12.20	3.27	0.11	0.10	1.70	3.75	2.64		99.62
Uncertainty (95%)	0.70	0.02	0.20	0.10	0.01	0.01	0.03	0.31	0.09		1.46
StHs6/80-G	63.70	0.70	17.80	4.37	0.08	1.97	5.28	4.44	1.29		99.63
Uncertainty (95%)		0.02	0.20	0.07	0.00	0.04	0.09	0.14	0.02		1.09
GOR132-G	45.50	0.31	11.00	10.10	0.15	22.40	8.45	0.83	0.03		98.77
Uncertainty (95%)	0.40	0.01	0.20	0.10	0.01	0.20	0.12	0.04	0.00		1.08
GOR128-G	46.10	0.29	9.91	9.81	0.18	26.00	6.24	0.57	0.04		99.13
Uncertainty (95%)	0.40	0.01	0.17	0.12	0.01	0.30	0.12	0.03	0.01		1.16

upon normalized data, show the comparison of POT-455 with the data from the Saksunarvatn type site (Mangerud *et al.*, 1986). The figures indicate a robust compositional match to our data on the SA, based on major, minor and trace element geochemistry. Subtle variations between POT-455 and type site SA are probably due to machine variability and differences in operating conditions. For details of SA type site analysis see Mangerud *et al.* (1984). Trace element analysis of the SA was previously undertaken by Merkt *et al.* (1993) using X-ray fluorescence (XRF). Our trace element analysis of the SA differs from the values of Merkt *et al.* (1993). This is largely due to the far greater precision and accuracy of single-grain LA-ICP-MS data presented by this study. Secondly, Merkt *et al.* (1993) commented on contamination issues within their XRF sample, with quartz and diatom frustules present within the sample leading to an elevation in SiO_2, therefore making normalization to SiO_2 problematic. The high SiO_2 given by XRF therefore yielded a tephra of dacite composition not basaltic as indicated by EPMA.

POT-446

Following repeated efforts to chemically characterize POT-446 using WD-EMPA, only a single geochemical analysis was produced. Whilst indicating a glass shard of rhyolitic composition, the total single grain glass total was 91.45% and therefore had to be rejected. As already discussed, due to the nature of the sediment, it was not possible to produce enough shards for WD-EPMA due to the amounts of material required. Secondly, the small size of a number of shards from POT-446 (<30 μm longest axis length) made WD-EPMA with a 10-μm spot problematic.

Discussion

Dating Potremser Moor

Positive correlation of POT-455 with the SA provides the first *in situ* calendar age estimate for the Potremser Moor chronology. We are therefore able to demonstrate that the deposition of the SA falls into the main expansion of *Corylus*. Similar observations by Merkt *et al.* (1993) in three sites from north-western Germany robustly demonstrate that the expansion of *Corylus* was synchronous in both areas of northern Germany.

Distribution of the Saksunarvatn Ash

Potremser Moor lies approximately 200 km east of Plußsee which hitherto marked the south-easterly extent of the SA within northern Europe (Merkt *et al.*, 1993). Our discovery of the SA as a cryptotephra layer within Potremser Moor therefore extends the known south-easterly margin of the ash fallout zone (Fig. 1).

Comparison of sites within northern Germany indicates that at the limits of the SA distribution, topography and basin size may influence the preservation of the SA. Plußsee, Eversener See and now Potremser Moor are hitherto the only sites within northern Germany with geochemically confirmed SA. All three sites are located in upland regions, with Plußsee and Potremser Moor located in hilly, former morainic landscapes. All three sites have relatively small basins of <15 ha located in topographic hollows. Micromorphological analysis of the SA deposits from Plußsee and Eversener See appeared to show one distinct tephra layer, interpreted as reflecting air fall

Copyright © 2013 John Wiley & Sons, Ltd.

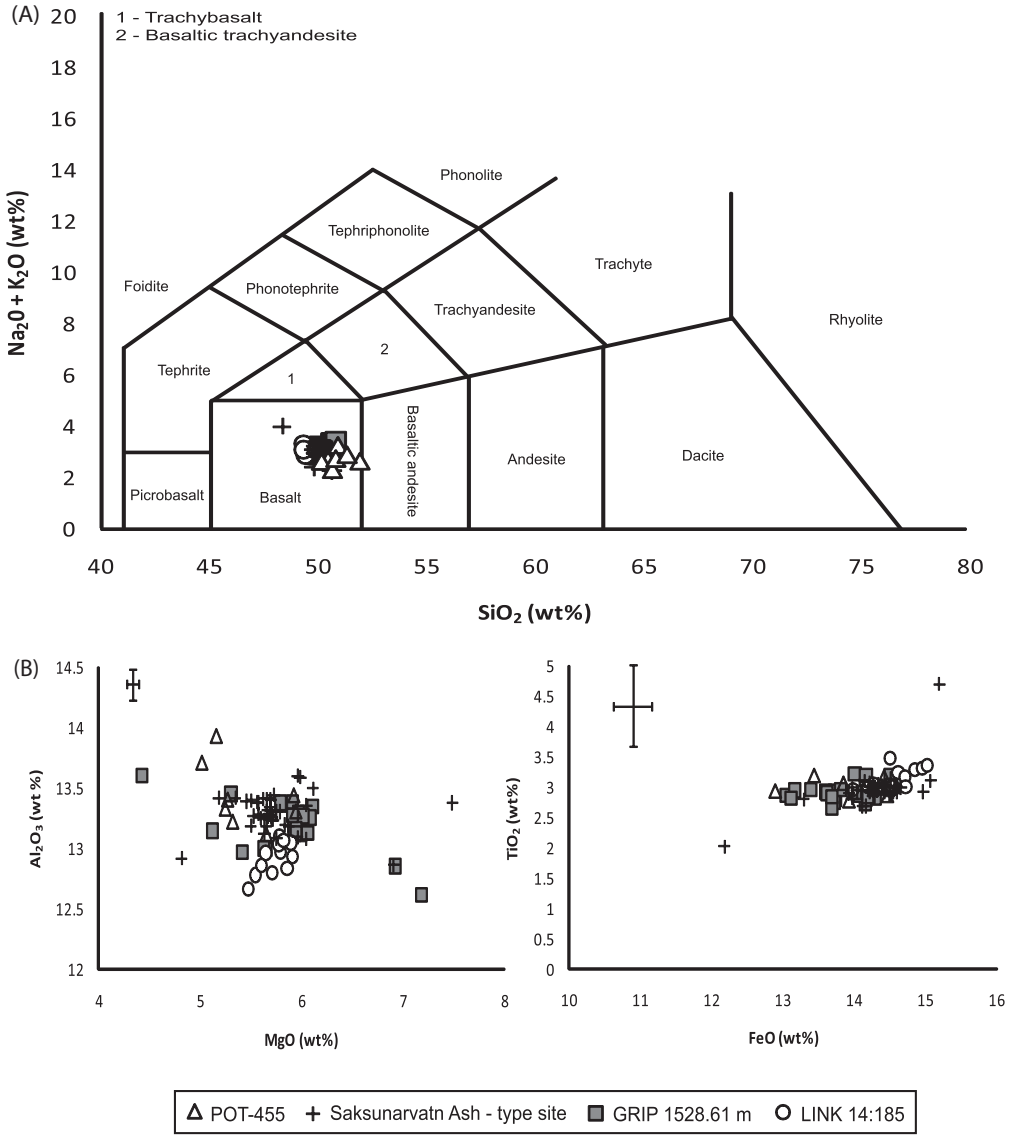


Fig. 3. POT-455, Saksunarvatn Ash, GRIP 1528.61 m and LINK 14:185 major and minor element plots. All major and minor data are plotted as normalized values. (A) Total alkali/silica (after Le Bas *et al.*, 1986) plot of POT-455 with comparison of Saksunarvatn Ash type site, GRIP 1528.61 m and LINK 15:185. (B) Selected bi-plots of POT-455 with comparison of Saksunarvatn Ash type site, GRIP 1528.61 m and LINK 15:185. Saksunarvatn Ash data from type site reported from in house data; Saksunarvatn Ash reported from GRIP 1528.61 m (Grönvold *et al.*, 1995; Davies *et al.*, 2012) and LINK 14:185 (Rasmussen *et al.*, 2011; Davies *et al.*, 2012). Representative 2σ are indicated for each bi-plot within B (upper left) based upon precision established from secondary standard analysis (Table 1).

deposition (Merkt *et al.*, 1993). It is likely that the small basin size of Potremser Moor effectively acted as a lens, concentrating air fall deposition within the small basin, and therefore allowing sufficient quantities of the Saksunarvatn Ash to be deposited, and allowing its detection within the sedimentary record.

Chemical characterization of the Saksunarvatn Ash

As with many Lateglacial–Early Holocene Icelandic distally described tephra layers, no proximal outcrop is known for the SA. Therefore, identification relies on compositional and stratigraphic correlation to other distal occurrences. It is possible to identify tephra deposits based solely on major element data when there is secure stratigraphy and additional chronological information, but many of the Icelandic volcanoes that erupted frequently during the Lateglacial and Holocene are known to have produced tephra with almost identical major elemental profiles from multiple eruptive events (Larsen *et al.*, 2001; Lowe *et al.*, 2008; Housley *et al.*, 2012; Lane *et al.*, 2012). The addition of trace element analysis is therefore an important step in confirming a correlation.

The major and minor element glass compositions of the ashes named Saksunarvatn Ash at POT-455, the type site SA, GRIP and LINK are all indistinguishable (within the quoted errors, see Table 1 and Fig. 3A,B). However, using single-grain glass trace element ratios, Davies *et al.* (2012) show a compositional distinction (based on Zr/Ce–Y/Ce ratios, Fig. 4C) between two tephra layers correlated to the SA from (i) the Greenland ice core GRIP 1528.61 m (Grönvold *et al.*, 1995) and (ii) North Atlantic marine core LINK 14:185 (Rasmussen *et al.*, 2011). The authors therefore suggest that two separate eruptions generated the tephra dispersed to the north-west and south-east. The composition of POT-455 and data from the type site SA is more consistent with the data from LINK 14:185 than with GRIP 1528.61 m, supporting this hypothesis (Fig. 4C).

Copyright © 2013 John Wiley & Sons, Ltd.

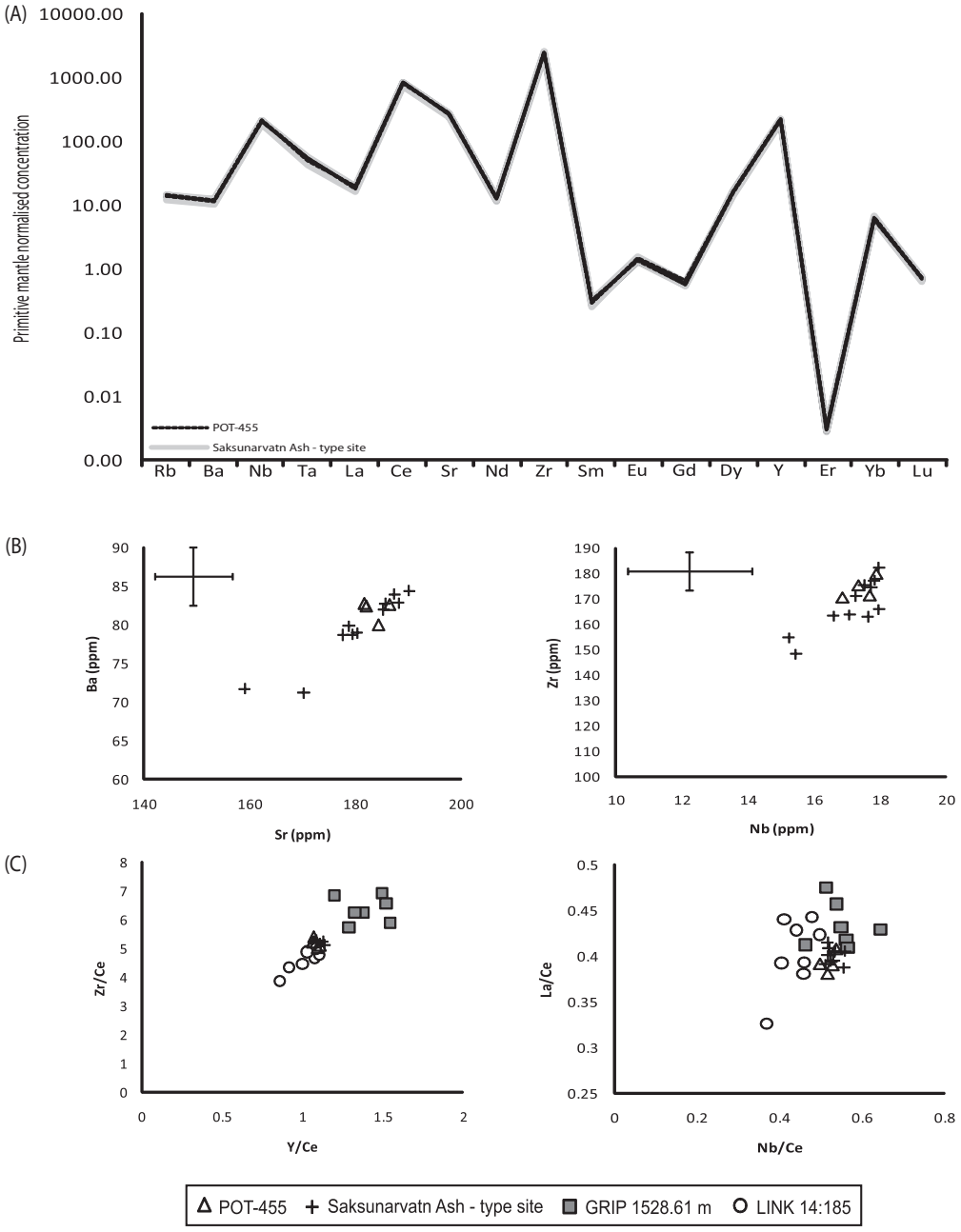


Fig. 4. POT-455, Saksunarvatn Ash, GRIP 1528.61 m and LINK 14:185 trace element plots. (A) Primitive mantle normalized trace element composition profile (after Sun and McDonough, 1989) of POT-455 and type site Saksunarvatn Ash. (B) Selected bi-plots of trace element concentrations showing comparison of POT-455 with type site Saksunarvatn Ash. Representative 2σ uncertainties are indicated for each bi-plot (upper left) based upon precision established from secondary standard analysis (Table 2). (C) Selected trace element ratio bi-plots for comparison of POT-455 and type site Saksunarvatn Ash with Saksunarvatn Ash reported from GRIP 1528.61 m (Grönvold *et al.*, 1995; Davies *et al.*, 2012) and LINK 14:185 (Rasmussen *et al.*, 2011; Davies *et al.*, 2012).

Comparison of age estimates for the SA from Greenland (10 297 ± 45 GICC05 a BP; Rasmussen *et al.*, 2006) and Norway (10 210 ± 35 cal a BP; Lohne *et al.*, 2013) also are consistent with the hypothesis of separate eruptions, with an initial, older eruption with a north-west dispersal axis followed by the Saksunarvatn eruption, which was dispersed to the south-east towards the Faroe Islands and continental Europe, forming the SA type ash. Evidence from Lake Hvítárvatn, central Iceland, is consistent with a multiple eruption hypothesis. Sediment cores from the site show three tephra layers of SA age and composition separated by 4- and 2-cm laminated sediment horizons (Jóhannesdóttir *et al.*, 2005). The lowest and middle ash layers are separated by 4 cm of sediment representing ~80–100 years, whilst the middle and top layers are separated by 2 cm of sediment representing ~30 years (Jóhannesdóttir *et al.*, 2005).

It is apparent from Fig. 4C that there is a difference in the precision of the two trace element datasets. This is attributed by Abbott *et al.* (2012) to the use of a smaller beam size during analysis of the very fine-grained tephra shards in the GRIP sample, therefore reducing the volume of material ablated during analysis. Fractionation effects due to the small beam size may have also impacted upon the accuracy of the analysis, thus preventing accurate quantification of the data and reliance upon elemental ratios. To confirm this chemical differentiation, a fully quantitative trace element analysis of the apparent SA in GRIP, or from other sites within the north-west axis is required. Nonetheless, with a lack of

Copyright © 2013 John Wiley & Sons, Ltd.

Table 2. LA-ICP-MS results for POT-455 from Potremser Moor. <LOD indicates samples below 6σ of the background. This may vary due to instrument sensitivity and between sample runs (Jochum *et al.*, 2005, 2006; http://georem.mpch-mainz.gwdg.de/).

	Rb	Sr	Y	Zr	Nb	Ba	La	Ce	Pr	Nd	Sm	Eu	Gd	Dy	Er	Yb	Ta	Th	U	Spot size (μm)
Tephra analysis																				
POT-455																				
	9	182	37	171	18	83	13	34	5	22	6	2	6	7	4	4	1	1	<LOD	25
	9	186	38	175	17	83	14	35	4	23	6	2	6	7	4	4	1	1	<LOD	25
	9	182	36	180	18	82	14	33	4	21	6	2	7	7	4	3	1	1	<LOD	25
	9	184	35	170	17	80	12	33	4	22	7	2	6	7	4	4	1	1	<LOD	25
Secondary standards																				
Atho-G																				
Observed	66	91	89	482	57	541	54	118	14	61	14	2	14	16	10	10	4	7	2	25
Certified	65	94	95	512	62	547	56	121	15	61	14	3	15	16	10	11	4	7	2	25
StHs6/80																				
Observed	30	469	11	110	6	293	11	25	3	11	<LOD	1	<LOD	2	1	<LOD	<LOD	2	1	25
Certified	31	482	11	118	7	298	12	26	3	13	3	1	3	2	1	1	0	2	1	25
Tephra analysis																				
Saksunarvatn Ash	9	190	38	182	18	84	14	34	5	23	6	2	6	7	4	4	1	1	0	25
	9	187	37	175	18	84	14	34	5	23	6	2	6	7	4	3	1	1	0	25
	8	159	33	148	15	72	12	29	4	20	6	2	6	6	4	3	1	1	<LOD	25
	9	178	35	163	17	79	13	32	4	21	6	2	7	7	4	3	1	1	<LOD	25
	9	185	36	171	17	82	13	34	5	22	6	2	6	7	4	4	1	1	0	25
	9	179	35	164	17	79	13	32	4	20	7	2	7	7	4	4	1	1	0	25
	9	180	35	163	18	79	13	32	4	22	6	2	7	7	4	3	1	1	0	25
	9	186	36	174	18	83	13	33	5	22	7	2	7	7	4	3	1	1	0	25
	8	170	33	155	15	71	12	29	4	21	5	2	6	6	4	3	1	1	0	25
	9	179	35	166	18	80	13	32	4	21	6	2	7	7	4	4	1	1	0	25
	9	188	36	177	18	83	13	34	4	22	6	2	7	7	4	4	1	1	0	25
Secondary standards																				
Atho-G																				
Observed	66	95	89	487	59	558	55	120	15	59	15	3	15	16	10	10	4	7	2	25
Certified	65	94	95	512	62	547	56	121	15	61	14	3	15	16	10	11	4	7	2	25
StHs6/80																				
Observed	30	465	11	111	6	299	11	24	3	12	3	1	3	2	1	1	0	2	1	25
Certified	31	482	11	118	7	298	12	26	3	13	3	1	3	2	1	1	0	2	1	25

corresponding proximal sources, the fully quantified and high-precision single-grain trace element data for the SA provided by this study from the type site will enable robust identification of future discoveries of the SA within northern Europe and elsewhere.

Implications for Early Holocene European tephrostratigraphy

The results from Potremser Moor significantly raise the potential of the SA as a well-characterized time-parallel stratigraphic marker within northern European environmental records. However, they raise questions over the correlation of the GRIP 1528.61 m layer to the same eruptive event.

The Early Holocene SA is well positioned to enable the synchronicity between climatic amelioration following the Younger Dryas and vegetation response in northern Europe to be tested. Crucially this can help elucidate whether lags in vegetation response are locally isolated, or form part of a pan-regional response (Lange *et al.*, 1986; De Klerk, 1998). Like the widespread Vedde Ash (Wastegård *et al.*, 2000; Davies *et al.*, 2005; Lane *et al.*, 2011b) the SA can further improve age modelling of individual sites by providing an independently dated isochrone at 10 210 ± 35 cal a BP, thus enabling greater precision at sub-centennial scales.

The trace element data presented here contribute further to our understanding of the timing and dispersal of the SA, showing that separate eruptions probably contributed to the two axes of dispersal. This detail will allow more precise and accurate correlation of this stratigraphically and chronologically important Early Holocene tephra across the North Atlantic and northern Europe.

The eastward extension of the SA as provided by the results from Potremser Moor raises the potential of the tephra being found further south into Germany and east into Poland. Following our results we predict that investigations into additional upland sites will yield further SA deposits, particularly those in the morainic zones of northern Germany and Poland.

Acknowledgements. C.B.L. is funded by a NERC studentship (NE/H524822/1) and M. T. is funded by ICLEA. We thank V. C. Smith for microprobe analysis and E. L. Tomlinson for LA-ICP-MS, which were both funded by the NERC consortium project 'Response of humans to abrupt environmental transitions' (RESET, NE/E015905/1 and NE/E015670/1). We also thank René Dommain who helped with the coring of Potremser Moor and Alexander Fields who helped with the processing of samples in the Laboratory. Two anonymous reviewers provided useful and constructive comments.

Abbreviations. LA-ICP-MS, laser ablation inductively coupled plasma mass spectrometry; SA, Saksunarvatn Ash; WD-EMPA, wavelength-dispersive electron microprobe analysis; XRF, X-ray fluorescence.

References

Aarnes I, Bjune AE, Birks HH, *et al.* 2012. Vegetation responses to rapid climatic changes during the last deglaciation 13, 500–8, 000 years ago on southwest Andøya, artic Norway. *Vegetation History and Archaeobotany* **21**: 17–35.

Copyright © 2013 John Wiley & Sons, Ltd.

Abbott PM, Davies SM, Steffensen J-P, *et al*. 2012. A detailed framework of Marine Isotope Stages 4 and 5 volcanic events recorded in two Greenland Ice-cores. *Quaternary Science Reviews* **36**: 59–77.

Alley RB, Meese DA, Shuman CA, *et al*. 1993. Abrupt increase in Greenland snow accumulation at the end of the Younger Dryas event. *Nature* **362**: 527–529.

Andrews JT, Geirsdóttir A, Hardardóttir J, *et al*. 2002. Distribution, sediment magnetism and geochemistry of the Saksunarvatn (10 180 ± 60 cal. yr BP) tephra in marine, lake, and terrestrial sediments, northwest Iceland. *Journal of Quaternary Science* **17**: 731–745.

Bennett KD, Boreham S, Sharp MJ, *et al*. 1992. Holocene history of environment, vegetation and human settlement on Catta Ness, Lunnasting, Shetland. *Journal of Ecology* **80**: 241–273.

Birks HH, Gulliksen S, Halflidason H, *et al*. 1996. New radiocarbon dates for the Vedde Ash and the Saksunarvatn Ash from Norway. *Quaternary Research* **45**: 119–127.

Björck S, Ingólfsson O, Haflidason H, *et al*. 1992. Lake Torfadalsvatn: a high resolution record of the North Atlantic ash zone I and the last glacial–Interglacial environmental changes in Iceland. *Boreas* **21**: 15–22.

Blockley SPE, Pyne-O'Donnell SDF, Lowe JJ, *et al*. 2005. A new and less destructive laboratory procedure for the physical separation of distal glass tephra shards from sediments. *Quaternary Science Reviews* **24**: 1952–1960.

Bondevik S, Mangerud J, Dawson S, *et al*. 2005. Evidence for three North Sea tsunamis at the Shetland Islands between 8000 and 1500 years ago. *Quaternary Science Reviews* **24**: 1757–1775.

Brooks SJ, Matthews IP, Birks HH, *et al*. 2012. High resolution Lateglacial and early-Holocene summer air temperature records from Scotland inferred from chironomid assemblages. *Quaternary Science Reviews* **41**: 67–82.

Boygle J. 1999. Variability of tephra in lake and catchment sediments, Svínavatn, Iceland. *Global and Planetary Change* **21**: 129–149.

Bunting MJ. 1994. Vegetation history of Orkney, Scotland: pollen records from two small basins in West Mainland. *New Phytologist* **128**: 771–792.

Caseldine C, Geirsdóttir A, Langdon P. 2003. Efstadalsvatn – a multi-proxy study of a Holocene lacustrine sequence from NW Iceland. *Journal of Paleolimnology* **30**: 55–73.

Dansgaard W, Johnsen SJ, Clausen HB, *et al*. 1993. Evidence for general instability of past climate from a 250-kyr ice-core record. *Nature* **364**: 218–220.

Davies SM, Hoek WZ, Bohncke SJP, *et al*. 2005. Detection of Lateglacial distal tephra layers in the Netherlands. *Boreas* **34**: 123–135.

Davies SM, Abbott PM, Pearce NJG, *et al*. 2012. Integrating the INTIMATE records using tephrochronology: rising to the challenge. *Quaternary Science Reviews* **36**: 11–27.

De Klerk P. 1998. Lateglacial and Early Holocene vegetation history in northern Vorpommern: a preliminary review of available pollen diagrams. Project report, Greifswald University.

Dugmore AJ, Newton AJ. 1998. Holocene Tephra layers in the Faroe Islands. *Fróðskaparrit* **46**: 191–204.

Eiríksson J, Knudsen KL, Haflidason H, *et al*. 2000. Lateglacial and Holocene palaeoceanography of the North Icelandic shelf. *Journal of Quaternary Science* **15**: 23–42.

Geirsdóttir Á, Andrews JT, Ólafsdóttir S, *et al*. 2002. A 36 Ky record of iceberg rafting and sedimentation from north-west Iceland. *Polar Research* **21**: 291–298.

Giesecke T, Bennett KD, Birks HJB, *et al*. 2011. The pace of Holocene vegetation change – testing for synchronous developments. *Quaternary Science Reviews* **30**: 2805–2814.

Grönvold K, Oskarsson N, Johnsen SJ, *et al*. 1995. Ash layers from Iceland in the GRIP ice core correlated with oceanic and land sediments. *Earth and Planetary Science Letters* **135**: 149–155.

Haflidason H, Sejrup HP, Jones GA. 1990. Tephra-, bio- and lithostratigraphy of an AMS dated core from the Norway basin, southern Norwegian Sea. *Geonytt* **17**: 52.

Haflidason H, Sejrup HP, Johannesson H, *et al*. 1995. The southern Norwegian Greenland Sea through the last 20 Ka: sedimentation, tephra layers and palaeoceanography. In: The Lateglacial Palaeoceanography of the North Atlantic Margins. Quaternary Research Association, Edinburgh, UK Annual Discussion Meeting. Abstract.

Haflidason H, Eiríksson J, van Kreveld S. 2000. The tephrochronology of Iceland and the North Atlantic region during the Middle and Late Quaternary: a review. *Journal of Quaternary Science* **15**: 3–22.

Housley RA, Lane CS, Cullen VL, *et al*. 2012. Icelandic volcanic ash from the Late-glacial open-air archaeological site of Ahrenshöft LA58 D, North Germany. *Journal of Archaeological Science* **39**: 708–716.

Ingólfsson Ó, Norddahl H, Haflidason H. 1995. Rapid isostatic rebound in southwestern Iceland at the end of the last glaciation. *Boreas* **24**: 245–259.

Jennings AE, Grönvold K, Hilberman R, *et al*. 2002. High-resolution study of Icelandic tephras in the Kangerlussuaq Trough, southeast Greenland, during the last deglaciation. *Journal of Quaternary Science* **17**: 747–757.

Jóhannesdóttir GE, Thordarson T, Geirsdóttir Á, *et al*. 2005. The widespread ~10 ka Saksunarvatn tephra: a product of three large basaltic phreatoplinian eruptions? Geophysical Research Abstracts 7. 05991 (SRef-ID: 1607–7962/gra/EGU05-A-05991).

Jóhansen J. 1975. Pollen diagrams from the Shetland and Faroe islands. *New Phytologist* **75**: 369–387.

Jóhansen J. 1978. Outwash of terrestric soils into Lake Saksunarvatn, Faroe Islands. *Danmarks Geologiske Undersøkelse, Årbok* **1977**: 31–37.

Jóhansen J. 1977. Outwash of terrestric soils into Lake Saksunarvatn, Faroe Islands. *Danmarks Geologiske Undersøgelse* **1977**: 31–37.

Jóhansen J. 1981. Vegetation Development in the Faroes from 10,000 BP to Present. *Danmarks Geologiske Undersøgelse* **1981**: 111–136.

Jóhansen J. 1985. *Studies in the Vegetation History of the Faroe and Shetland Islands*. Føroya Fróðskaparfelag: Tórshavn, Faroe Islands.

Jochum KP, Nohl U, Herwig K, *et al*. 2005. GeoReM: a new geochemical database for reference materials and isotopic standards. *Geostandards and Geoanalytical Research* **29**: 333–338.

Jochum KP, Stoll B, Herwig K, *et al*. 2006. MPI-DING reference glasses for in situ microanalysis: new reference values for element concentrations and isotope ratios. *Geochemistry Geophysics Geosystems* **7**: Q02008. doi: 10.1029/2005GC001060.

Kapsner WR, Alley RB, Shumann CA, *et al*. 1995. Dominant influence of atmospheric circulation on snow accumulation in Greenland over the past 18,000 years. *Nature* **373**: 52–54.

Koç N, Jansen E. 1992. A high resolution diatom record of the last deglaciation from the SE Norwegian Sea: documentation of rapid climatic changes. *Palaeoceanography* **7**: 499–520.

Lane CS, Andric M, Cullen VL, *et al*. 2011a. The occurrence of distal Icelandic and Italian tephra in the Lateglacial of Lake Bled, Slovenia. *Quaternary Science Reviews* **30**: 1013–1018.

Lane CS, De Klerk P, Cullen VL. 2011b. A tephrochronology for the Lateglacial palynological record of the Endinger Bruch (Vorpommern, north-east Germany). *Journal of Quaternary Science* **27**: 141–149.

Lane CS, Blockley SPE, Mangerud J, *et al*. 2012. Was the 12.1 ka Icelandic Vedde Ash one of a kind? *Quaternary Science Reviews* **33**: 87–99.

Lange E, Jeschke L, Knapp HD. 1986. Ralswiek und Rügen. Landschaftsentwicklung und Siedlungsgeschichte der Ostseeinsel. Teil I: Die Landschaftsgeschichte der Insel Rügen seit dem Spätglazial. Akademie Verlag, Berlin.

Larsen G, Newton AJ, Dugmore AJ, *et al*. 2001. Geochemistry, dispersal, volumes and chronology of Holocene silicic tephra layers from the Katla volcanic system, Iceland. *Journal of Quaternary Science* **16**: 119–132.

Lawson IT, Swindles GT, Plunkett G, *et al*. 2012. The spatial distribution of Holocene cryptotephras in north-west Europe since 7 ka: implications for understanding ash fall events from Icelandic eruptions. *Quaternary Science Reviews* **41**: 57–66.

Le Bas MJ, Le Maitre RW, Streckeisen A, *et al*. 1986. A chemical classification of volcanic rocks based on the total alkali-silica diagram. *Journal of Petrology* **27**: 745–750.

Copyright © 2013 John Wiley & Sons, Ltd.

Lind EM, Wastegård S. 2011. Tephra horizons contemporary with short early Holocene climate fluctuations: new results from the Faroe Islands. *Quaternary International* **24**: 157–167.

Lohne OS, Mangerud J, Birks HH. 2013. Precise ^{14}C ages of the Vedde and Saksunarvatn ashes and the younger Dryas boundaries from western Norway and their comparison with the Greenland Ice Core (GICC05) chronology. *Journal of Quaternary Science* (in press).

Lowe JJ, Rasmussen SO, Björck S, *et al*. 2008. Synchronisation of palaeoenvironmental events in the North Atlantic region during the Last Termination: a revised protocol recommended by the INTIMATE group. *Quaternary Science Reviews* **27**: 6–17.

Mangerud J, Lie SE, Furnes H, *et al*. 1984. A Younger Dryas ash bed in western Norway and its possible correlations with tephra in cores from the Norwegian Sea and the North Atlantic. *Quaternary Research* **21**: 85–104.

Mangerud J, Furnes H, Johansen J. 1986. A 9,000 year old ash bed on the Faroe Islands. *Quaternary Research* **26**: 262–265.

Merkt J, Muller H, Knabe W, *et al*. 1993. The early Holocene Saksunarvatn Tephra found in lake sediments in N.W. Germany. *Boreas* **22**: 93–100.

Mortensen AK, Bigler M, Grönvold K, *et al*. 2005. Volcanic ash layers from the Last Glacial Termination in the NGRIP ice core. *Journal of Quaternary Science* **20**: 209–219.

Müller W, Shelley M, Miller P, *et al*. 2009. Initial performance metrics of a new custom-designed ArF excimer LA-ICP-MS system coupled to a two-volume laser-ablation cell. *Journal of Analytical Atomic Spectrometry* **24**: 209–214.

Pyne-O'Donnell SDF. 2011. The taphonomy of Last Glacial–Interglacial Transition (LGIT) distal volcanic ash in small Scottish lakes. *Boreas* **40**: 131–145.

Rasmussen SO, Andersen KK, Svensson AM, *et al*. 2006. A new Greenland ice core chronology for the last glacial termination. *Journal of Geophysical Research* **111**: 1–15.

Rasmussen TL, Thomsen E, Nielsen T, *et al*. 2011. Atlantic surface water inflow to the Nordic seas during the Pleistocene-Holocene transition (mid-late Younger Dryas and Pre-Boreal periods, 12 450–10 000 a BP. 2011. *Journal of Quaternary Science* **26**: 723–733.

Sigurgeirsson MA, Leosson MA. 1993. Two early Holocene tephra layers in the Sogamyri peat deposit. Reykjavik. *Náttúrufrædingurinn* **62**: 129–137.

Sjøholm J, Sejrup HP, Furnes H. 1991. Quaternary volcanic ash zones on the Iceland Plateau, southern Norwegian Sea. *Journal of Quaternary Science* **6**: 159–173.

Steffensen JP, Andersen KK, Bigler M, *et al*. 2008. High-resolution Greenland ice core data show abrupt climate change happens in few years. *Science* **321**: 680–684.

Sun SS, McDonough WF. 1989. Chemical and isotopic systematics of oceanic basalts: implications for mantle composition and processes. *Geological Society of London* **42**: 313–345.

Tomlinson EL, Thordarson T, Müller W, *et al*. 2010. Microanalysis of tephra by LA-ICP-MS-strategies, advantages and limitations assessed using the Thorsmörk ignimbrite (Southern Iceland). *Chemical Geology* **279**: 73–89.

Turney CSM, Van Den Burg K, Wastegård S, *et al*. 2006. North European last glacial–interglacial transition (LGIT; 15–9 ka) tephrochronology: extended limits and new events. *Journal of Quaternary Science* **21**: 335–345.

Waagstein R, Jóhansen J. 1968. Tre vulkanske askelag fra Faeröerne. *Meddelelser fra Dansk Geologisk Forening* **34**: 257–264.

Wastegård S, Wohlfarth B, Subetto DA, *et al*. 2000. Extending the known distribution of the Younger Dryas Vedde Ash into northwestern Russia. *Journal of Quaternary Science* **15**: 581–586.

Wastegård S, Björck S, Grauert M, *et al*. 2001. The Mjauvotn tephra and other Holocene tephra horizons from the Faroe Islands: a link between the Icelandic source region, the Nordic Seas, and the European continent. *The Holocene* **11**: 101–109.

Zielinski GA, Mayewski PA, Meeker D, *et al*. 1997. Volcanic aerosol records and tephrochronology of the Summit, Greenland, ice cores. *Journal of Geophysical Research* **102**: 26,625–26,640.

Copyright © 2013 John Wiley & Sons, Ltd.